

**MATHEMATICS and
COMPUTERS in SCIENCE and
INDUSTRY**

MATHEMATICS and COMPUTERS in SCIENCE and INDUSTRY

Copyright © 2014, by the editors

All the copyright of the present book belongs to the editors. All rights reserved. No part of this publication may be reproduced, stored in a retrieval system, or transmitted in any form or by any means, electronic, mechanical, photocopying, recording, or otherwise, without the prior written permission of the editors.

All papers of the present volume were peer reviewed by no less than two independent reviewers. Acceptance was granted when both reviewers' recommendations were positive.

Series: Mathematics and Computers in Science and Engineering Series | 31

ISBN: 978-1-61804-247-7

ISSN: 2227-4588

**MATHEMATICS and
COMPUTERS in SCIENCE and
INDUSTRY**

Table of Contents

| | |
|---|----|
| Generalized Least-Squares Regressions IV: Theory and Classification Using Generalized Means | 19 |
| <i>Nataniel Greene</i> | |
| Convex Relaxation Methods for Nonconvex Polynomial Optimization Problems | 36 |
| <i>André A. Keller</i> | |
| An Inverse Calculation of Unimodular for Polynomial Matrices | 46 |
| <i>Wataru Kase</i> | |
| Formal Verification of Safety Control System based on GHENESYS NET | 51 |
| <i>Rodrigo Cesar Ferrarezi, Reinaldo Squillante Júnior, Jeferson A. L. Souza, Diolino J. Dos Santos Filho, José Reinaldo Silva, Paulo Eigi Miyagi, Lucas Antonio Moscato</i> | |
| Intelligent Border Security Interactive Simulation Tool (IBS-IST) | 57 |
| <i>Iyad Aldasouqi, Arafat Awajan</i> | |
| Parameter Estimate of Anisochronic Models Using Method of Moments | 62 |
| <i>Milan Hofreiter</i> | |
| Speech Processing Strategy in a Cochlear Implant Processing Unit based on a Combination of SNR and the Number of Frequency Bands in Amplitude and Frequency Modulation | 66 |
| <i>S. Antonov, G. Tsenov, V. Mladenov</i> | |
| Include Macbeth in the MCDA Models Suggested by Italian Legislation for the Selection of the Most Economically Advantageous Tender in Contracts for Public Works. Comparison and Application of MCDA Model to a Case Study | 70 |
| <i>Maria Rosaria Guarini, Claudia Buccarini, Fabrizio Battisti</i> | |
| Using Integral E-Portfolio to Learn Linear Algebra | 75 |
| <i>M. Isabel Garcia-Planas, Judit Taberna</i> | |
| Piezoelectric based Vibration Energy Harvester with Tip Attraction Magnetic Force: Modeling and Simulation | 80 |
| <i>Dauda Sh. Ibrahim, Asan G. A. Muthalif, Tanveer Saleh</i> | |

| | |
|---|-----|
| Data Mining in Medicine Domain Using Decision Trees and Vector Support Machine <i>Djamila Benhaddouche, Abdelkader Benyettou</i> | 87 |
| Conversion of the METCM into the Meteo-11 <i>Karel Šilinger, Ladislav Potužák, Jiří Šotnar</i> | 92 |
| Image Encryption based on Development of Hénon Chaotic Maps using Fractional Fourier Transform <i>Mona F. M. Mursi, Hossam Eldin H. Ahmed, Fathi E. Abd El-Samie, Ayman H. Abd El-Aziem</i> | 98 |
| Anti-Windup Approach for the Compensation of Slip Speed of Induction Motor <i>T. Benmiloud</i> | 107 |
| Multivalent Harmonic Mappings <i>Melike Aydogan, Durdane Varol</i> | 114 |
| The Development, Status and Trends of Recommender Systems: A Comprehensive and Critical Literature Review <i>Jin Xu, Karaleise Johnson-Wahrmann, Shuliang Li</i> | 117 |
| Using Simulation for Testing of Control Programs for Process Control Systems in Coal Mining <i>Victor Okolnishnikov, Sergey Rudometov, Sergey Zhuravlev</i> | 123 |
| The Influence of the Gear Cutting Dynamics upon the Shape and Position of the Replaceable Cutting Edges Made from Sintered Metallic Carbides <i>Cristian-Silviu Simionescu, Carmen Debeleac</i> | 127 |
| Optimization of Feeding Management on Small-Scale Dairy Systems of Central México <i>Adolfo Aarmando Rayas-Amor, Carlos Galdino Martínez-García, Octavio Alonso Castelán-Ortega</i> | 132 |
| Motion Capture Systems Overview and Accelerometer MoCaps Systems <i>Slava Milanova Yordanova, Nikolay Todorov Kostov, Yasen Dimchev Kalchev</i> | 138 |
| The Use of Psychometric Questionnaires in Security Community Members Evaluation <i>Alena Paduchova, Ludek Lukas</i> | 142 |
| The Analysis of Removable Cutting Tools from the Point of View of the Operating Properties <i>Cristian-Silviu Simionescu</i> | 146 |
| Investigation of Natural User Interfaces and their Application in Gesture-Driven Human-Computer Interaction <i>Bekim Fetaji, Majlinda Fetaji, Aleksandar Petrovski, Mirlinda Ebibi</i> | 152 |

| | |
|--|-----|
| Integrated Development Environment for Remote Application Platform <i>Omer Saleh, Xavier Patrick Kishore, P. Sagaya Aurelia</i> | 159 |
| 3D Numerical Optimization of Pollution Emission by Group of Source <i>V. V. Fedosov, Alina Fedossova</i> | 166 |
| Comparison between Functional Parameters of the Four Gear Automatic Gearbox and the Seven Gear Automatic Gearbox by a Kinematic Point of View <i>Veronica Argeșanu, Ion Silviu Borozan, Inocențiu Maniu, Raul Miklos Kulcsar, Mihaela Jula</i> | 168 |
| The Political Culture of Civic Type: Methodology of Formation <i>I. Dolinina</i> | 173 |
| Service Based Generation of Latex Graphical Dependencies <i>Pavol Buzák, Katarína Žáková, Zoltán Janík</i> | 179 |
| Entropy in Terms of Vehicular Distance under Driving Constraints <i>Caglar Kosun, Serhan Ozdemir</i> | 183 |
| Governance and Adaptation to Innovative Modes of Higher Education Provision <i>Silvia Florea, Cecile Hoareau McGrath</i> | 186 |
| Development and Analyses of “M-LearnSys” Mobile Learning Course Management System <i>Bekim Fetaji, Majlinda Fetaji, Jovica Saveski, Mirlinda Ebibi</i> | 191 |
| A Survey on Mobile Augmented Reality Based Interactive, Collaborative and Location based Storytelling <i>P. Sagaya Aurelia, Durai Raj, Omer Saleh</i> | 197 |
| Crowdsourcing Implementation Platform as Methodology in Process Management –BPM- of Services Information System in Health <i>Fernando Prieto Bustamante, Yaneth P. Caviatava, Yoan Manuel Guzman, Victor Manuel Castro Rodríguez</i> | 204 |
| Free Software for the Modelling and Simulation of a Mini-UAV <i>Tomáš Vogeltanz, Roman Jašek</i> | 210 |
| Algorithmic Analysis of the Marketing Mix in Metallic Materials Industry <i>Adrian Ioana, Augustin Semenescu</i> | 216 |
| Particle Shape Effect on Extraction in Vibration Screening: Ellipsoidal vs Spherical Particle Approximation <i>Kirill Sergeevitch Ivanov, Leonid Abramovitch Vaisberg</i> | 220 |
| Subdiffusive Dynamics of Istanbul Highway Traffic Flow <i>Caglar Kosun, Tunc Bilgincan, Serhan Ozdemir</i> | 224 |

| | |
|---|------------|
| Investigating Factors that Influence E-School Management in High Schools in Macedonia | 227 |
| <i>Majlinda Fetaji, Bekim Fetaji, Mirlinda Ebibi</i> | |
| | |
| Automatic Paint Mixing Process using LabView | 233 |
| <i>Mohamed A. Muftah, Abdulgani M. Albagul, Abdullah M. Faraj</i> | |
| | |
| Approach for Automated Person Identification from Any Type of Identification Document | 239 |
| <i>Krasimir Diyanov Dimitrov, Sivo Vladimirov Daskalov, Mariana Tsvetanova Stoeva</i> | |
| | |
| Advantages of the implementation of Service Desk based on ITIL Framework in Telecommunication Industry | 244 |
| <i>Anel Tanovic, Fahrudin Orucevic, Asmir Butkovic</i> | |
| | |
| An Improved Hybrid Distributed Image Compression Model | 259 |
| <i>Sherin M. Youssef, Ahmed Abou Elfarag, Noura S. Khalil</i> | |
| | |
| Comparison of Cryptographic Methods based on the Arithmetic of Elliptic Curves (ECC) with Symmetric Cryptography Methods on the Android Platform | 265 |
| <i>Milan Oulehla, David Malaník</i> | |
| | |
| Analysis of the Triple Correlation: Commerce – Sustainable Development – Risk Management | 270 |
| <i>Adrian Ioana, Augustin Semenescu</i> | |
| | |
| Adaptive Risk-Based Assessment of Security Investments | 274 |
| <i>M'hamed Chammem, Mohamed Hamdi</i> | |
| | |
| Knowledge Modelling of Electric Arc Furnace (EAF) | 282 |
| <i>Adrian Ioana, Augustin Semenescu</i> | |
| | |
| Videogame Design as Strengthening in Communicational and Cognitive Processes | 286 |
| <i>Yaneth P. Caviativa, María Inés Mantilla Pastrana, Yoan M. Guzmán, Adán Beltrán, Valentino Jaramillo, Ana Milena Rincón</i> | |
| | |
| Characterisation of High Carbon Ash from Captive Power Plant for Potential Utilisation | 290 |
| <i>Ruma Rano, A. Sarkar</i> | |
| | |
| Palm Vein Recognition and Verification System Using Local Average of Vein Direction | 298 |
| <i>Asmaa M. J. Abbas, Loay E. George</i> | |
| | |
| Inter Comparison of Classification Techniques for Vowel Speech Imagery using EEG Sensors | 309 |
| <i>Anaum Riaz, Sana Akhtar, Shanza Iftikhar, Amir Ali Khan, Ahmad Salman</i> | |
| | |
| Offline Detection of P300 in BCI Speller Systems | 314 |
| <i>Mandeep Kaur</i> | |

| | |
|--|-----|
| A Short Review of Location-Based Mobile Phone Emergency Systems: Current State and Future Guidelines | 321 |
| <i>Anas Aloudat</i> | |
| | |
| Relation and Attribute Fusion to Detect Communities of Online Social Networks | 326 |
| <i>Mohammad H. Nadimi, Mehrafarin Adami</i> | |
| | |
| Mobile Augmented Reality and Interactive Storytelling | 332 |
| <i>Sagaya Aurelia, Durai Raj, Omer Saleh</i> | |
| | |
| Concealing of Data Using Conjecturable Dissemination of Image | 338 |
| <i>J. Hari, S. Kalyani</i> | |
| | |
| Remoulded Dredged Marine Clay: A Study of Time Factor on Strength Recovery | 342 |
| <i>Chee-Ming Chan</i> | |
| | |
| A Robust Hash Scheme for Image Authentication System via Singular Value Decomposition | 348 |
| <i>Engr Faizullah, Ayaz Hussain</i> | |
| | |
| Power-Line Communication-Revisited in the Context of Smart Grid | 355 |
| <i>Saurabh Chaudhury, Sourav Bhattacharjee</i> | |
| | |
| Using DSML in Moodle Configuration to Support PBL-Pedagogy | 361 |
| <i>Khulood Khalil Al-Dous, Mohammed Samaka</i> | |
| | |
| Study of Enzymatic Hydrolysis and Liquid Glucose Production by Solid State Fermentation from Rice Hull using Trichoderma Species | 367 |
| <i>Arezou Ghadi, Azam Sinkakarmi</i> | |
| | |
| Comparative Analysis of Base Transceiver Station (BTS) and Power Transmission Lines Effects on the Human Body in Lagos Environs | 372 |
| <i>L. A. Akinyemi, N. T. Makanjuola, O. Shoewu, F. O. Edeko</i> | |
| | |
| A Study of Droplets Division in Circle Shape Micro Channel | 384 |
| <i>Maryam Ghelikhhani</i> | |
| | |
| AQP0 as an Atomic Machine | 388 |
| <i>Kunihiro Goto, Atsushi Suenaga, Takehiko Ogura, Makoto Taiji, Akira Toyama, Hideo Takeuchi, Mingyu Sun, Kazuyoshi Takayama, Masatoshi Iwamoto, Ikuro Sato, Jay Z. Yeh, Toshio Narahashi, Haruaki Nakaya, Akihiko Konagaya</i> | |
| | |
| Comparison of Segmentation Methods for Accurate Dental Caries Detection | 393 |
| <i>Jackson B.T. Pedzisai, Serestina Viriri</i> | |
| | |
| A Critical Study to Enhance the Competitiveness of Engineering Educational Institutions | 400 |
| <i>G. M. Ramesh, V. Jaiganesh</i> | |

Generalized Least-Squares Regressions IV: Theory and Classification Using Generalized Means

Nataniel Greene

Department of Mathematics and Computer Science

Kingsborough Community College, CUNY

2001 Oriental Boulevard, Brooklyn, NY 11235, USA

Email: ngreene.math@gmail.com

Abstract—The theory of generalized least-squares is reformulated here using the notion of generalized means. The generalized least-squares problem seeks a line which minimizes the average generalized mean of the square deviations in x and y . The notion of a generalized mean is equivalent to the generating function concept of the previous papers but allows for a more robust understanding and has an already existing literature. Generalized means are applied to the task of constructing more examples, simplifying the theory, and further classifying generalized least-squares regressions.

Keywords—Linear regression, least-squares, orthogonal regression, geometric mean regression, generalized least-squares, generalized mean square regression.

I. OVERVIEW

Ordinary least-squares regression suffers from a fundamental lack of symmetry: the regression line of y given x and the regression line of x given y are not inverses of each other. Ordinary least-squares $y|x$ regression minimizes the average square deviation between the data and the line in the y variable and ordinary least-squares $x|y$ minimizes the average square deviation between the data and the line in the x variable. A theory of generalized least-squares was described by this author for minimizing the average of a symmetric function of the square deviations in both x and y variables [7,8,9]. The symmetric function was referred to as a generating function for the particular regression method.

This paper continues the development of the theory of generalized least-squares, reformulated using the notion of generalized means. The generalized least-squares problem described here seeks a line which minimizes the average generalized mean of the square deviations in x and y . The notion of a generalized mean is equivalent to the generating function concept of the previous papers but allows for a more robust understanding and has an already existing literature.

It is clear from the name that geometric mean regression (GMR) seeks a line which minimizes the average geometric mean of the square deviations in x and y . Orthogonal regression seeks a line which minimizes the average harmonic mean of the square deviations in x and y . Therefore it is also called harmonic mean regression (HMR). Arithmetic mean regression (AMR) seeks a line which minimizes the average

arithmetic mean of the square deviations in x and y and was called Pythagorean regression previously. Here, logarithmic, Heronian, centroidal, identric, Lorentz, and root mean square regressions are described for the first time. Ordinary least-squares regression is shown here to be equivalent to minimum or maximum mean regression. Regressions based on weighted arithmetic means of order α and weighted geometric means of order β are explored. The weights α and β parameterize all generalized mean square regression lines lying between the two ordinary least-squares lines.

Power mean regression of order p offers a particularly simple framework for parameterizing all the generalized mean square regressions previously described. The p -scale has fixed numerical values corresponding to many known special means. All the symmetric regressions discussed in the previous papers are power mean regressions for some value of p . Ordinary least-squares corresponds to $p = \pm\infty$. The power mean is one example of a generalized mean whose free parameter unites a variety of special means as subcases. Other generalized means which do the same include: the Dietel-Gordon mean of order r , Stolarsky's mean of order s , and Gini's mean of order t . There are also two-parameter means due to Stolarsky and Gini. Regression formulas based on all these generalized means are worked out here for the first time.

II. REGRESSIONS BASED ON GENERALIZED MEANS

Generalized means are applied to the task of constructing more examples, simplifying the theory, and further classifying generalized least-squares regressions.

A. Axioms of a Generalized Mean

The axioms of a generalized mean presented here are drawn from Mays [13] and also from Chen [2].

Definition 1: A function $M(x, y)$ defines a generalized mean for $x, y > 0$ if it satisfies Properties 1-5 below. If it satisfies Property 6 it is called a homogenous generalized mean. The properties are:

1. (Continuity) $M(x, y)$ is continuous in each variable.
2. (Monotonicity) $M(x, y)$ is non-decreasing in each variable.

3. (Symmetry) $M(x, y) = M(y, x)$.
4. (Identity) $M(x, x) = x$.
5. (Intermediacy) $\min(x, y) \leq M(x, y) \leq \max(x, y)$.
6. (Homogeneity) $M(tx, ty) = tM(x, y)$ for all $t > 0$.

All known means are included in this definition. All the means discussed in this paper are homogeneous. The reader can verify that the weighted arithmetic mean or convex combination of any two generalized means is a generalized mean. The weighted geometric mean of any two generalized means is a generalized mean. More generally, the generalized mean of any two generalized means is itself a generalized mean.

The equivalence of generalized means and generating functions is now demonstrated.

Theorem 1: Let $M(x, y)$ be any generalized mean, then $\psi(x, y) = M(x^2, y^2)$ is the generating function for a corresponding generalized symmetric least-squares regression. Let $\psi(x, y)$ be any generating function, then $M(x, y) = \psi(\sqrt{|x|}, \sqrt{|y|})$ defines a generalized mean. The weight function is given by $g(b) = \psi(1, \frac{1}{b}) = M(1, \frac{1}{b^2})$.

From here it is clear that the theory of generalized least-squares can be reformulated using generalized means. The general symmetric least-squares problem is re-stated as follows.

Definition 2: (The General Symmetric Least-Squares Problem) Values of a and b are sought which minimize an error function defined by

$$E = \frac{1}{N} \sum_{i=1}^N M \left((a + bx_i - y_i)^2, \left(\frac{a}{b} + x_i - \frac{1}{b} y_i \right)^2 \right) \quad (1)$$

where $M(x, y)$ is any generalized mean. The solution to this problem is called generalized mean square regression.

Definition 3: (The General Weighted Ordinary Least-Squares Problem) Values of a and b are sought which minimize an error function defined by

$$E = g(b) \cdot \frac{1}{N} \sum_{i=1}^N (a + bx_i - y_i)^2 \quad (2)$$

or using Ehrenberg's formula

$$\begin{aligned} E &= g(b) \left(\sigma_y^2 (1 - \rho^2) + \sigma_x^2 \left(b - \rho \frac{\sigma_y}{\sigma_x} \right)^2 \right. \\ &\quad \left. + (a + b\mu_x - \mu_y)^2 \right) \end{aligned} \quad (3)$$

where $g(b)$ is a positive even function that is non-decreasing for $b < 0$ and non-increasing for $b > 0$.

The next theorem states that every generalized mean square regression problem is equivalent to a weighted ordinary least-squares problem with weight function $g(b)$.

Theorem 2: The general symmetric least-squares error function can be written equivalently as

$$E = g(b) \cdot \frac{1}{N} \sum_{i=1}^N (a + bx_i - y_i)^2 \quad (4)$$

or using Ehrenberg's formula

$$\begin{aligned} E &= g(b) \left(\sigma_y^2 (1 - \rho^2) + \sigma_x^2 \left(b - \rho \frac{\sigma_y}{\sigma_x} \right)^2 \right. \\ &\quad \left. + (a + b\mu_x - \mu_y)^2 \right) \end{aligned} \quad (5)$$

where

$$g(b) = M \left(1, \frac{1}{b^2} \right). \quad (6)$$

Proof: Substitute $\frac{a}{b} + x_i - \frac{1}{b} y_i$ with $\frac{1}{b}(a + bx_i - y_i)$ and then use the homogeneity property:

$$\begin{aligned} E &= \frac{1}{n} \sum_{i=1}^n M \left((a + bx_i - y_i)^2, \frac{(a + bx_i - y_i)^2}{b^2} \right) \\ &= \frac{1}{n} \sum_{i=1}^n (a + bx_i - y_i)^2 M \left(1, \frac{1}{b^2} \right). \end{aligned}$$

Define

$$g(b) = M \left(1, \frac{1}{b^2} \right),$$

factor $g(b)$ outside of the summation and replace using Ehrenberg's formula. ■

The theory now continues unchanged with all the same theorems and formulas involving the weight function $g(b)$. It is reviewed now. To find the regression coefficients a and b take first order partial derivatives of the error function E_a and E_b and set them equal to zero. The result is $a = \mu_y - b\mu_x$ and the First Discrepancy Formula:

$$b - \rho \frac{\sigma_y}{\sigma_x} = -\frac{1}{2} \frac{g'(b)}{g(b)} \left(\left(b - \rho \frac{\sigma_y}{\sigma_x} \right)^2 + \left(\frac{\sigma_y}{\sigma_x} \right)^2 (1 - \rho^2) \right). \quad (7)$$

To derive the slope equation for any generalized regression of interest, begin with the First Discrepancy Formula and substitute the specific expression for $g(b)$ into the formula, simplify and reset the equation equal to zero. What emerges is the specific slope equation. This is the procedure employed for all the slope equations presented in this paper.

Solving this equation for the discrepancy $b - \rho \frac{\sigma_y}{\sigma_x}$ using the quadratic formula yields the Second Discrepancy Formula:

$$b - \rho \frac{\sigma_y}{\sigma_x} = -\frac{g(b)}{g'(b)} \left(1 - \sqrt{1 - \kappa^2 \left(\frac{\sigma_y}{\sigma_x} \right)^2 \left(\frac{g'(b)}{g(b)} \right)^2} \right). \quad (8)$$

In order for the y-intercept a and slope b to minimize the error function the Hessian determinant $E_{aa}E_{bb} - (E_{ab})^2$ must be positive. Calculation of this determinant in the general case yields a function

$$G(b) = 2g'(b)/g(b) - g''(b)/g'(b) \quad (9)$$

called the indicative function. The Hessian determinant is positive provided that $G(b) \left(b - \rho \frac{\sigma_y}{\sigma_x} \right) > -1$. This differential equation for the weight function is solved to yield

$$g(b) = 1/(c + k \int \exp(- \int G(b) db) db). \quad (10)$$

B. The Exponential Equivalence Theorem Revisited

In the third paper of this series [9] the weight function

$$g_0(b) = \exp(-\gamma p_0 |b|) \quad (11)$$

was shown to generate all generalized least-squares regression lines as γ varies from 0 to 1. Here $p_0 = 1/\left(|\kappa|\frac{\sigma_y}{\sigma_x}\right)$ and $\kappa = \text{sgn } \rho \sqrt{1 - \rho^2}$ is the coefficient of scatter. The regression lines have the simple form described in the next theorem.

Theorem 3: (Fundamental Generalized Least-Squares Formula) The generalized least-squares regression line is given by $y = a + bx$ where

$$a = \mu_y - b\mu_x \quad (12)$$

and

$$b = (\rho + \lambda\kappa) \frac{\sigma_y}{\sigma_x}. \quad (13)$$

The parameters γ and λ are related by the equations

$$\lambda = \frac{\gamma}{1 + \sqrt{1 - \gamma^2}} \quad (14)$$

and

$$\gamma = \frac{2\lambda}{\lambda^2 + 1}. \quad (15)$$

Proof: Substitute $g_0(b)$ into the Second Discrepancy Formula and simplify. ■

Trigonometric formulas for the parameters γ and λ are now derived. It is shown that γ and λ are functions of a more fundamental parameter ϕ in $[0, \frac{\pi}{2}]$ or an equivalent parameter δ in $[0, 1]$ satisfying $\phi = \delta \cdot \frac{\pi}{2}$.

Lemma 4: If $\phi = \delta \cdot \frac{\pi}{2}$ with δ in $[0, 1]$ then

$$\gamma = \sin \phi = \sin\left(\delta \cdot \frac{\pi}{2}\right) \quad (16)$$

and

$$\lambda = \tan \frac{\phi}{2} = \tan\left(\delta \cdot \frac{\pi}{4}\right). \quad (17)$$

Proof: Substitute $\lambda = \tan \frac{\phi}{2}$ and $\gamma = \sin \phi$ into the formula relating γ and λ and verify that $\sin \phi = 2 \tan \frac{\phi}{2} / (\tan^2 \frac{\phi}{2} + 1)$. ■

Theorem 5: The parameters γ and λ are related by the trigonometric equations

$$\lambda = \tan\left(\frac{1}{2} \sin^{-1} \gamma\right) \quad (18)$$

and

$$\gamma = \sin(2 \tan^{-1} \lambda). \quad (19)$$

Proof: Solve for ϕ in each of the two equations and substitute into the other equation. ■

Corollary 6: The following inequality holds between the parameters.

$$0 \leq \lambda \leq \delta \leq \gamma \leq 1 \quad (20)$$

with equality only when all three parameters equal 0 or 1.

Proof: This is due to the concavity of the functions $\gamma(\delta)$ and $\lambda(\delta)$ with $\gamma(\delta)$ lying above the diagonal line $\gamma = \delta$ and $\lambda(\delta)$ lying below the diagonal line $\lambda = \delta$. ■

Corollary 7: Let $\rho = \cos \theta$ for θ in $[0, \pi]$. Then GMR corresponds to $\phi = \theta$ with $\gamma = \sin \theta$ and $\lambda = \tan \frac{\theta}{2}$. OLS $x|y$ corresponds to $\phi = 2\theta$ with $\gamma = \sin 2\theta$ and $\lambda = \tan \theta$.

Proof: It was shown [8] that for GMR, $\gamma = \kappa$ and $\lambda = \kappa / (1 + |\rho|)$. For OLS $x|y$, $\gamma = 2\kappa\rho$ and $\lambda = \kappa/\rho$. ■

To summarize, γ and λ are interrelated using simple trigonometric formulas. The parameter δ (or equivalently ϕ) generates both γ and λ using simple trigonometric formulas. As δ varies between 0 and 1, ϕ varies between 0 and $\frac{\pi}{2}$ and γ and λ vary between 0 and 1. All possible generalized least-squares lines are thereby generated. The case $\delta = 0$ corresponds to the ordinary least-squares line and $\delta = 1$ corresponds to the extremal line.

C. An Admissibility Criterion for Generalized Least-Squares

In order for the pair (a, b) to minimize the error function, the expression inside the radical of the Second Discrepancy Formula must be non-negative. This means that the following inequality must be satisfied:

$$\left(\frac{g'(b)}{g(b)}\right)^2 \leq 1 / \left(\left(\frac{\sigma_y}{\sigma_x}\right)^2 \kappa^2\right). \quad (21)$$

For specific choices of $g(b)$ and fixed ρ , this inequality can be solved for b . The result is an admissibility condition on the slope b : slopes which exceed a certain magnitude become inadmissible in the sense that they no longer lie on the spectrum between OLS $y|x$ and the extremal line and they no longer minimize the error function.

According to the exponential equivalence theorem, $g(b) = \exp(-\gamma p_0 |b|)$ for some γ in $[0, 1]$. This inequality is therefore equivalent to the statement $\gamma \leq 1$, which is in turn equivalent to $\lambda \leq 1$ and $\delta \leq 1$. Numerically, it suffices to compute any one of these parameters and check that it does not exceed 1. If it exceeds 1 then the line is inadmissible for the given data: the slope and y-intercept will fail to minimize the error function.

D. A Restriction on Ordinary Least-Squares $x|y$

It is known that as ρ^2 tends to zero, the OLS $x|y$ line becomes increasingly perpendicular to both the OLS $y|x$ line and to the data cloud itself. This suggests that for some critical value of ρ^2 , OLS $x|y$ ceases to be a model for the data. The above admissibility criterion when applied to ordinary least-squares $x|y$ produces this critical value which may not have been known. It is stated in the next theorem.

Theorem 8: The ordinary least-squares $x|y$ line

$$y = \left(\frac{1}{\rho} \frac{\sigma_y}{\sigma_x}\right) x + \left(\mu_y - \frac{1}{\rho} \frac{\sigma_y}{\sigma_x} \mu_x\right) \quad (22)$$

is admissible provided that

$$\frac{1}{2} \leq \rho^2 \leq 1. \quad (23)$$

In this case, the slope and y-intercept of the line minimize the error function. ■

Proof: Substitute $g(b) = \frac{1}{b^2}$ and simplify. Replace b with $\frac{1}{\rho} \frac{\sigma_y}{\sigma_x}$ and solve the inequality for ρ^2 . ■

This restriction was already stated in a chart in the previous paper [9] but without elaboration. To summarize, for data with $\rho^2 < \frac{1}{2}$ the OLS $x|y$ line is inadmissible: its slope and y-intercept will fail to minimize the error function and its graph no longer passes through the data cloud sufficiently for it to model the data.

E. A Symmetry Property of Least-Squares Lines

Without loss of generality, all the slope equations presented in this paper are for least-squares lines with positive slope, corresponding to data with a positive correlation coefficient. This restriction makes the slope equations less cumbersome to write. Least-squares lines with negative slope, corresponding to data with a negative correlation coefficient can be computed from a positive slope equation as follows.

1. Reflect the data across the x-axis: $(x_i, y_i) \rightarrow (x'_i, y'_i)$ where $x'_i = x_i$ and $y'_i = -y_i$.

2. Compute the regression line for the reflected data. This corresponds to replacing ρ with $|\rho|$ and b with $b \operatorname{sgn} b = b \operatorname{sgn} \rho$ in the original slope equation and solving for the relevant *positive* solution for b' . Note that $\mu_{x'} = \mu_x$, $\mu_{y'} = -\mu_y$, $\sigma_{x'} = \sigma_x$, and $\sigma_{y'} = \sigma_y$. Therefore the y-intercept for the reflected data is given by $a' = \mu_{y'} - b' \mu_{x'}$.

3. The regression line for the original data has slope $b = -b'$ and y-intercept $a = -a'$, which is the same as writing $a = \mu_y - b \mu_x$.

In practice, to write a general slope equation which is true for all b and ρ , take the positive slope equation presented here, replace b with $(\operatorname{sgn} b)(b) = (\operatorname{sgn} \rho)(b)$ and replace ρ with $|\rho|$ and simplify. For example, in the case of square perimetric regression (SPR), use Formula 77 with $p = \frac{1}{2}$ and obtain the positive slope equation:

$$b^3 - \rho \frac{\sigma_y}{\sigma_x} b^2 + \rho \frac{\sigma_y}{\sigma_x} b - \left(\frac{\sigma_y}{\sigma_x} \right)^2 = 0. \quad (24)$$

Replace b with $(\operatorname{sgn} b)(b) = (\operatorname{sgn} \rho)(b)$ and replace ρ with $|\rho|$ in this equation and obtain the general form which appears in the previous work [7], namely:

$$b^3 - \rho \frac{\sigma_y}{\sigma_x} b^2 + |\rho| \frac{\sigma_y}{\sigma_x} b - \operatorname{sgn} \rho \left(\frac{\sigma_y}{\sigma_x} \right)^2 = 0. \quad (25)$$

Similarly, for squared harmonic mean regression (SHR), again use Formula 77 with $p = -\frac{1}{2}$ and obtain the positive equation:

$$b = \frac{\sigma_y}{\sigma_x} \cdot \frac{\frac{\sigma_y}{\sigma_x} + \rho}{\rho \frac{\sigma_y}{\sigma_x} + 1} \quad (26)$$

Again make the above replacements and obtain the form which appears in the previous work:

$$b = \operatorname{sgn} \rho \frac{\sigma_y}{\sigma_x} \cdot \frac{\frac{\sigma_y}{\sigma_x} + |\rho|}{|\rho| \frac{\sigma_y}{\sigma_x} + 1}. \quad (27)$$

The focus of this paper is to derive slope equations for all the known special means, as well as the generalized means with free parameters which appear in the literature. The free parameters are used to classify the known special cases.

F. A Naming Convention for Generalized Regressions: XMR

A naming convention is adopted here for generalized mean regression following what is already done for geometric mean regression: take the letter already in use for denoting the given mean and add 'MR' after it. If X is the letter already in use to denote a particular generalized mean, then XMR is the corresponding regression. For example, the geometric mean is denoted by 'G', therefore the corresponding geometric mean regression is denoted GMR. What was called Pythagorean regression earlier, is now called AMR here since it minimizes the arithmetic mean of the square deviations in x and y . Similarly, orthogonal regression is also denoted here as HMR since it minimizes the average harmonic mean of the square deviations in x and y . Where the name is already established, as in the case of orthogonal regression, the convention here simply provides an alternative name.

G. Arithmetic, Geometric and Harmonic Mean Regression

The weight functions and slope equations are reviewed for arithmetic, geometric and harmonic regression.

For AMR, which was called Pythagorean regression previously, the mean is

$$M(x, y) = \frac{x + y}{2}, \quad (28)$$

the weight function is

$$g(b) = \frac{1}{2} \left(1 + \frac{1}{b^2} \right), \quad (29)$$

and the slope equation is

$$b^4 - \rho \frac{\sigma_y}{\sigma_x} b^3 + \rho \frac{\sigma_y}{\sigma_x} b - \left(\frac{\sigma_y}{\sigma_x} \right)^2 = 0. \quad (30)$$

Here the user selects the unique real solution that is greater than $\rho \frac{\sigma_y}{\sigma_x}$ when ρ is positive or less than $\rho \frac{\sigma_y}{\sigma_x}$ when ρ is negative.

For GMR, the mean is

$$M(x, y) = \sqrt{xy}, \quad (31)$$

the weight function is

$$g(b) = \frac{1}{|b|}, \quad (32)$$

and the slope equation is

$$b^2 - \left(\frac{\sigma_y}{\sigma_x} \right)^2 = 0, \quad (33)$$

so that

$$b = \operatorname{sgn} \rho \frac{\sigma_y}{\sigma_x}. \quad (34)$$

For HMR, which is the same as orthogonal regression, the mean is

$$M(x, y) = \frac{2xy}{x + y}, \quad (35)$$

the weight function is

$$g(b) = \frac{2}{1 + b^2}, \quad (36)$$

and the slope equation is

$$\rho \frac{\sigma_y}{\sigma_x} b^2 + \left(1 - \left(\frac{\sigma_y}{\sigma_x} \right)^2 \right) b - \rho \frac{\sigma_y}{\sigma_x} = 0. \quad (37)$$

The quadratic formula yields the well-known solutions.

H. Ordinary Least-Squares is Minimum or Maximum Mean Regression

It is now shown that ordinary least-squares regression is also generated by a generalized mean.

Theorem 9: Let $y = a + bx$ be a regression line generated by the minimum mean or the maximum mean. If $|b| \leq 1$, then $M(x, y) = \min(x, y)$ corresponds to OLS $y|x$ regression and $M(x, y) = \max(x, y)$ corresponds to OLS $x|y$ regression. If $|b| > 1$, then $M(x, y) = \min(x, y)$ corresponds to OLS $x|y$ regression and $M(x, y) = \max(x, y)$ corresponds to OLS $y|x$ regression.

Proof: It is a geometric fact that the vertical distance between a point and a line is always less than or equal to the horizontal distance when $|b| \leq 1$ and greater than the horizontal distance when $|b| > 1$. The error function is given by

$$E = \frac{1}{N} \sum_{i=1}^N M \left((a + bx_i - y_i)^2, \left(\frac{a}{b} + x_i - \frac{1}{b} y_i \right)^2 \right) \quad (38)$$

For minimum mean regression $M(x, y) = \min(x, y)$ and

$$\begin{aligned} & \min \left((a + bx_i - y_i)^2, \left(\frac{a}{b} + x_i - \frac{1}{b} y_i \right)^2 \right) \\ &= \begin{cases} (a + bx_i - y_i)^2, & |b| \leq 1 \text{ (OLS } y|x) \\ \left(\frac{a}{b} + x_i - \frac{1}{b} y_i \right)^2, & |b| > 1 \text{ (OLS } x|y) \end{cases}. \end{aligned}$$

Similarly, for maximum mean regression, $M(x, y) = \max(x, y)$ and

$$\begin{aligned} & \max \left((a + bx_i - y_i)^2, \left(\frac{a}{b} + x_i - \frac{1}{b} y_i \right)^2 \right) \\ &= \begin{cases} \left(\frac{a}{b} + x_i - \frac{1}{b} y_i \right)^2, & |b| \leq 1 \text{ (OLS } x|y) \\ (a + bx_i - y_i)^2, & |b| > 1 \text{ (OLS } y|x) \end{cases}. \end{aligned}$$

Alternatively, the result is obtained by examining the weight functions. Recall that OLS $y|x$ corresponds to $g(b) = 1$ and OLS $x|y$ corresponds to $g(b) = \frac{1}{b^2}$. For minimum mean regression the weight function is given by

$$g_{\min}(b) = \min \left(1, \frac{1}{b^2} \right) = \begin{cases} 1, & |b| \leq 1 \text{ (OLS } y|x) \\ \frac{1}{b^2}, & |b| > 1 \text{ (OLS } x|y) \end{cases}.$$

For maximum mean regression the weight function is given by:

$$g_{\max}(b) = \max \left(1, \frac{1}{b^2} \right) = \begin{cases} \frac{1}{b^2}, & |b| \leq 1 \text{ (OLS } x|y) \\ 1, & |b| > 1 \text{ (OLS } y|x) \end{cases}. \quad \blacksquare$$

III. MORE REGRESSION EXAMPLES BASED ON KNOWN SPECIAL MEANS

This section examines regressions based on several special means that are already known from the references. They are: the logarithmic, Heronian, centroidal, contraharmonic, root mean square and identric means. For each case, the weight function and the corresponding slope equation are derived.

A. Logarithmic Mean Regression (LMR)

The logarithmic mean is given by

$$L(x, y) = \begin{cases} (y - x) / (\ln y - \ln x), & x \neq y \\ x, & x = y. \end{cases} \quad (39)$$

Therefore, the weight function is given by

$$g(b) = L \left(1, \frac{1}{b^2} \right) = \frac{b^2 - 1}{b^2 \ln b^2}. \quad (40)$$

To find b one must solve the slope equation:

$$\begin{aligned} \ln(b^2) &= \left\{ b^4 - 2\rho \frac{\sigma_y}{\sigma_x} b^3 + \left(\left(\frac{\sigma_y}{\sigma_x} \right)^2 - 1 \right) b^2 \right. \\ &\quad \left. + 2\rho \frac{\sigma_y}{\sigma_x} b - \left(\frac{\sigma_y}{\sigma_x} \right)^2 \right\} / \\ &\quad \left\{ b^4 - \rho \frac{\sigma_y}{\sigma_x} b^3 - \rho \frac{\sigma_y}{\sigma_x} b + \left(\frac{\sigma_y}{\sigma_x} \right)^2 \right\}. \quad (41) \end{aligned}$$

It will be seen further on that it is useful to define here a second logarithmic mean

$$L_2(x, y) = \begin{cases} xy (\ln y - \ln x) / (y - x), & x \neq y \\ x, & x = y \end{cases} \quad (42)$$

and when necessary the first logarithmic mean is denoted by $L_1(x, y) = L(x, y)$. The second logarithmic mean satisfies the relation $L_2(x, y) = (G(x, y))^2 / L(x, y)$. The weight function for the second logarithmic mean is given by

$$g(b) = \frac{\ln(b^2)}{b^2 - 1}, \quad (43)$$

and the slope equation is given by

$$\begin{aligned} \ln(b^2) &= - \left\{ b^4 - 2\rho \frac{\sigma_y}{\sigma_x} b^3 + \left(\left(\frac{\sigma_y}{\sigma_x} \right)^2 - 1 \right) b^2 \right. \\ &\quad \left. + 2\rho \frac{\sigma_y}{\sigma_x} b - \left(\frac{\sigma_y}{\sigma_x} \right)^2 \right\} / \\ &\quad \left\{ \rho \frac{\sigma_y}{\sigma_x} b^4 - \left(1 + \left(\frac{\sigma_y}{\sigma_x} \right)^2 \right) b^2 + \rho \frac{\sigma_y}{\sigma_x} b \right\}. \quad (44) \end{aligned}$$

B. Heronian Mean Regression (NMR)

The Heronian mean is given by

$$N(x, y) = \frac{1}{3} (x + \sqrt{xy} + y). \quad (45)$$

The weight function is given by

$$g(b) = N\left(1, \frac{1}{b^2}\right) = \frac{1}{3} \left(1 + \frac{1}{|b|} + \frac{1}{b^2}\right). \quad (46)$$

To find b one must solve a quartic polynomial equation:

$$\begin{aligned} 0 &= b^4 + \left(\frac{1}{2} - \rho \frac{\sigma_y}{\sigma_x}\right) b^3 \\ &\quad + \left(\rho \frac{\sigma_y}{\sigma_x} - \frac{1}{2} \left(\frac{\sigma_y}{\sigma_x}\right)^2\right) b - \left(\frac{\sigma_y}{\sigma_x}\right)^2. \end{aligned} \quad (47)$$

C. Contraharmonic Mean Regression (CMR)

The contraharmonic mean is given by

$$C(x, y) = \frac{x^2 + y^2}{x + y}. \quad (48)$$

The weight function is given by

$$g(b) = 1 + \frac{1 - b^2}{b^4 + b^2}, \quad (49)$$

and the slope equation is a polynomial equation of degree eight:

$$\begin{aligned} 0 &= b^8 - \rho \frac{\sigma_y}{\sigma_x} b^7 + 2b^6 - 3\rho \frac{\sigma_y}{\sigma_x} b^5 \\ &\quad + \left(\frac{\sigma_y}{\sigma_x} - 1\right) b^4 + 3\rho \frac{\sigma_y}{\sigma_x} b^3 - 2 \left(\frac{\sigma_y}{\sigma_x}\right)^2 b^2 \\ &\quad + \rho \frac{\sigma_y}{\sigma_x} b - \left(\frac{\sigma_y}{\sigma_x}\right)^2. \end{aligned} \quad (50)$$

D. Centroidal Mean Regression (TMR)

The centroidal mean is given by

$$T(x, y) = \frac{2}{3} \left(\frac{x^2 + xy + y^2}{x + y} \right). \quad (51)$$

The centroidal mean is a convex combination of the contraharmonic mean and the harmonic mean: $T(x, y) = \frac{2}{3}C(x, y) + \frac{1}{3}H(x, y)$. It also satisfies the relation $T(x, y) = N(x^2, y^2)/A(x, y)$.

The weight function is given by

$$g(b) = T\left(1, \frac{1}{b^2}\right) = \frac{2}{3} \left(1 + \frac{1}{b^2(b^2 + 1)}\right). \quad (52)$$

The slope equation is a polynomial equation of degree eight:

$$\begin{aligned} 0 &= b^8 - \rho \frac{\sigma_y}{\sigma_x} b^7 + 2b^6 - 2\rho \frac{\sigma_y}{\sigma_x} b^5 \\ &\quad + 2\rho \frac{\sigma_y}{\sigma_x} b^3 - 2 \left(\frac{\sigma_y}{\sigma_x}\right)^2 b^2 - \left(\frac{\sigma_y}{\sigma_x}\right)^2. \end{aligned} \quad (53)$$

E. Root-Mean-Square Regression (RMR)

The root-mean-square is given by

$$R(x, y) = \left(\frac{x^2 + y^2}{2} \right)^{1/2}. \quad (54)$$

The weight function is given by

$$g(b) = \frac{1}{\sqrt{2}} \left(1 + \frac{1}{b^4}\right)^{1/2}. \quad (55)$$

The slope equation is a polynomial equation of degree six:

$$b^6 - \rho \frac{\sigma_y}{\sigma_x} b^5 + \rho \frac{\sigma_y}{\sigma_x} b - \left(\frac{\sigma_y}{\sigma_x}\right)^2 = 0. \quad (56)$$

F. Identric Mean Regression (IMR)

The identric mean is given by

$$I(x, y) = \begin{cases} \frac{1}{e} \cdot \left(\frac{x^x}{y^y}\right)^{1/(x-y)}, & x \neq y \\ x, & x = y. \end{cases} \quad (57)$$

The weight function is given by

$$g(b) = \frac{1}{e} \cdot b^{2/(b^2-1)}, \quad (58)$$

and the slope equation is given by

$$\begin{aligned} \ln(b^2) &= \left\{ b^6 - \rho \frac{\sigma_y}{\sigma_x} b^5 - b^4 \right. \\ &\quad \left. + \left(\frac{\sigma_y}{\sigma_x}\right) b^2 + \rho \frac{\sigma_y}{\sigma_x} b - \left(\frac{\sigma_y}{\sigma_x}\right)^2 \right\} / \\ &\quad \left\{ b^4 - 2\rho \frac{\sigma_y}{\sigma_x} b^3 + \left(\frac{\sigma_y}{\sigma_x}\right)^2 b^2 \right\}. \end{aligned} \quad (59)$$

IV. CLASSIFYING GENERALIZED REGRESSIONS USING WEIGHTED ARITHMETIC MEANS

Perhaps the simplest generalized mean is a weighted arithmetic mean of order α .

Definition 4: The weighted arithmetic mean of order α is defined for $x < y$ by

$$M_\alpha(x, y) = (1 - \alpha)x + \alpha y. \quad (60)$$

The standard arithmetic mean corresponds to $\alpha = \frac{1}{2}$. The weight function is given by

$$g_\alpha(b) = (1 - \alpha) + \alpha \left(\frac{1}{b^2}\right) \quad (61)$$

and the corresponding slope equation is given by

$$(1 - \alpha)b^4 - (1 - \alpha)\rho \frac{\sigma_y}{\sigma_x} b^3 + \alpha\rho \frac{\sigma_y}{\sigma_x} b - \alpha \left(\frac{\sigma_y}{\sigma_x}\right)^2 = 0. \quad (62)$$

The indicative function is given by

$$G_\alpha(b) = \frac{(1 - \alpha)3b^2 - \alpha}{b((1 - \alpha)b^2 + \alpha)}. \quad (63)$$

It is clear that α continuously parameterizes a spectrum of generalized regression lines with OLS $y|x$ corresponding to

$\alpha = 0$ and OLS $x|y$ corresponding to $\alpha = 1$. Due to intermediacy, every generalized mean lies between $x = \min(x, y)$ and $y = \max(x, y)$, corresponding to OLS $y|x$ and OLS $x|y$ respectively. Therefore every generalized mean-square regression can be assigned an effective parameter α in $[0, 1]$, classifying the line on the spectrum between OLS $y|x$ and OLS $x|y$. This is formalized in the next theorem.

Theorem 10: (Weighted Arithmetic Mean Equivalence Theorem) Let b be the slope of a generalized least-squares regression line lying between the two ordinary least-squares lines. Then the regression line is generated by an equivalent weighted arithmetic mean of order α in $[0, 1]$ where

$$\alpha(b) = \frac{b^3 \left(b - \rho \frac{\sigma_y}{\sigma_x} \right)}{b^3 \left(b - \rho \frac{\sigma_y}{\sigma_x} \right) - \left(\rho \frac{\sigma_y}{\sigma_x} b - \left(\frac{\sigma_y}{\sigma_x} \right)^2 \right)}. \quad (64)$$

Proof: Begin with the slope equation and solve for α in terms of b . ■

V. CLASSIFYING GENERALIZED REGRESSIONS USING WEIGHTED GEOMETRIC MEANS

Weighted geometric means allow for a similar parameterization of generalized least-squares lines.

Definition 5: The weighted geometric mean of order β is defined for $x < y$ by

$$M_\beta(x, y) = x^{1-\beta} y^\beta. \quad (65)$$

The standard geometric mean corresponds to $\beta = \frac{1}{2}$. The weight function is given by

$$g_\beta(b) = \frac{1}{b^{2\beta}} \quad (66)$$

and the corresponding slope equation is given by

$$(1 - \beta)b^2 + (2\beta - 1)\rho \frac{\sigma_y}{\sigma_x} b - \beta \left(\frac{\sigma_y}{\sigma_x} \right)^2 = 0. \quad (67)$$

The indicative function is given by

$$G_\beta(b) = \frac{1 - 2\beta}{b}. \quad (68)$$

It is again clear that β continuously parameterizes a spectrum of generalized regression lines with OLS $y|x$ corresponding to $\beta = 0$ and OLS $x|y$ corresponding to $\beta = 1$. Again, due to intermediacy, every generalized mean lies between $x = \min(x, y)$ and $y = \max(x, y)$ corresponding to OLS $y|x$ and OLS $x|y$ respectively. Therefore every generalized mean-square regression can be assigned an effective parameter β in $[0, 1]$, classifying the line on the spectrum between OLS $y|x$ and OLS $x|y$. This is formalized in the next theorem.

Theorem 11: (Weighted Geometric Mean Equivalence Theorem) Let b be the slope of a generalized least-squares regression line lying between the two ordinary least-squares

lines. Then the regression line is generated by an equivalent weighted geometric mean of order β in $[0, 1]$ where

$$\beta(b) = \frac{b \left(b - \rho \frac{\sigma_y}{\sigma_x} \right)}{b \left(b - \rho \frac{\sigma_y}{\sigma_x} \right) - \left(\rho \frac{\sigma_y}{\sigma_x} b - \left(\frac{\sigma_y}{\sigma_x} \right)^2 \right)}. \quad (69)$$

Proof: Begin with the slope equation and solve for β in terms of b . ■

VI. CLASSIFYING GENERALIZED REGRESSIONS USING POWER MEANS

It is now shown that the subset of lines lying between the two ordinary least-squares lines is also naturally parameterized using power means. The power mean parameter p is either an increasing or decreasing function of the slope.

A. Power Mean Regression

Definition 6: The power mean of order p is defined by

$$M_p(x, y) = \left(\frac{x^p + y^p}{2} \right)^{1/p} \quad (70)$$

where $-\infty < p < \infty$ and $p \neq 0$. The following special cases are defined separately:

$$M_{-\infty}(x, y) = \min(x, y), \quad (71)$$

$$M_\infty(x, y) = \max(x, y), \quad (72)$$

and

$$M_0(x, y) = \sqrt{xy}. \quad (73)$$

For $p > 0$, a power mean of order p is the arithmetic mean of x^p and y^p raised to the $\frac{1}{p}$ power. For $p < 0$, a power mean of order p is the harmonic mean of $x^{|p|}$ and $y^{|p|}$ raised to the $\frac{1}{|p|}$ power. The following conjugacy relation therefore holds:

$$M_{-p}(x, y) M_p(x, y) = (G(x, y))^2 \quad (74)$$

and therefore

$$G(M_{-p}(x, y), M_p(x, y)) = G(x, y). \quad (75)$$

The general weight function for power mean regression when $p \neq 0$ and $p \neq \pm\infty$ is given by

$$g_p(b) = M_p \left(1, \frac{1}{b^2} \right) = 2^{-1/p} \left(1 + \frac{1}{b^{2p}} \right)^{1/p}. \quad (76)$$

To find b one must solve the slope equation

$$b^{2p+2} - \rho \frac{\sigma_y}{\sigma_x} b^{2p+1} + \rho \frac{\sigma_y}{\sigma_x} b - \left(\frac{\sigma_y}{\sigma_x} \right)^2 = 0. \quad (77)$$

The equation is a polynomial when p is any whole number multiple of $\frac{1}{2}$. When $p = 0$ the power mean formula becomes undefined. Nevertheless, substituting $p = 0$ into the slope equation and solving for the slope yields $b = \pm \frac{\sigma_y}{\sigma_x}$ which corresponds to geometric mean regression. This explains the separate definition $M_0(x, y) = G(x, y)$.

The indicative function for power mean regression has a simple form:

$$G_p(b) = \frac{(2p+1)b^{2p} - 1}{b(b^{2p} + 1)}. \quad (78)$$

Note that if $|b| < 1$, then $p = -\infty$ corresponds to OLS $y|x$ and $p = \infty$ corresponds to OLS $x|y$. If $|b| > 1$, then $p = -\infty$ corresponds to OLS $x|y$ and $p = \infty$ corresponds to OLS $y|x$.

B. Power Mean Equivalence Theorem

Ordinary least-squares and geometric mean regression were already observed to be specific cases of power mean regression. The harmonic mean $H(x, y)$ is equivalent to $M_{-1}(x, y)$ and the arithmetic mean $A(x, y)$ is equivalent to $M_1(x, y)$. Square perimeter regression (SPR) (also called least-perimeter squared regression previously) is generated by $M_{1/2}(x, y)$ and squared harmonic mean regression (SHR) is generated by $M_{-1/2}(x, y)$. This suggests that it is natural to use the power mean parameter p to parameterize generalized least-squares regression lines. The next table summarizes these cases.

| Case | Mean $M(x, y)$ $x < y$ | Weight Function $g(b) = M\left(1, \frac{1}{b^2}\right)$ | Order p |
|-------------------|--|--|----------------|
| OLS $y x$ | x | 1 | $\pm\infty$ |
| OLS $x y$ | y | $\frac{1}{b^2}$ | $\pm\infty$ |
| HMR (Orthogonal) | $\frac{2xy}{x+y}$ | $\frac{2}{1+b^2}$ | -1 |
| SHR | $\left(\frac{2\sqrt{xy}}{\sqrt{x+y}}\right)^2$ | $\frac{4}{(1+ b)^2}$ | $-\frac{1}{2}$ |
| GMR | \sqrt{xy} | $\frac{1}{ b }$ | 0 |
| SPR | $\left(\frac{\sqrt{x+y}}{2}\right)^2$ | $\frac{1}{4}\left(1+\frac{1}{ b }\right)^2$ | $\frac{1}{2}$ |
| AMR (Pythagorean) | $\frac{x+y}{2}$ | $\frac{1}{2}\left(1+\frac{1}{b^2}\right)$ | 1 |

It is observed further on that Heronian mean regression (NMR) has a value for p that is slightly below $\frac{2}{3}$ and identric mean regression (IMR) has a value for p that is slightly above $\frac{2}{3}$. First and second logarithmic mean regressions have values for p that are close to $\pm\frac{1}{3}$ respectively. Power mean regression of order $\frac{1}{3}$ is also called Lorentz mean regression (ZMR).

Theorem 12: (Power Mean Equivalence Theorem) Let b be the slope of a generalized least-squares regression line. Then the regression line is generated by an equivalent power mean of order p where

$$p(b) = \frac{\ln\left(\frac{\rho\frac{\sigma_y}{\sigma_x}(\frac{1}{\rho}\frac{\sigma_y}{\sigma_x}-b)}{b(b-\rho\frac{\sigma_y}{\sigma_x})}\right)}{\ln(b^2)}. \quad (79)$$

Proof: Begin with the slope equation and solve for p in terms of b . ■

The next theorem describes how the power mean order continuously parameterizes a spectrum of generalized least-squares regression lines as p increases from $-\infty$ to $+\infty$.

Theorem 13: (The Power Mean Spectrum)

Case 1: For all b satisfying $0 < \rho\frac{\sigma_y}{\sigma_x} < b < \frac{1}{\rho}\frac{\sigma_y}{\sigma_x} \leq 1$, $p(b)$ is an increasing function and the inverse $b(p)$ is an increasing function over $(-\infty, \infty)$. OLS $y|x$ corresponds to $p = -\infty$ and OLS $x|y$ corresponds to $p = +\infty$.

Case 2: For all b satisfying $1 \leq \rho\frac{\sigma_y}{\sigma_x} < b < \frac{1}{\rho}\frac{\sigma_y}{\sigma_x}$, $p(b)$ is a decreasing function and the inverse $b(p)$ is a decreasing function over $(-\infty, \infty)$. OLS $x|y$ corresponds to $p = -\infty$ and OLS $y|x$ corresponds to $p = +\infty$.

Case 3: For all b satisfying $-1 \leq \frac{1}{\rho}\frac{\sigma_y}{\sigma_x} < b < \rho\frac{\sigma_y}{\sigma_x} < 0$, $p(b)$ is a decreasing function and the inverse $b(p)$ is a decreasing function over $(-\infty, \infty)$. OLS $y|x$ corresponds to $p = -\infty$ and OLS $x|y$ corresponds to $p = +\infty$.

Case 4: For all b satisfying $\frac{1}{\rho}\frac{\sigma_y}{\sigma_x} < b < \rho\frac{\sigma_y}{\sigma_x} \leq -1$, $p(b)$ is an increasing function and the inverse $b(p)$ is an increasing function over $(-\infty, \infty)$. OLS $x|y$ corresponds to $p = -\infty$ and OLS $y|x$ corresponds to $p = +\infty$.

Case 5: For all b satisfying $0 < \rho\frac{\sigma_y}{\sigma_x} < b < 1 < \frac{1}{\rho}\frac{\sigma_y}{\sigma_x}$ and $\frac{\sigma_y}{\sigma_x} < 1$, $p(b)$ is an increasing function over $(\rho\frac{\sigma_y}{\sigma_x}, 1)$. The inverse $b(p)$ is an increasing function over $(-\infty, \infty)$. OLS $y|x$ corresponds to $p = -\infty$ and the regression line with $b = 1$ corresponds to $p = +\infty$.

Case 6: For all b satisfying $\frac{1}{\rho}\frac{\sigma_y}{\sigma_x} < -1 < b < \rho\frac{\sigma_y}{\sigma_x} < 0$ and $\frac{\sigma_y}{\sigma_x} < 1$, $p(b)$ is a decreasing function over $(-1, \rho\frac{\sigma_y}{\sigma_x})$. The inverse $b(p)$ is a decreasing function over $(-\infty, \infty)$. OLS $y|x$ corresponds to $p = -\infty$ and the regression line with $b = -1$ corresponds to $p = +\infty$.

Proof: In all cases begin with the derivative

$$p'(b) = \frac{1}{(\ln b^2)^2} \left\{ \left(\frac{1}{b - \frac{1}{\rho}\frac{\sigma_y}{\sigma_x}} - \frac{1}{b - \rho\frac{\sigma_y}{\sigma_x}} \right) \ln b^2 - \ln \left(\frac{\rho\frac{\sigma_y}{\sigma_x} \left(\frac{1}{\rho}\frac{\sigma_y}{\sigma_x} - b \right)}{\left(b - \rho\frac{\sigma_y}{\sigma_x} \right)} \right)^2 \left(\frac{1}{b} \right) \right\}. \quad (80)$$

The critical values of the $p(b)$ occur at $b = \pm 1$, $b = \rho\frac{\sigma_y}{\sigma_x} = b_{OLS Y|X}$, $b = \frac{1}{\rho}\frac{\sigma_y}{\sigma_x} = b_{OLS X|Y}$ and when $p'(b) = 0$. The first derivative test is now applied between the critical values to determine whether $p(b)$ is increasing or decreasing. Choose the test value b_* to be the arithmetic mean of the two ordinary least-squares slopes. That is, choose

$$b_* = \frac{1}{2} \left(\rho + \frac{1}{\rho} \right) \frac{\sigma_y}{\sigma_x} \quad (81)$$

and obtain

$$p'(b_*) = -\frac{\ln\left(\rho\frac{\sigma_y}{\sigma_x}\right)^2}{b_* (\ln b_*^2)^2}. \quad (82)$$

For this choice, $|b_*| < 1$ whenever $\frac{\sigma_y}{\sigma_x} < 1$. According to the first derivative test when $p'(b_*)$ is positive, $p(b)$ is increasing over the interval. It follows that its inverse $b(p)$ is an increasing function over $(-\infty, \infty)$. When $p'(b_*)$ is

negative, $p(b)$ is decreasing over the interval. Its inverse $b(p)$ is therefore a decreasing function over $(-\infty, \infty)$.

In Case 1, $p'(b_*) > 0$, in Case 2, $p'(b_*) < 0$, in Case 3, $p'(b_*) < 0$, in Case 4, $p'(b_*) > 0$, in Case 5, b_* is in $(\rho \frac{\sigma_y}{\sigma_x}, 1)$ and $p'(b_*) > 0$, and in Case 6, b_* is in $(-1, \rho \frac{\sigma_y}{\sigma_x})$ and $p'(b_*) < 0$. ■

Corollary 14: Generalized least-squares lines follow the same order relations as their corresponding means. The slopes increase or decrease in the following order: *HMR, SHR, GMR, SPR, AMR.*

Proof: The power mean is a increasing function of p and the slope b is always either an increasing function or a decreasing of p . ■

Thus the order of the generalized least-squares regression lines is explained by the corresponding inequalities of the underlying special means. The reader can observe this order among the lines in the numerical examples below.

The case of $|b| = 1$ plays a special role in the previous theorem; therefore it is given a name.

Definition 7: Call a generalized regression line with $|b| = 1$ unitary least-squares (ULS). If $b = 1$ then $a = \mu_y - \mu_x$ and if $b = -1$ then $a = \mu_y + \mu_x$.

C. Power Mean Regressions of Order $-\frac{1}{3}$, $\frac{1}{3}$ and $\frac{2}{3}$

It is known and observed here that the Lorentz mean or power mean of order $\frac{1}{3}$, approximates the logarithmic mean well [12]. The power mean of order $-\frac{1}{3}$ approximates both the second logarithmic mean and the geometrically weighted harmonic-geometric mean $H^{1/3}G^{2/3}$, usually written as $(HG^2)^{1/3}$ [3,13]. The power mean of order $\frac{2}{3}$ approximates both the Heronian mean and the identric means well. Therefore the regression formulas for these power means deserve special consideration and are described now.

For the Lorentz mean regression (ZMR),

$$Z(x, y) = M_{1/3}(x, y) = \left(\frac{\sqrt[3]{x} + \sqrt[3]{y}}{2} \right)^3, \quad (83)$$

the weight function is given by

$$g_{1/3}(b) = \frac{1}{8} \left(1 + b^{-2/3} \right)^3, \quad (84)$$

and the slope equation is

$$b^{8/3} - \rho \frac{\sigma_y}{\sigma_x} b^{5/3} + \rho \frac{\sigma_y}{\sigma_x} b - \left(\frac{\sigma_y}{\sigma_x} \right)^2 = 0. \quad (85)$$

The slope equation is solved as a polynomial equation in q after setting $q = b^{1/3}$. The result is

$$q^8 - \rho \frac{\sigma_y}{\sigma_x} q^5 + \rho \frac{\sigma_y}{\sigma_x} q^3 - \left(\frac{\sigma_y}{\sigma_x} \right)^2 = 0 \quad (86)$$

and $b = q^3$.

For the power mean with $p = -\frac{1}{3}$,

$$M_{-1/3}(x, y) = \left(\frac{2 \sqrt[3]{xy}}{\sqrt[3]{x} + \sqrt[3]{y}} \right)^3, \quad (87)$$

the weight function is given by

$$g_{-1/3}(b) = 8 \left(1 + b^{2/3} \right)^{-3}, \quad (88)$$

and the slope equation is

$$b^{4/3} - \rho \frac{\sigma_y}{\sigma_x} b^{1/3} + \rho \frac{\sigma_y}{\sigma_x} b - \left(\frac{\sigma_y}{\sigma_x} \right)^2 = 0. \quad (89)$$

The slope equation is again solved as a polynomial equation in q after setting $q = b^{1/3}$. The result is

$$q^4 + \rho \frac{\sigma_y}{\sigma_x} q^3 - \rho \frac{\sigma_y}{\sigma_x} q - \left(\frac{\sigma_y}{\sigma_x} \right)^2 = 0 \quad (90)$$

and $b = q^3$.

For the power mean with $p = \frac{2}{3}$,

$$M_{2/3}(x, y) = \left(\frac{\sqrt[3]{x^2} + \sqrt[3]{y^2}}{2} \right)^3, \quad (91)$$

the weight function is given by

$$g_{2/3}(b) = \frac{1}{\sqrt[8]{8}} \left(1 + b^{-4/3} \right)^{3/2}, \quad (92)$$

and the slope equation is

$$b^{10/3} - \rho \frac{\sigma_y}{\sigma_x} b^{7/3} + \rho \frac{\sigma_y}{\sigma_x} b - \left(\frac{\sigma_y}{\sigma_x} \right)^2 = 0. \quad (93)$$

The slope equation is again solved as a polynomial equation in q after setting $q = b^{1/3}$. The result is

$$q^{10} - \rho \frac{\sigma_y}{\sigma_x} q^7 + \rho \frac{\sigma_y}{\sigma_x} q^3 - \left(\frac{\sigma_y}{\sigma_x} \right)^2 = 0 \quad (94)$$

and $b = q^3$.

VII. CLASSIFYING REGRESSIONS USING ALTERNATIVE GENERALIZED MEANS

Power means of order p were just shown in certain cases to naturally parameterize the regression lines lying between the two ordinary least-squares lines. This section explores the use of other known generalized means having free parameters which give alternative ways to parameterize generalized regression lines.

A. Dietel and Gordon's Generalized Mean

It was shown by Dietel and Gordon [3] that if $(x, f(x))$ and $(y, f(y))$ are two distinct points on the graph of a function f , then the tangent lines of f at these two points intersect at the arithmetic mean of x and y if $f(x) = x^2$, the geometric mean of x and y if $f(x) = \sqrt{x}$ and the harmonic mean of x and y if $f(x) = \frac{1}{x}$. The authors generalize this result to means $S_f(x, y)$ that are generated by an arbitrary function f satisfying certain conditions. When $f(x) = x^r$, the resulting means are parametrized by r and are given by

$$S_r(x, y) = \begin{cases} \frac{r-1}{r} \cdot \frac{y^r - x^r}{y^{r-1} - x^{r-1}}, & x \neq y, r \neq 0, 1 \\ x, & x = y. \end{cases} \quad (95)$$

The function $S_r(x, y)$ is called here the Dietel-Gordon mean of order r . The case $S_1(x, y) = \lim_{r \rightarrow 1} S_r(x, y)$ is given by

$$S_1(x, y) = (y - x) / (\ln y - \ln x) \quad (96)$$

and is the logarithmic mean. It is parameterized by $f(x) = x \ln x$. The case $S_0(x, y) = \lim_{r \rightarrow 0} S_r(x, y)$ is given by

$$S_0(x, y) = xy (\ln y - \ln x) / (y - x) \quad (97)$$

and is the second logarithmic mean. It is parameterized by $f(x) = \ln x$. The authors show that $\lim_{r \rightarrow -\infty} S_r(x, y) = x = \min(x, y)$ and $\lim_{r \rightarrow +\infty} S_r(x, y) = y = \max(x, y)$ and that $S_r(x, y)$ is an increasing function of r . Dietel and Gordon show that many of the special means mentioned here are specific cases of this generalized mean for particular values of r . The next chart summarizes this.

| Mean Type | Formula | Order r |
|--------------------|--|---------------|
| Minimum | $\min(x, y)$ | $-\infty$ |
| Harmonic | $H(x, y) = \frac{2xy}{x+y}$ | -1 |
| Second logarithmic | $L_2(x, y) = \frac{xy(\ln y - \ln x)}{y-x}$ | 0 |
| Geometric | $G(x, y) = \sqrt{xy}$ | $\frac{1}{2}$ |
| Logarithmic | $L(x, y) = \frac{y-x}{\ln y - \ln x}$ | 1 |
| Heronian | $N(x, y) = \frac{1}{3}(x + \sqrt{xy} + y)$ | $\frac{3}{2}$ |
| Arithmetic | $A(x, y) = \frac{x+y}{2}$ | 2 |
| Centroidal | $T(x, y) = \frac{2}{3} \cdot \frac{x^2 + xy + y^2}{x+y}$ | 3 |
| Maximum | $\max(x, y)$ | ∞ |

Since $S_r(x, y)$ is an increasing function of r , it follows that

$$H \leq L_2 \leq G \leq L \leq N \leq A \leq T. \quad (98)$$

Chen defines a related generalized mean $F_t(x, y) = S_{t-2}(x, y)$ in his paper and presents a similar classification [2]. Because of its simple relation to the already existing Dietel-Gordon mean, the Dietel-Gordon parameterization is preferred here.

B. Regression Formulas for the Dietel-Gordon Generalized Mean

The generalized mean $S_r(x, y)$ is now applied to the task of classifying and further understanding generalized least-squares regressions. The weight function is given by

$$g_r(b) = \frac{r-1}{r} \left(1 + \frac{b^2 - 1}{b^{2r} - b^2} \right), r \neq 0, 1. \quad (99)$$

As in the case of power mean regression, since $S_{-\infty}(x, y) = \min(x, y)$, it follows that when $|b| < 1$, $r = -\infty$ corresponds to OLS $x|y$ and when $|b| > 1$, $r =$

$-\infty$ corresponds to OLS $y|x$. Similarly, since $S_\infty(x, y) = \max(x, y)$, it follows that when $|b| < 1$, $r = \infty$ corresponds to OLS $x|y$ and when $|b| > 1$, $r = \infty$ corresponds to OLS $y|x$.

The slope equation is given by

$$\begin{aligned} 0 &= b^{4r} - \rho \frac{\sigma_y}{\sigma_x} b^{4r-1} - rb^{2r+2} \\ &\quad + (2r-1) \rho \frac{\sigma_y}{\sigma_x} b^{2r+1} \\ &\quad + (r-1) \left(1 - \left(\frac{\sigma_y}{\sigma_x} \right)^2 \right) b^{2r} \\ &\quad - (2r-1) \rho \frac{\sigma_y}{\sigma_x} b^{2r-1} + r \left(\frac{\sigma_y}{\sigma_x} \right)^2 b^{2r-2} \\ &\quad + \rho \frac{\sigma_y}{\sigma_x} b - \left(\frac{\sigma_y}{\sigma_x} \right)^2. \end{aligned} \quad (100)$$

Unlike power mean regression, the parameter r cannot be solved in terms of b explicitly. Nevertheless, it can always be done numerically. The slope profile $b = b(r)$ exhibits similar behavior to $b = b(p)$ and is plotted numerically for the examples below. Generalized least-squares lines follow the same order relations as the inequalities of their corresponding means. The slope b is either a strictly increasing function of r or a strictly decreasing function of r . Therefore the slopes increase or decrease in the following order: $HMR, L2MR, GMR, LMR, SPR, NMR, AMR, TMR$. The reader can observe this in the numerical examples presented further on.

C. Stolarsky's Generalized Logarithmic Mean

Mays [13] describes how the integral and differential forms of the mean value theorem of calculus can be used to define generalized means. The integral mean value theorem states that for f continuous and strictly monotone on $(0, \infty)$ there is a unique c in (x, y) such that

$$f(c)(y-x) = \int_x^y f(w) dw. \quad (101)$$

Therefore one can define the generalized mean

$$U_f(x, y) = f^{-1} \left(\int_x^y f(w) dw / (y-x) \right). \quad (102)$$

For $f(x) = x^{s-1}$ the generalized mean becomes Stolarsky's generalized logarithmic mean [3,13,14,15]:

$$U_s(x, y) = \left(\int_x^y w^{s-1} dw / (y-x) \right)^{1/(s-1)} \quad (103)$$

which can be written explicitly as

$$U_s(x, y) = \begin{cases} \left(\frac{1}{s} \cdot \frac{y^s - x^s}{y-x} \right)^{1/(s-1)}, & x \neq y, s \neq 0, 1 \\ x, & x = y. \end{cases} \quad (104)$$

The case $s = 0$ corresponds to the logarithmic mean and the case $s = 1$ corresponds to the identric mean. The weight

function for Stolarsky's mean is given by

$$\begin{aligned} g_s(b) &= U_s \left(1, \frac{1}{b^2} \right) \\ &= s^{-1/(s-1)} \left(1 + \frac{b^{2s-2} - 1}{b^{2s} - b^{2s-2}} \right)^{1/(s-1)} \end{aligned} \quad (105)$$

and the slope equation is given by

$$\begin{aligned} 0 &= (s-1)b^{2s+4} - (s-1)\rho \frac{\sigma_y}{\sigma_x} b^{2s+3} - sb^{2s+2} \\ &\quad + (s+1)\rho \frac{\sigma_y}{\sigma_x} b^{2s+1} - \left(\frac{\sigma_y}{\sigma_x} \right)^2 b^{2s} \\ &\quad + b^4 - (s+1)\rho \frac{\sigma_y}{\sigma_x} b^3 + s \left(\frac{\sigma_y}{\sigma_x} \right)^2 b^2 \\ &\quad + (s-1)\rho \frac{\sigma_y}{\sigma_x} b - (s-1) \left(\frac{\sigma_y}{\sigma_x} \right)^2. \end{aligned} \quad (106)$$

Again, the parameter s cannot be solved in terms of b explicitly, however it can always be done numerically. The slope profile $b = b(s)$ exhibits similar behavior to $b = b(p)$ and $b = b(r)$ and is plotted numerically in the examples below.

D. Gini's Mean

Gini's mean [6,11,13] is given by

$$G_t(x, y) = \frac{x^t + y^t}{x^{t-1} + y^{t-1}}. \quad (107)$$

The weight function for Gini's mean is:

$$g_t(b) = G_t \left(1, \frac{1}{b^2} \right) = 1 + \frac{1 - b^2}{b^{2t} + b^2} \quad (108)$$

and the slope equation is given by

$$\begin{aligned} 0 &= b^{4t} - \rho \frac{\sigma_y}{\sigma_x} b^{4t-1} + tb^{2t+2} \\ &\quad - (2t-1)\rho \frac{\sigma_y}{\sigma_x} b^{2t+1} \\ &\quad + (t-1) \left(\left(\frac{\sigma_y}{\sigma_x} \right)^2 - 1 \right) b^{2t} \\ &\quad + (2t-1)\rho \frac{\sigma_y}{\sigma_x} b^{2t-1} - t \left(\frac{\sigma_y}{\sigma_x} \right)^2 b^{2t-2} \\ &\quad + \rho \frac{\sigma_y}{\sigma_x} b - \left(\frac{\sigma_y}{\sigma_x} \right)^2. \end{aligned} \quad (109)$$

A related mean is Moskovitz's mean $M_t(x, y) = G_{1-t}(x, y)$ [13], given explicitly by

$$M_t(x, y) = \frac{xy^t + yx^t}{x^t + y^t}. \quad (110)$$

Because of its simple relation to Gini's mean and because Gini's mean parameterizes the specific cases in the same order as the power mean, the Dietel-Gordon mean, and Stolarsky's logarithmic mean, Gini's mean is preferred here. Moskovitz's mean parameterizes the specific cases in the reverse order. Again, the parameter t cannot be solved in terms of b explicitly, however it can always be done numerically. The slope profile $b = b(t)$ will be analyzed in greater detail in future work.

E. Two-Parameter Means

The two-parameter mean of Stolarsky [10,14] is given by

$$E_{r,s}(x, y) = \begin{cases} \left(\frac{r(x^s - y^s)}{s(x^r - y^r)} \right)^{1/(s-r)}, & x \neq y \\ x, & x = y. \end{cases} \quad (111)$$

Some properties include: $E_{r,s}(x, y) = E_{s,r}(x, y)$, $E_{r,-r}(x, y) = G(x, y)$. The power mean is a specific case: $M_p(x, y) = E_{p,2p}(x, y)$, as is Stolarsky's one-parameter mean: $U_s(x, y) = E_{s,1}(x, y)$. The weight function is given by

$$\begin{aligned} g_{r,s}(b) &= E_{r,s} \left(1, \frac{1}{b^2} \right) \\ &= \left(\frac{r}{s} \right)^{1/(s-r)} \left(1 + \frac{b^{2(s-r)} - 1}{b^{2s} - b^{2(s-r)}} \right)^{1/(s-r)} \end{aligned} \quad (112)$$

and the slope equation is given by

$$\begin{aligned} 0 &= (s-r)b^{2s+2r+2} - (s-r)\rho \frac{\sigma_y}{\sigma_x} b^{2s+2r+1} \\ &\quad - sb^{2s+2} + rb^{2r+2} + (s+r)\rho \frac{\sigma_y}{\sigma_x} b^{2s+1} \\ &\quad - (s+r)\rho \frac{\sigma_y}{\sigma_x} b^{2r+1} - \left(\frac{\sigma_y}{\sigma_x} \right)^2 rb^{2s} \\ &\quad + \left(\frac{\sigma_y}{\sigma_x} \right)^2 sb^{2r} + \rho \frac{\sigma_y}{\sigma_x} (s-r)b \\ &\quad - (s-r) \left(\frac{\sigma_y}{\sigma_x} \right)^2. \end{aligned} \quad (113)$$

Gini's two-parameter mean [6,13] is given by

$$G_{r,s}(x, y) = \left(\frac{x^s + y^s}{x^r + y^r} \right)^{1/(s-r)}. \quad (114)$$

Gini's two-parameter mean includes as specific cases the power means: $M_p(x, y) = G_{p,0}(x, y)$ and Gini's one-parameter mean: $G_s(x, y) = G_{s,s-1}(x, y)$. The weight function is given by

$$\begin{aligned} g_{r,s}(b) &= G_{r,s} \left(1, \frac{1}{b^2} \right) \\ &= \left(1 + \frac{1 - b^{2(s-r)}}{b^{2s} + b^{2(s-r)}} \right)^{1/(s-r)} \end{aligned} \quad (115)$$

and the slope equation is given by

$$\begin{aligned} 0 &= (s-r)b^{2s+2r+2} - (s-r)\rho \frac{\sigma_y}{\sigma_x} b^{2s+2r+1} \\ &\quad + sb^{2s+2} - rb^{2r+2} - (s+r)\rho \frac{\sigma_y}{\sigma_x} b^{2s+1} \\ &\quad + (s+r)\rho \frac{\sigma_y}{\sigma_x} b^{2r+1} + r \left(\frac{\sigma_y}{\sigma_x} \right)^2 b^{2s} \\ &\quad - s \left(\frac{\sigma_y}{\sigma_x} \right)^2 b^{2r} + (s-r)\rho \frac{\sigma_y}{\sigma_x} b \\ &\quad - (s-r) \left(\frac{\sigma_y}{\sigma_x} \right)^2. \end{aligned} \quad (116)$$

F. Relating the Mean Parameters Using Linear Approximations

The p, r, s , and t scales offer different ways of parameterizing and classifying the known special means. The actual functions $p = p(r)$, $r = r(p)$, etc. depend on the data (i.e. on ρ and $\frac{\sigma_y}{\sigma_x}$) and cannot be written explicitly. However, linear approximations are possible which give further insight and understanding. The linear relations presented here reveal that the Heronian and identric means are always approximate power means of order $\frac{2}{3}$, regardless of the data. The first and second logarithmic means are always approximate power means of order $\pm\frac{1}{3}$ respectively, regardless of the data. The geometrically weighted harmonic-geometric mean $H^{1/3}G^{2/3}$, usually written $(HG^2)^{1/3}$, has an exact Stolarsky parameter of $s = -2$, which corresponds approximately to a power mean of order $-\frac{1}{3}$ and to the second logarithmic mean.

Theorem 15: (Approximate Linear Relations) The power mean parameter p , the Dietel-Gordon parameter r , the Stolarsky parameter s and the Gini parameter t are interrelated according to the following pairs of linear approximations:

$$\begin{aligned} p &\approx \frac{2}{3}r - \frac{1}{3}, \quad r \text{ in } [-1, 2] \text{ and} \\ r &\approx \frac{3}{2}p + \frac{1}{2}, \quad p \text{ in } [-1, 1], \end{aligned} \quad (117)$$

$$\begin{aligned} s &\approx 2r - 2, \quad r \text{ in } \left[\frac{1}{2}, 2\right] \text{ and} \\ r &\approx \frac{1}{2}s + 1, \quad s \text{ in } [-1, 2], \end{aligned} \quad (118)$$

$$\begin{aligned} s &\approx 3p - 1, \quad p \text{ in } [0, 1] \text{ and} \\ p &\approx \frac{1}{3}s + \frac{1}{3}, \quad s \text{ in } [-1, 2], \end{aligned} \quad (119)$$

$$\begin{aligned} t &\approx \frac{1}{2}p + \frac{1}{2}, \quad p \text{ in } [-1, 1] \text{ and} \\ p &\approx 2t - 1, \quad t \text{ in } [0, 1], \end{aligned} \quad (120)$$

$$\begin{aligned} t &\approx \frac{1}{3}r + \frac{1}{3}, \quad r \text{ in } [-1, 2] \text{ and} \\ r &\approx 3t - 1, \quad t \text{ in } [0, 1], \end{aligned} \quad (121)$$

$$t \approx \frac{1}{6}s + \frac{2}{3}, \quad s \text{ in } [-1, 2] \text{ and} \quad (122)$$

$$s \approx 6t - 4, \quad t \text{ in } \left[\frac{1}{2}, 1\right].$$

Proof: In the (p, r) plane, regardless of the data, the harmonic mean corresponds to $(p, r) = (-1, -1)$, the geometric mean corresponds to $(p, r) = (0, \frac{1}{2})$, and the arithmetic mean corresponds to $(p, r) = (1, 2)$. There is a single straight line passing through these three points which approximates the values of p and r lying between the harmonic, geometric and arithmetic means.

In the (s, r) plane, the geometric mean corresponds to $(s, r) = (-1, \frac{1}{2})$, the logarithmic mean corresponds to $(s, r) = (0, 1)$ and the arithmetic mean corresponds to $(s, r) = (2, 2)$. The linear approximation is the single straight line which passes through these points.

In the (s, p) plane, the geometric mean corresponds to $(s, p) = (-1, 0)$, the power mean of order $\frac{1}{2}$ corresponds to $(s, p) = (\frac{1}{2}, \frac{1}{2})$, and the arithmetic mean corresponds to $(2, 1)$. The linear approximation is again the single straight line which passes through these points.

In the (p, t) plane, the harmonic mean corresponds to $(-1, 0)$, the geometric mean corresponds to $(0, \frac{1}{2})$, and the arithmetic mean corresponds to $(1, 1)$. The linear approximation is again the single straight line which passes through these points.

In the (r, t) plane, the harmonic mean corresponds to $(-1, 0)$, the geometric mean corresponds to $(\frac{1}{2}, \frac{1}{2})$, and the arithmetic mean corresponds to $(2, 1)$. The linear approximation is again the single straight line which passes through these points.

Finally, in the (s, t) plane, the harmonic mean does not have a fixed value, but the geometric mean corresponds to $(-1, \frac{1}{2})$, and the arithmetic mean corresponds to $(2, 1)$. The linear approximation is the straight line which passes through these points. ■

The next chart summarizes the approximate correspondences for all the notable cases. An asterisk by the number indicates that it is an approximate value obtained from the linear formulas. Two asterisks indicate that the approximate value is outside the domain of the linear formulas. Therefore the approximation will be less accurate than the values with single asterisks.

| Mean Type | Power $M_p(x, y)$ | Dietel-Gordon $S_r(x, y)$ | Stolarsky $U_s(x, y)$ | Gini $G_t(x, y)$ |
|--------------------|-------------------|---------------------------|-----------------------|------------------|
| Order | p | r | s | t |
| Harmonic | -1 | -1 | -4** | 0 |
| Power | $-\frac{1}{2}$ | $-\frac{1}{4}$ * | -2.5** | $\frac{1}{4}$ * |
| Second Logarithmic | $-\frac{1}{3}$ * | 0 | -2* | $\frac{1}{3}$ * |
| $(HG^2)^{1/3}$ | $-\frac{1}{3}$ * | 0* | -2 | $\frac{1}{3}$ * |
| Geometric | 0 | $\frac{1}{2}$ | -1 | $\frac{1}{2}$ |
| Logarithmic | $\frac{1}{3}$ * | 1 | 0 | $\frac{2}{3}$ * |
| Lorentz | $\frac{1}{3}$ | 1* | 0* | $\frac{2}{3}$ * |
| Power | $\frac{1}{2}$ | $\frac{5}{4}$ * | $\frac{1}{2}$ | $\frac{3}{4}$ * |
| Heronian | $\frac{2}{3}$ * | $\frac{3}{2}$ | 1* | $\frac{5}{6}$ * |
| Identric | $\frac{2}{3}$ * | $\frac{3}{2}$ * | 1 | $\frac{5}{6}$ * |
| Arithmetic | 1 | 2 | 2 | 1 |

Although there is no fixed value of the Stolarsky parameter s corresponding to the harmonic mean [13], there is always a variable value of s which depends in the data corresponding to orthogonal regression which is HMR. The linear approximation may no longer be a good fit for s outside the

domain $[-1, 2]$. Nevertheless, the equations suggest taking $s = -4$ as an initial guess. Similarly, root-mean-square regression corresponds to $p = 2$. Since this value is outside the domain $[-1, 1]$, the linear equations may no longer give a good fit. Nevertheless, the linear approximations suggest taking $r = \frac{7}{2}$, $s = 5$ and $t = \frac{3}{2}$ as initial guesses.

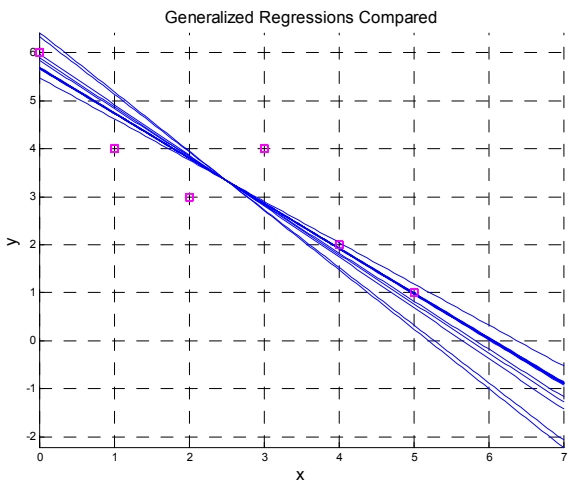
To summarize, the inequalities involving the known special means are due to the fact that they are parameterized by generalized means which are increasing functions of the parameter. The corresponding regression lines have the same order since their slopes are either increasing or decreasing functions of the parameter.

The approximate symmetry of all the special means about $p = 0$ on the power mean scale is striking. Power mean regression has a slope equation where the free parameter p can be solved explicitly in terms of the slope. Because of this, the power mean spectrum may be a preferred scale in which to work.

VIII. NUMERICAL EXAMPLES

This section revisits the examples explored previously. Regressions corresponding to all the special means are computed and the corresponding numerical values for the generalized mean parameters are computed for each regression line as well.

Example 1 Six data values are given: $(0, 6)$, $(1, 4)$, $(2, 3)$, $(3, 4)$, $(4, 2)$, and $(5, 1)$. The reader can verify that $\rho = -0.9157$, $\kappa = -0.4019$, $\mu_x = 2.5000$, $\mu_y = 3.3333$, $\sigma_x = 1.7078$, and $\sigma_y = 1.5986$. The generalized regression lines are plotted together with the extremal line thereby displaying the region containing all admissible generalized regression lines.



The equation of each line is presented along with the scatter parameter λ , the weighted arithmetic mean parameter α , and the weighted geometric mean parameter β . The parameters ϕ and δ defined earlier can be computed by the reader using

$$\phi = 2 \tan^{-1} \lambda \text{ and } \delta = \frac{4}{\pi} \tan^{-1} \lambda.$$

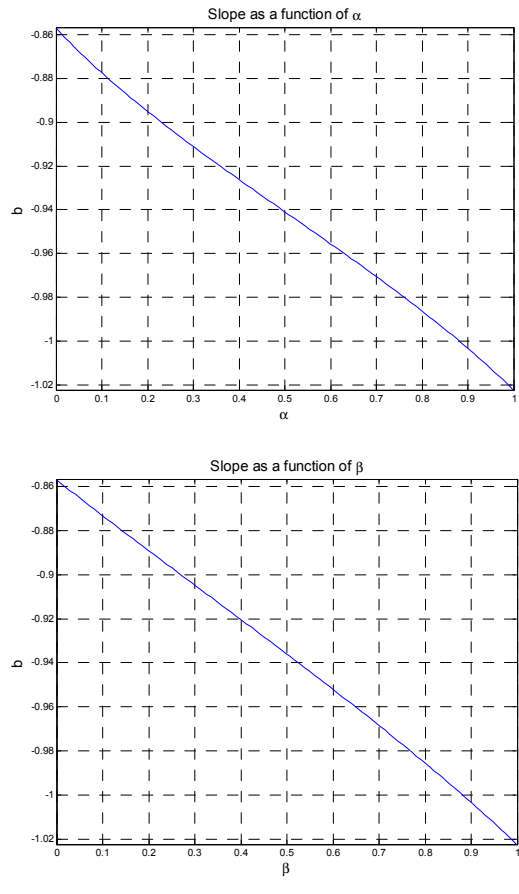
| Method | $y = a + bx$ | λ | α | β |
|--------------------|------------------------|-----------|----------|---------|
| Extremal | $y = 6.4166 - 1.2333x$ | 1.0000 | — | — |
| CMR | $y = 6.3335 - 1.2001x$ | 0.9117 | — | — |
| TMR | $y = 5.9729 - 1.0558x$ | 0.5282 | — | — |
| OLS $x y$ | $y = 5.8889 - 1.0222x$ | 0.4389 | 1.0000 | 1.0000 |
| USR | $y = 5.8333 - 1.0000x$ | 0.3798 | 0.8824 | 0.8824 |
| RMR | $y = 5.6958 - 0.9450x$ | 0.2335 | 0.5283 | 0.5563 |
| AMR | $y = 5.6855 - 0.9409x$ | 0.2226 | 0.5000 | 0.5304 |
| IMR | $y = 5.6817 - 0.9394x$ | 0.2185 | 0.4897 | 0.5209 |
| PMR | $y = 5.6817 - 0.9394x$ | 0.2185 | 0.4897 | 0.5208 |
| $p = \frac{2}{3}$ | | | | |
| NMR | $y = 5.6817 - 0.9394x$ | 0.2185 | 0.4896 | 0.5208 |
| SPR | $y = 5.6797 - 0.9386x$ | 0.2164 | 0.4842 | 0.5159 |
| ZMR | $y = 5.6777 - 0.9377x$ | 0.2143 | 0.4786 | 0.5107 |
| $p = \frac{1}{3}$ | | | | |
| LMR | $y = 5.6777 - 0.9377x$ | 0.2143 | 0.4786 | 0.5107 |
| GMR | $y = 5.6735 - 0.9361x$ | 0.2098 | 0.4670 | 0.5000 |
| L2MR | $y = 5.6690 - 0.9343x$ | 0.2050 | 0.4548 | 0.4887 |
| PMR | $y = 5.6690 - 0.9343x$ | 0.2050 | 0.4548 | 0.4887 |
| $p = -\frac{1}{3}$ | | | | |
| SHR | $y = 5.6667 - 0.9333x$ | 0.2026 | 0.4484 | 0.4828 |
| HMR | $y = 5.6593 - 0.9304x$ | 0.1947 | 0.4283 | 0.4640 |
| OLS $y x$ | $y = 5.4762 - 0.8571x$ | 0.0000 | 0.0000 | 0.0000 |

| Method | p | r | s | t |
|--------------------|-----------|-----------|-----------|-----------|
| USR | $+\infty$ | $+\infty$ | $+\infty$ | $+\infty$ |
| RMR | 2.0000 | 3.4990 | 5.0077 | 1.4984 |
| AMR | 1.0000 | 2.0000 | 2.0000 | 1.0000 |
| IMR | 0.6667 | 1.5001 | 1.0000 | 0.8335 |
| PMR | 0.6667 | 1.5001 | 1.0000 | 0.8335 |
| $p = \frac{2}{3}$ | | | | |
| NMR | 0.6666 | 1.5000 | 0.9998 | 0.8334 |
| SPR | 0.5000 | 1.2501 | 0.5000 | 0.7501 |
| ZMR | 0.3333 | 1.0000 | 0.0000 | 0.6668 |
| $p = \frac{1}{3}$ | | | | |
| LMR | 0.3333 | 1.0000 | 0.0000 | 0.6668 |
| GMR | 0.0000 | 0.5000 | -1.0000 | 0.5000 |
| L2MR | -0.3333 | 0.0000 | -2.0012 | 0.3332 |
| PMR | -0.3333 | 0.0000 | -2.0012 | 0.3332 |
| $p = -\frac{1}{3}$ | | | | |
| SHR | -0.5000 | -0.2501 | -2.5029 | 0.2499 |
| HMR | -1.0000 | -1.0000 | -4.0125 | 0.0000 |
| OLS $y x$ | $-\infty$ | $-\infty$ | $-\infty$ | $-\infty$ |

The parameter p is also computed using the explicit formula

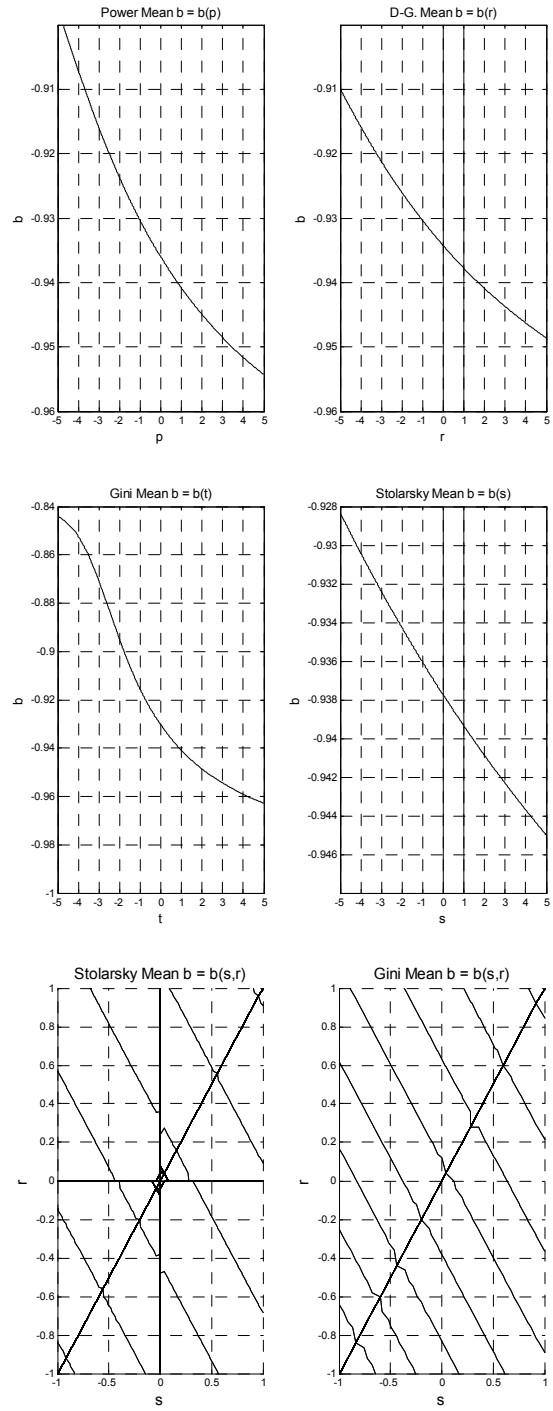
for $p(b)$ and the value for the slope. The parameters r , s , and t are computed by solving the slope equations numerically using the linear approximations $r_0 = \frac{3}{2}p + \frac{1}{2}$, $s_0 = 3p - 1$, and $t_0 = \frac{1}{2}p + \frac{1}{2}$ as initial guesses. For these data, the actual values for the parameters are in excellent agreement with the linear approximations.

The reader will observe that for this data set and level of accuracy, LMR and ZMR are indistinguishable as are NMR, PMR with $p = \frac{2}{3}$, and IMR. The slope profiles for weighted arithmetic mean regression and weighted geometric mean regression are displayed next.



This example corresponds to Case 6 of the Power Mean Spectrum: the slope decreases continuously from the unitary least-squares slope -1 down to the ordinary least-squares slope -0.8571 as p varies from $-\infty$ up to ∞ . The Dietel-Gordon mean, the Stolarsky mean, and the Gini mean, display similar behavior as is suggested by the next two pairs of slope profiles. In the Dietel-Gordon plot, $s = 0$ and $s = 1$, correspond to the two logarithmic mean regressions. In the Stolarsky plot, $s = 0$ corresponds to LMR and $s = 1$

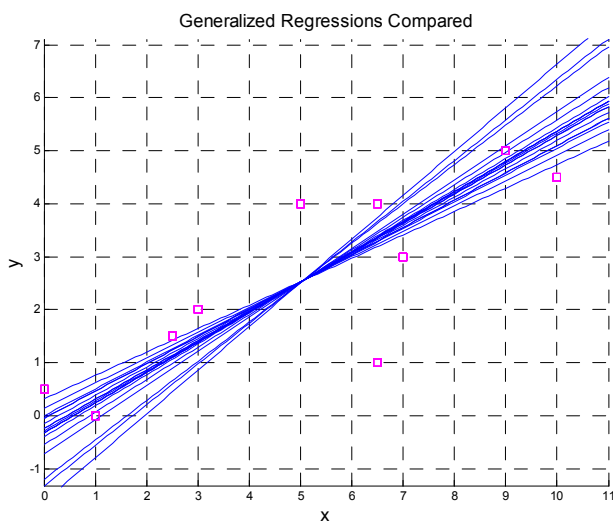
corresponds to IMR.



In the third pair of plots, slope contours are plotted in the (s, r) parameter plane for Stolarsky's two-parameter mean $E_{r,s}(x, y)$ and Gini's two-parameter mean $G_{r,s}(x, y)$. The line $r = s$ which appears in the graphs is a removable singularity. The contours are decreasing as s and r increase. For the Stolarsky slope equation, six contours $b = -0.9327, \dots, -0.9392$ are plotted in increments of -0.0013 . For the Gini equation, eight contours $b =$

$-0.9262, \dots, -0.9444$ are plotted in increments of -0.0026 . The jaggedness of the contours is an artifact of the plotting algorithm.

Example 2 Ten data values are given: $(0, 0.5)$, $(1, 0)$, $(2.5, 1.5)$, $(3, 2)$, $(5, 4)$, $(6.5, 4)$, $(6.5, 1)$, $(7, 3)$, $(9, 5)$, and $(10, 4.5)$. The reader can verify that $\rho = 0.8268$, $\kappa = 0.5625$, $\mu_x = 5.0500$, $\mu_y = 2.5500$, $\sigma_x = 3.1737$, and $\sigma_y = 1.6948$. The generalized regression lines are plotted together with the extremal line thereby displaying the region containing all admissible generalized regression lines.



The equation of each line is presented along with the scatter parameter λ , the weighted arithmetic mean parameter α , and the weighted geometric mean parameter β . The parameters ϕ and δ defined earlier can be computed by the reader using $\phi = 2 \tan^{-1} \lambda$ and $\delta = \frac{4}{\pi} \tan^{-1} \lambda$. The parameter p is also computed using the explicit formula and the value for the slope. The parameters r , s , and t are computed by solving the slope equations numerically using the linear approximations $r_0 = \frac{3}{2}p + \frac{1}{2}$, $s_0 = 3p - 1$, and $t_0 = \frac{1}{2}p + \frac{1}{2}$ as initial guesses. This example corresponds to Case 1 of the Power Mean Spectrum: the slope increases continuously from the OLS $y|x$ slope to the OLS $x|y$ slope as p increases from $-\infty$ to ∞ . TMR has the equation $y = -1.6144 + 0.8246x$ and CMR has the equation $-1.321 + 0.7665x$. Their slopes exceed the extremal line and their corresponding λ values exceed 1. These lines are therefore inadmissible by the criteria described

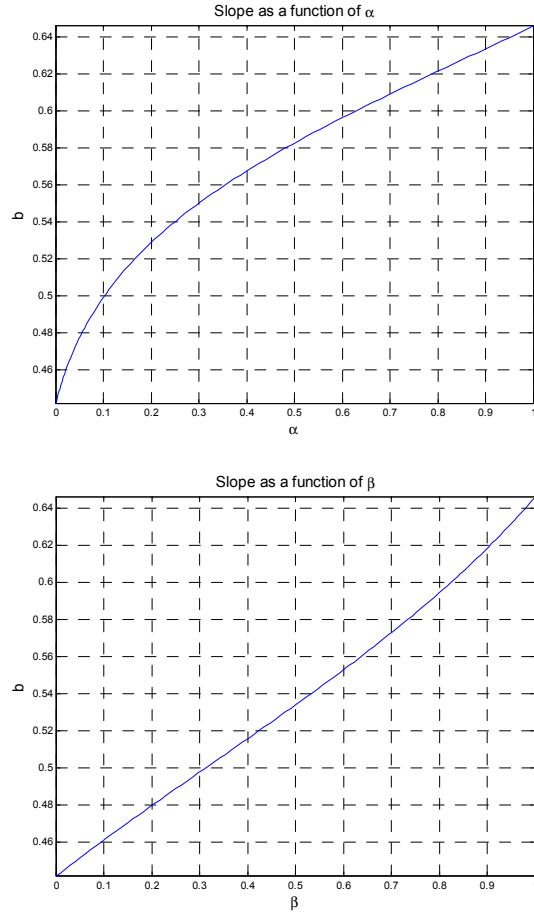
earlier.

| Method | $y = a + bx$ | λ | α | β |
|---------------------------|-------------------------|-----------|----------|---------|
| Extremal | $y = -1.1966 + 0.7419x$ | 1.0000 | — | — |
| OLS $x y$ | $y = -0.7116 + 0.6459x$ | 0.6803 | 1.0000 | 1.0000 |
| RMR | $y = -0.5431 + 0.6125x$ | 0.5691 | 0.7272 | 0.8766 |
| AMR | $y = -0.3924 + 0.5827x$ | 0.4698 | 0.5000 | 0.7466 |
| IMR | $y = -0.3227 + 0.5688x$ | 0.4238 | 0.4079 | 0.6804 |
| PMR $p = \frac{2}{3}$ | $y = -0.3220 + 0.5687x$ | 0.4233 | 0.4070 | 0.6797 |
| NMR | $y = -0.3211 + 0.5685x$ | 0.4228 | 0.4059 | 0.6789 |
| SPR | $y = -0.2824 + 0.5609x$ | 0.3972 | 0.3593 | 0.6407 |
| ZMR $p = \frac{1}{3}$ | $y = -0.2397 + 0.5525x$ | 0.3692 | 0.3119 | 0.5976 |
| LMR | $y = -0.2390 + 0.5523x$ | 0.3686 | 0.3110 | 0.5967 |
| GMR | $y = -0.1468 + 0.5340x$ | 0.3079 | 0.2219 | 0.5000 |
| L2MR | $y = -0.0478 + 0.5144x$ | 0.2426 | 0.1459 | 0.3923 |
| PMR $p = -\frac{1}{3}$ | $y = -0.0465 + 0.5142x$ | 0.2417 | 0.1451 | 0.3909 |
| SHR | $y = 0.0041 + 0.5041x$ | 0.2084 | 0.1136 | 0.3352 |
| HMR | $y = 0.1406 + 0.4771x$ | 0.1184 | 0.0493 | 0.1854 |
| OLS $y x$ | $y = 0.3202 + 0.4416x$ | 0.0000 | 0.0000 | 0.0000 |

| Method | p | r | s | t |
|---------------------------|-----------|-----------|-----------|---------|
| OLS $x y$ | $+\infty$ | $+\infty$ | $+\infty$ | 2.0113 |
| RMR | 2.0000 | 3.4396 | 5.6917 | 1.3952 |
| AMR | 1.0000 | 2.0000 | 2.0000 | 1.0000 |
| IMR | 0.6698 | 1.5103 | 1.0000 | 0.8445 |
| PMR $p = \frac{2}{3}$ | 0.6667 | 1.5057 | 0.9906 | 0.8430 |
| NMR | 0.6628 | 1.5000 | 0.9795 | 0.8411 |
| SPR | 0.5000 | 1.2562 | 0.5000 | 0.7604 |
| ZMR $p = \frac{1}{3}$ | 0.3333 | 1.0052 | 0.0101 | 0.6754 |
| LMR | 0.3299 | 1.0000 | 0.0000 | 0.6736 |
| GMR | 0.0000 | 0.5000 | -1.0000 | 0.5000 |
| L2MR | -0.3291 | 0.0000 | -2.1243 | 0.3247 |
| PMR $p = -\frac{1}{3}$ | -0.3333 | -0.0065 | -2.1404 | 0.3224 |
| SHR | -0.5000 | -0.2586 | -2.8197 | 0.2355 |
| HMR | -1.0000 | -1.0000 | -5.9780 | 0.0000 |
| OLS $y x$ | $-\infty$ | $-\infty$ | $-\infty$ | -0.3737 |

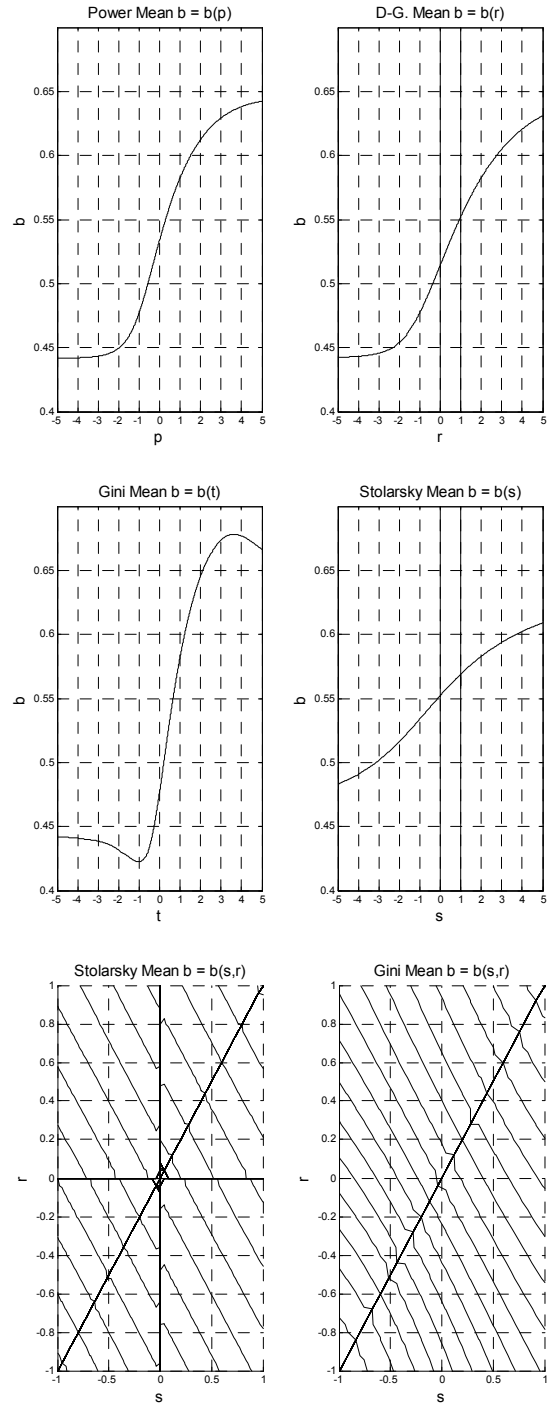
In the next diagrams slope profiles are plotted. The slope

profiles for weighted arithmetic mean regression and weighted geometric mean regression are displayed next.



For the power mean, the Dietel-Gordon mean and the Stolarsky mean, the slope equations are solved numerically, and the slope profile is plotted as a function of the parameter. For these cases, the slope is a strictly increasing function of the parameter with parameter values $\pm\infty$ corresponding to ordinary least-squares regression. The Gini mean has the same asymptotic behavior as the other generalized means, but it experiences an undershoot and an overshoot. This means that it is not one-to-one over $(-\infty, \infty)$. However, one can restrict the parameter t to the subinterval $[-0.3737, 2.0113]$ over which the slope is one-to-one and lies between the two OLS lines. Again, in the Dietel-Gordon plot, $s = 0$ and $s = 1$, correspond to the two logarithmic mean regressions. In the Stolarsky plot, $s = 0$ corresponds to LMR and $s = 1$

corresponds to IMR.



Again, in the third pair of plots, slope contours are plotted in the (s, r) parameter plane for Stolarsky's two-parameter mean and Gini's two-parameter mean. The line $r = s$ which appears in the graphs is a removable singularity. The contours are increasing as s and r increase. For the Stolarsky slope equation, thirteen contours $b = 0.496, \dots, 0.568$ are plotted in increments of 0.006. For the Gini equation, sixteen contours $b = 0.436, \dots, 0.616$ are plotted in increments of 0.012. The

jaggedness of the contours is again an artifact of the plotting algorithm.

IX. SUMMARY

Least-squares regressions arising from generalized means are explored. The notion of a generalized mean is equivalent to the generating function concept of the previous work but allows for a more robust understanding of what generalized least-squares is about. Generalized least-squares seeks a line which minimizes the average generalized mean of the square deviations in x and y .

The theory is reviewed and trigonometric formulas are also derived relating the parameters γ and λ in the fundamental generalized least-squares formula. An admissibility condition for least-squares lines in general and for the OLS $x|y$ line in particular is discussed. The OLS $x|y$ line is admissible, in the sense that its coefficients minimize the error function, provided that $\frac{1}{2} \leq \rho^2 \leq 1$.

The specific cases of arithmetic, geometric and harmonic mean regression were already explored in the previous papers with AMR called Pythagorean regression and HMR noted to be equivalent to orthogonal regression. Here, logarithmic, Heronian, centroidal, identric, Lorentz, and root mean square regressions are described for the first time. Ordinary least-squares regression is also shown here to be equivalent to minimum or maximum mean regression. Regressions based on weighted arithmetic means of order α and weighted geometric means of order β are explored. The weights α and β parameterize all generalized mean square regression lines lying between the two ordinary least-squares lines.

Power mean regression of order p is shown to be another particularly simple framework for parameterizing all the generalized mean square regressions previously described. The p -scale has fixed numerical values corresponding to many known special means. Since the power mean is an increasing function of p , the parameter p concisely explains the inequalities of the special means and why the same order is found among the corresponding regression lines. The parameter p has an explicit formula in terms of b , ρ , and $\frac{\sigma_y}{\sigma_x}$. Under certain conditions, every regression line lying between the two ordinary least-squares lines is generated by a power mean of order p for some p in $(-\infty, \infty)$ with the ordinary least-squares lines corresponding to $p = \pm\infty$.

The Dietel-Gordon mean of order r , Stolarsky's logarithmic mean of order s , Gini's mean of order t , Gini's two-parameter mean and Stolarsky's two-parameter mean each provide an alternative parameterization and classification. Linear approximations relating the parameters are derived. The parameter scales again have fixed numerical values corresponding to many known special means. The parameters again concisely explain the inequalities of the known special means and why the same order is found among the corresponding regression lines. Again under certain conditions, every regression line

lying between the two ordinary least-squares lines is generated by these generalized means for some value of the parameters.

REFERENCES

- [1] B. C. Carlson. "The Logarithmic Mean." *American Mathematical Monthly*, vol. 79, pp. 615-618, 1972.
- [2] H. Chen. "Means Generated by an Integral." *Mathematics Magazine*, vol. 82, p. 370, Dec. 2005.
- [3] B. C. Dietel and R. A. Gordon. "Using Tangent Lines to Define Means." *Mathematics Magazine*, vol. 76, pp.52-62, Feb. 2003.
- [4] S. C. Ehrenberg. "Deriving the Least-Squares Regression Equation." *The American Statistician*, vol. 37, p.232, Aug. 1983.
- [5] H. Eves. "Means Appearing in Geometric Figures." *Mathematics Magazine*, vol. 76, No. 4, pp.292-294, Oct. 2003.
- [6] C. Gini. "Di una formula comprensiva della medie." *Metron*, vol. 13, pp. 3-22, 1938.
- [7] N. Greene. "Generalized Least-Squares Regressions I: Efficient Derivations," in *Proceedings of the 1st International Conference on Computational Science and Engineering (CSE'13)*, 2013, pp. 145-158.
- [8] N. Greene. "Generalized Least-Squares Regressions II: Theory and Classification," in *Proceedings of the 1st International Conference on Computational Science and Engineering (CSE '13)*, 2013, pp. 159-166.
- [9] N. Greene. "Generalized Least-Squares Regressions III: Further Theory and Classification," in *Proceedings of the 5th International Conference on Applied Mathematics and Informatics (AMATHI '14)*, 2014, pp. 34-38.
- [10] E. B. Leach and M. C. Sholander. "Extended Mean Values." *American Mathematical Monthly*, vol. 85, pp. 84-90, 1978.
- [11] D. H. Lehmer. "On the compounding of certain means." *J. Math. Anal. Appl.*, vol. 36, pp. 183-200, 1971.
- [12] T.-P. Lin. "The power mean and the logarithmic mean." *American Mathematical Monthly*, vol. 81, pp. 879-883, 1974.
- [13] M. E. Mays. "Functions Which Parametrize Means." *American Mathematical Monthly*, vol 90, pp. 677-683, 1983.
- [14] K. B. Stolarsky. "Generalizations of the logarithmic mean." *Mathematics Magazine*, vol. 48, pp. 87-92, 1975.
- [15] K. B. Stolarsky. "The power mean and generalized logarithmic means." *American Mathematical Monthly*, vol. 82, pp. 545-548, 1980.

Convex Relaxation Methods for Nonconvex Polynomial Optimization Problems

André A. Keller

Université des Sciences et Technologies de Lille
 Laboratoire d’Informatique Fondamentale de Lille
 (LIFL) section SMAC, Cité Scientifique
 59650 Villeneuve-d’Ascq, France

Abstract— This paper introduces to constructing problems of convex relaxations for nonconvex polynomial optimization problems. Branch-and-bound algorithms are convex relaxation based. The convex envelopes are of primary importance since they represent the uniformly best convex underestimators for nonconvex polynomials over some region. The reformulation-linearization technique (RLT) generates LP (linear programming) relaxations of a quadratic problem. The LP-RLT yields a lower bound on the global minimum. RLT operates in two steps: a reformulation step and a linearization (or convexification) step. In the reformulation phase, the constraints (constraints and bounds inequalities) are replaced by new numerous pairwise products of the constraints. In the linearization phase, each distinct quadratic term is replaced by a single new RLT variable. This RLT process produces an LP relaxation. LMI formulations (linear matrix inequalities) have been proposed to treat efficiently with nonconvex sets. An LMI is equivalent to a system of polynomial inequalities. A semialgebraic convex set describes the system. The feasible sets are spectrahedra with curved faces, contrary to the LP case with polyhedra. Successive LMI relaxations of increasing size can be used to achieve the global optimum. Nonlinear inequalities are converted to an LMI form using Schur complements. Optimizing a nonconvex polynomial is equivalent to the LP over a convex set. Engineering application interests include system analysis, control theory, combinatorial optimization, statistics, and structural design optimization.

Keywords—convex relaxation; polynomial optimization; nonconvex optimization; LMI formulation; structural optimization

I. INTRODUCTION

This paper introduces to the problem of constructing convex relaxations for nonconvex polynomial optimization problems. Techniques such as outer-approximation, branch-and-bound (B&B) algorithms, reformulation-convexification methods are convex relaxation based [1].

Convex extensions and envelopes are of primary importance to the efficiency of global optimization methods. These notions reflect the capability to construct tight convex

relaxations¹. Locatelli [3] determines convex envelopes for quadratic and polynomial functions over polytopes. Convex underestimators of nonconvex functions over some region are essential to B&B techniques. However, computing convex envelopes is NP-hard, even for simple polynomials². The nuclear norm (i.e., the sum of singular values) heuristic is also used instead of the convex envelope of the objective function. The affine matrix rank minimizing problem (RMP) uses the nuclear norm of the rank function. In this case, the nonconvex objective rank function is replaced by its convex envelope (i.e., the nuclear norm) [4]. In statistics, this important practical problem may consist of finding the least complex stochastic model, which is consistent with observations and priors.

The reformulation-linearization technique (RLT) generates LP (linear programming) relaxations of a quadratic problem [5]. The LP-RLT yields a lower bound on the global minimum. RLT operates in two steps: a reformulation step and a linearization (or convexification) step. In the reformulation phase, the constraints (constraint and bound inequalities) are replaced by new pairwise products of the constraints (i.e., bound factor product, bound-constraint factor product, and constraint factor product inequalities). In the linearization phase, each distinct quadratic term is replaced by a single new RLT variable. This RLT process produces an LP relaxation.

LMI (linear matrix inequalities) formulations have been proposed to treat efficiently with nonconvex sets. An LMI is equivalent to a system of polynomial inequalities. A semialgebraic convex set describes the system. The feasible sets are spectrahedra with curved faces, contrary to the LP case with polyhedra. SOS (sum of squares) relaxations can be used to obtain good approximate SDP (semidefinite programming) descriptions of convex envelopes (e.g., computing the convex envelope of quadratic forms over polytopes via a semidefinite program). Successive LMI relaxations of increasing size can be used to achieve the global optimum³. Nonlinear inequalities are

¹ The theory of convex extensions is developed for lower semi-continuous functions in [2].

² A proposition may consist in computing the convex envelopes over simpler domains such as triangles. Some examples are proposed in [3].

³ The approach consists in approximating a programming problem (PP) by a sequence of easier relaxed problems, such that the sequence of solutions

converted to an LMI form using Schur complements. Optimizing a nonconvex polynomial is equivalent to the LP over a convex set.

Engineering application interests include system analysis, control theory, combinatorial optimization, statistics and structural design. As a practical illustration, one can mention the truss topology design problem. This problem can be set to an equivalent LMI, by using the Schur lemma for linearization.

This article is organized as follows. Section II introduces to some important convex transforms in practice, such as the eigen-transformation, the convex envelopes, the nuclear norm and the conjugacy transform. The basic reformulation-linearization technique is presented in Section III for nonconvex QP (quadratic programming) problems. An illustrative numerical example is solved in Appendix A. The effectiveness of semidefinite programming (SDP) in polynomial optimization is shown in Section IV. The following essentials aspects are introduced: the LMI feasibility sets, the LMI formulation of SOS (sum of squares) polynomials, and simplified engineering application to this approach. Appendix B is devoted to the SDP interpretation of quadratic optimization problems.

II. CONVEX TRANSFORMS

Convexification transformation methods can convert a nonconvex problem to an equivalent problem, such as a concave minimization problem, a reverse convex minimization problem or a difference convex (d.c.) programming problem. The followings are restricted to concepts such as the eigen-transformation, convex envelopes, nuclear norm and conjugacy transformations.

A. Eigen-Transformation [10]

Let the quadratic programming (QP) problem

$$\text{QP : minimize}_{\mathbf{x} \in \mathbb{R}^n} \mathbf{c}^T \mathbf{x} + \mathbf{x}^T \mathbf{Q} \mathbf{x}$$

subject to :

$$\mathbf{A} \mathbf{x} \leq \mathbf{b},$$

$$x_k \in [l_k, u_k], k = 1, \dots, n.$$

The eigen-transformation for the QP problem is a particular linear transformation based on the eigenstructure of the quadratic objective. Let $\mathbf{Q} = \mathbf{P} \mathbf{D} \mathbf{P}^T$ where \mathbf{D} is diagonal with eigenvalue elements of \mathbf{Q} , and \mathbf{P} column eigenvectors.

Define $\mathbf{x} = \mathbf{P} \mathbf{z}$, so that $\mathbf{z} = \mathbf{P}^T \mathbf{x}$. The resulting eigen-transformed QP is

converge to a global solution of the global optimization problem. This outer approximation method (known as the cutting plane method) was initially introduced by Kelley Jr (1960) in convex programming [6]. Kelley's cutting plane algorithm starts with a relaxed LP (linear programming) solution. Thereafter, it find the solution by successively adding constraints (i.e., constructed cuts) to the problem [7], pp. 463-465 and [8], pp. 316-323. The outer-approximate with increasingly tighter convex programs was extended by Tuy (1983) [9] to general nonconvex optimization problems.

$$\underset{\mathbf{z} \in \mathbb{R}^n}{\text{minimize}} \mathbf{c}^T \mathbf{P} \mathbf{z} + \mathbf{z}^T \mathbf{D} \mathbf{z}$$

subject to :

$$\mathbf{A} \mathbf{P} \mathbf{z} \leq \mathbf{b},$$

$$\mathbf{l} \leq \mathbf{P} \mathbf{z} \leq \mathbf{u}.$$

B. Convex Envelope

Definition 1. The convex envelope for a nonconvex function f and region X is the largest convex underestimator of f over X , so that

$$\text{conv}_{f,X} = \sup \{c(\mathbf{x}) : c(\mathbf{x}') \leq f(\mathbf{x}'), \forall \mathbf{x}' \in X\},$$

where $c(\cdot)$ is a convex function. \square

The convex envelope can be a convex polyhedral representation, i.e., the maximum of a finite number of affine underestimators. In [11], Locatelli and Schoen derive convex envelopes of bivariate functions $f(x, y)$ over general two-dimensional polytopes, assuming that some conditions on f are satisfied. Carathéodory's theorem yields the convex envelope of f at a point $K \in P$. Given a polytope $P \subset \mathbb{R}^n$ and a function f , we have the PP

$$\text{conv}_{f,P}(K) = \min \left\{ \sum_{i=1}^{n+1} \lambda_i f(Q_i) : Q_i \in P, i = 1, \dots, n+1 \right\},$$

subject to :

$$\sum_{i=1}^{n+1} \lambda_i = 1, \quad \sum_{i=1}^{n+1} \lambda_i Q_i = K, \quad \lambda_i \geq 0.$$

Theorem 1 [1], pp. 45-46. Let $f(\mathbf{x})$ be a lower semicontinuous function defined on the convex compact set $X \in \mathbb{R}^n$ and $\phi(\mathbf{x})$ be the convex envelope of f on X , then we have

$$(i) \underset{\mathbf{x} \in X}{\text{minimize}} f(\mathbf{x}) = \underset{\mathbf{x} \in X}{\text{minimize}} \phi(\mathbf{x}) = \hat{f}$$

$$(ii) \{ \mathbf{y} \in X : f(\mathbf{y}) = \hat{f} \} \subseteq \{ \mathbf{y} \in X : \phi(\mathbf{y}) = \hat{f} \}. \square$$

Hence, the theorem states that for each nonconvex PP on a convex feasible region, one can associate a convex PP for which we have the same optimal solution.

Example 1. Let the nonconvex polynomial of degree 4 in Fig.1

$$f(x) = 1.5 + 2.882x - 1.277x^2 + 0.096x^3 + 0.005x^4$$

where $x \in [0, 7]$. The convex envelope is

$$\text{conv } f(x) = \begin{cases} 1.5 - 0.489, & \text{if } x \in [0, 4.83] \\ f(x), & \text{if } x \in [4.83, 7]. \end{cases}$$

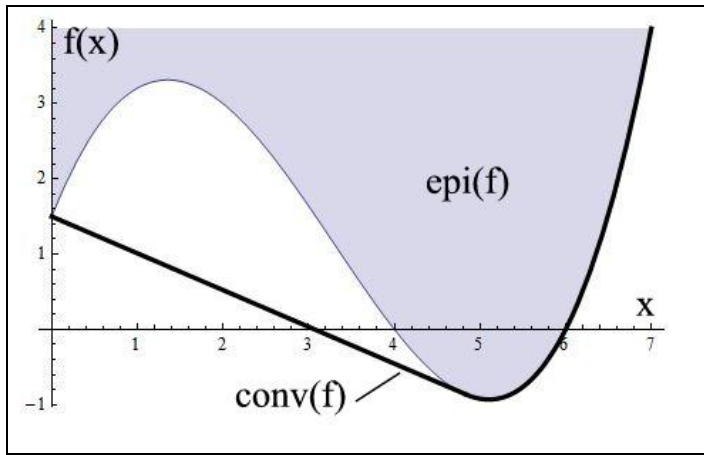


Fig 1. Convex envelope of a nonconvex polynomial over a closed convex interval.

C. Nuclear Norm

Complexity and dimensionality of the system can be expressed by means of the rank of a matrix. In [4] a low-rank matrix should correspond to different situations in statistics, system identification or control, e.g., a low-degree for a random process model, a low-order realization of a linear system. An affine rank minimization problem (RMP) consists of finding a matrix of minimum rank that satisfies a system of linear equality constraints[4].

Definition 2. The nuclear form of the $m \times n$ matrix \mathbf{X} (or Schatten 1-norm, or Ky Fan r -norm) is the sum of its singular values, i.e.,

$$\|\mathbf{X}\|_* = \sum_{i=1}^{\min\{m,n\}} \sigma_i(\mathbf{X}), \sigma_i(\mathbf{X}) = \sqrt{\lambda_i(\mathbf{X}^T \mathbf{X})}. \square$$

Let the RMP [4][12] be

$$\text{minimize } \text{rank}(\mathbf{X})$$

subject to :

$$\mathcal{A}(\mathbf{X}) = \mathbf{b},$$

where $\mathcal{A} : \mathbb{R}^{m \times n} \mapsto \mathbb{R}^p$ is a linear mapping. In statistics, RMP can refer to the problem of finding the least complex stochastic model according to the available observations and prior assumptions⁴ [12].

Theorem 2. The convex envelope of the rank function $\phi(\mathbf{X}) = \text{rank}(\mathbf{X})$ over the set of matrices with bounded norm $\mathcal{S} = \{\mathbf{X} \in \mathbb{R}^{m \times n} : \|\mathbf{X}\| \leq 1\}$ is $\phi_{\text{env}}(\mathbf{X}) = \|\mathbf{X}\|_*$. \square

⁴ Let the variance-covariance matrix $\mathbf{X} = E[(\tilde{\mathbf{z}} - E[\tilde{\mathbf{z}}])(\tilde{\mathbf{z}} - E[\tilde{\mathbf{z}}])^T]$ of the random $\tilde{\mathbf{z}}$. In this application, the rank of \mathbf{X} denotes the complexity of the stochastic model, i.e., the number of independent random variables needed to explain the variance-covariance matrix. The trade-off that we have in practice between the model complexity (i.e., $\text{rank}(\mathbf{X})$) and its accuracy $f(\mathbf{X})$ is illustrated in [12].

Proof⁵: See [12], pp. 54-60 \square

Since the nuclear norm is the convex envelope of rank, the problem is

$$\begin{aligned} & \text{minimize } \|\mathbf{X}\|_* \\ & \text{subject to :} \\ & \mathcal{A}(\mathbf{X}) = \mathbf{b}. \end{aligned}$$

D. Conjugacy Transformation [13]

Conjugacy transformation (or Legendre-Fenchel transform) associates with any function f a convex function f^* called convex conjugate. This important notion intervenes in the Lagrangian duality. It relates the dual with the primal function.⁶

Definition 3. Let the closed convex differentiable function $f : \mathbb{R}^n \mapsto (-\infty, \infty)$.

The Fenchel conjugate $f^* : \mathbb{R}^n \mapsto (-\infty, \infty)$ is⁷

$$f^*(\mathbf{y}) \triangleq \sup_{\mathbf{x} \in \mathbb{R}^n} \{\langle \mathbf{x}, \mathbf{y} \rangle - f(\mathbf{x})\}. \square$$

It is a generalization of the Legendre transform⁸. It expresses the maximum gap between the linear $\mathbf{x}^T \mathbf{y}$ and $f(\mathbf{x})$ [13] pp. 82-89.

The properties of the conjugate function are

- f^* is always convex, since it is the pointwise supremum of a family of convex functions of \mathbf{y} .
- If f and f^* are convex, and their epigraph is closed convex, then $f^{**} = f^*(f^*) = f$. Therefore, the conjugacy transform is a symmetric transformation.
- If f and f^* are convex, then they satisfy the Fenchel-Young inequality
$$f(\mathbf{x}) + f^*(\mathbf{y}) \geq \langle \mathbf{x}, \mathbf{y} \rangle \text{ for all } \mathbf{x}, \mathbf{y}.$$

Example 2. [16], pp. 72-74. Let the univariate exponential function $f(x) = e^x$ where $x \in \mathbb{R}$. If $y < 0$, the expression $yx - e^x$ is unbounded, so that $f^*(y) = +\infty$. For $y = 0$, we

⁵ The proof of the convex envelope theorem is using the conjugate functions.

⁶ On the conjugacy correspondence, see Bertsekas et al. [14], pp. 432-434.

⁷ The domain of the conjugate function consists of $\mathbf{y} \in \mathbb{R}^n$ for which the supremum is finite, i.e. the difference is bounded above on $\text{dom}(f)$.

⁸ The Legendre transform for invertible gradient of f is
$$f^*(\mathbf{s}) = \langle \mathbf{s}, \nabla^{-1} f(\mathbf{s}) \rangle - f(\nabla^{-1} f(\mathbf{s})).$$
 See [15].

have $\sup_x -e^x = 0$. If $y > 0$, the expression $yx - e^x$ reaches its maximum at $\hat{x} = \log_e y$. We deduce the convex conjugate $f^*(y) = y \log_e y - y$.⁹

Example 3. Let the negative entropy¹⁰ function $f(x) = x \log x$ on $\text{dom}(f) = \mathbb{R}_{++}$. The expression $yx - x \log x$ is bounded above on \mathbb{R}_+ for all y . Hence $\text{dom}(f^*) = \mathbb{R}$. We deduce $f^*(y) = e^{y-1}$. The epigraphs of the original function and that of its convex conjugate are pictured in Fig 2.

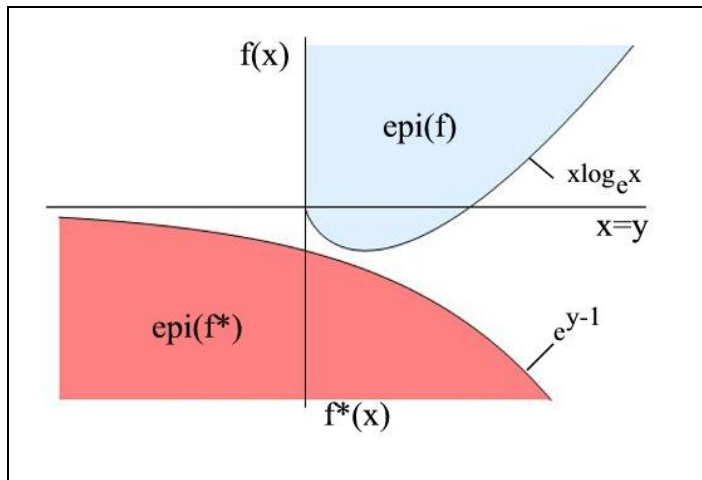


Fig 2 Convex conjugate of a negentropy function.

III. LP RELAXATIONS FOR NONCONVEX QUADRATIC POLYNOMIAL PROGRAMS

The Reformulation-Linearization Technique (RLT) by Sherali and Adams treats both discrete and continuous programming problems [5]. It is valuable for producing polyhedral outer approximations or LP relaxations for nonconvex polynomial programs having integral exponents for all nonlinear terms. RLT-LP relaxations of QP problems yield a lower bound on the global minimum [16][18]. New constraints and convex variables bounding types are introduced in [20][20] to obtain tighter lower bounds. The RLT procedure also benefits of various improvements of the implementation such as a range-reduction process, a constraint filtering technique, a new branching variable selection. Thus, filtering techniques have been proposed in [20] to accelerate the RLT

⁹ More generally, let $f(\mathbf{x}) = \sum_{i=1}^n c_i \exp(x_i)$, $c_i > 0$. From the definition we deduce that $f^*(\mathbf{y}) = \sum_{i=1}^n \sup_{x_i \in \mathbb{R}} \{x_i y_i - c_i \exp(x_i)\}$. Then

we obtain $f^*(\mathbf{y}) = \sum_{i=1}^n y_i \log_e(y_i / c_i) - \sum_{i=1}^n y_i$ for $\forall \mathbf{y} > \mathbf{0}$, i.e., the difference between the cross-entropy function and a linear function.

¹⁰ The entropy is an index about disorder in a system (e.g., wasted energy). The negative entropy or negentropy refers to the quantity that is exported by the system to keep its own entropy at a lower level.

search¹¹. The relaxations are embedded in a convergent branch-and-bound algorithm.

A. Nonconvex Quadratic Programming Problem [10]

Let a nonconvex quadratic programming problem (NQP) subject to linear equality constraints and box-constrained decision variables, such as

$$\text{NQP}(\Omega) : \underset{\mathbf{x} \in \Omega \subset \mathbb{R}^n}{\text{minimize}} \quad \mathbf{c}^T \mathbf{x} + \frac{1}{2} \mathbf{x}^T \mathbf{H} \mathbf{x}$$

subject to :

$$\mathbf{A} \mathbf{x} \leq \mathbf{b},$$

$$\mathbf{x} \in \Omega \equiv \left\{ \mathbf{x} : x_j \in [x_j^L, x_j^U], j = 1, \dots, n \right\},$$

where $\mathbf{x} \in \mathbb{R}^n$, $\mathbf{c} \in \mathbb{R}^n$ and $\mathbf{b} \in \mathbb{R}^m$. \mathbf{H} is an $n \times n$ indefinite symmetric matrix, \mathbf{A} is the $m \times n$ matrix of coefficients, and where the hyper-rectangle Ω defines finite lower and upper bounds on the variables, with $x_j^L < x_j^U$, $\forall j = 1, \dots, n$. All the linear $m + 2n$ inequality constraints, can be expressed by

$$\mathbf{G}_i \mathbf{x} \equiv \sum_{k=1}^n G_{ik} x_k \leq g_i, \quad i = 1, \dots, m + 2n.$$

Rewriting the NQP problem we have

$$\text{LP}(\Omega) : \underset{\mathbf{x} \in \Omega \subset \mathbb{R}^n}{\text{minimize}} \quad \sum_{k=1}^n c_k x_k + \frac{1}{2} \sum_{k=1}^n \sum_{l=1}^n h_{kl} x_k x_l$$

subject to :

$$g_i - \mathbf{G}_i \mathbf{x} \geq 0, \quad i = 1, \dots, m + 2n.$$

B. Reformulation-Linearization Technique

The reformulation-linearization technique (RLT) consists in the two following phases, the reformulation and the convexification phases

- In the reformulation phase, the constraints the constraints in (1) are replaced with a pairwise product such as $(g_i - \mathbf{G}_i \mathbf{x})(g_j - \mathbf{G}_j \mathbf{x}) \geq 0$, $1 \leq i \leq j \leq m + 2n$.
- In the linearization/ convexification phase, each distinct quadratic term $x_k x_l$ for $1 \leq k \leq l \leq n$ is replaced by a new RLT variable w_{kl} .

The RLT process yields the following LP relaxation of the NQP problem¹²

¹¹ Reduced size RLT (rRLT) [21] applies to nonconvex QP problems. rRLTs are obtained by replacing quadratic terms with linear constraints. An extension of the rRLT is proposed in [22] to general polynomial programs.

¹² The linearization of $[.]$ is denoted by $[.]_L$.

$$\underset{\mathbf{x}, \mathbf{w}}{\text{minimize}} \quad \sum_{k=1}^n c_k x_k + \frac{1}{2} \sum_{k=1}^n h_{kk} w_{kk} + \sum_{k=1}^{n-1} \sum_{l=k+1}^n h_{kl} w_{kl}$$

subject to :

$$[(g_i - \mathbf{G}_i \mathbf{x})(g_j - \mathbf{G}_j \mathbf{x})]_L \geq 0, \quad 1 \leq i \leq j \leq m + 2n.$$

C. Branch-and-Bound Algorithm

In the branch-and-bound procedure, a list of active nodes $q \in Q_s$ is maintained at each stage s of the algorithm. Each node q corresponds to some partitioned hyperrectangle $\Omega^q \subseteq \Omega$. The RLT algorithm to solve NQP consists in the following different steps [5], pp. 263-281 and [22], pp. 675-683.

- **Step 0 : Initialization.** Set $s = 1, Q_s = \{1\}, q(s) = 1$ and $\Omega^1 \equiv \Omega$. Solve $\mathbf{LP}(\Omega^1)$ and get a solution $(\bar{\mathbf{x}}, \bar{\mathbf{w}})$ for which the objective value is $LB_1 = \mathbf{LP}(\Omega^1)$. If $\bar{\mathbf{x}}$ is feasible to $\mathbf{NQP}(\Omega)$, update $\hat{\mathbf{x}} = \mathbf{x}^1$ and $\hat{v} = \mathbf{c}^T \hat{\mathbf{x}} + (1/2) \hat{\mathbf{x}}^T \mathbf{H} \hat{\mathbf{x}}$. If $LB_1 = \hat{v}$, then STOP. Otherwise, determine a branching variable x_p . The index p is such that $p \in \arg \max \{\theta_k, k = 1, \dots, n\}$

where

$$\begin{aligned} \theta_k &\equiv \max \left\{ 0, h_{kk} (\bar{x}_k^2 - \bar{w}_{kk}) \right\} \\ &+ \sum_{l=1}^n \max \left\{ 0, h_{kl} (\bar{x}_k \bar{x}_l - \bar{w}_{kl}) \right\}, \quad \theta_k > 0 \end{aligned}$$

for $k = 1, \dots, n$. Then, GO TO STEP 1.

- **Step 1 : Partitioning.** Partition the selected active node $\Omega^{q(s)}$ into two sub-hyperrectangles. Denote the lower and upper bounds by $l^{q(s)}$ and $u^{q(s)}$ respectively. Then, the bounding interval $[l_p^{q(s)}, u_p^{q(s)}]$ is divided for x_p at a value \bar{x}_p , say $[l_p^{q(s)}, \bar{x}_p]$ and $[\bar{x}_p, u_p^{q(s)}]$. Replace $q(s)$ by these two new nodes and revise Q_s .
- **Step 2: Bounding.** Solve the LP relaxation for each of the two nodes. Update the incumbent solution if possible. Determine a corresponding branching variable index, as in the initialization STEP 0.
- **Step 3: Fathoming.** Fathom non improving nodes by setting $Q_{s+1} = Q_s - \{q \in Q_s : LB_q + \varepsilon \geq \hat{v}\}$ where ε

denote a positive tolerance¹³. If $Q_{s+1} = \emptyset$, then STOP. Otherwise increment s by one and GO TO STEP 4.

- **Step 4: Node selection.** Select an active node $q(s) \in \arg \min \{LB_q : q \in Q_s\}$. RETURN TO STEP 1.

IV. LMI RELAXATIONS

Following the Shor's LMI formulation, [23][24] use LMI relaxations for solving nonconvex optimization problems. A hierarchy of LMI relaxations of increasing dimensions generates a monotone converging sequence of lower bounds to the global optimal solution. This section introduces to the LMI feasibility sets, SDP formulation of SOS polynomials, and illustrates these notions with a simplified engineering application, in structural optimization.

A. LMI Feasibility Sets

A linear matrix inequality (LMI) is of the canonical negative definite form [25]-[27]

$$\mathbf{F}(\mathbf{x}) = \mathbf{F}_0 + x_1 \mathbf{F}_1 + \dots + x_n \mathbf{F}_n \prec 0,$$

where $\mathbf{F}_0, \mathbf{F}_1, \dots, \mathbf{F}_n$ are symmetric $m \times m$ matrices (i.e. $\mathbf{F}_0, \mathbf{F}_i \in \mathbb{S}^m, i = 1, \dots, n$) and $\mathbf{x} \in \mathbb{R}^n$.

LMI is equivalent to semialgebraic sets of polynomial inequalities and equations. Converting an SDP to a semialgebraic set is illustrated as follows [28]

$$\left\{ \mathbf{X} \in \mathbb{S}^n : \mathbf{X} = \begin{pmatrix} 3-x & -(x+y) & 1 \\ -(x+y) & 4-y & 0 \\ 1 & 0 & -x \end{pmatrix} \succ 0 \right\} \quad (2)$$

where $x, y \in \mathbb{R}$ are parameters. Determine the principal minors of \mathbf{X} . Cone \mathbf{X} will satisfy (2) if and only if the parameters satisfy the polynomial inequalities¹⁴

$$\left. \begin{array}{l} 3-x > 0 \quad (a) \\ (3-x)(4-y) - (x+y)^2 > 0 \quad (b) \\ -x((3-x)(4-y) - (x+y)^2) - (4-y) > 0 \quad (c) \end{array} \right\} \quad (3)$$

The feasible set with curved faces (also called spectrahedra) of x and y is shown in Fig. 3.

¹³ An exact desired optimum requires $\varepsilon = 0$.

¹⁴ For a square $n \times n$ matrix \mathbf{X} , then $\mathbf{X} \succ \mathbf{0}$ if and only if $\det(\mathbf{X}_k) > 0$ for all $k = 1, \dots, n$, where \mathbf{X}_k denotes the $k \times k$ principal minor submatrices. In the case of semidefinite $\mathbf{X} \succeq \mathbf{0}$ the conditions include all the minors.

The Shur complement is used to reformulate quadratic convex inequality into the LMI form.

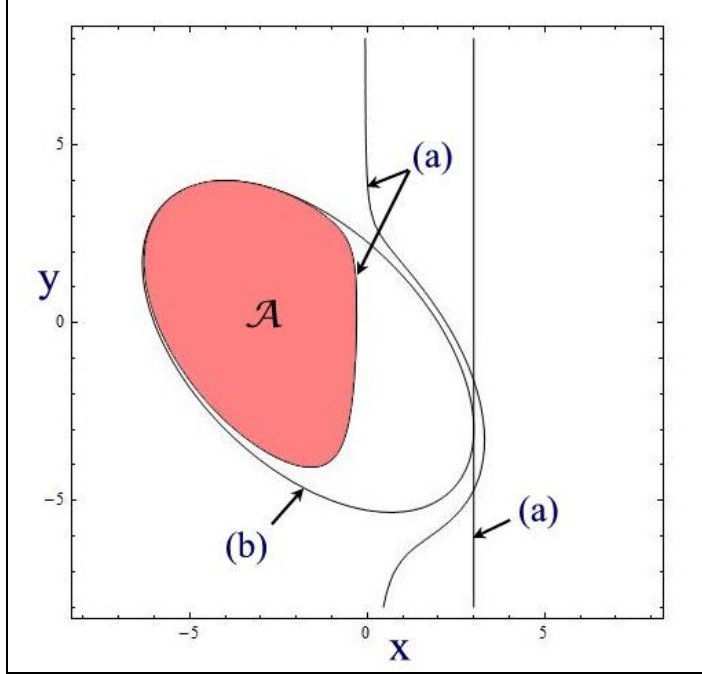


Fig. 3 . Example of a semialgebraic set.

Lemma 1. Shur Complement. Let the Hermitian block matrix

$$\mathbf{A} = \begin{pmatrix} \mathbf{B} & \mathbf{C}^T \\ \mathbf{C} & \mathbf{D} \end{pmatrix}$$

be a symmetric matrix with $k \times k$ block \mathbf{B}

and $l \times l$ block \mathbf{D} . Assume that $\mathbf{B} \succ \mathbf{0}$ (i.e., positive definite). Then, we have $\mathbf{A} \succ \mathbf{0}$, if and only if $\mathbf{D} - \mathbf{C}\mathbf{B}^{-1}\mathbf{C} \succ \mathbf{0}$.

The LMI is equivalent to n polynomial inequalities. In fact, $\mathbf{F}(\mathbf{x}) \succ 0$ if and only if all its principal minors $m_k(\mathbf{x})$ are positive. We have

$$m_k(\mathbf{x}) = \det \begin{pmatrix} F_{11}(\mathbf{x}) & \dots & F_{1k}(\mathbf{x}) \\ \vdots & \ddots & \vdots \\ F_{k1}(\mathbf{x}) & \dots & F_{kk}(\mathbf{x}) \end{pmatrix}, \quad k = 1, \dots, n$$

where $F_{kl}(\mathbf{x})$ denotes the entry on k -th and l -th column of $\mathbf{F}(\mathbf{x})$.

B. SDP Formulation of SOS Polynomials

Semidefinite programming (SDP) in polynomial optimization consists in approximating a hierarchy of convex semidefinite relaxations as in Shor [29]. These relaxations can be constructed by using an SOS representation of nonnegative polynomials and the dual theory of moments. Indeed, testing whether a polynomial is nonnegative can be reduced to the existence of an equivalent sum of squares (SOS) polynomial via semidefinite programming [30].

Definition 4. Let the multivariate polynomial be the following finite linear combination of monomials

$$p(\mathbf{x}) = \sum_{\alpha} c_{\alpha} \mathbf{x}^{\alpha} \equiv \sum_{\alpha} c_{\alpha} x_1^{\alpha_1} \dots x_n^{\alpha_n}, \quad c_{\alpha} \in \mathbb{R},$$

where $\alpha = (\alpha_1, \dots, \alpha_n), \alpha_i \in \mathbb{N}_0$. Recall that the total degree of a monomial \mathbf{x}^{α} is equal to $\alpha_1 + \dots + \alpha_n$ and that the total degree of the polynomial is the maximum degree of its monomials¹⁵.

Theorem 2. The existence of an SOS decomposition of a polynomial in n variables of degree $2d$, such as $p(\mathbf{x}) = \sum_i q_i^2(\mathbf{x})$ can result from a semidefinite programming feasibility problem [30][31].

The cone of SOS polynomials has an LMI formulation. A polynomial of degree $\alpha \leq 2d$ is SOS if and only if

$$p(\mathbf{x}) = \mathbf{z}^T \mathbf{Q} \mathbf{z}, \text{ with } \mathbf{Q} \succeq \mathbf{0},$$

where \mathbf{z} contains all monomials with degree not greater than d . The Cholesky factorization yields $\mathbf{X} = \mathbf{Q}^T \mathbf{Q}$, such that $p(\mathbf{x}) = \mathbf{z}^T \mathbf{L}^T \mathbf{L} \mathbf{z} = \sum_i (\mathbf{L} \mathbf{z})_i^2$. Then, we deduce that $p(\mathbf{x}) = \sum_{i=1}^{\text{rank}(\mathbf{X})} q_i^2(\mathbf{x})$.

Example 5. Let the following quartic form [30]

$$p(\mathbf{x}) = 2x_1^4 + 2x_1^3 x_2 - x_1^2 x_2^2 + 5x_2^4,$$

for which the monomial vector is $\mathbf{z} = (x_1^2, x_2^2, x_1 x_2)^T$. We have

$$\begin{aligned} p(\mathbf{x}) &= \begin{pmatrix} x_1^2 \\ x_2^2 \\ x_1 x_2 \end{pmatrix}^T \begin{pmatrix} q_{11} & q_{12} & q_{13} \\ q_{12} & q_{22} & q_{23} \\ q_{13} & q_{23} & q_{33} \end{pmatrix} \begin{pmatrix} x_1^2 \\ x_2^2 \\ x_1 x_2 \end{pmatrix}, \\ &= q_{11} x_1^4 + q_{22} x_2^4 + (q_{33} + 2q_{12}) x_1^2 x_2^2 \\ &\quad + 2q_{13} x_1^3 x_2 + 2q_{23} x_1 x_2^3. \end{aligned}$$

A positive semidefinite \mathbf{Q} that satisfies the linear equalities

$$q_{11} = 2, \quad q_{22} = 5, \quad q_{33} + 2q_{12} = -1, \quad 2q_{13} = 2 \text{ and } 2q_{23} = 0$$

is found by using SDP. A particular solution is

$$\mathbf{Q} = \begin{pmatrix} 2 & -3 & 1 \\ -3 & 5 & 0 \\ 1 & 0 & 5 \end{pmatrix} = \mathbf{L}^T \mathbf{L}, \quad \mathbf{L} = \frac{1}{\sqrt{2}} \begin{pmatrix} 2 & -3 & 1 \\ 0 & 1 & 3 \end{pmatrix}.$$

Therefore, we get the SOS decomposition

¹⁵ Special cases are homogeneous forms, where the monomials have the same total degree d . The polynomial is homogeneous of degree d , since $p(\lambda \mathbf{x}) = \lambda^d p(\mathbf{x})$.

$$p(\mathbf{x}) = \frac{1}{2} \left(2x_1^2 - 3x_2^2 + x_1 x_2 \right)^2 + \left(x_2^2 + 3x_1 x_2 \right)^2.$$

C. Truss Topology Design

A truss topology design (TTD) problem concerns a mechanical construction made up thin elastic bars linked to each other at nodes. The construction deforms under an external load until the tensions compensate the external forces. The goal is to design a truss of a given weight that best withstand the given weight. In other words, the compliance of the truss (i.e., potential energy resulting from the deformation) with regards to the load will be put as small as possible [25] pp. 21-29 and 227-247.¹⁶

Suppose that TTD problem consists in N bars of length $\mathbf{l} \in \mathbb{R}^N$ and cross-sections $\mathbf{x} \in \mathbb{R}^N$ for which lower and upper bounds are imposed, i.e., $\mathbf{a} \leq \mathbf{x} \leq \mathbf{b}$. Let v be the total volume of the construction, we must have $\mathbf{l}^T \mathbf{x} \leq v$. Let \mathbf{f} the external forces and \mathbf{d} the node displacements. Let the semidefinite stiffness matrix $\mathbf{A} \succeq \mathbf{0}$ be the following linear mapping $\mathbf{A}(\mathbf{x}) = \mathbf{A}_1 x_1 + \dots + \mathbf{A}_N x_N$. At the static equilibrium of the construction loaded by \mathbf{f} , we must have the nonlinear equality $\mathbf{A}(\mathbf{x})\mathbf{d} = \mathbf{f}$. The objective for the TTD problem being to minimize elastic stored energy $\mathbf{f}^T \mathbf{d}$ (i.e., maximize stiffness), the standard TTD optimization problem is

$$\begin{aligned} & \text{minimize}_{\mathbf{x} \in [\mathbf{a}, \mathbf{b}] \subset \mathbb{R}^N} \mathbf{f}^T \mathbf{d} \\ & \text{subject to :} \\ & \mathbf{A}(\mathbf{x})\mathbf{d} = \mathbf{f}, \quad (4) \\ & \mathbf{l}^T \mathbf{x} \leq v, \\ & \mathbf{A}(\mathbf{x}) \succeq \mathbf{0}. \end{aligned}$$

To obtain an equivalent LMI problem, we have to operate the following successive transformations to (4): eliminate the equilibrium constraint with $\mathbf{d} = \mathbf{A}^{-1}(\mathbf{x})\mathbf{f}$, place the objective to constraints with the auxiliary variable γ , and linearize with Schur lemma. We achieve the equivalent LMI formulation

$$\begin{aligned} & \text{minimize}_{\mathbf{x} \in [\mathbf{a}, \mathbf{b}] \subset \mathbb{R}^N} \gamma \\ & \text{subject to :} \\ & \mathbf{l}^T \mathbf{x} \leq v, \\ & \begin{pmatrix} \gamma & \mathbf{f}^T \\ \mathbf{f} & \mathbf{A}(\mathbf{x}) \end{pmatrix} \succ \mathbf{0}. \end{aligned}$$

¹⁶ The interests of SDP for structural design in engineering are presented and developed in [32], pp. 443-467.

V. APPENDIX A - EXAMPLE TO THE RLT PROCESS

A. Problem Formulation

Let the following nonlinear quadratic problem (NQP)¹⁷

$$\mathbf{NQP} : \underset{\mathbf{x} \in \Omega \subset \mathbb{R}^2}{\text{minimize}} \quad 24x_1 - x_1^2 - x_2^2$$

subject to :

$$-3x_1 + 4x_2 \leq 24,$$

$$3x_1 + 8x_2 \leq 120,$$

where $\mathbf{x} = (x_1, x_2)^T$ and $\Omega = [x_1^L, x_1^U] \times [x_2^L, x_2^U]$. Using RLT, NQP is reformulated as the linearized LP:

$$\underset{\mathbf{x} \in \mathbb{R}^2, \mathbf{w} \in \mathbb{R}^3}{\text{minimize}} \quad 24x_1 - w_{11} - w_{22}$$

subject to :

$$G1 \equiv (x_1^L)^2 + w_{11} - 2x_1^L x_1 \geq 0,$$

$$G2 \equiv -x_1^L x_1^U - w_{11} + x_1^L x_1 + x_1^U x_1 \geq 0,$$

$$G3 \equiv x_1^L x_2^L + w_{12} - x_2^L x_1 - x_1^L x_2 \geq 0,$$

$$G4 \equiv -x_1^L x_2^U - w_{12} + x_2^U x_1 + x_1^L x_2 \geq 0,$$

$$G5 \equiv (x_1^U)^2 + w_{11} - 2x_1^U x_1 \geq 0,$$

$$G6 \equiv -x_2^L x_1^U - w_{12} + x_2^L x_1 + x_1^U x_2 \geq 0,$$

$$G7 \equiv x_1^U x_2^U + w_{12} - x_2^U x_1 - x_1^U x_2 \geq 0,$$

$$G8 \equiv (x_2^L)^2 + w_{22} - 2x_2^L x_2 \geq 0,$$

$$G9 \equiv -x_2^L x_2^U - w_{22} + x_2^L x_2 + x_2^U x_2 \geq 0,$$

$$G10 \equiv (x_2^U)^2 + w_{22} - 2x_2^U x_2 \geq 0,$$

$$G11 \equiv -24x_1^L + 3w_{11} - 4w_{12} + 24x_1 - 3x_1^L x_1 + 4x_1^L x_2 \geq 0,$$

$$G12 \equiv -120x_1^L - 3w_{11} - 8w_{12} + 120x_1 + 3x_1^L x_1 + 8x_1^L x_2 \geq 0,$$

$$G13 \equiv 24x_1^U - 3w_{11} + 4w_{12} - 24x_1 + 3x_1^U x_1 - 4x_1^U x_2 \geq 0,$$

$$G14 \equiv 120x_1^U + 3w_{11} + 8w_{12} - 120x_1 - 3x_1^U x_1 - 8x_1^U x_2 \geq 0,$$

$$G15 \equiv -24x_2^L + 3w_{12} - 4w_{22} - 3x_2^L x_1 + 24x_2 + 4x_2^L x_2 \geq 0,$$

$$G16 \equiv -120x_2^L - 3w_{12} - 8w_{22} + 3x_2^L x_1 + 120x_2 + 8x_2^L x_2 \geq 0,$$

$$G17 \equiv 24x_2^U - 3w_{12} + 4w_{22} + 3x_2^U x_1 - 24x_2 - 4x_2^U x_2 \geq 0,$$

$$G18 \equiv 120x_2^U + 3w_{12} + 8w_{22} - 3x_2^U x_1 - 120x_2 - 8x_2^U x_2 \geq 0,$$

$$G19 \equiv 576 + 9w_{11} - 24w_{12} + 16w_{22} + 144x_1 - 192x_2 \geq 0,$$

$$G20 \equiv 2880 - 9w_{11} - 12w_{12} + 32w_{22} + 288x_1 - 672x_2 \geq 0,$$

$$G21 \equiv 14400 + 9w_{11} + 48w_{12} + 64w_{22} - 720x_1 - 1920x_2 \geq 0,$$

¹⁷ Adapted from [22], p.683.

where $\mathbf{w} = (w_{11}, w_{12}, w_{22})^T$. The first ten linear constraints are the linearized bound factor pairwise inequalities. The next eight linear constraints are the linearized bound-constraint factor pairwise inequalities. The last three constraints are linearized constraint factor pairwise inequalities.

B. Branch-and-Bound Resolution

Suppose the following lower and upper bounds $x_1^L = 0, x_1^U = 24, x_2^L = 0, x_2^U = 15$. Solving $LP(\Omega^1)$, we obtain $(\hat{x}_1, \hat{x}_2, \hat{w}_{11}, \hat{w}_{12}, \hat{w}_{22}) = (8, 6, 192, 48, 72)$ for which the objective value is $v(LP(\Omega^1)) = 92$. The solution $\hat{\mathbf{x}} = (8, 6)^T$ is feasible to NQP and produces an objective value of $\hat{v} = -72$. At this stage, we can observe that $\hat{w}_{12} = \hat{x}_1 \hat{x}_2$ is true, whereas $\hat{w}_{11} = 192 \neq \hat{x}_1^2 = 64$ and $\hat{w}_{22} = 72 \neq \hat{x}_2^2 = 36$ both differ. Hence, we need to split the interval for x_1 at $\hat{x}_1 = 8$ or for x_2 at $\hat{x}_2 = 6$.

Using the branching rule to decide, we obtain $\theta_1 = \max \{0, -(64 - 192)\} = 128$ and $\theta_2 = \max \{0, -(36 - 72)\} = 36$. Comparing the results, we select x_1 which achieves the best value. Then, we replace the interval Ω^1 with two sub-hyperrectangles $\Omega^2 = \{\mathbf{x} : x_1 \in [0, 8], x_2 \in [0, 15]\}$ and $\Omega^3 = \{\mathbf{x} : x_1 \in [8, 24], x_2 \in [0, 15]\}$. Thereafter, using the same procedure, we obtain results for the other steps in TABLE 1. We observe that the convergence is achieved at step 2 where $v(LP(\Omega^2)) = v(LP(\Omega^3)) = v^*$.

TABLE 1 SUCCESSIVE RELAXATIONS

| Relaxation # | Decision Variables | | | | | Objective Functions | |
|----------------|--------------------|-------|----------|----------|----------|---------------------|---------|
| | x_1 | x_2 | w_{11} | w_{12} | w_{22} | v | $v(\#)$ |
| $LP(\Omega^1)$ | 8 | 6 | 192 | 48 | 72 | -72 | 92 |
| $LP(\Omega^2)$ | 0 | 6 | 0 | 0 | 36 | -36 | -36 |
| $LP(\Omega^3)$ | 24 | 6 | 576 | 144 | 36 | -36 | -36 |

where $\Omega^1 = [0, 24] \times [0, 15]$, $\Omega^2 = [0, 8] \times [0, 15]$ and $\Omega^3 = [8, 24] \times [0, 15]$.

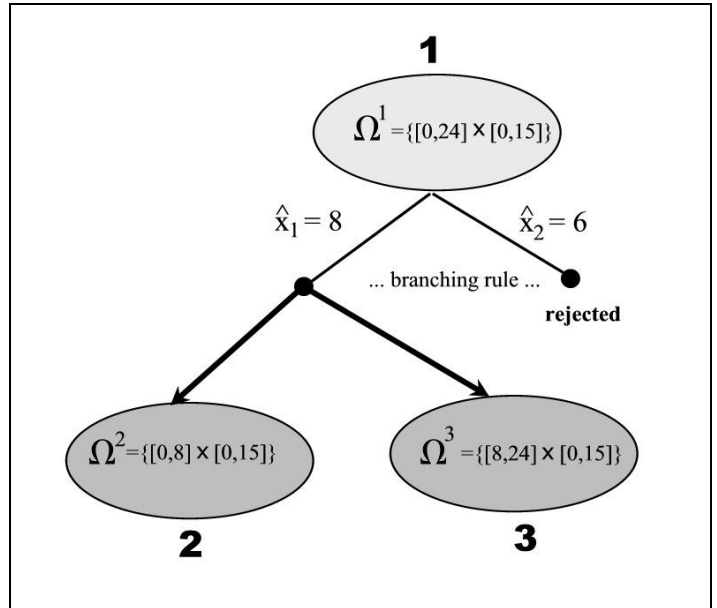


Fig. 1. Branch-and-bound decision tree.

VII. APPENDIX B - SEMIDEFINITE PROGRAMMING FOR QP PROBLEMS

QP problems can be interpreted as SDP problems by using the Schur complements with regular and singular matrices. The QP problems are extended by considering an unconstrained QP, a bilinear QP and a single constraint QP¹⁸. The complexity of nonconvex quadratic problems is studied in [36]. It is shown that even one negative eigenvalue makes the problem NB hard.

C. Unconstrained Quadratic Optimization Problem

Let the unconstrained nonconvex QP be

$$\underset{\mathbf{x} \in \mathbb{R}^n}{\text{minimize}} \quad \frac{1}{2} \mathbf{x}^T \mathbf{P} \mathbf{x} + \mathbf{q}^T \mathbf{x} + r,$$

where $\mathbf{P} \in \mathbb{S}^n$. For $\mathbf{P} \succ \mathbf{0}$, the optimal value is $p^* = -(1/2) \mathbf{q}^T \mathbf{P}^{-1} \mathbf{q} + r$. More generally, we have

$$p^* = \begin{cases} -(1/2) \mathbf{q}^T \mathbf{P}^\dagger \mathbf{q} + r, & \text{for } \mathbf{P} \succeq \mathbf{0}, \mathbf{q} \in \mathcal{R}(\mathbf{P}) \\ -\infty, & \text{otherwise,} \end{cases}$$

where \mathbf{P}^\dagger is the pseudo-inverse of \mathbf{P} , and $\mathcal{R}(\mathbf{P})$ denotes the range of \mathbf{P} .

D. Binary Quadratic Optimization Problem

Let the bilinear QP problem be

¹⁸ This presentation is inspired from Boyd and Vandenberghe [33]. A large number of real-world applications, e.g., in engineering models, design and control can be QPs with a quadratic objective and a linear set of constraints. The properties of QPs and the different techniques for solving QPs are reviewed in [34]. The theory of nonconvex QP problems via SDPs is discussed in Nesterov *et al.* [35]. Lagrangian relaxations are used to derive good approximate solutions.

$$\underset{\mathbf{x} \in \mathbb{R}^n}{\text{minimize}} \quad \frac{1}{2} \mathbf{x}^T \mathbf{A} \mathbf{x} + 2 \mathbf{y}^T \mathbf{B}^T \mathbf{x} + \mathbf{y}^T \mathbf{C} \mathbf{y} \quad (5)$$

Suppose that we have a regular matrix \mathbf{A} . The solution is $\hat{\mathbf{x}} = -\mathbf{A}^{-1} \mathbf{B} \mathbf{y}$.

The initial QP problem (5) is rewritten as

$$\inf_{\mathbf{x}} \begin{pmatrix} \mathbf{x} \\ \mathbf{y} \end{pmatrix}^T \begin{pmatrix} \mathbf{A} & \mathbf{B} \\ \mathbf{B}^T & \mathbf{C} \end{pmatrix} \begin{pmatrix} \mathbf{x} \\ \mathbf{y} \end{pmatrix}.$$

The Schur complement of \mathbf{A} in the partitioned matrix is $\mathbf{S} = \mathbf{C} - \mathbf{B}^T \mathbf{A}^{-1} \mathbf{B}$. Using the optimal expression for \mathbf{x} , we find the optimal value

$$p^* = \mathbf{y}^T (\mathbf{C} - \mathbf{B}^T \mathbf{A}^{-1} \mathbf{B}) \mathbf{y}.$$

Suppose that we have a singular matrix \mathbf{A} . If $\mathbf{A} \geq \mathbf{0}$ and the range condition¹⁹ $\mathbf{B} \mathbf{y} \in \mathcal{R}(\mathbf{A})$, then the QP problem is solvable, and the optimal value for this problem is generalized as follows

$$p^* = \mathbf{y}^T (\mathbf{C} - \mathbf{B}^T \mathbf{A}^\dagger \mathbf{B}) \mathbf{y}.$$

E. Single Constraint Quadratic Optimization Problem

Let the nonconvex QP be constrained with a quadratic inequality

$$\begin{aligned} & \underset{\mathbf{x} \in \mathbb{R}^n}{\text{minimize}} \quad \mathbf{x}^T \mathbf{A}_0 \mathbf{x} + 2 \mathbf{b}_0^T \mathbf{x} + c_0 \\ & \text{subject to :} \quad (6) \\ & \mathbf{x}^T \mathbf{A}_1 \mathbf{x} + 2 \mathbf{b}_1^T \mathbf{x} + c_1 \leq 0. \end{aligned}$$

where $\mathbf{A}_i \in \mathbb{S}^n$, $\mathbf{b}_i \in \mathbb{R}^n$, and $c_i \in \mathbb{R}$ for $i = 0, 1$. Since the quadratic terms $\mathbf{x}^T \mathbf{A}_i \mathbf{x}$ can be expressed as $\text{tr}(\mathbf{A} \mathbf{x} \mathbf{x}^T)$, a new variable \mathbf{X} is defined by $\mathbf{X} = \mathbf{x} \mathbf{x}^T$. Relaxing this constraint by $\mathbf{X} \geq \mathbf{x} \mathbf{x}^T$ and using the Schur complement, the QP problem (6) is now expressed as

$$\begin{aligned} & \underset{\mathbf{x}}{\text{minimize}} \quad \text{tr}(\mathbf{A}_0 \mathbf{X}) + \mathbf{b}_0^T \mathbf{x} + c_0 \\ & \text{subject to :} \\ & \text{tr}(\mathbf{A}_1 \mathbf{X}) + \mathbf{b}_1^T \mathbf{x} + c_1 \leq 0, \\ & \begin{pmatrix} \mathbf{X} & \mathbf{x} \\ \mathbf{x}^T & 1 \end{pmatrix} \geq \mathbf{0}. \end{aligned}$$

The Lagrangian of problem (6) is

$$\mathcal{L}(\mathbf{x}, \lambda) = \mathbf{x}^T (\mathbf{A}_0 + \lambda \mathbf{A}_1) + 2(\mathbf{b}_0 + \lambda \mathbf{b}_1)^T \mathbf{x} + c_0 + \lambda c_1.$$

The dual function is $g(\lambda) = \inf_{\mathbf{x}} \mathcal{L}(\mathbf{x}, \lambda)$, so that

$$g(\lambda) = \begin{cases} c_0 + \lambda c_1 - (\mathbf{b}_0 + \lambda \mathbf{b}_1)^T (\mathbf{A}_0 + \lambda \mathbf{A}_1)^\dagger (\mathbf{b}_0 + \lambda \mathbf{b}_1), \\ \text{for } \mathbf{A}_0 + \lambda \mathbf{A}_1 \geq \mathbf{0}, \mathbf{b}_0 + \lambda \mathbf{b}_1 \in R(\mathbf{A}_0 + \lambda \mathbf{A}_1), \\ -\infty, \text{ otherwise.} \end{cases}$$

The dual problem and its equivalent hypograph form are

$$\begin{cases} \underset{\lambda}{\text{maximize}} \quad g(\lambda) \\ \text{subject to :} \\ \lambda \geq 0. \end{cases} \Leftrightarrow \begin{cases} \underset{t}{\text{maximize}} \quad t \\ \text{subject to :} \\ g(\lambda) \geq t, \\ \lambda \geq 0. \end{cases}$$

Using the Schur complement of $\mathbf{A}_0 + \lambda \mathbf{A}_1$, the dual problem is expressed as the following SDP

$$\underset{\lambda}{\text{maximize}} \quad t$$

$$\text{subject to :}$$

$$\lambda \geq 0,$$

$$\begin{pmatrix} \mathbf{A}_0 + \lambda \mathbf{A}_1 & \mathbf{b}_0 + \lambda \mathbf{b}_1 \\ (\mathbf{b}_0 + \lambda \mathbf{b}_1)^T & c_0 + \lambda c_1 - t \end{pmatrix} \geq \mathbf{0}.$$

REFERENCES

- [1] C.A. Floudas, Deterministic Global Optimization: Theory, Methods and Applications, Dordrecht, NL: Kluwer Academic Publishers, 2000.
- [2] M. Tawarmalani and V. Sahinidis, "Convex extensions and envelopes of lower semi-continuous functions", Math. Program., ser. A, vol. 93, pp. 247-263, 2002.
- [3] M. Locatelli, "Convex envelopes for quadratic and polynomial functions over polytopes", 2010. Available at http://www.optimization-online.org/DB_FILE/2010/11/2788.pdf.
- [4] B. Recht, M. Fazel, and P.A. Parrilo, "Guaranteed minimum-rank solutions of linear matrix equations via nuclear norm minimization", SIAM Rev., vol.52, no. 3, pp. 471-501, 2010.
- [5] H.D. Sherali and W.P. Adams, A Reformulation-Linearization Technique for Solving Discrete and Continuous Nonconvex Problems, Dordrecht, NL: Kluwer Academic Publishers, 1999.
- [6] J.E. Kelley Jr., "The cutting plane method for solving convex programs", J.SIAM, vol. 8, no. 4, pp. 703-712, 1960.
- [7] D.G. Luenberger and Y. Ye, Linear and Nonlinear Programming, 3rd ed., New York: Springer Science+Business Media, 2008, pp. 491-497.
- [8] D.P. Bertsekas, Convex optimization theory: supplementary Chapter 6 on Convex Optimization Algorithms, Belmont, MA: Athena Scientific, 2014. Available at <http://www.athenasc.com/convexdualitychapter.pdf>.
- [9] H. Tuy, "On outer approximation methods for solving concave minimization problems", Acta Math.Vietnam., vol. 8, no. 2, pp. 3-34, 1983.
- [10] H.D. Sherali and C.H. Tuncbilek, "A reformulation-convexification approach for solving nonconvex quadratic programming problems", J. Global Optim., vol. 7, no. 1, pp. 1-31, 1995.
- [11] M. Locatelli and F. Schoen, "On convex envelopes for bivariate functions over polytopes", Math. Program., ser. A, vol. 144, no 1-2, pp. 65-91, 2014. Available at http://www.optimization-online.org/DB_FILE/2009/11/2462.pdf.
- [12] M. Fazel, Matrix Rank Minimization with Applications, Ph.D. Thesis, Stanford University, 2002. Available at <https://faculty.washington.edu/mfazel/thesis-final.pdf>.
- [13] D.P. Bertsekas, Convex Optimization Theory, Belmont, MA: Athena Scientific, 2009.
- [14] D.P. Bertsekas, A. Nedic, and A.E. Ozdaglar, Convex Analysis and Optimization, Belmont, MA: Athena Scientific, 2003.

¹⁹ The range condition is also given by $(\mathbf{I} - \mathbf{A} \mathbf{A}^T) \mathbf{B} \mathbf{y} = \mathbf{0}$.

- [15] Y. Lucet, "What shape is your conjugate?", SIAM Rev., vol. 52, no. 3, pp. 505-542, 2010. Available at http://www.optimization-online.org/DB_FILE/2007/12/1863.pdf.
- [16] H. Tuy, Convex Analysis and Global Optimization, Dordrecht- Boston-London: Kluwer Academic Publishers, 1998.
- [17] H.D. Sherali and C.H. Tuncbilek, "A global optimization algorithm for polynomial programming problems using a reformulation-linearization technique", J. Global Optim., vol. 2, no. 1, pp. 101-112, 1992.
- [18] H.D. Sherali and C.H. Tuncbilek, "Comparison of two reformulation-linearization technique based linear programming relaxations for polynomial programming problems", J. Global Optim., vol. 10, no. 4, pp. 381-390, 1997.
- [19] H.D. Sherali and C.H. Tuncbilek, "New reformulation linearization/convexification relaxations for univariate and multivariate polynomial programming problem", Oper. Res. Lett., vol. 21, no. 1, pp. 1-9, 1997.
- [20] H.D. Sherali, E. Dalkiran, and L. Liberti, "Reduced RLT representations for nonconvex polynomial programming problems", J. Global Optim., vol. 52, no. 3, pp. 447-469, 2012.
- [21] S. Cafieri, P. Hansen, L. Létocart, L. Liberti, and F. Messine, "Reduced RLT constraints for polynomial programming", European Workshop on Mixed Integer Nonlinear Programming (EWMINLP10), Marseille, FR, 2010.
- [22] M.S. Bazaraa, H.D. Sherali, and C.M. Shetty, Nonlinear Programming: Theory and Algorithms, 3rd ed, Hoboken, NJ: John Wiley & Sons, 2006.
- [23] D. Henrion and J.-B. Lasserre, "Detecting global optimality and extracting solutions in GloptiPoly", in Positive polynomials in control, D. Henrion and A. Garulli, Eds. Berlin Heidelberg: Springer Verlag, LNCIS, vol. 312, pp. 293-310, 2005.
- [24] D. Henrion and J.-B. Lasserre, "Convergent relaxations of polynomial matrix inequalities and static output feedback", IEEE Trans. Automat. Control, vol. 51, no. 2, pp. 192-202, 2006.
- [25] A. Ben-Tal and A. Nemirovski, Lectures on Modern Convex Optimization: Analysis, Algorithms, and Engineering Applications, Philadelphia, PA: SIAM, 2001.
- [26] B. Suliowski and W. Paszke, "Linear Matrix Inequalities in Control", Institute of Control and Computation Engineering, University of Zielona Gora, Poland, 2005. Available at http://www.uz.zgora.pl/~wpaszke/materiały/ts/slides_1print.pdf
- [27] S. Boyd, L. El Ghaoui, E. Feron, and V. Balakrishnan, Linear Matrix Inequalities in System and Control Theory, Philadelphia, PA: SIAM, 1994.
- [28] P.A. Parrilo and S. Lall, "Semidefinite programming relaxations and algebraic optimization in control", Eur. J. Control, vol. 9, no 2-3, pp. 307-321, 2003.
- [29] N.Z. Schor, "Quadratic optimization problems", Soviet J. Comput. Syst. Sci., vol. 25, pp. 1-11, 1987.
- [30] P.A. Parrilo, "Semidefinite programming relaxations for semialgebraic problems", Math.Program, Ser.. B 96, pp. 293-320, 2003.
- [31] P.A. Parrilo, Structured Semidefinite Programs and Semialgebraic Geometry Methods in Robustness and Optimization, Ph.D. Thesis, Pasadena, CA: California Institute of Technology, 2000. Available at <http://www.mit.edu/~parrilo>
- [32] A. Ben and A. Nemirovski, "Structural design", in Handbook of Semidefinite Programming: Theory, Algorithms, and Applications, H. Wolkowicz, R. Saigal, and L. Vandenberghe, Eds., Norwell, MA: Kluwer Academic Publishers, 1998, pp. 443-467.
- [33] S. Boyd and L. Vandenberghe, Convex Optimization, Cambridge, UK: Cambridge University Press, 2004.
- [34] C.A. Floudas and V. Visweswaran, "Quadratic optimization", in Handbook of Global Optimization, R. Horst and P.M. Pardalos, Eds., Dordrecht, NL: Kluwer Academic Publishers, pp. 217-269, 1995.
- [35] Y. Nesterov, H. Wolkowicz, and Y. Ye, "Semidefinite programming relaxations of nonconvex quadratic optimization", in Handbook of Semidefinite Programming: Theory, Algorithms, and Applications, H. Wolkowicz, R. Saigal, and L. Vandenberghe, Eds., Norwell, MA: Kluwer Academic Publishers, 1998, pp. 361-419.
- [36] P.M. Pardalos and S.A. Vavasis, "Quadratic programming with one negative eigenvalue is NP-hard", J. Global Optim., vol. 1, pp. 15-22, 1991.

An Inverse Calculation of Unimodular for Polynomial Matrices

Wataru Kase

Department of Electrical and Electronic Systems Engineering
 Osaka Institute of Technology
 5-16-1 Omiya, Asahi-ku, Osaka 535-8585 JAPAN
 Email: kase@ee.oit.ac.jp

Abstract—The polynomial matrix approach is important for control system analysis and synthesis. In the approach, it sometimes needs the inverse calculation of unimodular. In this paper, we will propose an inverse calculation method of unimodular for polynomial matrices. Application to the solution of the generalized Bezout identity and zeros assignment of interactor will be also considered.

I. INTRODUCTION

The control system analysis and synthesis by polynomial matrix approach are important especially in the area of parameter adaptive control systems [1], [2] and descriptor systems [3]. In the course of analysis and synthesis, it sometimes needs the inversion calculation of polynomial matrices. If the polynomial matrix is row (or column) proper [4], it can be easy to represent the inverse using the Structure Theorem [4]. If a given polynomial matrix is unimodular, then it is not easy to represent the inverse.

In this paper, we propose a calculation of inverse for unimodular matrices. The basic idea of the calculation is a derivation method for interactor matrices [5], [6]. So our proposed method can be carried on by calculating Moore-Penrose pseudoinverse for some real matrices. Since there exists a program to calculate pseudoinverse in some standard software package for control systems, the method is simple and numerically stable.

The paper is organized as follows. In the next section, the problem statement will be given. In section 3, a calculation method will be presented using pseudoinverse. As applications, a solution of the generalized Bezout identity [7] and zeros assignment of interactor matrix will be considered in section 4. Concluding remarks will be given in section 5.

II. PROBLEM STATEMENT

A unimodular matrix $U(s)$ for polynomial matrices is defined as any square matrix which can be obtained from the identity matrix I by a finite number of elementary row and column operations on I , where the elementary row (column) operations on the polynomial matrix $D(s)$ with coefficients belongs in the set of real number \mathfrak{R} are defined by

- 1) Interchange of rows (columns) i and j .
- 2) Multiplication of row (column) i by a nonzero scalar in \mathfrak{R} .
- 3) Replacement of row (column) i by itself plus any polynomial multiplied by any other row (column) j .

The determinant of a unimodular matrix is a nonzero scalar in \mathfrak{R} , and conversely, any polynomial whose determinant is a nonzero scalar in \mathfrak{R} is a unimodular matrix. Therefore, the inverse of a unimodular matrix is also a unimodular matrix.

Define an $m \times m$ unimodular matrix $U(s)$ by

$$U(s) = U_0 + sU_1 + \cdots + s^wU_w \quad (1)$$

where w is a natural number and U_i ($i = 0, 1, \dots, w$) are $m \times m$ real matrices. The problem considered in this paper is to propose a calculation method of the inverse of $U(s)$. If $U^{-1}(s)$ is given by

$$U^{-1}(s) = V_0 + sV_1 + \cdots + s^wV_w, \quad (2)$$

for real matrices V_i ($i = 0, 1, \dots, w$), the problem becomes to find real matrices V_i . In the next section, it will be presented a calculation method of V_i .

III. AN INVERSE CALCULATION

From eqns.(1) and (2),

$$U(s)U^{-1}(s) = I \quad (3)$$

$$= [\begin{matrix} I & sI & \cdots & s^{2w}I \end{matrix}] \left[\begin{matrix} U_0 & 0 & \cdots & 0 \\ U_1 & U_0 & \cdots & 0 \\ \vdots & \vdots & \ddots & \vdots \\ U_w & U_{w-1} & \cdots & U_0 \\ 0 & U_w & \cdots & U_1 \\ \vdots & \vdots & \ddots & \vdots \\ 0 & 0 & \cdots & U_w \end{matrix} \right] \left[\begin{matrix} V_0 \\ V_1 \\ \vdots \\ V_w \end{matrix} \right].$$

Since the above equation holds for any s ,

$$\left[\begin{matrix} U_0 & 0 & \cdots & 0 \\ U_1 & U_0 & \cdots & 0 \\ \vdots & \vdots & \ddots & \vdots \\ U_w & U_{w-1} & \cdots & U_0 \\ 0 & U_w & \cdots & U_1 \\ \vdots & \vdots & \ddots & \vdots \\ 0 & 0 & \cdots & U_w \end{matrix} \right] \left[\begin{matrix} V_0 \\ V_1 \\ \vdots \\ V_w \end{matrix} \right] = \left[\begin{matrix} I \\ 0 \\ \vdots \\ 0 \end{matrix} \right] \quad (4)$$

must hold. Especially, $U_0 V_0 = I$ must hold and the solutions of the above equation are given by

$$\begin{aligned} V_0 &= U_0^{-1} \\ V_1 &= -U_0^{-1}U_1V_0 \\ V_2 &= -U_0^{-1}(U_2V_0 + U_1V_1) \\ &\vdots \\ V_w &= -U_0^{-1}(U_wV_0 + U_{w-1}V_1 + \cdots + U_1V_{w-1}) \end{aligned} \quad (5)$$

and the following relation must hold

$$\begin{bmatrix} U_w & U_{w-1} & \cdots & U_1 \\ 0 & U_w & \cdots & U_2 \\ \vdots & \vdots & \ddots & \vdots \\ 0 & 0 & \cdots & U_w \end{bmatrix} \begin{bmatrix} V_1 \\ V_2 \\ \vdots \\ V_w \end{bmatrix} = 0. \quad (6)$$

Conversely, the above condition can be used for the confirmation where a given polynomial matrix is unimodular or not.

Theorem 1 For a given polynomial matrix $U(s)$, which has coefficient matrices like eqn.(1), define real matrices V_0, V_1, \dots, V_w by eqn.(5). If V_i satisfy eqn.(6), then $U(s)$ is a unimodular matrix.

Example 1 Consider the following polynomial matrix $U(s)$:

$$U(s) = \begin{bmatrix} s+1 & s+2 \\ s+3 & s+4 \end{bmatrix}.$$

Define U_0 and U_1 by

$$U_0 = \begin{bmatrix} 1 & 2 \\ 3 & 4 \end{bmatrix}, \quad U_1 = \begin{bmatrix} 1 & 1 \\ 1 & 1 \end{bmatrix}.$$

Then, V_0 and V_1 are given by

$$\begin{aligned} V_0 &= U_0^{-1} = \begin{bmatrix} 2 & -1 \\ -1.5 & 0.5 \end{bmatrix}, \\ V_1 &= -U_0^{-1}U_1V_0 = \begin{bmatrix} -0.5 & 0.5 \\ 0.5 & -0.5 \end{bmatrix} \end{aligned}$$

and $U^{-1}(s)$ is given by

$$\begin{aligned} U^{-1}(s) &= V_0 + sV_1 \\ &= -\frac{1}{2} \begin{bmatrix} s+4 & -s-2 \\ -s-3 & s+1 \end{bmatrix} \end{aligned}$$

IV. APPLICATIONS

A. The Generalized Bezout Identity

Let $(D(s), N(s))$ be right coprime polynomial matrices, with $D(s)$ nonsingular. Then, there exist polynomial matrices $\tilde{D}(s), \tilde{N}(s), X(s), Y(s), \tilde{X}(s)$ and $\tilde{Y}(s)$ such that

$$\begin{bmatrix} X(s) & Y(s) \\ \tilde{N}(s) & -\tilde{D}(s) \end{bmatrix} \begin{bmatrix} D(s) & \tilde{Y}(s) \\ N(s) & -\tilde{X}(s) \end{bmatrix} = \begin{bmatrix} I & 0 \\ 0 & I \end{bmatrix}. \quad (7)$$

Moreover, the block matrices in the above equation will all be unimodular. The above equation is called the generalized Bezout identity. In this section, we will consider a solution method of the above equation.

Assume that $D(s)$ is column proper and $N(s)D^{-1}(s)$ is strictly proper. Then, by the Structure Theorem [4], a controllability canonical realization of $N(s)D^{-1}(s)$, say (A, B, C) can be obtained, i.e.,

$$sx(s) = Ax(s) + Bu(s), \quad (8)$$

$$y(s) = Cx(s) \quad (9)$$

where $u(s), y(s)$ and $x(s)$ are input, output and state vector respectively. Let c_i denote the i -th row of C , and ν_1, \dots, ν_m be observability indices of (C, A) . Define $\nu := \max \nu_i$. Multiplying s eqn.(8) successively, employing eqn.(9) for substitution, we have

$$S_I^\nu(s)y(s) = \mathcal{O}_\nu(C, A)x(s) + \hat{T}_{\nu-1}(C, A, B)S_I^{\nu-1}(s)u(s) \quad (10)$$

where

$$\begin{aligned} S_I^\nu(s) &= \begin{bmatrix} I \\ sI \\ \vdots \\ s^\nu I \end{bmatrix}, \quad \mathcal{O}_\nu(C, A) = \begin{bmatrix} C \\ CA \\ \vdots \\ CA^\nu \end{bmatrix}, \\ \mathbf{T}_\nu(C, A, B) &= \begin{bmatrix} CB & 0 & \cdots & 0 \\ CAB & CB & \cdots & 0 \\ \vdots & \vdots & \ddots & \vdots \\ CA^\nu B & CA^{\nu-1}B & \cdots & CB \end{bmatrix}, \\ \hat{T}_\nu(C, A, B) &= \begin{bmatrix} 0_{m \times m(\nu+1)} \\ \mathbf{T}_\nu(C, A, B) \end{bmatrix}. \end{aligned} \quad (11)$$

Since (A, B, C) is a controllability canonical realization of $N(s)D^{-1}(s)$, there exists a partial state $\eta(s)$ such that

$$\begin{aligned} x(s) &= S^{\mu_i-1}(s)\eta(s), \\ D(s)\eta(s) &= u(s), \quad y(s) = N(s)\eta(s) \end{aligned} \quad (12)$$

where $S^{\mu_i-1}(s) = \text{block diag} \left\{ \begin{array}{c} 1 \\ s \\ \vdots \\ s^{\mu_i-1} \end{array} \right\}$. Substituting the above relations to eqn.(10) gives

$$\begin{aligned} S_I^\nu(s)N(s)\eta(s) \\ = \mathcal{O}_\nu(C, A)\eta(s) + \hat{T}_{\nu-1}(C, A, B)S_I^{\nu-1}(s)D(s)\eta(s). \end{aligned} \quad (13)$$

Define

$$\hat{\mathcal{O}} = \begin{bmatrix} c_1 \\ \vdots \\ c_1 A^{\nu_1-1} \\ c_2 \\ \vdots \\ c_m A^{\nu_m-1} \end{bmatrix}, \quad \tilde{\mathcal{O}} = \begin{bmatrix} c_1 A^{\nu_1} \\ \vdots \\ c_m A^{\nu_m} \end{bmatrix}. \quad (14)$$

Then, from the definition of the observability indices, there exists a matrix A such that

$$\tilde{\mathcal{O}} = A\mathcal{O}. \quad (15)$$

Using A , define

$$\tilde{D} = [-A \quad I] J, \quad (16)$$

where J is a row selection matrix such that

$$J\mathcal{O}_\nu = \begin{bmatrix} \hat{\mathcal{O}} \\ \tilde{\mathcal{O}} \end{bmatrix}. \quad (17)$$

Theorem 2 The polynomial matrices

$$\tilde{D}(s) = \tilde{\mathbf{D}}S_I^\nu(s), \quad \tilde{N}(s) = \tilde{\mathbf{D}}\hat{\mathbf{T}}_{\nu-1}(C, A, B)S_I^{\nu-1}(s) \quad (18)$$

are minimal degree solutions of

$$\tilde{D}(s)N(s) - \tilde{N}(s)D(s) = 0, \quad (19)$$

and $\tilde{D}(s)$ is a column proper polynomial matrix.

Now, choose linearly independent row vectors $c_1, \dots, c_1A^{\nu_1-1}, c_2, \dots, c_mA^{\nu_m-1}$, where

$c_1A^{\nu_1}$ is row span of $c_1, \dots, c_1A^{\nu_1-1}$,

$c_2A^{\nu_2}$ is row span of $c_1, \dots, c_1A^{\nu_1-1}, c_2, \dots, c_2A^{\nu_2-1}$,

\vdots

$c_mA^{\nu_m}$ is row span of $c_1, \dots, c_mA^{\nu_m-1}$.

Now we use the above procedure for polynomial matrices $D(s)$ and $\begin{bmatrix} N(s) \\ I \end{bmatrix}$. Let (A, B, C_1) and (A, B, C_2) denote a controllability canonical realization of $N(s)D^{-1}(s)$ and $D^{-1}(s)$ respectively. Since $D(s)$ and $N(s)$ are right coprime, C_2 is row span of $\tilde{\mathcal{O}}$. Therefore, $\tilde{\mathcal{O}}$ is given by

$$\tilde{\mathcal{O}} = \begin{bmatrix} c_1A^{\nu_1} \\ \vdots \\ c_mA^{\nu_m} \\ C_2 \end{bmatrix} \quad (20)$$

and thus $\tilde{\mathbf{D}}S_I^\nu(s)$ has the following structure:

$$\tilde{\mathbf{D}}S_I^\nu(s) = \begin{bmatrix} \tilde{D}(s) & 0 \\ -Y(s) & I \end{bmatrix}. \quad (21)$$

Then, a left annihilating polynomial matrix for $[D^T(s) \ N^T(s) \ I]^T$ has the following structure:

$$\begin{bmatrix} \tilde{N}(s) & -\tilde{D}(s) & 0 \\ X(s) & Y(s) & -I \end{bmatrix}. \quad (22)$$

Example 2 Consider the following $D(s)$ and $N(s)$:

$$D(s) = \begin{bmatrix} (s+1)(s+3) & 0 \\ 0 & (s+2)(s+4) \end{bmatrix},$$

$$N(s) = \begin{bmatrix} s+1 & s+2 \\ s+3 & s+4 \end{bmatrix}.$$

Then, a controllability canonical realization of $\begin{bmatrix} N(s) \\ I \end{bmatrix}D^{-1}(s)$ is given by

$$A = \begin{bmatrix} 0 & 1 & 0 & 0 \\ -3 & -4 & 0 & 0 \\ 0 & 0 & 0 & 1 \\ 0 & 0 & -8 & -6 \end{bmatrix}, \quad B = \begin{bmatrix} 0 & 0 \\ 1 & 0 \\ 0 & 0 \\ 0 & 1 \end{bmatrix},$$

$$C = \begin{bmatrix} 1 & 1 & 2 & 1 \\ 3 & 1 & 4 & 1 \\ 1 & 0 & 0 & 0 \\ 0 & 0 & 1 & 0 \end{bmatrix},$$

Then, by [9],

$$\begin{bmatrix} -\tilde{D}(s) & 0 \\ Y(s) & -I \end{bmatrix} = \mathbf{D} \begin{bmatrix} I_4 \\ sI_4 \\ s^2I_4 \end{bmatrix} = \begin{bmatrix} -s^2 - 7s - 12 & 0 & 0 & 0 \\ 0 & -s^2 - 3s - 2 & 0 & 0 \\ -0.5s - 2 & 0.5s + 1 & -1 & 0 \\ 0.5s + 1.5 & -0.5s - 0.5 & 0 & -1 \end{bmatrix}$$

where

$$\mathbf{D} = \begin{bmatrix} 12 & 0 & 0 & 0 & 7 & 0 & 0 & 0 & 1 & 0 & 0 & 0 \\ 0 & 2 & 0 & 0 & 0 & 3 & 0 & 0 & 0 & 1 & 0 & 0 \\ -2 & 1 & -1 & 0 & -0.5 & 0.5 & 0 & 0 & 0 & 0 & 0 & 0 \\ 1.5 & -0.5 & 0 & -1 & 0.5 & -0.5 & 0 & 0 & 0 & 0 & 0 & 0 \end{bmatrix}.$$

On the other hand, $\begin{bmatrix} \tilde{N}(s) \\ X(s) \end{bmatrix}$ is given by

$$\begin{bmatrix} \tilde{N}(s) \\ X(s) \end{bmatrix} = \mathbf{D} \begin{bmatrix} \begin{bmatrix} 0 \\ C \\ I \end{bmatrix}B & 0 \\ \begin{bmatrix} C \\ I \end{bmatrix}AB & \begin{bmatrix} C \\ I \end{bmatrix}B \end{bmatrix} \begin{bmatrix} I \\ sI \end{bmatrix} = \begin{bmatrix} s+4 & s+3 \\ s+2 & s+1 \\ 0 & 0 \\ 0 & 0 \end{bmatrix}.$$

Therefore, the unimodular matrix $\begin{bmatrix} X(s) & Y(s) \\ \tilde{N}(s) & -\tilde{D}(s) \end{bmatrix}$ is given by

$$\begin{bmatrix} X(s) & Y(s) \\ \tilde{N}(s) & -\tilde{D}(s) \end{bmatrix} = \begin{bmatrix} 0 & 0 & -0.5s - 2 & 0.5 + 1 \\ 0 & 0 & 0.5s + 1.5 & -0.5s - 0.5 \\ s+4 & s+3 & -s^2 - 7s - 12 & 0 \\ s+2 & s+1 & 0 & -s^2 - 3s - 2 \end{bmatrix} = \begin{bmatrix} 0 & 0 & -2 & 1 \\ 0 & 0 & 1.5 & -0.5 \\ 4 & 3 & -12 & 0 \\ 2 & 1 & 0 & -2 \end{bmatrix} + s \begin{bmatrix} 0 & 0 & -0.5 & 0.5 \\ 0 & 0 & 0.5 & -0.5 \\ 1 & 1 & -7 & 0 \\ 1 & 1 & 0 & -3 \end{bmatrix} + s^2 \begin{bmatrix} 0 & 0 & 0 & 0 \\ 0 & 0 & 0 & 0 \\ 0 & 0 & -1 & 0 \\ 0 & 0 & 0 & -1 \end{bmatrix} =: U_0 + sU_1 + s^2U_2.$$

Define $\begin{bmatrix} X(s) & Y(s) \\ \tilde{N}(s) & -\tilde{D}(s) \end{bmatrix}^{-1} = V_0 + sV_1$ by

$$\begin{bmatrix} X(s) & Y(s) \\ \tilde{N}(s) & -\tilde{D}(s) \end{bmatrix}^{-1} = V_0 + sV_1 + s^2V_2.$$

for some V_0 , V_1 and V_2 , then from the previous section,

$$\begin{aligned} V_0 &= U_0^{-1} = \begin{bmatrix} 3 & 0 & -0.5 & 1.5 \\ 0 & 8 & 1 & -2 \\ 1 & 2 & 0 & 0 \\ 3 & 4 & 0 & 0 \end{bmatrix}, \\ V_1 &= -U_0^{-1}U_1V_0 = -U_0^{-1}U_1U_0^{-1} \\ &= \begin{bmatrix} 4 & 0 & -0.5 & 0.5 \\ 0 & 6 & 0.5 & -0.5 \\ 1 & 1 & 0 & 0 \\ 1 & 1 & 0 & 0 \end{bmatrix}, \\ V_2 &= -U_0^{-1}(U_1V_1 + U_2V_0) \\ &= U_0^{-1}(U_1U_0^{-1}U_1 - U_2)U_0^{-1} \\ &= \begin{bmatrix} 1 & 0 & 0 & 0 \\ 0 & 1 & 0 & 0 \\ 0 & 0 & 0 & 0 \\ 0 & 0 & 0 & 0 \end{bmatrix}. \end{aligned}$$

For the above matrices, $U_2V_1 + U_1V_2 = U_2V_2 = 0$. Thus,

$$\begin{aligned} &\begin{bmatrix} X(s) & Y(s) \\ \tilde{N}(s) & -\tilde{D}(s) \end{bmatrix}^{-1} \\ &= \begin{bmatrix} 3 & 0 & -0.5 & 1.5 \\ 0 & 8 & 1 & -2 \\ 1 & 2 & 0 & 0 \\ 3 & 4 & 0 & 0 \end{bmatrix} + s \begin{bmatrix} 4 & 0 & -0.5 & 0.5 \\ 0 & 6 & 0.5 & -0.5 \\ 1 & 1 & 0 & 0 \\ 1 & 1 & 0 & 0 \end{bmatrix} \\ &\quad + s^2 \begin{bmatrix} 1 & 0 & 0 & 0 \\ 0 & 1 & 0 & 0 \\ 0 & 0 & 0 & 0 \\ 0 & 0 & 0 & 0 \end{bmatrix} \\ &= \begin{bmatrix} s^2 + 4s + 3 & 0 & -0.5s - 0.5 & 0.5s + 1.5 \\ 0 & s^2 + 6s + 8 & 0.5s + 1 & -0.5s - 2 \\ s + 1 & s + 2 & 0 & 0 \\ s + 3 & s + 4 & 0 & 0 \end{bmatrix} \end{aligned}$$

B. Zeros Assignment of Interactor Matrix

For a given $m \times m$ nonsingular transfer function matrix $G(s)$, there exists a nonsingular polynomial matrix $L(s)$ such that

$$\lim_{s \rightarrow \infty} L(s)G(s) = I. \quad (23)$$

$L(s)$ is called an interactor matrix for $G(s)$ [5]. The authors presented a simple derivation method of an interactor, which zeros lie at the origin. In this subsection, we will propose a method to assign the zeros of interactor arbitrary.

Let (A, B, C) denote a realization of a given $G(s)$ Assume that $L(s)$ has the following structure:

$$L(s) = sL_1 + s^2L_2 + \cdots + s^wL_w := s\mathbf{L}S_I^{w-1}(s), \quad (24)$$

where w is the positive integer. Then, the coefficient matrix \mathbf{L} is given by

$$\mathbf{L} = [I \ 0_{m \times m(w-1)}] \mathbf{T}_{w-1}^\dagger(C, A, B) \quad (25)$$

(detail discussion can be found in [6]).

The feedback gain matrix F which makes the closed-loop transfer function matrix $G_{cl}(s) = L^{-1}(s)$ (after possibly poles-zeros cancellation) is given by

$$F = \mathbf{L}\mathcal{O}_{w-1}(C, A)A \quad (26)$$

[10]. Define

$$A_F := A - BF. \quad (27)$$

Then, $G_{cl}(s) = C(sI - A_F)^{-1}B$. Let nu denote the observability index for (C, A_F) . Calculate a minimal left annihilating matrix \tilde{D} for $\mathcal{O}_\nu(C, A_F)$ as in the previous subsection. Then,

$$\tilde{D}(s) := \tilde{\mathbf{D}}S_I^\nu(s) \quad (28)$$

is column proper and

$$\tilde{N}(s) := \tilde{\mathbf{D}}\hat{\mathbf{T}}_{\nu-1}(C, A_F, B)S_I^{\nu-1}(s) \quad (29)$$

is a unimodular matrix, and $L(s)$ can be written by

$$L(s) = \tilde{N}^{-1}(s)\tilde{D}(s). \quad (30)$$

Calculate a right coprime factorization of $\tilde{D}^{-1}(s)\tilde{N}(s)$, say, $N(s)D^{-1}(s)$ where $D(s)$ is column proper. So the above equation can be rewritten by

$$L(s) = D(s)N^{-1}(s). \quad (31)$$

Note that $N(s)$ is a unimodular matrix. Set a desired polynomial matrix $D_*(s)$ which has the same column degree with $D(s)$, i.e.,

$$\lim_{s \rightarrow \infty} D(s)D_*^{-1}(s) = K \text{ (nonsingular)}. \quad (32)$$

Define

$$L_*(s) = D_*(s)N^{-1}(s). \quad (33)$$

Then,

$$\begin{aligned} \lim_{s \rightarrow \infty} L_*(s)G(s) &= \lim_{s \rightarrow \infty} D_*(s) \cdot D^{-1}(s)D(s) \cdot N^{-1}(s)G(s) \\ &= \lim_{s \rightarrow \infty} D_*(s)D^{-1}(s) \cdot L(s)G(s) \\ &= K \text{ (nonsingular)} \end{aligned} \quad (34)$$

i.e., $L_*(s)$ is an interactor matrix with desired zeros. Therefore, the inverse calculation given in section III for $N(s)$ is useful.

V. CONCLUSIONS

In this paper, we consider an inverse calculation of unimodular matrix for polynomial matrices. Since the method is based on the pseudoinverse calculation, it is numerically stable. Application to the solution of the generalized Bezout identity and the zeros assignment of interactor matrix were also considered.

REFERENCES

- [1] H. Elliott and W. A. Wolovich, "Parametrization Issues in Multivariable Adaptive Control", *Automatica*, vol.**20**, pp.533-545, 1984.
- [2] W. Kase and K. Tamura, "Design of G-Interactor and its Application to Direct Multivariable Adaptive Control", *International Journal of Control*, vol.**51**, pp.1067-1088, 1990.
- [3] G.-R. Duan, *Analysis and Design of Descriptor Linear Systems*, Advances in Mechanics and Mathematics 23, Springer-Verlag, 2010.
- [4] W. A. Wolovich, *Linear Multivariable Systems*, Springer-Verlag, 1974.
- [5] W. A. Wolovich and P. L. Falb, "Invariants and Canonical Forms under Dynamic Compensations", *SIAM Journal of Control and Optimization*, vol.**14**, pp.996-1008, 1976.
- [6] W. Kase and Y. Mutoh, "A Simple Derivation of Interactor Matrix and its Applications", *International Journal of Systems Sciences*, vol.**40**, pp.1197-1205, 2009.
- [7] T. Kailath, *Linear Systems*, Prentice-Hall, 1980.
- [8] W. Kase, "Regularization for Polynomial Matrices and its Application to Descriptor Systems" *Proceedings of 38th Annual Conference of IEEE Industrial Electronics*, pp.2427-2432, 2012.
- [9] W. Kase, "A Solution of Polynomial Matrix Equations using Extended Division Algorithm and Another Description of All-Stabilizing Controllers", *International Journal of Systems Science*, vol.**30**, pp.95-104, 1999.
- [10] Y. Mutoh and P. N. Nikiforuk, "Inversed Interactorizing and Triangularization with an Arbitrary Pole Assignment using the State Feedback", *IEEE Transactions on Automatic Control*, vol.**37**, pp.630-633, 1992.

Formal verification of safety control system based on GHENESYS NET

Rodrigo Cesar Ferrarezi, Reinaldo Squillante Júnior, Jeferson A. L. Souza, Diolino J. Dos Santos Filho, José Reinaldo Silva, Paulo Eigi Miyagi, Lucas Antonio Moscato

Abstract—Due to the high complexity of the actual Productive Systems, the current industrial standards, and the possible negative impacts on the human being, on the environment and on equipment in case of faults, the development of control solutions that are both secure and stable – as some systems have to operate nonstop – is much demanded. In this context, the development of safety control systems which simultaneously present high reliability and availability is required. The concepts of SIS, according to experts, may be one solution to these problems. Due the complexity of these systems, project mistakes are expected during their development and thus, validation and verification processes became an imperative – as well as a normative requirement – before the actual deployment of the control software on site. One of the most outstanding system verification techniques is the Model Checking, which performs an exhaustive search on the state space of an event driven system and checks some specific properties written in temporal logic. The GHENeSys environment will be used as computational tool, as it provides a complete solution for modelling and verifying systems based on the GHENeSys network. The proposed methodology will then be applied to the development of a SIS control system to be implemented on a flexible manufacture system, which simulates assembly and handling of parts.

Keywords—GHENeSys nets, Model Checking, Safety Instrumented System, Verification.

I. INTRODUCTION

The growing demand on cost and quality of products and services, the highly competitive market with several players, the increasing hardware storage capacity, processing power and networks speeds, and above all, the concern with the environment, the foundation of all current suitability policies caused an implementation of more complex control systems in the most diverse areas, from the production of consumer products to services [1].

The increasing implementation of processes automation, mandatory for costs reductions and quality improvements, key factors to the survival of a company in a highly competitive market, induced an ever increasing complexity of the control systems required for these systems [2] [3]

The authors would like to thank the Brazilian governmental agencies CNPq, FAPESP, and CAPES for their financial support to this work.

All authors are with Polytechnic School – Department of Mechatronics Engineering and Mechanical Systems - University of São Paulo - São Paulo, Brazil (phone: +55 11 3091-5337 ; e-mail: rferrarezi@usp.br, reinaldo.squillante@usp.br, jeferson.souza@usp.br, diolinos@usp.br, reinaldo@usp.br, pemiyagi@usp.br, lamoscat@usp.br).

Being the control software increasingly complex, and the quality requirements more and more severe, there is a demand for more detailed and concise specification as well as a better control of the development process. It is also required a deeper understanding of the system to be controlled, including details regarding all relevant sub-systems and furthermore, how several system interacts and communicates with each other and with the environment, as the behavior of an interconnected system depends not only of its internal variables, but also of external events originated from the surrounds of the system [4] [5].

Additionally, any industrial system, as modern and innovative as it can be, still may pose serious risks to equipment, to operators and to the environment, in the event of a fault failing to be diagnosed and treated correctly [6]. Although many studies have been presented for diagnosis and treatment of faults, accidents still occur. The main problem is that there is no zero risk in process industries since: (i) physical devices do not have zero risk of fault, (ii) human operators do not have zero risk of error and (iii) there is no computational system that can predict all the reachable states by the system [7].

According to experts, the concepts of safety instrumented systems (SIS), is one solution to these types of issues. They strongly recommend the implementation of layers of risk reduction based on control systems organized hierarchically in order to manage risks by either preventing or mitigating faults, bringing the process to a safe state. In this sense, some safety standards such as IEC 61508 [8], IEC 61511 [9] among others, guide different activities related with a SIS Safety Life Cycle (SLC), such as design, installation, operation, maintenance, tests and others [10][11].

On this context, the processes of understanding, specifying, modelling and validating these systems became a highly complex task, resulting in great hardships on their development. Due all this, project mistakes are associated with the development of these systems and thus, validation and verification processes became an imperative before the actual deployment of the control software on the actual plant [3] [4]. Besides the obvious necessity of verifying and validating critical systems, these activities are required by the safety standard IEC 61511 [9] as part of the safety program development cycle, also known as “V-model”.

Model Checking is a verification technique for finite state concurrent systems, and thanks to this restriction, the

verification processes can be performed semi-automatically, being human interaction only needed for the analysis of the results. The basic procedure performs an exhaustive search of the space state of an event driven system, verifying properties specified from propositions described using some temporal logic. Given enough time and computational power, the procedure will always finish with a positive or negative result, in case of a negative result; a counterexample is given by the system, helping the designer to find the source of error [12].

In this work we propose the first steps towards the development of a framework for the modelling and formal verification of SIS control programs based on the IEC 61511 standard. On the framework, we expect to propose methods, techniques and systematics to comply with all phases of the “V model” according to the IEC 51511 standard. With the complete framework we expect to aid the control engineers to develop SIS control programs in a structured and well defined way as well as fulfilling the requirements of the IEC 51511 standard.

The GHENeSys environment will be used as computational tool modelling and verification processes, the environment is a proposal of the DesignLab from USP and was originally designed as unified approach to cover several types of Petri Nets as well as its extensions, support for timed nets was implemented later on.

This paper is organized as follows: Section 2 presents the main concepts of Model Checking, GHENeSys nets and TCTL. Section 3 presents the SIS Control System Modelling proposal. Section 4, presents the application example. Section 5 presents the conclusion. References are presented thereafter.

II. MAIN CONCEPTS

A. Model checking

The Model Checking technique is composed by the following main tasks [12]:

- Modelling: First the system is converted to a formalism accepted by the chosen verification tool.
- Specification: Before the verification process, it is necessary to list the required system properties. These specifications must also be supplied in some kind of formalism. Usually temporal logic is used to specify the system behavior.
- Verification – Usually the verification process is performed automatically by the tool, except by the results analysis – in case of errors being found. In this case, the tool will supply counterexamples for the verified property, helping the designer finding the source of error on the system.

Concurrent systems can frequently interact with their environments and usually are operating non-stop, therefore, these systems cannot be properly modelled by their input output behavior. The first feature of these systems that must be taken into account is the state. A state can be defined as an instantaneous description of the system, containing the value of every system variable in a single instant. Also it is important to understand how the states change as result of

some action of the system. This change can be described as the state of the system before and after the some action, this pair of states determines a transition of the system [12].

In order to represent the behavior of concurrent systems several types of used graphs might be used, among them we have Kripke structures [12], automata [13], Petri Nets [14] and its extensions, as the GHENeSys nets [15].

There are many different types of concurrent systems (synchronous and asynchronous systems, sequential systems, parallel process, etc.) and due to this diversity, it is necessary to adopt unifying formalism in which these systems can be represented regardless of its type. For such representations will be used first order logic formulas, which are able to represent a great variety of systems [12].

In order to write specifications to describe the properties of a concurrent system it is necessary to define a set of atomic propositions AP. Such propositions have the form $v = d$ where $v \in V$ and $d \in D$, an atomic proposition $v = d$ is said to be true in a state s if $s(v) = d$ [12].

Temporal logic was proved to be very useful for specifying concurrent systems due to its capacity to describe the ordering of events without introducing time explicitly, and thanks to this feature, it was possible to develop completely automated verification algorithms.

B. Timed Computation Tree Logic (TCTL)

TCTL [16] was proposed as an extension of the CTL (Computation Tree Logic) proposed in [12], for the interpretation of temporal formulas over computational trees for systems modelled by temporized graphs. TCTL can be defined semantically related to a structure $\mathcal{M} = (\mathcal{S}, \mu, f)$, where \mathcal{S} is the set of states, $\mu : \mathcal{S} \rightarrow 2^{AP}$ the labelling function which labels each state with the set of atomic prepositions that hold on this state and f the mapping that assigns for each $s \in \mathcal{S}$ a set of s -paths through \mathcal{S} that obey the closure properties [16].

The formula ϕ of TCTL can be inductively defined as [16]:

$$\begin{aligned} \phi ::= & p \mid \text{false} \mid \neg\phi \mid \phi_1 \rightarrow \\ & \phi_2 \mid \phi_1 \wedge \phi_2 \mid \exists[\phi_1 U_{\sim c} \phi_2] \mid \forall[\phi_1 U_{\sim c} \phi_2], \text{ where } p \in AP \text{ and } c \in \mathbb{N}. \end{aligned}$$

TCTL formulas are composed of path quantifiers and temporal operators. There are two path quantifiers:

- \forall (for all computation paths)
- \exists (for some computation path)

Quantifiers are used to specify if from some state, if all paths or just some paths must have some propriety. Temporal operators are used to describe the properties of a path belonging to some computational tree and were defined by adding timing limitations to the classical CTL operators [16]:

- $\Diamond_{\sim c} \phi = \text{true} U_{\sim c} \phi$ (ϕ must hold eventually in some state of the computational path for $\sim c$ time units);
- $\Box_{\sim c} \phi$ (ϕ must hold in all states of the computational path for $\sim c$ time units);
- $\phi_1 U_{\sim c} \phi_2$ (ϕ_2 must hold in some state and ϕ_1 must hold in all previous states of the computational path for $\sim c$ time units).

Where \sim may represent any of the following binary operators $<, \leq, =, >, \geq$. It is important to note that TCTL, as opposed to CTL, does not define the temporal operator that requires that some property must hold on the next state, because as the time is considered dense, by definition, there is not only one next state [16].

Given a TCTL structure $\mathcal{M} = (\mathcal{S}, \mu, f)$ and a state $s \in \mathcal{S}$, a TCTL formula ϕ holds $(\mathcal{M}, s) \models \phi$ if [16]:

- $s \models p$ if $p \in \mu(s)$
- $s \neq \text{false}$;
- $s \models (\phi_1 \rightarrow \phi_2)$ if $s \neq \phi_1$ or $s \models \phi_2$;
- $s \models \exists(\phi_1 U_{\sim c} \phi_2)$ if for some $\rho \in f(s)$, for some $t \sim c$, $\rho(t) \models \phi_2$, and for all $0 \leq t' < t$, $\rho(t') \models \phi_1$.
- $s \models \forall(\phi_1 U_{\sim c} \phi_2)$ if for each $\rho \in f(s)$, for some $t \sim c$, $\rho(t) \models \phi_2$, and for all $0 \leq t' < t$, $\rho(t') \models \phi_1$.

C. GHENeSys environment

A SIS control system can be seen as an event driven system and presents functional characteristics as asynchronism, possibility of reset, parallelism, concurrence, etc., thus this class of system can be classified as a discrete event system (DES), and thus be modelled through Petri Nets [14] [17] and its extensions.

The GHENeSys environment was developed as an extended Petri net with object orientation and abstraction mechanisms defined through hierarchy concepts, which are included as well as synthesis mechanisms that are implemented through a structured approach supported by the encapsulation introduced by the use of objects [15].

The GHENeSys environment is being developed with the goal of representing, in a unified way, classical Petri Nets, its extensions defined on the ISO/IEC 15909 standard, as well as High Level Petri Nets. The GHENeSys environment is composed of the following basic modules. The GHENeSys nets, the Editor tool, the simulation module and the verification tool [18].

The GHENeSys environment implements also several concepts to aid the modeling process, such as: Pseudoboxes that allow the modelling of the exchange of information between different parts of the system; Hierarchy that allows the encapsulation of subnets without losing any properties by using macro elements; The representation of non-deterministic time durations, where a set of time intervals can be defined for each transition.

The GHENeSys net is the tuple $G = (L, A, F, K, \Pi, C_0, \tau)$, where:

- $L = B \cup P$ is the set of places, which can be boxes or pseudoboxes;
- A are the activities, or active elements;
- $F \subseteq (L \times A \rightarrow \mathbb{N}) \cup (A \times L \rightarrow \mathbb{N})$ is the flux relation;
- $K : L \rightarrow \mathbb{N}^+$ is the capacity function;
- $\Pi : (B \cup A) \rightarrow \{0,1\}$ is the function that identify the macro elements or the hierarchy;
- $C_0 = \{(l, \sigma_j) | l \in L, \sigma_j \in \mathbb{R}^+ | l | < K(l)\}$ is the set of initial marks;
- $\tau : (B \cup A) \rightarrow \{\mathbb{Q}^+, \mathbb{Q}^+ \cup \{\infty\}\}$ is the function that maps

the dense time intervals for each element.

The set of markings is the pair (l, σ_j) with $l \in L$, defining which place each token can be found and σ_j defining for how long this token will remain in place. The time measurement is globally synced and updated after each transition.

The GHENeSys verification tool performs the formal verification of real time concurrent systems modelled as GHENeSys net through Model Checking [12] techniques. The space state is constructed using the enumerative approach based on the state class [19] concept. The tool has options to build SCG, SSCG and CSCG state graph types. Checked properties are specified through TCTL [20].

The GHENeSys environment will be used in this work due to several reasons: (i) Due characteristics of the SIS, the amount of checked properties can be very large, so it might be desirable that the space state is generated through the enumerative approach instead of being generated “on the fly” several times. As the space state generation is done in exponential space and time, and the verification of a property is performed in polynomial time, if the space state is already constructed. (ii) The use of the dense time approach, as several SIS properties are time dependent. (iii) PNML [21] is implemented as the default transfer format, thanks to that, the interchange of information between the GHENeSys tools is possible, as well as with external tools that support the standardized format. (iv) The environment allows that all modelling and verification tasks to be performed without the need of external modules or tools. (v) The space state generation and the specification of the tested properties are done on the same tool.

D. Requirements for safety control programs

According to [9] and [22], safety control programs must be developed according to the development cycle proposed by the IEC 61511 standard as shown on Fig. 1 and using modularity concepts.

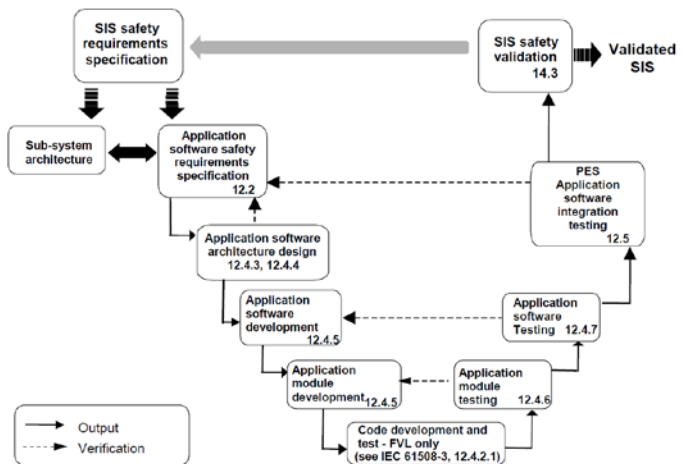


Fig. 1. Safety program development cycle or "V-model"

The development cycle is the combination of several phases ranging from the requirements analysis to the formal verification of the entire control program. The development phases, located on the left, also include steps related with the

description of the operation of each SIS module, the choice of methods and tools to aid the development, the development of the control program and its modules integration and the control code development. The verification phases, located on the right, include the formal verification of the modules and their integration and the final tests of the control program and hardware integration.

III. SIS CONTROL PROGRAM MODELING

The initial step towards the proposed framework has already been done on the previous section. There, the GHENeSys environment was chosen as the modelling and verification tool, as well as the choice was justified as required by the standard as part of the second phase of the development cycle.

Through the concepts of modularity, we can break the SIS control program in two parts. The prevention module is responsible to detect dangerous events represented as critical faults and deploy the suitable treatment to degenerate the system leading it to a safe state. The mitigation module is responsible to detect the effects of a fault not being treated correctly – or even not being detected by the prevention module – and deploy the suitable treatment to degenerate the system and to extinguish the effects before they disseminate to other parts of the plant. The definition of the main control program modules and thus the high level control program architecture are the second part of the second phase of the development cycle.

The development of the framework will be performed according to the Model Based Design (MbD) approach [3]. Although this approach is not referred in the IEC 61511 standard, as according to the standard, all control programs are directly developed in an implementation language. The standard requires that a final validation shall be carried out by the end of the development cycle, and modeling is one of the recommended tools for validation. Thus by adopting the MbD, the framework will be not only complying with the standard but also improving the modularity of the SIS control programs.

The third and fourth phases of the development cycle are related with de control program development. On these phases must be chosen methodologies for the development of the prevention and mitigation modules. These methodologies must be based on formal models and must have been proposed according the requirements of the IEC 61508 and IEC 61511 standards.

The prevention module development methodology must first be able to define which faults the SIS will treat. This definition can be made through HAZOP reports, cause-effect matrix or other applicable technique. With knowledge of the faults, formal methods to discover the causal relations leading to each fault, that is, how – by which sensors – each fault can be detected must be presented. The methodology then must be able to propose actions to deal with each fault, through the actuation of some component – such as control valves – and/or the shutdown of an endangered component.

Now a mitigation module development methodology must

be chosen. The same methodology as used on prevention can be adopted; as well as other methodology can be adopted, as long as the same criteria – as described on the previous paragraph – are used.

As opposite as the prevention activity, the mitigation activity does not need to define the treated faults through documents or reports. The mitigation activity shall treat the prevention activity faults, that is, the system will mitigate the consequences of the prevention system not being able to lead the plant or process to a safe state.

The sixth and seventh phases of the development cycle are related with the formal verification of the models. Due to the Model Based approach, the verifications are performed on the control program models and not on the control code. All properties specified no natural language shall be translated to TCTL according to the patterns proposed in [23].

IV. APPLICATION EXAMPLE

Now we will present a simple application example of the development of a prevention SIS control program according with the IEC 61511 phases already covered by the presented framework. We will begin the application example by choosing the methodology to develop the prevention SIS module, then the methodology will be applied and the resulting control program model will be verified.

The systematic proposed in [24] was chosen. Briefly, the faults that will be treated by the prevention SIS are extracted from the HAZOP report. The detection models are generated from cause-effect matrixes, where those matrixes are converted on Bayesian Networks, which are finally converted on Petri Nets. The treatment models, that is, the actuators related with each treated fault are generated from the HAZOP report.

The systematic was then applied to a flexible manufacturing system prototype. This prototype is composed by three manufacture cells: feeder, inspection and assembly. The cells are connected by a conveyor belt transportation system. On this example, the prevention SIS control system was developed for the assembly cell. This cell is composed of a three axis manipulator robot [24].

| Case | X_Axis_Fail | S9.1 | S9.2 | X_Encoder_Fail | B9.2 |
|------|-------------|------|------|----------------|------|
| 1 | 1 | 0 | 0 | 0 | 1 |
| 2 | 1 | 0 | 0 | 1 | 0 |
| 3 | 1 | 0 | 0 | 1 | 1 |
| 4 | 1 | 0 | 1 | 0 | 0 |
| 5 | 1 | 0 | 1 | 0 | 1 |
| 6 | 1 | 0 | 1 | 1 | 0 |
| 7 | 1 | 0 | 1 | 1 | 1 |
| 8 | 1 | 1 | 0 | 0 | 0 |
| 9 | 1 | 1 | 0 | 0 | 1 |
| 10 | 1 | 1 | 0 | 1 | 0 |
| 11 | 1 | 1 | 0 | 1 | 1 |
| 12 | 1 | 1 | 1 | 0 | 0 |
| 13 | 1 | 1 | 1 | 0 | 1 |
| 14 | 1 | 1 | 1 | 1 | 0 |
| 15 | 1 | 1 | 1 | 1 | 1 |

Where:

X_Axis_Fail: X axis movement fail
S9.1: External limit sensor 1 fail
S9.2: External limit sensor 2 fail
X_Encoder_Fail: Encoder fail
B9.2: Initial position sensor fail

Fig. 2. Cause-effect Matrix "X Axis Movement Fault"

The first step of the systematic was the construction of the cause-effect matrix together with the definition of which fault will be treated by the SIS. On Fig. 2 is displayed the cause-effect matrix for 15 cases of “X axis movement fault” on the manipulator robot. For each case the combination of the four sensors that can detect this type of fault is presented.

On the next step, the data Fig. 2 was inputted into the proper algorithms for construction of the Bayesian Network. The resulting Bayesian Network for the diagnostic model was then converted on the GHENeSys net presented on Fig. 4 .The grayed places displayed on the models are pseudo-boxes. These boxes carry the marking information of their master elements. The master element can be identified by the name of each pseudo-box.

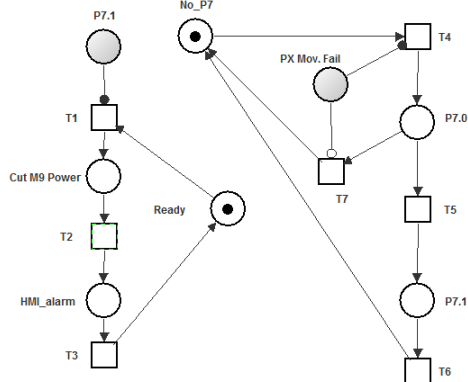
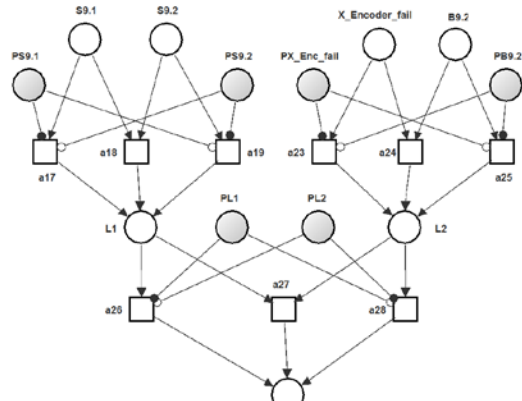


Fig. 3. GHENeSys net coordination model (left) and treatment model (right)

On the final step, the Safety Instrumented Function (SIF) for the manipulator robot “X” axis is determined based on the risk analysis HAZOP, and then the SIF treatment and coordination models were constructed as displayed Fig. 3. The function of each transition and place used on the treatment and coordination models is explained on Fig. 5.



| Place | Transition | Description |
|----------|------------|--|
| S9.1 | - | "X" axis limit sensor 1 |
| S9.2 | - | "X" axis limit sensor 2 |
| X_Encod | - | "X" axis encoder fail signal |
| B9.2 | - | "X" axis position sensor |
| A1 | - | Intermediate Place 1 |
| A2 | - | Intermediate Place 1 |
| X_Axis_F | - | "X" axis movement fail diagnostic |
| - | T1 | Logical (S9.1 OR S9.2) transition |
| - | T2 | Logical (X_Encode_Fail OR B9.2) transition |
| - | T3 | Logical (A1 OR A2) transition |

Fig. 4. Diagnostic model for “X axis movement fault”

A spurious events filter was implemented on the coordination model. This filter prevents the activation of the treatment model during a preset time, thus avoiding the degeneration of the plant and the costs associated with restarting the plant in case of spurious readings from some sensor.

SIF-01 treatment model.

| Place | Transition | Description |
|-------|------------|--|
| P7.1 | - | Failure cause found: X axis movement error |
| P2 | - | Action: Cut M9 motor power |
| P3 | - | HMI Alarm: X axis movement error |
| P4 | - | Error acknowledgment signal |
| Ready | - | Sistem ready for fail treatment |
| | T1 | T1 fired if (X_Axis_Fail AND Ready) |
| - | T2 | After the power for M9 is cut, T2 is fired |
| - | T3 | T3 fired if (HMI alarm AND fail is acknowledged) |

SIF-01 coordination model

| Place | Transition | Description |
|-------|------------|--|
| P7 | - | X axis fail diagnosed through the BPN |
| No_P7 | - | No X axis fail detected |
| P7.0 | - | Enable the call the SIF-01 treatment model |
| P7.1 | - | Calls the SIF-01 treatment model after Δt |
| - | T1 | T1 fired if (X_Axis_Fail & No_P7 ==1) |
| - | T2 | T2 fired if (P7.0==1)&(P7==0) |
| - | T3 | T3 fired if (P7.0==1)& $\Delta t \geq \text{preset}$ |

Fig. 5. Models elements descriptions

Currently there is no template or standard to determine a set of the system properties to be tested, thus, these properties usually are chosen by the control engineers based on previous knowledge and expertise [3] .

Table I. Checked Properties

| | |
|---|---|
| 1 | If any of the sensors B9.2, S9.1, S9.2 or X_Encoder_Fail are triggered for longer than the pre-set time the treatment model is called. $\forall \square_{\geq 10} ((B9.2 \vee S9.1 \vee S9.2 \vee X_Encoder_Fail) \rightarrow \forall \Diamond_{\geq 0} (\text{X Mov. Fail}))$ |
| | The motor remain turned off until no sensor is detecting the fault anymore $\neg \exists ((B9.2 \vee S9.1 \vee S9.2 \vee X_Encoder_Fail) U_{\geq 10} ((\text{Cut M9 Power}) \wedge (B9.2 \vee S9.1 \vee S9.2 \vee X_Encoder_Fail)))$ |
| 2 | Motors are not turned off until a fault is detected by the sensors $\neg \forall (\neg (B9.2 \vee S9.1 \vee S9.2 \vee X_Encoder_Fail) U_{\geq 0} (\text{Cut M9 Power}))$ |
| | |
| 3 | |
| | |

Thus, we propose do extract the basic properties from the SIFs descriptions, through that we have the main properties that the system was designed to fulfil. Besides the properties the system must fulfil, as we are working with safety systems, it is also imperative to check if the system reaches undesirable – or unsafe – states. So we have the following natural language properties and their respective translated TCTL propositions on Table I.

The verification tool displays the results in a colored square

besides the formula: (i) green if the formula holds, or (ii), red if the formula does not hold. On Fig. 6 all tested formulas are presented with their verification results on a extract of the verification tool output window. All formulas were verified with satisfactory results.

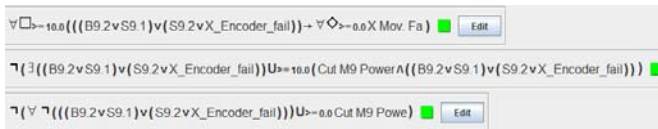


Fig. 6. TCTL Propositions and verification results

V. CONCLUSIONS

In this work, the first steps towards a framework for modeling and verifying SIS control programs were presented, the framework is based on the safety software development cycle from the IEC 61511 standard associated with the model based design approach. As demanded by the IEC 61511 standard, tools and methodologies to comply with some phases of development cycle were chosen, the initial high level control architecture was proposed, guidelines to choose the methodologies for developing the prevention and mitigation activities were also proposed. Also guidelines for TCTL propositions mapping from natural language properties – which we consider one of the most difficult tasks when using model checking techniques – were chosen.

SIS control program, as the one developed on this work, are critical to the systems they protect, as they responsible for the identification and treatment of critical faults. These faults, if not treated might lead to severe accidents and the loss of human lives. Frameworks as the one introduced on the present work, became crucial in order to enable these systems to be correctly interpreted and developed allowing the SIS to present a lesser probability of faults.

The next steps on the development of the framework might include more detailed modules architecture and functionalities, as well as systematics for the refinement of the high level modules; Methodologies for automatic isomorphic transformation of the models in IEC 61131-3 code; Methodologies for the integration of the prevention and mitigation modules, as well as modules for the treatment of several faults; And finally, systematics to verify the integrated SIS models and the study the relation between its modules.

REFERENCES

- [1] M. Bani Younis and G. Frey, "Formalization of Existing PLC Programs: A survey," , Kaiserslautern, 2003.
- [2] Leonardo Rodrigues Sampaio, *Validação Visual de Programas Ladder Baseada em Modelos*. Campina Grande: Universidade Federal de Campina Grande, 2011.
- [3] Mauro Mazzolini, Alessandro Brusaferri, and Emanuele Carpanzano, "An Integrated Framework for Model-based Design and Verification of discrete Automation Solutions," in *Proceedings 2011 9th IEEE International Conference on Industrial Informatics*, Milan, 2011, pp. 545-550.
- [4] Michel Diaz, *Petri Nets - Fundamental Models, Verification and Applications*. London: John Wiley & Sons, 2009.
- [5] Peter Hoffmann, Reimar Schumann, Talal M.A Maksoud, and Giuliano C. Premier, "Virtual Commissioning of Manufacturing Systems," in *24th European Conference on Modelling and Simulation*, Kuala Lumpur, Malaysia, 2010, pp. 175-181.
- [6] M. Sallak, C. Simon, and J.-F. Aubry, "A Fuzzy Probabilistic Approach for Determining Safety Integrity Level," *IEEE Transactions on Fuzzy Systems*, vol. 16, no. 1, pp. 239-248, 2008.
- [7] Reinaldo Squillante Jr., Diolino J. Santos Filho, Jeferson A. L. de Souza, Paulo E. Miyagi, and Fabricio Junqueira, "Safety in Supervisory Control for Critical Systems," in *Technological Innovation for the Internet of Things*, Costa de Caparica, 2012, pp. 261-270.
- [8] IEC, "IEC 61508 - Functional safety of electrical/electronic/programmable electronic safety-related systems," International Electrotechnical Commission, Geneva, Switzerland, 2010.
- [9] IEC, "IEC 61511 - Safety instrumented systems for the process industry sector," International Electrotechnical Commission, Geneva, 2003.
- [10] Mary Ann Lundteigen and Marvin Rausand, "Architectural constraints in IEC 61508: Do they have the intended effect?," *Reliability Engineering & System Safety*, vol. 94, no. 2, pp. 520-525, 2009.
- [11] Laihua Fang and Lijun Wei and Ji Liu Zongzhi Wu, "Design and Development of Safety Instrumented System," in *Proceedings of the IEEE International Conference on Automation and Logistics*, Qingdao, 2008, pp. 2685 - 2690.
- [12] Edmund M. Clarke, Orna Grumberg, and Doron A. Peled, *Model Checking*, 1st ed. Cambridge: MIT Press, 1999.
- [13] Rajeev Alur and David L. Dill, "A theory of timed automata," *Theoretical Computer Science*, vol. 126, no. 2, pp. 183-235, 1994.
- [14] T. Murata, "Petri nets: Properties, analysis and applications," *Proceedings of IEEE*, vol. 77, no. 4, pp. 541-580, 1989.
- [15] Pedro M. Gonzalez del Foyo and José Reinaldo Silva, "Towards a unified view of Petri nets and object oriented modeling," in *In 17th International Congress in Mechanical Engineering*, São Paulo, 2003, pp. 518-524.
- [16] Rajeev Alur, Costas Courcoubetis, and David Dill, "Model-Checking in Dense Real-time," *Information and Computation*, vol. 104, no. 1, pp. 2-34, 1993.
- [17] Richard Zurawski and MengChu Zhou , "Petri nets and industrial applications: a tutorial," *IEEE Transactions on Industrial Electronics*, vol. 41, no. 6, pp. 567-583, 1994.
- [18] Pedro M. G. del Foyo, A. S. P. José Miralles, and José Reinaldo Silva, "UM VERIFICADÓR FORMAL EFICIENTE PARA SISTEMAS DE TEMPO REAL," in *X SBAI – Simpósio Brasileiro de Automação Inteligente*, vol. X, São João del-Rei, 2011, pp. 1220-1225.
- [19] Bernard Berthomieu and Miguel Menasche, "An Enumerative Approach For Analyzing Time Petri Nets," in *Proceedings IFIP*, Paris, 1983, pp. 41-46.
- [20] Rajeev Alur, Costas A. Courcoubetis, and David L. Dill, "Model-checking for real-time systems," in *Proceedings of the Fifth Annual IEEE Symposium on Logic in Computer Science*, Philadelphia, 1990, pp. 414-425.
- [21] ISO/IEC, "Software and Systems Engineering - High-level Petri Nets, Part 2: Transfer Format, International Standard WD ISO/IEC 15909. Wd version 0.9.0," 2005.
- [22] Alois Mayr, Reinhold Plösch, and Matthias Saft, "Towards an Operational Safety Standard for Software - Modelling IEC 61508 Part 3," in *18th IEEE International Conference and Workshops on Engineering of Computer-Based Systems*, Las Vegas, 2011, pp. 97-104.
- [23] Matthew B. Dwyer, George S. Avrunin, and James C. Corbett, "Property Specification Patterns for Finite-state Verification," in *Proceedings of 2nd Workshop on Formal Methods in Software Practice*, Clearwater Beach, 1998, pp. 7-15.
- [24] Reinaldo Squillante Júnior, Diolino Jose Santos Filho, Fabricio Junqueira, and Paulo Eigi Miyagi, "Development of Control Systems for Safety Instrumented Systems," *IEEE (Revista IEEE America Latina Latin America Transactions*, vol. 9, no. 4, pp. 451-457, 2011.

Intelligent Border Security Interactive Simulation Tool (IBS-IST)

Iyad Aldasouqi
 Royal Scientific Society
 The Middle East Scientific Institute for Security
iyad@mesis.jo

Arafat Awajan
 Princess Sumaya University for Technology
 The King Hussein School for Information Technology
awajan@psut.edu.jo

Abstract:

This paper describes an intelligent tool that simulate border security interactive system. The proposed system consist of a tool that assists in the understanding of ground sensors and their uses the simulation of sensor behavior, vehicle movement and environmental conditions in order to promote cooperative monitoring. Furthermore, the proposed tool helps security personnel to understand the performance of a border or checkpoint monitoring system. The expected response of the monitoring system to the movement of vehicles and other intruders, under a variety of environmental conditions, can be simulated in real time. The use of this tool will lead to improved monitoring system design.

Keywords

Security, Seismic sensors, wireless, Ad hoc, wireless sensors

1. Introduction:

Many experts around the world are developing monitoring systems that demonstrate a wide range of advanced surveillance techniques: real-time moving object detection and tracking from stationary and moving camera platforms, recognition of generic objects (human, sedan and truck). Border Security is a very important issue, but also an extremely difficult task daily performed by a limited number of officials. In an effort to find ways to develop expertise more efficiently, a detailed description of expert performance is presented and contrasted with beginner and intermediate routine.

The method of imitating modeling is one of the most powerful and effective methods of research of processes and systems, covering the most various natures and degree of complexity. The essence of this method consists in developing the software for simulating process of functioning systems. In order to assess statistical characteristics of modeled system, it is necessary to carry out many experiments.. Results of imitating modeling enable to describe the behavior

of the system, to estimate influence of various parameters of the system on its characteristics, to reveal advantages and lacks of Offered changes and to predict behavior of the system [11].

If attitudes, which form a model, are simple enough to access the exact information on questions interesting us, then it is possible to use mathematical methods.

Computer simulations constitute the main research tools in the field of artificial life. Some of the many advantages include the possibility to choose an appropriate level of abstraction, to possess permanent control over and access to every aspect of the simulated world, as well as to conduct series of experiments in a highly efficient and reproducible way. Furthermore, the simulation environment can be interactively controlled via both conventional and custom developed hardware interfaces as shown in figure 1.

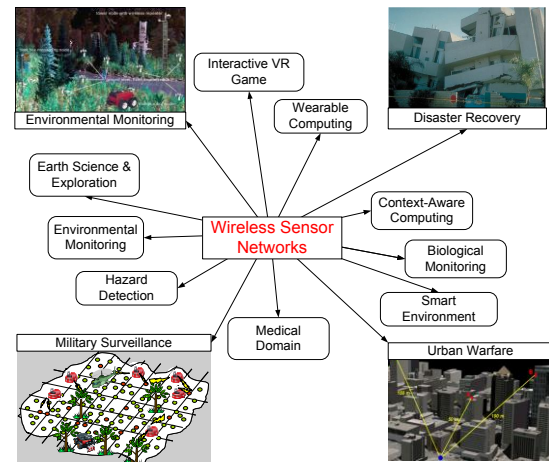


Figure1: Ad Hoc applications

1.1. Mobile wireless ad hoc networks

Mobile wireless ad hoc networks consist of wireless hosts that communicate with each other in the absence of a fixed infrastructure. Some examples of the possible uses of ad hoc networking include soldiers on the battlefield, emergency disaster relief personnel, and networks of laptops. The mobile devices can communicate to each other either through the access points closest to them, or as on

a peer-to-peer basis by forming wireless ad hoc networks.

The Two main uses of location services in mobile ad hoc networks are to provide information regarding a geographic location of the nodes in the network and to locate content.

In Figure 2, an example of wireless sensor networks and sensors node is illustrated. This example shows the role of the sensor network to monitor and track the movement of the truck. The wireless sensor networks can be viewed in two levels. One is the network level which provides information about connectivity, routing, channel characteristics and protocols. The other is node level which consists of hardware and software components, radio, CPU, sensors, embedded software and limited energy.

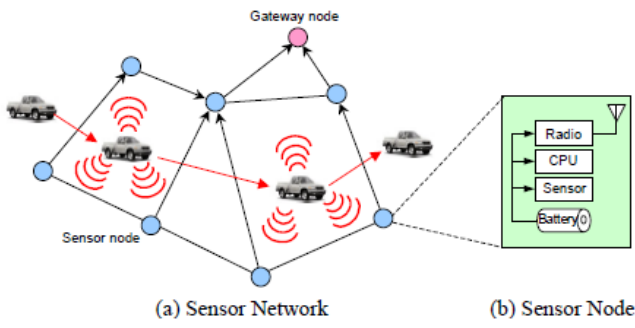


Figure 2: An Example of Sensor Network (a) and Sensor Node (b)

1.2. Border security concerns

Depending on the border situation, there are several working assumptions in order to test demanded changes:[2]

1. The border must be secured against any unwelcomed disturbance to the agreed territory.
2. A secure border must be protected from terror and crime altogether, all the roads that are used by criminals, are used by terrorists too.
3. There must be a similar interest core between different territories, allies, in order to maintain any laws and rules for a secure border.
4. An aerial, naval and land defense space, and in the near future also in the space.
5. There is no 100% secure border, especially against rockets, media networks and the internet.
6. The organizations those are responsible for border security, crime and terror (Terrocrime) foiling on the global level, are not efficient enough at the moment/ or have still tremendous room for progress in term of the efficiency of their work

7. Intelligence is the most important tool for terror and crime (Terrocrime), and has to be used more efficiently on the level is not put in good use on the global level.
8. And has to be used more efficiently on the global level
9. The best examples for control and global action are in private finances, industry and economy.
10. A border must stand as an obstacle and a checkpoint to hold and react against any action on the agreed territory.

1.3 Incentives:

There are many motivations in this field such as; the land navigator incorporates elements dealing with small unit tactics, group leadership, and military mission planning that do not exist for the civilian orienteer [3]. Also cognitive model is another related motivation, which is a virtual environment based training to improve infantry leader's tactical navigation skills. Another example is the Recognition Primed Decision (RPD) model, which is used to explain the performance of experts in a wide variety of activities, including urban and rural firefighting, flight control in commercial airlines, chess tournament play, and intensive care unit nursing [7].

2. Problem Statement:

One of the main concerns in every country is to secure their borders as much as they can, but many factors impact on this concern, such as the geographical texture, long borders line, budget and cooperation with neighbor countries.

The purpose of this paper is to present a detailed description of an expert intelligent border security interactive system, then to show how a portion of this expertise may be represented.

From this model, future work may develop a more complete model of comprehensive expert border security system.

3. Related work

This topic is very important since it deals with one of the most crucial issues for national security (border security). Furthermore, it is a wide subject and related to many other applications that used the same or similar technologies, such as environment and earthquake early warning system or fire detection systems.

In border security, some related works about detecting motion and securing borders against intruders, have been done and others are still under development such as medium access control protocols for ad hoc wireless networks [16]. This work presented a broad overview of the research work conducted in the field of ad hoc wireless networks with respect to MAC protocols, and it discussed many schemes and identified their salient features, it also focused on collision resolution, power conservation, multiple channels, advantages of using directional antennas and QoS.

Other groups discussed the subject from another prospective as the Location Services in Wireless Ad Hoc and Hybrid network [17]. They presented a taxonomy of location services and survey on techniques for constructing such a service in wireless ad hoc and hybrid networks. Another example is the Unified Network and Node Level Simulation Framework for Wireless Sensor Networks [18], they presented a unified simulation framework for network and node level, suitable for energy profiling of wireless sensor networks.

As seen in the above related works, all of them have focused on the security and up to date technologies issues without considering the cost reduction, except the first example. They have focused on power conservation, but they have not considered saving on number of nodes or sensors.

4. Our work:

In our work, the main concern will focus on lowering the cost by reducing the number of nodes to a minimum and keeping the security issue as a top priority. For testing and demonstration purposes we used seismic sensors and developed a computer application as a tool.

As known seismic sensors signal is divided into two parts (Primary and secondary) as shown in figure 3, which can help us to build an early detection system or early warning system as in our previous research tool “Earthquake Monitoring System Using Ranger Seismometer Sensor” [13].

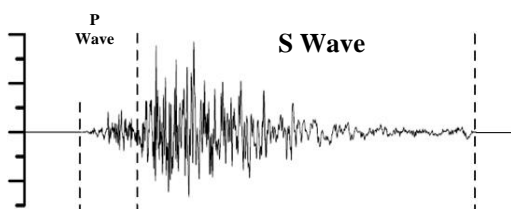


Figure 3: Secondary and Primary seismic sensor signals

The objective of this tool is to present the optimum scenario for distributing the sensors that can guide to fully secure the monitored area and determine the most suitable location of the sensor in order to detect intruders.

In this paper, I used a traditional way of seismology (the same technique used in earthquake) to determine the location of the intruder. This technique is used, at least, by three seismic stations.

This work is divided into two phases, Phase I is navigation, and Phase II is Implementation. In phase I, a photo from the sky or satellite image (2D or 3D is preferable, as in figure 4) is needed to determine the texture of the monitored area.



Figure 4: Sample photo

Then a study for the features and textured of monitored area should be conducted to know the most appropriate sensor for that area. As shown in figure 5

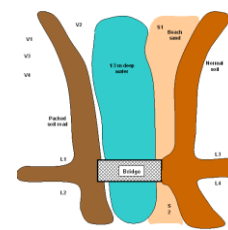


Figure 5: Photo after analysis

Drawing of some suggested scenarios can help in building images of what may be happening as in figure 6.



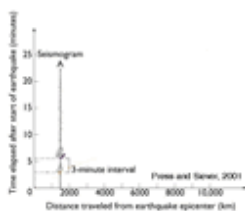
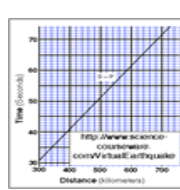
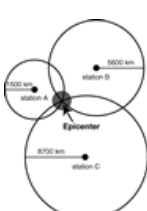
Figure 6: suggested scenario

In the implementation phase (Phase II), and after we identify the monitored area and know its features, we have to choose the best locations for the seismic sensors (it should be rocky or not moisture, since Primary waves can travel through solids and liquids,

where Secondary waves can only travel through solids)

We can locate the threat by following these four simple steps:

Table 1: Algorithm base lines

| | |
|--|---|
| 1. Measure the time difference between P and S wave arrivals on a seismogram. |  |
| 2. Use a travel-time graph to get the distance from the threat to the seismic station. |  |
| 3. Draw a circle on a map that represents this distance. | 3 minutes P-S time = 1500 km distance  |
| 4. At least three stations are needed in order to "triangulate" one, or more location(s) from different seismic stations, which should intersect at the threat's location. |  |

In our work the following algorithm of threat location determination is used:

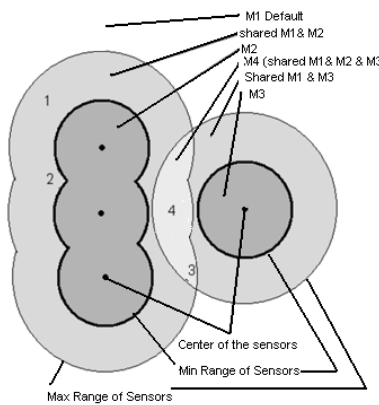


Figure 6: Scenario of sensors installation as an example of defining the areas for two shared areas

We have four Models (four Different Areas)(M1, M2, M3 and M4)

- Intrusion in the dark gray areas (M2, M3) within the inner circles uses one model, in which we can detect every motion within sensor zoon.
- Intrusion in the white area surrounding all of the circles (M1) uses the default model not covered.
- Intrusion in the lighter gray transition areas (shared area between M2 and M3) that can detect motion by two sensors, and can cover more area. One week point is when one of the sensors stop working.
- Intrusion in the lighter white transition regions M4 (when we have shared area between three sensors or more, in which we can not only cover more area, but we can determine the exact location of the threat, and we can use them for other maintenance purposes (when one of the sensors stop working))

5. Conclusion and future work:

IBSIST provides a realistic, reliable tool for modeling human decision-making and organizational behavior, which can help to determine the best location and type of sensors in order to find the optimal solution to secure the monitored area. This work is divided into two phases, Navigation, which can be done via different techniques (simulation tool is used), and a detection tool, built upon a narrative algorithm.

The IBSIST reference case demonstrated the ability to model individual decision-making in an unsure environment. It used multiple rules and could be easily modified to allow selection and finding of the "best" rule sets, given a specific personality and environment.

Future work on IBSIST could be to improve this system to make it a comprehensive tool for decision makers, such as: Add GPS data, to specify the location, add the ability of agent software to self-organize into pre-determined relationships and select from competing goals.

6. References:

- [1] Integrating Intelligence for Border Security, Dale N. Anderson, Sandra E. Thompson, Charles E. Wilhelm, Ned A. Wogman, January 2004

- [2] The Importance of Border Security in the Age of Globalization, Dubi Yung, 15/04/2009
- [3] Representing Tactical Land Navigation Expertise, Jason L. Stine, September 2000
- [4] Ferber, J., Multi-agent Systems, Addison Wesley Longman, 1999
- [5] Holland, J. H., Hidden Order: How Adaptation Builds Complexity, Perseus Books, 1995.
- [6] Dreyfus, H., Intuitive, Deliberative, and Calculative Models of Expert Performance, in Zsambok, C., and Klein, G. (Eds.), Naturalistic Decision Making, Lawrence Erlbaum, 1997.
- [7] Klein, G., and others, "Characteristics of Skilled Option Generation in Chess," Organizational Behavior and Human Decision Processes, 62 (1), 1995.
- [8] Carver, N. and Lesser, V.R. 1991. A new framework for sensor interpretation: Planning to resolve sources of uncertainty. In Proceedings of the Ninth National Conference on Artificial Intelligence. 724-731.
- [9] Durfee, E.H.; Lesser, V.R.; and Corkill, D.D. 1987. Coherent cooperation among communicating problem solvers. IEEE Trans. on Computers 36(11): 1275-1291.
- [10] Durfee, E.H. and Lesser, V.R. 1991. Partial global planning: A coordination framework for distributed hypothesis formation. IEEE Trans. on Systems, Man, and Cybernetics 21(5): 1167-1183.
- [11] Averill M.Law, W. David Kelton. Simulation modeling and analysis.Third edition.McGraw-Hill, Osborne, 2003.
- [12] Sycara K.P. Multiagent systems.<http://www.cs.cmu.edu/~softagents/papers/multiagentsystems.PDF>
- [13] Iyad Aldasouqi and Adnan Shaout, Earthquake Monitoring System Using Ranger Seismometer Sensor, INTERNATIONAL JOURNAL of GEOLOGY, , Issue 3, Volume 3, 2009
- [14] Y. M. Wu and H. Kanamori, "Development of an earthquake early warning system using real-time strong motion signals," Sensors, Vol.8, pp. 1-9, 2008.
- [15] HEPOINVIRSE-2000, Fred W. Klein, 2002
- [16] Sunil Kumar, Vineet S. Raghavan b, Jing DengMedium, Access Control protocols for ad hoc wireless networks: A survey, 2004 Elsevier
- [17] Roy Friedman and Gabriel Kliot Location Services in Wireless Ad Hoc and Hybrid network, Dependable Systems and Networks With FTCS and DCC, 2008. DSN 2008. IEEE International Conference
- [18] Park, H., Liao, W., Tam, K.H., Srivastava, M.B. and He, L. (2003) A Unified Network And Node Level Simulation Framework For Wireless Sensor Networks, Technical report, Center for Embedded Network Sensing, University of California.
- [19] R. Beuran, K. Chinen, K.T. Latt, T. Miyachi, J. Nakata, L.T. Nguyen, Y. Shinoda, Y. Tan, "Application Performance Assessment on Wireless Ad Hoc Networks", Asian Internet Engineering Conference (AINTEC) 2006, Bangkok, Thailand, November 28-30, 2006.

Parameter Estimate of Anisochronic Models Using Method of Moments

Milan Hofreiter

Abstract—This paper presents an original approach to parameter estimation of the anisochronic model containing delays in both input and state, which is suitable for control design. This model is very universal because it can be used for modeling both overdamped and underdamped processes, which are conventionally described by a serial combination of a rational transfer function and a transportation delay. In this paper it is described how to transfer the conventional linear models of various orders into the linear anisochronic models with the fixed plain structure. It is also shown how to estimate parameters of the anisochronic models from the step responses. The simple computational formulas for parameter estimation are derived and then used for these purposes. The applicability of the suggested methodology is presented in the Matlab/Simulink programming environment.

Keywords—Anisochronic model, approximation, average residence time, parameter estimation.

I. INTRODUCTION

If we want to control a process, we must get to know its properties. Mostly, a model is obtained through system identification and the obtained model is then used for the control design. In most cases, the controllers maintain process variables around operating points; therefore linear dynamical models of plants are predominantly used for control design. The models are usually expressed by a serial combination of rational transfer function and a transfer function of transport delay [1], [6], [7].

In comparison with this standard model, the transfer function of the anisochronic model contains delays in both input and state. The very universal anisochronic model was described in [2], [4], [8], [9]. The transfer function $G_a(s)$ of this model contains only five parameters, see (1),

$$G_a(s) = \frac{K \cdot e^{-s\tau_u}}{(\tau_1 \cdot s + 1)(\tau_2 \cdot s + e^{-s\tau_y})}, \quad (1)$$

where K is the process static gain, τ_u is the pure input time delay, τ_1 and τ_2 are the time constants and τ_y is the

feedback time delay. The variable s represents the complex argument defined by the Laplace transform. The parameters are depicted in Fig. 1, where I represents the position of the inflex point, p is the tangent at the inflex point I , see [3], [4].

Because the delay τ_y is in the denominator of transfer function (1), then the characteristic equation is transcendental in s and has an infinite set of roots [7], [9]. For this reason, it can be expected to be a better approximation of the dynamics of high-order systems.

Model (1) is stable if $\tau_y/\tau_2 < \pi/2$, overdamped if $\tau_y/\tau_2 < 1/e$, critically damped if $\tau_y/\tau_2 = 1/e$ and underdamped if $\tau_y/\tau_2 > 1/e$. Therefore model (1) may be used both for nonoscillatory and oscillatory processes [4], [9].

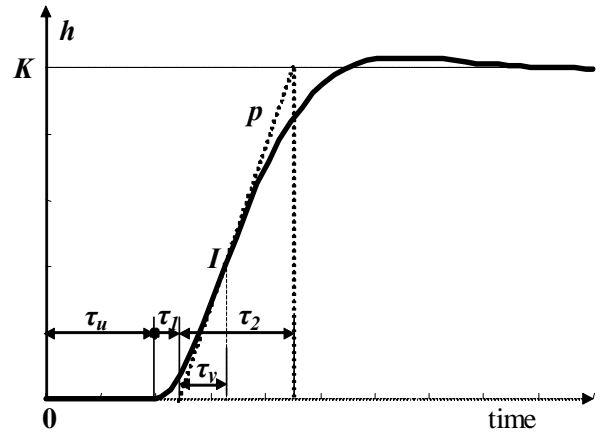


Fig. 1 Unit step response $h(t)$ of model (1)

The parameters K , τ_1 , τ_2 , τ_u and τ_y can be estimated from the unit step response $h(t)$ by the graphical method, see Fig. 1. But this approach is based on local measurements at a few points. If the signals are corrupted with noise then this graphical construction may lead to large errors. The position of the inflex point I is also vague. To improve the estimates, the method of moments is further applied.

II. METHOD OF MOMENTS

The method of moments [1], [5] is based on the computation of some integral quantities. The two integrals (2), and (3) can be determined for a more reliable estimate of the parameters of anisochronic model (1).

$$M_0 = \int_0^\infty (K - h(\tau)) d\tau \quad (2)$$

$$M_1 = \int_0^\infty \tau \cdot (K - h(\tau)) d\tau \quad (3)$$

Integrals (2) and (3) can be determined using the Laplace transform and the theorem of the final value.

$$\begin{aligned} M_0 &= \lim_{t \rightarrow \infty} \int_0^t (K - h(\tau)) d\tau = \lim_{s \rightarrow 0} \left(\frac{K}{s} - \frac{G_a(s)}{s} \right) = \\ &= \lim_{s \rightarrow 0} \left(\frac{K}{s} - \frac{K e^{-s \tau_u}}{s(\tau_1 s + 1)(\tau_2 s + e^{-s \tau_y})} \right) = K \cdot \tau_{ar} \quad (4) \\ \tau_{ar} &= \tau_1 + \tau_2 - \tau_y + \tau_u = \tau_p - \tau_y \quad (5) \end{aligned}$$

where τ_{ar} is the average residence time and τ_p is the transient time of anisochronic model (1), see Fig. 2.

Similarly integral (2) can be determined.

$$\begin{aligned} M_1 &= \lim_{t \rightarrow \infty} \int_0^t \tau (K - h(\tau)) d\tau = \\ &= \lim_{s \rightarrow 0} \left(-\frac{d}{ds} \mathcal{L}\{K - h(\tau)\} \right) = \\ &= \lim_{s \rightarrow 0} \left(-\frac{d}{ds} \left(\frac{K}{s} - \frac{G_a(s)}{s} \right) \right) = \\ &= -K \cdot \lim_{s \rightarrow 0} \frac{d}{ds} \left(\frac{1}{s} - \frac{e^{-s \tau_u}}{s(\tau_1 s + 1)(\tau_2 s + e^{-s \tau_y})} \right) = \\ &= K \left(\frac{\tau_{ar}^2 + \tau_1^2 + \tau_2^2}{2} - \tau_2 \cdot \tau_y \right). \quad (6) \end{aligned}$$

where \mathcal{L} denotes the Laplace transform.

For anisochronic model (1) with respect to (4) and (5) it holds

$$K(\tau_1 + \tau_2 + \tau_u) - M_0 = K \cdot \tau_y, \quad (7)$$

which may be used for the determination of parameter τ_y . The area $K \cdot \tau_y$ is depicted in Fig. 2.

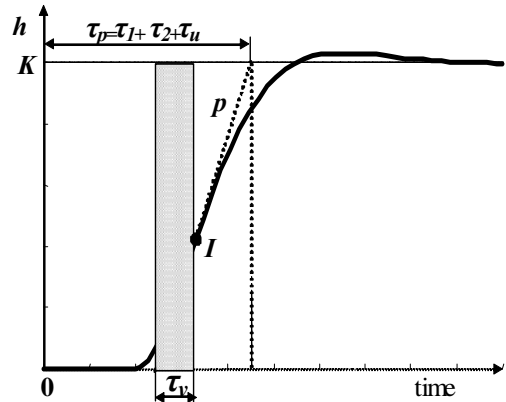


Fig. 2 The marked area $K \cdot \tau_y$

III. ESTIMATION OF PARAMETERS

Without the knowledge of the exact position of inflex point I in the step response, one can construct the tangent p and calculate by numerical integration moments (2) and (3). Then the parameters of anisochronic model (1) can be found in according to the following steps.

1. Determine the static gain K from a graphical construction or through static tests.
2. Determine the time constant τ_2 from a graphical construction, see Fig. 1.
3. Compute the average residence time τ_{ar} from (4)

$$\tau_{ar} = \frac{M_0}{K}. \quad (8)$$

4. Determine the transient time τ_p from a graphical construction, see Fig. 2, where

$$\tau_p = \tau_1 + \tau_2 + \tau_u. \quad (9)$$

5. Compute the time constant τ_y

$$\tau_y = \tau_p - \tau_{ar} \quad (10)$$

6. Compute the time constant τ_1 from (6)

$$\tau_1 = \sqrt{2 \cdot \frac{M_1}{K} - \left(\tau_{ar}^2 + (\tau_2 - \tau_y)^2 - \tau_y^2 \right)}. \quad (11)$$

7. Compute the apparent dead time τ_u

$$\tau_u = \tau_p - \tau_1 - \tau_2. \quad (12)$$

One will notice that in this method only the time constants τ_p and τ_2 are obtained directly from the graphical construction and they are easily determined by tangent p . The others constants τ_1 , τ_u and τ_y are calculated using the values M_0 and M_1 . This procedure easily enables the estimation of delays τ_u and τ_y .

IV. DETERMINATION OF MOMENTS

Since digital computers are used for data processing, continuous measurements are converted into digital form. The moments M_0 and M_1 can be obtained from a sampled data record $h(k\Delta t)$, $k=1,2,\dots,N$ of the unit step response, where Δt represents the sampling period and N relates to the last sample, when the unit step response achieved the new steady state. The integrals (2) and (3) can be computed by a numerical integration, e.g. a trapezoidal or rectangular integration algorithm.

V. DETERMINATION OF MOMENTS

A system with the transfer function

$$G(s) = \frac{e^{-10s}}{(5s+1)^5} \quad (13)$$

is described by the step response, see Fig. 3. Find parameters of anisochronic model (1) using the presented method.

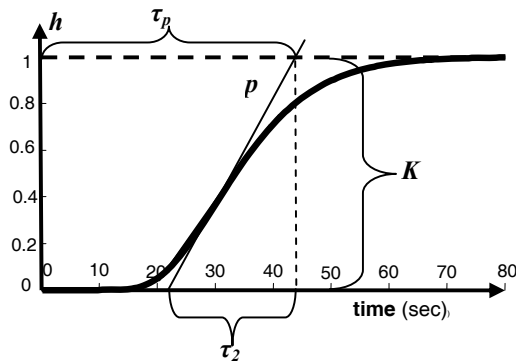


Fig. 3 The unit step response $h(t)$ of a system

Solution:

The following parameters are estimated by graphical analysis of the unit step response $h(t)$ depicted in Fig. 3: $K=1$, $\tau_2=22s$, $\tau_p=44s$. The values of integrals (1) and (2) are obtained by the numerical integration: $M_0=35s$, $M_1=675s^2$.

The other estimated parameters obtained by the procedure described in section 3 are: $\tau_1=6s$, $\tau_y=9s$, $\tau_u=16s$. The transfer function of anisochronic model (1) is then

$$G_a(s) = \frac{e^{-16s}}{(6s+1)(22s+e^{-9s})}. \quad (14)$$

The unit transfer functions of both the system and model (13) are in Fig. 4.

Although there is very good conformity between the step response h of the identified system and the step response h_a of the anisochronic model, the transfer functions (13) and (14) are different. The Bode diagrams of system (13) and model (14) are depicted in Fig. 5. The Bode diagrams display very

good conformity for frequencies $\omega < 1\text{ rad}\cdot\text{s}^{-1}$ and for higher frequencies $A(\omega)=A_a(\omega)\approx 0$.

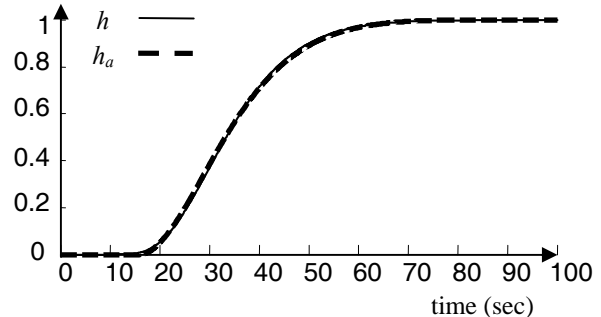


Fig. 4 The unit step response h of the system and the unit step response h_a of anisochronic model (13).

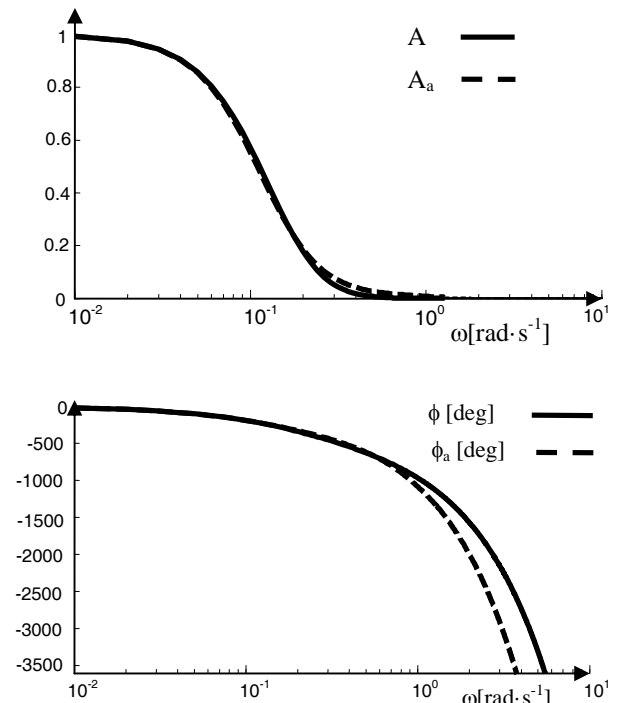


Fig. 5 The Bode diagrams for system (13) and model (14), where $A(\omega)=|G(j\omega)|$, $\phi(\omega)=\angle G(j\omega)$ and $A_a(\omega)=|G_a(j\omega)|$, $\phi_a(\omega)=\angle G_a(j\omega)$.

VI. CONVERSION OF TRANSFER FUNCTIONS

Moments (2) and (3) can also be used for a conversion of a transfer function in the form

$$G(s) = K \frac{(1-T_0s) \cdot e^{-T_0 s}}{(T_1 s + 1)(T_2 s + 1) \cdots (T_n s + 1)}. \quad (15)$$

to the anisochronic model in form (1).

Moments (2) and (3) can be determined for transfer function (15) and the result is [5]

$$M_0 = K \cdot T_{ar}, \quad (16)$$

$$M_1 = K \left(\frac{T_{ar}^2 + T_1^2 + T_2^2 + \dots + T_n^2 - T_0^2}{2} \right), \quad (17)$$

where the average residence time

$$T_{ar} = T_u + T_0 + T_1 + T_2 + \dots + T_n.$$

It follows from formulas (4) and (16)

$$T_{ar} = \tau_{ar}, \quad (19)$$

and from formulas (6) and (17)

$$\begin{aligned} & \frac{\tau_{ar}^2 + \tau_1^2 + \tau_2^2}{2} - \tau_2 \cdot \tau_y = \\ & = \frac{T_{ar}^2 + T_1^2 + T_2^2 + \dots + T_n^2 - T_0^2}{2} \end{aligned} \quad (20)$$

For example, moments (2) and (3) for transfer function (13) can be calculated using (16) and (17) by the following way

$$M_0 = K \cdot T_{ar} = 1 \cdot (5 \cdot 5 + 10) = 35s, \quad (21)$$

$$M_1 = 1 \cdot \frac{(35^2 + 5 \cdot 5^2)}{2} = 675s^2. \quad (22)$$

The moments M_0 and M_1 for anisochronic model (14) are approximately the same but they are calculated by derived formulas (4) and (6).

$$M_0 = K \cdot \tau_{ar} = 1 \cdot (6 + 22 - 9 + 16) = 35s \quad (23)$$

$$M_1 = 1 \cdot \left(\frac{35^2 + 6^2 + 22^2}{2} - 22 \cdot 9 \right) = 674.5s^2 \quad (24)$$

VII. GENERALIZATION

The transfer function $G_a(s)$ can be factored

$$G_a(s) = {}^1G_a(s) \cdot {}^2G_a(s) \quad (25)$$

where the static gain $K = G_a(0) = {}^1G_a(0) \cdot {}^2G_a(0)$. Then using the MacLaurin series one can obtain

$$\begin{aligned} \frac{M_0}{K} &= \lim_{t \rightarrow \infty} \int_0^t \left(1 - \frac{h(\tau)}{K} \right) d\tau = \lim_{s \rightarrow 0} \left(\frac{G_a(0) - G_a(s)}{s \cdot G_a(0)} \right) = \\ &= \lim_{s \rightarrow 0} \frac{1}{s} \left(-\frac{G'_a(s)}{G_a(0)} s - \frac{G''_a(s)}{G_a(0)} \frac{s^2}{2} - \frac{G'''_a(s)}{G_a(0)} \frac{s^3}{6} - \dots \right) = \end{aligned}$$

$$= -\frac{G'_a(0)}{G_a(0)} = -\left(\frac{{}^1G'_a(0)}{{}^1G_a(0)} + \frac{{}^2G'_a(0)}{{}^2G_a(0)} \right). \quad (26)$$

Hence with respect to (4)

$$\tau_{ar} = {}^1\tau_{ar} + {}^2\tau_{ar}, \quad (27)$$

where ${}^i\tau_{ar}$ is the average residence time, which relates to the transfer function ${}^iG_a(s)$, $i=1, 2$.

A system with transfer function (29) has, due to (4), (5), (18) and (27), the average residence time

$$\tau_{ar} = \tau_u + \sum_{j=1}^{N_1} \tau_j + \sum_{k=1}^{N_2} ({}_a\tau_k - {}_y\tau_k) - \sum_{i=1}^{N_3} T_i \quad (28)$$

$$G_a(s) = \frac{e^{-s \cdot \tau_u} \cdot \prod_{i=1}^{N_3} (T_i \cdot s + 1)}{\prod_{j=1}^{N_1} (\tau_j \cdot s + 1) \cdot \prod_{k=1}^{N_2} ({}_a\tau_k \cdot s + e^{-s \cdot y\tau_k})} \quad (29)$$

$N_1, N_2, N_3 \in \mathbb{N}$; $\tau_j, {}_a\tau_k, {}_y\tau_k, T_i, \tau_u \in \mathbb{R}^+$ for $\forall i, j, k$.

For transfer function (29) the moment M_0 is

$$M_0 = K \cdot \tau_{ar}. \quad (30)$$

VIII. CONCLUSION

This paper presents an original approach to parameter estimation of anisochronic model (1) that is suitable for the description of most industrial processes. For this purpose using the moment method, the simple computational formulas were derived for parameter estimation of the anisochronic model from a step response or for conversion of a transfer function from form (15) into the transfer function of anisochronic model (1).

REFERENCES

- [1] K., J. Åström and B. Wittenmark, *Adaptive Control*. Addison-Wesley Publishing Company, Inc., 1995.
- [2] M. Hofreiter, *Parameter Identification of Anisochronic Models*, DAAAM International Scientific Book 2002. Vienna: DAAAM International, Editor B. Katalanic, 2002, pp. 247-252.
- [3] M. Hofreiter, "Discretization of continuous linear anisochronic models," *Studies in Informatics and Control*, vol. 12, no. 1, 2003, pp. 69-76.
- [4] M. Martináková, "Control of hereditary DIDO systems using anisochronic models." Thesis in Czech, CTU in Prague, FME, 2000.
- [5] P. Klán, R. Gorez, in *Process Control*, FSS Public s.r.o., Prague, 2011.
- [6] Seborg, D. E., T.F. Edgar, and D. A. Mellichamp, *Process Dynamics and Control*. John Wiley & Sons, Inc., 2011.
- [7] T. Vyhídal, P. Zitek, "Control System Design Based on Universal First Order Model with Time Delays," *Acta Polytechnica*, vol. 41, no. 4-5, 2001, pp. 49-53.
- [8] P. Zitek, J. Hlava, "Anisochronic Internal Model Control of Time Delay Systems," *Control Engineering Practice*, vol. 9, no. 5, 2001, pp. 501-516.
- [9] P. Zitek, "Time Delay Control System Design Using Functional State Models," *CTU Reports*, CTU Prague, no. 1, 1998.

Speech processing strategy in a cochlear implant processing unit based on a combination of SNR and the number of frequency bands in amplitude and frequency modulation

S. Antonov, G. Tsenov and V. Mladenov

Abstract — The human hearing system can be estimated as a nonlinear functioning organ. The proposed research combines different type of modulations- amplitude and frequency modulation of speech audio signals in various conditions related to the processing method of a cochlear implant and the sex of the talker as a speech sound signal source. The aforementioned combination of different conditions of signal modulation is performed in various signal to noise ratio and different number of the frequency channels in the processing strategy. The numeric simulation of the proposed algorithm is used as a base for a comparison between the usage of 1-32 frequency channels in computing the mean squared error and varying the signal to noise ratio.

Keywords — Audio signal modulation, cochlear implant, coding, nonlinear signal processing, speech processing.

I. INTRODUCTION

THE acoustic characteristics in speech signals deliver identification and localization of a human speaker or an animal. Some other characteristics allow listeners to get the meaning of the speech but also the speaker's emotion and intention. Some studies using artificially synthesized speech or naturally produced whispered speech [1]. They have discovered several important acoustic parameters for speech recognition. This can be achieved on the base of the Organ of Corti's structure, way of frequency analyses and signal amplifying [10].

The main aim of this study is to conclude for the best conditions in the processing strategy of a cochlear implant based on a comparison between the usage of different number of frequency channels in computing the mean squared error and varying the value of the signal to noise ratio.

A speech signal produced by a male talker is chosen for the

S. I. Antonov is with the Technical university Sofia, bul. "Kliment Ohridski" 8, Building 12, office 12502, Sofia 1000, Bulgaria (e-mail: svantonov@yahoo.com).

G. Tsenov, is with the Technical university Sofia, bul. "Kliment Ohridski" 8, Building 12, office 12504, Sofia 1000, Bulgaria (e-mail: gogotzenov@tu-sofia.bg).

purpose. The results are compared with a MSE in case of male singer source of sound A combination of slowly varying amplitude modulation (AM) and frequency modulation (FM) from a number of frequency bands in speech signals is proposed and testing their contribution to speech recognition in cochlear implant hearing device. The frequency modulation used here tracks gradual changes around a fixed frequency in a frequency subchannel which is different from other studies using relatively "fast" FM to track formant changes in speech production [4], or fine structure in speech acoustics [5]. It is estimated amplitude modulation only and amplitude plus frequency modulation, and the original unprocessed speech signal in different conditions to compare the results of the processing, and to extract the mean-squared error and the distortion. This experiment tests the relative contribution of the added frequency modulation in the speech signal processing method in the cochlear implants in quiet environment (no masker/noise signal added) and noise environment (a song fragment). The comparison of the amplitude modulation only and amplitude plus frequency modulation and the sex of the talker depending on the number of frequency channels is presented. Than the results of processing by the same algorithm is used to compare depending of signal to noise ratio.

II. METHODS

A. Physical model

The human ear is an organ of hearing. It is used for the audition of sound oscillations. The general purpose of the ear is to transfer the sound oscillations in neural impulse. It is receptor and analyzer of the sound. The studies up so far show that it consists of three parts: outer, middle, and inner ear (cochlear).

The cochlear is about 35mm long and has conical shape. Represents a tube rotated 2.5 times around bone axis. This shape of the cochlear based on [10] is presented in Figure 1.

The significant part of the cochlear is basilar membrane in the middle of this kind of pipe. Its length is about 33 mm. It consists of thousands of elastic fibers which are short and closely packed in the basal region. Being under tension, the

fibers can vibrate like the strings of a musical instrument. This leads our study to the idea of a resonance in a point on the basilar membrane depending on the investigated frequency. This helps us to separate the frequency channels in our processing strategy in a cochlear implant processing unit.

The proposed algorithm represents the function of the basal

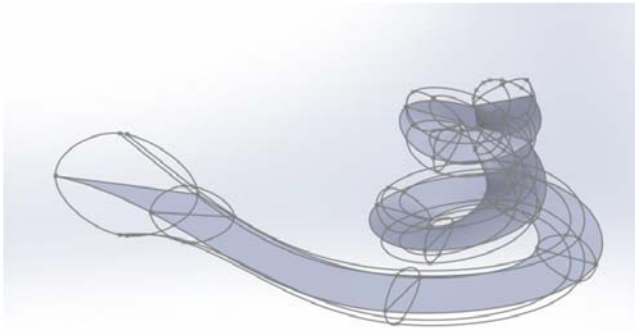


Fig. 1 Three-dimensional view of the inner ear showing the basal membrane [10]

membrane in the Organ of Corti.

B. Signal processing

In this experiment the processed stimuli contains the amplitude modulation only and the both amplitude and frequency modulation cues. A speech signal produced by a male talker (4 s.), a speech signal produced by a female talker (4 s.) and a fragment of a song (5 s) is used. The main parameters are the number of frequency bands varying from 1 to 32 (matching the number of auditory filters estimated psychophysically over the 80 Hz to 8800 Hz bandwidth [6]), type of the signal modulation (amplitude modulation only or the both amplitude modulation and frequency modulation) and signal to noise ratio varying from 1 dB to 20 dB.

Fig. 2 shows the block diagram of the processing strategy in general [3]. To produce the amplitude modulation only or amplitude plus frequency modulation processing, the signal is filtered into a number of some frequency bands ranging from 1 to 32. The distribution of the cutoff frequencies of the bandwidth pass filters is logarithmic according to the

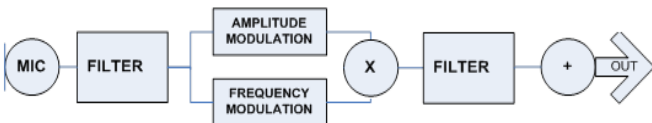


Fig. 2 Block diagram of the processing strategy in general [3]

Greenwood map [10]. The band-limited signal is then decomposed by the Hilbert transform into a slowly varying temporal envelope and a relatively fast-varying fine structure [6]. The slowly varying FM component is derived by removing the center frequency from the instantaneous frequency of the Hilbert fine structure and additionally by limiting the

frequency modulation rate to 400 Hz and the frequency modulation depth to 500 Hz [7].

The amplitude modulation-only is obtained by modulating the temporal envelope to the subchannels's center frequency and then summing the modulated subchannels signals [2]. The amplitude plus frequency modulation is obtained by additionally frequency modulating each band's center frequency and subchannels adding. Before that, both the amplitude modulation and the amplitude plus frequency modulation processed subchannels are subjected to the same bandwidth pass filter as the corresponding previous bandwidth pass filter to prevent crosstalk between bands and the introduction of additional spectral cues produced by frequency modulation.

C. Amplitude and frequency modulation

A signal, $s(t)$, can be approximated by a sum of N band-limited components, $x_k(t)$, containing both amplitude and frequency modulations [7]:

$$s(t) \approx \sum_{k=1}^N x_k(t) \quad (1)$$

The same signal can be presented as [7]:

$$s(t) = \sum_{k=1}^N A_k(t) \cos \left[2\pi f_{ck} t + 2\pi \int_0^t g_k(\tau) d\tau + \theta_k \right] \quad (2)$$

where,

A_k and $g_k(\tau)$ are the k-th band's amplitude and frequency modulations,

f_{ck} and θ_k are the k-th band's center frequency and initial phase.

If $x_k(t) = m(t) \cos [2\pi f_{ck} t + \varphi(t)]$, where $m(t)$ is the amplitude, and $\varphi(t)$ is the phase, then the in-phase signal can be derived [8]:

$$\begin{aligned} x_k(t) \cos(2\pi f_{ck} t) &= \\ \frac{1}{2} m(t) \cos[2(2\pi f_{ck})t + \varphi(t)] + \frac{1}{2} m(t) \cos \varphi(t) \end{aligned} \quad (3)$$

D. Mean squared error and signal to noise ratio

Mean squared error (MSE) is essentially a signal fidelity measure [9]. The goal of a signal fidelity measure is to compare two signals by providing a quantitative score that describes the degree of similarity/ fidelity or, conversely, the level of error/ distortion between them. Usually, it is assumed that one of the signals is a pristine original, while the other is distorted or contaminated by errors.

Suppose that $x = \{x_k | k = 1, 2, \dots, N\}$ and $y = \{y_k | k = 1, 2, \dots, N\}$ are two finite-length, discrete signals, original and processed. The MSE between the signals is given by the following Eq. (4) [10].

$$MSE(x, y) = \frac{1}{N} \sum_{k=1}^N (x_k - y_k)^2 \quad (4)$$

where,

N – number of signal samples,
 x_k – value of the k -th sample in x ,
 y_k – value of the k -th sample in y .

Signal-to-noise ratio (SNR) is defined as the power ratio between a signal (meaningful information) and the background noise (unwanted signal) [10]:

$$SNR = \frac{P_{signal}}{P_{noise}} \quad (5)$$

where,

P is average power.

Either signal and noise power must be measured at the same or equivalent points in the system, and within the same system bandwidth. If the signal and the noise are measured across the same impedance, then the SNR can be obtained by calculating the square of the amplitude ratio [10]:

$$SNR = \left(\frac{A_{signal}}{A_{noise}} \right)^2 \quad (6)$$

where,

A is root mean square (RMS) amplitude.

III. RESULTS

Fig. 3 shows the results of the numerical simulation of the signal processing the speech male and female sound sources in case of missing masking sound source.

On Fig.3 are visible the differences in the magnitude of the

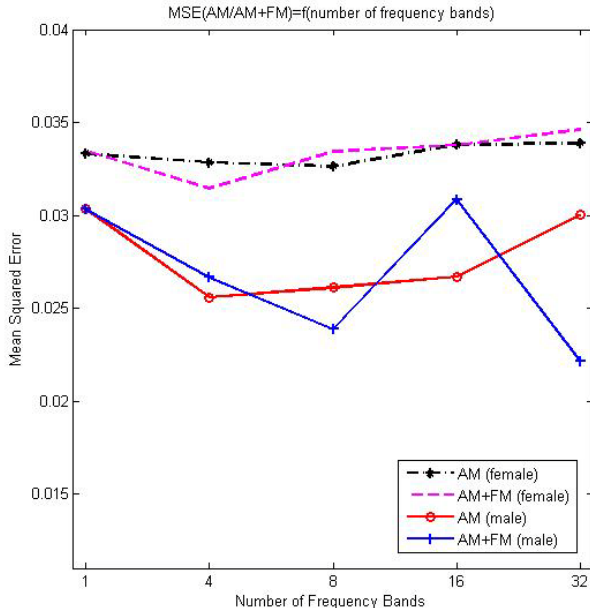


Fig. 3 Results of the numerical simulation of the signal processing the speech male and female sound sources in case of missing masking sound source.

mean squared error between male and female processed sound signals in case of amplitude modulation only and in case of combined amplitude and frequency modulation. The main conclusion here is that the processing strategy in case of

combined amplitude and frequency modulation and the case of amplitude modulation only are almost equally beneficial to the level of the mean squared error. In case of female sound source the MSE is slightly variable depending on the number of frequency bands. Compared to the results for the male sound source it leads to the conclusion that the best case for speech sound processing is 32 number of frequency bands by means of the combined amplitude and frequency modulation.

Fig. 4 shows the results of the numerical simulation of the signal processing of the speech male and female sound sources in case of masking sound source for 32 number of frequency bands.

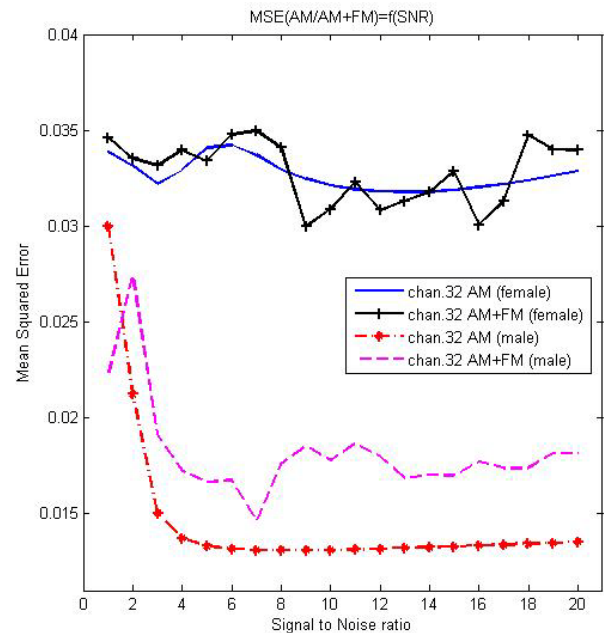


Fig. 4 Results of the numerical simulation of the signal processing of the speech male and female sound sources in case of masking sound source for 32 number of frequency bands .

On Fig. 4 are visible the same trends in the differences in the magnitude of the mean squared error between male and female processed sound signals. Here the curves in case of amplitude modulation only look more linear when $SNR > 8$ dB. A noise signal can make worse the processing strategy results in case of $SNR < 8$ dB for male sound source with amplitude modulation. In case of $SNR = 1$ dB or $SNR = 2$ dB it's better to be used combined amplitude and frequency modulation and then for $SNR > 8$ dB automatically to be switched to amplitude modulation only. The results for the female sound source the MSE is slightly variable depending on the level of SNR between AM and AM+FM conditions. In general the processing strategies in both conditions of modulation are almost equally beneficial to the level of the mean squared error separately for the male and for the female sound source. The result for the male sound source leads to the conclusion that

the best case for speech sound processing in 32 number of frequency bands by means of the amplitude modulation. This conclusion can be used for deciding how to process the speech signal in case of female sound source. It can be chosen to process all speech sound sources with amplitude modulation only in case of noise signal.

IV. CONCLUSION

Some conclusions are mentioned in the preview paragraph. Related to the presented results from the numerical simulations and considering to the different analyses in this paper it can be made a general conclusion how to process different speech sound signals from male and female sound sources in the world around. All of the investigations were made by real signal processing.

In general the presented results lead to the conclusion that mean squared error is lower when the speech sound signal source is from a male talker. This can be explained by the theory of the spectral differences between the both speech signals. The frequency modulation has a contribution to the strategy performance when conditions are with no masker/noise signal source (in quiet environment). Different speakers lead to different level of mean squared error, but the trends in results of the both modulations depending on the speaker's sex are kept.

REFERENCES

- [1] Tartter, V. C., Identifiability of vowels and speakers from whispered syllables, *Percept. Psychophys* 49, pp. 365–372, 1991
- [2] Wilson B. S., Finley C. C., Lawson D. T., Wolford R. D., Eddington D. K., Rabinowitz W. M., Better speech recognition with cochlear implants, *Nature*, vol. 352, pp. 236-238, 1991
- [3] Shannon R. V., Zeng F. G., Kamath V., Wygonski J. Ekelid M., Speech recognition with primarily temporal cues, *Science*, vol. 270, pp. 303–304, 1995
- [4] Alexandros P., Maragos P., Speech analysis and synthesis using an AM-FM modulation model, *Journal Speech Communication*. Vol. 28, Issue 3, pp. 195–209, 1999
- [5] Smith Z. M., Delgutte B., Oxenham A. J., *Nature*, vol. 416, pp. 87–90, 2002
- [6] Moore B. C., Glasberg B. R., Formulae describing frequency selectivity as a function of frequency and level and their use in calculating excitation patterns, *Hearing Research Journal*, vol. 28, pp. 209–225, 1987
- [7] Nie, K., Stickney, G. & Zeng, F. G., Encoding frequency modulation to improve cochlear implant performance in noise. *IEEE Trans. on Biomedical Engineering*, vol. 52, pp. 64-73, 2005
- [8] Chen, H. & Zeng, F. G., Frequency modulation detection in cochlear implant subjects, *Journal of the Acoustical Society of America*, vol. 116, pp. 2269–2277, 2004
- [9] Casella G., Lehmann E. L., *Theory of Point Estimation*. New York: Springer Verlag, 1998
- [10] Antonov S., Development of methods and algorithms for analysis and processing of audio signals in modeling auditory perception, Dissertation, Technical university Sofia, 2013

Include Macbeth in the MCDA Models Suggested by Italian Legislation for the Selection of the Most Economically Advantageous Tender in Contracts for Public Works. Comparison and Application of MCDA Model to a Case Study¹

Maria Rosaria Guarini

Department of Architecture and Design (DIAP)
Faculty of Architecture, "Sapienza" University of Rome
Rome, Italy
mariarosaria.guarini@uniroma1.it

Claudia Buccarini

Department of Architecture and Design (DIAP)
Faculty of Architecture, "Sapienza" University of Rome
Rome, Italy
claudia.buccarini@uniroma1.it

Fabrizio Battisti

Department of Architecture and Design (DIAP)
Faculty of Architecture, "Sapienza" University of Rome
Rome, Italy
fabrizio.battisti@uniroma1.it

Abstract—Directive 2004/18/EC of the European Parliament and of the Council of 31 March 2004 on the coordination of procedures for the award of public works contracts, public supply contracts and public service contracts, (2004/18/EC), provides that in Member States the commissioning body may base the choice of contractor on two award criteria

- the lowest price, where only the economic aspect is evaluated;
- the most economically advantageous tender, where a number of factors are evaluated.

In Italy, the 2004/18/EC directive has been adopted by the Code of Public Contracts for works, services and supplies, Legislative Decree No 163 of 2006 and subsequent amendments (Legislative Decree No 163/2006) and its implementing decree, Presidential Decree No 207 of 2010 (P.D. 207/2010), which, in

accordance with European case law, indicate complete equivalence between the two award criteria.

In accordance with the 2004/18/EC directive, Italian legislation provides that, between the two award criteria, the commissioning body must choose the most appropriate one depending on the nature of the contract. This decision by the commissioning body must be made by applying the criteria and objectives, and by ensuring compliance with the principles of transparency, non-discrimination and competition.

In order to rank the different tenders for the award of public works contracts using the criterion of the most economically advantageous tender, Legislative Decree No 163/2006 and P.D. No 207/2010 require the use of a Multicriteria Decision Analysis (MCDA) model.

Five MCDA models are suggested:

- Weighted Sum Model (WSM, Einhorn and McCoach, 1977);
- Analytic Hierarchy Process (AHP, Saaty, 1977);
- ELimination Et Choix Traduisant la RÉalité (ELECTRE, Roy, 1968);
- EVAluation of MIXed criteria (EVAMIX, Voogd, 1982);
- Technique for Order of Preference by Similarity to Ideal Solution (Topsis, Hwang and Yoon, 1981).

¹ This article is a revised and expanded version of a paper entitled "Proposta per l'utilizzo di un nuovo modello di analisi multicriteriale per scegliere l'offerta economicamente più vantaggiosa nei contratti di appalto dei lavori pubblici" presented at "Società Italiana Estimo e Valutazione" (SIEV) Seminary: Analisi Multicriteri, Valutazione, Processi decisionale, Torino, 29-30 maggio 2014

But the possibility of using any of the methods to be found in scientific literature is also indicated.

The aim of the text is to propose the application of a new MCDA model: the Measuring Attractiveness by a Categorical Based Evaluation Technique (MACBETH, Bana e Costa, Vansnick, 1994) has not yet been applied in the approximate evaluative field, in verifying either similarities/differences with other MCDA methods suggested by Italian legislation, or with reference to a case study, the advantages/disadvantages arising from the operational application of different MCDA methods considered.

Keywords— Multicriteria Decision Analysis, MACBET, Most economically advantageous tender, Appraisal, Public Works

CRITERIA FOR THE AWARD OF PUBLIC WORKS CONTRACTS IN ITALY

Directive 2004/18/EC of the European Parliament and of the Council of 31 March 2004 on the coordination of procedures for the award of public works contracts, public supply contracts and public service contracts, (2004/18/EC) [9] governs, for all Member States, the procedures that the commissioning body must follow when choosing the contractor, indicating that the criterion for the award can be referred to:

- the lowest price;
- the most economically advantageous tender.

The criterion of lowest price only considers the economic aspect of the tender and is adequate for meeting the requirements of the commissioning body when the work covered by the contract does not have by a particular technological value, or the commissioning body has already determined the qualitative and time specifications that are most modifiable.

The criterion of most economically advantageous tender permits evaluation of a number of aspects of the tender; it can be adopted when the objective characteristics of the contract suggest the relevance, for the purposes of the award, also of other factors: technical merit, aesthetic, technical, functional and time characteristics.

In Italy, Directive 2004/18/EC has been adopted in the Code of Public Contracts for works, services and supplies, Legislative Decree No 163 of 2006 and subsequent amendments (Legislative Decree No 163/2006) [10] which indicates the selection criteria for tenders, and its implementing decree, Presidential Decree No 207 of 2010 and subsequent amendments (P.D. No 207/2010) [8], which defines in detail the methodologies to be applied to make this selection.

The choice of the award criterion falls under the technical discretion of commissioning bodies, which must assess its adequacy with respect to the objective characteristics of the contract, applying criteria which ensure compliance with the principles of transparency, non-discrimination and equal treatment.

With regard to the award of public works contracts using the criterion of the most economically advantageous tender, P.D. No 207/2010:

- stipulates that it is necessary to employ a Multicriteria Decision Analysis² (MCDA) model but without giving instructions on the method of choice;
- tentatively suggests five possible MCDA models for developing in detail their structure and mode of application; refer to the consolidated bibliography:
 - Weighted Sum Model (WSM³, Einhorn and McCoach, 1977) [11];
 - Analytic Hierarchy Process (AHP, Saaty, 1977) [21], [22];
 - ELimination Et Choix Traduisant la REalitè (ELECTRE, Roy, 1968) [18], [19], [20];
 - EVAluation of MIXed criteria (EVAMIX, Voogd, 1982) [26], [27];
 - Technique for Order of Preference by Similarity to Ideal Solution (Topsis, Hwang and Yoon, 1981) [14], [15];
- still leaves the commissioning body the possibility of using any of the MCDA methods to be found in scientific literature.

In practice, the model most used by commissioning bodies appears to be the WSM, which is considered the easiest to use. The aim of the text is to propose application of the Measuring Attractiveness by a Categorical Based Evaluation Technique (MACBETH, Bana e Costa, Vansnick, 1994) [2], [3], [4], [5], [6] for the choice of the most economically advantageous tender in contracts for public works contracts, in order to highlight at operational level the possible advantages and disadvantages of its use in comparison with other adoptable MCDA models.

In the text, an introductory framework section will be followed first by a comparison between the structure of MACBETH and of other MCDA models suggested by Italian legislation (WSM, AHP, ELECTRE, EVAMIX, TOPSIS), to explain the differences and similarities; the different models will then be applied to a concrete case study; the results obtained from their application will be briefly explained in such a way as to highlight in the comparison the similarities and possible advantages/disadvantages in their operational use.

THE MCDA MODELS INDICATED BY ITALIAN LEGISLATION FOR THE AWARD OF PUBLIC WORKS CONTRACTS AND THE MACBETH MODEL

Building a comparative framework for comparison (Fig. 1) of the configuration and division into phases of MACBETH and of the MCDA models suggested by Italian legislation, the similarities and differences in the method to be used in data processing emerge.

² MCDA are multi-parametric evaluation tools of a mathematical nature used to support decision-making processes. They make it possible to perform comparative evaluations of alternatives through the definition of a scale of preference, defined as a function of the synthesis of complex and heterogeneous information that is both qualitative and quantitative.

³ In P.D. No 207/2010, the model is indicated with the Italian term Aggregativo Compensatore (Aggregative Compensator) (AC)

All major MCDA models considered are divided into phases that are successive and preliminary among themselves:

- Construction of the evaluation matrix;
- A1. Standardisation of data of the evaluation matrix (only for certain models);
- B. Application of weights to standardised data;
- C. Ranking of alternatives.

A. Construction of the evaluation matrix (EM)

Construction of a square type matrix (alternatives $j \times$ criteria i) whose elements E_{ji} represent the performance that the different alternatives j possess with respect to each of the criteria i considered (quantitative and/or qualitative); these elements, depending on the MCDA model applied, can be expressed as:

- coefficients from 0 to 1 (WSM, AHP);
- absolute values (MACBETH);
- mixed values: coefficients (0 to 1) and absolute values (ELECTRE, EVAMIX, TOPSIS);

Therefore depending on the model used, the EM will be constituted by elements E_{ji} expressed with values that are:

- homogeneous, immediately comparable (WSM, AHP): matrix of coefficients;
- non-homogeneous and therefore not comparable: performance matrix (ELECTRE, EVAMIX, TOPSIS) and data matrix (MACBETH). In order to then proceed with comparison between the data entered in these two matrices, these data must be "standardised".

A1. Standardisation of the EM data (only for ELECTRE, EVAMIX, TOPSIS, MACBETH)

Application of mathematical functions, which differ according to the model used, to make the elements E_{ji} of the EM homogeneous and comparable; structuring of the standardised data N_{ji} EM in:

- standardisation matrices (SM): square type (alternatives $j \times$ criteria i) whose elements N_{ji} consist of the EM data made dimensionless through linear functions (ELECTRE, EVAMIX, TOPSIS);
- criteria scales (CS): whose steps consist of cardinal values N_{ji} that represent the ranking of the alternatives for each criterion considered, obtained through readjustment functions (MACBETH).

The complexity of the linear functions used for the construction of the SM makes application of automated computer supports necessary.

Fig. 1 Comparison between the structure of MCDA models listed in P.D. No 207/2010 and the MACBETH model

B. Application of weights to standardised data

Weigh the standardised values N_{ji} by applying, according to the model used, mathematical formulae/logical steps that make it possible to assign to each criterion the weight W_i of the importance that it assumes for persons who must make judgmental evaluations.

| MCDA MODELS P.D. No 207/2010 | | | | | |
|--|--|---|---|---|-----------------|
| PHASES | ELECTRE | EVAMIX | TOPSIS | WSM | AHP |
| CONSTRUCTION OF THE EVALUATION MATRIX (EM) | | Performance matrix | | Matrix of coefficients | Data matrix |
| square type matrix (alternatives $j \times$ criteria i) | quantitative | Absolute values | | Coefficients (0-1) | Absolute values |
| Whose elements E_{ji} considered criteria: | qualitative | | | | |
| STANDARDISATION OF THE EM DATA | Standardisation matrices (SM) square type matrix ($j \times i$) whose elements N_{ji} made dimensionless through linear functions: Divide E_{ji} for the larger value of E_i $N_{ji} = \frac{E_{ji}}{E_i(>)}$ | | Already standardised | Criteria scales (CS) whose steps consist of cardinal values (0-100) N_{ji} obtained through readjustment functions | |
| Elements (E_{ji}) of the EM have to make homogeneous and comparable (N_{ji}) structuring of the standardised data N_{ji} in: | | Divide E_{ji} for the square root of the sum of squares of E_i $N_{ji} = \frac{E_{ji}}{\sqrt{\sum E_i^2}}$ | | | |
| APPLICATION OF WEIGHTS (W) | Logical steps Define the differences between the alternatives | Multiply each element of the SM/EM for its W $Nw_{ji} = N_{ji} \times W_i$ | Multiply the EM for the vector weights $Nw_{ji} = [MV] \times [W]$ | Multiply each element of the CS for its W $Nw_{ji} = N_{ji} \times W_i$ | |
| Calculate the total score (TS_j) by applying: | | | | Weighted sum | |
| RANKING OF ALTERNATIVES | Indices of concordance and discordance pairwise comparison of all the alternatives j and measurement of concordance and discordance indices | Weighted sum Sum of the weighted elements (Nw_{ji}) Relative to the alternative j -th $TS_j = \sum Nw_{ji}$ | Indices of concordance and discordance pairwise comparison of all the alternatives j and measurement of concordance and discordance indices | Weighted sum Sum of the weighted elements (Nw_{ji}) Relative to the alternative j -th $TS_j = \sum Nw_{ji}$ | |

C. Ranking of alternatives

Calculate the total score (TS_j) of each alternative j taking into account the different criteria considered. Depending on the MCDA model used:

- weighted sum: sum of the weighted elements NW_{ji} relative to the alternative J -th; (WSM, AHP, EVAMIX, MACBETH);
- indices of concordance and discordance: pairwise comparison of all the alternatives j and measurement of concordance and discordance indices that quantify respectively the satisfaction/regret with choosing one alternative over another (ELECTRE, TOPSIS).

From comparison of the MCDA models, it emerges that (Fig. 2) MACBETH permits processing the data in the EM more quickly than with other models (ELECTRE, TOPSIS, AHP), whose methods require complex logical/mathematical steps. Even compared with models (WSM, EVAMIX) whose application requires simple steps, the MACBETH model presents the advantage of requiring only absolute values for construction of the EM.

This simplicity of processing makes the model manageable and usable without invoking computer support for the management and processing of input data.

The MACBETH model also enables formulation of a complete ranking of the alternatives with respect to ELECTRE which, instead, defines a partial ranking.

Compared with other MCDA models, the MACBETH model requires the evaluator to provide a preferential judgment with respect to the difference in attractiveness among the alternatives; such a subjective type evaluation could affect the final result of the processing of the model, making it unverifiable.

| MCDA MODELS P.D. No 207/2010 | | | | | |
|---|---------|--------|--------|-----|---------|
| LIMITS | ELECTRE | EVAMIX | TOPSIS | WSM | MACBETH |
| Long processing times of the model | x | | x | | |
| Permits a partial ranking of tenders | x | | | | |
| Does not directly provide a ranking of tenders, expressed on a cardinal scale, compared on the basis of the individual criteria considered | | | x | | |
| Does not require the evaluator to provide a preferential judgment | | | | x | |
| POTENTIAL | | | | | |
| Short processing times of the model | | x | | | |
| Permits a complete ranking of tenders | | | x | | |
| Provides for each criteria a ranking of tenders, expressed on a cardinal scale from 0 to 100, by evaluating the different appreciation for tenders on the basis of the individual criteria considered | | | x | | |
| Requires the evaluator to provide a preferential judgment with respect to the difference in attractiveness among the alternatives | | | x | | |

Fig. 2 Limits and potential of MCDA models indicated in P.D. No 207/2010 and the MACBETH model

APPLICATION OF DIFFERENT MCDA MODELS TO A CASE STUDY FOR THE SELECTION OF THE MOST ECONOMICALLY ADVANTAGEOUS TENDER

The case study assumed for operational application of the different MCDA models indicated by P.D. No 207/2010 (WSM, ELECTRE, EVAMIX, TOPSIS) and MACBETH is the invitation to tender for an “integrated contract through a procedure open to the most economically advantageous tender for award of design and construction of changing rooms with

grandstand at the sports centre in the municipality of Rho, Milan”⁴

For the case study, the following were assumed for operational application of the models (Fig. 3):

- the set of criteria and their weights, obtained from the invitation to tender;
- the scores assigned by the selection board to the four tenders submitted (A, B, C, D);

| CRITERIA | WEIGHTS | SCORES OF TENDERS | | | |
|---------------------|---------|-------------------|------|------|------|
| | | A | B | C | D |
| Architectural value | 20 | 15 | 10 | 12,5 | 13,5 |
| Technical value | 25 | 12 | 14,5 | 14,5 | 11 |
| Functional value | 25 | 9,2 | 11,2 | 16 | 11 |
| Economic offer | 20 | 15 | 9 | 4 | 50 |
| Time | 10 | 90 | 120 | 120 | 120 |

Fig. 3 Criteria, weights and scores of tenders

The EM for the different models considered was constructed on the basis of these data, applying the procedures formalised for each one (Fig. 4).

| MODELS | CRITERIA | TENDERS | | | |
|-----------------------------|---------------------|---------|------|------|------|
| | | A | B | C | D |
| WSM | Architectural value | 1 | 0,67 | 0,83 | 0,9 |
| | Technical value | 0,83 | 1 | 1 | 0,76 |
| | Functional value | 0,57 | 0,7 | 1 | 0,68 |
| | Offerta economica | 0,3 | 0,18 | 0,08 | 1 |
| | Time | 0,75 | 1 | 1 | 1 |
| EVAMIX TOPSIS ELECTRE | Architectural value | 1 | 0,67 | 0,83 | 0,9 |
| | Technical value | 0,83 | 1 | 1 | 0,76 |
| | Functional value | 0,57 | 0,7 | 1 | 0,68 |
| | Economic offer | 15 | 9 | 4 | 50 |
| | Time | 90 | 120 | 120 | 120 |
| MACBETH | Architectural value | 15 | 10 | 12,5 | 13,5 |
| | Technical value | 12 | 14,5 | 14,5 | 11 |
| | Functional value | 9,2 | 11,2 | 16 | 11 |
| | Economic offer | 15 | 9 | 4 | 50 |
| | Time | 90 | 120 | 120 | 120 |

Fig. 4 Evaluation matrix

Subsequently, the non-homogeneous data contained in the EM were standardised, constructing the SM (WSM, EVAMIX, ELECTRE, TOPSIS) and the CS (MACBETH); weights (taken from the invitation to tender) were then applied to the standardised data.

Finally, through the operations of processing of the weighted data, a ranking of the tenders according to each

⁴ All the information relating to the invitation to tender are present on <http://www.comune.rho.mi.it/Bandi-Aaggiudicati/Bandi-di-gara-e-Concorsi/Bandi-Aaggiudicati/Archivio-Bandi-2011/Gara-dappalto-con-procedura-aperta-ad-offerta-economicamente-piu-vantaggiosa-per-l'affidamento-della-progettazione-e-realizzazione-spoliatoi-con-tribuna-presso-il-centro-spor>

MCDA method was obtained (Fig. 5).

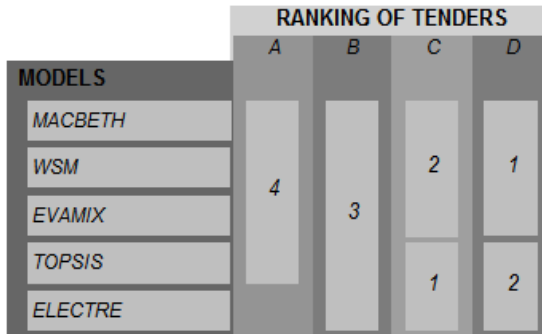


Fig. 5 Ranking of tenders

By comparing the results obtained from application of the models indicated by P.D. No 207/2010 and the MACBETH model, it was possible to find similarities and differences and possible advantages/disadvantages in their operational use.

It was also possible to verify, from the operational point of view, the validity of MACBETH as a tool for selection of the most economically advantageous tender in public works contracts.

Observing the different rankings of the alternatives produced by application of the models, it can be seen that, by applying the same methodology of data aggregation, WSM, EVAMIX and MACBETH permit formulation of results that are consistent with each other.

Compared with other MCDA models, ELECTRE permits only a partial ranking of tenders, eliminating those that are completely dominated [28].

In addition, the MACBETH model makes it possible to define the quantification of appreciation of the alternatives on the basis of the individual criteria considered, expressed on a cardinal scale from 0 to 100.

REFERENCES

- [1] D. Albonetti, S. Degli Espositi, "L'offerta economicamente più vantaggiosa e l'analisi multicriteri", Maggioli Editore, 2011
- [2] C. Bana e Costa, J. Vansnick "MACBETH: An interactive path to-wards the construction of cardinal value functions" in Operational Research, 1, 1994, pp. 387-500
- [3] C. Bana e Costa, L. Ensslin, E.C. Corrúa, J. Vansnick, "Decision Support Systems in action: Integrated application in a multicriteria decision aid process" in European Journal of Operational Research, 113, 1999, pp. 315-335
- [4] C. Bana e Costa, "The use of multi-criteria decision analysis to support the search for less conflicting policy options in a multi-actor context: case study" in Journal of Multi-Criteria Decision Analysis, 10, 2001, pp. 111-125
- [5] C. Bana e Costa, J. Ramos, J. Vansnick, "Multicriteria approach for strategic town planning: the case of Barcelos" in Kluwer Academic Publishers, Book Series: International Series in Operations Research e Management Science, vol. 44, 2002, pp. 429-456
- [6] C. Bana e Costa, J. Vansnick "On the mathematical foundations of MACBETH. Multiple Criteria Decision Analysis: State of the Art Surveys", Springer, New York, pp 409-442
- [7] G. Dandri, "L'offerta economicamente più vantaggiosa. Tecniche economiche e procedimenti estimativi", in Performance, 22, 1992, pp. 51-74
- [8] Decreto Presidente della Repubblica 5 ottobre 2010, 207, Regolamento di esecuzione ed attuazione del decreto legislativo 12 aprile 2006, n. 163
- [9] Directive 2004/18/EC of the European Parliament and of the Council of 31 March 2004 on the coordination of procedures for the award of public works contracts, public supply contracts and public service contracts
- [10] D.Lgs 12 aprile 2006, n. 163, Codice dei contratti pubblici relativi a lavori, servizi e forniture
- [11] H. J. Einhorn, W. McCoach, "A simple multiattribute utility procedure for evaluation", in Behavioral Science, 22, 1977, pp. 270-282,
- [12] J. Figueira, S. Greco, M. Ehrgott, "Multiple Criteria Decision Analysis: The State of the Art Surveys" Springer ScienceBusiness Media, New York, 2005.
- [13] J. Figueira, B. Roy "Determining the weights of criteria in the ELECTRE type methods with a revised Simos' procedure" in European Journal of Operational Research, 139, 2002, pp. 317-326
- [14] C. L. Hwang, K. Yoon, "Multiple attribute decision making: Methods and applications", Heidelberg Springer, New York, 1981
- [15] C. L. Hwang, K. Yoon, "TOPSIS for MODM" in European Journal of Operational Research, 76, 1994, pp. 486-500
- [16] P.Mori, "Il metodo aggregativo-compensatore come criterio di aggiudicazione di aste," in SIPI Spa, 1, 2012, pp 311-346
- [17] F. Romano, F. Sbicca, A. Zaino, Direzione Generale Osservatorio dei Contratti Pubblici - Analisi e studio dei mercati, Autorità per la vigilanza sui contratti pubblici di lavori, servizi e forniture, Quaderno, "il criterio dell'offerta economicamente più vantaggiosa", Dicembre 2011
- [18] B. Roy, "Classement et choix en présence de points de vue multiples: La méthode ELECTRE", in Revue Française d'Informatique et de Recherche Opérationnelle, 8, 1968, pp. 57-75
- [19] B. Roy, "Optimisation et aide à la décision", in Journal de la Société de Statistique de Paris, 3, 1976, pp 208-215
- [20] B. Roy, "A multicriteria analysis for trichotomic segmentation problems", in P. Nijkamp and J. Spronk, editors, Multiple Criteria Analysis: Operational Methods, Gower Press, 1981, pp. 245-257
- [21] T. Saaty, "A scaling Method for priorities in herarchical structures" in Math psychology, 15, 1977, pp. 234-281
- [22] T. Saaty. "The analytic hierarchy process", McGraw Hill, New York, 1980
- [23] W. Tonietti, "Le gare con l'offerta economicamente più vantaggiosa", IPSOA, 2007
- [24] O. Vaidya, S. Kumar, "Analytic Hierarchy Process: an overview of applications" in European Journal of Operational Research, 169, 2004, pp. 1-29
- [25] A. Violano, "Metodi multicriterio di supporto alle decisioni. Applicazione del metodo Evamix con l'approccio del punto ideale" in Atti del convegno Matematica e Architettura, Firenze, 2002
- [26] H. Voogd, "Multicriteria Evaluation with Mixed Qualitative and Quantitative data" in Environment and Planning, 9, 1982, pp. 221-236
- [27] H. Voogd, "Multicriteria Evaluation for urban and regional planning", Pion Limited, London, 1983
- [28] Morano, P., Un modello multicriterio «fuzzy» per la valutazione degli interventi di riqualificazione urbana. Aestimum, (39), Firenze, 2009

Using Integral E-Portfolio to learn Linear Algebra

M.Isabel García-Planas

Departement de Matemàtica Aplicada I

Universitat de Politècnica Catalunya

Barcelona, Spain

maria.isabel.garcia@upc.edu

Judit Taberna

Departament d'Expressió Gràfica Arquitectònica I

Universitat Politècnica de Catalunya

Barcelona, Spain

judit.taberna@gmail.com

Abstract—The use of e-portfolio is becoming common in the learning and assessment of students. This is due to the need of teachers to enhance student autonomy making them to reflect on the process of learning. Lately, we have worked with different software, facilitating its generation and use. In this paper, the recent experience in the use of e-portfolio for undergraduate students of the Universitat Politècnica de Catalunya are set.

Index Terms—E-portfolio, integral e-portfolio, linear algebra.

1. INTRODUCTION

Throughout history the use of portfolios was more common in other areas of knowledge than mathematics in general and linear algebra in particular, as, for example, in architecture and arts fields. The emergence of Information and Communication Technology (ICT) has caused a change in the world of education and one tool in within the ICT context is the use of e-portfolio.

In recent years is becoming habitual use of the electronic portfolio for learning and assessment of students. This is due to the need for teachers empower students through reflection on their own learning processes ([17]). The electronic portfolio not only is an electronic learning portfolio, its great potential could be used in other professional fields. In the field of education has extended its use as a technique for gathering evidence and competencies rather than integrating evaluation in the teaching-learning process by collecting samples of learning activities at key moments and reflecting on achievements and difficulties encountered in the scope of both generic and specific competencies that had been proposed, showing their ability and progress.

In the last years several authors work in introducing the e-portfolio at the higher education, as

we can see in [2], [4], [5], [8], [10],[11], [13], [17] and [16] for example.

2. LINEAR ALGEBRA FOR UNDERGRADUATES

It is well known that Linear algebra is fundamental in different areas of sciences. Because of multiple problems can be modelled by means linear systems where linear algebra became essential to obtain and discuss the solution.

Nevertheless, one of the main difficulties to overcome in the first year courses of university students enrolled in different programs other than the career math is that they do not see the importance that mathematics may have in their fields of interest. This can seriously affect their motivation in the course, and its ultimate success. This effect appears to be more pronounced in the first year of linear algebra due to its abstract factor, while the calculus find it easier to think that may be useful.

To address the question that every teacher of linear algebra often heard: why do we need to know that? we can make use of new technologies and in particular we can use the e-portfolio.

After to propose several projects about real life problems, students can place their progress in the e-portfolio. Through the e-portfolio, the students can discuss among peers and with the teacher.

In this paper we present a model of e-portfolio for the subject of linear algebra. This model will be implemented in engineering studies of the higher technical School of Engineering at the Universitat Politècnica de Catalunya.

To prepare this e-portfolio has been essential define the goals which we want that the students reach as well as the topics that we consider basic to overcome objectives.

The topics include linear system equations, vector spaces, matrices, linear maps, the matrix of a linear transformation, change of basis, eigenvalues and eigenvectors (see [12] and [15] for an undergraduate course of linear algebra).

3. E-PORTFOLIO

Portfolio is a word of French origin “portefeuille” meaning briefcase for carrying books, papers, etc. In the field in question, the university teaching, the word comes from “Portfolio Assessment” or “Portfolio process”, so it has the sense of “assessment folder” or a broader form of “learning portfolio”. In the case where this activity takes place on a digital platform called an e-portfolio. More specifically in our context, the portfolio is a method of teaching, learning and assessment is the contribution of different types of productions by students through which they can judge their abilities in the context of a discipline or field of study. These productions staff report process followed by the student, allowing him and others to see their efforts and achievements in relation to the learning objectives and evaluation criteria previously established.

A. Different ways of using the e-Portfolio

The e-portfolio allows students and teachers, create and manage a virtual space with both personal, academic and professional (see [3]); turn incorporating a review and justification of the importance of these activities have.

a) E-Portfolio Evaluation:

It allows to assess the achievement of specific criteria to obtain a degree or work.

b) E-Learning Portfolio:

Allows providing information on learning objectives incorporating both self-reflection and the student and the teacher

c) E-Portfolio “Demonstration of best practices”:

Allows submit information to specific audiences or achievements.

d) E-Portfolio Transition:

Let us bring evidence and records useful in times of transition or passage of an academic level to another

Regardless of the mode of use of e-portfolio, the process of design, creation and development in-

volves data collection, organization, reorganization and presentation.

Hellen C. Barrett in [6] proposes a balance between all the possibilities of use of e-Portfolio and is represented by means the graphic Figure 1. Specifically in the graph, the author proposes a

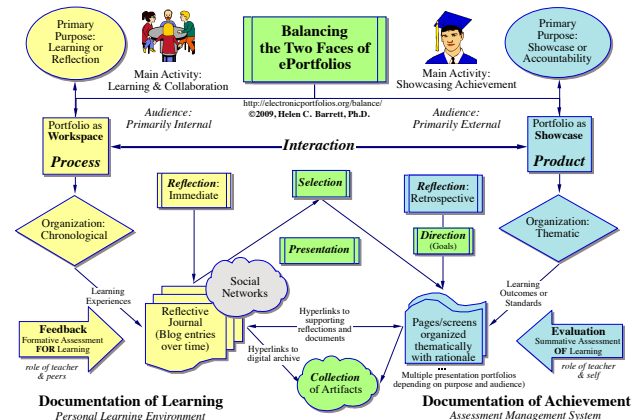


Figure 1. Balancing the Two Faces of ePortfolios [6]

balance between different aspects of the e-Portfolio that interact along a continuum such as: Process-Product, Immediate reflection-Reflection retrospective, Reflective journal-Organized web pages, Formative evaluation-Summative evaluation, Learning documentation-Documentation of achievements, among others.

4. THE E-PORTFOLIO AND LINEAR ALGEBRA COURSE

After analyzing the different types of e-portfolio, firstly we thought that the most appropriate model of e-portfolio would be used in a course of linear algebra is the “e-Portfolio as a repository of learning experiences”

By means this kind of e-portfolio, teachers and students can work activities and teaching and learning using the Internet. More specifically

a) The student uses the e-portfolio for:

- 1) Collect, systematically, the learning achievements,
- 2) Self-assess how to acquire and develop the skills required in the subjects they are studying.

- 3) Self-assess their learning outcome.
- b) The teacher uses the e-portfolio for:
 - 1) Collect and place the work done by students in their courses.
 - 2) Evaluate how to acquire and develop skills by students through the implementation of some activities (with the tutor, with the peer group, independently, etc.).
 - 3) Evaluate the outcome of learning.

But finally and after observing that the different uses of e-portfolio are not exclusive and all of them can be used simultaneously, we believe that the most appropriate is to use the “integral e-portfolio”, that is to say an e-portfolio that integrates all the different uses.

With this type of e-portfolio, cooperative learning is stimulated, this type of learning is very important for engineering studies (see [1]).

5. INTEGRAL E-PORTFOLIO EDITION

To implement the integral e-portfolio we use the integrated Moodle and Mahara (Mahoodle) platform, as well as the simultaneous use of platforms Exabis inside Moodle and Google Sites.

Different authors as for example Diana Bri, Miguel García, Hugo Colls, Jaime Lloret in [7]), analyze educational platforms in order to facilitate the decision about platform on which to choose.

“Mahoodle is the usual name given to the joining of the systems Mahara and Moodle. Mahara is an open source e-Portfolio and social networking web application and Moodle it is an open source e-learning platform, also known as a Learning Management System, or Virtual Learning Environment. Both systems have built-in support for each other in the form of single sign-on and transfer of content or export different types of objects from Moodle to Mahara (API Portfolio) and to import objects from Mahara to Moodle (API repository). You can only link one to one Moodle Mahara either place the level of an individual institution or individual institution. You can not link Moodle in various institutions in Mahara. Exabis is also an open source of e-Portfolio able to be connected to Moodle by means of a plug. We are using the e-portfolio 4.1 version for Moodle, “My Portfolio” in Exabis, let us users upload files,



Figure 2. E-portfolio Mahoodle model,

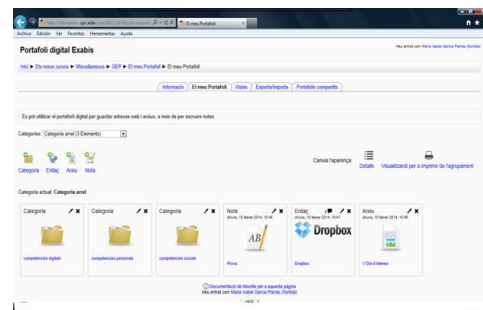


Figure 3. E-portfolio Exabis inside Moodle

In figures 2 and 3, images of two models of e-portfolios that have been made using Mahoodle and Exabis + Moodle respectively have been presented.

With respect Figure 2 we have included different sections to help to the students to configure their e-portfolio. The selected model is in such a way that fits the needs of the course, although students can add more paragraphs to make visible their portfolio and can display more information of the minimum required for the course. In the left side appear the icons to introduce the profile and curriculum, a place to put files and a place to keep a journal. In the center the icons that allow you to organize personalized portfolio and the right side is the place to share (links to discussion groups) set the privacy level of each part of the portfolio.

In Figure 3 different pictures called categories where each of them gives access to different competencies are observed. It is possible to access to multiple frames and assign different categories. In this particular case, we have chosen three categories for storing information, one of one is for the student profile, there is also access to a table that is used for notes and drafts and also there is network access.

The Exabis platform is simpler than Mahara however is easier to import and export materials

from Moodle.

6. EXPERIENCES IN USING E-PORTFOLIO

In our experience with students from the Universitat Politècnica de Catalunya has been taken into account that the learning activities for the development of an electronic portfolio are setting learning objectives, data collection, peer review, feedback from peers, reflection, and sharing of materials. These activities include gathering knowledge, organization, reorganization, presentation, sharing, application, knowledge accumulation and management.

During the year 2012-13 started a pilot implementation of the e-portfolio in the student test using Mahoodle management system within the Athena Labs platform. This project is developing and testing with a selected few number of student participation. In the year 2013-14 the pilot has expanded to the use of Exabis + Moodle. With this assay we can compare advantages and disadvantages according with Mahara or Exabis was used.

The academic results obtained by the students who have participated in this pilot have been better than those of other students. However, the small number of students who have participated not allow to extrapolate results. The next academic year 2014-15 will launch this pilot but in this case the assay will involve all students enrolled in the first year of undergraduate degrees in Industrial Technology, Chemical Engineering and Materials Engineering.

The study has been performed on the portfolio to be used in the subject of algebra can be applied to other materials, but the structure of the portfolio must be adapted to the subject. In fact, during the academic year 2011-12, we conducted a pilot study for the subject of drawing, but in this case the online application used to be Google Sites. Participants were chosen from among students of the School of Architecture of Barcelona of Universitat Politècnica de Catalunya, studying the subject of drawing I corresponding to the first year of studies. The pilot test was conducted in two groups called M13 and T21 with a share of 82.19% and 92.14% of students, respectively. The procedure followed was to integrate an e-portfolio in their academic activities distinguishing traditional teaching of distance teaching. Students also introduce its curriculum and

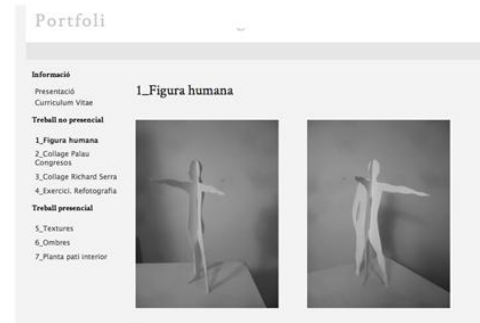


Figure 4. Source: ETSAB, Drawing Course I, year 2011-12

the work, should develop a short summary including both text and images summarizing the results of the activities. The instrument used as we discussed was the Google Sites platform.

7. CONCLUSION

As a conclusion we show some advantages of using portfolio

- Promotes global formative assessment
- Integrate generic and specific skills
- It allows the student to demonstrate the depth of their learning,
- Provides opportunities to reflect on their learning and how far they have come
- Learning to learn and take more responsibility in their learning process
- Provides opportunities and evidence to evaluate teaching
- Facilitates horizontal and vertical coordination of content (feedback from colleagues, department, etc.).

Through our experiences we can conclude that the e-portfolio through Mahoodle is a good tool to link teachers with students and vice versa, and to optimize this tool is necessary to improve the interconnection between Mahara and Moodle platforms, and also Exabis and Moodle.

In order to enable students to actively use the e-portfolio is necessary for teachers to prepare guidelines and provide a reference template.

Moreover teachers must prepare and plan the course comprehensively in order to coordinate the different tasks carried out in the classroom with the work of the e-portfolio.

REFERENCES

- [1] I. Asshaari, H. Othman, N. Razali, N.M. Tawil, F.H.M. Ariff, *Comparison between Level of Students' Responses toward Cooperative Learning in Mathematics Engineering Courses at UKM*. Wseas Transactions on Advances in Engineering Education, **8**, (2), (2011), pp. 53-61.
- [2] M.A. Bairral, R.T. dos Santos, *E-Portfolio Improving Learning in Mathematics Pre-Service Teacher*. Digital Education Review, **21**, (2012), pp. 1-12.
- [3] E. Barberà, G. Bautista, A. Espasa, T. Guasch, *Portfollio electrónico: desarrollo de competencias profesionales en la red*. (2006). http://www.uoc.edu/rusc/3/2/dt/esp/barbera_bautista_espasa_guasch.pdf
- [4] R. Barragán, *El portafolio, metodología de evaluación y aprendizaje de cara al nuevo espacio Europeo de Educación superior. Una experiencia práctica en la Universidad de Sevilla*. Revista Latinoamericana de Tecnología Educativa, **4** (1),(2005), pp. 121139.
- [5] H. Barrett, *Create Your Own Electronic Portfolio (using off-the-shelf software)*. Learning and Leading with Technology, (2000).
- [6] H. Barrett, *Balancing the Two Faces of ePortfolios*. Educação, Formação & Tecnologias, **3** (1), (2010), pp. 6-14.
- [7] D. Bri, M. García, H. Coll, J. LLoret, *A Study of Virtual Learning Environments*. Wseas Transactions on Advances in Engineering Education, **6**, (1), (2009), pp. 33-43.
- [8] G.M. Brandes, N. Boskic, *E-portfolios: From description to analysis*. International Review of Research in Open and Distance Learning, **9**, (2),(2008), pp. 1-17.
- [9] F. Campos Sánchez, F. Abarca Álvarez, (2014) *La rúbrica como herramienta de enseñanza, aprendizaje y evaluación del urbanismo*. Innovaggogia 2014.
- [10] S.C. Cismas, *Effective Foreign Language Portfolios in Engineering Education* . Wseas Transactions on Advances in Engineering Education **6**, (11), (2009), pp. 383-398.
- [11] R. C. Costa, *The use of the e-portfolios in the student's learning at the Federal e Institute of Education, Science and Technology of Maranhão/Campus Codó*. Seropédica, Rio de Janeiro, UFRRJ/PPGEA (Master Dissertation in Education). (2009). <http://www.ia.ufrrj.br/ppgea/dissertacao/Ronaldo%20Campelo%20da%20Costa.pdf>
- [12] M.I. Garcia-Planas, J.L. Domínguez, "Introducción a la teoría de matrices positivas. Aplicaciones. Ed. Iniciativa Digital Politécnica, Barcelona, (2013).
- [13] S. Jones, (2008). *E-portfolios and how they can support Personalisation. Improving learning through technology*. Becta UK (2008).
- [14] M. Kimball, (2002) "The Web Portfolio Guide: Creating Electronic Portfolios for the Web", Longman.
- [15] D.C. Lay, *Linear Algebra and Its Applications*. Addison-Wesley, (1994).
- [16] C. Mccowan, W. Harper, K. Hauville, (2005). *Student E-Portfolio: The Successful Implementation of an E-Portfolio across a Major Australian University*. Australian Journal of Career Development. **14**, (2), pp. 40-51.
- [17] A. Pitarch, A. Alvarez, J. Monferrer, *El ePEL: la gestión del aprendizaje a lo largo de la vida. Portafolios electrónicos y Educación Superior en España*.http://www.um.es/ead/Red_U/m3/. (2009).

Piezoelectric based vibration energy harvester with tip attraction magnetic force: modeling and simulation

Dauda Sh. Ibrahim¹, Asan G.A. Muthalif^{2*}, Tanveer Saleh

Department of Mechatronics Engineering
 International Islamic University Malaysia (IIUM)
 Jalan Gombak, 53100, Kuala Lumpur, Malaysia
¹ sidauda85@gmail.com, ^{2*} asan@iium.edu.my

Abstract— In recent times, vibration based energy harvesting has drawn attention of many researchers worldwide. This is due to advancement in Microelectromechanical (MEM) devices and wireless sensors with power requirements in range of microwatts-milliWatts; hence vibration energy sources have promising potentials for such demands. Thus, many attempts were made by researchers to develop different system configurations for effective utilization of vibrations that happen all around us. Cantilever beams with piezoelectric patches are used to harness kinetic energy from mechanical vibrations. This paper is aimed at studying the effect of adding a magnetic force at the tip mass, which is also a magnet with opposite pole, on power output of the energy harvester. The additional attraction force between the tip mass and the fixed magnet influences stiffness of the system, whilst tuning the natural frequency. Mathematical equation to depict the relationship between tuned natural frequency and distance between permanent magnet is derived. The lumped parameter model for the harvester with single fixed magnets aligned with magnetic tip mass is derived. MATLAB software is used to perform the simulation study on influence of the magnet on the harvester.

Keywords— Piezoelectric; Magnet; Vibration energy harvester

I. INTRODUCTION

Recent interest in developing micro and macro electromechanical systems for harvesting ambient vibration energy has increased immensely as reviewed in [1, 2]. This is as a result of rapid development in technology of small electronic devices with very low power requirements. Piezoelectric based vibration energy harvester among other forms of transduction mechanisms such as electromagnetic and electrostatic harvesters [3] has stood the test of time in providing required energy to power these devices. Due to that, many efforts were made by researchers to develop mathematical models of different piezoelectric, beam configurations for effective estimation of power output of the harvesters. Diyana et al.[4] derived the mathematical model of a single and comb-shaped piezoelectric beam

structure based on Euler-Bernoulli beam theory. The model used to estimate the influence of the proposed structure (i.e. Comb-shaped beam) in generating voltage output when excited at the base. Erturk et al.[5] proposed a model of an L-shaped piezoelectric beam energy harvester. This configuration is modeled as a linear distributed parameter model for predicting the electromechanical couple voltage response and displacement response for the energy harvesting structure. De Marqui junior C. et al.[6] presented an electromechanical coupled finite element (FE) plate model for the estimation of power output of piezoelectric energy harvester plates.

It is noteworthy that Modeling techniques are not limited to the aforementioned; several other approaches are available for the derivation of mathematical models of piezoelectric beam energy harvester configuration. Rayleigh Ritz method, Hamilton Principle and single degree of freedom (SDOF) to mention but few, are some of the techniques that can be employed to derive the equation of motion of harvesters for good estimate of their output power. In view of that, SDOF model is adopted in this paper for developing the model of the proposed harvester. Although, some literatures adopt continues system model approach (for example [5, 7]) to develop the equation of motion of the piezoelectric beam structures, however, higher vibration mode yield low magnitude of the voltage output and are usually far away from the fundamental mode.[3, 8]. Therefore, SDOF model is sufficient enough for estimating the power output of a piezoelectric energy harvester (PEH). Magnetic interactions are extensively used in piezoelectric energy harvesters (PEHs) to achieve a broadband frequency bandwidth as reported in [9-13]. The permanent magnets are often used to tune the natural frequency of the harvesting system so as to coincide with the excitation frequency (as it is a well known fact that maximum output of PEH is achieved at resonance frequency). Challa et al.[9] employed magnetic force to tune the resonance frequency of a harvester by altering its stiffness. The harvester consists of a spring-screw as tuning mechanism which was used to alter the distance between aligned magnetic forces. Ayala-Garcia

et al.[13] proposed a vibration energy harvester(VEH) by employing same tuning mechanism used by[9]. The novel kinetic energy harvester uses close loop control to detect the phase difference between the base and the harvester which in turn, detects the direction to tune the magnet. Also, the non-linearity introduced by magnet interactive force can benefit wideband frequency as well (for example [10-12]). In spite of the fact that, wide frequency bandwidth have been achieved in the reported literatures [9-13] by employing magnetic interactions in the proposed PEHs. However, the effect of magnetic force on the power out has not been addressed.

The main focus of this paper is to study the effect of magnetic force on the power output of a PEH subjected to base excitation. A model of a conventional PEH and a single fixed magnets aligned with magnetic tip mass of PEH are used for the study. For efficient utilization of magnetic force in widening the bandwidth of PEHs, through resonance tuning approach, an equation relating the distance for a given tuned resonance frequency is also derived.

II. MATHEMATICAL MODELLING OF THE PIEZOELECTRIC ENERGY HARVESTERS

A. Conventional Cantilever PEH

A typical configuration of a conventional PEH is shown in Fig .1, with a piezoelectric layer bonded to the root of an aluminum beam with tip mass (M_t) subjected to base excitation $x_0(t)$. The system can be modelled as a SDOF system depicted in Fig. 2. The discrete parameter electromechanical equation of PEH in Fig. 2 is derived by applying Newton's second law in the mechanical domain and Kirchoff's law in the electrical domain[5]

$$M_{eq}\ddot{x}(t)+C_{eq}\dot{x}(t)+K_{eq}x(t)+\Theta_b V(t)=-\mu M_{eq}\ddot{x}_0(t) \quad (1)$$

$$I(t)+C^S \dot{V}(t)-\Theta_f \dot{x}(t)=0 \quad (2)$$

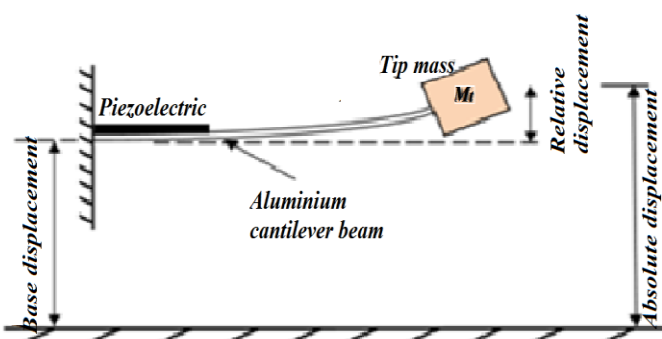


Figure 1 A conventional piezoelectric Harvester (PEH)

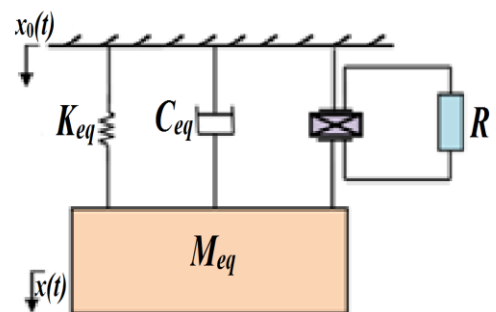


Figure 2 A single degree of freedom model of PEH

Equation (1) and (2) represent mechanical and electrical domain of the PEH respectively, where $x(t)$ is the relative displacement of the tip mass (M_t) and M_{eq}, C_{eq} , and K_{eq} are equivalent mass, damping and stiffness of the PEH, respectively; $\Theta_b V(t)$ is the force feedback of the induce voltage while (Θ_b and Θ_f are forward and backward electromechanical effects respectively). μ is amplitude correction factor for improving the lumped parameter model [14]

$$\mu = \frac{\left(\frac{M_t}{M_b}\right)^2 + 0.603\left(\frac{M_t}{M_b}\right) + 0.08955}{\left(\frac{M_t}{M_b}\right)^2 + 0.4637\left(\frac{M_t}{M_b}\right) + 0.0571} \quad (3)$$

Where $\left(\frac{M_t}{M_b}\right)$ is the ratio of the tip mass to distributed mass of the beam; $I(t)$ and $V(t)$ are the current and the voltage output from the PEH; C^S is the clamp capacitance of the piezoelectric transducer. From ohms law, $V(t) = I(t)R$, therefore $I(t)$ in (1) can be substituted by $V(t)/R$; where R can be considered as the load resistance.

B. PEH with magnetic tip mass aligned to fixed magnet at enclosure

To develop the model of the PEH configuration shown in Fig. 3 , having a fixed magnet aligned with magnetic tip mass in an enclosure (where the Magnets are used to implement resonance tuning by adjusting the distance D_o or introduce non linearity in the harvester for broad bandwidth frequency [9-13]), the electromechanical coupling equations in (1) and (2) can be extended by introducing the magnetic force (F_m) into the system dynamic equation

$$M_{eq}\ddot{x}(t) + C_{eq}\dot{x}(t) + K_{eq}x(t) + \Theta_b V(t) + F_m = -\mu M_{eq}\ddot{x}_0(t) \quad (4)$$

$$\frac{V(t)}{R} + C^S \dot{V}(t) - \Theta_f \dot{x}(t) = 0 \quad (5)$$

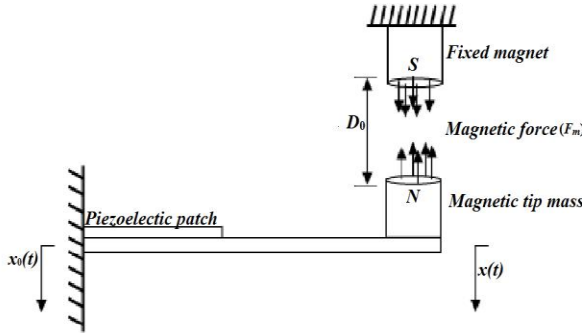


Figure 3 A PEH with magnetic tip mass aligned to a fixed magnet at enclosure.

Where, the magnetic force (F_m) can be established based on the assumptions that there is a dipolar coupling (magnetic dipole-dipole interaction) between the magnets and the magnetic dipoles are always vertically aligned when the PEH vibrates. Based on the aforementioned assumptions, the magnetic force (F_m) between cylindrical magnets is expressed as [15]

$$F_m = \left[\frac{\beta^2 A^2 (l+r)^2}{\pi \tau_0 l^2} \right] \left[\frac{1}{D_0^2} + \frac{1}{(D_0 + 2l)^2} - \frac{2}{(D_0 + l)^2} \right] \quad (6)$$

With τ_0 as the permeability of the medium (air); D_0 is the distance between the magnetic tip mass and the fixed magnet; A is the area of the magnets; l is the height of the magnet; r is the radius and β is the magnetic flux density (magnetic field). When $l \ll D_0$ the approximation of the magnetic force (F_m) on point dipole is reduced to

$$F_m = -\frac{3\tau_0 m_1 m_2}{2\pi[D_0]^4} \quad (7)$$

m_1 and m_2 are the moments of the magnetic dipoles, which is mathematically represented as

$$m = \frac{2\beta V}{\tau_0} \quad (8)$$

Where V is the volume of magnet which depends on the geometry of the magnets. With tip displacement $x(t)$ of the

PEH system, the magnetic force in equation (7) can be written as

$$F_m = -\frac{3\tau_0 m_1 m_2}{2\pi[x(t) + D_0]^4} \quad (9)$$

The electromechanical coupled governing equation of the system can therefore be written as,

$$M_{eq}\ddot{x}(t) + C_{eq}\dot{x}(t) + K_{eq}x(t) + \Theta_b V(t) - \frac{3\tau_0 m_1 m_2}{2\pi[x(t) + D_0]^4} = -\mu M_{eq}\ddot{x}_0(t) \quad (10)$$

$$\frac{V(t)}{R} + C^S \dot{V}(t) - \Theta_f \dot{x}(t) = 0 \quad (11)$$

It is worthmentioning that for a attractive magnets, $m_1=-m_2$ while $m_1=m_2$ for repulsive magnets.

C. State space equation

The discrete parameter models depicting the dynamics of the proposed harvesters in (1)(2) and (10)(11) can be represented in state space form as shown in (12) which is without tip magnetic force and (13) with tip magnetic force respectively; By Letting, $z_1(t)=x(t)$, $z_2(t)=\dot{x}(t)$ and $z_3(t)=V(t)$ where $z_1(t)$, $z_2(t)$ and $z_3(t)$ are the state variables. Therefore,

$$\begin{aligned} \dot{z}_1(t) &= z_2(t) \\ \dot{z}_2(t) &= -\frac{C_{eq}}{M_{eq}} z_2(t) - \frac{K_{eq}}{M_{eq}} z_1(t) - \frac{\Theta_b}{M_{eq}} z_3(t) - \mu \ddot{x}_0(t) \\ \dot{z}_3(t) &= \frac{\Theta_f}{C^S} z_2(t) - \frac{1}{RC^S} z_3(t) \end{aligned} \quad (12)$$

$$\begin{aligned} \dot{z}_1(t) &= z_2(t) \\ \dot{z}_2(t) &= -\frac{C_{eq}}{M_{eq}} z_2(t) - \frac{K_{eq}}{M_{eq}} z_1(t) - \frac{\Theta_b}{M_{eq}} z_3(t) + \frac{3m_1m_2}{M_{eq}2\pi[z_1(t)+D_0]^4} - \mu \ddot{x}_0(t) \\ \dot{z}_3(t) &= \frac{\Theta_f}{C^S} z_2(t) - \frac{1}{RC^S} z_3(t) \end{aligned} \quad (13)$$

D. Natural frequency tunning with dsitance between magnet

The mathematical equation relating the tuned resonance frequency and distance between magnets is developed in this subsection. As earlier mentioned, the magnetic force (F_m) is used to tune the natural frequency (ω_n) of the PEHs so as to match the excitation frequency, which amounts to resonance phenomena (a desirable property in vibration based energy harvesting) and broadband frequency. In practice, this can be achieved by altering the stiffness of the

PEHs through magnetic force by adjusting the distance between the magnets. For a cylindrical magnets, by adjusting the distance D_0 , the magnetic force (F_m) as shown in our proposed harvester in Fig. 3 introduces stiffness unto the system, therefore, change in F_m in (6) with respect to D_0 yield

$$\bar{K}_m = \left| \frac{\partial F_m}{\partial D_0} \right| = \left| \frac{\beta^2 A^2 (l+r)^2}{\pi r_0 l^2} \left[-\frac{2}{D_0^3} - \frac{2}{(D_0+2l)^3} + \frac{4}{(D_0+l)^3} \right] \right| \quad (14)$$

Where \bar{K}_m is the magnitude of the stiffness introduced, therefore the effective stiffness of the PEH is given by

$$K_{eff} = K_{eq} + \bar{K}_m \quad (15)$$

Whereas, K_{eq} is the original stiffness of the harvester without the magnetic force. The tuned resonance frequency of the PEH (ω_t) can be obtained by the equation:-

$$\omega_t = \sqrt{\frac{K_{eff}}{M_{eq}}} = \sqrt{\frac{K_{eq} \pm \bar{K}_m}{M_{eq}}} \quad (16)$$

It is worth mentioning that \bar{K}_m can be either negative or positive depending on the nature of magnetic force (attractive or repulsive). A sign convention of (-ve) for attractive is adopted in this paper. By substituting (14) into (15), the relationship between tuned resonance frequency and the distance between magnets experiencing attractive force is given by;

$$\omega_t = \sqrt{\frac{K_{eq} - \left| \frac{\beta^2 A^2 (l+r)^2}{\pi r_0 l^2} \left(-\frac{2}{D_0^3} - \frac{2}{(D_0+2l)^3} + \frac{4}{(D_0+l)^3} \right) \right|}{M_{eq}}} \quad (17)$$

III. SIMULATION RESULTS AND DISCUSSION

The Geometrical parameters of the beam and material properties used in the simulation are given in Table 1. It is assumed that the piezoelectric material used is of type Micro Fiber Composite (MFC).

TABLE 1 Parameter Descriptions and their values

| Description | Symbols | Value | Units |
|--------------------------|---------|---------------------------|---------|
| Aluminum Beam dimension | - | $80 \times 10 \times 0.6$ | mm^3 |
| Distributed mass of beam | M_b | 1.676 | grams |
| Young's Modulus of beam | E_b | 70×10^9 | N/m^2 |

| | | | |
|--|-----------------------|--------------------------|------------|
| Damping ratio | ξ | 0.0085 | - |
| Tip mass | M_t | 3.995 | grams |
| Piezoelectric material dimension. | - | $42 \times 7 \times 0.3$ | mm^3 |
| Clamp capacitance | C^s | 12.45×10^{-9} | Farad |
| Electro mechanical coupling coefficient. | $\Theta_b = \Theta_f$ | 1.496×10^{-4} | $N V^{-1}$ |
| Young's Modulus of piezoelectric patch. | E_p | 30×10^9 | N/m^2 |
| Length of magnet | l | 3.0 | mm |
| Diameter of magnet | d | 4.0 | mm |
| Surface flux (magnetic field) | β | 1.4 | Tesla |
| Distance between magnets | D_0 | 10 | mm |
| Permeability of medium | τ_0 | $4\pi \times 10^{-7}$ | $H m^{-1}$ |

The equivalent mass M_{eq} of the proposed cantilever PEH can be estimated by

$$M_{eq} = \frac{33}{140} M_b + M_t \quad (18)$$

Also, the equivalent stiffness can be approximated using the following relation

$$K_{eq} = K_{beam} + K_{patch} = \left(\frac{3E_b I_b}{L_b^3} \right)_{beam} + \left(\frac{3E_p I_p}{L_p^3} \right)_{patch} \quad (19)$$

$$\omega_n = \sqrt{\frac{K_{eq}}{M_{eq}}} \quad (20)$$

The equivalent damping of the PEH is calculated using the estimated value of damping ratio by

$$C_{eq} = 2\xi M_{eq} \omega_n \quad (21)$$

The state-space equations developed for the PEHs are used to perform 3-D simulation of power output versus increase in tip mass for a range of frequency using (MATLAB ode45). The output power is computed by

$$P = \frac{V^2 R_{load}}{(R_{source} + R_{load})^2} \quad (22)$$

Where R_{source} and R_{load} are the impedance of PEH and load resistance respectively. For maximum power output of the PEHs, $R_{source} = R_{load}$ a phenomenon known as impedance matching. Therefore an optimal load resistor R_{load} can be estimated by

$$R_{load} = \frac{1}{\omega_n \cdot C^S} \quad (23)$$

A. Power output and frequenc sweep for the PEHs configuration

The 3-D simulation results of power generated from the configurations presented in Fig. 1 and 3 by increasing tip mass (M_t) over a range of frequency from 0-100 Hz is performed on MATLAB software as shown in Fig 4 and 6. The z-x axis dimension of the 3-D simulation which constitute of power on z-axis and frequency sweep on x-axis are presented for analysis. In the simulation for conventional PEH shown in Fig. 5, a maximum power output of 1.88mW is achieved at a frequency of 87Hz. Whereas, for PEH with a single fixed magnet at enclosure, a power output of 1.25mW is produced at the same frequency of 87Hz as shown in Fig. 7. By comparing the power outputs for the different configurations presented, it is observed that conventional PEH yeilds more power output by about 33.5% more than PEH with a fixed magnet at the enclosure of the systems.

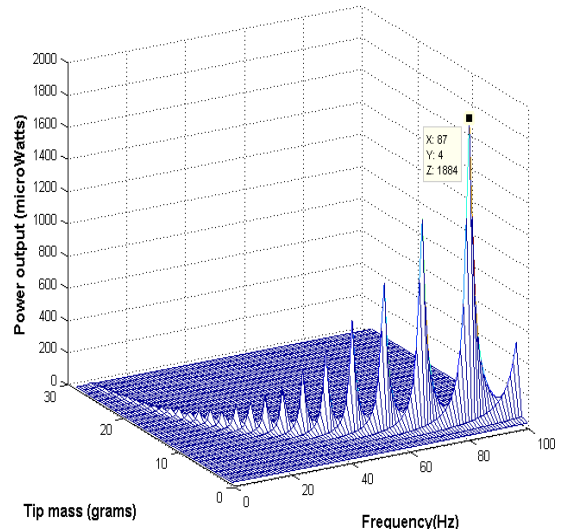


Figure 4 A 3-D simulation of power output versus tip mass and frequency for conventional PEH

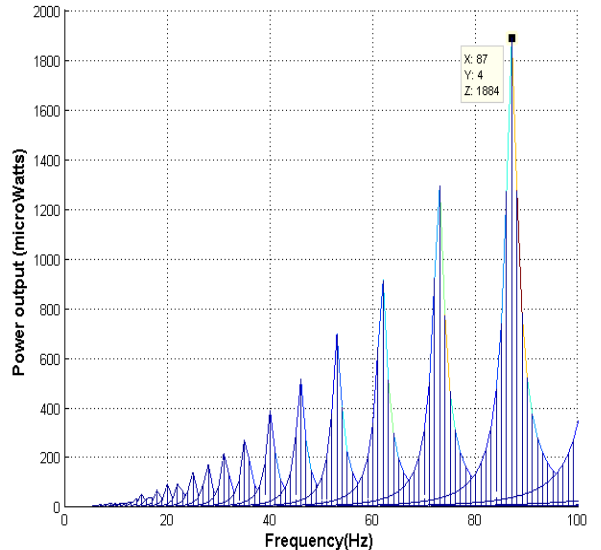


Figure 5 plot f the power versus frequency for conventional PEH

It is evident that the pronounced difference in power output is attributed to damping introduced by the magnetic force which dissipates some of the energy produced by the harvester configuration in Fig 3. Also, it is observed that the non uniformity of the power output in harvester with the magnet is as a result of non linearity introduced by the magnet, making the response slightly tilt to the right as seen in Fig. 7.

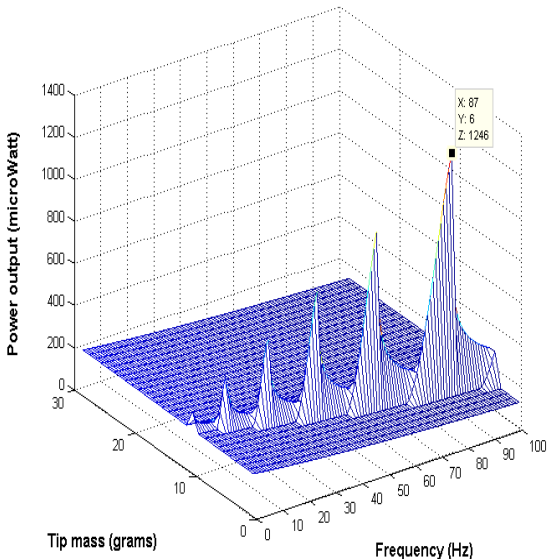


Figure 6 A 3-D simulation of the power output versus tip mass and frequency for PEH with fixed magnet

However, when a wider frequency bandwidth is considered, the later harvesters outperform the conventional PEH.

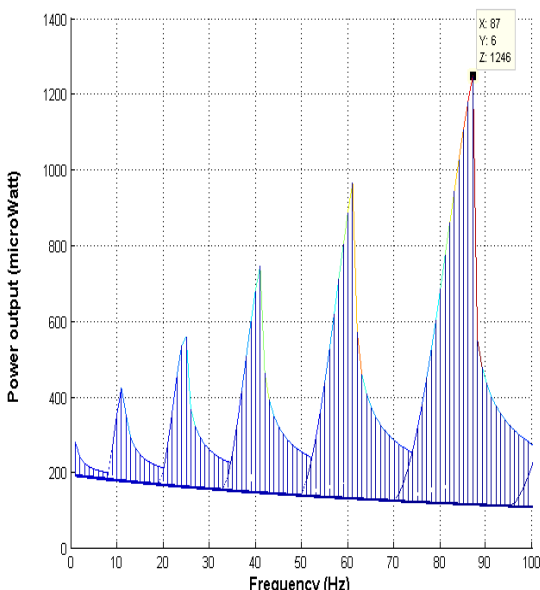


Figure 7 plot of the power output versus frequency for PEH with fixed magnet.

A half power bandwidth analysis is performed for this study. The analysis is done by taking $(P_{\max}/\sqrt{2})$ of the maximum power output obtained from the simulation plots. A horizontal line is drawn from the point where power equals $P_{\max}/\sqrt{2}$ on the plot. Two lines are then projected to the frequency axis forming points of frequency f_1 and f_2 respectively. The difference between f_1 and f_2 is referred to as *Half power bandwidth*. By analysing the half power bandwidth of the conventional PEH, it is observed that the difference in frequency $\Delta f = f_2 - f_1$ is 0.91Hz (less than 1 Hz) which signifies a very narrow power bandwidth. Conversely, for PEH with single fixed magnet, $\Delta f = 5.02\text{Hz}$.

It is worthmentioning that the half power bandwidth analysis revealed the fact that when designing a PEH, a trade off needs to be done between high power output and wide frequency bandwidth. However, when a perfect design of PEH is carried out, a balance of relatively high power output and wide frequency bandwidth can be achieved.

B. Tuned resonance frequency and distance between magnets

The application of magnetic force in vibration based energy harvesters is to introduce stiffness in harvesters which in turn tuned the resonace frequency of the PEH, making a device a broadband energy scavenger. By applying an attractive magnetic force as seen in Fig. 3, the natural frequency of the PEH beam can be tuned to lower frequencies with respect to the initial natural frequency of the harvester (ω_n), while the distance required for a given tuned resonance frequency can be obtained by using the plot in Fig 8. The tuned resonance frequency versus distance is plotted in log-linear scale.

We observed that the distance for a specified tuned frequency depends on the magnetic field (β) induced by the magnets as shown in Fig. 7. For lower magnetic field (Example $\beta_1=1.4$ Tesla), the distance between the magnets is lower compared to when $\beta_2=2.8$ Tesla.

In nut shell, the distance for a given tuned resonance frequency increases with increase in magnetic field. If the distance (D_0) between the magnets is zero, the tuned resonance frequency will approach infinity, meaning that the magnets snaped making the PEH extremely stiff. As D_0 increases, the stiffness introduced by magnetic force on the harvester decreases upto a point where there will be no influence of magnetic force on the stiffness of the system.

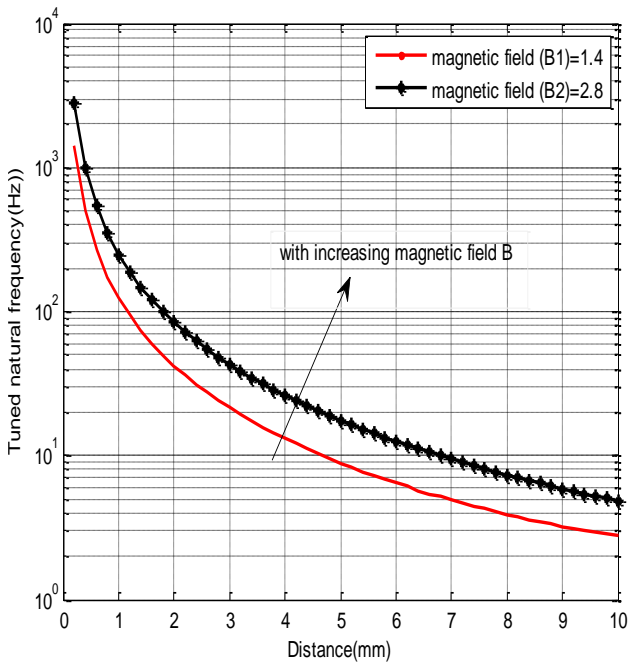


Figure 8 Plot of tuned resonance frequency versus distance between magnets in Log - scale

IV. CONCLUSION

This paper presents the mathematical model of single fixed magnet in an enclosure of piezoelectric energy harvester system. The simulation studies of power output over a range of frequency are performed. We observed that magnetic force undermines the power output of the piezoelectric energy harvester systems. However, when wider frequency bandwidth is required, Linear PEH has a very narrow bandwidth compared to harvester with magnetic influence. Therefore, in designing a PEH, a balance should be aimed between high power output and wide frequency bandwidth. Mathematical equation relating the tuned resonance frequency and the distance between magnets is established. We also realized that the distance required for tuning is directly proportional to magnetic field induced by the magnets. This could be an important design relationship when developing a broadband vibration energy harvester.

references

- [1] L. Tang, Y. Yang, and C. K. Soh, "Toward Broadband Vibration-based Energy Harvesting," *Journal of Intelligent Material Systems and Structures*, vol. 21, pp. 1867-1897, 2010.
- [2] D. Zhu, M. J. Tudor, and S. P. Beeby, "Strategies for increasing the operating frequency range of vibration energy harvesters: a review," *Measurement Science and Technology*, vol. 21, p. 022001, 2010.
- [3] O. Qing, C. Xiaoqi, S. Gutschmidt, A. Wood, and N. Leigh, "A two-mass cantilever beam model for vibration energy harvesting applications," in *Automation Science and Engineering (CASE), 2010 IEEE Conference on*, 2010, pp. 301-306.
- [4] N. H. Diyana, A. G. A. Muthalif, M. N. Fakhzan, and A. N. Nordin, "Vibration Energy Harvesting using Single and Comb-shaped Piezoelectric Beam Structures: Modeling and Simulation," *Procedia Engineering*, vol. 41, pp. 1228-1234, // 2012.
- [5] A. Erturk and D. J. Inman, "On Mechanical Modeling of Cantilevered Piezoelectric Vibration Energy Harvesters," *Journal of Intelligent Material Systems and Structures*, vol. 19, pp. 1311-1325, 2008.
- [6] C. De Marqui Junior, A. Erturk, and D. J. Inman, "An electromechanical finite element model for piezoelectric energy harvester plates," *Journal of Sound and Vibration*, vol. 327, pp. 9-25, 2009.
- [7] M. N. Fakhzan and A. G. A. Muthalif, "Harvesting vibration energy using piezoelectric material: Modeling, simulation and experimental verifications," *Mechatronics*, vol. 23, pp. 61-66, 2013.
- [8] M. Arafa, W. Akl, A. Aladwani, O. Aldrahem, and A. Baz, "Experimental implementation of a cantilevered piezoelectric energy harvester with a dynamic magnifier," 2011, pp. 79770Q-79770Q-9.
- [9] V. R. Challa, M. G. Prasad, Y. Shi, and F. T. Fisher, "A vibration energy harvesting device with bidirectional resonance frequency tunability," *Smart Materials and Structures*, vol. 17, p. 015035, 2008.
- [10] A. Erturk, J. Hoffmann, and D. J. Inman, "A piezomagnetoelastic structure for broadband vibration energy harvesting," *Applied Physics Letters*, vol. 94, p. 254102, 2009.
- [11] S. C. Stanton, C. C. McGehee, and B. P. Mann, "Reversible hysteresis for broadband magnetopiezoelectric energy harvesting," *Applied Physics Letters*, vol. 95, p. 174103, 2009.
- [12] L. Tang and Y. Yang, "A nonlinear piezoelectric energy harvester with magnetic oscillator," *Applied Physics Letters*, vol. 101, p. 094102, 2012.
- [13] I. N. Ayala-Garcia, D. Zhu, M. J. Tudor, and S. P. Beeby, "A tunable kinetic energy harvester with dynamic over range protection," *Smart Materials and Structures*, vol. 19, p. 115005, 2010.
- [14] A. Erturk and D. J. Inman, "Issues in mathematical modeling of piezoelectric energy harvesters," *Smart Materials and Structures*, vol. 17, p. 065016, 2008.
- [15] D. Vokoun, M. Beleggia, L. Heller, and P. Šittner, "Magnetostatic interactions and forces between cylindrical permanent magnets," *Journal of Magnetism and Magnetic Materials*, vol. 321, pp. 3758-3763, 11// 2009.

Data Mining in Medicine Domain Using Decision Trees and Vector Support Machine

Djamila Benhaddouche

Department of Computer Science, University of
Science and
Technology of Oran “Mohammed Boudiaf” USTO
USTO, 31000 Bir El Djir Oran Algérie
benhaddouche.djamil@gmail.com

Abdelkader Benyettou

Department of Computer Science, University of
Science and
Technology of Oran “Mohammed Boudiaf” USTO
USTO, 31000 Bir El Djir Oran Algérie
a_benyettou@yahoo.fr

Abstract - In this paper, we used data mining to extract biomedical knowledge. In general, complex biomedical data collected in studies of populations are treated by statistical methods, although they are robust, they are not sufficient in themselves to harness the potential wealth of data. For that you used in step two learning algorithms: the Decision Trees and Support Vector Machine (SVM). These supervised classification methods are used to make the diagnosis of thyroid disease. In this context, we propose to promote the study and use of symbolic data mining techniques.

Keywords- biomedical data, learning; classifier, Algorithms decision tree; knowledge extraction

I. INTRODUCTION

The quality of the data recorded in the great biomedical data bases is not guaranteed by the strict procedures of “dated management”, as it is the case for the clinical trials. It thus appears necessary to set up specific methods of pre-treatment of the data before carrying out analyses that it is by traditional statistical methods or recent methods of excavation of data. In general, the biomedical complex data collected at the time of the studies of populations are treated by statistical methods, which constitute the reference for the majority of the biologists, epidemiologists or doctors confronted with the analysis of the results. However, the technological projection in medicine implies a volume of data to be treated increasingly large. The statistical methods are robust but they are not alone enough to exploit all the potential richness of the data. The principal problems are to extract from the units of knowledge starting from

these data, which are new and potentially useful. In this context, we propose to promote the

study and the use of the techniques symbolic systems in excavation of data

II. DATA MINING

The term of excavation of the data, more known under the name “Data mining” is often employed to indicate the whole of the tools making it possible the user to reach the data of the company and to analyse them. One could define the excavation of the data like a step having the aim of discovering relations and facts, at the same time new and significant, on great sets of data. The data are without value if they are not interpreted. By interpreting data, one obtains information, and it is necessary that information is received, included/understood and classified to obtain knowledge from them. [2]

A. Processes

There are five great stages which it is necessary to traverse in a project of excavation of the data. [5] :

- ✓ To pose the problem
- ✓ Seek and selection of data
- ✓ the Préparation data
 - ❖ Reduction
 - ❖ cleaning
 - ❖ Transformation
- ✓ Development of the model (modeling)
- ✓ Application of the model

B. Tasks

Contrary to the generally accepted ideas, the excavation of the data is not the miracle cure able to solve all the difficulties or needs for the company. However, a multitude of problems of a intellectual, economic or commercial nature can

be gathered, in its formalization, one of the following tasks: Classification, estimate, prediction, grouping by similarities, segmentation (or clusterisation), description, optimization. [4]

C. Methods

We adopt only certain methods which come to supplement the traditional tools which are requests SQL, the requests of crossed analysis, the tools for visualization, the descriptive statistics and the analysis of the data. The methods are the algorithm for the segmentation, the rules of association, the closest neighbours (reasoning starting from case), the decision trees, the networks of neurons, the genetic algorithms, the networks Bayesians, support vector machine (SVM), the methods of regression, the analysis discriminating.

III. SUPPORT VECTOR MACHINES (SVM)

Support Vector Machines (SVM) are new discriminating techniques in the theory of the statistical training. For the data processing specialists, the SVM is a linear classifier with broad margin in a space with core. For the statisticians, the SVM is a nonparametric estimator. It is based on a minimization of the empirical risk regularized on a functional space of Hilbert and with a linear function of loss per pieces.

A. Mathematical principle & general

SVM are algorithms based on the three following mathematical principles [1]:

- principle of Fermat (1638)
- principle of Lagrange (1788)
- principle of KuhnTucker (1951)

Principle general

: The principle general is the construction of a classifier with actual values and the division of the problem in two pennies problems:

- ▶ Nonlinear transformation of the entries;
- ▶ Choice of a linear separation "optimal". [6]

B. Concepts of bases

1) Problem of training

One is interested in a phenomenon F (possibly not determinist) which starting from a certain set of entries X product an exit $y = f(x)$ generally, only the case ($Y = \{-1, 1\}$) interests us

in SVMs but one can easily extend to the case $|y| = m > 2$).

The goal is to find this function F starting from the only observation of a sample
 $S = \{(X_1, Y_1), \dots, (X_n, Y_n)\}$ of n independent copies of (X,Y).

2) Optimal hyper plane

One calls optimal hyper plane the separating hyper plane which is located at the maximum distance from the vectors X closest among the unit to the examples; one can also say that this hyper plane maximizes the margin.

3) Supports Vectors (SV)

The Vectors Supports (term which one could translate by points of support) are the vectors X_i for which equality: $Y_i((W^0 X_i) + b^0) = 1$ is checked, concretely, they are the points closest to the optimal hyper plane.

4) The margin

The margin represents the smallest distance between the various data of the two classes and the hyper plane.

C. Construction of the optimal hyper plane

For describing well the technique of construction of the optimal hyper plane separating from the data belonging to two different classes in two different cases: The case of the linearly separable data and the case of the data not linearly separable. We consider the following formalism Is the unit D such as:

$$D = \{(X_i, Y_i) \in \mathbb{R}^n \times \{-1; 1\} \text{ for } i = 1, \dots, m\}$$

D. Principle of the SVM

Classifiers SVM use the idea of HO (Optimal Hyper plane) to calculate a border between groups of dots. They project the data in space of characteristics by using nonlinear functions. In this space, one builds the HO which separates the transformed data. The principal idea is to build a linear surface of separation in the space of the characteristics which corresponds to a nonlinear surface in the space of entry.

For any function $g \neq 0$ with:

$$\int g^2(z)dz \geq 0$$

One calls these functions the cores of Hilbert-Schmidt. Several cores were used by the researchers; here are some (table 2.1): [1]

IV. DECISION TREES

The decision trees are most popular of the methods of training, the popularity of the method rests mainly on its simplicity. A decision tree is the chart of a procedure of classification. Indeed, with any complete description only one sheet with the decision tree is associated. This association is defined while starting with the root of the tree and while going down according to answers' to the tests which label the internal nodes [7]. The associated class is then the class by defect associated with the sheet which corresponds to description. The procedure of classification obtained has an immediate translation in term

A. Principe fundamental *

One gives oneself a unit X of N examples

noted \mathcal{X}_i whose P attributes are quantitative or qualitative. Each example X is labelled, i.e. it is associated for him a "class" or a "target attribute" which one notes $y \in Y$.

From these examples, one builds a tree such as: [3]

- ▶ **Node :** each non final node corresponds to a test (IF....THEN...) on the value of one or more attributes;
- ▶ **Arc :** each branch on the basis of a node corresponds to one or more values of this test;
- ▶ **Break into leaf:** with each final node called sheet a value with the target attribute is associated (class).

B. Construction of a decision tree

The best method is that which consists in testing all the possible trees, but this solution is not possible.

Example: If one has NR attributes which can take on average V values, the number of trees studied:

$$\sum_{i=1}^N (n-i+1)^{V^{i-1}}$$

Thus 4 attributes with 3 values gives 526 possible trees.

One thus seeks to build the tree by a downward induction (top-down induction of decision tree). [8]

C. Problems

This apparent simplicity should not mask real difficulties which arise during the construction of the tree.

- Choice of the discriminating attribute (choice of the attribute of segmentation)
 - Stop of the segmentation (choice depth of the tree)
- There are two various techniques:
- pré-pruning
 - post-pruning
- Décision

D. Algorithms

1) Algorithme CART

Algorithme CART is published by L.briemen and associates (1984).

2) Algorithm CHAID

Algorithm CHAID is published by J.A.Hartigan (1975).

3) Algorithm ID3

Algorithm ID3 of R. Quinlan proposed in 1986.

4) Algorithm C4.5

Algorithm C4.5 was worked out by Quinlan 1993, this algorithm is in fact only one improvement of ID3.

V. CONCEPTION AND REALISATION

A. Description of the base of the data

We will use in our application the base of the data «hypo py» published on the site http://axon.cs.byu.edu/~martinez/classes/470/ML_DB/thyroid-disease/hypothyroid.data.

TABLE1. CORES OF HILBERT-SCHMIDT

| Noyau | Formule |
|------------|---|
| Linéaire | $K(x, y) = x \cdot y$ |
| Sigmoïde | $K(x, y) = \tanh(ax \cdot y + b)$ |
| Polynomial | $K(x, y) = (ax \cdot y + b)^d$ |
| RBF | $K(x, y) = \exp(-\ x - y\ ^2 / \sigma^2)$ |
| Laplace | $K(x, y) = \exp(-\gamma \ x - y\)$ |

It contains 3163 biomedical recordings connected of the patients hypothyroïdiens with 25 attributes and a result of diagnosis. By using this base of the data, we can show some models related on the age of the patient, the kind, the questions, the pregnancies, the thyroid treatment, the surgery and the drug, as well as their clinical test results, such as the disease, the tumour, lithium, the goitre, and measurements of TSH, T3, TT4, T4U, FTI, levels of TBG.

We asked for the opinion of an expert who proposed to us to eliminate some attributes from the original base of the data which do not have impact on the result of the diagnosis, and another examination which are not available in our laboratories. Thus one obtained another data base more adapted to the problems

B. Structure of the data used

1) Entries

Age: concerning the age of the patient, oldest are touched by the hypothyroid.
 Sex: this disease more frequently assigns the women.
 Enclosure: if the woman is pregnant or not.
 Patient: if the patient is already sick or not.
 Test TSH: if the test were carried out or not.
 TSH (THYROGLOBULINE): anti-hypophyseal hormone simulating the thyroid one.
 Test T3: if the test were carried out or not.
 T3 (TRIIODOTHYRONINE): iodized hormone secreted by the thyroid one, also coming from the peripheral desiodation of T4.
 Tt4 test: if the test were carried out or not.
 Tt4 (THIROXINE): iodized hormone secreted by the thyroid one, the free form (T4L or free-T4 or FT4), which presents 0.02 A 0.04% of T4 total, and only activates it.
 Test TBG: if the test were carried out or not.
 TBG (THYROXIN BINDING GLOBULIN): protein of transport of the thyroid hormone

2) Résults

Class: there are two classes:

- Hypothyroid: the case where the diagnosis is confirmed positive.
- Négative : as the word indicates it, they is the nonsick people.

C. Scheme of work

To be able to treat our data base, one was obliged to pass by the following stages which enter the processes of excavation of the data:

1) The comprehension of the problem

For this spot, one tried to control well our problems concerning the disease "Hypothyroid" using the experts in the field..

2) Selection of the data

Our original data base contains 25 attributes where according to the expert the majority of them are unutilised for our diagnosis; thus one filtered the original data base by selecting only the useful fields.

3) Cleaning

Cleaning consists with

- ✓ to eliminate the doubled blooms appeared in our data base.
- ✓ filling of the missing values.
- ✓ the replacement of the disturbed data.

4) The algorithm general of SVM

Entry a labelled unit X.

Algorithm

That w, b=0;

That is to say unit X for the whole of training.

That is to say together of the labels of Y.

Beginning

For i=1 j until L do :

For j=1 j until L do:

To learn:

$$\max \left[\sum_{i=1}^L \alpha_i - \frac{1}{2} \sum_{i,j=1}^L y_i y_j \alpha_i \alpha_j K(x_i, x_j) \right]$$

With the constraints

$$0 \leq \alpha_i \leq C, \quad i = 1, \dots, L$$

$$\sum_{i=1}^L \alpha_i y_i = 0$$

$$H = \sum_{i,j=1}^L y_i y_j K(x_i, x_j)$$

To solve the problem of optimization with QP such as the function to be minimized is:

$$\text{Min} \quad -1/2 \alpha' * H * \alpha + c^t * \alpha$$

C: control level of error in classification

After the resolution of this problem, one obtains which is used for the calculation of the function of decisions as follows:

$$f(x) = \text{sign} \left(\left(\sum_{i=1}^L \alpha_i y_i K(x_i, x_j) \right) + b \right)$$

To evaluate the number of support vector.

To evaluate the value of B.

End

5) The algorithm general of C4.5

Entry: language of description: sample S;

Beginning

To Initialize with the empty tree; the root is the current node;

To repeat

To calculate the entropies for each value of each attribute;

To calculate the profit for each attribute;

The choose the maximum profit;

The choose the test for the current node;

To decide if the node courant is final;

If the node is final then to affect a class;

If not to select a test and create the under tree;

End if

To passe to the following node not explored if there are;

Until obtaining a decision tree;

End.

6) Results

| | SVM | Décisions tree |
|----------------------|-------|----------------|
| The time of training | 16h | 8h |
| The error rate | 0.054 | 0.061 |

VI. CONCLUSIONS

Both methods gave satisfactory results of both: that of Support Vector Machines (SVM) gave a better classification compared to decision trees, this is due to its simplicity and mathematical rigor, so the SVM can better generalization and time despite significant learning as opposed to the method of decision.

REFERENCES

- [1] N. E. Ayat, "Automatic selection of model of the machines with vectors of support application to the recognition of images and handwritten figures", These Jan 2004.
- [2] J-F Boulicaut, "State of the art on the extraction of frequent reasons.", Paris, Nov. 2002.
- [3] L. Bougrain, "Decision Trees."
- [4] G. Bouchard, "Generative models in supervised classification and applications to the categorization of images and industrial reliability", These 2005.
- [5] W. Jouini, "Methods and techniques of Retrieval of Knowledge of Data bases.", 2003.
- [6] J. Kharroubi, "Methods and techniques of Retrieval of Knowledge of Data bases.", July 2002
- [7] R. Marée, "Automatic classification of images by decision trees.", These Feb 2005.

Conversion of the METCM into the Meteo-11

Karel Šilinger

University of Defense

Department of fire support control

Brno, Czech Republic

karel.silinger@unob.cz

Ladislav Potužák

University of Defense

Department of fire support control

Brno, Czech Republic

Jiří Šotnar

University of Defense

Department of fire support control

Brno, Czech Republic

Abstract—This article deals with a proposed method of conversion of the METCM meteorological message into the METEO-11 format. This method is designed for artillery of these armies that are using the METEO-11 meteorological message during a spare (manual) method of firing data calculation. The proposed method is based on the simulation of temperature and wind sounding by radiosonde from the values of the METCM meteorological message. Then the values of the METEO-11 meteorological message are calculated with using carried out simulation of temperature and wind sounding by radiosonde. The conversion of the METCM meteorological message into the METEO-11 format consists of the recalculating of the meteorological message header, recalculating of meteorological data in the METCM meteorological message onto the units used in the METEO-11 meteorological message, conversion of the ground meteorological data, conversion of the meteorological data from the particular zones used in METCM meteorological message into the needed heights above an artillery meteorological station used in the METEO-11 meteorological message and the calculation of the meteorological data average values in the individual layers of the METEO-11 meteorological message.

Keywords—Artillery; METCM meteorological message; METEO-11 meteorological message; conversion of meteorological message

I. INTRODUCTION

Two standard types of meteorological messages are used in the North Atlantic Treaty Organisation (NATO) during the firing data calculation – METCM meteorological-computer message and the METBK meteorological-ballistic message [1, 2]. The METCM is used in automated artillery fire control systems and the METB3 during spare (manual) methods of firing data calculation.

Artilleries of NATO armies have to be able to provide meteorological messages to each other. The compatibility in using of the same meteorological messages is currently achieved only in the automated mode – in using of the METCM. Some artillery of NATO armies still use the non-standardized format of the METEO-11 meteorological message in case of the classic (spare, manual) mode is used. The transition to the exclusive use of standard meteorological messages is not often possible (because of implemented weapon systems and their firing tables, due to the implemented firing data calculation methods, for economic reasons, etc.)[3 - 5].

If the artillery, uses the METEO-11, could not realize own comprehensive meteorological sounding of atmosphere for various reasons, some other artillery can provide the METCM for this artillery. If this artillery cannot carry out the firing data

calculation with using of automated artillery fire control system, it has to be capable to transpose (convert) the METCM into the METEO-11 format. However, the algorithm of this conversion has not been defined yet [6 - 9].

The proposed method of conversion of the METCM into the METEO-11 format can be divided into three consecutive phases:

- 1.) header (baseline data) of the meteorological message recalculations;
- 2.) ground meteorological data conversion;
- 3.) meteorological data average values in the individual layers conversion.

II. HEADER OF THE METEOROLOGICAL MESSAGE RECALCULATION

The header of the METCM consists of the following symbols:

METCMQ L_{AL}L_{AL}L₀L₀ YYG₀G₀G₀ hhP_dP_dP_d,

where: METCM is signification (type) for the meteorological message;

Q is the designation of the earth octant;

L_{AL}L_A is the latitude of centre of the valid area in tens, unit and tenths of degree;

L₀L₀L₀ is the longitude of centre of the valid area in tens, units and tenths of degree. The hundreds digits are leaving out for longitude 100-180° including.

YY is the day of that month in which the time validity starts beginning;

G₀G₀G₀ is the world time GMT of the time validity beginning in tens, units and tenths of hours. It is used the 24hours interval from 000 to 239;

G is the time of meteorological message validity in hours. The time validity is determining in the interval from 1 to 8 hours. The number 9 designates the time validity of 12 hours;

hh is the altitude of the artillery meteorological station (AMS) in tens of meters;

P_dP_dP_d is the air pressure at the level of the AMS in units of millibars. If the air pressure is more than 1000 millibars, thousands digits are leaving out [9].

The header of the METEO-11 consists of the following symbols (different countries can use different letters):

METEO-11CC-DDHHM-VVVV,

where: METEO-11 is signification (type) for the meteorological message;
 CC is meteorological unit number which compiled the meteorological message;
 DD is the day of the end of meteorological sounding;
 HH is the hour of the end of meteorological sounding;
 M are tens of time minutes of the end of meteorological sounding;
 VVVV is the altitude of the AMS in meters[9].

The recalculation of METCM header into the METEO-11 format will be carried out according to the following rules:

- the label of the METEO-11 is always the same – „METEO-11“;
- CC – this information is not possible to get from the METCM, as a result it must always be fill in manually;
- DD – it corresponds to the YY data in the METCM;
- HH – it corresponds to the first two symbols $\mathbf{G}_0\mathbf{G}_0\mathbf{G}_0$ in the METCM;
- M – it corresponds to the third symbol $\mathbf{G}_0\mathbf{G}_0\mathbf{G}_0$ in the METCM. Tenth of an hour will be converted to the tens of minutes as follow:

$$M = G_0 \cdot \frac{6}{10}, \quad (1)$$

- VVVV – it corresponds to the hhh in the METCM. The altitude of AMS (hhh) will be multiplied by 10 for getting the altitude in meters:

$$VVVV = hhh \cdot 10 \quad (2)$$

III. GROUND METEOROLOGICAL DATA CONVERSION

The ground meteorological data are listed in the METCM in the line (zone) 00, which consists of the following symbols:

00dddFFFFTTTTPPPP,

where: 00 shows the line in the meteorological message (zone code 00);
 ddd is the wind direction – from which the wind vector is coming (from where the wind is blowing) – in tens of mils (in the METCM is usually used the division of the circle into the 6400 mils);
 FFF is the wind speed in units of knots;
 TTTT is the virtual air temperature in tenths of Kelvin degrees;
 PPPP is the air pressure in units of millibars[9].

The ground meteorological data are shown in the METEO-11 by following symbols:

$B_0B_0B_0T_0T_0$,

where: $B_0B_0B_0$ is the change of the ground air pressure due to the tabular value in the altitude of AMS;

T_0T_0 is the change of the virtual ground air temperature due to the tabular value in units of Celsius degrees[9].

The conversion of METCM ground meteorological data into the METEO-11 format will be carried out according to the following rules:

- $B_0B_0B_0$ will be converted from PPPP indication of the zone 00 at first by determining the value of auxiliary change of the ground air pressure due to tabular value ($B_0B_0B_0'$) as follows:

$$B_0B_0B_0' = 0,750064 \cdot PPPP_{00} - 750, \quad (3)$$

where: PPPP₀₀ is the air pressure in the 00 zone (in the AMS altitude).

Then the $B_0B_0B_0$ value will be determined by the follow relation:

$$B_0B_0B_0 = \begin{cases} (-1) \cdot B_0B_0B_0' + 500, & \text{pro } B_0B_0B_0' < -0,5 \\ B_0B_0B_0, & \text{pro } B_0B_0B_0' \geq -0,5 \end{cases}. \quad (4)$$

- T_0T_0 will be converted from TTTT of zone 00 at first by determining the value of auxiliary change of the virtual ground air temperature due to tabular value (T_0T_0') as follows:

$$T_0T_0' = \left(\frac{TTTT_{00}}{10} - 273,15 \right) - 15,9, \quad (5)$$

where: TTTT₀₀ is the virtual air temperature in the 00 zone (in the AMS altitude).

Then the T_0T_0 value will be determined by the follow relation:

$$T_0T_0 = \begin{cases} (-1) \cdot T_0T_0' + 50, & \text{pro } T_0T_0' < -0,5 \\ T_0T_0, & \text{pro } T_0T_0' \geq -0,5 \end{cases}. \quad (6)$$

IV. METEOROLOGICAL DATA AVERAGE VALUES IN THE INDIVIDUAL LAYERS CONVERSION

Meteorological data in the individual zones of the METCM are listed in the relevant lines of the meteorological message and they are expressed by the following symbols:

ZZdddFFFFTTTTPPPP,

where: ZZ is the line number indicating the zone code (tableI);
 ddd is the wind direction;
 FFF is the wind speed in units of knots;
 TTTT is the virtual air temperature in tenths of Kelvin degrees;
 PPPP is the air pressure in units of millibars[9].

Virtual air temperature, wind direction and wind speed are expressed as average values of the appropriate zone in the METCM. Therefore it was established an assumption – these meteorological data average values correspond to the meteorological data in the medium height of particular zones (table I). Hence the courses of the virtual air temperature,

wind direction and wind speed are linear in the interval from the bottom to the upper boundary of the appropriate zone.

The air pressure in the individual heights above AMS is not considered during the firing data calculation (its effect is

included in the virtual air temperature)[10]. Therefore the air pressure in the individual heights above AMS is not converted.

TABLE I. HEIGHTS INTERVALS OF INDIVIDUAL METCM ZONES

| Zone code | Zone height above AMS [m] | Medium height of zone [m] | Zone code | Zone height above AMS [m] | Medium height of zone [m] |
|------------------|----------------------------------|----------------------------------|------------------|----------------------------------|----------------------------------|
| 01 | 0 - 200 | 100 | 14 | 14 000 - 16 000 | 15 000 |
| 02 | 200 - 500 | 350 | 15 | 16 000 - 18 000 | 17 000 |
| 03 | 500 - 1 000 | 750 | 16 | 18 000 - 20 000 | 19 000 |
| 04 | 1 000 - 1 500 | 1 250 | 17 | 20 000 - 22 000 | 21 000 |
| 05 | 1 500 - 2 000 | 1 750 | 18 | 22 000 - 24 000 | 23 000 |
| 06 | 2 000 - 3 000 | 2 500 | 19 | 24 000 - 26 000 | 25 000 |
| 07 | 3 000 - 4 000 | 3 500 | 20 | 26 000 - 28 000 | 27 000 |
| 08 | 4 000 - 5 000 | 4 500 | 21 | 28 000 - 30 000 | 29 000 |
| 09 | 5 000 - 6 000 | 5 500 | 22 | 30 000 - 32 000 | 31 000 |
| 10 | 6 000 - 8 000 | 7 000 | 23 | 32 000 - 34 000 | 33 000 |
| 11 | 8 000 - 10 000 | 9 000 | 24 | 34 000 - 36 000 | 35 000 |
| 12 | 10 000 - 12 000 | 11 000 | 25 | 36 000 - 38 000 | 37 000 |
| 13 | 12 000 - 14 000 | 13 000 | 26 | 38 000 - 40 000 | 39 000 |

Meteorological data in the individual layers of the METEO-11 are expressed by the following symbols:

hhTTSSRR,

where: hh is the layer code;
 TT is the average change of virtual air temperature due to tabular value;
 SS is the average wind direction in hundreds of mils (in the METEO-11 it is usually used the division of the circle into the 6000 mils);

RR is the average wind speed in meters per second[9].

The average change of virtual air temperature due to tabular value corresponds to the entire high interval from the AMS altitude up to the medium height of appropriate layer above AMS (table II).

The average wind direction and the average wind speed correspond to the entire high interval from the AMS altitude up to the upper boundary of appropriate layer above AMS (table II).

TABLE II. HEIGHTS INTERVALS OF INDIVIDUAL METEO-11 LAYERS

| Zone code | Zone height above AMS [m] | Medium height of zone [m] | Zone code | Zone height above AMS [m] | Medium height of zone [m] |
|------------------|----------------------------------|----------------------------------|------------------|----------------------------------|----------------------------------|
| 02 | 0 - 200 | 100 | 40 | 3 000 - 4 000 | 3 500 |
| 04 | 200 - 400 | 300 | 50 | 4 000 - 5 000 | 4 500 |
| 08 | 400 - 800 | 600 | 60 | 5 000 - 6 000 | 5 500 |
| 12 | 800 - 1 200 | 1 000 | 80 | 6 000 - 8 000 | 7 000 |
| 16 | 1 200 - 1 600 | 1 400 | 10 | 8 000 - 10 000 | 9 000 |
| 20 | 1 600 - 2 000 | 1 800 | 12 | 10 000 - 12 000 | 11 000 |
| 24 | 2 000 - 2 400 | 2 200 | 14 | 12 000 - 14 000 | 13 000 |
| 30 | 2 400 - 3 000 | 2 700 | 18 | 14 000 - 18 000 | 16 000 |

For each METEO-11 layer is need to calculate:

- a) the average change of virtual air temperature due to tabular value in Celsius degrees (TT);

- b) the average wind direction in hundreds of mils (SS);
- c) the wind speed in meters per second (RR).

A. The Average Changes of Virtual Air Temperature due to Tabular Value (TT) Calculation

The average virtual air temperatures in the individual METCM zones (TTT_{ZZ}) correspond to the virtual air temperature values in the medium heights of appropriate zones. The average virtual air temperatures in the individual METCM zones in tenths of Kelvin degrees (TTT_{ZZ}) have to be converted to Celsius degrees as follow:

$$T_{(^\circ C)}_{ZZ} = \frac{TTT_{ZZ}}{10} - 273,15 , (7)$$

where: $T_{(^\circ C)}_{ZZ}$ is the virtual air temperature in the medium height of appropriate zone (ZZ) in Celsius degrees.

It is necessary to carry out a simulation (budgeting) of temperature (and also wind) sounding in the particular heights above AMS from the values established according to the (7) relation for calculation of the average changes of virtual air temperature (and also the average wind directions and the average wind speeds) in the individual METEO-11 layers – as if they were actually measured by radiosonde. The radiosonde sends the measured meteorological data at specified intervals after approximately 25-50 meters (depending on the speed of meteorological balloon ascent and on the used meteorological sets). The simulation (budgeting) of temperature and wind soundings can be carried out on the basis of linear interpolations of particular meteorological data in the appropriate heights above AMS from the meteorological data mentioned in the METCM. For these simulations it is sufficient to calculate the meteorological data at intervals of 50 m (in heights above AMS)[11 - 13].

For each height (v) above AMS (after 50 meters) it necessary to calculate the appropriate changes of virtual air temperature due to tabular value (ΔT_v) according to (8) to (13):

- for $v=50$ m:

at first it is needed to determine the virtual air temperature at the height of 50 m above AMS in Celsius degrees:

$$T_{50} = \frac{T_{(^\circ C)}_{00} + T_{(^\circ C)}_{01}}{2} , (8)$$

where: $T_{(^\circ C)}_{00}$ is the virtual air temperature in the height of 50 m above AMS and it corresponds to $T_0 T_0'$ value,
 $T_{(^\circ C)}_{01}$ is the virtual air temperature in the

medium height of the 01 zone (100 m) determined according to (7)

and then it can be calculated the change of virtual air temperature in the height of 50 m above AMS due to tabular value in Celsius degree (ΔT_{50}):

$$\Delta T_{50} = T_{50} - (15,9 - 0,006328 \cdot v) , (9)$$

- for $v=100$ m:

$$T_{100} = T_{(^\circ C)}_{01} , (10)$$

$$\Delta T_{100} = T_{100} - (15,9 - 0,006328 \cdot v) , (11)$$

- for $v=150$ m:

$$T_{150} = [T_{(^\circ C)}_{02} - T_{100}] \cdot \frac{50}{v_{02} - (v-50)} + T_{100} , (12)$$

where v_{02} is the medium height of the METCM 02 zone ($v_{02} = 350$ m) – table I,

$$\Delta T_{150} = T_{150} - (15,9 - 0,006328 \cdot v) , (13)$$

Analogously it is needed to carry out the calculation of all changes of virtual air temperature in the heights after 50 m above AMS due to tabular value in Celsius degree – up to required height above AMS.

Then it will be calculated auxiliary average changes of virtual air temperature due to tabular value in the particular METEO-11 layers (TT'_{hh}) according to (14) to (16):

$$TT'_{02} = \frac{\sum_{n=1}^2 \Delta T_{50 \cdot n}}{2} , (14)$$

where $50 \cdot n$ is the height (v) above AMS in meters,

$$TT'_{04} = \frac{\sum_{n=1}^6 \Delta T_{50 \cdot n}}{6} , (15)$$

$$TT'_{08} = \frac{\sum_{n=1}^{12} \Delta T_{50 \cdot n}}{12} , (16)$$

etc.

The average changes of virtual air temperature due to tabular value in the particular METEO-11 layers (TT'_{hh}) will be determined according to the follow relation:

$$TT'_{hh} = \begin{cases} (-1) \cdot TT'_{hh} + 50, & \text{pro } TT'_{hh} < -0,5 \\ TT'_{hh}, & \text{pro } TT'_{hh} \geq -0,5 \end{cases} , (17)$$

where hh is the code of the METEO-11 layer.

B. The Everage Wind Direction (SS) Calculation

The average wind directions in the individual METCM zones (ddd_{ZZ}) correspond to the wind directions in the medium heights of appropriate zones. The average wind directions in the medium heights of appropriate zones (ddd_{ZZ}) is needed to convert to mil (usually used in the METEO-11 – 6000 mils for one circle) as follow:

$$\alpha'_{w(dc)}_{ZZ} = ddd_{ZZ} \cdot 10 \cdot \frac{15}{16} , (18)$$

where $\alpha'_{w(dc)}_{ZZ}$ is the wind direction in the medium height of appropriate zone (ZZ) in mils;

ddd_{ZZ} is the average wind direction in the appropriate zone (ZZ) in tens of mils.

Then it will be compared the course of the wind direction. If the wind direction crosses the kilometre north direction (from left or right) the particular wind direction values must be adjusted. If the wind direction crosses the kilometre north direction from the left during a movement from one layer to the next (higher), the 60-00 value must be added to the $\alpha'_{w(dc)}_{ZZ}$ value. If the wind direction crosses the kilometre

north direction from the right during a movement from one layer to the next (higher), the $\alpha'_{w(dc)ZZ}$ value must be deduced from the 60-00 value. By this way will be got all adjusted wind direction values in the individual METCM zones $\alpha_{w(dc)ZZ}$ in units of mils. If the wind direction does not cross the kilometre north direction with increasing height above AMS, then the wind direction will be:

$$\alpha_{w(dc)ZZ} = \alpha'_{w(dc)ZZ}. \quad (19)$$

For each height (v) above AMS it is necessary to calculate the wind directions (α_v) in hundreds of mils from the $\alpha_{w(dc)ZZ}$ values according to (20) to (22):

$$\alpha_{50} = \frac{\alpha_{w(dc)00} + \alpha_{w(dc)01}}{2} \cdot 0,01, \quad (20)$$

$$\alpha_{100} = \alpha_{w(dc)01} \cdot 0,01, \quad (21)$$

$$\alpha_{150} = \left\{ [\alpha_{w(dc)02} - \alpha_{100}] \cdot \frac{50}{v_{02} - (v-50)} + \alpha_{100} \right\} \cdot 0,01, \quad (22)$$

etc.

Then auxiliary average wind directions (in hundreds of mils) in the particular METEO-11 layers (SS'_{hh}) will be calculated according to (23) to (24):

$$SS'_{02} = \frac{\sum_{n=1}^4 \alpha_{50 \cdot n}}{4}, \quad (23)$$

$$SS'_{04} = \frac{\sum_{n=1}^8 \alpha_{50 \cdot n}}{8}, \quad (24)$$

etc.

The average wind directions in the particular METEO-11 layers (SS_{hh}) will be determined according to the follow relation:

$$SS_{hh} = \begin{cases} (-1) \cdot SS'_{hh} + 50, & \text{if } SS'_{hh} < -0,5 \\ SS'_{hh}, & \text{if } SS'_{hh} \geq -0,5 \end{cases}. \quad (25)$$

C. The Average Wind Speeds (RR) Calculation

The average wind speeds in the individual METCM zones (FFF_{ZZ}) correspond to the wind speed values in the medium heights of appropriate zones. The wind speeds in the medium heights of appropriate zones in meters per second (FFF_{ZZ}) is needed to convert to meters per second as follow:

$$w_{(m \cdot s^{-1})ZZ} = 0,51 \cdot FFF_{ZZ}, \quad (26)$$

where $w_{(m \cdot s^{-1})ZZ}$ is the wind speed in the medium height of appropriate zone (ZZ) in meters per second.

For each height (v) above AMS it is necessary to calculate the wind speeds (w_v) in meters per second from the $w_{(m \cdot s^{-1})ZZ}$ values according to (27) to (29):

$$w_{50} = \frac{w_{(m \cdot s^{-1})00} + w_{(m \cdot s^{-1})01}}{2}, \quad (27)$$

- [8] Blaha, M. & Sobarňa, M. Some Develop aspects of perspective fire support control system. In The 6th WSEAS International Conference on DYNAMICAL SYSTEMS & CONTROL (CONTROL '10): WSEAS Press, Tunisia, 2010. pp 179-183.

$$w_{100} = w_{(m \cdot s^{-1})01}, \quad (28)$$

$$w_{150} = \left[w_{(m \cdot s^{-1})02} - w_{100} \right] \cdot \frac{50}{v_{02} - (v-50)} + w_{100}, \quad (29)$$

etc.

Then the average wind speeds in the particular METEO-11 layers (RR_{hh}) (in meters per second) will be calculated according to (30) to (31):

$$RR_{02} = \frac{\sum_{n=1}^4 w_{50 \cdot n}}{4}, \quad (30)$$

$$RR_{04} = \frac{\sum_{n=1}^8 w_{50 \cdot n}}{8}, \quad (31)$$

etc.

V. CONCLUSION

The conversion of the METCM into the METEO-11 format is needed to be carried out by using the computer because the manual conversion is time-consuming and can leads to errors. It is advantageous to use the defined mathematical apparatus for the conversion in the own software application or to use it in some program – for example in the MS Excel.

Philosophy of the conversion of the METCM into the METEO-11 format can be also used to develop mathematical apparatuses for other conversions of meteorological messages (as METB3 into METEO-11 format or METCM into METB3 format) in the future.

REFERENCES

- [1] NATO Standardization Agency. AArtyP-1 (A) – Artillery Procedures. Brussels, Belgium, 2004. 102 p.
- [2] NATO Standardization Agency. AArtyP-5 (A) – NATO Indirect Fire Systems Tactical Doctrine. Brussels, Belgium, 2013. 121 p.
- [3] Mukhedkar, R. J. & Naik, S. D. Effects of different meteorological standards on projectile path. *Def. Sci. J.* 2013, **63** (1), 101-107.
- [4] Chusilp, P.; Charubhun, W. & Ridluan, A. Developing firing table software for artillery projectile using iterative search and 6-DOF trajectory model. In the Second TSME International Conference on Mechanical Engineering, Krabi, 19-21 October 2011.
- [5] Chusilp, P.; Charubhun, W. & Nuktumhang, N. Investigating and iterative method to compute firing angles for artillery projectiles. In the 2012 IEEE/ASME International Conference on Advanced Intelligent Mechatronics, Kaohsiung, Taiwan, 11-14, July 2012, pp 940-945.
- [6] Vondrák, J. A Complex utilization of artillery reconnaissance assets in a reconnaissance data acquisition for artillery requirements. University of Defence, Brno, Czech Republic, 2008. PhD Thesis.
- [7] Blaha, M. A complex utilization of artillery reconnaissance assets in a reconnaissance data acquisition for artillery requirements. University of Defence, Brno, Czech Republic, 2012. PhD Thesis.
- [9] Preparation Department of ACR. Meteorological preparation of the Czech Artillery. ACR, Prague, Czech Republic, 1998. 112 p.
- [10] Jirsák, Č. & Kodym, P. External ballistics and theory of artillery fire. Prague, Czech Republic, 1984. 399 p.

- [11] Bartolucci, L.; Chang, M.; Anuta, P. & Graves, M. Atmospheric effects on Landsat TM thermal IR data. *IEEE Trans. Geosci. Remote Sensing*, 1988, **26** (2), 171-176.
- [12] Taeho, L.; Sangjin, L.; Seogbong, K. & Jongmoon, B. A distributed parallel simulation environment for interoperability and reusability of models in military applications. *Def. Sci. J.* 2012, **62** (6), 412-419.
- [13] Jameson, T. Computer met message accuracy studies relating to the met measuring set – profiler; ARL-Project report; U.S. Army Research Laboratory: White Sands Missile Range, NM, 2003.

Image Encryption Based on Development of Hénon Chaotic Maps Using Fractional Fourier Transform

Mona F. M. Mursi¹, Hossam Eldin H. Ahmed², Fathi E. Abd El-samie³, Ayman H. Abd El-aziem⁴

¹*Prof. Dept. Of Electrical Engineering, Shubra Faculty of Engineering, Benha University, Egypt.*

²*Dept. Of Electronics Comm. Eng., P. Dean of the Faculty of Electronic Eng. Menouf-32952, Menufiya University, Egypt.*

³*Assoc. Prof. Dept. Of Electronics& Communication Engineering, Faculty of Electronic Eng - Menufiya University, Egypt.*

⁴*Ph. D Student, Dept. Of Electrical Engineering, Shubra Faculty of Engineering, Benha University, Egypt.*

¹monmursi@yahoo.com, ²hhossamkh@yahoo.com, ³fathi_sayed@yahoo.com, ⁴eng_aymnhassn@ yahoo.com

Abstract:

In this paper, we propose an image encryption scheme based on the development of a Hénon chaotic map using fractional Fourier transform (FRFT) which is introduced in order to satisfy the necessity of high secure image transfer. This proposed algorithm combines the main advantages of fractional Fourier transform domain (FRFT), chaotic Arnold cat map encryption algorithm for confusion and our proposed Hénon chaotic map for diffusion.

Our proposed algorithm is compared with some different chaotic maps as Arnold cat map, Baker map, Hénon map and RC6 algorithm. We perform a comparison between them in several experimental, statistical analyses, processing time and key sensitivity tests. We find from these comparison tests that our proposed algorithm demonstrates good result even better than RC6 and other chaotic maps in some cases.

Keywords: Image encryption, chaotic map, FRFT

1. Introduction

The development of image security become very important to satisfied the different requirements of good security, in recent there are many algorithms introduce the image security in different principle as [1-2-3]. Chaos based encryption algorithms are considered good for practical use as it provide a good combination of high speed, good security, and computational power.

In our proposed algorithm, an image is first subjected to the fractional Fourier transform

domain. Secondly, the transformed image is encrypted using two stages encryption scheme of confusion presented by Arnold Cat map and diffusion presented by Hénon map or one of the proposed Hénon maps for diffusion. Finally the encrypted image is obtained. The confusion algorithm (Arnold Cat map) has been applied ten times on the plain-image to produce shuffled-image. The diffusion algorithm has been applied once in the shuffled-image to produce the ciphered-image.

The rest of the paper is organized as follow, in section 2 we describe an analysis of different 2-D chaotic maps. Section 3 presents an overview of FRFT. Our proposed algorithm and experimental results are explained in sections 4, 5 respectively. The conclusions of the paper are presented in section 6.

2. Two Dimensional Chaotic Maps

We introduce some different chaotic maps and analyze the resulting simulation by using MATLAB (R 2013b), with processor Core2 Duo (2.16 GHz) and 2 GB RAM on Windows 8.

2.1 Arnold Cat Map

The Arnold cat map is a two-dimensional invertible chaotic map [4-5], it is used to shuffle the pixel positions of the plain image. Without loss of generality, we assume the dimension of the original image to be $N \times N$. The 2-D Arnold cat map can be described as follows:

$$\begin{bmatrix} x_{m+1} \\ y_{m+1} \end{bmatrix} = A \begin{bmatrix} x_m \\ y_m \end{bmatrix} \pmod{N} \quad (1)$$

$$= \begin{bmatrix} 1 & p \\ q & pq+1 \end{bmatrix} \begin{bmatrix} x_m \\ y_m \end{bmatrix} \pmod{N}$$

Where p and q are positive integers, Determinant (A) = 1. When Arnold cat map is performed once. The new position of pixel (x_m, y_m) will be in the new position (x_{m+1}, y_{m+1}) , after applying Arnold Cat map with number of iteration iterating R, it satisfied that $(x_{m+1}, y_{m+1}) = (x_m, y_m)$ until it reach its original case. The number of iteration R to satisfied that depends on the parameters p , q and the size N of the original image. Thus the parameters p , q , and the number of iterations R, all can be used as the secret keys. Since the 2-D Arnold cat map has only a linear transformation and mod function, it is very efficient to shuffle the pixel positions using Arnold cat map. After several iterations, the correlation among the adjacent pixels can be completely disturbed.

2.2 Hénon Chaotic System

The Hénon map is two dimensional chaotic maps. It takes a point (x_i, y_i) and maps it to a new point in the same plane. It can be describing as follows [6-7]:

$$\begin{aligned} x_{i+1} &= 1 - rx_i^2 + y_i \\ y_{i+1} &= bx_i \quad , i = 0, 1, 2, \dots \end{aligned} \quad (2)$$

Hénon map, which presents a simple 2-D chaotic map with quadratic nonlinearity, depends on two parameters, r and b , which for the canonical Hénon map have values of $r = 1.4$ and $b = 0.3$. For the canonical values the Hénon map is chaotic. This map has chaotic behavior in range $[1.07, 1.4]$, for other values it behave as periodic or convergence to constant value. The initial value and the value of parameter r are very important to make the Hénon strange attractor, or diverge to infinity. Hénon map gave a first example of the strange attractor with a fractal structure. Because of its simplicity, the Hénon map easily lends itself to numerical studies. Thus a large amount of computer investigations followed. Nevertheless, the complete picture of all possible bifurcations under the change of the parameters r and b is far from completeness.

In the Hénon chaotic map, there are two variables that are adopted to encrypt the image. The encryption process consists of three steps of operations [18]:

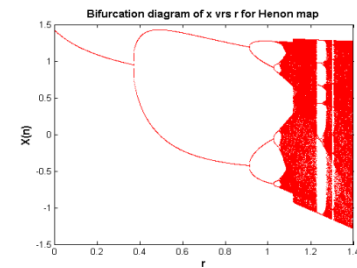
Step1: The Hénon chaotic system is converted into one-dimensional chaotic map. The one dimensional Hénon chaotic map is defined as:

$$x_{i+2} = 1 - rx_{i+1}^2 + bx_i \quad (3)$$

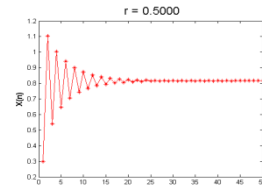
Where $b = 0.3$, $r \in [1.07, 1.4]$. The parameter r , the parameter b , initial value x_0 and initial value x_1 may represent the key.

Step2: We adopt a Hénon chaotic map to change the pixel values of the image. First, the Hénon chaotic map is obtained by the equation (2). Then a transform matrix of pixel values is created.

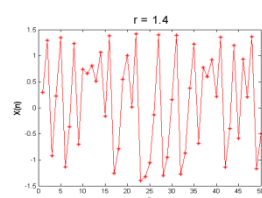
Step3: The exclusive OR operation will be completed bit-by-bit between the transform matrix of pixel values and the values of pixel of the image. The result is the cipher-image. The parameters are selected as $b = 0.3$, $r = 1.4$, $x_0 = 0.01$ and $x_1 = 0.02$.



a) The bifurcation diagram b) The bifurcation diagram
for $r \in [0, 1.4]$, for $r \in [1.07, 1.4]$,



c) Iteration property when d) Iteration property when
 $r = 0.5$ $r = 1$



e) Iteration property when f) Iteration property when
 $r = 1.4$ $r = 1.6$

Fig.1 Analysis of Hénon chaotic map

2.3 Our Proposed Hénon Chaotic Map 1

Our proposed Hénon chaotic map 1 is developed to give a chaotic function which can be used in cryptography applications. This Hénon map 1 is expressed as,

$$\begin{aligned} x_{i+1} &= (r \times x_i + y_i) \bmod 1 \\ y_{i+1} &= 1 - \frac{b}{x_i} , i = 0, 1, 2 \end{aligned} \quad (4)$$

The development of the Hénon chaotic map 1 increases the chaotic range of parameter r to be from the range 1.1 to 1.4 to be from 0 to ∞ except from 0.15 to 0.3 and except using by multiple of value 10 as shown in figure 3.2, that will increase the available chaotic value of parameters that are to be used in encryption.

Our proposed chaotic map is applied under the following conditions:

- x_n takes a value from interval 0, 1, $X_n \in [0,1]$.
- r is variable and $r \in [0, \infty]$.
- $b = 0.3$, initial value $x_0 = 0.01$, $x_1 = 0.02$.

The simulation is shown in figure 2, it is divided into two parts; one is a bifurcation diagram which draws the relation between x_i for all values of r incremented by 0.001 to show the chaotic behavior of the function and the second part shows the iteration property of chaotic functions at different values of r to determine which value is suitable for use in encryption. Figure 2 (c, d, e, f) shows that we can use any integer value of r except the range from 0 to 1 and the multiples of value 10.

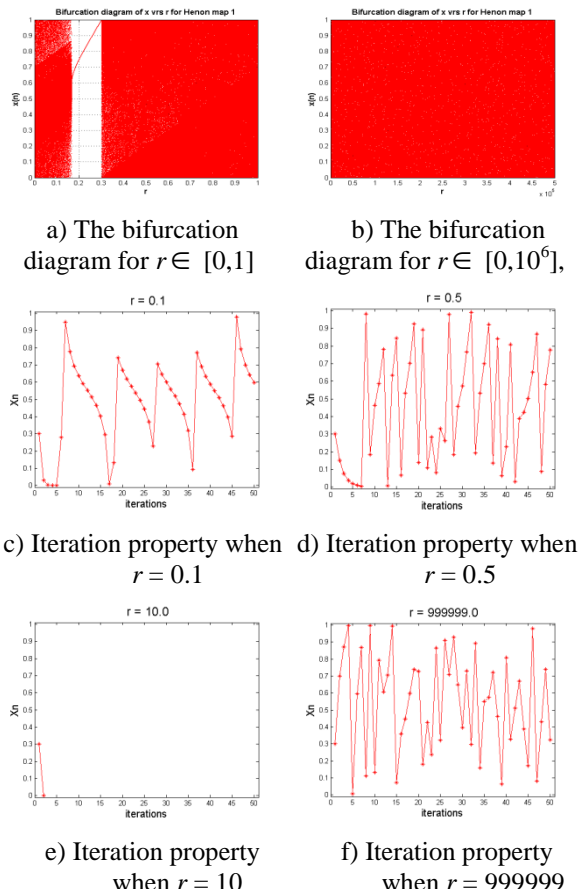


Fig.2 Analysis of Hénon chaotic map1

We introduce another development of Hénon chaotic map as can be shown in table 1.

Finally, we collect the entire previous proposed Hénon map in table 1 to compare among them in the available chaotic range of variable r as shown in the table 1.

Table 1 The different Hénon chaotic maps

| Chaotic map | Function chaotic map | Range of chaotic for variable r |
|-------------|---|-----------------------------------|
| Hénon map | $x_{i+1} = 1 - r \times x_i^2 + y_i$ $y_{i+1} = b \times x_i$ | [1.07, 1.4] |
| Hénon map 1 | $x_{i+1} = (r \times x_i + y_i) \bmod 1$ $y_{i+1} = 1 - \frac{b}{x_i}$ | [0.3, ∞] - multiple of 10 |
| Hénon map 2 | $x_{i+1} = (r \times x_i + y_i) \bmod 1$ $y_{i+1} = b \times x_i$ | [0.7, ∞] |
| Hénon map 3 | $x_{i+1} = (r \times x_i + y_i) \bmod 1$ $y_{i+1} = \frac{b}{1 - x_i}$ | [0, ∞] |
| Hénon map 4 | $x_{i+1} = (r \times x_i + y_i) \bmod 1$ $y_{i+1} = x_i - b$ | [0.6, ∞] |

3. Fractional Fourier Transform (FRFT)

The FRFT can be seen as a linear transformation, which rotates the signal through any arbitrary angle into a mixed frequency – space domain. It can be applied to the entire field where Fourier transform is applied with better results like image processing, quantum physics and communication. We can define the expression for the p -th FRFT of a signal is defined as [8],

$$X_\alpha(u) = \int_{-\infty}^{\infty} x(t) k_\alpha(t, u) dt \quad (5)$$

Here α is the angle at which FRFT is to calculate. Where K_p is the kernel defined as [8]

$$K_\alpha(t, u) = \begin{cases} \sqrt{\frac{1-j \cot \alpha}{2\pi}} \cdot \exp(j \frac{t^2 + u^2}{2} \cot \alpha - j \frac{tu}{\sin \alpha}) & \text{if } \alpha \neq n\pi \\ \delta(u-t) & \text{if } \alpha = 2n\pi \\ \delta(u+t) & \text{if } \alpha = (2n+1)\pi \end{cases} \quad (6)$$

The FRFT is periodic with the equation 6, the transform order can be limited in the interval [-2, 2]. The fractional of Fourier transform of a function x , with an angle α , is defined as the function $R^\alpha = X^\alpha$. One of them is a kernel-based integral transformation of the form:

$$\begin{aligned} f_\alpha(u) &= F^\alpha[f(x)] \\ &= C_\alpha \int f(x) \exp[i\pi \frac{u^2 + x^2}{\tan \alpha} - 2i\pi \frac{ux}{\sin \alpha}] dx \end{aligned} \quad (7)$$

$$\text{where } \alpha = \frac{\alpha\pi}{2}, \text{ and } C_\alpha = \frac{\exp[-i(\frac{\pi \cdot \text{sign}(\sin(\alpha))}{4} - \frac{\alpha}{2})]}{|\sin \alpha|^{1/2}}$$

4. A Proposed Scheme Based on The Development of Hénon Chaotic System Using Fractional Fourier Transform.

We propose a new image encryption algorithm based on the development of Hénon chaotic map using FRFT. The proposed algorithm is divided into two parts; first applying FRFT to original image, then combine the confusion with diffusion. The confusion algorithm is the Arnold Cat map which is applied on the FRFT image. This procedure achieves shuffling of the positions of the pixels of the plainimage. The diffusion algorithms are using Hénon chaotic map or one of the proposed Hénon chaotic maps which are presented in the section 2, it changes the value of the gray scale of each pixel depending on the function of the chaotic map used in the diffusion algorithm. The image, which will be encrypted with the diffusion algorithm, is the shuffled-image. The proposed algorithm cryptosystems have high security performance to fulfill the classic Shannon requirements of confusion and diffusion.

The Diagram of our proposed algorithm can be shown in figure 3.

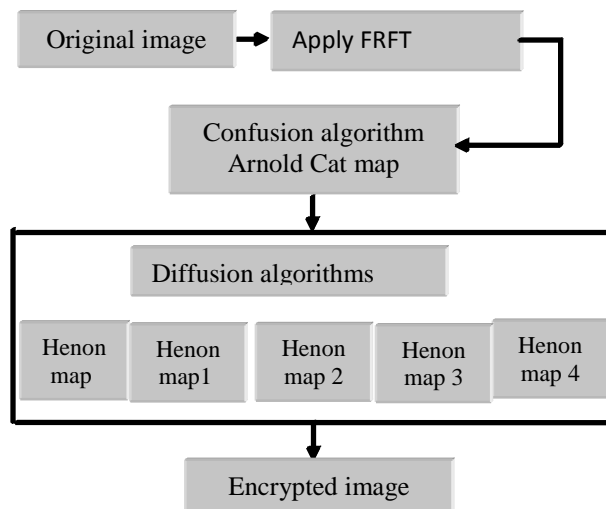


Fig. 3 Diagram of encryption for the proposed algorithm

The proposed algorithm can be described in the following steps:

1. Applying the fractional Fourier transform to the original image.
2. The transformed image is encrypted using chaotic Cat map for confusion.
3. The shuffled transformed image is applied to the second stage of chaotic encryption for

diffusion (Hénon map or one of the proposed Hénon maps), to obtain the ciphered image.

5. Experimental Result and Its Analysis

Our proposed algorithm has been applied to the image (lena.bmp) of size 512×512 as plainimage, which is shown in Figure 4(a).Our proposed algorithm is compared with some different chaotic maps as Arnold cat map, Baker map, Hénon map and RC6 algorithms [11-12-13].One of the important examinations of encrypted image is the visual inspection, where, the more hidden features of the image are, the better the encryption algorithm. The visual inspection of encrypted image for different algorithms in SD and FRFT domain can be shown in the following figures (4-7). It is clear that the different algorithms show hidden details of the image. It gives good results for encryption, but we can't determine which of these algorithms give better results; hence we perform different tests to the algorithms to determine the best. But depending on the visual inspection only, is not enough in judging the complete hiding of the content of the image. So that it should to measure other metrics to evaluate the degree of encryption quantitatively. The security analysis in this paper includes the statistical analysis, the histogram analysis, the correlation coefficient metric, the maximum deviation metric, the irregular deviation metric and the processing time [9-10].

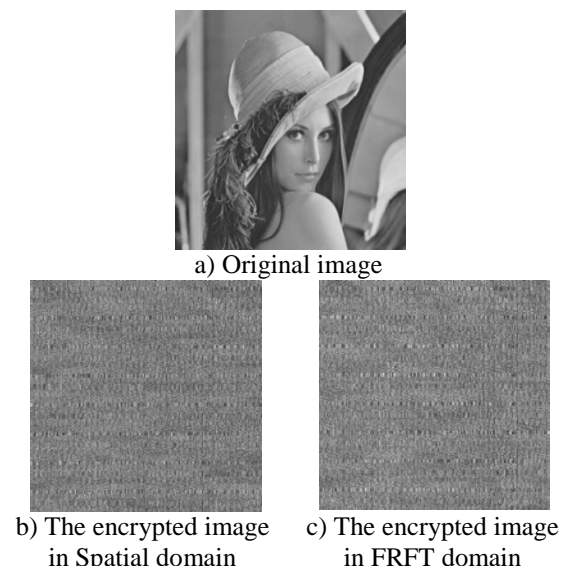


Fig 4 The encrypted image using chaotic Baker map

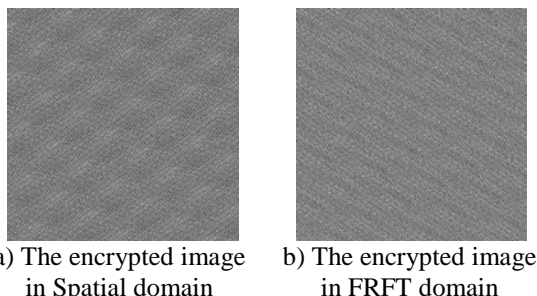
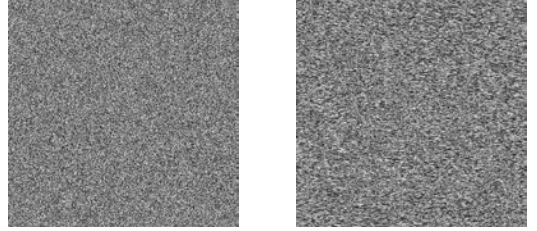


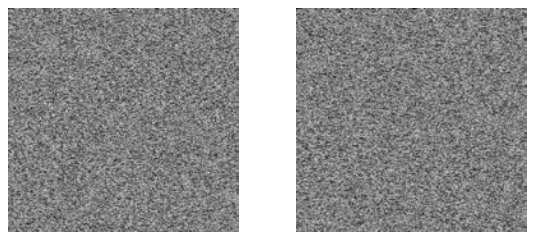
Fig.5The encrypted image using chaotic Cat map

Fig.5 The encrypted image using chaotic Cat map

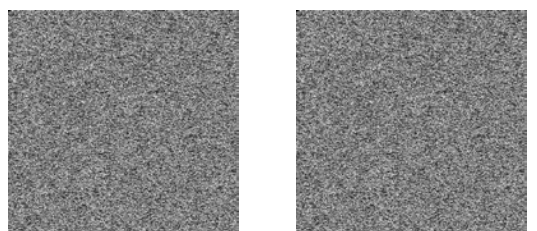


a) The encrypted image in Spatial domain b) The encrypted image in FRFT domain

Fig. 6 The encrypted image using chaotic Hénon map



a) The encrypted image using proposed algorithm using Hénon1 map with FRFT b) The encrypted image using proposed algorithm using Hénon2 map with FRFT



c) The encrypted image using proposed algorithm using Hénon3 map with FRFT

d) The encrypted image using proposed algorithm using Hénon4 map with FRFT

Fig. 7 The encrypted image using our proposed algorithm using with FRFT domain

5.1 Statistical Analysis.

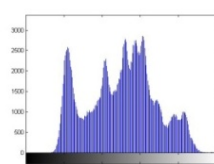
To examine the quality of encryption and

the stability via statistical attacks, the histogram is calculated for all images, correlation coefficient (CC) between original image and cipherimage, maximum deviation factor (MD), and irregular deviation factor (ID), unified average change intensity (UACI), and number per change rate (NPCR).

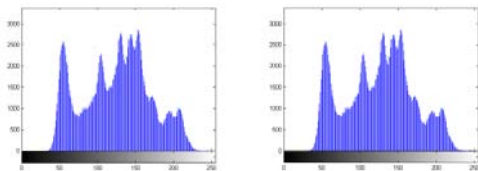
5.1.1 Histogram Analysis.

The histogram of the original-image is shown in figure 8(a), the histogram of shuffled-image by using the Baker Chaotic map in the spatial domain and FRFT is shown in figure 8 (b), (c) respectively, using key (10, 5, 12, 5, 10, 8, 14, 10, 5, 12, 5, 10, 8, 14, 10, 5, 12, 5, 10, 8, 14, 10, 5, 12, 5, 10, 8, 14, 10, 5, 12, 5, 10, 8, 14, 10, 5, 12, 5, 10, 8, 14, 10, 5, 12, 5, 10, 8, 14, 10, 5, 12, 5, 10, 8, 14, 10, 5, 12, 5, 10, 8, 14). The ciphering key of Chaotic Baker map consists of the following sequence of 56 divisors of 512. It is clear that the baker map doesn't change the histogram of the encrypted image from the original image in the SD and in FRFT because it makes only permutation to the pixels of the image.

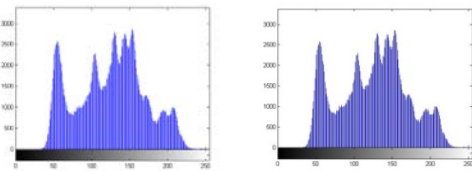
Figure 9(a) And (b) is the shuffled-image by using an Arnold Cat map in SD and FRFT domain, the histogram of this shuffled- image, such that the Arnold cat map is chosen as $p = 1$, $q = 2$ and $R = 10$ times. As we can see, the histograms of the ciphered images in Arnold cat map encryption in FRFT transforms domain and spatial domain is the same as the original image as this algorithm depends only on permutation. In figure 10(a),(b), we can see the histogram of the encrypted image using Hénon map which is fairly uniform distribution and it is completely different from the histogram of the original image that is because of diffusion caused by this map. Figure 11 illustrate our proposed algorithm using our proposed Hénon map 1, 2, 3, 4, it is uniformly distributed and totally different from the original histogram. As we can see from the visual inspection, our proposed algorithm improves the encrypted image as their hiding information and has no symmetric blocks. Also, they improve the histogram of the encrypted image as they are uniformly distributed and totally different from the original histogram.



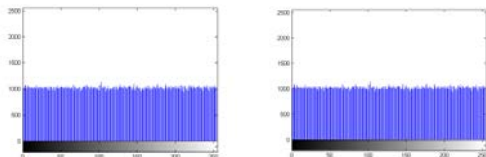
a- The histogram of the original image



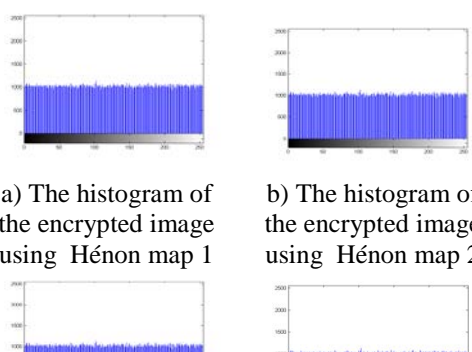
b) The histogram of the encrypted image in SD
c) The histogram of the encrypted image in FRFT domain
Fig. 8 The histogram of encrypted image using the chaotic Baker map.



a) The histogram of the encrypted image in SD
b) The histogram of the encrypted image in FRFT domain
Fig. 9 The histogram of encrypted image using the Arnold cat map



a) The histogram of the encrypted image in SD
b) -The histogram of the encrypted image in FRFT domain
Fig. 10 The histogram of encrypted image using the Hénon map



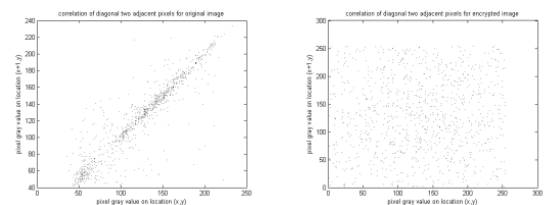
c) The histogram of the encrypted image using Hénon map 1
d)The histogram of the encrypted image using Hénon map 2
e) The histogram of the encrypted image using Hénon map 3
f)The histogram of the encrypted image using Hénon map 4

Fig. 11The histograms of the encrypted image using our proposed algorithm with proposed Hénon map 1,2,3,4 in FRFT domain

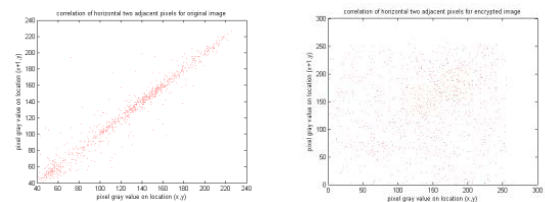
5.1.2 Correlation Coefficient

We analyzed the correlation between two vertically adjacent pixels, two horizontally adjacent pixels and two diagonally adjacent pixels in original image/cipher image respectively, using our proposed algorithm using Hénon map 3 in the FRFT domain, as an example to test the correlation coefficient of our proposed algorithm. We made these tests in the three directions. We tested that by selecting 1000 pairs randomly of two adjacent pixels from an image. Then, we calculated their correlation coefficient [13]. Figure 12 shows the diagonal, vertical, horizontal correlation coefficient of the original and encrypted image in the FRFT domain.

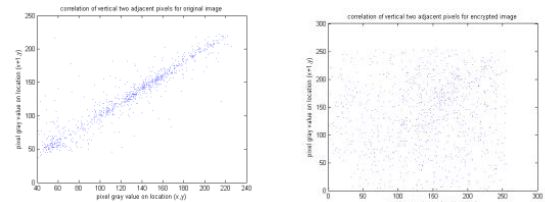
In the following figure, it is clear that there is a close correlation between pixels in the original image, but when the chaotic maps applied in the FRFT domain there is no correlation between adjacent pixels in the encrypted images. We can see that, our used proposed algorithm has a small correlation coefficient.



a) CC of diagonal two pixels for original image
b) CC of diagonal two pixels for encrypted image



c) CC of horizontal two pixels for original image
d) CC of horizontal two pixels for encrypted image



e) CC of vertical two pixels for original image
f) CC of vertical two pixels for encrypted image

pixels for original
image pixels for encrypted
image

Fig 12 The CC of the original and encrypted image using proposed using Hénon 3with FRFT

Table 2 The encryption evaluation measurements of the encrypted images in SD and FRFT domains.

| | | CC | MD | ID | Time | UACI | NPCR |
|-------------------------------------|-------------|-----------|-----------|-----------|-------------|-------------|-------------|
| Chaotic Baker Map | SD | 0.0032 | 0 | 256816 | 3.66 | 20.23 | 99.28 |
| | FrFT | 0.00 | 56029 | 248988 | 3.65 | 20.77 | 99.35 |
| Arnold Cat Map | SD | 0 | 0 | 256968 | 0.6412 | 20.28 | 99.33 |
| | FrFT | 0.0008 | 56029 | 252780 | 0.6303 | 20.63 | 99.33 |
| Hénon map | SD | 0.0062 | 184176 | 186122 | 1.08 | 28.05 | 99.58 |
| | FrFT | 0 | 184218 | 185158 | 1.06 | 28.20 | 99.62 |
| Hybrid system (Cat +Hénon) | FrFT | 0 | 187860 | 183718 | 1.6714 | 28.12 | 99.6002 |
| Hybrid system (Cat + Hénon1) | FrFT | 0.0044 | 187020 | 184454 | 1.6809 | 28.25 | 99.6082 |
| Hybrid system (Cat +Hénon2) | FrFT | 0.0026 | 188628 | 184022 | 1.7187 | 28.34 | 99.61 |
| Hybrid system (Cat + Hénon3) | FrFT | 0 | 187430 | 183490 | 1.77 | 28.55 | 99.6418 |
| Hybrid system (Cat + Hénon4) | FrFT | 0.0042 | 187570 | 184902 | 1.7221 | 28.31 | 99.62 |
| RC6 | SD | 0.0013 | 186907 | 184910 | 800 | 22.31 | 99.60 |

The rest of all tests are applied and the results of measuring factors of the proposed algorithm with FRFT domain and other algorithms are given in Table 2 where CC indicates the correlation coefficient between the original image and encrypted one, MD indicates the maximum deviation measures, ID indicates the irregular deviation measures, T indicates the processing time in seconds, UACI indicate Unify average change intensity between original image and encrypted one and NPCR indicate number per change rate between original image and encrypted one. Based on this table, we can conclude that:

- 1) The correlation coefficient CC is measuring factor: In this test, in general, all the algorithms have a good correlation. But the encrypted image has the best results with our proposed algorithm using Hénon map 3, The correlation coefficient between the original image and the encrypted image, has been improved through our proposed algorithm besides FRFT improves the CC with any algorithm.
- 2) The Maximum deviation MD measuring factor: proposed algorithm using Hénon map 3 achieved the highest result. But the baker and cat map in spatial domain and fractional

Fourier transform domain has the worst result compared to all algorithms.

- 3) The irregular deviation ID measuring factor: In this test, our proposed algorithm using Hénon map 2 has the best result. FRFT domain improves the results with each algorithm. But the spatial domain with cat and baker maps has the worst results in the proposed algorithms.
- 4) The NPCR: in general, all the algorithms have a good NPCR, the best result with our proposed algorithm using Hénon map3 and the worst case with baker map at spatial domain.
- 5) In UACI, the best result is with the proposed algorithm using Hénon map 3 and the worst case obtained with baker map in spatial domain.
- 6) It is clear that RC6 algorithm has a very large computational time that made it unsuitable for real time applications.
- 7) The processing time, in our proposed algorithm, takes much more time because of the complexity of the system. In general, to improve the processing time. We use the

proposed Hénon map 2, 3 in the FRFT domain, which give good results than the single algorithms and provide higher encryption quality.

In general, all maps in FR FT domains have results better than RC6 algorithm.

5.2 Security Analysis

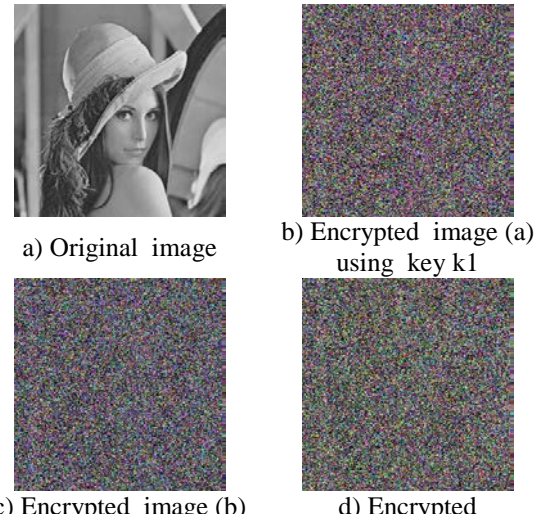
A good encryption scheme should resist most kinds of known attacks, it should be sensitive to the secret keys, and has large key space to make brute force attacks infeasible. In the proposed scheme, the parameters r and b , the initial values x_0 and x_I , and extra parameter p , q of the Arnold cat map, parameter a which represent the angle of rotation of FRFT chaotic maps encryption, are used as secret keys. The key space it should be very large to can resist all kinds of brute-force attacks.

5.2.1 Key Sensitivity Analysis

The sensitivity of key is more important in the measuring of security of the image cryptosystem, which means that the cipher image cannot be decrypted correctly if there is only a very small difference between the keys used for encryption and decryption. For testing the sensitivity of key for our proposed image encryption algorithm by using Hénon chaotic map 3, we have performed the following steps:

- As shown in figure 13(a), (b) is original image and encrypted image (A) respectively by applying our proposed algorithm using the following parameter of Hénon map 4 using the secret key 1 as follows: $r=11$, $b = 0.3$, $x_0=0.01$, $x_1 = 0.02$, $p=1$, $q=2$ and iteration = 10.
- We make slight modification at parameter r to be 11.1 and apply the proposed algorithm at this in case the key called k2, the encrypted image (B) is shown in figure 13 (c)
- Again, the same original image is encrypted by making the slight modification in the secret key 3 to become $r=11.2$ as shown in figure 13 (d) encrypted image (C).
- Finally, we compare among three encrypted images A, B and C.

We have shown the original image and the three encrypted images produced, it is clear that it not sufficient to judge the difference between the three encrypted images by visual inspection. So that, we have calculated the CC between the corresponding pixels in the three encrypted images, also we measure the NPCR between the three encrypted images. All these results are tabulated in table 3.



c) Encrypted image (b)
using key k2
d) Encrypted
image(c)using key k3

b) Encrypted image (a)
using key k1

Fig. 13 Key sensitive result with using proposed
Hénon chaotic map 3

It is clear from the following results in table 3 there are no correlation exists among three encrypted images and the value of NPCR are larger than %99.6 which mean that our algorithm are very sensitive for any small change in the key.

Table 3 Correlation coefficients and NPCR
between the three different encrypted images

| Image 1 | Image 2 | C.C | NPCR |
|-------------------|-------------------|-----|---------|
| Encrypted image A | Encrypted image B | 0 | 99.6132 |
| Encrypted image B | Encrypted image C | 0 | 99.6155 |
| Encrypted image | Encrypted image A | 0 | 99.6239 |

Moreover, in figure 14, we have shown the results of some attempts to encrypted and decrypted images by using small different secret keys, in figure 14(a), (b) is the original image and encrypted image produced respectively. Small changes in key fail completely to reproduce the original image as it is clear in figure 14(d). High key sensitivity is required by secured image cryptosystems, which means that the cipher image cannot be decrypted correctly although there is only a slight difference between encryption and decryption keys. From previous figures and table it is clear that our proposed algorithm is high key sensitive.



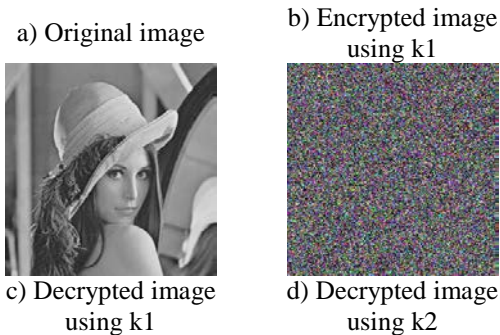


Fig. 14 Key sensitive result by using Hénon chaotic map 3

6. Conclusion

This paper focuses on presenting an efficient image cryptosystem based on combination of confusion and diffusion with FRFT to provide the best performance. Our proposed algorithm use Arnold cat map for confusion and our proposed development Hénon chaotic map for diffusion in FRFT. The experimental results and analysis show that the proposed cryptosystem is the good and has high security compared with baker map and Arnold cat map in spatial and FRFT domain.

According to the results obtained in this paper, we can conclude that:

- 1) The diffusion chaotic cryptosystem (Hénon map) has better performance than confusion chaotic crypto systems (Baker map and Arnold Cat map) and RC6.
- 2) The Fractional Fourier Transform domain improves the performance of chaotic maps.
- 3) Our proposed algorithm using Hénon map 3 provide higher performance compared to the other algorithms.
- 4) It has a large enough key space to resist most kinds of brute force attacks; it is very sensitive to all members of the secret keys.
- 5) Its results with all tests of statistical analysis are better than the results of a baker, Arnold cat map, Hénon and Rc6 and for the same tests.
- 6) Using our proposed Hénon map1, 2, 3, 4 increase the available range of chaotic to be used in encryption compare to limited range of Hénon map.
- 7) As demonstrated in the simulation, our proposed scheme is suitable image encryption in real time application.

References

- [1] Komal D Patel, SonalBelani "Image Encryption Using Different Techniques: A Review" International Journal of Emerging Technology and Advanced Engineering www.ijetae.com (ISSN 2250-2459, Volume 1, Issue 1, November 2011).

[2] Varsha S. Nemade, R. B.Wagh "Review of different image encryption techniques" National Conference on Emerging Trends in Computer Technology (NCETCT-2012).

[3] Rajinder Kaur, Er. KanwalpritSingh "Image Encryption Techniques: A Selected Review" IOSR Journal of Computer Engineering (IOSR-JCE) e-ISSN: 2278-0661, p- ISSN: 2278-8727Volume 9, Issue 6 (Mar. - Apr. 2013), PP 80-83 www.iosrjournals.org

[4] Zhenwei Shang, Honge Ren, Jian Zhang. 2008. A Block Location Scrambling Algorithm of Digital Image Based on Arnold Transformation. the 9th International Conference for Young Computer Scientists, 978-0-7695-3398-8/08/\$25.00 © IEEE.

[5] Zhu Liehuang, Li Wenzhuo, Liao Lejian, Li Hong. 2006. "A Novel Algorithm for Scrambling Digital Image Based on Cat Chaotic Mapping" Proceedings of the 2006 International Conference on Intelligent Information Hiding and Multimedia Signal Processing (IIH-MSP'06), 0-7695-2745-0/06 © IEEE.

[6] L. Guo-hui, Z. Shi-ping, X. De-ming, L. Jian-wen, "An Intermittent Linear Feedback Method for Controlling Hénon-like Attractor" Journal of Applied Sciences, pp. 288–290, Dec 2001.

[7] Chen Wei-bin, Zhang Xin, "Image Encryption Algorithm Based on Hénon Chaotic System" 978-1-4244-3986-7/09© IEEE 2009.

[8] Ashutosh, Deepak Sharma" Image Encryption Using Discrete Fourier Transform and Fractional Fourier Transform" International Journal of Engineering and Advanced Technology (IJEAT) ISSN: 2249 – 8958, Volume-2, Issue-4, April 2013.

[9] Nawal El-Fishawy, Osama M. Abu Zaid Quality of Encryption Measurement of Bitmap Images with RC6, MRC6, and Rijndael Block Cipher Algorithms. International Journal of Network Security, 5(3): 241–251, Nov. 2007.

[10] Osama S. Faragallah , E. M. Nigm , Nawal A. El-Fishawy , Osama M. Abu Zaid, " A Proposed Encryption Scheme based on Hénon Chaotic System (PESH) for Image Security" International Journal of Computer Applications (0975 – 8887) Volume 61– No.5, January 2013 .

[11] J. Fridrich "Symmetric ciphers based on two-dimensional chaotic maps" Int. J Bifurcation and Chaos 8 (6): 1259 – 1284 -1998.

[12] J. Fridrich, "Image encryption based on chaotic ma.ps" In Proc. IEEE Int. Conference on systems, Man and Cybernet-ics, volume 2, pages 1105–1110, 1997.

[13] H. E. H. Ahmed, H. M. Kalash, and O. S. Faragallah, "Encryption Efficiency Analysis and Security Evaluation of RC6 Block Cipher for Digital Images", International Conference on Electrical Engineering (ICEE '07), pp. 1-7, 11-12 April 2007.

Anti-windup approach for the compensation of slip speed of induction motor

T. Benmiloud

IUT institute of Technology - University of Tiaret -Algeria

Laboratoire de Développement des Entrainements Electriques (LDEE)- Oran University of Sciences and Technology

Abstract – This paper present a new technique for the compensation of slip speed of induction motor using anti-windup approach. The slip speed change when we have parametric variation of rotor resistance in presence of load torque. Otherwise, the effects of parametric variations of induction motor appears most because the windup due to the non-linearity of the model of static inverter. So, we can use the anti-windup action to make the compensation of slip speed of induction motor. Simulation results have shown the effectiveness of the new anti-windup technique of compensation of slip speed of induction motor, which will improve the performances and the robustness of direct field oriented control of induction motor.

Keywords: *direct filed oriented control, anti-windup strategy, slip speed of induction motor, parametric variations of induction motor*

I. Introduction

The direct field oriented control (DFOC) technique is widespread used in high performance induction motor (IM) drives [1, 2]. It allows, by means a coordinate transformation, to separate the electromagnetic torque control from the rotor flux one, and, hence to manage induction motor as DC motor. Voltage vector control improves the dynamics and stability of the speed control of IM, both when the speed reference is changed and in relation to the load torque. The main problem that occurs in induction motor drives is drop of speed because the speed depends on motor load [3]: that is caused by the finite limit of the inverter output voltage [4, 5]. This phenomenon is defined as the windup problem [6, 7].

The windup problem generates an error on the dynamic between real and calculated control of IM. Then, windup problem will increase the effects of some disturbances (such as variation of resistances or the magnetic saturation), which provide a drop of speed when the load torque is applied. So, the drop of speed in the direct filed control is the result of association of the three several elements (windup phenomena, parametric variation, application of load torque). So, several works have been oriented to improve the performances of the DFOC control of IM either to;

- overcome windup problem [7, 8, 9],

- or to make the adaptation of the parametric variations [10, 11, 12],
- or to make the compensation of load torque [13],
- or to make compensation of slip speed of IM [3].

The calculation of the slip speed in the direct vector control involves the rotor time constant, which may vary considerably over the operational range of the motor mainly due to changes in rotor resistance with temperature. An error in the slip speed calculation gives an error in the rotor flux position, resulting in coupling between the flux and torque-producing currents due to axis misalignment [14]. In this paper, we improve the performances of direct field oriented control of IM using the compensation of slip speed of induction motor using the anti-windup action. This will combine two among the four methods mentioned previously. Then, we propose to add the back of the anti-windup of the control voltages of IM not to make the correction of currents or to make the correction of the speed, but to add the anti-windup action to the slip speed of IM.

This paper is organized as follows. In Section II, the principle of the DFOC control of IM is presented. Section III presents the proposed technique for the new anti-windup strategy to make the compensation of the slip speed of IM, for a DFOC strategy. In Section IV, the effectiveness of the proposed technique is discussed via simulation results. Section V presents the final remarks.

II. Direct Field Oriented Control

The IM model, in space vector notation, established in $d-q$ coordinate system rotating at synchronous speed ω_s is given by the following equations [15, 16, 17];

$$\begin{bmatrix} \dot{i}_{sd} \\ \dot{i}_{sq} \\ \dot{\phi}_{rd} \\ \dot{\phi}_{rq} \\ \dot{\omega}_r \end{bmatrix} = \begin{bmatrix} -\gamma i_{sd} + \omega_s i_{sq} + \frac{K}{T_r} \phi_{rd} + p \omega_r K \phi_{rq} + \frac{1}{\sigma L_s} u_{sd} \\ -\omega_s i_{sd} - \gamma i_{sq} - p \omega_r K \phi_{rd} + \frac{K}{T_r} \phi_{rq} + \frac{1}{\sigma L_s} u_{sq} \\ \frac{L_m}{T_r} i_{sd} - \frac{1}{T_r} \phi_{rd} + (\omega_s - p \omega_r) \phi_{rq} \\ \frac{L_m}{T_r} i_{sq} - (\omega_s - p \omega_r) \phi_{rd} - \frac{1}{T_r} \phi_{rq} \\ \frac{p^2 L_m}{J L_r} (\phi_{rd} i_{sq} - \phi_{rq} i_{sd}) - \frac{f}{J} \omega_r - \frac{p}{J} T_L \end{bmatrix} \quad (1)$$

Where:

$$\sigma = 1 - \frac{L_m^2}{L_s L_r}, \quad \gamma = \left(\frac{R_s}{L_s} + \frac{R_r (1-\sigma)}{\sigma L_r} \right) \text{ and } K = \frac{(1-\sigma)}{\sigma L_m} \quad (2)$$

The state variables are the two components of stator current (i_{sd}, i_{sq}), the two components of the rotor flux (ϕ_{rd}, ϕ_{rq}), and the electrical rotor speed ω_r . The vector input u is represented by the stator voltages v_{sd}, v_{sq} , the load torque is generally considered like external disturbance. There are many categories of vector control strategies. We are interested in this study to the DFOC control technique. Equation (1) shows that the electromagnetic torque expression, presents a coupling between stator current and rotor flux. The main objective of the vector control of induction motor is, as in direct current (DC) machines, to independently control the torque and the flux. This is done by using a d - q rotating reference frame synchronously with the rotor flux space vector. The d -axis is aligned with the rotor flux space vector. Under this condition we have: $\phi_{rd} = \phi_r$ and $\phi_{rq} = 0$. In this case the torque equation becomes:

$$T_e = p \cdot \frac{M}{L_r} \phi_{rd} \cdot i_{sq} \quad (3)$$

It is right to adjust the flux while acting on the component i_{sd} of the stator current and to adjust the torque while acting on the i_{sq} component. We have two variables of action then as in the case of a DC machine. Using equation (1), we obtain the following d and q -axis stator currents:

$$i_{ds} = \frac{(1+T_r s)}{L_m} \phi_r \quad (4)$$

$$i_{qs} = \frac{T_r}{L_m} \omega_{sl} \phi_r \quad (5)$$

Where T_r is the rotor constant; $T_r = \frac{L_r}{R_r}$,

L_m and ω_{sl} are mutual inductance and sleeping pulsation respectively. Using Eq (1), we obtain the following voltage equations [1]:

$$\begin{aligned} u_{sd} &= (R_s + \sigma L_s s) i_{sd} + \frac{L_m}{L_r} p \phi_r - \sigma L_s \omega_s i_{sq} \\ u_{sq} &= (R_s + \sigma L_s s) i_{sq} + \sigma L_s \omega_s i_{sd} + \frac{L_m}{L_r} \omega_s \phi_r \end{aligned} \quad (6)$$

These equations are functions of some structural electric parameters of the induction motor (R_s, R_r, L_s, L_r, L_m), which are in reality approximate values. We will come back thereafter to the influence of the bad knowledge of most interest parameter ($T_r=L_r/R_r$) on the control of the machine [18]. The rotor flux amplitude can be obtained by solving Eq. (1), and its spatial position is given by:

$$\theta_s = \int \left(\omega_r + \frac{L_m i_{sq}}{T_r \phi_r} \right) dt \quad (8)$$

$$\omega_s = \omega_r + \omega_{gl}, \quad \omega_{gl} = \frac{L_m i_{sq}}{T_r \phi_r} \quad (9)$$

The mechanical speed is: $\Omega_m = \frac{\omega_r}{p}$.

These equations are functions of some structural electric parameters of the IM (R_s, R_r, L_s, L_r, L_m), which are in reality approximate values. We will come back thereafter to the influence of the bad knowledge of most interest parameter ($T_r=L_r/R_r$) on the control of IM [19].

III. The new anti-windup strategy

This new proposition of compensation of slip speed of induction motor is motivated by the following items;

1- equation (9) shows that slip speed of induction motor is function of the value of rotor resistance.

2- the variation in slip speed affect several variables of IM, because the synchronous speed is function of slip speed which is not the case of the variables of induction motor. So, by adapting the slip speed we will act on all variables at the same time.

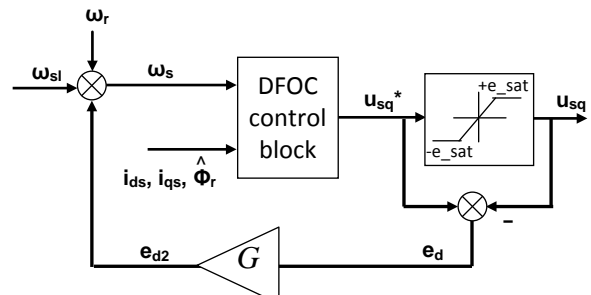


Fig.1: Block diagram of the anti-windup compensation of ω_{sl}

Because the effects of parametric variations appear in the presence of windup action, then, we can make the compensation of variation of rotor resistance by the anti-windup action. The anti-windup compensation (AWC) is made in the following way: the difference between the

calculated control and the real voltage control is used to make the slip speed of induction motor.

Anti-windup compensation is generally used to make compensation of integral action, because it is precisely the integral action that creates a problem of regulation in the case of the windup phenomenon [20, 21, 6]. In our case, the anti-windup action is not used to make limitation of the integral action of PI corrector. Figure 1 shows that AWC uses the difference between input and output saturation block of u_{sq} voltage of IM to make adaptation of the slip speed $\Delta\omega_{gl}$ [20, 21]: When difference between Saturation's input and output e_d appears, we have an adaptation of the value of slip speed equal to e_{d2} . When the input and output Saturation difference vanishes, there is not adaptation of slip speed. We write:

$$\Delta\omega_{gl} = \begin{cases} ed_2 & \text{if } ed \neq 0 \\ 0 & \text{if } ed = 0 \end{cases} \quad (10)$$

The diagram of the AWC includes a gain G , its value is chosen so as to obtain a best compensation of parametric variations [22]. This gain controls the drop of speed of induction motor.

IV. Simulation results

Simulations, using MATLAB Software Package, have been carried out to show the test of the proposed anti-windup compensation of slip speed of induction motor. Classical Proportional-Integral controllers are used for speed, flux and stator current loops. The sampling time of simulation is set to 1ms. The induction motor parameters used in simulation are given in Table I. The reference trajectories of speed, flux, and stator currents are given in Fig. 2. Flux reference is set to its rated value of 1Wb.

TABLE I. PARAMETERS OF THE INDUCTION MOTOR.

| <i>Parameter</i> | <i>Notation</i> | <i>Value</i> |
|--------------------------|-----------------|-------------------------|
| Rotor resistance | R_r | 3.805 |
| Stator resistance | R_s | 4.85 |
| Mutual inductance | l_m | 0.258 H |
| Stator inductance | L_s | 0.274 H |
| Rotor inductance | L_r | 0.274 H |
| Rotor inertia | J_m | 0.031 kg/m ² |
| Pole pair | P | 2 |
| Viscous friction | f_m | 0.008 N m sec |
| Mechanical power | P_{max} | 1.5 KW |
| Nominal voltage | U_n | 220 V |
| Nominal current | I_{sn} | 3.1 A |
| Nominal mechanical speed | Ω_{mn} | 1500 Nm |

This benchmark shows that the load torque appears at the nominal speed (157 rad/s), and the load torque is varied 3 times; at 1.3 s from 0 to 10 Nm, at 2.6 s from 10 to 0 Nm, at 5.3 s from 0 Nm to -10 Nm, and at 6.6 s from -10 Nm to 0 Nm.

We have first made the simulation of DFOC control of induction motor with AWC, without then with application of 100 % of rotor resistance variation. Fig2. shows that we make control of induction motor with a nominal speed and with application of nominal load torque. Secondly, we make the simulation of DFOC control of induction motor with AWC, also without then with application of 100 % of rotor resistance variation. In this case we apply the same nominal speed and nominal load torque to IM. To make the estimation of rotor flux we use a classic estimator given by Eq (4).

Fig. 3 shows that we have good tracking of speed when we have not parametric variation, with very small static error. The drop in speed after the application or the elimination of the load torque reached a value of 18 rad/s.

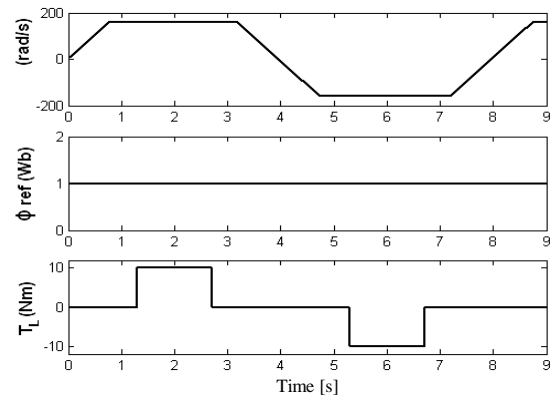


Fig. 2. Reference trajectories

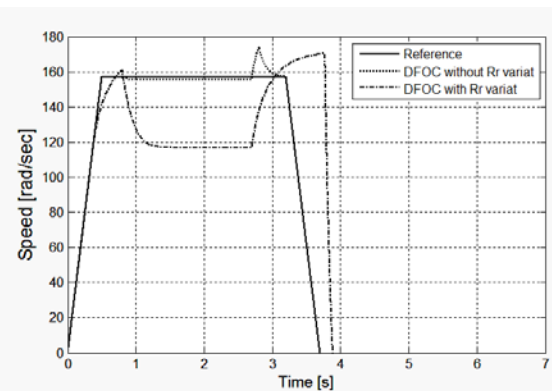


Fig. 3. Speed tracking using DFOC control of IM with and without rotor resistance variation

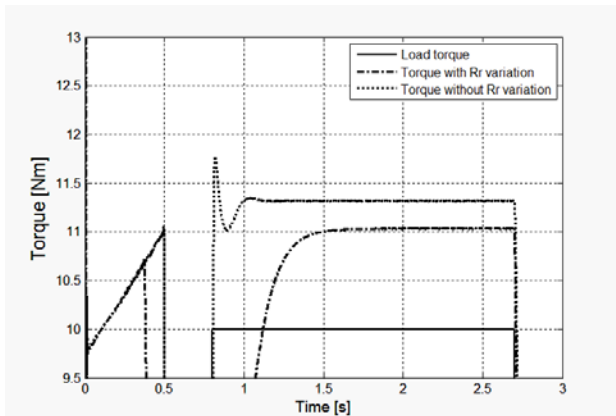


Fig. 4. Motor and load torques using DFOC control of IM with AWC compensation - with and without rotor resistance variation

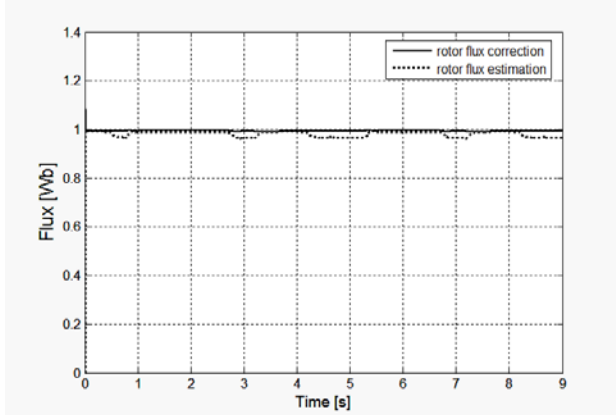


Fig. 5. Rotor flux correction and rotor flux estimation for DFOC control of IM without AWC compensation and without rotor resistance variation

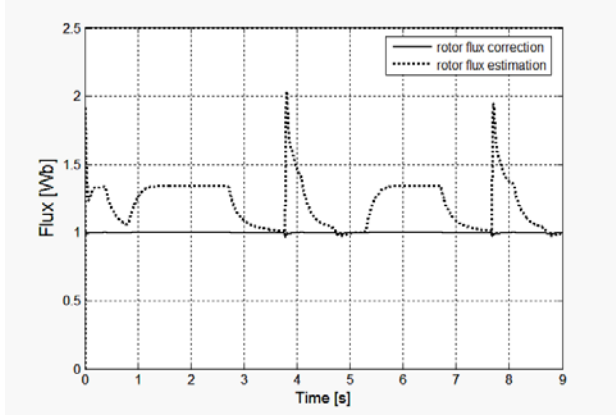


Fig. 6. Rotor flux correction and rotor flux estimation for DFOC control of IM without AWC compensation with rotor resistance variation

But when we have rotor variation, we obtain big drop in mechanical speed of IM (due also the application of load torque). Fig. 4 shows good performances tracking of the load torque, in the two cases; with and without application of rotor resistance variation, with some peaks in the curve of the torque.

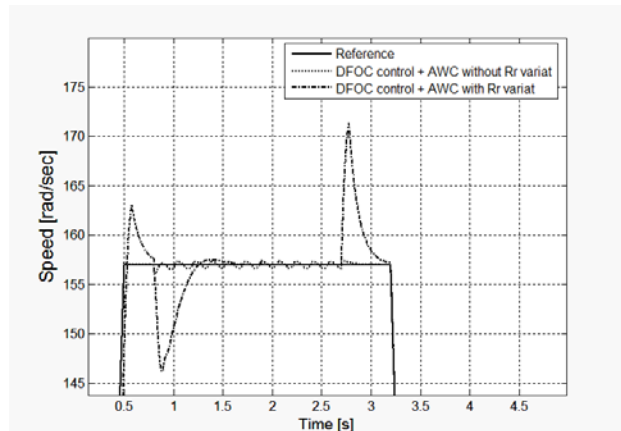


Fig. 7. Speed tracking using DFOC of IM with AWC compensation - with and without rotor resistance variation

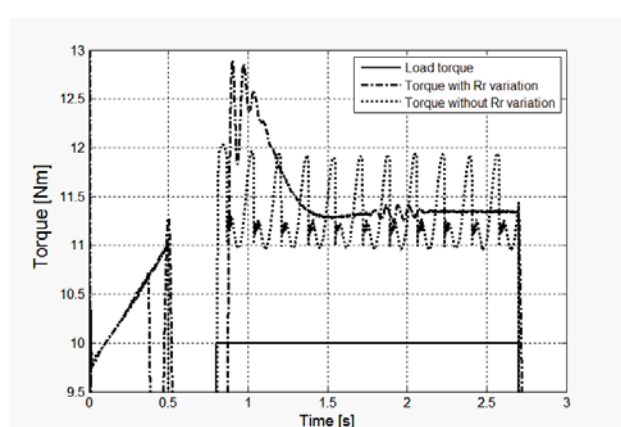


Fig. 8. Motor and load torques using DFOC of IM with AWC compensation - with and without rotor resistance variation

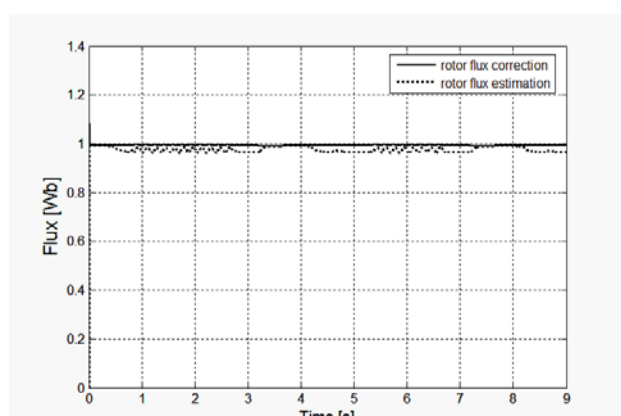


Fig. 9. Rotor flux correction and rotor flux estimation for DFOC control with AWC compensation and without rotor resistance

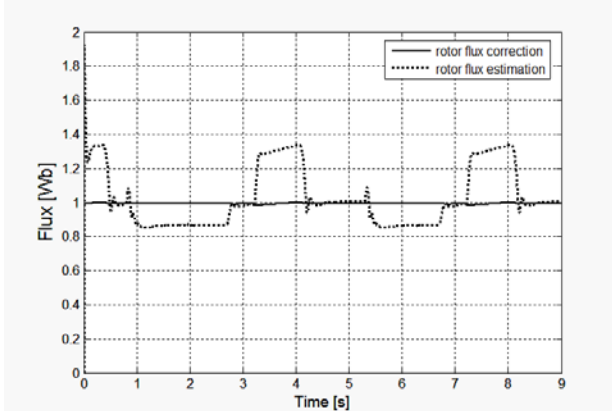


Fig. 10. Rotor flux correction and rotor flux estimation for DFOC control of IM with AWC compensation with rotor resistance variation

Fig. 5 and Fig. 6 show that we have good correction and good estimation of rotor flux without AWC compensation with big overshoot in the case of application of rotor resistance. Fig. 7 shows that by using the anti-windup compensation of slip speed of IM we doesn't obtain a drop of tracking of speed of induction motor in the presence of rotor resistance variation.

The DFOC control with AWC compensation technique allows keeping good same regulation performances despite the change of the value of the rotor resistance. However, we note the presence of small oscillation of speed when we haven't rotor resistance variation. Fig. 8 shows that we have most important oscillations in the curve of the torque of IM when there is not rotor resistance variation. Fig. 9 and Fig. 10 show good performances tracking of the load torque, in the two cases; with and without application of rotor resistance variation.

The obtained results of the proposed AWC compensation of slip speed are interests except the presence of oscillations in the tracking speed and the torque of IM. These oscillations are dues to feedback action of the windup of voltage of induction motor in the value of slip speed of induction motor. So, to perform these results, we propose to make filtering of the anti-windup action on the slip speed of induction motor. To make the filtering we use classic second order filter associated with proportional derivative action (PD) with small value of derivative action. The formula of the second order filter is given by the following transfer function:

$$FT_{filter} = \frac{K_1}{s^2 + K_2 s + K_1} \quad (11)$$

with: $K_1 = 2200$, and $K_2 = 480$.

The final scheme of AWC compensation of slip speed of induction motor is showed the following figure.

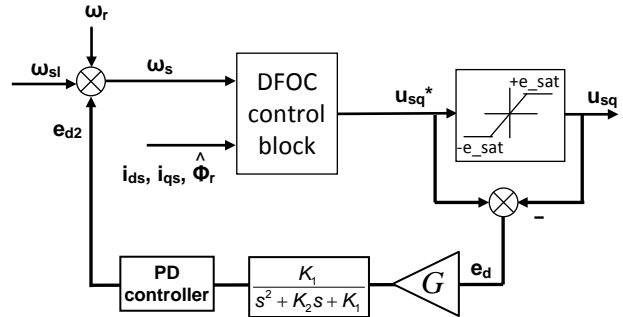


Fig. 11. Final block diagram of AWC compensation of ω_{sl}

Followed figures give simulation results of DFOC control of IM with modified AWC compensation of slip speed of IM. Fig. 12 shows that we obtain good tracking of speed with and without rotor resistance variation. Fig. 13 and Fig. 14 show good tracking of torque with limited oscillations in the case of non application of rotor resistance variation. Fig. 15 and fig. 16 show good tracking and good estimation of rotor flux of IM in the two cases, with and without rotor resistance variation.

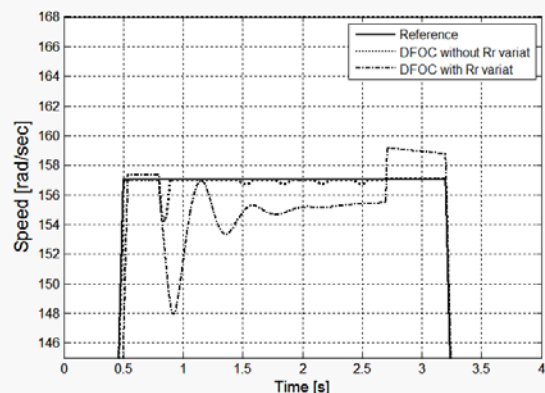
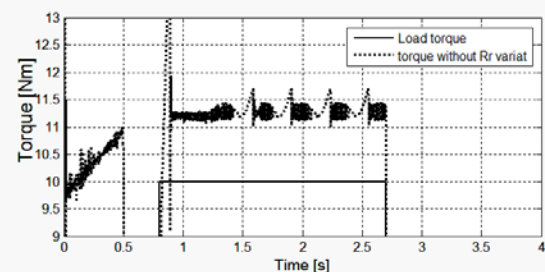


Fig. 12. Motor and load torques using DFOC of IM with modified AWC compensation - with and without rotor resistance variation



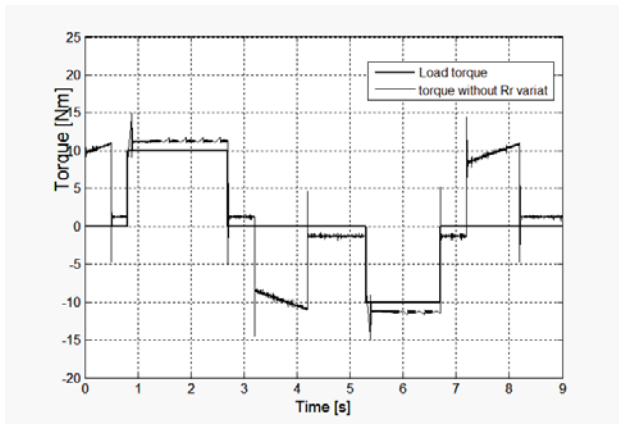


Fig. 13. Motor and load torques using DFOC of IM with modified AWC compensation - without rotor resistance variation

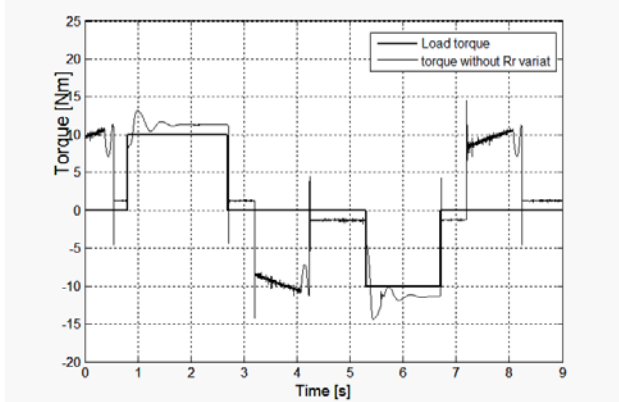


Fig. 14. Motor and load torques using DFOC control of IM with AWC compensation - with rotor resistance variation

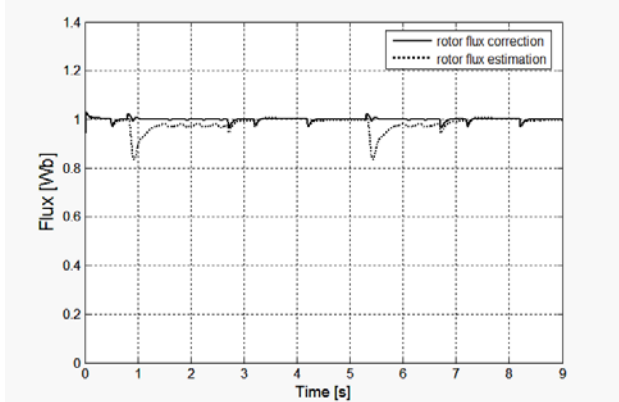


Fig. 15. Rotor flux correction and rotor flux estimation for DFOC of IM with modified AWC compensation - without rotor resistance variation

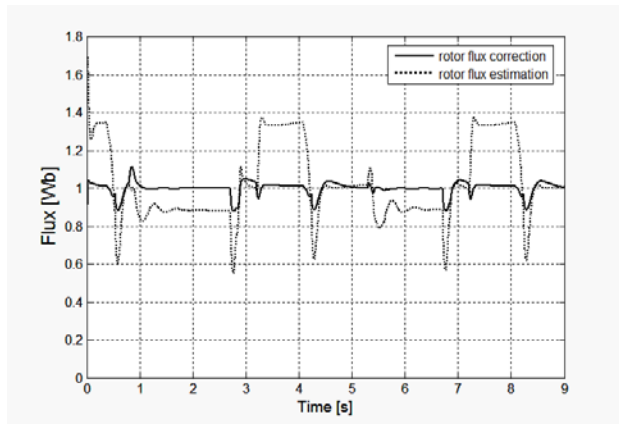


Fig. 16. Rotor flux correction and rotor flux estimation for DFOC of IM with modified AWC compensation with rotor resistance variation

Conclusion

In this paper, we presented a new approach anti-windup compensation of slip speed of induction motor. The proposed anti-windup strategy is based on the evaluation of the difference between input and output saturation block of voltage of IM to make adaptation of the slip speed. The compensation of slip speed will improve the performances and the robustness of the DFOC control of induction motor. The results of simulation show that the proposed anti-windup compensation gives better performances while tracking the speed and the flux, even in presence of rotor resistance. Future works concern real true implementation of the proposed scheme to validate these theoretical results.

References

- [1] J. P. Caron, J. P. Hautier, Modeling and Control of Induction Machine. *Technip Edition*.
- [2] M. A. Ouhrouche and C. Volat, Simulation of a Direct Field-Oriented Controller for an Induction Motor Using Matlab/Simulink. *Proceeding of the IASTED International Conference Modelling and Simulation* (Pittsburgh, Pennsylvania, USA).
- [3] Jerkovic Vedrana, Spoljaric Zeljko, Valter Zdravko, Optimal Control of Induction Motor Using High Performance Frequency Converter, *IEEE 13th International Power Electronics and Motion Control Conference*, pp. 690-694, 2008.
- [4] T. G. Habetler, R. G. Harley, Power Electronic Converter and System Control, *Proceedings of the IEEE*, Vol.89, and Issue: 6, pp.913 –925, Jun 2001.
- [5] Ye Zhongming, Wu Bin, A Review on Induction Motor Online Fault Diagnosis, *The Third International Power Electronics and Motion Control Conference Proceedings. PIEMC 2000*, Vol.3, pp.1353 -1358 vol.3, 2000.
- [6] Karl J. Åström and Tore Hägglund, PID Controllers: *Theory, Design, and Tuning*. Instrument Society of America, 1995.
- [7] Shen Yan-xia, Chen Zhong-wei. Induction motor vector control system based on anti-windup controller. *Industrial Electronics and Applications (ICIEA)*. 6th IEEE Conference on. 2011: 2729-2732.
- [8] Kumar S, Negi R. A comparative study of PID tuning methods using anti-windup controller. Power, *Control and Embedded Systems (ICPCES)*. 2nd International Conference on. 2012: 1-4.

- [9] Hwi-Beom Shin, Jong-Gyu Park. Anti-windup PID Controller with Integral State Predictor for Variable-Speed Motor Drives. *Industrial Electronics, IEEE Transaction on*. 2012: 1509-1516.
- [10] Garces.L.J, Parameter adaptation for the speed controlled static AC drive with a squirrel cage induction motor, *IEEE Trans. IA*, Vol.IA- 16, No.2, Mar./Apr., 1980, pp.173-178.
- [11] T. Rowan, R. Kerkman and D. Leggate, A simple on-line adaptation for indirect-field orientation of an induction machine, *IEEE Trans. IA, VoLIA-37, July/August, 1991*, pp.720-727.
- [12] T. Matsu and T. A. Lipo, A rotor parameter identification scheme for vector controlled induction motor drives, *IEEE Trans. Ind. Applicat, July/Aug. 1985. vol. IA-21*, pp. 624–632.
- [13] Gastaldini, C. & Grundling, H. (2009). Speed-sensorless induction motor control with torque compensation, *13th European Conference on Power Electronics and Applications, EPE '09*, pp. 1 –8.
- [14] I. K. Bousserhane, A. Hazzab, M. Rahli, M. Kamli and B. Mazari, Direct field-oriented control using back-stepping strategy with fuzzy rotor resistance estimator for induction motor speed control. *Information Technology and Control*, vol. 4, no. 4, pp.403-411, 2006.
- [15] Soltani, Y.Abdolmaleki and M. Hajian, Adaptive fuzzy sliding-mode control of speed sensorless universal field oriented induction motor drive. *Iranian Journal of Science & Technology, Transaction B, Engineering*, Vol. 29, No. B4.
- [16] A. Bouhenna, A. Mansouri, M. Chenafa, A. Belaidi, Feedback Gain Design Method for the Full-Order Flux Observer in Sensorless Control of Induction Motor. *Int. J. of Computers, Communications & Control, IJCCC*, Vol. III , No. 2, pp. 135-148.
- [17] A. Mansouri, M. Chenafa, A. Bouhenna and E. Etien, Powerfull nonlinear observer associated with field-oriented control of an induction motor. *Int. J. Appl. Math. Comput. Sci*, Vol. 14, No. 2, 209–220.
- [18] M. Alamir, Sensitivity analysis in simultaneous state/ parameter estimation for induction motors. *Int. J. Of Control*, vol. 75, n°10, pp. 753-758.
- [19] T. Pana and C. Rusu, Speed and rotor flux estimation in speed sensorless control of induction motor. The annals of "Dunarea Dejose", *Electrotechnics, Electronics, Automatic Control, Informatics* (University of Galati Fascicle III, ISSN 1221-454X).
- [20] C. Bohm and D.P Atherton, A Simulink package for comparative studies of PID Anti-windup Strategies, *IEEE/IFAC joint Symposium, 7 March 1994*.
- [21] P. March and M. Turner, "Anti-windup Compensator Designs for Permanent Magnet Synchronous Motor Speed Regulation, *The IEEE International Electric Machines & Drives Conference, IEMDC 2007*. Vol. 1, 3-5 May 2007 Antalya. Turkey.
- [22] Y. Cao, Z. Lin , D. G. Ward: An Anti-windup Approach to Enlarging Domain of Attraction for Linear Systems Subject to Actuator Saturation, *IEEE Transaction on Automatic Control*, Vol. 47, No. 1, Jan. 2002, pp. 140 – 145.

Multivalent Harmonic Mappings

Melike Aydoğ̃an, Durdane Varol

Abstract—In the present paper, we investigated the class of multivalent harmonic mappings in the simply connected domain. In general passing from the harmonic univalent function to the harmonic multivalent function turns out to be quite non-trivial. This passing is guaranteed by the argument principle which was obtained by Duren, Hengartner and Laugesen [1].

Keywords—Harmonic multivalent mappings, Close-to-convex functions, Distortion theorem, Growth theorem, Subordination principle.

I. INTRODUCTION

LET $\mathbb{D} = \{z \mid |z| < 1\}$ be the open unit disc in the complex plane \mathbb{C} . A complex-valued harmonic function $f : \mathbb{D} \rightarrow \mathbb{C}$ has the representation

$$f(z) = h(z) + \overline{g(z)} \quad (1)$$

where $h(z)$ and $g(z)$ are analytic in \mathbb{D} and have the following power series expansions

$$h(z) = \sum_{n=0}^{\infty} a_n z^n, \quad g(z) = \sum_{n=0}^{\infty} b_n z^n, \quad z \in \mathbb{D},$$

where $a_n, b_n \in \mathbb{C}$, $n = 0, 1, 2, \dots$ chose, i.e., $b_0 = 0$, so the representation is unique in \mathbb{D} and is called the canonical representation of f .

For the univalent and sense-preserving harmonic function f in \mathbb{D} it is convenient to make further normalization (without loss of generality) $h(0) = 0$, i.e., $a_0 = 0$ and $h'(0) = 0$, i.e., $a_1 = 1$. The family of such functions f is denoted by S_H [3]. The family of all functions $f \in S_H$ with the additional property that $g'(0) = 0$, i.e., $b_1 = 0$ is denoted by S_H^0 [3]. Observe that the classical family of univalent functions S consists of all functions $f \in S_H^0$ such that $g(z) \equiv 0$. Thus it is clear that $S \subset S_H \subset S_H^0$ [3]. Under the guarantee argument principle which was mentioned in abstract we can define the class of multivalent harmonic functions $S_{H(p)}$. A function f in $S_{H(p)}$ can be expressed $f(z) = h(z) + \overline{g(z)}$, where $h(z)$ and $g(z)$ are of the form

$$\begin{aligned} h(z) &= z^p + \sum_{n=2}^{\infty} a_{n+p-1} z^{n+p-1}, \\ g(z) &= \sum_{n=1}^{\infty} b_{n+p-1} z^{n+p-1}, \quad |b_p| < 1. \end{aligned}$$

The Jacobian J_f of $f(z) = h(z) + \overline{g(z)}$ is defined by $J_f = |f_z|^2 - |f_{\bar{z}}|^2$. If $J_f > 0$, then f is called sense-preserving multivalent harmonic function in \mathbb{D} , and the

M. Aydoğ̃an is with the Department of Mathematics, İ̄sik University, Meşrutiyet Koyu, Şile İstanbul, Turkey email: melike.aydogan@isikun.edu.tr
D. Varol is with İ̄sik University.

Manuscript received September 02, 2014; revised September 02, 2014.

class of all sense-preserving multivalent harmonic functions with $b_p = 0$ is denoted by $S_{H(p)}^0$. For convenience, we will investigate sense-preserving harmonic functions that are functions for which $J_f > 0$. If $J_f < 0$, then \overline{f} is sense-preserving. The second analytic dilatation of a harmonic function is given by $\omega(z) = \frac{g'(z)}{h'(z)}$. We also note that if f is locally univalent and sense-preserving then $|\omega(z)| < 1$ and $J_f \neq 0$ for every $z \in \mathbb{D}$ and f is the solution of the non-linear partial differential equation $\overline{f_{\bar{z}}} = \omega(z) f_z$ [3].

Let Ω be the family of functions $\phi(z)$ which are regular and analytic in \mathbb{D} and satisfying the conditions $\phi(0) = 0$, $|\phi(z)| < 1$ for every $z \in \mathbb{D}$. Denote by $P(p)$ the class of functions $p(z) = p + p_1 z + p_2 z^2 + \dots$ analytic in \mathbb{D} and satisfying the conditions $p(0) = p$, $Re p(z) > 0$ for all $z \in \mathbb{D}$ and such that $P(p)$ if and only if

$$p(z) = p \frac{1 + \phi(z)}{1 - \phi(z)} \quad (2)$$

for some function $\phi(z) \in \Omega$ and every $z \in \mathbb{D}$. Let $s(z) = z^p + c_{p+1} z^{p+1} + c_{p+2} z^{p+2} + \dots$ be an analytic function in \mathbb{D} and satisfies the condition

$$Re \left(z \frac{s'(z)}{s(z)} \right) > 0, \quad z \in \mathbb{D} \quad (3)$$

then we say that $s(z)$ is p -valent starlike function. The class of such functions is denoted by $S^*(p)$. Let $s_1(z) = z + \alpha_2 z^2 + \dots$ and $s_2(z) = z + \beta_2 z^2 + \dots$ be analytic functions in \mathbb{D} . If there exists a function $\phi(z) \in \Omega$ such that $s_1(z) = s_2(\phi(z))$ for all $z \in \mathbb{D}$, then we say that $s_1(z)$ is subordinate to s_2 and we write $s_1(z) \prec s_2(z)$. We also note that if $s_2(z)$ is univalent in \mathbb{D} , then $s_1(z) \prec s_2(z)$ if and only if $s_1(\mathbb{D}) \subset s_2(\mathbb{D})$, $s_1(0) = s_2(0)$ implies $s_1(\mathbb{D}_r) \subset s_2(\mathbb{D}_r)$ where $\mathbb{D}_r = \{z \mid |z| < r, 0 < r < 1\}$. (Subordination and Lindelöf principle [4])

In the present paper we will investigate the following class

$$\begin{aligned} S_{H(p)}^* &= \left\{ f(z) = h(z) + \overline{g(z)} \mid f \in S_{H(p)}, \right. \\ &\quad \left. \omega(z) = \frac{g'(z)}{h'(z)} \prec b_p \frac{1+z}{1-z}, \quad h(z) \in S^*(p) \right\}. \end{aligned}$$

For the aim of this paper, we will need the following lemma and theorems.

Lemma 1. ([5]) Let $\phi(z)$ be regular in the unit disc \mathbb{D} with $\phi(0) = 0$, then if $|\phi(z)|$ attains its maximum value on the circle $|z| = r$ at a point z_0 , we can write $z_0 \phi'(z_0) = k \phi(z_0)$, where k is real and $k \geq 1$.

Theorem 2. ([2]) Let $s(z)$ be an element of $S^*(p)$, then

$$\frac{r^p}{(1+r)^{2p}} \leq |s(z)| \leq \frac{r^p}{(1-r)^{2p}},$$

$$\frac{r^{p-1}(1-r)}{(1+r)^{2p+1}} \leq |s'(z)| \leq \frac{r^{p-1}(1+r)}{(1-r)^{2p+1}},$$

$$|a_n| \leq \prod_{k=0}^{n-(p+1)} \frac{|2p-k|}{k+1}, \quad n \geq p+1.$$

September 02, 2014

II. MAIN RESULTS

Theorem 3. Let $f(z) = h(z) + \overline{g(z)}$ be an element of $S_{H(p)}^*$, then

$$\frac{g(z)}{h(z)} \prec b_p \frac{1+z}{1-z}, \quad z \in \mathbb{D}. \quad (4)$$

Proof: Since $f \in S_{H(p)}^*$, then we have

$$\begin{aligned} \omega(z) &= \frac{g'(z)}{h'(z)} \\ &= \frac{b_p + (p+1)b_{p+1}z + (p+2)b_{p+2}z^2 + \dots}{z} + \dots \\ &+ 1 + (p+1)a_{p+1}z + (p+2)a_{p+2}z^2 + \dots \\ &\Rightarrow \omega(0) = b_p, \end{aligned}$$

$|b_p| < 1$, $|\omega(z)| < 1$. Thus we define the function

$$\phi(z) = \frac{\omega(z) - \omega(0)}{1 - \overline{\omega(0)}\omega(z)}.$$

Then $\phi(z)$ is analytic and satisfies the condition of Schwarz lemma and we have

$$\omega(z) = \frac{b_p + \phi(z)}{1 + \overline{b_p}\phi(z)}. \quad (5)$$

The equality (5) shows that $\omega(z)$ is subordinate to $w(z) = \frac{b_p + z}{1 + \overline{b_p}z}$. On the other hand, the transformation $w(z) = \frac{b_p + z}{1 + \overline{b_p}z}$ maps $|z| = r$ onto the disc with the centre

$$C(r) = \left(\frac{(1-r^2)Reb_p}{1-|b_p|^2r^2}, \frac{(1-r)^2Imb_p}{1-|b_p|^2r^2} \right)$$

and the radius

$$\rho(r) = \frac{(1-|b_p|^2)r}{1-|b_p|^2r^2}.$$

Therefore we can write

$$\left| \omega(z) - \frac{b_p(1-r^2)}{1-|b_p|^2r^2} \right| \leq \frac{(1-|b_p|^2)r}{1-|b_p|^2r^2}. \quad (6)$$

The inequality (6) shows that

$$\begin{aligned} \omega(\mathbb{D}_r) &= \left\{ \frac{g'(z)}{h'(z)} \mid \left| \frac{g'(z)}{h'(z)} - \frac{b_p(1-r^2)}{1-|b_p|^2r^2} \right| \leq \frac{(1-|b_p|^2)r}{1-|b_p|^2r^2}, \right. \\ &\quad \left. 0 < r < 1 \right\}. \end{aligned} \quad (7)$$

Now we define the function

$$\frac{g(z)}{h(z)} = b_p \frac{1+\phi(z)}{1-\phi(z)}, \quad (8)$$

thus $\frac{g(0)}{h(0)} = b_p = b_p \frac{1+\phi(0)}{1-\phi(0)} \implies \phi(0) = 0$, $\phi(z)$ is analytic and if we take derivative from (8) we obtain

$$\frac{g'(z)}{h'(z)} = b_p \frac{1+\phi(z)}{1-\phi(z)} + b_p \frac{2z\phi'(z)}{(1-\phi(z))^2} \frac{h(z)}{zh'(z)}. \quad (9)$$

On the other hand, since $h(z) \in S^*(p)$ then the boundary value of $z \frac{h'(z)}{h(z)}$ on \mathbb{D}_r is

$$\frac{h'(z)}{h(z)} = p \frac{1+2re^{i\theta}+r^2}{1-r^2}.$$

Therefore using the equality, (9) can be written in the following form

$$\frac{g'(z)}{h'(z)} = b_p \left(\frac{1+\phi(z)}{1-\phi(z)} + \frac{2z\phi'(z)}{(1-\phi(z))^2} \frac{1-r^2}{p(1+2re^{i\theta}+r^2)} \right). \quad (10)$$

Now it is easy to realise that the subordination $\frac{g(z)}{h(z)} \prec b_p \frac{1+z}{1-z}$ is equivalent to $|\phi(z)| < 1$ for all $z \in \mathbb{D}$. Indeed assume to the contrary; that there exists a $z_0 \in \mathbb{D}_r$ such that $|\phi(z_0)| = 1$, then by Lemma 1 $z_0\phi'(z_0) = k\phi(z_0)$, $k \geq 1$ for such $z_0 \in \mathbb{D}_r$ we have

$$\begin{aligned} \omega(z_0) &= \frac{g'(z_0)}{h'(z_0)} \\ &= b_p \left(\frac{1+\phi(z_0)}{1-\phi(z_0)} + \frac{2k\phi(z_0)}{(1-\phi(z_0))^2} \frac{1-r^2}{p(1+2re^{i\theta}+r^2)} \right) \notin \omega(\mathbb{D}_r) \end{aligned}$$

because $k \geq 1$ and $|\phi(z_0)| = 1$. But this is a contradiction to the condition $\frac{g'(z)}{h'(z)} \prec b_p \frac{1+z}{1-z}$ and so our assumption is wrong, i.e., $|\phi(z)| < 1$ for all $z \in \mathbb{D}$. ■

Corollary 4. Let $f(z) = h(z) + \overline{g(z)}$ be an element of $S_{H(p)}^*$, then

$$\frac{|b_p|r^p(1-r)}{(1+r)^{2p+1}} \leq |g(z)| \leq \frac{|b_p|r^p(1+r)}{(1-r)^{2p+1}}, \quad (11)$$

$$\frac{|b_p|r^{p-1}(1-r)^2}{(1+r)^{2(p+1)}} \leq |g'(z)| \leq \frac{|b_p|r^{p-1}(1+r)^2}{(1-r)^{2(p+1)}}. \quad (12)$$

Proof: Using the definition of $S_{H(p)}^*$ and Theorem 3 we can write

$$\frac{g'(z)}{h'(z)} \prec b_p \frac{1+z}{1-z} \implies \left| \frac{g'(z)}{h'(z)} - \frac{b_p(1+r^2)}{1-r^2} \right| \leq \frac{2|b_p|r}{1-r^2},$$

$$\frac{g(z)}{h(z)} \prec b_p \frac{1+z}{1-z} \implies \left| \frac{g(z)}{h(z)} - \frac{b_p(1+r^2)}{1-r^2} \right| \leq \frac{2|b_p|r}{1-r^2}.$$

Then these inequalities give

$$|h(z)| \frac{|b_p|(1-r)}{1+r} \leq |g(z)| \leq |h(z)| \frac{|b_p|(1+r)}{1-r}, \quad (13)$$

$$|h'(z)| \frac{|b_p|(1-r)}{1+r} \leq |g'(z)| \leq |h'(z)| \frac{|b_p|(1+r)}{1-r}. \quad (14)$$

Using Theorem 3 in the inequalities (13) and (14) we get (11) and (12). ■

Corollary 5. If $f(z) = h(z) + \overline{g(z)} \in S_{H(p)}^*$, then

$$\frac{(1-|b_p|^2)r^{2(p-1)}(1-r)^3}{(1+|b_p|r)^2(1+r)^{4p+1}} \leq J_f \leq \frac{(1-|b_p|^2)r^{2(p-1)}(1+r)^3}{(1-|b_p|r)^2(1-r)^{4p+1}}. \quad (15)$$

Proof: Since

$$\left| \omega(z) - \frac{b_p(1-r^2)}{1-|b_p|^2r^2} \right| \leq \frac{(1-|b_p|^2)r}{1-|b_p|^2r^2},$$

then we have

$$\frac{(1-r^2)(1-|b_p|^2)}{(1+|b_p|r)^2} \leq 1 - |\omega(z)|^2 \leq \frac{(1-r^2)(1-|b_p|^2)}{(1-|b_p|r)^2}. \quad (16)$$

On the other hand

$$\left. \begin{aligned} J_f &= |h'(z)|^2 - |g'(z)|^2 = |h'(z)|^2 - |\omega(z)h(z)|^2 \\ &= |h'(z)|^2(1 - |\omega(z)|^2) \end{aligned} \right\} \quad (17)$$

Using Theorem 2, inequality (16) and the inequality (17) we get (15). ■

Corollary 6. Let $f(z) = h(z) + \overline{g(z)}$ be an element of $S_{H(p)}^*$, then

$$\begin{aligned} (1-|b_p|) \int_0^r \frac{\rho^{p-1}(1-\rho)^2}{(1+\rho)^{2p+1}(1+|b_p|\rho)} d\rho &\leq |f| \\ &\leq (1-|b_p|) \int_0^r \frac{\rho^{p-1}(1+\rho)^2}{(1-\rho)^{2p+1}(1+|b_p|\rho)} d\rho \end{aligned} \quad (18)$$

Proof: Since

$$\left| \omega(z) - \frac{b_p(1-r^2)}{1-|b_p|^2r^2} \right| \leq \frac{(1-|b_p|^2)r}{1-|b_p|^2r^2},$$

$$\frac{(1-r)(1-|b_p|)}{1+|b_p|r} \leq 1 - \omega(z) \leq \frac{(1+r)(1-|b_p|)}{1-|b_p|r}, \quad (19)$$

$$\frac{(1-r)(1+|b_p|)}{1-|b_p|r} \leq 1 + \omega(z) \leq \frac{(1+r)(1+|b_p|)}{1+|b_p|r}, \quad (20)$$

and

$$(|h'(z)| - |g'(z)|)|dz| \leq |df| \leq (|h'(z)| + |g'(z)|)|dz| \implies$$

$$|h'(z)|(1-|\omega(z)|)|dz| \leq |df| \leq |h'(z)|(1+|\omega(z)|)|dz|. \quad (21)$$

Using Theorem 2, inequality (19) and (20) in the inequality (21) and after integrating we get (18). ■

Theorem 7. Let $f(z) = h(z) + \overline{g(z)}$ be an element of $S_{H(p)}^*$, then

$$|b_{n+1}| \leq 2p \sum_{k=0}^n \left(\prod_{m=0}^{k-(p+1)} \frac{|2p+m|}{m+1} \right). \quad (22)$$

Proof: Using Theorem 3 we write

$$\begin{aligned} \frac{g(z)}{h(z)} &\prec b_p \frac{1+z}{1-z} \\ &\Rightarrow \frac{g(z)}{h(z)} = b_p \frac{1+\phi(z)}{1-\phi(z)} \\ &\Rightarrow \frac{g(z)}{h(z)} = b_p p(z) \\ &\Rightarrow g(z) = b_p h(z)p(z) \end{aligned} \quad (23)$$

$$\begin{aligned} b_p z^p + \dots + b_{p+m} z^{p+m} + \dots &= b_p (z^p + a_{p+1} z^{p+1} + \dots) \\ &\quad + a_{p+m} z^{p+m} + \dots)(p + p_1 z + \dots + p_n z^n + \dots) \end{aligned}$$

$$\left. \begin{aligned} b_{n+p} &= b_p p_n + b_p p_{n-1} a_{p+1} + \dots + b_p p_1 a_{p+n-1} + b_p p a_{p+n} \\ &= \sum_{k=0}^n b_p p_{n-k} a_{p+k} \end{aligned} \right\} \quad (24)$$

Using the coefficient inequalities of the classes $P(p)$ and p -valent starlike functions in the inequality (24) we obtain (22). ■

REFERENCES

- [1] Ahuja Om. P., *Planar Harmonic Univalent and Related Mappings*, Journal of inequalities in pure and Applied Mathematics, Vol. 6 issue 4 Article 122 (2005).
- [2] Aouf, M. K., *On a Class of p -valent Starlike Functions of order α* , Internat. J. Math. and Math. Sci Vol 10 No 4, 733-744.
- [3] P. L. Duren, *Harmonic Mappings in the Plane*, Cambridge Tracts In Mathematics Vol 156, Cambridge Univ. Press, Cambridge UK, 2004.
- [4] Goodman A. W. , *Univalent Functions*, Volume I and Volume II, Mariner publishing Company INC, Tampa Florida, (1984).
- [5] Jack, I. S. , *Functions Starlike and Convex of Order α* , J. London Math. Soc. 3 (1971) No.2, 469-474.

The Development, Status and Trends of Recommender Systems: A Comprehensive and Critical Literature Review

Jin Xu¹, Karaleise Johnson-Wahrmann¹, Shuliang Li^{1,2}

¹ School of Economics & Management, Southwest Jiaotong University, Chengdu, Sichuan, 610031, China
xj_james@126.com

² Westminster Business School, University of Westminster, 35 Marylebone Road, London NW1 5LS, UK
shuliangliuk@gmail.com

Abstract—Recommender systems have been used in many fields of research and business applications. In this paper, a comprehensive and critical review of the literature on recommender systems is provided. A classification mechanism of recommender systems is proposed. The review pays attention to and covers the recommender system algorithms, application areas and data mining techniques published in relevant peer-reviewed journals between 2001 and 2013. The development of the field, status and trends are analyzed and discussed in the paper.

Keywords-Recommender Systems; Recommendation Systems; Comprehensive and Critical Literature Review; Research Status and Trends

I. INTRODUCTION

With the increasing availability of large volumes of data, it has become cumbersome to wade through all available options in the hopes of finding what one desires. Even with advancements in searching capabilities, the user may still have many options that do not necessarily fit their personal preferences. This information overload problem as given rise to recommender systems.

Recommender Systems (RS, or Recommendation Systems) track past actions of a group of users to make recommendations to individual members of the group [1]. A recommender system is one of the most interesting research areas for investigating information overload [2]. The recommender system's task is to turn users' current preference data into predictions of future likes and interests [3]. Recommender systems are responsible for providing users with a series of personalized suggestions (recommendations) on particular items. A recommender system extracts the user's relevant characteristics to form user profile, it then determines the set of items that may be of interest based on those characteristics [4]. In most recommender systems, users provide recommendations as input that the system can then aggregate and redirect to other appropriate users [5].

Recommender systems have had extensive application in ecommerce where there are a high volume of products for shoppers to choose from. Recommender systems have become a necessary part of the online shopping experience

not just for consumers but retailers as well [6]. Popular websites such as Amazon.com, Ebay.com, Taobao.com among many others, use recommendations to suggest products to their users based on past activities. They are also popular in other domains such as mobile applications, movie recommendations, social networks, document recommendations etc...

However, there is still lack of effort on conducting a comprehensive literature review of the past 10 years' research on recommender systems. Therefore, in this paper, we are going to propose a classification mechanism to figure out the blueprint of recommender systems' research and give an analysis and critical evaluation on development, status and trends .

II. RECOMMENDER SYSTEMS APPROACHES

Recommender systems produce recommendations either through a collaborative filtering approach (CF) or a content-based filtering approach (CBF) [2]. It is a process by which information on the preference and actions of a group of users is tracked by the system [1]. It is an emerging technology to deal with information overload by using customer interests to guide them to products they might like [7].

CF recommender systems work by storing relevant information in a database that contains the ratings of a large number of users on a large number of items (films, books, jokes, study material, holiday destinations, etc.). CF aims to determine similarity between users and then to recommend to the active user the items preferred by users similar to him or her [4].

CBF recommender systems make suggestions to users based on a profile learnt from previously rated items [8]. CBF recommendation systems typically (1) build an item profile from extracted attributes from each item in the set, (2) build a content-based user profile based on the attributes of the items which each user has purchased, (3) calculate the similarity between users and items based on profile information using similarity functions and (4) make recommendations of top n items with highest similarity scores [9]. The content-based filtering methods analyzes the content of items and try to understand the similarities between items for generating relevant recommendations.

Thus, a user is offered recommendations of those items which have high similarity to the ones the user showed preference for in the past [10].

Both recommender approaches can be augmented with context awareness, that is, the ability for the recommender to be aware of the environment in which the activity is taking place. Context awareness is about capturing a wide range of contextual attributes (such as location and surrounding environments) to better understand what the user is trying to accomplish, and what services the user might prefer [11].

Although both approaches can generate reasonable recommendations, each of them has its own drawbacks. CBF recommendations do not necessarily include preference similarity across individuals while CF do not necessarily incorporate feature information and must face the sparsity and cold-start problems [3]. Cold start problems occur when not enough information is available to make recommendations for new users. CBF relies heavily on textual descriptions, leading to other spinoff problems such as limited information retrieval, new user issues, and overspecialized recommendations [12]. Many hybrid methods that combine the two main approaches have been explored to find solutions to these problems.

The research into recommender systems has strong focus on finding solutions to the above mentioned problems, however a complete solution has not yet been created and the research trend shows continued efforts to find both new applications for recommender systems as well as applying multi-disciplinary methods to solve its existing problems.

III. REVIEW METHODOLOGY

A. Review Process

The review methodology employed involved examining articles on recommender systems published in relevant peer-reviewed journals over a 12 year period between the years 2001 and 2013. The purpose of the review is to understand the development, status and trends that exist in the field and to explore the algorithms used that may be of benefit for its application some domains. The following relevance criteria were employed: *Algorithms used in recommender systems, prototypes of recommender systems, validation and evaluation and performance of recommender systems*. The algorithms would give details of the research done in recommender algorithms that can be applied in further researches, the prototypes will give insights in the fields of applications and the evaluation will give information on the research on recommendation system performance.

To accomplish this, a search was done on major research database for the terms *Recommender System, Recommendation System, Personalization System, Collaborative Filtering and Content Based Filtering*. Of the papers returned; the titles and abstracts were read to determine relevance. Excluded from consideration were the following results: Conference papers, Masters and PHD Dissertations, Unpublished working papers, Editorials, and Reports. Once a paper was considered of relevance, then it is classified according to the area of focus of the paper. The

classifications were then analyzed, with the results collated and reported.

B. Classification Mechanism

An abundance of papers related to recommender systems exists and are scattered across different disciplines and in different journal databases. Therefore it was very difficult to classify papers according to disciplines.

Park et al [13] had previously done a literature review of recommender systems between the years 2001 and 2010. Their study had similar relevance criteria but lacked granularity in categorizing the recommender system approaches and did not specify the focus areas of the papers in their review. Since 2010 some of the data mining techniques have evolved and others have become more popular thus requiring their own categories. New algorithms have been incorporated and researchers have found new application fields for recommender systems.

For these reasons it was not possible to simply extend the study by Park et al to 2013, but rather to revisit the literature from 2001 in order to make the classifications that were of interest for this research. The study by Park et al was therefore very useful as a guide and for validation purposes but the articles presented in this review were individually analyzed and classified to match the criteria described in the classification methodology.

The classification mechanism employed is as follows:

1) Application Areas

The application area refers to the type of items that is being recommended in the articles. These can fall into the following categories:

- E-commerce - recommenders of products and services for purchase online
- Education - recommendations relating to learning such as courses, research papers etc...
- Entertainment - recommendations of multimedia such as movies, music, images etc...
- Book/Documents - recommendations on documents and books
- Tourism/Travel - recommendations for travel destinations and tourist activities
- Health Care - recommendations on medical items
- Social Media - recommendations on social activities
- Web pages/ Online News - recommendations of web sites and news feeds
- Other - all other application areas not listed above

2) Algorithm Type

The algorithms type refers to the recommendation algorithm that the paper discussed. These were grouped in the categories:

- Collaborative Filtering
- Content Based Filtering
- Context Aware
- Hybrid

The hybrid category is given to those papers that discuss the use of a combination of any of the three previous categories.

3) Information Retrieval Technique

Information Retrieval techniques refer to the data mining technique discussed in the paper that is used in determining the similarity of items or users that generate the recommendations. The categories are taken from the most popular data mining techniques and are as follows:

- K- Nearest Neighbour (KNN) - This algorithm calculates a set of k users whose similarities are most comparable to the user for whom a recommendation is intended (the active user) [14]. The algorithm searches for users similar to the active user in terms of ratings for the previously seen items. Then, ratings predictions are made for the unknown item based on the ratings that were assigned to this item by other similar users [15].
- Association Rule Mining (ARM) - The aim of ARM is to uncover inter-relationships of two or more items included in a transaction. An association rule is expressed as “If U, then V (UV)”, interpreted as “If event U occurs, then event V also occurs”. Rules generated by ARM are easily to understand, and easy to deploy in practice [16].
- Clustering - Data clustering determines a group of patterns in a dataset that are homogeneous in nature. It is an unsupervised pattern classification technique that defines a group of n objects into m clusters without any prior knowledge [17]. The objective is to develop an automatic algorithm that is able to accurately classify unleveled datasets into groups [18]. The clustering problem addresses the partitioning of datasets into n patterns in a d-dimensional space into K distinct set of clusters, in such a way that the data within the same cluster have a higher similarity to each other than to data in other clusters [19].
- Fuzzy Set - Fuzzy sets deal with subjective rather than precise reasoning. For example: a buyer might consider an item to be expensive but the linguistic label “expensive” is not precise and may differ depending on the buyer. “The fuzzy linguistic approach is based on the representation of qualitative aspects as linguistic values by means of linguistic variables” [20]. It is also concerned with approximate reasoning under uncertainty with certain level of confidence or a degree of certainty.
- Singular Value Decomposition (SVD) - SVD is used fundamentally in dealing with noisy data [21]. The SVD of an $m \times n$ real matrix A is to mathematically transform A to a diagonal matrix, with nonnegative diagonal elements, through a transformation of the form PAQ with an $m \times m$ orthogonal matrix P and an $n \times n$ orthogonal matrix Q [21]. An important feature of SVD, that is useful for recommender systems, is that it provides the best low-rank approximation of the original matrix [22].
- Latent Semantic Analysis (LSA) - LSA is an automatic mathematical/statistical technique for extracting meaning and inferring relationships of expected contextual usage of words [23]. LSA is originally an information retrieval method, however, it is also widely used in text categorization [24]. “The purpose of LSA is to extract a smaller number of dimensions that are more robust indicators of meaning than the individual terms” [17].

- Naïve Bayes / Bayesian Network (BN) - BN is a probabilistic model that provides a representation of a joint probability distribution [25]. BN nodes are graphically represent attributes and arcs represent attribute dependencies. Attribute dependencies are quantified by conditional probabilities for each node given its parents. Bayesian networks are often used for classification problems. With BN a learner attempts to construct a classifier from a given set of training instances with class labels [26].

- Other – All other techniques.

4) Focus Area

The areas of focus of the papers reviewed will be classified in the following 9 categories:

- Review/Survey - Papers that conduct literature reviews, surveys, and overviews of recommender systems without specific interest in any particular domain application.
- Empirical Studies - Papers that focus mainly on empirical evidence gathered in recommendation system usage studies.
- Performance/Evaluation - Papers that focus on the evaluation of recommender systems algorithms and performance metrics.
- Algorithm Improvement - Papers that focus on improving the main algorithm types and showing the merits of their improved approach.
- Prototype/Simulation - Papers that present a working prototype of a recommender system or a simulation of that system.
- New technique - Papers that focus on applying a new cross discipline techniques to improving recommendations.
- User Behavior - Papers focusing on the human actions and reactions when interacting with recommender systems.
- Mobile Specific - Papers that focus specifically on recommender systems for a mobile channel.
- Data Capture - Papers that focus on the explicit or implicit methods of capturing the preference data used to generate recommendations.

IV. THE FINDINGS AND RESULTS

The results revealed a total of 403 articles of relevance between that periods. Each of the relevant papers were reviewed and classified according to the methodology and mechanism proposed. The papers were analyzed as follows:

A. Distribution by Year of Publication

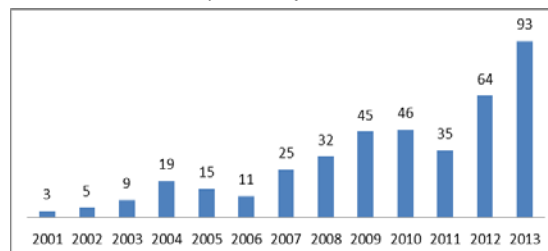


Figure 1. Article distribution by year of publication

The results showed that recommender system is still popular among researchers despite over 20 years since the first recommender system publication. The trends show a steady rise in research publishing since 2001 with 93 papers published in 2013 accounting for the highest number of publishing so far in any one year. This demonstrated that recommender systems is still a hot research topic and has captured the attention of researchers for some time. The full distribution by year is shown in Figure 1.

B. Distribution by Journals

The review resulted in 403 articles published between 2001 and 2013 from peer reviewed journals that match the relevance criteria. The results revealed papers from a total of 72 different journals across various disciplines. The top publishing journal for recommender system articles was *Expert Systems with Applications* with a total of 129 articles accounting for 32.8%. *Knowledge Based Systems* journal as well as *Decision Support Systems*, *Information Sciences* and *IEEE Intelligent Systems* were also amongst the top publishers accounting for between 5.3% to 7.6% of the total papers. The gap between the second highest publishing journal, *Knowledge Based Systems* at 7.6% and *Expert Systems with Applications* is very wide thus indicating that the latter plays a leading role in publishing research on recommender systems. Distributions of the research by top 15 journals is shown in Table 1.

Table 1. Paper distribution by Journal

| Journal | Amount |
|---|--------|
| Expert Systems with Applications | 129 |
| Knowledge-Based Systems | 30 |
| Decision Support Systems | 25 |
| Information Sciences | 24 |
| IEEE Intelligent Systems | 21 |
| Information Processing & Management | 16 |
| ACM Transactions on Information Systems | 12 |
| Electronic Commerce Research and Applications | 10 |
| IEEE Transactions on Consumer Electronics | 10 |
| IEEE Transactions on Knowledge and Data Engineering | 10 |
| IEEE Transactions on Internet Computing | 9 |
| International Journal of Electronic Commerce | 7 |
| Journal of Systems and Software | 7 |
| Computers in Human Behavior | 5 |
| International Journal of Human-Computer Studies | 5 |

C. Distribution by Application Field

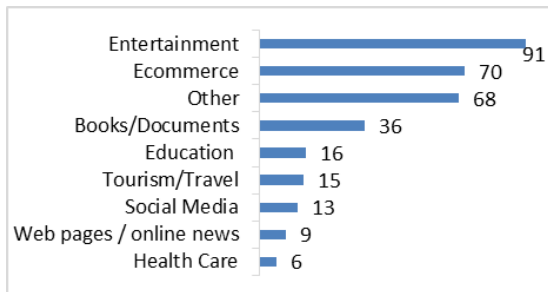


Figure 2. Article distribution by application field

There were many articles that discussed recommender system but did not mention a specific field of application. Of

the ones that did specify an application field, the results are shown in Figure 2. As seen the majority of the article discussed application to entertainment particularly movie and music recommendations, however there were also those articles that discussed image and other video recommendations that were also classified in the entertainment category. E-commerce was also very popular among researchers and a total of 70 articles were found that discussed recommending products for online shoppers. The categories of ‘other’ grouped recommenders of varying items include real estates, restaurants, stocks, digital ecosystems and others.

D. Distribution by Algorithm

There were many articles that discussed recommender systems but did not get into a specific algorithm, such articles mainly gave an overview of the recommendations generated. Of the articles that specified the algorithm type, collaborative filtering was by far the most popular among researchers, followed by hybrid algorithms. Context aware algorithms became more popular in later years since 2008. In 2001 there was a complete absence of papers that focused on any of these algorithms. The distribution of papers by algorithm type can be seen in Figure 3.

There was a clear interest by researchers in collaborative filtering algorithms and much effort was expended in developing new ways to improve such algorithms in various areas of application. Many existing data mining techniques were used including popular techniques such as K-nearest neighbor, association rule and clustering, however many more were discussed but were too numerous to itemize so there were categorized as other. Some of these other data mining techniques explained in the papers included: vector space model, matrix factorization, neural networks, genetic algorithms, product taxonomy and others.

E. Distribution by Focus Area

The review results show that the majority of papers written on recommender systems during the years of study were about improving the algorithms making up 35% of the total papers analyzed. Prototypes and simulations were also popular as researchers demonstrated the utility of the recommender systems they had developed, this accounted for 25% of the papers. Evaluations of the performance of recommender systems was also of interest to researcher accounting for 13%. The full distribution of the focus areas can be seen in Figure 4.

V. CONCLUSIONS AND DISCUSSIONS

It is clear from the review that recommender systems have captured the attention of researchers since its inception and is still doing so. The application fields for recommender systems seems to be ever expanding, however e-commerce and entertainment has still remained the most popular. Throughout the years of the review, collaborative filtering algorithms were the main approaches used in building recommender systems especially for their social value and particularly for movie, music and product recommendations. In the later years, researchers have shifted more towards

travel and tourism recommendations. Content based algorithms are mainly applied in situations where collaborative filtering may not be feasible such as in education. Context aware systems are gaining in popularity amongst researchers and during the period studied, papers discussing context aware systems were mainly for the mobile channel.

The review revealed the evolution of algorithms over the period. With each application field, a new method is applied to existing algorithms and in some case new algorithms are invented. It was very difficult to categorize all the algorithms as they were so diverse and dynamic in nature. It also showed that no one technique fits all application fields and businesses often change algorithms to match their specific needs. There was also an increase in survey and review papers addressing user behavior and consumer psychology for users interacting with a recommender system. There were also a few papers that discussed the privacy concerns regarding recommender systems.

Of great importance is the almost complete lack of papers focusing on business processes using recommender systems. From an organizational point of view, very little interest was expressed by researchers in improving business operations with recommenders, the focus has been on consumers' needs, users' needs and in one case business-to-business needs. However, almost no interest in improving internal operations with recommender systems has been found. This may be recognized as one of the future research areas.

Another issue is that each of the methods or techniques mentioned in the literature review has its own weaknesses or limitations. Therefore, a hybrid approach [27, 28, 29] integrating the strengths and advantages of various techniques, technologies and methods for developing and applying recommender systems is required. One topic of the studies in this area will be concerned with the creation and use of hybrid intelligent recommender systems.

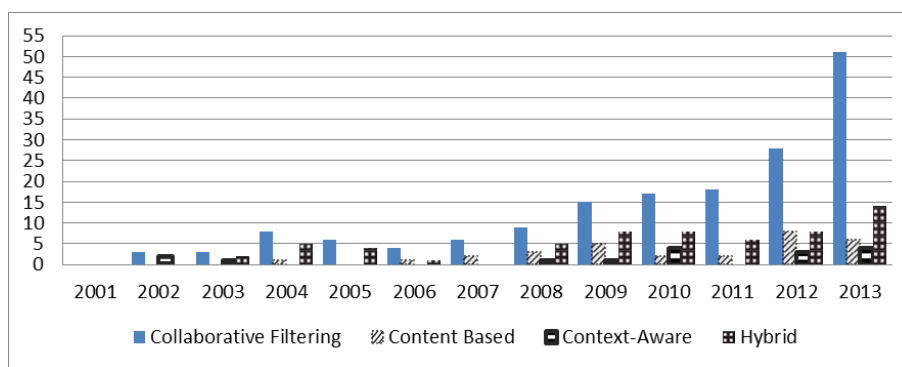


Figure 3. Article distribution by algorithm type

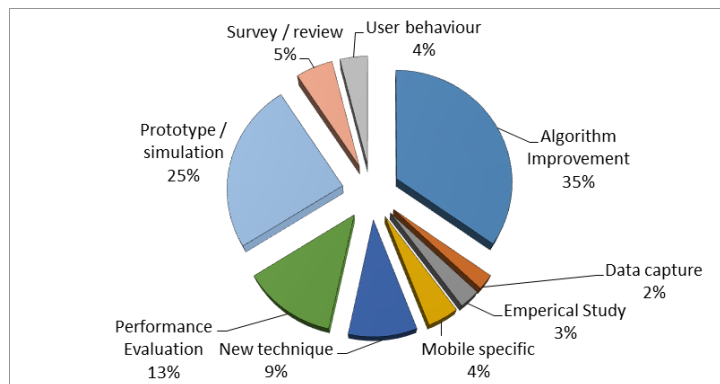


Figure 4. Article distribution by focus area

ACKNOWLEDGEMENT

This study is supported by grants from National Natural Science Foundation of China (71002064 & 71090402), the Fundamental Research Funds for the Central Universities of China (2682013CX075), the Soft Science Research Plan of Sichuan Province (2013ZR0043), the Experimental Teaching and Technique Project of Southwest Jiaotong

University (SYJS201324), and Sichuan 100-Talent Scheme (bai ren ji hua) grant.

REFERENCES

- [1] R. Kumar, P. Raghavan, S. Rajagopalan and A. Tomkins, "Recommender Systems a probabilistic Analysis," Journal of Computer and System Sciences, pp. 42-61, 2001.

- [2] X. Z. Hongchen Wu, "Div-clustering:Exploring active users for social collaborative recommendation," Journal of Network and Computer Applications, pp. 1642 - 1650, 2013.
- [3] L. Lü, M. Medo, C. H. Yeung, Y.-C. Zhang, Z.-K. Zhang and T. Zhou, "Recommender Systems," Physics Reports, pp. 1-49, 2012.
- [4] F. Ortega, J.-L. Sánchez, J. Bobadilla and A. Gutiérrez, "Improving collaborative filtering-based recommender systems results using Pareto dominance," Information Science, pp. 50-61, 2013.
- [5] P. Resnick and H. R. Varian, "Recommender systems. (Special section: recommender systems)(Cover story)," Association of the ACM, pp. 56-58, 1997.
- [6] S. R. L. C. N. Paloma Ochia, "Predictors of user perceptions of web recommender systems: How the basis for generating experience and search product recommendations affects user responses," International Journal of Human-Computer Studies , pp. 472-482, 2013.
- [7] C. Kalel, "An entropy-based neighbor selection approach for collaborative filtering," Knowledge-Based Systems, pp. 273-280, 2014.
- [8] R. Mooney, N. P. Bennett and R. Loriene, "Book Recommending Using Text Categorization with Extracted Information," in Workshop on Recommender Systems, Madison, 1998.
- [9] Y. S. Keunho Choi, "A new similarity function for selecting neighbors for each target item in collaborative filtering," Knowledge-Based Systems, pp. 146-153, 2013.
- [10] K. ShwetaTyagi, "Enhancing collaborative filtering recommendations by utilizing multi-objective particles warm optimization embedded association rule mining," Swarm and Evolutionary Computation, pp. 1-12, 2013.
- [11] E.-H. S. J. K. S. K. Jongyi Hong, "Context-aware system for proactive personalized service based on context history," Expert Systems with Applications, pp. 7448-4457, 2009.
- [12] Z. Zhang, H. Lin, K. Liu, D. Wu, G. Zhang and J. Lu, "A hybrid fuzzy-based personalized recommender system for," Information Sciences, pp. 117-129, 2013.
- [13] H. H. Park, K. H. Kyeong, C. I. Young and K. J. Kyeong, "A literature review and classification of recommender system research," Expert Systems with Applications, pp. 10059-10072, 2012.
- [14] J. Bobadilla, F. Ortega, A. Hernando and G. Glez-de-Rivera, "A similarity metric designed to speed up, using hardware, the recommender systems k-nearest neighbors algorithm," Knowledge-Based Systems, pp. 27-34, 2013.
- [15] M. Nilashi, O. b. Ibrahim and N. Ithnin, "Hybrid recommendation approaches for multi-criteria collaborative filtering," Expert Systems with Applications, pp. 3879-3900, 2014.
- [16] Y. S. Kim and B.-J. Yum, "Recommender system based on click stream data using association rule mining," Expert Systems with Applications, pp. 13320-13327, 2011.
- [17] W. Song and S. C. Park, "Genetic algorithm for text clustering based on latent semantic indexing," Computers and Mathematics with Applications, pp. 1901-1907, 2009.
- [18] S. J. Nanda and G. Panda, "A survey on nature inspired metaheuristic algorithm for partitional clustering," Swarm and Evolutionary Computation, pp. 1-18, 2014.
- [19] I. Saha and U. Maulik, "Incremental learning based multiobjective fuzzy clustering for categorical data," Information Sciences, pp. 35-57, 2014.
- [20] J. Serrano-Guerrero, E. Herrera-Viedma and J. A. Olivas, "A google wave-based fuzzy recommender system to disseminate information in University Digital Libraries 2.0," Information Sciences, pp. 1503-1516, 2011.
- [21] T. Maehara and K. Murota, "Simultaneous singular value decomposition," Linear Algebra and its Applications, pp. 106-116, 2011.
- [22] A. B. Barragáns-Martínez, E. Costa-Montenegro, J. C. Burguillo, M. Rey-López, F. A. Mikic-Fonte and A. Peleteiro, "A hybrid content-based and item-based collaborative filtering approach to recommend TV programs enhanced with singular value decomposition," Information Sciences, pp. 4290-4311, 2010.
- [23] Y. Tonta and H. R. Darvish, "Diffusion of latent semantic analysis as a research tool: A social network analysis approach," Journal of Informetrics, pp. 166-174, 2010.
- [24] B. Yu, Z.-b. Xu and C.-h. Li, "Latent semantic analysis for text categorization using neural network," Knowledge-Based Systems, pp. 900-904, 2008.
- [25] H. Langseth and T. D. Nielsen, "A latent model for collaborative filtering," International Journal of Approximate Reasoning, pp. 447-466, 2012.
- [26] L. Jian, Z. Cai, H. Zhang and D. Wan, "Not so greedy: Randomly Selected Naive Bayes," Expert Systems with Applications, pp. 11022-11028, 2012.
- [27] S. Li, "The development of a hybrid intelligent system for developing marketing strategy", Decision Support Systems, 27(4), 2000, pp. 395-409.
- [28] S. Li & J. Z. Li, Li, "AgentsInternational: integration of multiple agents, simulation, knowledge bases and fuzzy logic for international marketing decision making", Expert Systems with Applications, 37(3), 2010, pp. 2580-2587, 2010.
- [29] S. Li & J. Z. Li, Li, WebInternational: combining Web knowledge automation, fuzzy rules and online databases for international marketing planning, Expert Systems with Applications, 37(10), 2010, pp.7094-7100.

Using Simulation for Testing of Control Programs for Process Control Systems in Coal Mining*

Victor Okolnishnikov, Sergey Rudometov, and Sergey Zhuravlev

Design Technological Institute of Digital Techniques

Novosibirsk, Russia

okoln@mail.ru

Abstract—This article describes the use of the model integrated with an actual process control system for debugging and testing of the system. Three ways how to use the integrated model are considered. Control programs of the process control pumping system for a coal mine were debugged and tested using hardware-software test bench which includes the integrated model. The integrated model has been developed using a new visual interactive discrete simulation system specialized in simulation of technological processes.

Keywords—visual interactive simulation; process control system; coal mining

I. INTRODUCTION

Technological Institute of Digital Techniques of Siberian Branch of the Russian Academy of Sciences in Novosibirsk develops process control systems for coal mining. Arising problems are the following:

- The complete testing of control system using the programmer's tools is almost impossible because of inability to connect to real equipment.
- There is no way to make the complete testing of control system on-site because of inability to reproduce alarm situations or emergency situations.
- Startup and live testing time of control system on-site is limited.

The most suitable way to solve these problems is simulation. A means for solving these problems is a model integrated with an actual process control system. The model can be run as a part of the actual process control system. On the other hand, the model can use software components of the actual process control system, for example, control programs, the operator workstation, and others. The model can emulate processing equipment of the actual process control system.

There are many examples of the use of emulation models for testing automated production lines or automated material handling systems [1].

This paper describes the use of integrated models for developing of industrial process control systems for underground coal mines in Kuznetsk Coal Basin (Russia, Western Siberia).

This work is supported by the Russian Foundation for Basic Research (Project 13-07-98023 r_siberia_a).

These models were built with the help of the new visual interactive discrete simulation system intended for the development and execution of models of technological processes.

Section 2 gives the review of architecture and capabilities of this simulation system.

Section 3 presents the use the model, integrated with the actual control system in the framework of hardware-software test bench.

II. THE OVERVIEW OF ARCHITECTURE AND CAPABILITIES OF THE SIMULATION SYSTEM

At present, simulation tools are required for rapid development of simulation and emulation models for various industrial applications [2]. Such models can be used as parts of the actual process control system for developing, testing, optimization, and operator training. They can be also used in marketing to present some industry solutions to the customers.

One of the requirements is to reduce or to exclude the participation of specialists in industrial simulation in the process of the simulation model contraction. It is required to ensure transparent access to simulation system for the specialists from application area having minimal knowledge in information technologies [3].

These requirements were taken into account while designing a new visual interactive simulation system of manufacturing processes MTSS (Manufacturing and Transportation Simulation System) [4, 5, 6]. MTSS is a set of program interfaces for building specialized libraries of *elementary models* and then for construction of complex models using elementary ones.

The elementary model is a simulation model of an object of equipment in a technological system. It consists of the following parts:

- Two-dimensional and three-dimensional graphic images.
- Input and output parameters.
- Functionality algorithm describing dependence between parameters.

- States which the elementary model can reach during the simulation process.
- Control commands defining switching process between elementary models states.

The process of development of the elementary model consists of creation a conceptual model of an equipment unit and its translation into Java in accordance with the structure of the elementary model in MTSS.

Images of different elementary models can be connected to each other, with the help of graphical port mechanism. Such approach allows building simulation models of complex technological systems using elementary models.

The elementary model is a model of an equipment unit and its low-level control for it. The model in MTSS is constructed by graphical connection of elementary models images. MTSS is also the system for running of complex models built from elementary models. The running model ensures the advances of the model time and visualization. Statistics are also being gathered.

Industrial process control systems often have two levels: the low level of equipment and simple control logic and the upper level of complex control of production. Therefore one of the features of MTSS architecture is a forced split of the logic of the simulation into two parts: low-level logic and an upper level one.

Such division in architecture allows not only correspond to the usual structure of the process control systems but use such models for embedding them into actual process control systems in the following ways: to emulate equipment, to simulate upper level logic, and to send signals to actual systems for the visualization. This division into upper and lower logics allows also organizing a switch between various implementations of the decomposition. It allows coexisting simulation of upper level logic and a proxy that allows communicating with the upper level logic of actual process control systems.

The upper level logic executes coordinated control of all elementary models or of a group of elementary models. The possible difficulty of such approach is that each elementary model must be detailed to allow easy creating as many models as possible. This approach requires elementary models simulate rather exactly the units of equipment. In the case of such approach there is a good chance to have an exact simulation model.

MTSS is effective in solving the task for the rapid building of correct simulation model by engineers in their fields. Usually engineers have no enough experience and qualification to build a simulation model in details, but they are good at connecting correctly elementary models to build the required topology.

The architecture of the system consists of the next main components: a simulator, libraries of elementary models, a graphical engine, visual interactive interface, and etc.

III. HARDWARE-SOFTWARE TEST BENCH

In order to debug and test control programs for actual process control pumping system we use the model, integrated with the actual control system in the framework of hardware-software test bench.

A fragment of the model of pumping system is shown in Fig. 1. This system refers to mine safety systems. It averts mine flood. Pumping system model consists of pumps, tubes, tanks, water flows and requires elements of electricity system. Pumping simulation is based on two parts: fluid distribution and energy consumption simulation.

The simulation model of this system provides technological and underground water pumping out processes and energy consumption simulation. The main settings are the following: pump efficiency, tube throughput, pump energy consumption, tanks capacity, and etc.

The following problems were solved with the help of the model of pumping system:

- Pumps centralized turning on.
- Pump turning on in according with selected control mode.
- Selection of optimized control mode for pumps.

The integrated model is developed and performs in simulation system MTSS. The usual structure of the actual process control system is shown in Fig. 2. The hardware-software test bench is shown in Fig. 3.

While carrying out the task three ways of the hardware-software test bench were used.

A. Autonomous model

This model isn't restricted by the actual control system. The processing equipment of the actual control system is substituted for an emulation model of processing equipment. The control programs are light versions of control programs for the actual control system. An autonomous model can be used to achieve the following goals:

- Design of a non-existent system.
- Solution for optimization problems.
- Experiments with the model of the system when the experiments with simulated system are expensive or dangerous.
- Definition of performance boundary conditions of simulated system.
- System improvement.

Using the simulation environment MTSS the models of two systems of a coal mine in Kuznetsk Coal Basin (Russia, Western Siberia) were made: the system of underground coal pipeline system and the pumping system.

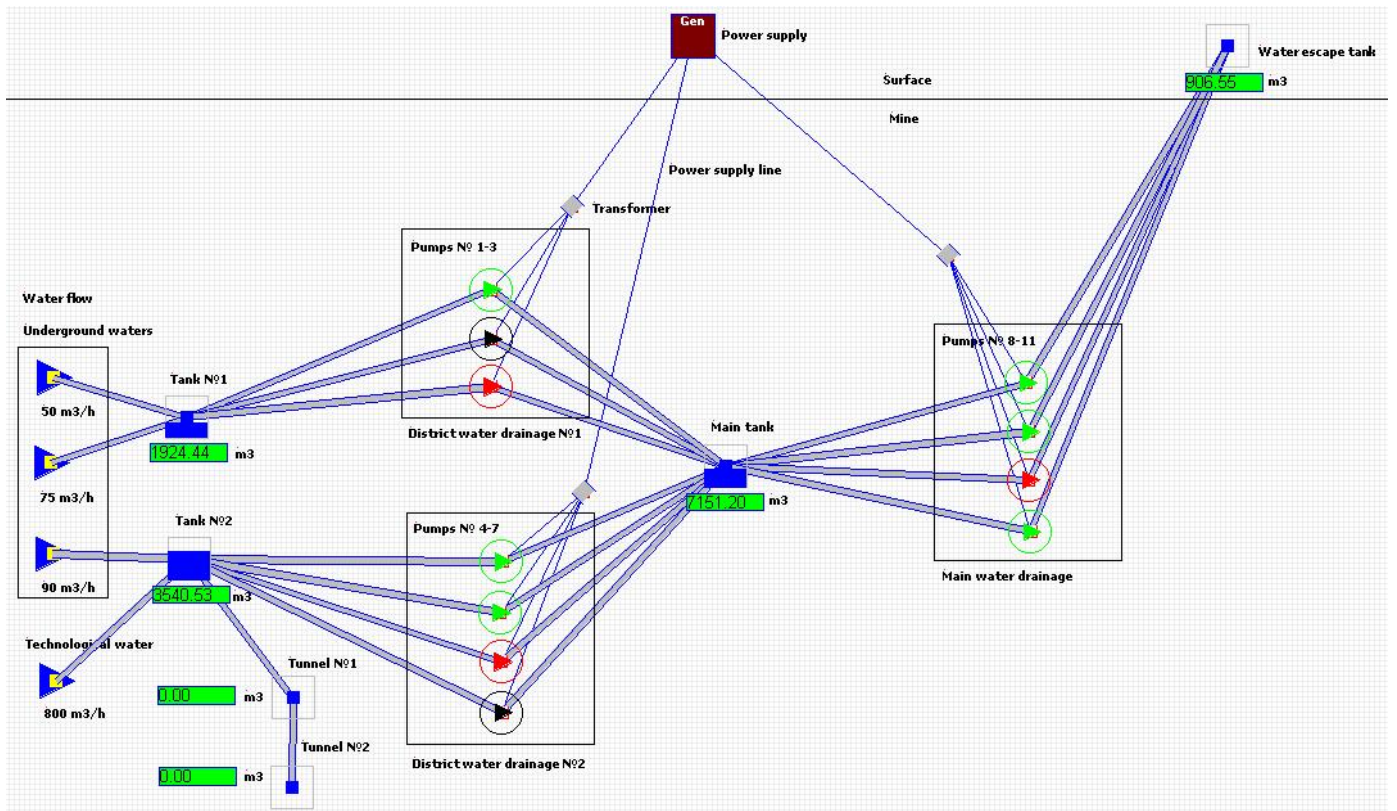


Fig. 1. Fragment of the model of pumping system.

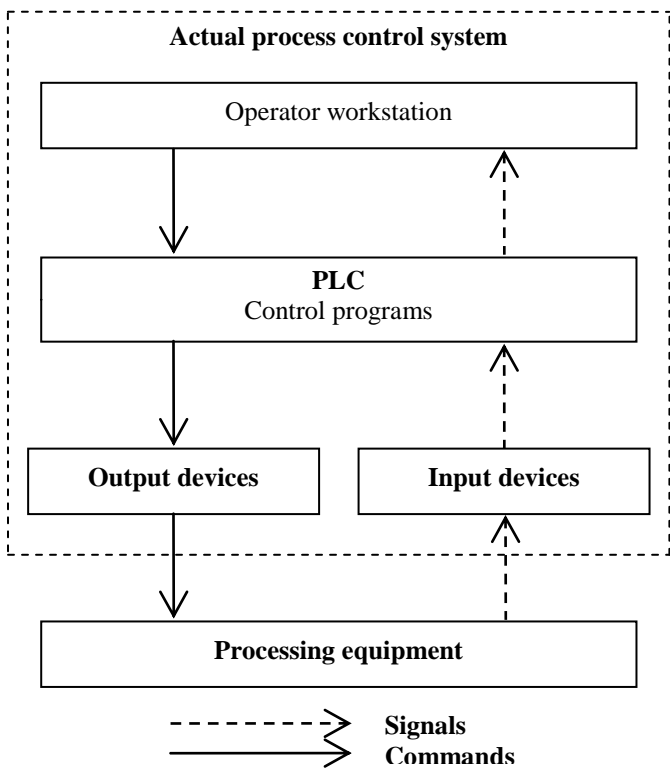


Fig. 2. Structure of usual process control system.

B. Data integrated model

The data integrated model is a source of signals for the actual control system instead of the actual processing equipment. The structure of the data integrating model is given in Fig. 3 without the loop of a control programs exchange.

The data model is designed to debug and test all software of the actual control system (upper and lower levels) excluding the control programs. In order to debug the lower level of the actual control system and input and output devices a part of signals generated by the model is transformed to the form of signals from actual sensors of processing equipment. In order to debug the upper level of the actual control system a part of signals generated by the model is transformed to the form of signals transmitted through local area network of the actual control system.

The data integrated model can be used to achieve the following goals:

- Debugging of software of upper and lower levels of the actual control system.
- Simulation of emergency and accident-related situations.
- Demo for a customer;
- Simulator for training of operators.

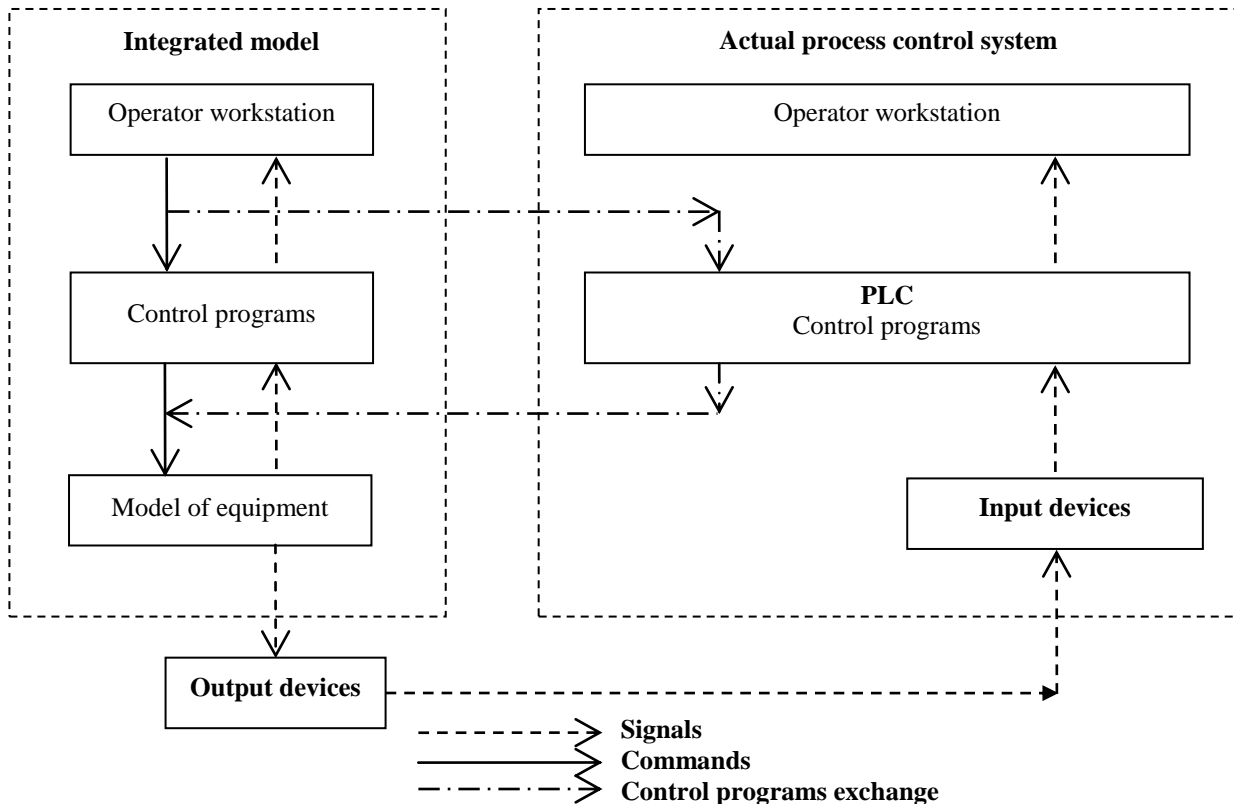


Fig. 3. Model integrated with the actual process control system.

C. Controlling integrated model

The controlling integrated model is aimed to debug and test all software of the actual control system (upper and lower levels) including the control programs. The structure of the controlling integrated model is given in Fig. 3. In the controlling integrated model a light version of control programs is substituted while execution for a release version performed in a programmable logic controller of the actual control system. Control programs “don’t know” in what environment they perform in an actual system or an integrated model. This way the validation of the model is obtained.

The controlling integrated model can be used to achieve the above mentioned goals for the data integrated model but also for additional ones:

- Maintenance of the actual control system during its life cycle, design, development, debugging, testing, commissioning, operational testing, optimization, evolution.
- Predictable conduct of the actual control system depending on situation and activity (non-activity) of the operator.
- Use of the model of external environment.

IV. CONCLUSION

Using hardware-software test bench with the integrated model control programs of the process control pumping

system for a coal mine in Kuznetsk Coal Basin was debugged and tested.

The usage of the integrated model let us reduce the time and cost of the development of process control pumping system.

Hardware-software test bench can be used not only for simulation of existing coal mining techniques but also for perspective robotized techniques.

References

- [1] N. Koflanovich and P. Hartman, “Live Modernizations of Automated Material Handling Systems: Bridging the Gap between Design and Startup Using Emulation,” in Proc. 2010 Winter Simulation Conference, Baltimore, 2010, pp. 1716-1726.
- [2] D. Carroll, “Rapid-Prototyping Emulation System Co-emulation Modelling Interface for SystemC Real-Time Emulation,” in Proc. of the 12th WSEAS International Conference on Systems, Heraklion, Greece, July 22-24, 2008, pp. 691-697.
- [3] E. Ginters, “Plenary Lecture 4: Simulation Highway – Step by Step to Common Environment,” in Proc. of the 11th WSEAS International Conference on Automatic Control, Modelling and Simulation, Istanbul, Turkey, May 30-June 1, 2009, p. 19.
- [4] V. Okolnishnikov, “Use of simulation for Development of Process Control System,” in Proc. of the 2008 IEEE Region 8 International Conference, Novosibirsk, Russia, 2008, pp. 248-251.
- [5] V. Okolnishnikov, S. Rudometov, and S. Zhuravlev, “Simulation environment for industrial and transportation systems,” in Proc. of the International Conference on Modelling and Simulation, Prague, Czech Republic, 2010, pp. 161-165.
- [6] V. Okolnishnikov, S. Rudometov, and S. Zhuravlev, “Monitoring System Development Using Simulation,” in Proc. of the 2010 IEEE Region 8 International Conference, Irkutsk, Russia, July 11-15, 2010, vol. II, pp. 736-739.

The influence of the gear cutting dynamics upon the shape and position of the replaceable cutting edges made from sintered metallic carbides

Cristian-Silviu SIMIONESCU, Carmen DEBELEAC

Faculty of Engineering form Braila

"Dunărea de Jos" University of Galati

Romania

cristian.simionescu@ugal.ro, carmen.bordea@ugal.ro

Abstract: The purpose of the present paper is to analyse the manner in which the positioning of the plates on the cutting edge influences the value of the cutting efforts. The analysed object is the worm cutter module with sintered metallic carbides. For this purpose we analysed the variation of the tooth advance and of the manufacturing schemes of the cutting edge made from hard plates upon the cutting dynamics for the gear cutting using worm cutters.

Keywords: gear cutting, worm cutters, cutting dynamics

1. Introduction

The worm cutter that is studied during the current analysis is considered to be made according to the following assumptions:

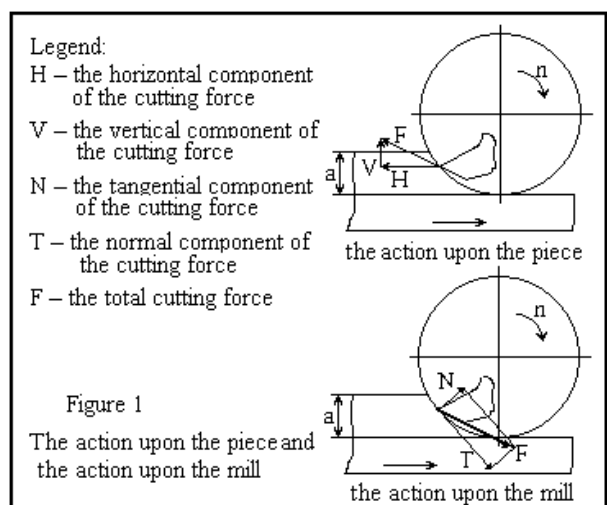
- the manufacturing of the cutting edges using removable plates made from sintered metallic carbides, an element suggested by the topic;
- the base worm of the cutter is an involute worm;

2. The influence of the change in the tooth advance upon the cutting force

In figure 1 there are presented the forces that act upon the piece and the reactions that act upon the tool during normal milling.

For the comfortable calculation of the efforts and of the power required for milling, meaning the load of the milling machine, the variation of the chip cross-section requires some simplifications. Thus in (figure 2), the

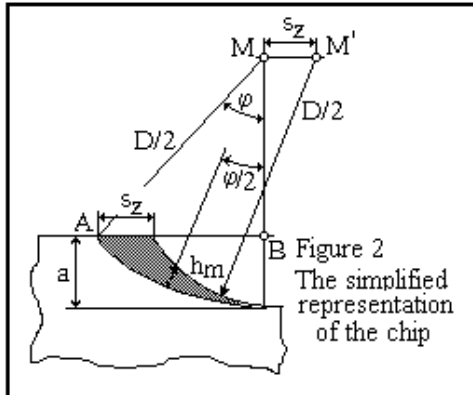
To establish the shape and the position of the cutting edges means to determine their length and especially, the possibility to make fragmented cutting edges mainly for practical manufacturing reasons. In the case of the fragmented cutting edges, an immediate consequence is the increase of the tooth advance which leads to the increase of the chip thickness. Therefore it is required to make a study of these consequences.



chip having a comma shape was represented simplified using two circle arcs.

The angle φ represents the contact angle for a single tooth of the milling machine.

The thickness of the chip for the angle $\varphi/2$ is called "average thickness" and will be noted with h_m .



If we take into account a milling width $b = 1\text{mm}$, we can obtain the average cross-section of the chip:

$$A_m = h_m b = h_m \quad (1)$$

By using figure 2 we can calculate the average thickness in this manner:

$$h_m = s_z \cdot \sin \frac{\varphi}{2} ; \quad \cos \varphi = \frac{\frac{D}{2} - a}{\frac{D}{2}} ; \quad \text{but}$$

$$\sin \frac{\varphi}{2} = \sqrt{\frac{1 - \cos \varphi}{2}} , \text{ so } \sin \frac{\varphi}{2} = \sqrt{\frac{a}{D}} \quad \text{and}$$

$$\text{then, } h_m = s_z \cdot \sqrt{\frac{a}{D}} \quad [\text{mm}]$$

Values for the specific pressure according to the average thickness of the chip

Table 1

| Material | The average thickness of the chip h_m in mm | | | | |
|----------------|--|------|------|------|------|
| | 0,02 | 0,04 | 0,08 | 0,15 | 0,3 |
| | The specific cutting pressure k_m in N/mm ² | | | | |
| Grey cast iron | 36,5 | 30 | 24 | 20 | 16,5 |
| Steel OL50 | 42 | 35 | 29 | 24,5 | 20,5 |
| Steel VCN15h | 49 | 41,5 | 35 | 300 | 26 |

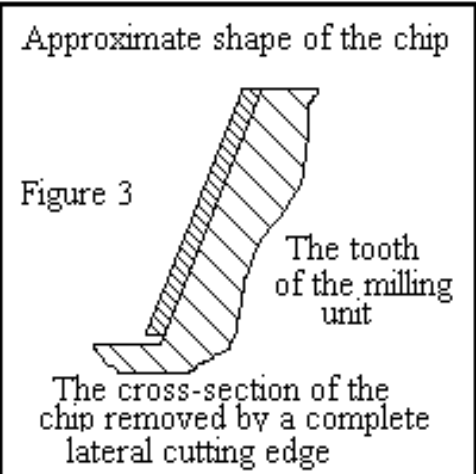
Values for the consumed power, N_z , specific pressure, k_m , according to the tooth advance, s_z

Table 2

| s_z | mm/tooth | 0,055 | 0,086 | 0,137 | 0,22 | 0,34 | 0,55 | 0,86 |
|--------|-------------------|----------|-------|--------------------|------|------|------|------|
| Fc 250 | v = | 80 m/min | , | $h_m = 1\text{mm}$ | | | | |
| k_m | N/mm ² | 22,6 | 19,4 | 16,6 | 14,1 | 12,1 | 10,3 | 8,8 |
| N_z | k_m/z | 0,084 | 0,11 | 0,15 | 0,21 | 0,28 | 0,38 | 0,52 |
| OL 60 | v = | 80 m/min | , | $h_m = 1\text{mm}$ | | | | |
| k_m | N/mm ² | 22,5 | 21,1 | 19,7 | 18,4 | 17,4 | 16,2 | 15,2 |
| N_z | k_m/z | 0,13 | 0,2 | 0,29 | 0,44 | 0,65 | 0,97 | 1,44 |
| OLT52 | v = | 80 m/min | , | $h_m = 1\text{mm}$ | | | | |
| k_m | N/mm ² | 31,9 | 29,4 | 27,1 | 25 | 23,1 | 21,2 | 19,5 |
| N_z | k_m/z | 0,19 | 0,28 | 0,4 | 0,6 | 0,86 | 1,27 | 1,84 |

| Al, Mg | | $v =$ | 80 m/min | $, h_m =$ | 1mm | | | |
|--------|-------------------|-------|----------|-----------|------|------|------|------|
| k_m | N/mm ² | 7,4 | 6,3 | 5,4 | 4,6 | 4,0 | 3,4 | 2,9 |
| N_z | k_m/z | 0,33 | 0,44 | 0,8 | 0,82 | 1,12 | 1,53 | 2,06 |

We have noticed that the size of the tooth advance s_z , has a favourable effect from the point of view of its influence upon the specific pressure, the main cutting force and the consumed power for gear cutting.



Due to the fact that the width of the chip, h , does not influence the specific pressure, we can conclude that if we maintain a constant cross-section of the chip, $h_{mb} = ct$, smaller cutting forces can be obtained if we increase the average thickness, and also the advance, at the expense of the width. Maintaining a constant cutting force can be done even if we increase the cross-section of the chip, with the condition that the increase of the cross-section must be done by increasing the advance and less reducing the width. The increase of the advance has also effects upon the productivity.

The volume of the detached chips in the unit of time is calculated using the relation:

$$Q = \frac{a \cdot b \cdot s}{1000} \quad [\text{cm}^3/\text{min}] \quad (6)$$

If a and b are considered to be constant, the volume of the chips can be increased only by increasing the advance speed, s . But: $s = s_z \cdot n \cdot z$, so

$$Q = \frac{a \cdot b \cdot n \cdot z \cdot s_z}{1000} \quad (7)$$

The parameters that can be increased are then s_z , n and z .

Due to the fact that the number of teeth cannot be increased, these as we can obviously

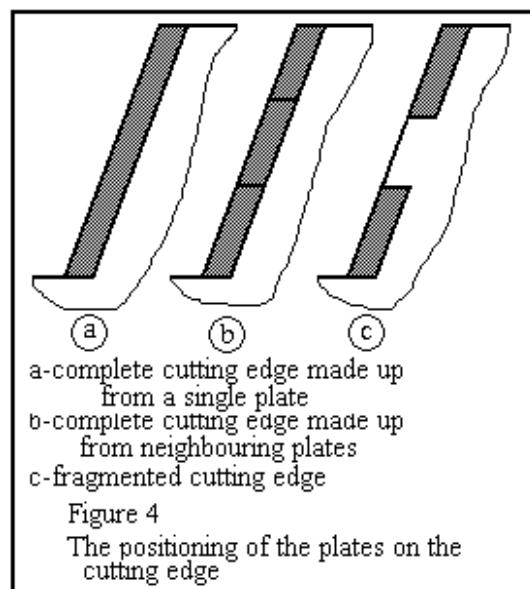
see are very well positioned, and the cutting speed is limited by the time and the rigidity of the gear cutting machine, *the only possible solution to increase the productivity is by increasing the tooth advance.*

3. The influence of the positioning of the plates upon the cutting force

Hereinafter, we want to highlight the manner in which the positioning of the plates can influence the size of the cutting force, in the conditions in which all the other parameters (rotation, advance) remain constant.

In figure 3 we can notice the cross-section of the chip removed by a complete lateral cutting edge.

For a tooth the same as the one shown



in figure 3 it corresponds a positioning of the plates like the one shown in figure 4.

The positioning of the plates same like in figure 5 a, represent a single piece cutting edge and it has the disadvantage that it uses non-standard metallic carbide plates with a relatively large length, these are likely to break, among other attachment difficulties. Furthermore, this type of plates requires specialized pressing and sintering

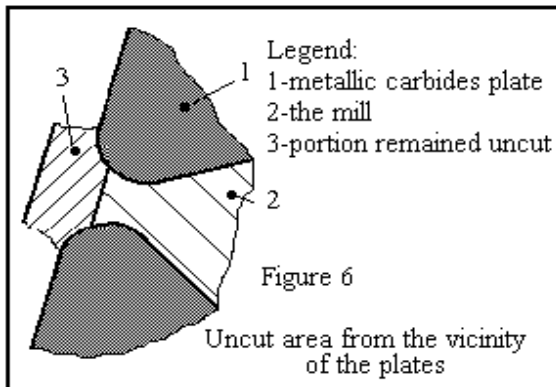
technologies, an expensive aspect that limits their use.

The positioning of the plates same like in figure 5 b, represents a single cutting edge made up from many pieces. In this case the cutting edge is made up from square shaped plates or triangular shaped plates as it can be seen in the figure 5.

A cutting edge similar to the one from figure 5 a cannot be made because it is not recommended the fixation of two plates one next to the other due to the existence of vibrations and oscillations during the cutting process. The version from figure 5 b removes this aspect but has technological fixing difficulties.

Also, due to the impossibility to achieve the continuity of the cutting edge in the neighbouring area of the plates, it results an uncut surface similar to the one from fig. 6.

Taking into account the positioning of the



plates on the flank with the purpose to totally cover the cutting edge, this is the same on every tooth, means that the uncut protuberance is transmitted to the next tooth, leading to an impossibility to continue the cutting process, due to the contact between the piece and the tool in an area where there is no cutting edge.

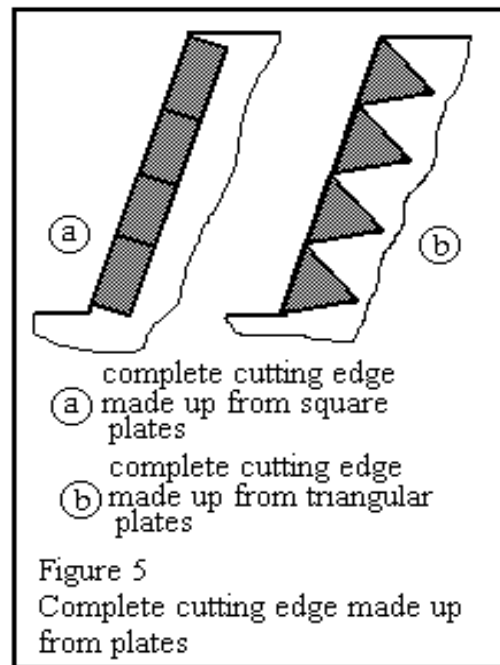
The positioning of the plates according to the scheme from figure 4 c is detailed hereinafter. As it can be seen from figure 7, obtaining a complete contour of the flank is possible with cinematically overlapped cutting edges, the tooth $i+1$ always removing the area uncut by the tooth i .

There are also possible other positioning solutions for the plates, obtaining a flank by using three or more cutting edges. In order to see the effect of the fragmentation of the cutting edge upon the sizes of the cutting

forces, we start from the relation:

$$k_m = F_m / h_m \cdot b \quad [Nmm^{-2}] \quad (8)$$

If we maintain constant the cutting

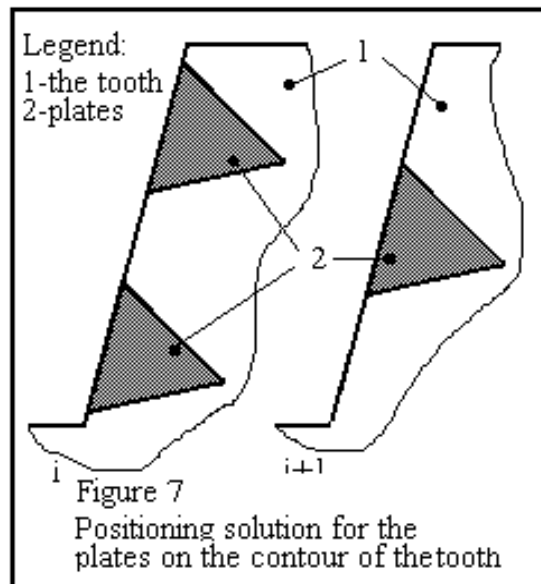


area, A , and we modify the elements h and b , we obtain:

$$A = ct = h_{m1} \cdot b_1 = h_{m2} \cdot b_2 \quad (9)$$

If $h_{m1} < h_{m2}$ and $b_1 > b_2$, then, for

$$A = h_{m2} \cdot b_2 \text{ we obtain: } k_m = \frac{F_m}{h_{m2} \cdot b_2}$$



(10)

4. Conclusions

From table 1 we can notice that the specific pressure, so the cutting force decreases once with the increase of the average thickness.

Therefore, if we manage to increase the cutting thickness in the same time with maintaining constant the cross-section of the chip, then the cutting force decreases. This thing can be accomplished by using a positioning of the plates in such a way to make a cutting width $b_a \cong \frac{1}{2}b$, when the entire cutting process is made with two teeth.

For such a positioning we obtain an average cutting thickness h_m de $h_{ma} = 2 \cdot h_m$.

So

$$A = h_m \cdot b = \frac{1}{2} \cdot b_a \cdot 2 \cdot h_{ma} = b_a \cdot h_{ma}$$

We can then notice the fact that the average thickness of the chip increased, but the cutting force decreased.

Finally we can conclude the following:

- the base worm for the mill must be the involute worm;
- the cutting edges will be made straight, by placing them in planes tangent to the base cylinder ;
- the cutting edges will be made fragmented, fact that will lead to a reduction of the cutting efforts.

5. Bibliography

1. **Bartelss, N.** - *Cutting Tools Now*. "Gear Technology" vol. 13, nr. 3, May-Jun 1996, p 16-21.
2. **Colbourne, J.R.,** - *Curvature of Surfaces Formed by a Cutting Edge* - "Mechanism & Machine Theory", vol.29, nr. 5, Jul 1994. p 767 - 775.
3. **Gimpert, D.-** *Gear Hobbing Process*. "Gear Technology", vol. 11, nr.1, Jan-Feb 1994, p 38 - 44, 1994.
4. **Simionescu, C.S.** – *Determining the optimal position of the cutting edge for modular worm mills*. "The bulletin of the second Interdisciplinary National Technical Colloquium", Brăila, 1995, p 58 - 64.
5. **Simionescu, C.S.-** *The calculation of the cutting force for variable thickness gear cutting* . "The bulletin of the second Interdisciplinary National Technical Colloquium", Brăila, 1995, p 64 - 68.

Optimization of feeding management on small-scale dairy systems of central México

Optimization of feeding management

Adolfo Aarmando Rayas-Amor

Departamento de Ciencias de la Alimentación
Universidad Autónoma Metropolitana Unidad Lerma
Lerma de Villada, México
a.rayas@correo.ler.uam.mx

Carlos Galdino Martínez-García

Instituto de Ciencias Agropecuarias y Rurales
Universidad Autónoma del Estado de México
Toluca, México
cgmartinezg@uaemex.mx

Octavio Alonso Castelán-Ortega

Facultad de Medicina Veterinaria y Zootecnia
Universidad Autónoma del Estado de México
Toluca, México
oaco@uaemex.mx

Abstract— For the last 20 years, developing countries have been attempting to develop the domestic milk production sector but due to their characteristics their profitability is low and there is little room for improving profitability by increasing milk yield. These systems must improve the efficiency of utilisation of all on-farm resources and turn them into milk production if they want to be competitive in the domestic market. This study consisted in the optimization of the biological components of the system through a modelling approach. Information from literature was used for developing a linear programming model and then it was used to simulate and evaluate management strategies of on-farm resources in order to improve energy/protein supply and minimize the use of purchased concentrates. Three scenarios were evaluated, 1) farms with 0.6 (ha), farms with 4 (ha) and 3) farms with 10 (ha). The optimal plan suggested grazing of cultivated pastures complemented with forages like oats (fresh or hay) harvested at vegetative stage, maize (fresh or silage) and moderate supplementation with concentrate based on maize grain (1 to 1.5 kg DM day⁻¹) and bread waste (1 to 2.5 kg DM day⁻¹). The low cost feeding strategies were; 1) grazing pasture + fresh oat + mixture of maize grain and bread waste and 2) grazing pasture + maize silage + mixture of maize grain and bread waste; the highest expenditure was observed when fresh maize was incorporated in the diet (US\$19 and US\$20 kg⁻¹ DM). It is conclude that in order to optimize small-scale dairy systems in Mexico, farmers should change the way they have managed their limited resources for decades implying that these systems must be redefined, from forage and concentrate buyers (external inputs) to pasture-based and conserved forage systems.

Keywords— optimization, feeding, management, systems

I. INTRODUCTION

In 2007 milk production passed from seven millions to 10 millions of tonnes per year [22], this was the result of improvements in management of intensive dairy farms; nonetheless, the costs of inputs used in large dairy farms increased also, but milk prices did not growth at the same rate, therefore many large dairy farms stopped production and small-scale dairy systems (SSDS) in Mexico were considered as an emergent alternative for the domestic milk supply.

Small-scale dairy systems in Mexico supplied 2.8 millions of tonnes in 2007 [22], but due to their characteristics in terms of small farms and herd size, low investment in facilities and machinery and the current negative market conditions, their profitability is low. Milk prices in SSDS have remained low over the last 20 years. On the contrary, input costs have increased substantially. Hence, there is little room for improving profitability by increasing milk yield with current input costs and management practices.

Maize is the main crop for SSDS in central Mexico; it provides grain, stover and weeds to feed dairy cattle [19], [13]. Other forages used less frequently include oats, alfalfa and cultivated pastures. Native pastures communally grazed are considered important for farmers in SSDS since they believe that these pastures are an important resource of feed that they can use without any cost.

Commercial concentrate supplementation is common among farmers; some farmers formulate their own concentrates that include maize grain mixed with poultry waste or feed industry by-products as an attempt to reduce their milk production costs [19].

The challenge of maximizing farm profit by means of improving farm-grown forage production and their efficient utilization is a common goal of dairy farming systems all over the world [5], and the SSDS must improve the efficiency of utilisation of all on-farm resources and turn them into milk if they want to be competitive in the domestic market.

Linear programming (LP) can augment intuitive decision making by providing more rigorously generated information to assist farmers [20] and [18]; therefore there are many examples of the use of LP technique applied to farm management, [16] used a multiperiod LP model for evaluating the profit maximizing mix of forages for a farm that calves year-round at constant milk prices, [19] and [6] used LP for maximising the gross margin of dairy farms in central Mexico but the later studies did not take into consideration the utilization of communal pastures (native pastures), their nutrient supply and the impact on profitability.

It is understood that integrating system modelling with field research is an essential step to facilitate management decisions in dairy farms either for developed and developing countries. Therefore, the objective of the present study was to develop an LP model that explores alternative changes on-farm's management strategies in order to improve the nutrient supply to dairy herd and to evaluate the impact of the suggested changes on the farms' profitability.

II. MATERIAL AND METHODS

Geographical location of the study

The study area was situated in the central highlands of Mexico ($19^{\circ} 04'$ and $19^{\circ} 28'N$ and $99^{\circ} 31'$ and $99^{\circ} 47'W$), at an altitude of 2,600 m. The climate is temperate sub-humid, dominated by summer-autumn rainfall (June to October) the annual rainfall is 750-990 mm and the mean annual temperature is $13.5^{\circ}C$ with a range of annual maximums of -5 to $25^{\circ}C$.

Selection of case studies

From a total of 205 small-scale dairy farms in Toluca valley [11], five percent of the farms were randomly selected and pre-interviewed in order to take into account the willingness of the farmers to supply technical and economic information. It was verified if the farmers considered the milk production as their largest single income, the selected farms had to show the most frequent land size (main constraint) in the studied area as well as herd size, thus, at the end only seven farms took part as case studies. The small-scale dairy systems supplies 37% of the total Mexican milk production [10].

A formal questionnaire was applied at the beginning of the study (July 2006) and updated every single month until the end of the study (June 2007). The questionnaire compiled

detailed information in seven sections such as: household characteristics; farm characteristics; the management of crops, pastures and livestock; farm inputs and their costs as well as farm's outputs and their sale prices.

Forages and feeds sampling

In order to know the supply of energy and protein within the system, samples of forage crops, grazing pastures and concentrates were collected as well as external feeds (concentrates and forages). Twelve sampling periods were established, the first sampling period started in July 2006 and the sampling procedure was repeated in each month until the end of June 2007.

Samples were transported to the laboratory for analyses of chemical composition and *in vitro* fermentation. The dry matter content was determined according to [2]. Crude protein content was calculated as nitrogen content \times 6.25 [2]. The estimation of metabolisable energy and metabolisable protein content of feeds were determined according to the Technical Committee on Responses to Nutrients (AFRC) [1].

Improvement of dry matter and nutrient supply

A mixed integer-linear programing model (LP) was built based on structural variables before mentioned; being the land size of farms the main constraint of the system, therefore the LP model was constructed using data of previous studies [4], [19], [13].

The objective function of the LP model was to maximize the farm net income in a year by means of maximizing sales of milk, cheese, yogurt, forage and heifers. The coefficients for milk, cheese and yogurt represented the sale price per kg; the coefficients of conserved oats represented the sale price of a hay bale, and the coefficients of heifers rearing represented the sale price of a heifer; the output of the objective function gave the combination of sale activities that maximized farm net income after variable costs, fixed costs and family labour costs were met. In this work, family labour costs (opportunity costs) were assigned to the family member that participated in the farm activities more than 8 hours per day (full time) and according with the farmers, the opportunity costs of family labour was US\$10.1/person.day; at the very least, since it was the wage paid to hired labour during the evaluation period.

The matrix of the mathematical model was developed in the standard form of an LP model that consisted in 166 activities grouped into nine categories and 188 constraints from which 177 were balance constraints (\leq or ≥ 0). The model integrates sale activities, rearing activities, production of forage crops and pastures, fertilizer application and balanced diets for dairy cows and heifers.

$$\text{Maximize } Z = f(x) = \sum_{j=1}^n c_j X_j, \quad (1)$$

Constrained to:

$$\sum_{j=1}^n a_{ij} X_j \leq \text{or } \geq = b_i; x_j \geq 0;$$

$j=1$

Where Z represents the net farm income. X_j is the level of the j th farm activity; let n denote the number of possible activities, then $j=1$ to 166. c_j is the coefficient of a unit of the j th farm activity. a_{ij} is the coefficient of the i th resource required to produce one unit of the j th farm activity; let m denote the number of resources, then $i=1$ to 188, b_i is the amount of the i th resource available (right hand side values).

Simulation of scenarios in small-scale dairy systems

The criteria for simulation were the availability of arable land on-farm since the average land size is 5.5 hectares with a range of 0 to 30 hectares, we attempted to work with the most common scenarios within the region; these scenarios (SC) were farms with less than one hectare of land, farms with four hectares of arable land and farms with up to 10 hectares of arable land; all of them depended greatly in grazing of communal pastures and external inputs; the grazing of communal pastures was an activity that used one family member for looking after the cattle while grazing every day and during 365 days of the year, therefore the opportunity costs of this activity increased substantially the total costs.

Three scenarios were simulated; the first scenario (SC1) described farms with 0.5 to 0.75 hectares and 1 family member that participated in the farm activities full time, the second scenario (SC2) described farms with 4 hectares and two family members that worked full time and the third scenario (SC3) described farms with 10 hectares of land and three family members working full time.

The farmers' existing plan in SC1 comprised two farms with 0.6 (± 0.2) hectares of land on average; of which 0.4 (± 0.3) and 0.3 (± 0.2) hectares were allocated to oats and maize crops respectively, mainly used as straws for animal feeding, the mean number of mature dairy cows was five heads and no replacements were observed; the estimated farm net income (FNI) was US\$-520 cow $^{-1}$ year $^{-1}$ (\pm US\$382). The farmers' existing plan in SC2 comprised two farms with 4 (± 0.05) hectares of land on average; of which 0.6 (± 0.9), 2.0 (± 0.1), 0.12 (± 0.2), 1.3 (± 1.1) hectares allocated to oats, maize, alfalfa and cultivated pastures, respectively; the average number of mature dairy cows was 11 (± 5) heads with 4 (± 1) replacements; and the FNI was US\$631 cow $^{-1}$ year $^{-1}$ (\pm US\$1269). The farmers' existing plan in SC3 comprised three farms with 10 (± 0.3) hectares of land; 1.3 (± 1.5), 7.5 (± 2.2), 1.5 (± 1.4) hectares of oats, maize and cultivated pastures, respectively; the average number of mature dairy cows was 14 (± 5) and 5 (± 1) replacements; and the FNI was US\$-758 cow $^{-1}$ year $^{-1}$ (\pm US\$226).

Additionally to on-farm resources mentioned above, all scenarios included grazing of communal pastures (native pastures) which is an important forage resource and farmers use freely all year-round.

The optimal plan derived from LP model was referred as the changes at farm level in order to improve the quality of dry

matter, energy and protein that were required for herd feeding and to diminish expenses in external inputs.

Software for model development

The model was developed in LINGO software v.10, which uses a windows platform. LINGO is a simple tool for utilizing linear and nonlinear optimization to formulate large problems concisely, solve them, and analyse the solution [15].

III. RESULTS

Land allocation to forage crops and pastures

Table 1 shows the optimal plan of land allocation, rent of land and grazing of communal pastures of the three scenarios, on average the ratio of land allocated to cultivated pastures and maize crop was 27:41 respectively; rather than 14:69 as farmers showed doing it. An important change that is suggested in the optimal plan is that grazing of communal pastures should not be carried out because the nutrient supply is lower than ryegrass- white clover pasture (Fig.1), another reason is that it represents an opportunity cost of family labour for looking after the cattle when grazing, therefore the cost of this activity is unprofitable.

TABLE I. OPTIMAL PLAN OF LAND ALLOCATION, RENT OF LAND AND GRAZING OF COMMUNAL PASTURE

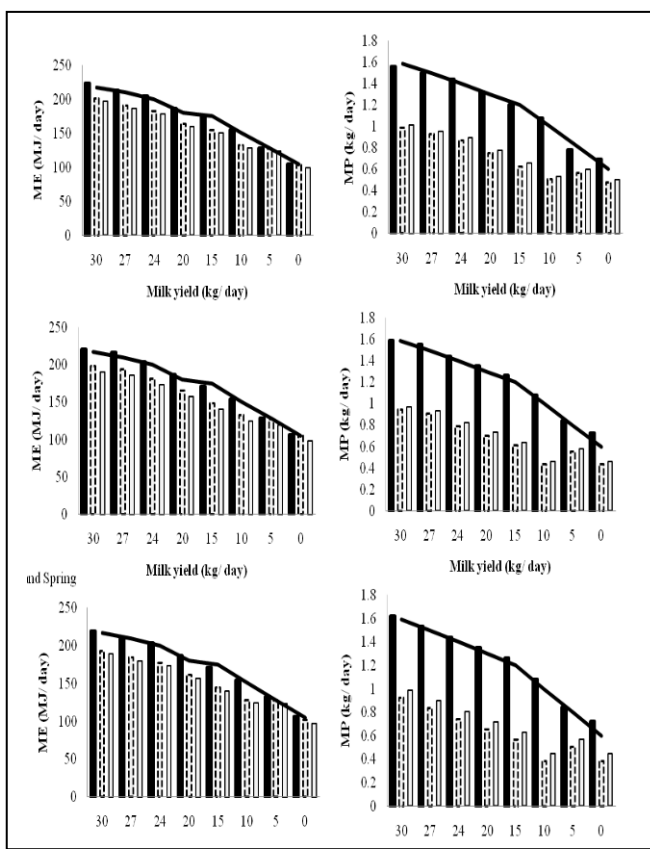
| Scenarios | Land Allocation | | | | | | |
|-----------|-----------------|-------|---------|--------------------|-----------|--------------|------------------------------|
| | Oat | Maize | Alfalfa | Cultivated pasture | Farm land | Rent of land | Grazing of Communal pastures |
| | (Hectares) | | | | | | |
| SC 1 | 1.5 | 2.0 | 0 | 1.2 | 0.6 | 3.5 | Na |
| SC 2 | 1.0 | 2.0 | 0 | 1.0 | 4.0 | 0 | Na |
| SC 3 | 1.7 | 2.7 | 6.6 | 2.2 | 10 | 0 | Na |

Na. Activity not suggested in the optimal plan

The changes mentioned above, in relation to land allocation, allowed to improve the DM supply in SC1 (3 kg DM/ herd.day) but not for SC2 and SC3, thus FEP was superior in these two scenarios (Table 1); in terms of nutrients, the OPI improved the ME supply in SC1 and SC2 (59 and 18 MJ/ herd.day; respectively); on the other hand, the MP supply was improved in SC1 and SC3 (2, kg herd $^{-1}$ day $^{-1}$), while in SC2, the MP supply remained unchanged.

The feeding strategies for dairy herd were based on quality forages grown on-farm, in Table 2 is presented the requirements of DM, ME and MP as well as the percentages that were met when the optimal plan or farmers' existing plan was followed. Although DM supply in SC2 derived from optimal plan was lower than farmers' existing plan, the ME supply was one percent higher and the MP supply did not show changes, indicating that forage management was improved; in SC3, 81% of the MP requirement was achieved.

Fig. 1. Metabolisable energy and metabolisable protein supply of three pastures in summer (a), autumn (b), winter and spring (c)



Solid black line: requirements of ME. Black bars: ME of ryegrass-white clover pasture.

Bars with broken line: ME of communal pasture in F6.

Bars with solid line: ME of communal pasture in F7

Solid black line: requirements of MP.

Black bars: MP supply of ryegrass-white clover pasture

Bars with broken line: MP of communal pasture in F6

Bars with solid line: MP of communal pasture in F7

Feeding strategies for all scenarios

Grazing of ryegrass-white clover pastures were used in all scenarios but grazing time was a constraint (up to 12 h day⁻¹) therefore DM intake was complemented with forage crops grown on-farm. Table 3 shows the feeding strategies that were common for all scenarios and the cost per kg of dry matter. Three diets were offered to lactating cattle by season, the diets were balanced according to the stage of lactation.

During summer; the available forages that complement grazing were; fresh oats and fresh maize, for cows in early lactation (EL) and middle lactation (ML), when cows were in late lactation (LL), the oats hay complemented the grazing of cultivated pastures; during autumn, grazing was complemented with fresh maize in EL only, and cows in ML and LL were complemented with maize silage and oats hay; during winter and spring season, grazing was complemented with maize silage in EL and ML; while for LL, the diet was the same as in autumn (Table 3).

TABLE 2. NUTRIENT SUPPLY (DM, KG DM/HERD.DAY); ME, MJ HERD.DAY; MP, KG HERD⁻¹ DAY⁻¹), ON-FARM FORAGES (%) AND NET FARM INCOME (\$ COW⁻¹ YEAR⁻¹) DERIVED FROM OPTIMAL PLAN OF LP AND FARMER'S ACTUAL PLAN IN THREE SCENARIOS

| SC | Herd | requirements | Nutrient supply | | On-farm | | Net farm | |
|-----|------|--------------|-----------------|------|---------|-----|-------------------|--------------|
| | | | | | (%) | | Income | |
| | | | OPI | FEP | OPI | FEP | OPI | FEP |
| SC1 | DM | 72 | 30 | 27 | 42 | 38 | 279 ±20 | -52 ±382 |
| | | ME | 785 | 251 | 192 | 32 | 25 | |
| | | MP | 6 | 2 | 1 | 34 | 20 | |
| SC2 | DM | 200 | 118 | 134 | 59 | 67 | 464 ±421 | 310 ±1723 |
| | | ME | 2198 | 1089 | 1071 | 50 | 49 | |
| | | MP | 16 | 10 | 10 | 64 | 64 | |
| SC3 | DM | 265 | 185 | 314 | 70 | 100 | 73 738 ±304 | -544 ±544 |
| | | ME | 2905 | 1681 | 2451 | 58 | 84 | |
| | | MP | 21 | 17 | 15 | 81 | 75 | |

In terms of supplementation, the optimal plan suggested a mixture of maize grain and bread waste (a concentrate made on-farm) rather than commercial compounds bought out of the farm for all scenarios. The proportion of supplements in the diet for lactating cows were 22% in EL and 21% in ML and LL throughout all seasons, for dry cows the proportion was 18%.

TABLE 3. FEEDING STRATEGIES BY SEASON AND STAGE OF LACTATION.

| Feeding strategy | Fodder crops | | | | Supplements | | Grazing pasture [#] (Ryegrass-white clover) | | | | \$ kg ⁻¹ DM | |
|------------------|--------------|----|----|----|-------------|-----|--|----|----|----|------------------------|------|
| | FO | FM | MS | OH | Mg | Bw | SU AU WI SP | | | | | |
| | | | | | | | (kg DM day ⁻¹) | | | | | |
| Summer | | | | | | | | | | | | |
| Autumn | EL | 7 | | | | 1.5 | 2.5 | 10 | 11 | 12 | 11 | 0.17 |
| | ML | 4 | | | | 1 | 2 | 10 | 11 | 12 | 11 | 0.19 |
| | LL | 2 | 1 | | 1 | 2 | | 10 | 11 | 12 | 11 | 0.17 |
| Winter-Spring | EL | 7 | | | | 1.5 | 2.5 | 10 | 11 | 12 | 11 | 0.20 |
| | ML | 4 | | | | 1 | 2 | 10 | 11 | 12 | 11 | 0.17 |
| | LL | 2 | 1 | 1 | 1 | 2 | | 10 | 11 | 12 | 11 | 0.17 |

EL: early lactation; ML: middle lactation; LL: late lactation; Mg: maize grain, Bw: bread waste; FO: fresh oat; FM: fresh maize; MS: maize silage; OH: oat hay; SU: summer; AU: autumn; WI: winter; SP: spring; [#] A minimum of 7 kg of dry matter intake in grazing pastures was assumed (Albarrán-Portillo, 2013)

Differences between seasons and forage sources influenced the cost of diet (Table 3). The lowest cost was attained when the optimal plan included oat hay and maize silage as forage complements of pastures, whereas fresh maize incremented costs in summer and autumn (11.7% in ML and 17.6% in EL,

respectively), supplementation with a mixture of maize grain and bread waste (Mg and BW) allowed a saving of 30% per cow/day.

The Fig. 1 shows the nutrient supply of cultivated pastures and communal pastures by season. Fig 1(a) shows that requirements of ME and MP were met when optimal plan included cultivated pastures in all seasons; on the other hand, the communal pastures achieved the ME requirements of cows in LL and dry cows (white bars; broken and solid line). When the optimal plan was forced to include communal pastures as activity for all scenarios, higher amounts of maize grain and bread waste were required.

Economic performance of the optimal plan

The economic performance of the optimal plan was presented in Table 2, it showed that optimal plan allowed an increment of US\$331 (cow year⁻¹), US\$130 (cow year⁻¹) and US\$633 (cow year⁻¹) with respect to farmers' existing plan; in SC1, SC2 and SC3 respectively.

IV. DISCUSSION

During the past decades inexpensive energy and protein enabled the development of systems based on feeds produced out of the farms (purchased feeds), unfortunately this has changed and SSDS needs to be re-defined because rising production costs and static milk prices have highlighted the advantage of grazing and hence maximizing the proportion of forages produced on-farm.

Feeding is financially the single most important element of animal production along with constituents of feeds and their consumption that affect animal productivity. In central Mexico the rainfall pattern do not permit year-round grazing systems, therefore the use of feeding strategies combining grazing of pastures plus fodder crops and supplementation with by-products are required [8].

Adoption of the suggested management

A key part of guiding farmers for adopting new management strategies without compromising time, efforts and money is the use of simulation models, such modelling can be applied to show the improvements they may have in terms of the economic benefit. The implementation of the suggested management is highly dependent of the farmers' willingness and education has been mentioned in [12] and [9] as very important driver about adoption of complex management [3] and as discussed by [14], the adoption of new management relies on the positive impact of the new management on the producer's net return, the applicability of such management to the producer's operations and the possession of the economic means to adopt new management.

Farmers in all scenarios believed that communal grazing was a free forage resource; however they did not realize that communal grazing had two aspects that influenced this activity; i) it used family labour for looking after the cattle while grazing, therefore the model assigned an opportunity costs for such activity and it was unprofitable, this is in line with [21] they found that net profit per litre of milk was

reduced between 25% and 75% when family labour costs are considered, additionally they mentioned that in Latin-American and African countries, family labour costs represents between 50% and 100 % of total labour costs in which women provide up to 22% of labour force having a fundamental role in the profits obtained in dairy farms. The second issue ii) communal pastures had lower nutritive value than cultivated pastures and feeding is financially the single most important element of animal production besides nutrients of feeds and their consumption that affect animal productivity.

In this way, the optimal plan suggested grazing of cultivated pastures complemented with fodder crops (fresh oat or as hay) harvested at vegetative stage, maize (fresh or silage) and moderate supplementation with concentrate based on maize grain (1 to 1.5 kg DM day⁻¹) and bread waste (1 to 2.5 kg DM day⁻¹); the supplementation of concentrates was 3 % lower to that reported by [7], they found a mean of 25% of concentrate in the diets of Western districts of Australia.

The optimal plan suggested two low cost feeding strategies; 1) grazing of pasture + oats (as fresh matter) + mixture of maize grain and bread waste and 2) grazing of pasture + maize silage + mixture of maize grain and bread waste. The feeding strategy 1 supplied up to 233 MJ of ME and up to 1771 g of MP and the feeding strategy 2 supplies up to 227 MJ of ME and up to 1625 of MP, the highest diet cost was observed when fresh maize was incorporated in the diet of cows in EL (Table 3, US\$19 and US\$20 kg⁻¹ DM); however, [17] observed that offering fresh maize as complement to grazing dairy cows had no benefits in milk production per cow but had benefits on milk production per hectare. Therefore, with the latter comment, a question was raised for exploring the management that optimize FNI per cow or per hectare.

V. CONCLUSIONS

In order to optimize the farm net income in small-scale dairy systems, farmers should change the way they have managed their limited resources for centuries implying that they must develop higher skills for managing efficiently the on-farm resources, thus small-scale dairy systems should be redefined; from forage and concentrate buyers (external inputs) to pasture-based and conserved forage systems.

ACKNOWLEDGMENT

Authors would like to thank to CONACYT, México; for supporting financially this study and all farmers involved in the field work, to Universidad Autónoma Metropolitana Unidad Lerma for supporting financially the presentation of this work in the MCSI14.

REFERENCES

- [1] Agriculture and Food Research Council, "The Nutrient Requirements of Ruminants". CAB, Wallingford, UK, 1995.
- [2] Association of Official Agricultural Chemist, "Official Method of Analysis". Assoc. Off. Analytic Chemists, 15th ed. Arlington, VA, USA, 1990.

- [3] A. Bernués, and M. Herrero, "Farm intensification and drivers of technology adoption in mixed dairy-crop systems in Santa Cruz, Bolivia". Spanish Journal of Agricultural Research, vol 6 (2), pp. 279-293, 2008.
- [4] C. M. Arriaga-Jordan, B. Albaran-Portillo, A. Espinoza-Ortega, A. Garcia-Martinez, and O. A. Castelan-Ortega, "On-farm comparison of feeding strategies based on forages for small-scale dairy production systems in the highlands of central Mexico". *Experimental Agriculture* vol. 38, pp. 375-388, 2003.
- [5] D. F. Chapman, S. N. Kenny, D. Beca, and I. R. Johnson, "Pasture and forage crop systems for non-irrigated dairy farms in southern Australia. 1. Physical production and economic performance". Agricultural Systems, vol 97, pp. 108–125, 2008.
- [6] D. Val-Arreola, E. Kebreab, J. Mills, S. L. Wiggins, J. France, "Forage production and nutrient availability in small-scale dairy systems in central Mexico using linear programming and partial budgeting". Nutrient Cycling in Agroecosystems, vol 69, pp. 191-201, 2004.
- [7] E. Bramley, I. J. Lean, W. J. Fulkerson, and N. D. Costa, "Feeding management and lean on dairy farms in New South Wales and Victoria". Animal Production Science, vol 52 1, pp. 20-29, 2011.
- [8] F. Bargo, D. H. Rearte, F. J. Santini, and L. D. Muller, "Ruminal digestion by dairy cows grazing winter oats pasture supplemented with different levels and sources of protein". Journal of Dairy Science, vol 84, pp. 2260–2272, 2001.
- [9] G. M. Bazzani "An integrated decision support system for irrigation and water policy design: DSIRR". Environmental Modelling & Software, vol 20, pp. 153-163, 2005.
- [10] Hemme T, "IFCN Dairy Report 2007". International Farm Comparison Network, IFCN Dairy Research Center, Kiel, Germany, 2007.
- [11] INEGI, "Censo Agrícola, Ganadero y Forestal". Instituto Nacional de Estadística y Geografía. Available at: <http://www3.inegi.org.mx/sistemas/tabuladosbasicos/default.aspx?c=17177&s=est>, 2007.
- [12] I. Baltenweck, S. Staal, M. N. M. Ibrahim, M. Herrero, F. Holmann, V. Manyong, M. B. R. Jabbar Patil, P. K. Thornton, T. Williams, M. M. Waithaka, and T. De Wolf, "Crop-livestock intensification and interaction across three continents". Final Project Report. CGIAR SystemWide Livestock Programme, ILRI, Addis Ababa, Ethiopia. pp. 133, 2003.
- [13] J. G. Estrada-Flores, M. Gonzales-Ronquillo, F. L. Mould, C. M. Arriaga-Jordan and O. A. Castelán-Ortega, "Chemical composition and fermentation characteristics of grain and different parts of stover from maize land races harvested at different growing periods in two zones of central Mexico". Animal Science, vol 82, pp. 845-852, 2006.
- [14] J. Gillespie, S. A. Kim, and K. Paudel, "Why don't producers adopt best management practices? an analysis of the beef cattle industry". Agricultural Economics, vol 36, pp. 89-102, 2007.
- [15] LINGO users guide Copyright © by LINDO Systems Inc. Chicago, Illinois 60642, pp. 820, 2006.
- [16] M. Neal, J. Neal, and W. J. Fulkerson, "Optimal choice of dairy forages in eastern Australia. Journal of Dairy Science, vol 90, pp. 3044–3059, 2007.
- [17] M. Ramírez-Mella, O. Hernández-Mendo, A. Améndola-Massiotti, E. J. Ramírez-Bribiesca, G. D. Mendoza-Martínez, and J. A. Burgueño-Ferreira, "Productive response of grazing dairy cows to fresh chopped maize supplementation under small farming system in the Mexican highlands". *Tropical Animal Health and Production*, vol 42, pp.1377-1383, 2010.
- [18] N. Andrieu, C. Poix, E. Josien and M. Durud, "Simulation of forage management strategies considering farm-level land diversity: Example of dairy farms in the Auvergne". Computers and Electronics in Agriculture, vol 55, pp. 36–48, 2007.
- [19] O. A. Castelan-Ortega, R. H. Fawcett, C. M. Arriaga-Jordan, and M. Herrero, "A Decision Support System for smallholder campesino maize-cattle production systems of the Toluca Valley in Central Mexico. Part II—Emulating the farming system". Agricultural Systems, vol 75, pp. 23–46, 2003.
- [20] P. B. R. Hazell, and R. D. Norton, "Mathematical programming for economic analysis in agriculture. (Macmillan Publishing Company, USA), 1986.
- [21] R. R. Posadas-Domínguez, C. M. Arriaga-Jordán, and F. E. Martínez-Castañeda, "Contribution of family labour to the profitability and competitiveness of small-scale dairy production systems in central Mexico", Tropical Animal Health and Production, vol 46, pp. 235-240, 2014.
- [22] SIAP-SAGARPA, "Resumen Nacional Pecuario. Servicio de Información Agroalimentario y Pesquero". Secretaría de Agricultura, Ganadería, Desarrollo Rural, Pesca y Alimentación. Available at: http://www.siap.gob.mx/index.php?option=com_wrapper&view=wrapper&Itemid=369, 2008.

Motion Capture Systems Overview and Accelerometer MoCaps Systems

Slava Milanova Yordanova

Department of Computer Science and Engineering,
Faculty of Computing and Automation, Technical
University of Varna,
1 Studentska Str., Varna 9010, Bulgaria
E-mail: slava_y@abv.bg

Nikolay Todorov Kostov

Department of Communication Technologies,

Faculty of Electronics, Technical University of Varna,
1 Studentska Str., Varna 9010, Bulgaria
e-mail: n_kostov@abv.bg

Yasen Dimchev Kalchev

Department of Communication Technologies,
Faculty of Electronics, Technical University of Varna,
1 Studentska Str., Varna 9010, Bulgaria
e-mail: yasenkalchev@mail.ru

Abstract — The Mocap system with accelerometers is quite practical to use and offers great advantages over the other systems. One must know that no system is perfect and every one of these three is good for certain project. MoCap with accelerometers is used for movies and game animation because of the great possibility of real-time animation.

Keywords — *Mocap, motion capturing, 3D, 2D, animation, movies, games, industry, technology, accelerometers, systems, recording, dsp;*

I. INTRODUCTION

In the last 20 years the popularity of Motion Capturing (MoCap) technique in animation has increased rapidly. MoCap system in animation refers to recording the movements of an actor and then using that information to animate digital character models in 2D or 3D computer animation. MoCap gives some great opportunities to animators such as timesaving, simplifying the process of animation and others. MoCap can be applied in many other fields : sport (analyzing movements), military, robotics, game industry, medicine (orthopedic analysis, surgical manipulation) and others. This report is focused on MoCap in computer animation.

II. MOCAP PARAMETERS AND TYPES

There are many MoCap techniques, but three of them have practical application in animation industry. The next paragraph reveals the most important parameters of the MoCap system and three most used MoCap techniques with short analysis of advantages and disadvantages. The important parameters of Mocap systems are:

- Accuracy: the error of measuring the movements of

the actor. This is a basic problem to solve. It's the reason for unrealistic and unpleasing animated characters.

- Animation in real-time: the possibility of the computer model to follow the actor's movements with a very short (negligible) time delay. This is a quite important because the actor can see how the character responds to the movements at the same moment. Then the actor could experiment with different movements without waiting a long time for the system to analyze the data. Only a few systems can work in real-time. Its quite important for the pipeline animation when time is the most important parameter.
- Freedom of movement: how complicated are the movements the actor is able to do. Its very important for the actor to be able to move freely. Freedom gives an opportunity for rich and interesting animation.
- Frames per second: the recording speed. The greater the speed the better the system will capture fast movements like running, jumping, waving etc.
- Possible interruption in recording: recording the movement with no interruption in the process of measuring the movements. In some systems an interruption could occur and the movement of some parts of the body could not be recorded.
- Identification: each part of the body must be identified. In some systems the parts of the body couldn't be identified. The problem is even more complicated when more than one actor are involved in the scene.
- External influence: the independence of the system from external influence. Some systems are sensitive to magnetic fields or light. This leads to errors and requires

more complicated software for analyzing the data and correcting the error.

- Price: the less the better. Some systems require expensive devices to work properly. As one can guess the goal is to make high quality system with affordable price.
- Training: training the actors to work with the system. Some systems require special awareness when acting. The less training is needed the better, because training takes time and efforts that the actor must be paid for.
- Portability: the ability of the system to be moved. Sometimes the scene must be moved and not all the MoCap systems can be moved easily. For example in first scene the actor must crawl on the ground, for the second he must jump down the stairs and in third he must climb up the wall.
- Software complexity: the complexity of the software developed for data analyzing and character animating. This parameter is important for time saving in the process of animating and the price of the system.

The three basic MoCap systems are :

- **Mocap with markers.**

Markers are fixed to the face and the body of the actor. Then the actor is shot by cameras. After that a software analyzes the position of the markers in each frame and calculates the movement of each part of the body. After that the data is sent to the animating software. The markers could be made in different shape and fixed on different places on the body depending on the software and the algorithm for analyzing the movements. For identification of the markers they are made in different colors. For better detection they are made from fluorescent or light reflecting material. An important for practice type of MoCap with markers is LED (light emitting diod) MoCap. Leds are easily detected and could be modulated for identification. The advantages of this system are the accuracy and the freedom of movements. Unlike the two other type of MoCap this one could record the movement of the face quite accurately [6]. The system could even record the movement of the eyelids. The markers don't interfere with the movements of the actor which gives him a great freedom of movement. The system gives the position of the body directly unlike some of the other systems that give only the movement vector. The cameras are able to shoot very fast so the system could capture high speed movements. In more advanced systems a

real-time animating is possible. Disadvantage is that the system is expensive due to the complicated software for analysis and the amount of high resolution cameras needed to shoot the markers from different angles. Another disadvantage is that the markers could be covered (blocked) from parts of the body, other actors or object on the scene. The analysis become more complicated when more than one actor are shot. The system is vulnerable to lights coming from other source than the marker. The system is not easy to move. In Table 1 are shown the advantages and disadvantages of Mocap with markers.

TABLE I. ADVANTAGES AND DISADVANTAGES OF MOCAP WITH MARKERS

| Advantages | Disadvantages |
|----------------------------|--------------------------------|
| High accuracy | High Price |
| High recording speed | Recording interruption |
| Actors movement freedom | Complicated software |
| Real-time | Not portable |
| Face expressions recording | Great amount of higher cameras |
| Position indication | |
| Most popular | |
| Many applications | |

- **Mocap with magnetic field.**

Sensors are placed on the body of the actor to measure the low-frequency magnetic field generated by a transmitter source. The sensors report position and rotational information. The system is relatively not expensive and provides data with high accuracy [1]. The software is less complicated than the MoCap with markers. The system gives information for 6 degrees of freedom (6DOF – right/left, up/down, back/forward, pitch, yaw, roll) [2]. The markers are independent from covering that means no recording interruption could occur. A great disadvantage is that the system is vulnerable to magnetic fields and metal objects. Every single sensor is identified and no aliasing is possible. Since most buildings are made with some metal objects a special place for the scene should be chosen. The recording speed is relatively low – about 100 frames per second [2]. That means faster movements can't be captured. The actor can move only in the field covered by the transmitter. The advantages and disadvantages are shown in table 2.

TABLE II. ADVANTAGES AND DISADVANTAGES OF MAGNETIC FIELD MOCAP

| Advantages | Disadvantages |
|-------------------------------------|--------------------------|
| High accuracy | Limited movement freedom |
| Gives orientation and position data | External interference |
| Low price | Low recording speed |
| No complicated software | Noise |
| 6DOF | |
| No occlusion | |
| Sensor Identification | |

- **Mocap with accelerometers.**

Accelerometer devices are fixed on the body of the actor. In the recent years this technique became more popular due to the better parameters of accelerometers and lower market price. Great advantages are – high accuracy, movement and orientation data, simple software, portability, no occlusion, 6DOF, sensor identification, high recording speed, independence from magnetic field and lights and others. Great disadvantage is that the hardware does not report information about position. In Table 3 are shown the advantages and disadvantages of the system.

TABLE III. ADVANTAGES AND DISADVANTAGES OF MOCAP WITH ACCELEROMETERS

| Advantages | Disadvantages |
|---|------------------|
| High accuracy | No position data |
| Real time | |
| Affordable price | |
| Simple software | |
| High recording speed | |
| Sensor identification | |
| 6DOF | |
| Portability | |
| No occlusions | |
| Independence from magnetic fields and light sources | |

There are other systems like – acoustic, markless, radio frequency and others. They are not reviewed in this report because they have rare practical use due to great disadvantages. Comparing the systems it is obvious why there is a growing popularity of the MoCap with accelerometers. In the next paragraph will take a closer look on this system.

III. MOCAP WITH ACCELEROMETERS

There are some new accelerometers at the market. For example ADXL 345. Its high resolution (3.9 mg/LSB) enables measurement of inclination changes less than 1.0° [3]. Lets look at the worst case – one sensor placed at the end of one of the longest part of the body – lower leg (350mm length). ADXL will indicate movement if it is more than 6mm at the end of the leg. Now lets see what will happen for a phalanx of a finger with length 30mm. ADXL 345 will indicate movement if this part moves with more than 0.5mm at the end. That means even the trembling of a finger will be captured. Thats why the accelerometer system has great accuracy.

The dimensions of ADXL 345 are 3x5x1 mm. The sensor can be placed on small parts of the body like hands and fingers. The system cannot measure the movement of face with high accuracy, but it could measure some basic changes like smiling , lower jaw movements, lips movement and brow movement.

ADXL345 cant measure absolute position [3]. It must be calculated . That leads to errors and a need for corrections.

ADXL345 measures the acceleration in three axes [3]. That gives enough data for easy calculating the movement and the software will be simpler than the marker system where a great amount of calculation for every camera and frame must be made.

ADXL345 measures the orientation to the ground [3] which gives important information for the absolute orientation of the body parts. That makes the calculations for the absolute position more simple.

ADXL345 is based on inertial elements and that's why the system cant be affected by magnetic fields and light.

ADXL345's consummation is as low as 23 μ A in measurement mode and 0.1 μ A in standby mode at VS = 2.5 V (typical) [3]. With this consummation all the sensors on the body can be powered by battery and the data can be send wireless. That way the actor will be free to move and the system will be easily portable.

Like all the other systems this one needs some data analysis for correction. The good thing here is that Mocap with accelerometers provides the most needed data right form the sensors, so there is no need for complicated software. The software will be focused on some errors fix and making the movements more pleasant to watch.

An interesting problem to solve is that the sensors are sliding over the skin [4] - The alignment with the bones can change due to relative movements of muscles and skin. This misalignment can result in large errors of angles. The trackers must be placed close to the bones where there is less muscles and fat. On the other hand, the rotations of the joints must also be limited to stay in the human limitations.

IV. CONCLUSION

As can be seen from this information the Mocap system with accelerometers is quite practical to use and offers great advantages over the other systems. One must know that no system is perfect and every one of these three is good for

certain project. MoCap with accelerometers is used for movies and game animation because of the great possibility of real-time animation.

REFERENCES

- [1] Ashish Sharma, Mukesh Agarwal, Anima Sharma, Pankhuri Dhuria, "Motion capture process, techniques and Applications", International Journal on Recent and Innovation Trends in Computing and Communication, Volume 1, Issue 4, pp. 251–257, 2013.
- [2] <http://www.metamotion.com/motion-capture/magnetic-motion-capture-1.htm>
- [3] http://www.analog.com/static/imported-files/data_sheets/ADXL345.pdf
- [4] David Fontaine, Dominique David, Yanis Caritu, "Sourceless Human Body Motion Capture", [Online] <http://www.minatec.com/grenoble-soc/proceedings03/Pdf/30-fontaine.pdf>
- [5] Katherine Ann Pullen, "Motion capture assisted animation: texturing and synthesis", PhD Thesis, STANFORD UNIVERSITY, July 2002.
- [6] Chris Bregler, "Motion Capture Technology for Entertainment", *Signal Processing Magazine*, IEEE, 24(6), pp. 160 -158, November 2007.

The Use of Psychometric Questionnaires in Security Community Members Evaluation

Alena Paduchova

Department of Security Engineering
Tomas Bata University in Zlin
Zlin, Czech Republic
paduchova@fai.utb.cz

Ludek Lukas

Department of Security Engineering
Tomas Bata University in Zlin
Zlin, Chczech Republic
lukas@fai.utb.cz

Abstract— Each user of information technologies prefers different type of work environment, especially in the security area. There exists a hypothesis of the relationship between personality typology and this work environment. We will use a dispositional framework of the Five Factor Model based on questionnaires in personality psychology for research in this area. After the analysis of the information environment of the user we will observe the personal type and the connection between these two problems. The paper presents the state of knowledge in personality typology area and results of the first part of research – Information environment analysis.

Keywords— Attributes, Hogan's Tests, MBTI Inventory, Pairwise Comparison, Psychometric Questionnaire, Personality Typology

I. INTRODUCTION

An information management of organization should ensure conditions to fulfill information needs. The use of information depends on their skills and literacy, on the basis of their knowledge and skills, information activities implemented thus ensuring the desired operation of the organization.

Each user prefers a different type of the information environment. There exists a hypothesis of relationship between personality typology and the information environment.

Current information technology enables it to be assessed in many ways. Study of the available literature leads to the conclusion that there are no research results of the relationship between personality typology and information support.

Our research consists of 3 main parts. In the first part we will observe chosen attributes of information environment of our respondents from security area. In the second part we will use questionnaires based on Big Five theory for the personality typology. Hogan's tests and Myers-Briggs Inventory were chosen for testing of our respondents. These questionnaires were chosen after the psychologist consultation. We will observe the relationship between these two areas after the analysis of personality typology of our respondents.

This paper includes the state of knowledge in personality typology area. Especially in Big Five theory based questionnaires. We chose 2 types of questionnaire for our research after the consultation with psychologist. It is MBTI inventory and Hogan's tests. Another section of paper describes the analysis of information environment of our respondents.

II. FIVE FACTOR MODEL IN PERSONALITY PSYCHOLOGY

One of the most dynamic areas of personality research during the past two decades has been that of personality structure. Studies on the structure of personality characteristics use a lexical approach in order to determine the major personality dimensions. The lexical approach rests on the assumption that the most meaningful personality attributes encoded in language as single-word description. The results of such studies supported the validity of the 'Five Factor Model' with factors identified as: (1) SURGENCY or EXTRAVERSION (talkative, assertive energetic), (2) AGREEABLENESS (good-natured, cooperative and trustful), (3) CONSCIENTIOUSNESS (conscientious, responsible and orderly), (4) EMOTIONAL STABILITY or its opposite NEUROTICISM (calm, neurotic, not easily upset), (5) CULTURE and INTELLECT or in one inventory representation OPENNESS TO ECPERIENCE (cultured, intellectual, unconventional). [4]



Fig. 1: Five Factor Model

There are two approaches in the framework of the Five Factor Model: lexical (taxonomic) and dispositional (based on questionnaires). We chose dispositional approach based on questionnaires after the consultation. We will use MBTI and Hogan's questionnaires for our research.

A. MBTI

The Myers-Briggs Type Indicator (MBTI) assessment is a psychometric questionnaire designed to measure psychological preferences in how people perceive the world and make decisions. These preferences were extrapolated from the typological theories proposed by Carl Gustav Jung and first published in his 1921 book *Psychological Types*. Jung theorized that there are four principal psychological functions by which we experience the world: sensation, intuition, feeling, and thinking. One of these four functions is dominant most of the time.

The original developers of the personality inventory were Katharine Cook Briggs and her daughter, Isabel Briggs Myers; these two, having studied extensively the work of Jung, turned their interest of human behavior into a devotion of turning the theory of psychological types to practical use. They began creating the indicator during World War II, believing that knowledge of personality preferences would help women who were entering the industrial workforce for the first time to identify the sort of war-time jobs that would be "most comfortable and effective". The initial questionnaire grew into the Myers-Briggs Type Indicator, which was first published in 1962. The MBTI focuses on normal populations and emphasizes the value of naturally occurring differences. Robert Kaplan and Dennis Saccuzzo believe "the underlying assumption of the MBTI is that we all have specific preferences in the way we construe our experiences, and these preferences underlie our interests, needs, values, and motivation". [4]

The identification and description of the 16 distinctive personality types that result from the interactions among the preferences.

| | | | |
|-------------|-------------|-------------|-------------|
| ISTJ | ISFJ | INFJ | INTJ |
| ISTP | ISFP | INFP | INTP |
| ESTP | ESFP | ENFP | ENTP |
| ESTJ | ESFJ | ENFJ | ENTJ |

Fig. 2 The 16 personality types of the MBTI

From MBTI Manual: Favorite world: Do you prefer to focus on the outer world or on your own inner world? This is called Extraversion (E) or Introversion (I).

Information: Do you prefer to focus on the basic information you take in or do you prefer to interpret and add meaning? This is called Sensing (S) or Intuition (N).

Decisions: When making decisions, do you prefer to first look at logic and consistency or first look at the people and special circumstances? This is called Thinking (T) or Feeling (F).

Structure: In dealing with the outside world, do you prefer to get things decided or do you prefer to stay open to new information and options? This is called Judging (J) or Perceiving (P).

Personality Type: When you decide on your preference in each category, you have your own personality type, which can be expressed as a code with four letters.

The 16 personality types of the Myers-Briggs Type Indicator® instrument are listed here as they are often shown in what is called a "type table." [4]

B. Hogan's tests

Hogan is an international authority in personality assessment and consulting, Hogan has over 30 years of experience helping businesses dramatically reduce turnover and increase productivity by hiring the right people, developing key talent, and evaluating leadership potential. Hogan's Select, Develop and Lead series of reports represent an integrated system of scientifically-validated tools that are specifically designed to help you to better manage your human resource capital and retain top talent.



Fig. 3 Hogan's tests

1) Hogan Personality Inventory

The Hogan Personality Inventory describes normal or bright-side personality – qualities that describe how we relate to others when we are at our best. Whether your goal is to find the right hire or develop stronger leaders, assessing normal personality gives you valuable insight into how people work, how they lead, and how successful they will be.

The HPI measures normal personality along seven scales:

1. Adjustment
2. Ambition
3. Sociability
4. Interpersonal Sensitivity
5. Prudence
6. Inquisitive
7. Learning Approach.

2) The Hogan Development Survey

The Hogan Development Survey describes the dark side of personality – qualities that emerge in times of increased strain and can disrupt relationships, damage reputations, and derail peoples' chances of success.

By assessing dark-side personality, you can recognize and mitigate performance risks before they become a problem.

The HDS measures dark side personality along 11 scales.

The following describe high scorers:

1. Excitable
2. Skeptical
3. Cautious
4. Reserved
5. Leisurely
6. Bold
7. Mischievous
8. Colorful
9. Imaginative
10. Diligent
11. Dutiful.

This HDS survey could be significant for our research because we will assess behavior in stressed situations.

3) The Motives, Values, Preferences Inventory (MVPI)

The Motives, Values, Preferences Inventory describes personality from the inside – the core goals, values, drivers, and interests that determine what we desire and strive to attain. The MVPI measures values along 10 primary scales. High scorers are described as:

1. Recognition
2. Power
3. Hedonism
4. Altruistic
5. Affiliation
6. Tradition
7. Security
8. Commerce
9. Aesthetics
10. Science

By assessing values, we can understand what motivates candidates to succeed, and in what type of position, job, and environment they will be the most productive. [4]

The research in this area is currently in progress. Results of this project will be evaluated in second part of our research.

II. INFORMATION ENVIRONMENT ANALYSIS

Information environment is an integral part of the social environment. Its structure consists of a human factor, which is an originator, intermediary and the user of the communication process. There is also information and communication processes which provide certain information flows and generate information products. All this ensures are provided by a material-technical base which consists of information institutions, libraries but also information technology and computing. We must deal with a space-time dimension which determines the direction, speed and novelty of the information communicated. It is clear that the most important element of the information environment is a human.

People represent an individual IT environment with cognitive and social aspects of personality.

Thus, there is a presumption that the type and arrangement of the information environment may depend on the typology of personality.

A. Attributes of information environment

We chose 10 major attributes for environment evaluation:

1. Complexity – satisfied the maximum of requests,
2. Friendliness- easy to use,
3. Orderliness- with some order,
4. Mobility-easily movable,
5. Resistance- able to provide a function in terms of the action of negative factors,
6. Maintainability- ease of maintenance,
7. Intricacy- given by number of elements and complexity,
8. Transparency- easy for understanding of order, easy orientation,
9. Effectivity-practical effectiveness,
10. Simplicity- from minimum of elements, without complications and problems.

We used the table of Pairwise Comparison for evaluation of these attributes.

III. METHODS

We have used The Method of Pairwise Comparison for the analysis of information environment of our respondents. Pairwise comparison generally refers to any process of comparing entities in pairs to judge which of each entity is preferred, or has a greater amount of some quantitative property. The method of pairwise comparison is used in the scientific study of preferences, attitudes, voting systems, social choice and public choice. In psychology literature, it is often referred to as paired comparison.

IV. RESULTS

This section of paper deals with results of attributes evaluation. Our respondent processed a table of pairwise comparison method. We have chosen 10 attributes of information environment. Our respondents evaluated their own work environment. As can be seen in Table 1 Effectivity is the attribute with the highest score.

TABLE I. Pairwise Comparison

| | Complexity | Friendliness | Orderliness | Mobility | Resistance | Maintainability | Intricacy | Transparency | Effectivity | Simplicity | Total |
|-----------------|------------|--------------|-------------|----------|------------|-----------------|-----------|--------------|-------------|------------|-------|
| Complexity | x | 1 | 0 | 1 | 0 | 0 | 1 | 1 | 0 | 1 | 5 |
| Friendliness | 0 | x | 1 | 0 | 0 | 0 | 1 | 0 | 0 | 0 | 2 |
| Orderliness | 1 | 0 | x | 0 | 0 | 1 | 1 | 1 | 0 | 0 | 4 |
| Mobility | 0 | 1 | 1 | x | 0 | 0 | 1 | 0 | 0 | 0 | 3 |
| Resistance | 1 | 1 | 1 | 1 | x | 1 | 1 | 1 | 0 | 1 | 8 |
| Maintainability | 1 | 1 | 0 | 1 | 0 | x | 0 | 0 | 0 | 0 | 3 |
| Intricacy | 0 | 0 | 0 | 0 | 0 | 1 | x | 0 | 0 | 0 | 1 |
| Transparency | 0 | 1 | 0 | 1 | 0 | 1 | 1 | x | 0 | 1 | 5 |
| Effectivity | 1 | 1 | 1 | 1 | 1 | 1 | 1 | 1 | x | 1 | 9 |
| Simplicity | 0 | 1 | 1 | 1 | 0 | 1 | 1 | 0 | 0 | x | 5 |

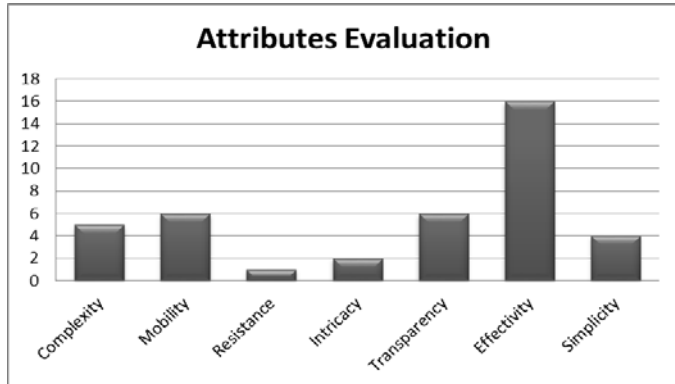


Fig.4 Attributes Evaluation

The graph shows that 'Effectivity' is the most important attribute of our respondents. They need effective and practical work with their environment. But there could be a problem of ineffective work with available information. We are talking about information fragmentation.

A. The problem of Information Fragmentation

In our point view, information fragmentation indicates a state when the user manages more data storages simultaneously. There is the problem of ineffective work with an ever-increasing volume of data and the growing number of media that he manages. User often does not realize that his data are stored on the flash drive and another are in a laptop or in a mobile phone. He is working with a version of the document at the flash drive which is not refreshed while the recent version is stored in his computer. Information is stored at the end of channels and this is a problem. The user does not get into end channels. For example, the member does not get

to the end with the requisite documents folder outside the barracks and the like. The worst case of scenario is irreversible loss of any of the media and thus the data stored on it. In this case, it is really difficult to quantify the value of the lost data. This problem of information fragmentation could be caused by personality typology.

V. CONCLUSION

The high rate of increase in the amount of data is causing that users store their data randomly to individual media. It leads to a situation where the user manages more and more data storages. There arises the problem of information fragmentation. User often does not realize that some of the data are stored on the flash drive and another are in a laptop or in a mobile phone. The worst case is irreversible loss of any of the media and thus the data stored on it. In this case, it is really difficult to quantify the value of the lost data.

Each user of information technologies prefers different type of work environment, especially in a security area. There exists a hypothesis of relationship between personality typology and this work environment. We will use a dispositional framework of the Five Factor Model based on questionnaires in personality psychology for a research in this area.

The first part of our research was the analysis of information environment. We analyzed chosen attributes by using the pairwise comparison method. This analysis showed that effectivity is the most important attribute for our respondents. This means that they need effective and practical information environment for their work. We want suggest this type of work environment. But our first problem is that each user is a different type of personality. This will be the second part of our research. In our future research we will try to design a connection between personality typology and work environment.

ACKNOWLEDGMENT

With support of the Grant No. IGA/FAI/2014/018 from Internal Grant Agency of Tomas Bata University in Zlín.

REFERENCES

- [1] LUKAS, L., HRUZA, P., *The Concept of C2 Communication and Information Support*. "Presented at CCRTS 2004 Conference, June 15 – 17, 2004, San Diego USA, pp 7.
- [2] LUKAS, L., HRUZA, P., Kny, M. *Information management in security services*. Praha: MO AVIS, 2008.
- [3] Stryja, P. *The Evaluation of Level of Information Support by Using Web Applications*. Zlín : UTB, 2012.
- [4] SNYDROVA, Ivana. *Psychodiagnosis*. Praha: Grada Publishing, 2008. ISBN 978-80-247-2165-1.
- [5] LUKAS, L. and team. *Security technologies, systems and management II*. Zlín: VeRBuM, 2012. ISBN 978-80-87500-19-4.
- [6] Lukas, L. and team. *Security technologies, systems and management II*. Zlín: VeRBuM, 2012. ISBN 978-80-87500-19-4

The Analysis of Removable Cutting Tools from the Point of View of the Operating Properties

Cristian-Silviu SIMIONESCU
 Faculty of Engineering form Braila
 "Dunărea de Jos" University of Galati
 Romania
cristian.simionescu@ugal.ro

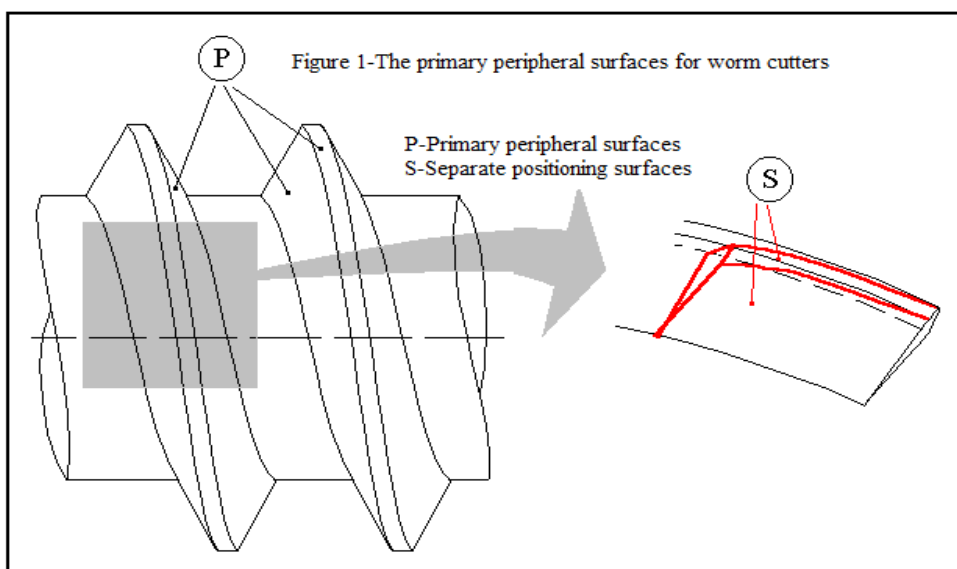
ABSTRACT: The present paper suggests a classification of all the properties of the cutting edges, according to the geometric criterion and according to the necessary usage requirements. Further developing, we make an analysis of the tools according to the second classification criterion, which is according to the necessary usage requirements.

1. General concepts

In the manufacturing process of a rotation tool it is impossible to obtain the cutting edge starting from previously obtaining a precise peripheral surface and *the detachment of the respective edge* out of it,

surfaces we need to take into account the following requirements:

- these contain the cutting edges;
- the clearance front must allow a convenient evacuation of the chip, a detaching of the chip with the smallest effort



except for the unusable case in which the clearance and the positioning angles are chosen at a null value.

The cutting edges are obtained only due to the intersection of the clearance front with the positioning fronts, each of these two surfaces being separately processed using different technological processes. In order to establish the shape of these two types of

and a comfortable sharpening of the tool;

- the positioning fronts must have primary a certain angle compared to the primary peripheral surface (respectively compared to the cutting surface that the edge goes through) –a positioning angle with a certain value–in order to avoid the friction between the positioning front and the surface generated by the part that is obtained;

- the intersection between the two fronts must lead to a cutting edge that must belong to a third surface, that is the primary peripheral surface.

Customizing this for the case of the worm cutters, while the primary peripheral surfaces to which the cutting edge must belong are cylindrical helixes with a straight or curved generator, according to the usage of the tool, containing cutting edges (see also figure 1), the positioning fronts are conic helical surfaces (in the case of the mono-block tools) plane or cylindrical surfaces (for the tools with removable combs), and the clearance fronts are helix surfaces (for the mono-block tools) or plane surfaces (for the tools with removable combs or teeth).

A special situation is represented by the tools for which the manufacturing of the cutting edges in a removable configuration. These cutting edges are made outside the tool, the clearance fronts and the positioning fronts have usually plane or ruler like shapes and lead to obtaining a cutting edge with a profile, with shapes and sizes that must correspond to the desired purpose, respectively to be able to overlap on a line belonging to the primary peripheral surface.

The positioning of the cutting edge on the tool must ensure a good mechanical fixing as well as the condition that the cutting edge must be positioned on the primary peripheral surface, or to deviate from this with an acceptable value in order to obtain the precision required by future manufacturing with the tool made in this manner.

In order for a cutting edge of a tool to fulfil its function this is required to have the following characteristics:

- to ensure a cutting edge with a proper shape size and position adequate for a requirement imposed by the complexity of the cinematic generation of the surface of the tool. We will call this characteristic *geometric property*;

- characteristics that depend upon the physical, mechanical and technological properties of the material from which the tool is made, depending upon the

manufacturing of surface by removing the chips. We will call this overall characteristic the *usage properties* of the tool.

The paper proposes to analyse the tools with removable cutting edges according to the usage properties.

2. The analysis of the tools from the usage properties point of view

The main usage properties necessary for the cold processing of the tools, determined when establishing the material for the cutting edge are the following:

- **the strength at the working temperature**; this property conditions the strength of the material under mechanical efforts at high temperatures, in other words, ensuring the creep strength. Many times this property is called thermal stability;

- **resistance to wear**; this property is closely related to the strength of the material, it depends also from other factors like: the structure, the nature and the refinement of the metallographic constituents, especially from carbides;

- **tenacity**; this property combines strength and ductility, two characteristics with effects that vary in opposite ways. For this reason, the tenacity represents a compromise by which we want to achieve the best strength possible without an excessive fragility.

- **the behaviour of the cutting edge**, or the cutting amplitude; this property can be defined as the property of the tool to maintain the integrity of the cutting edge. The cutting amplitude is a consequence of the first three basic properties mentioned above, the working temperature strength of the tool, the resistance and the tenacity.

- **the resistance to mechanical shocks**. Represents an important property for the tools using the hitting processing or when the chipping is intermittent, being directly related to the tenacity of the tool.

- **the resistance to thermal wear** and the sensitivity to thermal shock.

The presence of the alloying elements required necessary to achieve the above mentioned properties has also an important

disadvantage, respectively it diminishes the thermal conductivity and increases the temperature differences (thermal gradient) between different points from the transversal sections of the tools. The intense thermal gradients produce very different deformation stages in neighbouring areas, which lead to tensions that can exceed the tensile strength of the material, so cracks can appear.

- **the cutting processing easiness** of the cutting edges, in order to process and sharpen them – depends upon the chemical composition and the metallographic constituents.

- the corrosion resistance.

In order to fulfil the extremely varied working conditions, the materials used for the cutting edges of the tools represent extremely complex chemical compounds, starting from carbon steels, to allied steels (with maximum 30% alloying elements) and to sintered plates from metal carbides or ceramic plates.

Hereinafter we make an analysis according to the strength, thermal stability and durability.

a) Strength

In figure 2 we present the main categories of materials used for chipping.

From the strength point of view we can notice the obvious benefits of the

metallic carbides, mineral-ceramic materials or diamond.

b) The thermal stability

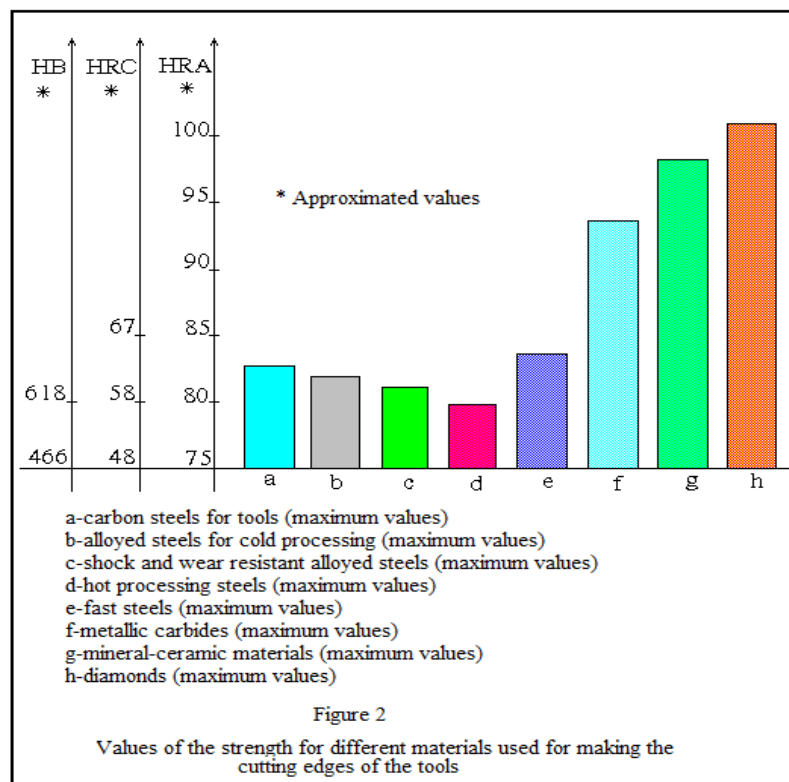
The thermal stability for metallic materials that are used for making the cutting edges of the tools is manifested up to 650°C for the fast steels, it exceeds 250°C for the carbon steels designed for tools and 350°C for the alloyed steels used for tools.

The temperature threshold is determined by the temperature at which structural changes appear, with a direct effect upon the strength of the material. In the case of sintered metallic carbides, the thermal stability is manifested up to 850°C , and for the mineral-ceramic materials the value of the thermal stability goes up to 1000°C .

For the synthetic diamond the thermal stability exceeds 1000°C .

c) Wear and durability

Durability represents the actual chipping time of the cutting edge of a tool between 2(two) consecutive sharpening processes or between two changes of the cutting edges. The durability of the cutting tools is mainly determined by the wear from the positioning surface, respectively the change in the cutting edge shape, figure 3.



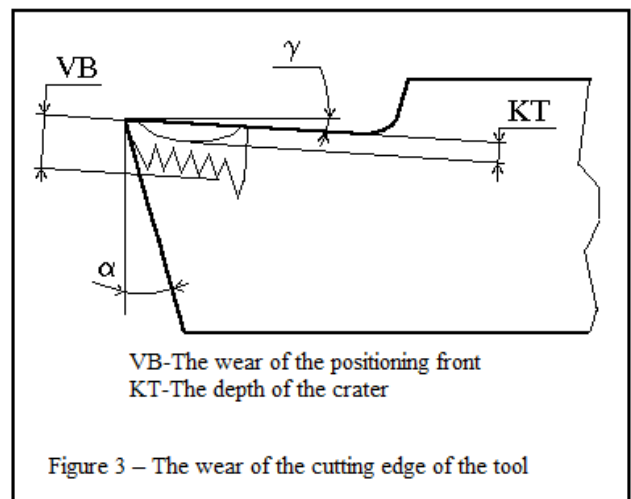
In the case of metallic carbides, we present in table 1 the values of the wear for different types of plates and the chipping conditions that lead to these specific values.

The wear of the strong alloy plates depends upon many parameters. Among these there are the chipping speed and the feed. Usually the favourable wear appears on the positioning front – figure 3.

During the processing, due to the wear, on the clearance front it appears a crater with the depth KT

(Kratertiefe = the depth of the crater), but the appearance of wear on this front does not render the tool obsolete.

For different materials we present in figure 4 different values of the wear VB (Verschleissmarken-breite = the width of the wear), according to the values of the chipping speed.



As it can be noticed from this figure, at chipping speeds smaller than the usual ones, especially in the case of metallic carbides, mineral-metallic materials and fast steel, the wear of the tool is larger.

Consequently, the use of high and very high speeds has as an effect a significant increase of the productivity, requires the choosing of the metallic carbides and mineral-ceramic materials.

3. Conclusions

From those showed above, we can conclude, that from the point of view of the strength, wear and thermal stability, we recommend the choosing of the cutting edges made from metallic carbides or mineral-ceramic materials.

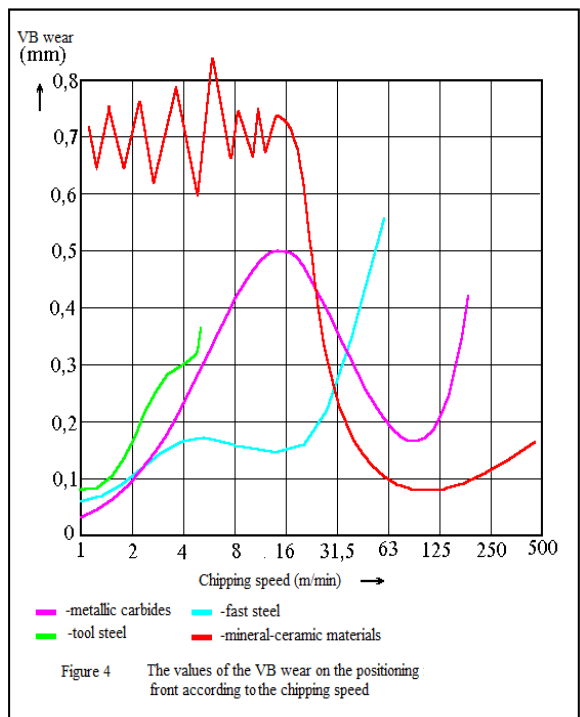


| Table 1 The variation of the wear according to the applied chipping regimes | | | | | | |
|--|-------|-------|-------|-------|-------|-------|
| | P01 | 0,12 | 0,05 | | | |
| P10 | | 0,18 | 0,08 | 0,05 | | |
| P20 | | 0,29 | 0,21 | 0,13 | 0,05 | |
| P40 | | 0,37 | 0,28 | 0,20 | 0,13 | 0,05 |
| P50 | | | | | 0,09 | 0,05 |
| [s [mm/U]] | 0,15 | 0,30 | 0,45 | 0,90 | 1,3 | 2,0 |
| [v [m/min]] | 300 | 150 | 100 | 50 | 35 | 22,5 |
| [t [min]] | 2,5 | 2,5 | 2,5 | 2,5 | 2,5 | 2,5 |
| [V [cm ³ /min]] | 112,5 | 112,5 | 112,5 | 112,5 | 112,5 | 112,5 |

The time it takes to reach the wear: 10 minutes

■ - materials with increasing wear resistance
 ■ - materials with increased tenacity

References

1. Hoyashita, S. - *Calculation Method of Cutting-Edge Profile of Shaving Cutter for Finishing Gear With Arbitrary Tooth Profile.* Nippon Kikai Gakkai Ronbunshu, C Hen/ Transactions of the Japan Society of Mechanical Engineering", Part C, vol. 61, nr. 584, Apr 1995, p 1677 - 1684.
2. Kim, S.- *Material Properties of Ceramic Cutting Tools.* "Key Eng. Mater. 96", p 33 - 80, 1994.
3. Kopac, J., Dolonsek, S. - *Advantages of Experimental Research Over Theoretical Models in the Field of Metal Cutting.* "Experimental Techniques", vol. 20, nr. 3, May-Jun 1996, p 24-28.
4. Oproescu, Gh., Simionescu, C.S. - *Aschiera neconventională.* "Buletinul Asociatiei române de prelucrări neconventionale", Galati, 1994, p 265 -269.
5. Repenning, D.- *Hardmaterial Coatings for Plastic-Working Tools-Against Abrasive Wear and Corrosion,* "Technische Rundschau", 83, (20), p 54-55, 1991.

Investigation of Natural User Interfaces and their application in gesture-driven human-computer interaction

Bekim Fetaji¹

South East European University,
Contemporary Sciences and Technologies, Computer
Science
Ilindenska bb, 1200 Tetovo, Republic of Macedonia
b.fetaji@seeu.edu.mk

Majlinda Fetaji² Aleksandar Petrovski² Mirlinda Ebibi²

South East European University,
Contemporary Sciences and Technologies, Computer
Science
Ilindenska bb, 1200 Tetovo, Republic of Macedonia
m.fetaji@seeu.edu.mk, ap102578@seeu.edu.mk,
m.ebibi@ibu.edu.mk

Abstract - The research study tries to contribute with the programmed several new gesture driven natural interface recognition gestures. The study as outcome developed a software application and analyzed a set of tools supporting the spectrum of software engineering natural user interfaces to be used in University promotion and marketing. This research study tries to foster several contributions. Firstly, this system is built on basis of separate library used for the gesture recognition part of the application, which can also work separately from the system and can be used in different contexts. It is very extendable and allows the users to implement new gestures on top of the library, thus enriching its context and provides easy start for the user allowing him to concentrate to the business logic instead of the low level programming of the gesture recognition algorithms. Secondly, in addition to the basic gestures, created are several other gestures that add additional value to the library itself. New gestures that are added to the library are DownSwipe, UpSwipe, ClockwiseCircle, CounterClockwiseCircle, Push gestures, ManualDoorOpen gesture, AutomaticDoorOpen gesture and WalkingGesture. Thirdly, this research also contributes to researchers and professionals who are dedicated to a research in the area of natural user interfaces and their efforts in finding an effective algorithm for human gesture recognition. This research investigates different approached to gesture recognition, such as Record and recognize approach, Neural Networks approach and Gesture composition approach, presented which are their advantages and weaknesses and presented why chosen is the Gesture Composition approach.

Keywords— *Natural User Interfaces, gesture-driven human-computer interaction, conceptual development of natural user interfaces*

I. INTRODUCTION

The research study investigates the effectiveness and efficiency of the several gesture recognition approaches.

Natural user interfaces as discussed in [5] are continually becoming important part of the contemporary human-computer interaction. They are introduced in almost every new device [2] easing the interaction between the user and the device itself. According to [6] from touch-sensitive displays to 3D cameras and infrared

sensors, natural user interfaces make the electronic devices usage much easier, faster and more intuitive. Some of the natural user interfaces require minimal contact between the human and the device [2].

The most advanced interfaces don't require any contact and they combine different kinds of cameras and sensors to use the human body as an input source [1].

II. BACKGROUND RESEARCH

Since the beginning of the computer era, many computer engineers were searching for a solution to improve and ease the way people interact with the computer systems [1]. Good user interface will improve user experience with the computer and other mobile devices [3] and will make the interaction as discussed in [12] easier, accessible and more optimal.

One of the most important devices [5] that take the NUI usage on the next level is the appearance of the Microsoft Kinect for Xbox and Microsoft Kinect for Windows [8]. This device allows the player to control the system using his/her body movements. The user doesn't have any direct interaction with the system, but his body is captured and gestures are recognized using one RGB and one Infrared camera. Kinect quickly became interesting device for the programmers worldwide. Many people have found a lot of interesting applications of Kinect in the real world environments.

The concept of Natural User Interface (or NUI) is firstly introduced by Steve Mann [8]. Steven Mann is a researcher and inventor best known for his work on computational photography, particularly wearable computing and high dynamic range imaging. According to [10] Mann holds degrees from the Massachusetts Institute of Technology (PhD in Media Arts and Sciences '97) and McMaster University, where he was also inducted into the McMaster University Alumni Hall of Fame, Alumni Gallery, 2004, in recognition of his career as an inventor and teacher. In the period of 1970s – 1990s he developed many different devices which were meant to replace the standard command line interface and graphical user interface. For his projects he had used several terms,

including ‘Natural User Interfaces’, ‘Direct User Interfaces’ and ‘Metaphor-Free Computing’ [7].

According to [8] August de los Reyes, Director for Surface Computing in Microsoft firstly mentioned the Natural User Interface as the next phase in the user interface evolution. Although natural user interfaces can’t replace graphical user interfaces, since most of the NUIs use graphical user interface to show the result, natural user interface tries to replace the WIMP (window, icon, menu and pointing device) principal. Later, on several conferences, representatives from Microsoft talked about the importance of the natural user interfaces and their efforts in providing best experience to the users using NUI features. According to [6] gesture recognition system is natural user interface which tries to follow the body movement and produce input out of this information. According to [11] there are two kinds of gesture recognitions systems: systems which require physical contact with the body and systems which can follow the body without physical contact.

In 2012 Microsoft released a new Kinect device meant to work only with personal computers. Unlike the older version which was originally published for Xbox 360, the new version had better resolution of the RGB camera and the depth infrared sensor.

Together with the new Kinect for Windows device, Microsoft released a new version of the software development kit. The new version of the SDK included improved skeleton recognition in different positions, better stabilization algorithm and additional tools for easier development of Kinect enabled applications.

According to [7] Kinect device is composed of several parts. Main parts of the device are the RGB camera and the infrared sensor.

The RGB camera is retrieving RGB video of the objects in front of the device. It supports resolution up to 1280x960 at 30 FPS. The resolution that will be used is programmable using the software development kit.

Next to the RGB camera is located the infrared sensor [7]. The infrared sensor is consisted of infrared transmitter and infrared receiver. When the infrared wave is transmitted, it is reflected from the objects in the front, and it is returned to the receiver. The time that the wave needed to return to the sensor can determine the distance between the object and the Kinect device [7].

Each Kinect device also has 4 microphones located on different places on the device, 3 in the front and 1 in the back of the device.

Using the 4 microphones, Kinect supports advanced audio features, such as beam formation to detect the audio source, noise suppression and echo cancelation and easy integration with Microsoft’s speech recognition platform.

Kinect also has a motorized tilt, which together with the gyroscope is responsible for vertical angle position of the Kinect sensor.

III. RESEARCH METHODOLOGY

The research study is fundamental research focusing on exploratory research and then action research developing a software solution to implement the insights gained from the fundamental research. The research investigation is focused on the Kinect sensor, programming new gesture recognitions and their features. The Kinect sensor allows users to interact with the system without any physical contact with it. The user stays in front of the sensor (2-4 meters away). The Kinect uses its RGB and Infrared cameras to capture the user position in the space. This information can be retrieved easily from the sensor, but what is missing in the Kinect software is the gesture recognition part.

The research study investigates the effectiveness and efficiency of the several gesture recognition approaches. The primary focus of research is the test for accuracy, speed and correctness of the different algorithms. The final system is implemented in Microsoft .NET technologies. Researched is how the gesture recognition system can be implemented in the .NET framework and be reused in many different projects. Participants were students, teaching and administrative staff of the Contemporary Sciences and Technologies Faculty of the South East European University.

IV. GESTURE RECOGNITION APPROACHES

Gestures and gesture recognition systems are main power driver for the Kinect device and Kinect enabled applications. Kinect for Windows SDK provides full skeleton information about the people in front of the device including location information about each joint on the skeleton, but the real power and value of the Kinect is fulfilled using the gestures and gesture recognition systems.

Since its beginning and first appearance on the market, Kinect became main topic of research of many computer professionals and enthusiasts all around the world [7]. Many of them researched how it can recognize a gesture and do specific action for each gesture. Few different approaches were discovered, each of them with several advantages and disadvantages.

A. Record and Recognize Approach

According to [6] one of the very first approaches to gesture recognition systems was the ‘record and recognize’ approach. With this approach each gesture is recorded once and is memorized by the underlying application. After the gesture is memorized as a valid gesture, then it can be used to recognize other movements and perform an action if the specified gesture is recognized.

The advantage of this algorithm is that it can be easily implemented [4]. The complete procedure consists of two phases. One phase is to follow the gesture, convert it to computer-understandable information and save the gesture in the memory or the database. The second phase is to record the algorithm, convert it to computer-understandable information using the same algorithm as in the first phase and search for that information in the

data store. If the algorithm is recognized, perform the desired action.

This approach has several disadvantages when applied to a real application. First, this approach has no fault tolerance. Even very small distortions will prevent the algorithm from recognizing the gesture. Several error and distortion correction algorithms can be applied to this approach to minimize or reduce the error, but since the data is very sensitive and not deterministic, it will still contain different data and the algorithm will fail.

Second problem with the approach is that when one gesture is recorded and saved in the data store, it would hardly be possible to use the same gesture model for different person. People have different body structure, size and natural movements and the gestures that are naturally performed by one person, are not same for another person.

B. Neural Networks Approach

According to [9] Neural networks approach was also used as one of the first algorithms for gesture recognition. Neural networks are used for different pattern recognition algorithms, including optical character recognition and are proven to be reliable and intelligent approaches to different real world problems.

Neural networks approach for gesture recognition is reliable and proven mechanism. Its advantage is that after sufficient training with different data sets it can recognize simple gestures. However, although this approach is good for academic and research environments, it's not very useful in a production, application environments, when the training time should be avoided.

Main disadvantage of the neural networks approach is that they require big input, training dataset [4]. The dataset should contain different gestures from big number of people, with different body structure, different size and different cultures because they have different natural movements. This is hardly achievable, and besides research environments it is hardly usable and effective in application environments.

Another disadvantage is the initial effort time for creating the neural network. The developer will need a lot of time to research and conclude which type of network and network structure is more suitable for the gestures that are needed to be recognized by the system.

C. Gesture Composition Approach

According to [6] gesture composition approach was introduced in its initial version by a group of employees at Microsoft Corporation in United Kingdom. Right after the appearance of the Kinect for Windows Software Development Kit, they had made internal research about what is missing as part of the development kit. They found out that in order to make a Kinect enabled application, one of the main parts of the system should be gesture recognition system. They provided a simple gesture recognition approach which was based on creating a composition or a model of the gesture upon which the application is able to recognize the gesture.

Gesture Composition Approach is a complete and reliable approach that is proven to work with different people in the same way. We tested this approach on 50 different employees in our company. We found out that each of them would require 5-10 minutes in order to learn and practice the gestures that we have made in our system. After the learning time, each user was able to efficiently use our application and play our games.

During our analysis we found out that the gesture is made of parts. Each gesture could be effectively divided in different parts. Each part presents a position in which specific body parts or joints are located in the space and relative to the other body parts which are relevant for the gesture. When these parts of the gesture are executed in a specific order in a specific time frame, we can say that the gesture is performed.

V. DEVELOPMENT OF NEW GESTURE RECOGNITIONS

Gesture Recognition Library is developed in .NET Framework, which is the framework on which Kinect for Windows SDK works and on which most Kinect enabled applications are developed. In its base it uses the libraries and APIs from the Kinect for Windows SDK in order to communicate with the Kinect, send commands to the device and get the input streams for the RGB and depth sensing cameras [9].

Skeletal recognition function enables the Kinect to recognize the human body (skeleton) in front of the device and track its movements. Kinect recognizes the skeleton and provides the position of the skeleton together with the body joints to the programmer. There are several body joints provided by default: AnkleLeft, AnkleRight, ElbowLeft, ElbowRight, FootLeft, FootRight, HandLeft, HandRight, Head, HipCenter, HipLeft, HipRight, KneeLeft, KneeRight, ShoulderLeft, ShoulderCenter, ShoulderRight, Spine, WristLeft, WristRight [10]. For each joint its position in meaning of x, y and z coordinates in the space is provided [12].

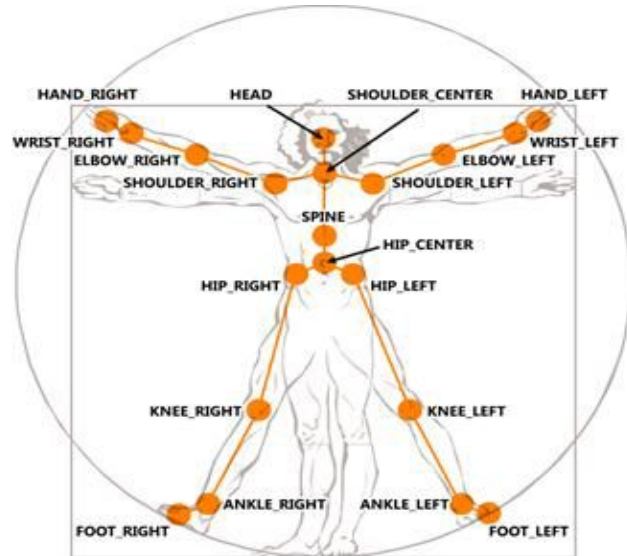


Figure 1. Body Joints that are recognized by the Kinect SDK Framework

Within the research study developed are several gestures that were needed for experimenting and for the development of the University Exploration System.

All these gestures are included in the library and are presented in the following parts. However, its design is very extensible and anyone with no huge effort can develop additional gestures that can be added to the library and very easily integrated.

The library is consisted of several main classes, such as KinectManager and GestureManager which are the main components of the library. Apart from that, there is class for each part of a gesture that is defined in the library.

The current implementation within the research study of the GestureType contains 13 gestures which are already implemented in the library: WaveRight, WaveLeft, DownSwipe, UpSwipe, ClockwiseCircle, CounterClockwiseCircle, PushLeft, PushRight, ShortLeftSwipe, ShortRightSwipe, ManualDoorOpen, AutomaticDoorOpen and Walking.

VI. CONCEPTUAL DESIGN OF THE UNIVERSITY EXPLORATION SYSTEM

One of the applications developed on top of the gesture recognition library is the university exploration system. This application is targeted to the new students and all the people who are interested in the university structure, study programs on different faculties and all additional information about the university itself. Using natural user interfaces as primary input source, this application provides extraordinary user experience, especially for the future students. Providing natural user interface as a first contact between the student and the university, it's promoting the university in the best way to the future students and introduce them to the advanced topics of the information technology.



Figure 2. GUI of the University Exploration system

The University Exploration and Presentation System is implemented in .NET framework version 4.5 and works in the same runtime environment together with the gesture recognition system. It utilizes all the features that the gesture recognition library provides and is complete example of the usage of the library.



Figure 3. Faculty Exploration System

The application is implemented as a Windows Presentation Foundation (WPF) application. The main application object is the MainWindow which implements the IPageSwitcher interface. There is one Switcher static class which is responsible for switching the content of the main application window. The idea behind this approach is to have one MainWindow which can display any WPF user control in its content. In this way there will be single window application which can just switch between different components and only show the currently active component. Every component, such as menu component, panorama component and HTML view component is implemented as separate WPF user control.

Complete configurability of the application allows extensibility and easy maintenance of the application during its lifecycle. The backend user is allowed to change the structure, content, texts and image resources at any time, and with one quick restart of the application complete new system state could be achieved.

Modularity and configurability of the application allow the application to be distributed to different locations and configured remotely from centralized system. The university is able to set different points on different locations that will perform individually and at the same time the administrator is able to control and configure the content and the behavior of the application.

A. Implementation of Menu Component

Menu component is one of the main components and the entry point of the application. Upon starting with the usage of the application, the user is able to select from one of the three official languages of the university as a main language and to continue to use the application with the selected language.

This component provides easy and intuitive navigation through the menu using swiping gestures with the hands and selection of the menu items with performing push gesture with the right hand or performing a walking gesture. Every menu item is configurable and different image can be assigned per item. The action is also configurable and based on the configuration it can open another menu, open a HTML view component or can start different component, such as panorama view component.

The configuration of the component is done using XML files stored in the same directory with the application executable. This allows the application to be easily configurable and extendable with new content and resources. The XML file contains configuration for the current menu and can also contain link to different XML file which defines another menu which is specified using the action attribute of the item configuration.

Location of the main menu or entry menu configuration for the application is specified in the applications app.config file, which is XML configuration file intended for a .NET application. When the application is started, it looks for the location of the entry point configuration, loads the configuration and renders the menu (shown in figure 6.1). One simple menu configuration is shown below.



Figure 4. Menu component

B. Implementation of the Web View

Web View component presents any HTML content to the user, which is able to navigate in the content using hand swipe gestures. This component is very useful for presenting rich content to the user, including text resources, images, animations and any other objects which can be displayed using Hypertext Markup Language.

The user is able to navigate or scroll through the content of the HTML view using the hand swipe gestures. The advantage of this component is that the content is configurable and it can be stored locally or if the client has internet access it can be stored on any place on the web. This allows real time content update and centralized content location for all distributed clients. In the background, this application uses Internet Explorer engine for rendering the HTML content, so it is able to show any content that is compatible with Microsoft Internet Explorer web browser.

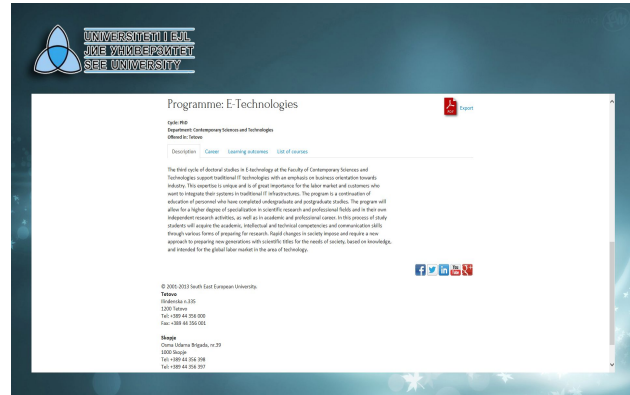


Figure 5. Web View Component Implementation

HTML view component is widely used in the University Exploration and Presentation application for showing different type of content. Study programs, text resources and additional information for different topics are all shown using the HTML view component. It allows easy and consistent rendering of the information equally to all the clients. Additionally, the feature for showing HTML content from a web page allows some part of the information to be directly get from the university website (www.seeu.edu.mk), in that way providing easy update of the application and keeping the content consistent between the website presentation and application presentation of the university.

C. Panorama View Component

The third component of the base application components is the panorama view component, which shows panoramic images to the user in interactive way. The user is able to move the image to the left or right using hand gestures and move the panoramic view to the left or right, thus allowing the user to explore the space in 360 degrees view.



Figure 6. Panorama View Component Implementation

This component allows the user to see the objects nearby his current location and get more information about each object in the current view. Easier navigation is achieved using the hand gestures which allow moving from one object to another one.

VII. RESULTS

After the completion of the system, different kinds of tests were performed in order to ensure the system performance, functionality and stability.

Usability testing that was performed on the system ensured that the system is usable and responds to the user behavior as expected during the design phase. Testing of the system was performed by people from different age ranges with different habits in order to test the system for its stability and acceptability.

The results from the testing show that the users learn the gestures very fast and they start to effectively use the system in a very short amount of time.

TABLE I. Time needed for people from different age to start to effectively use the system

| Age Range | Up to 2 minutes | 2-7 minutes | 7+ minutes |
|-----------|-----------------|-------------|------------|
| < 15 | 40% | 52% | 8% |
| 15-20 | 77% | 19% | 4% |
| 20-25 | 68% | 23% | 9% |
| 25-30 | 63% | 24% | 13% |
| 30-35 | 45% | 39% | 16% |
| 35-40 | 22% | 40% | 38% |
| > 40 | 14% | 34% | 52% |

From the table above we can see that 78% of the people from before-university grade will start to effectively use the application features in less than 2 minutes. Also, most of the people in the age range of 15-30 years will master the system in less than 2 minutes.

From all the people younger than 30 years which tested the system, more than 90% of them learnt how to use it in less than 7 minutes, while more than 50% of all the tested people achieve the same goal in less than 7 minutes.

WaveLeft and WaveRight gestures also have high percentage of recognition, about 90%. They are natural to the user but are composed of more gestures and are more complex for the system. At the bottom of the list are ClockwiseCircle and CounterClockwiseCircle which are the most complex gestures. They are consisted of 4 different positions which should be performed in a specific order. These movements are not so natural to the user, they are not present in the everyday movements and they are not so easily performed by the person.

This concludes that the gestures which are composed of smaller number of states are much easier for performing. The gestures should also be natural to the user and intuitive enough so the person doesn't need much time for learning the gesture. Before composing a new gesture, user behavior should be monitored and taken in mind, the gesture should be designed with as little states as possible and it should be natural to the performer.

VIII. CONCLUSION

This research tries to make several contributions in the development and application of Natural User Interfaces and university promotion and presentation providing a new approach.

First, it presents different approach for presenting the university and any of its internal institutions to the outside people and future students. Besides the traditional brochure and TV/radio marketing campaigns, with this system the university is able to present itself to the public in different, remarkable and distributed way throughout the whole university year, with little or no costs at all. The highly interactive way of communication between the user and the system will leave high impression and great mark at the user experience.

Second, this system is built on basis of separate library used for the gesture recognition part of the application, which can also work separately from the system and can be used in different contexts. Since this application thesis will remain in the university library, it can be basis for any other future research papers and systems that utilize the Kinect device for gesture recognition systems. It is very extendable and allows the users to implement new gestures on top of the library, thus enriching its context and provides easy start for the user allowing him to concentrate to the business logic instead of the low level programming of the gesture recognition algorithms.

In addition to the basic gestures provided by the employees at Microsoft department in United Kingdom, I created several other gestures that add additional value to the library itself. New gestures that I added to the library are DownSwipe, UpSwipe, ClockwiseCircle, CounterClockwiseCircle, Push gestures, ManualDoorOpen gesture, AutomaticDoorOpen gesture and WalkingGesture. After additional testing and small code improvements, I plan to send the new gesture library to Microsoft team working on the Kinect SDK and also to publish it online as an open source contribution to the community of programmers who are working on natural user interfaces improvements..

For the future work intended is to add more common functionality, such as course based real time chat, messaging, file sharing, library and wiki panel. Also will try to introduce new gestures and implement new components.

The future research will focus on head-driven gestures, i.e. gestures which are performed only with movements of the head. One of the main challenges is also configuration of the gestures using XML files instead of the programmatic approach which will also improve the extensibility of the application and new gestures could be added without modifying the application code.

REFERENCES

- [1] Brin, Sergey (2012) Project Glass Demo at Google I/O – Google I/O conference
- [2] De los Reyes, August (2008) Predicting the Past – Conference Presentation

- [3] Fetaji Majlinda., and Fetaji, Bekim., "Universities go mobile: Case study experiment in using mobile devices" – ITI IEEE conference, Dubrovnik, Croatia, 2008
- [4] George R. and Joshua B. (2010) Objects, Containers, Gestures, and Manipulations: Universal Foundational Metaphors of Natural User Interfaces
- [5] Jetter H., Gerken J. and Reiterer H. (2010) Natural User Interfaces: Why We Need Better Model-Worlds, Not Better Gestures – University of Konstanz
- [6] Kavanagh, Sam (2013) Facilitating Natural User Interfaces through Freehand Gesture Recognition – University of Auckland
- [7] Kean, S., Hall, J., Perry, P. (2011) Meet the Kinect: An Introduction to Programming Natural User Interfaces – Apress
- [8] Knies, Rob (2010) New, Natural User Interfaces – Microsoft Research Paper
- [9] Liu, Zhaochen (2013) Design a Natural User Interface for Gesture Recognition Application – University of California – Berkely, EECS Department, Technical Report No. UCB/EECS-2013-101
- [10] Moore, Christian (2006) New community Open – Natural User Interface Foundation Community Article
- [11] Widgor, D. and Wixon, D. (2011) Brave NUI World: Designing Natural User Interfaces for Touch and Gesture – Morgan Kaufmann
- [12] Xu, Wenkai and Lee, Eung-Joo (2013) A New NUI Method for Hand Tracking and Gesture recognition Based on User Experience - International Journal of Security and Its Applications, Vol. 7, No. 2, March, 2013

Integrated Development Environment for Remote Application Platform

Eclipse Rap –Review and Analysis

Omer Saleh

Department of Computer Science
Faculty of Education
Beniwalid, Libya
immer.jomah@gmail.com

Xavier Patrick Kishore

Department of Computer Science
Faculty of Education
Beniwalid, Libya
Patrick.kishore@gmail.com

P. Sagaya Aurelia

Department of Computer Science
Faculty of Education
Beniwalid, Libya
Sagaya.aurelia@gmail.com

Abstract - An integrated development environment (IDE) (also known as integrated design environment, integrated debugging environment or interactive development environment) is a software application that provides comprehensive facilities to computer programmers for software development. Eclipse is a community for individuals and organizations who wish to collaborate on open source software.

Eclipse Remote Application Platform (RAP 2.1.0M2) is a framework for modular business applications that can be accessed from different types of clients including web browsers, rich clients, and mobile devices. This paper reviews and analysis Eclipse RAP and its features.

Keywords-- IDE; Eclipse; RAP; RWT

I. INTRODUCTION

An integrated development environment (IDE) is a programming environment that has been packaged as an application program, typically consisting of a code editor, a compiler, a debugger, and a graphical user interface builder. The IDE may be a standalone application or may be included as part of one or more existing and compatible applications. Eclipse projects are focused on building an open development platform comprised of extensible frameworks, tools and runtimes for building, deploying and managing software across the lifecycle.

In general, the Eclipse provides four services 1) IT Infrastructure, 2) IP Management, 3) Development Process, and 4) Ecosystem Development. Eclipse Remote Application Platform (RAP) provides a powerful, multi-platform widget toolkit with SWT API that enables developers to write applications entirely in Java and re-use the same code on different platforms. The paper proceeds as follows in section 2, we will present about IDE. In Section 3, we will present Eclipse IDE.

Dr. M. Durai Raj

We follow in Section 4 with Eclipse RAP its architecture, life cycle phase, protocols how it works as a server and for embedded system. Finally suggestions along with conclusions are stated in section 5.

II. INTERGRATED DEVELOPMENT ENVIRONMENT

IDE is an integrated development environment, the handy, dandy piece of software that acts as text editor, debugger and compiler all in one sometimes-bloated but generally useful package [11]. Most common features, such as debugging, version control and data structure browsing, help a developer quickly execute actions without switching to other applications. Thus, IDE helps maximize productivity by providing similar user interfaces (UI) for related components and reduces the time taken to learn the language. An IDE supports single or multiple languages [12].

Selecting a good IDE is based on factors, such as language support, operating system (OS) needs and costs associated with using the IDE etc. Visual Studio, Delphi, JBuilder, FrontPage and DreamWeaver are all examples of IDEs. There are so many features an IDE can contain that the following list contains only a selected few [9].

- A. *Code completion or code insight:* The ability of an IDE to know a language's keywords and function names is crucial. The IDE may use this knowledge to do such things as highlight typographic errors, suggest a list of available functions based on the appropriate situation, or offer a function's definition from the official documentation.
- B. *Resource management:* When creating applications, languages often rely on certain resources, like library or header files, to be at specific locations. IDEs should be able

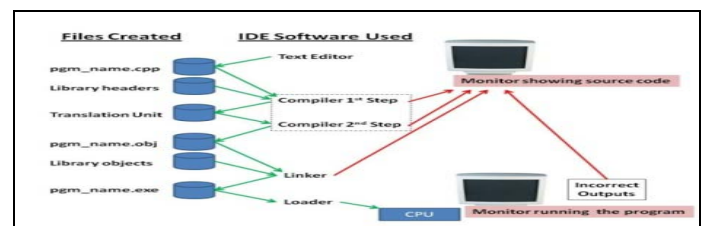


Fig 1: The role of IDE in development stage[19]

- C. to manage these resources. An IDE should be aware of any required resources so that errors can be spotted at the

development stage and not later, in the compile or build stage.

- D. *Access Databases*: To help connect Java applications to databases IDEs can access different databases and query data contained within them.
- E. *Optimization*: As Java applications become more complex, speed and efficiency become more important. Profilers built into the IDE can highlight areas where the Java code could be improved.
- F. *Project management*: This can be twofold. First, many IDEs have documentation tools that either automate the entry of developer comments, or may actually force developers to write comments in different areas. Second, simply by having a visual presentation of resources, it should be a lot easier to know how an application is laid out as opposed to traversing the file system for arcane files in the file system.

III. ECLIPSE –IDE

Eclipse is a universal platform for integrating development tools. Eclipse is the free and open-source editor upon which many development frameworks are based. The overview of Eclipse is shown in figure 2. Eclipse began as a Java development environment and has greatly expanded through a system of lightweight plugins. Eclipse is created by an Open Source community and is used in several different areas, e.g. as a development environment for Java or Android applications. The Eclipse Open Source community has over 200 Open Source projects covering different aspects of software development [10].

The Eclipse ++ can be extended with additional software components. Eclipse calls this software components *plug-ins*. Several Open Source projects and companies have extended the Eclipse IDE [18]. The extended overview of eclipse is shown in figure 2.

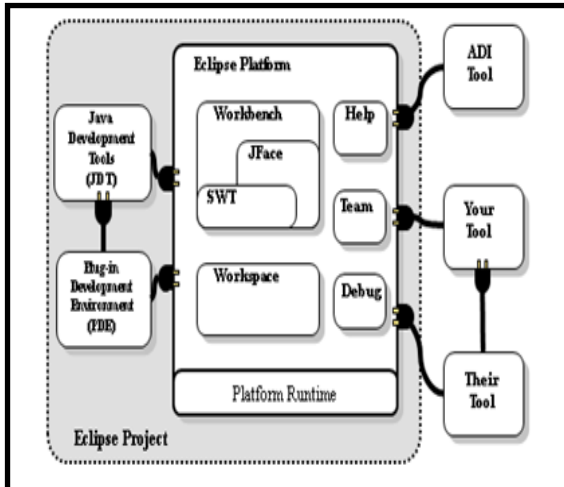


Fig. 2. Overview of eclipse [10]

IV. ECLIPSE BASED APPLICATIONS [20]

An Eclipse application consists of individual software components as shown in figure 3 and 4. The Eclipse IDE can be viewed as a special Eclipse application with the focus on supporting software development.

The components of the Eclipse IDE are primarily the following. Please note that the graph should display the concept, the displayed relationship is not 100 % accurate.

OSGi is a specification which describes a modular approach for Java application. Equinox is one implementation of OSGi and is used by the Eclipse platform. The Equinox runtime provides the necessary framework to run a modular Eclipse application.

SWT is the standard user interface component library used by Eclipse. JFace provides some convenient APIs on top of SWT. The workbench provides the framework for the application. The workbench is responsible for displaying all other UI components.

On top of these base components, the Eclipse IDE adds components which are important for an IDE application, for example the Java Development Tools (JDT) or version control support (EGit).

On top of these base components, the Eclipse IDE adds components which are important for an IDE application, for example the Java Development Tools (JDT) or version control support (EGit).

Eclipse 4 has a different programming model than Eclipse 3.x. Eclipse 4 provides the 3.x *Compatibility Layer* component which maps the 3.x API to the 4.0 API. This allows Eclipse 3.x based components to run unmodified on Eclipse 4.

Eclipse based applications which are not primarily used as software development tools are called Eclipse RCP applications. An Eclipse 4 RCP application typically uses the base components of the Eclipse platform and adds additional application specific components.

The programming model of OSGi (Equinox) allows you to define dynamic software components, i.e. OSGi services, which can also be part of an Eclipse based application.

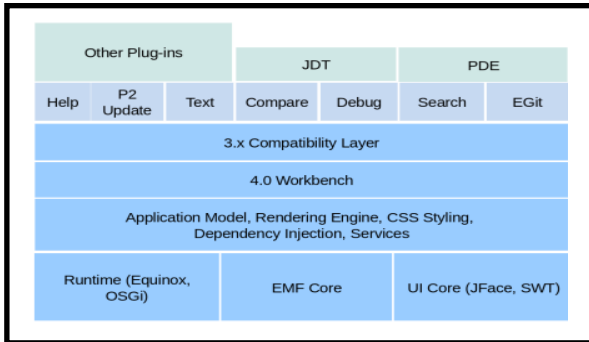


Fig. 3. Eclipse based application [20]

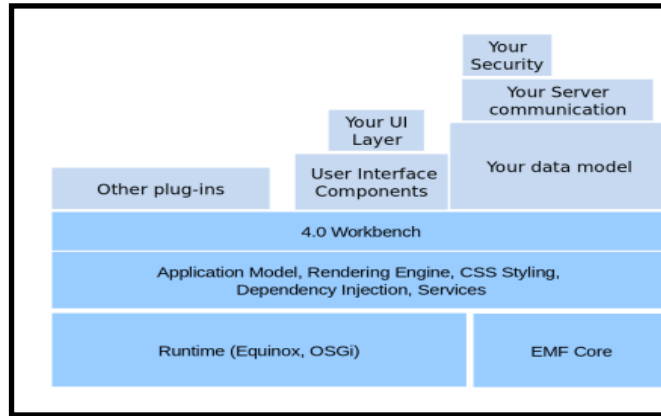


Fig. 4. Eclipse based application [20]

V. THE ECLIPSE PLATFORM PROVIDES A TOOL INTEGRATION FRAMEWORK [8]

The Eclipse Platform reduces the cost of tool integration by providing a large number of services, APIs, and frameworks that enable effective and scalable tool integration. Wherever possible, Eclipse uses open standards to limit tool vendor investment and reduce time to market. The Platform provides a focal point for integrating and configuring best-of-breed tools in a manner that best fits the end user's development process and Web application architecture. The Eclipse Workbench provides a central integration point for project control and an integration mechanism for resource-specific tools. The Eclipse Platform can also provide services common to different tools including user interface frameworks, managing relationships between components, component version management, and publishing services. Using Eclipse simplifies tool integration by allowing tools to integrate with the platform instead of each other. This significantly reduces the number of integration problems that must be solved, and provides a more consistent environment for the end user [8].

The eclipse IDE consists primarily of plug-ins built on the Eclipse base. A typical development system has more than

shown here. Building a non -IDE application on Eclipse is a matter of adding Application specific plug-ins as shown in figure 5. Developers ultimately gain a plug-in architecture and a common graphical interface.

VI. ECLIPSE RAP REMOTE APPLICATION PLATFORM

The Remote Application Platform (RAP) formerly Rich Ajax Platform is a framework for modular business applications that can be accessed from different types of clients including web browsers, rich clients, and mobile devices as shown in figure 6. It provides a powerful, multi-platform widget toolkit with SWT API that enables developers to write applications entirely in Java and re-use the same code on different platforms. It enables developers to build rich user interfaces using the Eclipse tools and common APIs [4].

Regardless of the client platform, RAP applications run on a server that communicates with its clients over HTTP.

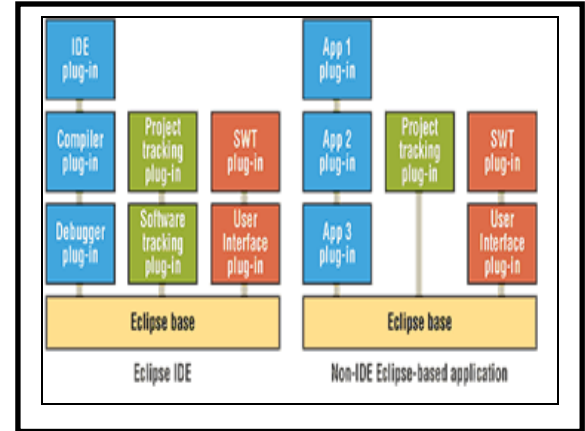


fig. 5 Plugin fo Eclipse IDE and Non IDE Eclipse based application.[1]

It can be considered a counterpart for web development to the Rich Client Platform (RCP). RAP encourages sharing source code between RCP and RAP applications as shown in figure 7 to reduce the development effort for business applications that need both desktop-based and web-based front ends.

VII. RAP ARCHITECTURE

RAP is to the web as RCP to the desktop. It inherits all the goodness from RCP such as workbench extension points model, event-driven SWT/JFace APIs, and componentized OSGi design. As indicated in figure 8 (a), the only difference between the architecture of RAP and that of RCP is the implementation of SWT/RWT. RWT is actually a bundle providing web-specific implementation of SWT's widgets based on the **qooxdoo** toolkit. In RAP, almost no SWT API is changed [15].

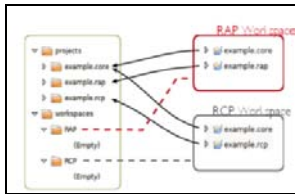


Fig. 6. RAP is a Multiuser

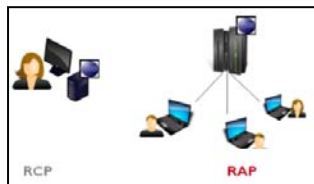


Fig. 7. Sharing Projects

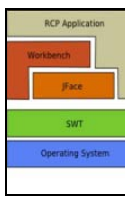


Fig.8 (a) RAP Architecture

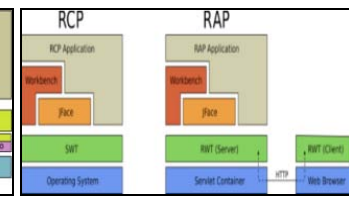


Fig. 8 (b) Architecture of RAP in Server Centric Framework

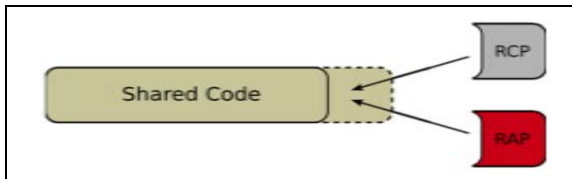


Fig. 9 a). Fragments

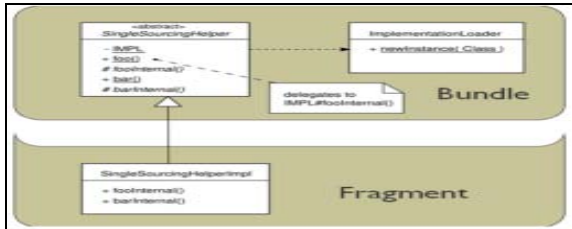


Fig. 9 b). Delegation

As indicated in figure 8(b), in a server-centric framework, the application is hosted on the application server and all processing is done on the server. The client browser is only used for data presentation. Consequently, it leaves small footprints on browsers: it waits for instructions from the server to create corresponding widgets on demand [15].

When the data has to be shared fragments are added to the shared codes. Fragments are a sort of patches as shown in figure

9a. The concepts of fragments are used both in RCP and RAP. Some of the fragment properties are fragment id, version, name, provider and the class path and the host plugin also has properties as plug-in ID, minimum and maximum version. Fig. 9b shows the delegation process where after the fragment process it is bundled together.

Like building a RCP application, building a RAP application is a process of building plug-ins and bundles: On the UI side, contributing widget plug-ins; On the server side, since it is powered by server-side Equinox, contributing servlet plug-ins. Unsurprisingly, it also inherits the benefits of any OSGi application such as dynamically adding/removing bundles[15]. As shown in the below figure eclipse rap works as server figure 10 and also for embedded system as shown in figure 11. It provides a complete target platform based on Equinox, including subsets of SWT, JFace, and Workbench APIs. With the RAP OSGi integration, they can be composed of modules and



Fig 10. Eclipse RAP as server



Fig. 11. Eclipse RAP for embedded system

using the OSGi service model. The core library can also be used in traditional web applications without OSGi [16].

Applications or components (coming in the form of bundles for deployment) can be remotely installed, started, stopped, updated, and uninstalled without requiring a reboot; management of Java packages/classes is specified in great detail. Application life cycle management (start, stop, install, etc.) is done via APIs that allow for remote downloading [14].

The default web client uses JavaScript to render the UI in the browser.

VIII. ECLIPSE RAP CONSIST OF [1]

1. Widget Toolkit

With RAP, you don't create UIs with HTML and browser technologies, but with the Java API of SWT, the widget toolkit used in Eclipse. The RAP Widget Toolkit (RWT) provides a

comprehensive set of powerful SWT widgets, also including layout managers and event listeners. RWT architecture is shown in figure 12.

1.1 The RWT Lifecycle Phases[5]

The phases are: as follows and shown in figure 13

- Prepare UI Root*: Responsible for invoking entry points.
- Read Data* :Reading request parameters and applying the contained status information to the corresponding widgets. As an example, if a user has entered some characters into a Text control, the characters are transmitted and applied to the text attribute of the Text instance.
- Process Action* : Events are processed which trigger user actions. As an example, when a Button has been pushed, the Selection Listeners attached to the Button are called.

Render: JavaScript code is generated for the response that applies the state changes to the client. Only those

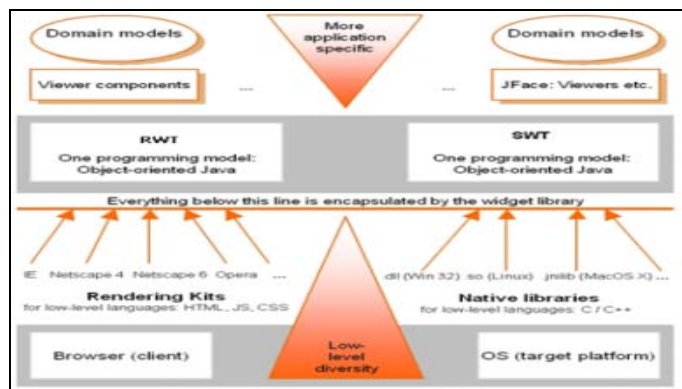


Fig . 12. RWT Architecture[17]

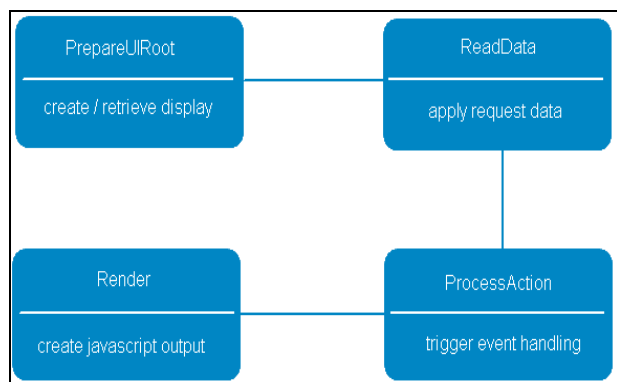


Fig. 13. RWT Life Cycle Phases

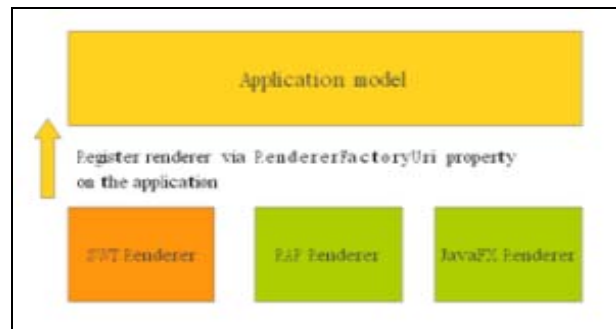


Fig. 14. Creating your own renderer[3]



Fig. 15. Renderers for different platform

widget attributes that were changed during the processing of the current request are being rendered. This results in a minimal amount of data that needs to be transferred to the client. The widget tree is not manipulated in this phase anymore.

User can create their own desired as shown in figure 14 and sample renderers for different platforms are shown in figure 15.

2. Cross Platform[2]

The default RAP Web client supports these browsers:

- Internet Explorer 7+
- Google Chrome 7+
- Firefox 3.5+
- Safari 4+
- Opera 10+
- iOS 5+
- Android 3 (Limited)

No browser plug-ins is required by the default client, only JavaScript needs to be enabled. However, custom widgets are free to build on any third-party API. Support on mobile browsers has some limitations. Other platforms can be supported by alternative RAP clients connecting to RAP's open protocol.

2.1 RAP Protocol [2]

The term RAP Protocol is used to describe the JSON-based message format used in the HTTP communication

between a RAP client and a RAP server. This protocol was introduced in RAP 1.5 to replace the plain JavaScript responses that have been used in previous releases. As of RAP 2.0, the entire communication between client and server uses this protocol. The idea of the RAP Protocol is to fully decouple RAP server and RAP client with the intention of making the client exchangeable. At this point of development, the most interesting use cases have been RAP clients for mobile devices (Android and iOS), written in the client's native language. As a consequence, all logic that is specific to the default RAP client has been moved from the server to the client.

The protocol does not only enable clients in other programming languages, it also opens the door to a new class of applications – applications that need to address a wide range of hardware from desktops to specialized devices (e.g. mobile data entry or point of sales solutions). Or applications that require integration with attached hardware devices. We think that this is a major new achievement for RAP warranting a major release – and a feature that sets RAP apart from other frameworks [6].

3. Integration

Making it possible to integrate RAP with other Java technologies is one of our main objectives. We're doing so by making RAP compatible with JEE and OSGi and by limiting dependencies to the necessary minimum. A partial list of compatible technologies:

- RAP applications can be deployed directly as OSGi bundles
- The JEE compatibility mode in RAP makes it possible to use clustering
- Equinox Security Integration ensures your data is safe at all times.

4. Single Sourcing

RAP allows to address different platforms with a shared code base. Applications can be developed for the desktop, the web browser, and even mobile clients without duplicating code. Due to RAP's high compatibility with the Eclipse UI technologies, a lot of existing code targeted at the desktop can be re-used for the user's web application with minimal changes.

Typical scenarios are:

- Porting an existing SWT/RCP application to the web.
- Developing a new application that can run on the desktop and in the browser.
- Re-using existing libraries developed for previous applications.
- Utilize RCP-compatible open source libraries and frameworks. Open Source

Notable Additional Features[2]

- *Client Class and Client Services*

All features specific to the RAP client (which is exchangeable as of RAP 2.0) are handled by the client class and the client services. This includes support for browser history, JavaScript execution and retrieving the clients time zone offset.

- *HTTP File Upload*

Unlike SWT, RWT cannot simply access the user's file system and read data from it. As an alternative, the File Upload widget can be used. The widget looks like a button, but when clicked will open the file picker dialog of the user's browser. After a file has been selected, it can programmatically be send to any HTTP server.

- *Fixed Columns*

It is possible in RWT to exclude some columns from Tree or Table from scrolling.

- *Multi-User Environment*

RAP operates in a multi-user environment and provides some additional API that helps dealing with the consequences. Notable Limitations

Notable Limitations[2]

- Few Unimplemented Features
- Unimplemented Widgets such as StyledText, Tracker, TaskBar, Tray
- Painting Limitations Some methods are unimplemented, including copyArea, drawPath, setClipping, setTransform, setInterpolation, setLineDash and setXORMode
- Limitations in Dialogs: Dialog, ColorDialog, FontDialog, MessageBox
- Limitations of the Browser widget :Since the Browser widget is based on the HTML iframe element, there are some restrictions
- Limitations in Mouse and Key Events
- Limitations in Verify and Modify Events
- Limitations in Drag and Drop
- Limitations when using background threads

IX. CONCLUSION

But integrated tools require a platform of services, frameworks, and standards that allow vendors to focus on their value-add while reusing common infrastructure. The platform must include a workbench that provides a common view of the whole application across all resource types and the entire team. And the platform must be accessible to tool vendors under an acceptable license. Eclipse not only provides such a platform, but its architecture also provides flexibility in how tool vendors integrate their tools and at what level. This allows vendors to

match their integration investment with their product needs and market window.

For simple integration, use invocation integration to provide users navigation, access, editing, and management of file-based resources. Use data integration to share data between tools that are otherwise unconnected [8]. When data integration isn't enough, use API integration to provide secure access to encapsulated data. Eclipse RAP

Is not only useful for software industry but also for academic. It can be used to integrate all colleges and furthermore all universities to introduce a centralized education system.

REFERENCES

- [1] www.electronicdesign.com
- [2] www.eclipse.org/rap
- [3] http://www.eclipsecon.org/europe2012/sites/eclipsecon.org.europe2012/files/Eclipse4_RAP.pdf
- [4] [Http://developer.eclipsesource.com/technology/crossplatform/#rap](http://developer.eclipsesource.com/technology/crossplatform/#rap)
- [5] <http://download.eclipse.org/rt/rap/doc/2.0/guide/reference/api/org/eclipse/rap/rwt/lifecycle/ILifeCycle.html>
- [6] <http://eclipsesource.com/blogs/2012/11/26/rap-becomes-the-remote-application-platform/>
- [7] <http://eclipse.org/rap/developers-Guide/devguide.php?topic=scopes.html&version=2.0>
- [8] <http://www.eclipse.org/articles/Article-Levels-Of-Integration/levels-of-integration.html>
- [9] <http://salfarisi25.wordpress.com/2010/12/22/advantage-and-disadvantage-of-using-ide/>
- [10] www.eclipse.org/
- [11] <http://mashable.com/2010/10/06/ide-guide/>
- [12] http://en.wikipedia.org/wiki/Integrated_development_environment
- [13] <http://help.eclipse.org/juno/>
- [14] <http://en.wikipedia.org/wiki/OSGi>
- [15] <http://owenou.com/2010/07/08/introducing-eclipse-rap.html>
- [16] <http://dev.eclipse.org/mhonarc/lists/rt-pmc/pdfmFx7CiT7Ma.pdf>
- [17] <http://www.pjug.org/docs/RAP.pdf>
- [18] <http://en.wikipedia.org/wiki/Eclipse>
- [19] <http://cnx.org/content/m18920/latest/graphics1.jpg>
- [20] <http://www.vogella.com/articles/EclipseRCP/article.html>

3D numerical optimization of pollution emission by group of source

Fedosov V.V.

freelance researcher
Moscow, Russia
vlr.fds@gmail.com

Alina Fedossova

Departamento de Matemáticas
Universidad Nacional de Colombia
Bogotá, Colombia
afedossova@unal.edu.co

Abstract—We present a model with variable parameters of emission group of sources for 3D area. We construct a numerical solution of the optimization problem when unequal norms of pollution loads in the subareas. The simulation results are presented by using of MATLAB graphics and help for the analysis in the 3D area.

Keywords—3D region; emission sources; pollution standards; semi-infinite optimization; stochastic algorithms; nonlinear programming.

I. INTRODUCTION

This paper considers a minimization problem of conflict emissions sources (industry or individual units) with the rest of the general infrastructure 3D area where environmental standards of security must be fulfilled. If environmental infrastructure has a priority then to have limit emissions or enhance the filtering technology. The difficulty consists in finding the required vector of of emission limits when we have a group of sources with different coordinates, unequal powers, structure and different modes of emissions, as well as, 3D map objects (zones).

This class of problems corresponds to the stochastic semi-infinite optimization algorithms (SIP, Semi-Infinite Programming). SIP allows XYZ coordinate attachment of the points, which allows us to consider 3D formulation.

The results of numerical solution of the conflict was made for the 3D area. MATLAB was used and the numerical solution was illustrated with maps of the environment pollution.

II. PROBLEM DEFINITION

In 3D area we have: the reformed group, permanent sources of emissions group, as well as, a group of treatment of contamination. Composition of emissions, including K components, which are used for dissimilar sets of different sources and devices.

The problem consists in finding of the necessary adjustment capacity vector sources for which the function of the overall pollution based on the work of the fence devices contaminants does not violate pollution standards defined at all points.

Spreads (fences) pollution point sources were described with the parabolic type functions.

The model parameters are size, capacity, location, components sets and the variation coefficient:

- * / Location and subareas configuration (3D matrix);
- * / Reformed emission sources (RS, H, tN, kod1, a1);
- * / Unreformed emission sources (NRS, NH, tNN, kod2, a2);
- * / Intake section (E, F, tE, kod3, a3).

For any point s of declared area we have restrictions:

$$\begin{aligned} g(s) = & \sum_{j=1}^{RS} \sum_{k=1}^K \text{kod1}(k, j) \left(-a1(k)r(s, j)^2 \right. \\ & + (1 - x(j))H(j) \Big) \\ & + \sum_{j=1}^{NRS} \sum_{k=1}^K \text{kod2}(k, j) (-a2(k)r(s, j)^2 \\ & + NH(j)) \\ & - \sum_{j=1}^E \sum_{k=1}^K \text{kod3}(k, j) (-a3(k)r(s, j)^2 \\ & + F(j)) - \text{Norm}(\omega(s)) \leq 0 \quad (1) \end{aligned}$$

where: $x(j)$ - reform coefficient of power source j , $r(s, j)$ - the distance from the source s to the j (unit), k - component number, $\omega(s)$ – subarea number, $\text{Norm}(\omega(s))$ – pollution norm for point s of subarea (s) .

Solution algorithm provides:

1. Stochastic search for common areas where the constraint (1) does not fulfill.

2. Maximize of function (1) to detect the coordinates of local maxima.

3. Formation of the parameters (local maxima) like matrix coefficient matrix and restrictions.

4. Solve the nonlinear programming problems.

The objective function $f(x)$ (2) is aimed to reduce the valuation of integrated emission sources by solving the problem ($0 \leq x(j) \leq 1$). Integrated emissions were calculated by summing the volumes of spheres component spread contamination sources (2).

$$\min \left\{ f(x) = \frac{4}{3} \pi \left[\sum_{j=1}^{RS} \sum_{k=1}^K k \text{od1}(k,j) m_p(j) \left(\frac{H(j)}{a(k)} \right)^{3/2} - \sum_{j=1}^{RS} \sum_{k=1}^K k \text{od1}(k,j) m_p(j) \left(\frac{(1-x(j))H(j)}{a(k)} \right)^{3/2} \right] \right\} \quad (2)$$

where: $m_p(j)$ - the unit cost of contingent losses from lowering integral power j .

III. NUMERICAL EXPERIMENTS AND GRAPHICS

After optimization emissions of sources 1, 6 found like incompatible, and 3, 9 fully correspond to the task. Power of other emission sources requires adjustments.

Modeling allows us quickly translate an array of input data to a comparative pollution graph before and after optimization. Pollution maps are available for viewing in all sections of the vertical and horizontal fields. There is an opportunity to examine in detail the cloud emissions, fences or dirt residues for some study area.

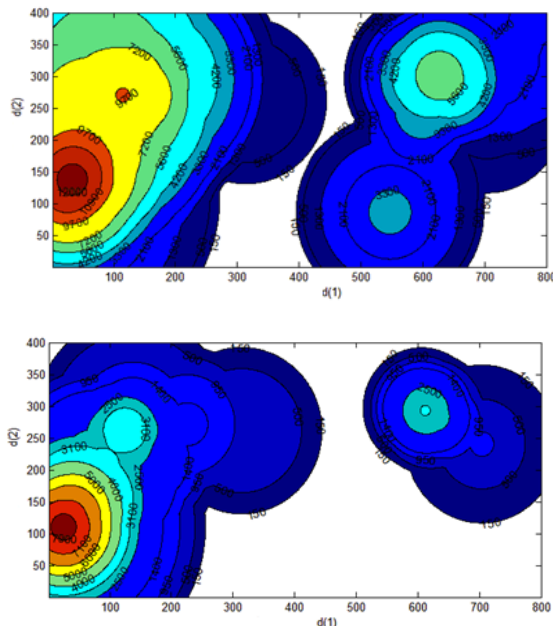


Fig. 1. Initial (a) and optimal (b) maps of the total pollution.

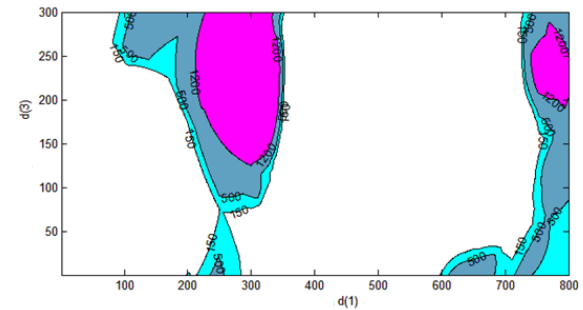
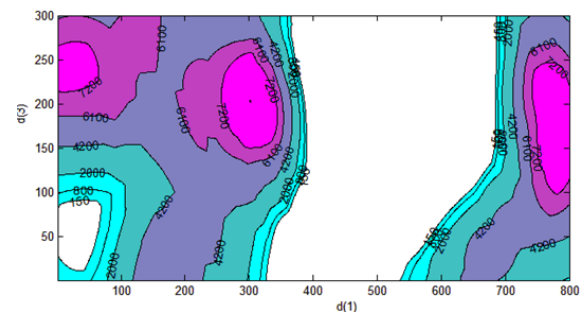


Fig. 2. Initial (a) and optimal (b) maps of total pollution in section $d(2) = 300$.

Detailed discussion of initial parameters and the optimization results in 3D area show their logical connection. Numerical results of the solution can be the basis for the calculation and analysis of many derivatives criteria.

IV. CONCLUSIONS

A numerical solution of the optimization problem of pollution in the area of simultaneous 3D group pollution emissions and fences, as well as unequal norms of pollution loads in the subareas.

Developed software package can be used for the estimation of anthropogenic situations in the design or development of the territories and the adjacent environment.

REFERENCES

- [1] S. K. Zavriev, N. N. Novikova and A. V. Fedossova, "Stochastic algorithm for solution of convex semi-infinite programming problem with equality and inequality constraints," Vestnik of Moscow University, Ser. 15, vol. 4, pp. 30-35, 2000.
- [2] V.V. Fedosov and A. Fedossova, "Semi-infinite limit emissions model enterprises in areas with mixed landscape", Herald of Computer and Information Technologies, vol. 8. pp.14-22, 2011.
- [3] I. Vaz and E. C. Ferreira, "Air pollution control with semi-infinite programming," Applied Mathematical Modeling, vol. 33, pp. 1957-1969, 2009.

Comparison between functional parameters of the four gear automatic gearbox and the seven gear automatic gearbox by a kinematic point of view

Veronica ARGEŞANU, Ion Silviu BOROZAN, Inocențiu MANIU, Raul Miklos KULCSAR, Mihaela JULA

Abstract— Kinematic analysis conducted with reverse motion method (Willis), for the automatic gearboxes with four and seven gears reveals both the evolution and state of the elements of these types of automatic gearboxes in operation. The dependency of the energy consumption and the value of the gearboxes final ratios it is also highlighted. Dynamic performances and fuel consumption of an automobile depend on the engine that is used on it and the performance of its transmission.

Keywords—automatic gearbox, fuel, kinematics, transmission, energy.

I. INTRODUCTION

THE acceleration, fuel consumption and reliability are important factors for the development and optimization of the gearboxes. In sporty vehicles the gearboxes are adapted to a dynamic driving style, which allows faster accelerations in each gear. It is known that the dynamic performance and the fuel consumption of an automobile are influenced by the engine and gearbox ratios.

The optimization of the gearbox is made based on a single criterion-acceleration or fuel consumption and this two criterions cannot be satisfied simultaneously.

It is well known that there are two criterions of calculating gear ratios.

Dynamic performances and fuel consumption of an automobile depend on the engine that is used on it. Also, a considerable effect on the vehicle performance is created by the gear ratios.

According to the construction and functioning of the gearbox, the main elements of a gearbox are the gears that form the transmission. The variation of the gear ratios from one gear to another one represents the gearing of the gearbox.

The gear ratios in the gearbox allow the automobile to meet the following criterions:

- drive in difficult condition (road with a very steep incline)
- reach the maximum speed
- to function in the minimum consumption domain of the internal combustion engine

II. KINEMATIC ANALYSIS OF THE 4 SPEED AUTOMATIC GEARBOX

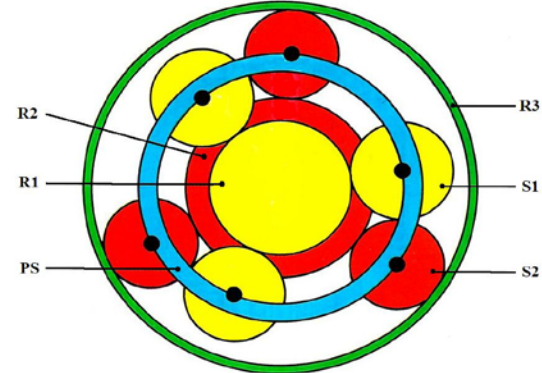


Figure 1. „Ravigneaux” planetary gear system

In figure 1 we can identify the following elements: two sun gears R_1 and R_2 , the R_3 crown gear, the carrier PS and two planet gears S_1 and S_2 .

The “Ravigneaux” type planetary system has 4 forward gear ratios, and one reverse gear ratio. The input elements are different type of combinations of two by two pairs of the elements R_1 , R_2 and PS, and the output element is the crown gear, R_3 with inner teeth [1; 2; 7; 8; 9; 10].

The main advantages of the „Ravigneaux” planetary gear system are:

- compact and space-saving, because the energy transfer is performed in parallel in many ways divided
- it can realize wide gear ratios
- high reliability, ensured by the good lubrication conditions

For the kinematic analysis of a automatic 4 gear transmission, we choose a Renault A R4 automatic transmission with 4 gear plus one reverse gear.

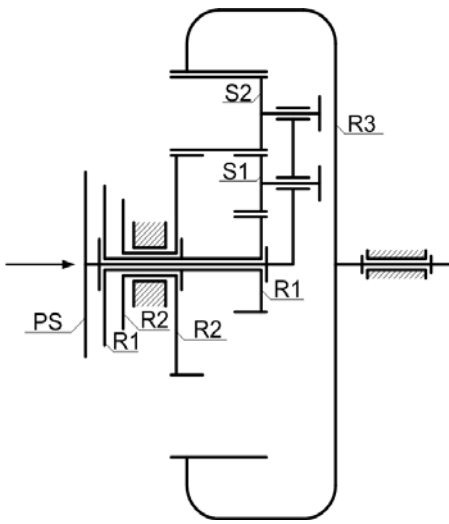


Figure 2. Kinematic scheme of a „Ravigneaux” planetary gear system

There are three known methods to determine the ratio of a planetary gear system :

-the reverse motion method (Willis method) and the transformation of the planetary transmission system into an ordinary transmission with fixed axis

-decomposition of composed movements into simple movements using the decomposition method (Swamp method);

-graphic-analytical method (method of instantaneous centers or method Kutzbach). The most utilized method is “the Willis method”

First gear: PS-fixed, R₁-input, R₂-output

Second gear: PS-free, R₁-input, R₂-fixed

Third gear: PS-free, R₁-input, R₂-input

Fourth gear: PS-input, R₁-free, R₂-fixed

The reverse gear: PS-fixed, R₁-free, R₂-input

For the following steps of the kinematic calculus it is used only the Willis method.

Next, we calculate the gear ratio on each gear, using the teeth numbers

First gear kinematic calculation:

The transmission ratio between R₁ gear and R₂ gear is the ratio between the angular speed $\overline{\omega_{R_1}}$ and $\overline{\omega_{R_2}}$

$$\frac{\overline{\omega_{R_1}}}{\overline{\omega_{R_2}}} = \left(+ \frac{z_{R_3}}{z_{S_2}} \right) \cdot \left(- \frac{z_{S_2}}{z_{S_1}} \right) \cdot \left(- \frac{z_{S_1}}{z_{R_1}} \right) = \frac{z_{R_3}}{z_{R_1}} = i_1 \quad (1)$$

For the second gear we will use “The Willis method” (inversion movement method)

Table 1. Willis Method table

| MOTION | R ₁ | R ₂ R ₂ (FIXED ELEMENT) | PS | R ₂ |
|-------------------------------|--|---|--------------------------|--|
| Real | $\overline{\omega_{R_1}}$ | 0 | $\overline{\omega_{PS}}$ | $\overline{\omega_{R_2}}$ |
| With ω_{PS} overlapped | $\overline{\omega_{R_1}} - \overline{\omega_{PS}}$ | $-\overline{\omega_{PS}}$ | 0 | $\overline{\omega_{R_2}} - \overline{\omega_{PS}}$ |

From the planetary cycloidal gear train the transfer is made into an ordinary gear train by immobilizing the carrier (equation 2):

$$\frac{\overline{\omega_{R_1}} - \overline{\omega_{PS}}}{-\overline{\omega_{PS}}} = \left(- \frac{z_{R_2}}{z_{S_2}} \right) \cdot \left(- \frac{z_{S_2}}{z_{S_1}} \right) \cdot \left(- \frac{z_{S_1}}{z_{R_1}} \right) = - \frac{z_{R_2}}{z_{R_1}} \quad (2)$$

$$\frac{\overline{\omega_{R_1}}}{-\overline{\omega_{PS}}} + 1 = - \frac{z_{R_2}}{z_{R_1}} \quad (3)$$

$$\frac{\overline{\omega_{R_1}}}{\overline{\omega_{PS}}} = 1 + \frac{z_{R_2}}{z_{R_1}} \quad (4)$$

Using “The Willis method”, we have the same calculation, but this time the input is on the R₃ gear

$$\frac{\overline{\omega_{R_3}} - \overline{\omega_{PS}}}{-\overline{\omega_{PS}}} = \left(- \frac{z_{R_2}}{z_{S_2}} \right) \cdot \left(+ \frac{z_{S_2}}{z_{R_3}} \right) = - \frac{z_{R_2}}{z_{R_3}} \quad (5)$$

$$\frac{\overline{\omega_{R_3}}}{\overline{\omega_{PS}}} - 1 = \frac{z_{R_2}}{z_{R_3}} \quad (6)$$

$$\frac{\overline{\omega_{R_3}}}{\overline{\omega_{PS}}} = 1 + \frac{z_{R_2}}{z_{R_3}} \quad (7)$$

Returning to the second gear transmission ratio we have:

$$i_1 = \frac{\overline{\omega_{R_1}}}{\overline{\omega_{R_3}}} = \frac{1 + \frac{z_{R_2}}{z_{R_1}}}{1 + \frac{z_{R_2}}{z_{R_3}}} = \frac{\frac{z_{R_1} + z_{R_2}}{z_{R_1}}}{\frac{z_{R_2} + z_{R_3}}{z_{R_3}}} = \frac{z_{R_1} + z_{R_2}}{z_{R_2} + z_{R_3}} \cdot \frac{z_{R_3}}{z_{R_1}} \quad (8)$$

Third gear calculation:

$$\frac{\overline{\omega_{R_1}}}{\overline{\omega_{R_3}}} = \frac{\overline{\omega_{R_1}}}{\overline{\omega_{R_3}}} ; \quad \frac{\overline{\omega_{R_1}}}{\overline{\omega_{R_3}}} = 1 = i_3 \quad (9)$$

Using “The Willis method”, but this time the input is element PS, the relation for the fourth gear is the following:

$$\frac{-\overline{\omega_{PS}}}{\overline{\omega_{R_3}} - \overline{\omega_{PS}}} = \left(+ \frac{z_{R_3}}{z_{S_2}} \right) \cdot \left(- \frac{z_{S_2}}{z_{R_2}} \right) = - \frac{z_{R_3}}{z_{R_2}} \quad (10)$$

$$\frac{\overline{\omega_{R_3}} - \overline{\omega_{PS}}}{-\overline{\omega_{PS}}} = - \frac{z_{R_2}}{z_{R_3}} \quad (11)$$

$$-\frac{\overline{\omega_{R_3}}}{\overline{\omega_{PS}}} = - \frac{z_{R_2}}{z_{R_3}} - 1 \quad (12)$$

$$\frac{\overline{\omega_{PS}}}{\overline{\omega_{R_3}}} = \frac{z_{R_3}}{z_{R_3} + z_{R_2}} = i_4 \quad (13)$$

The reverse gear calculation:

$$\frac{\omega_{R_3}}{\omega_{R_2}} = \left(+ \frac{z_{R_3}}{z_{S_2}} \right) \cdot \left(- \frac{z_{S_2}}{z_{R_2}} \right) = - \frac{z_{R_3}}{z_{R_2}} = i_R \quad (14)$$

By having the teeth number of all gears for the „Ravigneaux” system for the Renault AR4 automatic gear box we can easily verify the transmission ratios [14].

Given: $z_{R_1} = 21$, $z_{R_2} = 27$, $z_{R_3} = 57$, $z_{S_1} = 15$, $z_{S_2} = 14$

We have the next calculus relation for the transmission ratios:

$$i_1 = \frac{z_{R_3}}{z_{R_1}} = 2,71 \quad (15)$$

$$i_2 = \frac{z_{R_1} + z_{R_2}}{z_{R_2} + z_{R_3}} \cdot \frac{z_{R_3}}{z_{R_1}} = 1,55 \quad (16)$$

$$i_3 = \frac{\omega_{R_1} + \omega_{R_2}}{\omega_{R_3}} = 1 \quad (17)$$

$$i_4 = \frac{z_{R_3}}{z_{R_3} + z_{R_2}} = 0,68 \quad (18)$$

$$i_R = -\frac{z_{R_3}}{z_{R_2}} = -2,11 \quad (19)$$

Table 2. Gear speed and transmission ratios for four speed automatic gear box

| Gear | Transmission ratio | | State of motion of the input elements | | | |
|------------------|----------------------------------|---|---------------------------------------|----|----|---|
| | Relation | Value | R1 | R2 | PS | |
| Forward movement | 1 | $i_1 = \frac{z_{R_3}}{z_{R_1}}$ | 2,71 | 1 | - | 0 |
| | 2 | $i_2 = \frac{z_{R_1} + z_{R_2}}{z_{R_2} + z_{R_3}} \cdot \frac{z_{R_3}}{z_{R_1}}$ | 1,55 | 1 | 0 | - |
| | 3 | $i_3 = 1$ | 1 | 1 | 1 | - |
| | 4 | $i_4 = \frac{z_{R_3}}{z_{R_3} + z_{R_2}}$ | 0,68 | - | 0 | 1 |
| Reverse gear | $i_R = -\frac{z_{R_3}}{z_{R_2}}$ | -2,11 | - | 1 | 0 | |

Analyzing the upward table we can see that the automatic gearbox in four gears has one amplifier transmission ratio, which means that in the fourth gear it has a lower energetic consumption.

III. 7G TRONIC AUTOMATIC GEARBOX KINEMATIC ANALYSIS

As stated in the technical literature, the automatic gearbox 7G Tronic with 7 gears of forward movement and 2 reverse gears is divided in 3 planetary systems: the „Ravigneaux” type planetary system of gears and two simple planetary systems, named specifically to their positioning: Simple front

planetary system – SPSF and simple rear planetary system – SPSS (Figure 3) [2; 3; 10; 15].

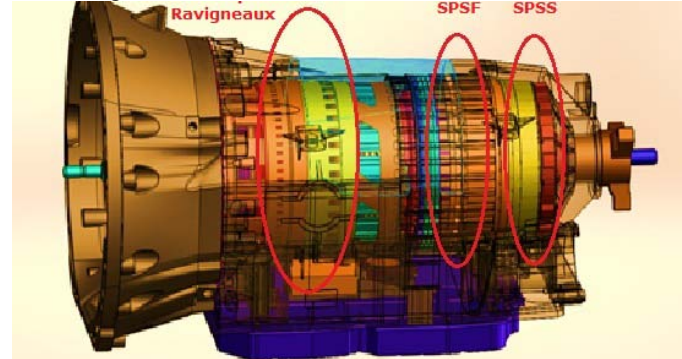


Figure 3. 7G Tronic automatic gearbox

There are three distinct cases of reduction transmission ratios and three amplifier transmission ratios for a simple planetary transmission. Two of these cases have an inversion role, for the reverse gear.

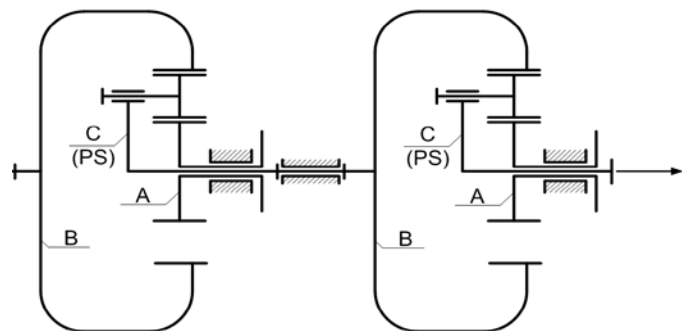


Figure 4 simple front planetary system SPSF and simple rear planetary system SPSS (A-central sun gear, B-crown gear, C<PS>-carrier)

Knowing all technical data for the 7G Tronic transmission, means that we also have all the transmission ratios. We can extract the final drive ratio, by dividing the transmission ratios like below [7]:

$$i_{\text{Final}} = \frac{i_{1,7G}}{i_{1,4R}} = \frac{4,377}{2,71} \approx 1,617$$

$$i_{\text{Final}} = \frac{i_{R,1}}{i_{R,4R}} = \frac{-3,416}{-2,11} \approx 1,617$$

These values are given by the transmission ratios of the two simple planetary system.

In the case of a simple reduction planetary system, the calculation formula for that kind of system is:

$$i = 1 + \frac{z_A}{z_B} \quad (20)$$

For a simple reductive planetary system with the ratio between [1,25;1,67], and in the case of 7G Tronic gear box, having the final ratio $i_{\text{Final}} = 1,617$ on both simple planetary system. That means that for an individual simple planetary system we have:

$$i_{\text{SPSF}} = i_{\text{SPSS}} = \sqrt{i_{\text{Final}}} \quad (21)$$

From where we have:
 $i_{\text{SPSF}} = i_{\text{SPSS}} = \sqrt{1,617} = 1,272$

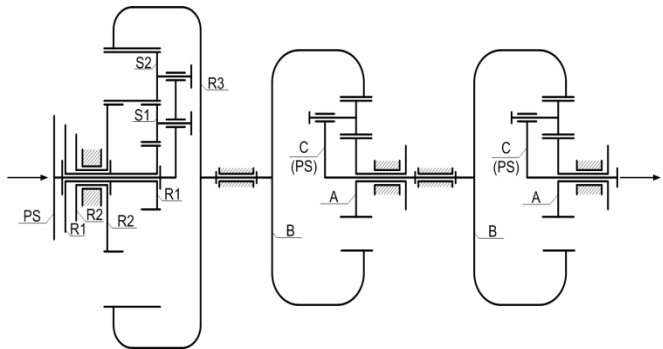


Figure 5. Kinematic scheme of the 3 planetary systems of the 7G Tronic automatic gearbox

According to these data and figure 4 and 5, we can notice that in both cases(SPSF and SPSS) the input is in the crown gear B, the output is on carrier C, and the blocked element, the central sun gear A, using the same notation for both simple planetary system [3; 5; 10].

Comparing the data from table 3 we can notice that the composition of the transmission ratios of the 7G Tronic gearbox by the "Ravigneaux" planetary system, of which kinematic calculation was determined before for the Renault A R4 automatic gearbox and combination of one, two or none simple planetary system.

Table 3. Comparison between the gear ratios of a „Ravigneaux” planetary system and the ones of the 7G Tronic automatic gearbox

| Relations for calculating the ratios of 7G Tronic | Calculated values | 7G Tronic Ratios |
|---|---|-------------------|
| $i_{17G} = i_{Final} \cdot i_{14R}$ | $i_{17G} = 4,377 \cong 1,617 \cdot 2,71$ | $i_2 = 4,377$ |
| $i_{27G} = i_{SPSS} \cdot i_{14R}$ | $i_{27G} = 2,859 \cong 1,272 \cdot 2,71$ | $i_2 = 2,859$ |
| $i_{37G} = i_{SPSS} \cdot i_{24R}$ | $i_{37G} = 1,921 \cong 1,272 \cdot 1,55$ | $i_3 = 1,921$ |
| $i_{47G} = i_{24R}$ | $i_{47G} = 1,368 \cong 1,55$ | $i_4 = 1,368$ |
| $i_{57G} = i_{34R}$ | $i_5 = 1$ | $i_5 = 1$ |
| $i_6 = i_{SPSF} \cdot i_{44R}$ | $i_6 = 0,821 \cong 1,272 \cdot 0,68$ | $i_6 = 0,821$ |
| $i_7 = i_{44R}$ | $i_7 = 0,728 \cong 0,68$ | $i_7 = 0,728$ |
| $i_{R1} = i_{Final} \cdot i_{R4R}$ | $i_{R1} = -3,416 \cong 1,617 \cdot (-2,11)$ | $i_{R1} = -3,416$ |
| $i_{R2} = i_{R4R}$ | $i_{R2} = -2,23 \cong -2,11$ | $i_{R2} = -2,23$ |

According to www.gearsmagazine.com in Gear Ratios section there is a calculating algorithm, which defines

the number of teeth for the gears of the planetary system, according to the transmission ratios.

Using figure 5 we can optimize the planetary gear sets SPSF and SPSS with the following teeth numbers: 71, 14, 28, 60.

| Ravigneaux Tooth Counts | Simpson Tooth Counts |
|-------------------------|----------------------|
| Small Sun Gear | 21 |
| Large Sun Gear | 27 |
| Ring Gear | 57 |
| Input Ring Gear | 71 |
| Input Sun Gear | 14 |
| Reaction Sun Gear | 28 |
| Reaction Ring Gear | 60 |

| Ratios | |
|-------------|------|
| First Gear | 2.71 |
| Second Gear | 1.55 |
| Third Gear | 1.00 |
| Fourth Gear | 0.68 |
| Reverse | 2.11 |

| Ratios | |
|-------------|------|
| First Gear | 1.62 |
| Second Gear | 1.20 |
| Third Gear | 1.00 |
| Reverse | 2.14 |

Figure 6. Teeth number using the given transmission ratios [16]

IV. CONCLUSION

If we realize the ratio between two consecutive gears, we obtain the jump from one gear to the other. This coefficient lets us evaluate the quality of the process of changing between gears for a specifically gearbox. The jump between gears is calculated for each gear change by dividing the values of the current gear to the values of the neighbor gear. For example for the automobile equipped with the gasoline engine the jump between the first and second gear is $i_2/i_1=4,377/2,859$.

The more the jump has lower values between the gears, the more the gear changes are made more easily and more comfortably. Also the dissipated energy of the process of the synchronization depends on the value of the jump between gears. If the jump between gears has high values, then synchromesh must eliminate a bigger difference of revolutions between shafts, and that results in more intense friction in the gear change process.

From the example presented above, we observe that the jump between gears drops as we approach higher gears, so that the process of changing the higher gears is more comfortable and easier.

Usually manufacturers opt for a compromise, respectively fast accelerations in the first gears and good fuel consumption in the higher gears.

REFERENCES

- [1] Argeșanu V., „Organe de mașini” Vol.1, Editura Eurostampa, Timișoara, 2003.
- [2] Borozan I. S., Maniu I., Kulcsar R. M., Argeșanu V., „Ergonomic analysis on driving an Automatic Gearbox equipped vehicle”, IEEE 7th International Symposium on Applied Computational Intelligence and Informatics, May 24-26, 2012, Timișoara, Romania.

- [3] Bostan I., Dulgheru V., Grigoraș S., „Transmisii planetare, precesionale și armonice”, Editura Tehnică Chișinău, 1997.
- [4] Budynas R.-Nysbett J. K., „Shigley's mechanical engineering design”, eighth edition, Mc Graw-Hill Science, 2006.
- [5] Gheorghiu N. S., Ionescu N., Mădăras L., Dobra A. „Transmisii prin Angrenare. Elemente de Proiectare” Editura Orizonturi Universitare, Timișoara, 1997.
- [6] Gligor, O. „Structuri Mecatronice” Editura Politehnica Timișoara – 2003.
- [7] Greiner J., C. Doerr, H. Nauerz, M. Graeve, The New '7G-TRONIC' of Mercedes-Benz: Innovative Transmission Technology for Better Driving Performance, Comfort, and Fuel Economy. SAE Technical Paper No. 2004-01-0649, SAE International, Warrendale, PA, USA, 2004.
- [8] Maniu I., „Le Circuit Hydraulique De Commande D'une Boite De Vitesses Automatique” The Seventh IFTOMM International Symposium on Linkages and Computer Aided Design Methods – Theory and Practice of Mechanisms, Bucharest, 1997, Vol. 4, pp. 85-90.
- [9] Maniu I., Varga S., „Les Trains Cycloidaux Qui Equipent Les Boites De Vitesses Automatiques” Tenth World Congress On The Theory Of Machine And Mechanisms, Oulu, Finland, June 20-24, 1999
- [10] Maniu I., Varga S., „Cinematica, acționarea și comanda unei cutii de vitează automată cu 3+1 trepte de rulare”, 6th Conference on fine mechanic and Mechatronic COMEFIM'6, 2002, Brașov, Romania, 10-12 October, 2002.
- [11] Maniu I., Varga S., „Structura, cinematica și comanda unei cutii de vitează automată pentru autovehicule”, Simpozionul național cu participare internațională Proiectarea asistată de calculator, PRASIC'02, Vol. III, Design de produs, 7-8 Noiembrie 2002, Brașov, România, ISBN 973-635-076-2.
- [12] Sonsino CM, Kaufmann H, Foth J, Jauch F. Fatigue strength of driving shafts of automatic transmission gearboxes under operational torques. SAE paper 970706 (1997); SAE Transactions Section 5. J Mater Manufact, USA 1997, 635–48.
- [13] Sonsino CM. Structural durability of cast aluminium gearbox housings of underground railway vehicles under variable amplitude loadings. International Journal Fatigue 2005;27:944–53.
- [14] Stander C. J., P.S. Heyns, Instantaneous angular speed monitoring of gearboxes under non-cyclic stationary load conditions, Mechanical Systems and Signal Processing 19 (2005) 817–835.
- [15] Yip L. ,Analysis and Modeling of Planetary Gearbox Vibration Data for Early Fault Detection. Phd Thesis,Department of Mechanical and Industrial Engineering University of Toronto,2011.
- [16] *** „La transmission automatique Type A R4”, Technologie Automobile, Régie Nationale des Usines Renault, 1988
- [17] www.gearsmagazine.com;

The Political Culture of Civic Type: Methodology of Formation

I. Dolinina

Abstract - This research makes the lack of methodological development problems of state citizens in a democratic state. Civic information is paradigm of education required in modern Russia described. We carried out the design of pedagogical theory, which was carried out under the three main stages of scientific pedagogical knowledge. On the ground - empirical methodology formed inductively through observation, arrangement and description of facts. The second - on the basis of the facts and explain their understanding of the principles formulated, context category, the criteria put forward hypotheses and designing educational space. The third - accomplished active transformation of education at schools, universities and public organizations.

Keywords- Political culture, methodology, civic information paradigm of education, competence, levels.

I.INTRODUCTION

Methodology of pedagogy as a theory of knowledge about the process of its creation is in demand today, more than ever before in connection with the development of civic society and rules of law in Russia. Currently, structures and function of pedagogical knowledge is poorly defined.

There is need to study methodology in the direction of the political culture of civic type, defining public order law "On Education" - "content of education should ensure the formation of human and citizen, integrated into contemporary society and aimed at the improvement of the society". The idea was developed in the subsequent regulations of the Russian Federation, which is recognized by us as a pedagogical goal - building a civic political culture, upbringing a citizen being prepared for civilian political participation in society - self-enrolled in the socio-political space, self-assessed of one's own qualities, properties and capabilities as an active subject of politics, responding to political actions and events with the aim to influence them [1].

II. LEGISLATIVE RESEARCH FOUNDATIONS

The relevance to civic political culture is determined by international organizations and the Ministry of Education of the Russian Federation.

A number of documents regulating principles of work in this direction have been published. Regulatory framework research were conducted: the International Covenant on Civic and Political Rights , the International Covenant on Economic, Social and Cultural Rights, the UN Convention on the Rights of the Child , the "Declaration of Principles on Tolerance", the RF Law "On Education", "Concept of the Russian education for the period up to 2010", "Strategy for modernizing the content of general education",

This work was supported the Russian Humanitarian Foundation project "Legal education and the formation of a civil competent youth Perm edge" 14-16-59004.

"National doctrine of Education in the Russian Federation", covering the period up to 2025 "State Youth Policy Strategy of the Russian Federation", the Federal Law "On Public Associations", Federal Law "Higher and postgraduate Professional Education ", Federal Target Program "Formation of tolerance and preventing extremism in Russian society (2001-2005)".

III.THE CIVIC INFORMATION PARADIGM OF EDUCATION

Ideally modern society is characterized as civic and informative, as its fundamentals are the substantive information and human responsibility for their own actions.

Therefore, the Russian society needs civil information paradigm of education. "Civic" means the goal of development, and "information", providing adequate conditions, establishing the means for the implementation of the rights and freedoms in citizens of modern Russia, and their responsibility for their actions. The combination of citizenship and information is the process offering a content paradigm shift of education as an integral phenomenon, and its parts would have an independent existence; differ from one another, and would be related socially determined.

The study the interrelationship of education and upbringing synthesized educational and training components for the preparation for political participation is necessary. Educational objectives of the formation of the political culture are implemented as a complex effect on learners (pupils, students, members of public organizations) to influence the worldview, values and personal qualities of a sovereign and responsible citizen. The effectiveness of methodology is built on the basis of the information paradigm verifying civic practice, solution of scientific and practical tasks that are implemented [3, 4, and 5].

IV. "POLITICAL CULTURE" - THE TERM POLITICAL SCIENCE

The political culture is a vast scope of the whole cultures of mankind. At the same time it is one of the fundamental categories in modern political science, as a scientific category it is ill-defined, amorphous, so she scientists "easily attach to one thing or another" [6]. The

phrase “political culture” was first introduced in the scientific revolution in the broad philosophical sense, the by German philosopher and educator J. Herder (1744 - 1803) in his work “Ideas to the philosophy of history“in 1784.

As a categorical status, the term “political culture” is found in Western literature in 1956 in the work of American political scientists G. Almond and S. Verba. They believed that the political culture was a special type of political orientation, reflecting the specificity of each of the political system. Political culture is the action of the general culture, closely associated with a particular political system.

“When we talk about the political culture of a society, we refer to the political system, to internalize knowledge, feelings and evaluation of its members” (G. Almond and S. Verba) [7].

The political culture is a part of the general culture, the rate of political experience, the level of political knowledge, patterns of political behavior and functioning political actors; it characterizes the life of a state, a social group, and individuals. Political culture is a system historically, relatively stable, embodying the experience of previous generations units, orientations and behaviors (functioning), manifested in the immediate activity of subjects of the political process, fixing the principles of their relationship to the process as a whole, its main elements and thereby ensuring the reproduction of the political life of the society. The analysis of theoretical and methodological approaches to the concept of political culture, seems possible to be generalized in the following scheme (Fig. 1) [1].

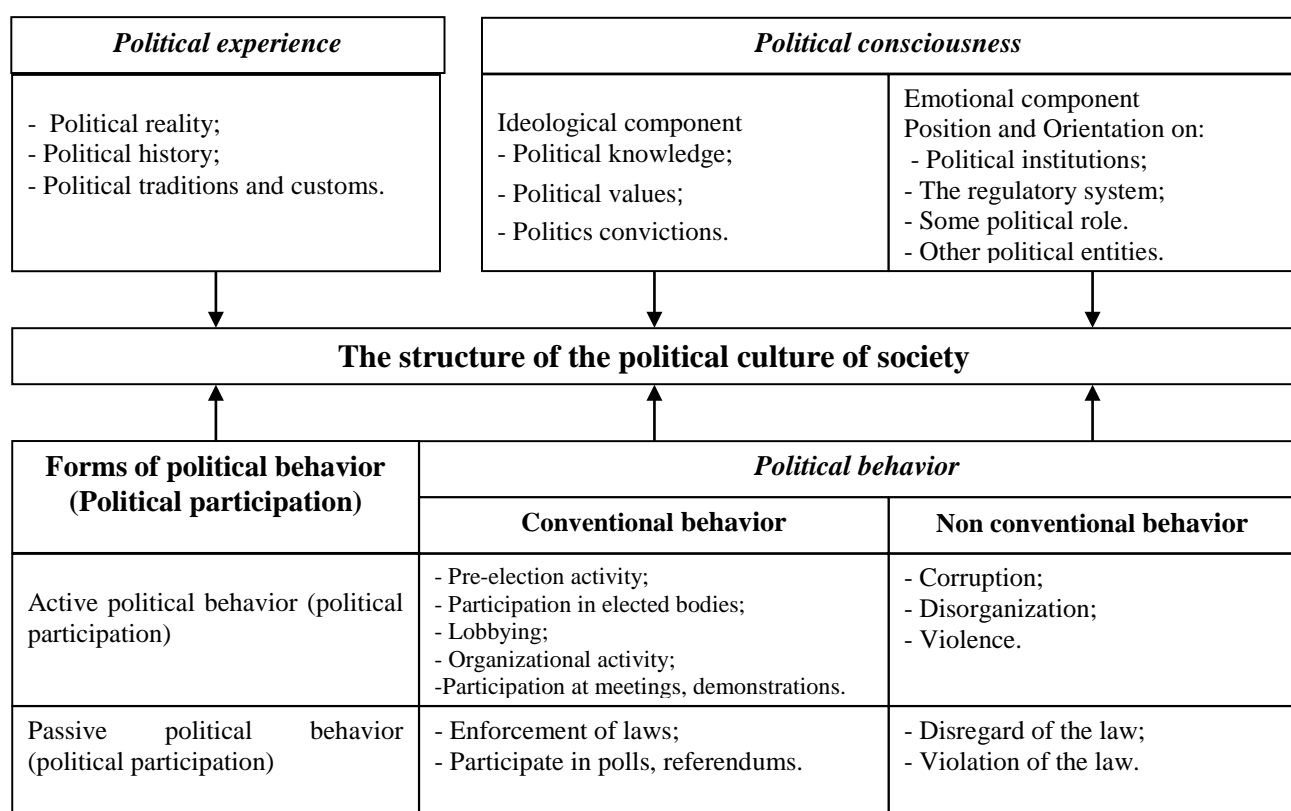


Fig. 1. The structure of the political culture of the society

Political experience, transmitted from one generation to another, making political culture dynamic, evolving as it is exposed to external influences that can either stabilize the level of political culture, or change it. Political consciousness is determined by two components: ideological and psychological. The first is the political knowledge, political values and political beliefs.

Political knowledge - it is knowledge of people about politics, the state and its political system and institutions. People need to have a sufficient level of political knowledge, in order to participate in the political processes of the society. Political values are normative notions and judgments about people's political life. Social justice, law and order are the political values. Political beliefs reflect the views of people about the ideals of

political systems. Usually people compare their political knowledge, values and beliefs with real political system, its institutions and their functioning. Psychological perceptions and attitudes to the political system and its parts (approved or condemned), the regulatory system (to perform or neglect laws), political events and specific politicians.

The non-participation of citizens in the political life may be due to political behavior is determined as both conscious and unconscious reactions of political activities of the educational system aimed at expanding the scope of value-conscious individual oriented behavior and its predominance over the spontaneous, unconscious behavior. Individual state political culture

determines the form of political behavior - active or *and the capacity for interacting with social and governmental institutions [11]*.

V.THE CONCEPT “THE CIVIC PARTICIPATION”

The modern state of society, when the civic society paradigm replaces significantly the idea of public participation, which is a continuous process of interaction between institutions (organizations) responsible for the decision, and the citizens whose interests may be affected by the direct or indirect consequences of the planned solutions, as well as public authorities at different levels, regulating this kind of activity.

“Participation” involves a number of characteristics: action and inaction, promotion and opposition (protest), and the length of time of an action or activity. “Participation” is dotters from “civic participation” which internalization of individual civic values, inner freedom and responsibility, respect for rights and freedoms, protection of the rights and freedoms of others, respect for human dignity, tolerance towards each other, harmonious manifestation of patriotism, culture communication, responsibility for the fate of the country and the world community as a whole, the ability to compromise, tolerate, respect for each personality, peaceful conflict resolution, human rights and advocacy mechanisms, respect for minority rights. For effective implementation of citizen participation on the one hand, institutional experience is necessary, on the other citizens of the actual practice of acting [8]. “Civic participation” is possible only in the regulation of involvement in the development of the state, society and human. The regulation is carried out when the declaration and guarantee of fulfillment of civil, political and social rights is [9]. Close to each other and largely integrated three types of participation: political, civic and social. The boundaries between them are blurred and do not gain sufficient conceptualization currently.

Civic participation is closer to political participation by its cognitive, - affective and behavioral components [10].

VI.THE CONCEPT OF “THE POLITICAL CULTURE OF STUDENTS”

The modern educational practice requires a new interpretation of the concept of “the political culture of the students”, which allows to produce the bass of the pedagogical impact; arrange a purposeful process of the formation of the political culture. Otherwise, the learning curve might be reduced mainly to the amount of the political knowledge, which is not the civic informational paradigm of education.

In our research it is scientifically substantiated that *“Political culture of students” is the aggregating result of upbringing and instruction; it is that part of the individual’s total character that is marked by the appropriation an institutional experience, by the developed political awareness, and by conventional political behavior, with the following dominant features: interest in solving significant sociopolitical problems, preparedness to participate in the political life of society,*

The established system provides increased efficiency of the formation of the political culture of students that can have a wide range of applications: from the creation of educational practice to the individual diagnosis, counseling and correction. Educational methodological basis of implementing the system of the formation of the political culture of students includes:

- 4 monographs describing the methodological research of the author and practical implementation of the research results;

- Syllabi for students and members of non-governmental organizations (“Democracy: state and society: the social studies on elective course program (civics)”, “Suffrage.

- Election Processes: special course program”, “Fundamentals of the constitutional system of the Russian Federation”, “Basics of civil political culture”);

- Tutorials (“Worksheet on social, Fundamental Political Science”, “Workbook on social science. Basic provisions of the Constitution of the Russian Federation”, “Elections at the Russian Federation and the Perm region. Workbook”, “Russian parliament”, “We are learning to democracy”, “Fundamental of civil political culture”, “Pedagogy: formation of political culture of students in the educational space of school (materials to prepare students for teaching practice)”;

- Prepared and tested in practice the diagnostic complex based on the test materials to verify the results of the pedagogical process (4 tests, 2 scales, 7 questionnaires).

VII.METHODOLOGY: PRINCIPLES, ELEMENTS, STRUCTURE

We carried out the design of the pedagogical theory, which was carried out under the three main stages of scientific the pedagogical knowledge. Firstly, empirical methodology based on inductive observation, arrangement and description of facts. Secondly, on the basis of the facts and explain of the understanding, the principles were formulated: contextual category, criteria were put forward designing educational space. Thirdly, - active transformation stipulated in advance was accomplished and was used at schools, universities, public organizations [1].

We consider methodology as theoretical work that provides production of pedagogically appropriate ideas and practice, focused on solving the problems of the formation of the political culture as purposeful civic type of educational space. Theoretical Foundations are the perfect representation of the system of the formation of civic political culture of learning, practical - structural-dynamic model of educational technology, “methodological software”.

The methodological structure is represented by: 1. Methodology is contextual analysis of philosophical, political science and pedagogical knowledge about the political culture; 2. Specific activities: systems analysis, design, identifying features, principles and conditions for the formation of political culture in educational space; 3. Structural activity: subject-subject interaction between students and teacher, the result of

the activity - preparedness for civil political participation; dynamics of political culture; 4. Temporary structure of activity: steps of structural dynamic model and pedagogical research program studying political culture; 5. Technology consists of content and procedural components.

Methodology of designing educational space relies on pedagogical principles: consistent designing objective and social readiness for civic and political participation; democratization and humanization of education, personal organization and activity of educational space; values expressed in the formation of human and civic values; socialization and self-determination of priorities on the basis of individual choice.

Having the dynamics - changing educational measures having specified a content definition of pedagogical discourse allowed developing same criteria. Criteria are integrated in nature and allow us to judge on the degree of preparedness of future citizens for the political participation in society, to the conventionally political behavior in the active or passive forms.

Criteria for determining the individual level of political culture are concerned with the events in the political life (city, country, international relations), willingness to participate in civic and political life, the ability and desire to interact with society and the state. Each of the criteria includes a number of indicators.

Experimentally confirmed the need for compliance with the methodology of designing educational space [8].

VIII. ACKNOWLEDGEMENT

This article was prepared under a grant from the Russian Humanitarian Foundation project "Legal education and the formation of a civil competent youth Perm edge" 14-16-59004.

REFERENCES

- [1] Dolinina, I.G. Formation of political culture: the experience of the methodological design / I.G. Dolinina. - Perm, 2011. - 366.
- [2] Dolinina, I.G. The Activity of Student Public Organizations in the Formation of Civic Political Culture. 17 World Sociological Congress Sociology on the Move, Russian Society of Sociologists (issue 1), 2010. pp: 583-584.
- [3] Dolinina, I.G. Consciousness and behavior of young people in the context of civil political culture // I.G. Dolinina // Social and Humanities. - 2011. - № 1. pp: 162 - 170.
- [4] Dolinina, I.G., "Must be a citizen ..." - formation of political culture. // I.G. Dolinina.// High education today. - 2013 - № 1. pp: 71 - 74.
- [5] Dolinina, I.G., Student's Political Culture Willingness to Civic Participation. // I.G. Dolinina. // Authority. 2013 - № 5. pp: 135 -139.
- [6] Toffler, Al. Power shift: knowledge, wealth and violence at the edge of the XXI – st. century / Al. Toffler. – New York; London, 1990. - 299 s.
- [7] Almond, G. The Civic Culture. Political attitudes and democracy in five nations, Princeton, 1963.
- [8] Turner B.S. The Erosion of Citizenship // British Journal of Sociology, 2001. Vol. 52. No 2. pp: 189-209.
- [9] Marshal T.H. Citizenship and Social Class. Concord, MA: Pluto Press, 1992.
- [10] Newton K., Deth J. van. Foundation of Comparative Politics[^] Democracies of the Modern World, Cambridge: Cambridge University Press, 2005.
- [11] Dolinina, I.G., The state of civil political culture among youth: goals and results of education. 2014 International Conference on Educational Technologies and Education, EUROPMENT (issue 4), 2014. pp: 57-60.
- [12] Chashchin E.V. Modern thinking in terms of social transformations and the emergence of global problems: diss. ... Cand. Philosophy. Sciences. - Perm: PSU, 2010. – 185 p.
- [13] Battistoni, R. Public Schooling and the Education of Democratic Citezens / R. Battistoni. - Jacson : University Press of Mississippi. -1985. P. 187.
- [14] Teaching about society, passing on values/A Secondary Education for Europe Council for Cultural Co-operation: Council of Europe Press,1993
- [15] Condliffe Lagemann E. Renewing Civic Education. Time to restore American higher education's lost mission // Harvard Magazine. March-April 2012. pp: 42-45. <http://harvardmagazine.com/2012/03/renewing-civic-education>
- [16] Vasilyeva L. A, Shustova K. D. Boyar Legal education as one of the areas of socialization in the modern world . // Adukatar . - 2011 . - № 2. P. 2
- [17] The Universal Declaration of Human Rights : approved and carried out by UN General Assembly on December 10 . 1948 - Moscow: UN Association - USSR, 1989. – P. 8
- [18] Dolinina, I.G. Shakirov E.A . Legal education: conceptual bases / IG Dolinina, EA Shakirov // Higher education today. - 2013. - № 3 . pp: 49 - 52.
- [19] Dolinina, I.G., Shakirova, E.A. Legal culture as the goal of legal education. / And. G. Dolinina, EA Shakirova // Formation of the humanitarian environment in higher education: Innovative educational technologies . Competence approach . Proceedings of XIII All-Russian scientific - practical conference. - Perm, 2013. pp: 166 - 170.
- [20] Convention on the Rights of the Child: Adopted by Resolution 44/25 of the General Assembly of 20 November 1989. URL: <http://www.znaem-mozhem.ru/node/601> (date accessed: 05.12.13)
- [21] Alexeev V.N., Dolinina I.G. The formation of civic competence. Perm, 2012, p. 122.
- [22] Butler J.E. Democracy, diversity and civic engagement/ J.E.Butler // Academe. -2000. -T.86. - N 4. pp: 52-55.
- [23] Cecchini M. Education for democratic citizenship/ M. Cecchini, Voelkner K. // Newsletter education. - 1999. -N 7. pp: 7-9.

- [24] Dixon A. Fire blankets or depth charges: choices in education for citizenship/ A. Dixon // Forum for promoting 3-19 comprehensive education. - 2000. -T.42. -N 3. pp: 95-99.
- [25] Gibbon P.X. Giving students the heroes they need/ P.H. Gibbon // The education digest. -Ann Arbor. -2003. -Vol.68. -№8. pp: 12-19.
- [26] Husen T. An agenda for the education of world citizens/ T. Husen // Prospects. -1997. -T. 27. - N2. - pp: 201-205.
- [27] Kalb P.E. Verantwortung uebernehmen// Paedagogik. -Weinheim. -2004. Jg.56. - H.5. pp: 6-35.
- [28] Patrick J.J. Civic Education in Pre-Service Training Program for Teachers and Children Welfare Professionals. Giedrė Kviesienė, Vilnius Pedagogical University. Vol 11, No 1, 2013. Available: <http://www.socwork.net/sws/article/view/181/580>
- [29] Rosen L. Elementary school civic education gets good citizens started/ L. Rosen // The education digest. -2000. -T.65. -N 6. pp: 19-22.
- [30] Audigier Teaching about society, passing on values. Council of Europe Publishing, 1996. - P. 34.
- [31] Lagemann E.C. Renewing Civic Education. Time to restore American higher education's lost mission // Harvard Magazine. March-April 2012. pp: 42-45.
- [32] McMurray A. Building bridging social capital in a divided society: The role of participatory citizenship education. // Education, Citizenship and Social Justice July 2012 7. pp: 207-221.
- [33] Purnel J. Get students started on social change/ J. Purnell // The education digest. -2000. T. 65. N 7. pp: 33-36.
- [34] Bolotina, T.V. On the state of civic education in Russia / T.V.Bolotina. – Moscow, 2004, p. 1
- [35] Botalova A. A. Formation of tolerance means of local lore. In Sat: Articles IV Interregional Scientific and Practical Conference "City Tchaikovsky from antiquity to the present day" and X interregional scientific-practical conference "Ethnic culture and modern school" – Izhevsk: IPC "Bon Anza", 2011.
- [36] Botalova A. A. The role of the school museum in civic education students. // International scientific and practical conference "Man. Society. State". Perm. 2009.
- [37] Dolinina I.G. Formation of political culture: the experience of the methodological design: diss. ... Doc. Philosophy. Sciences. - Perm, 2011. – 336 p.
- [38] Alekseev V.N., Dolinina I.G. Foster civic competence. Perm, 2013. 122 p.
- [39] Modernization strategy withholding general education / / Materials for the development of instruments of general education. Moscow, 2001
- [40] Alekseev V.N., Dolinina I.G. Pedagogical conditions formation of civil competence of students// Higher education today. - 2013 . - № 8 . pp: 34 - 38.
- [41] Dolinina, I.G., 2014. The state of civil political culture among youth: goals and results of education. 2014 International Conference on Educational Technologies and Education, EUROPMENT (issue 4), pp: 57-60.
- Irina G. Dolinina** is currently a doctor of pedagogical sciences, professor of department philosophy and law at Perm national research university. In her PhD thesis (1997-2002) studied the conceptual model of the civic culture of students. Subsequently, conducted extensive research the methodology of universities education, schools and community organizations (2002 - 2011). Both her research and her applied work, the prime interest involves the dynamics of behavioral change within social systems, the training of the civilian political participation.
- Public and professional recognition
- 2014 - Awards Medal. John Locke (Medal of John Locke) by the European scientific and industrial consortium (www.euscienc.info) recognized by the international community for the contribution to the teaching of science and education. (Protocol 463 / 10.06.2014).
- 2012 - Monograph "Formation of political culture: the experience design methodology" by the All-Russian competition for the best scientific book in 2011, the winner of the Development Fund of the national education and the Education Committee of the State Duma of the Russian Federation.
- 2013 - Monograph "Formation of civic competence" (co-author V. Alexeev) at the All-Russian competition for the best scientific book in 2012 Winner of the Fund for the Development of national education and the Education Committee of the State Duma of the Russian Federation.
- Diploma of the All-Russian contest "The best scientific book in the humanitarian sphere - 2013."
- 2014 1 "Constitutional Law of the Russian Federation. Teaching manual (electronic educational resource) "in the" Jurisprudence "by the All-Russian competition for the best scientific book in 2013 Winner of the Fund Development of National Education and the Education Committee of the State Duma of the Russian Federation.
- 2 Teaching Materials discipline "intellectual property protection" in the "Humanities" by the All-Russian competition for the best scientific book of 2014. Winner of the Development Fund of the national education and the Education Committee of the State Duma of the Russian Federation.
- 3 Winner of the Golden World Science Foundation for the best scientific and methodological publication at the industry.
- Professor I. Dolinina leading expert work in the social scientific and political institutions:
- 1 Council of Federation of the Russian Federation.



2 The Public Chamber of the Perm region.

3 Public Council for Civic Education Perm edge

developer of the concept of the target program of

civic education Perm region.

Service Based Generation of Latex Graphical Dependencies

Pavol Buzák, Katarína Žáková and Zoltán Janík

Abstract—As it is known, LaTeX enables typesetting of medium-to-large technical or scientific documents that includes not only text and mathematical expressions but also graphical objects. There exist several packages for generation LaTeX graphics that are based on PostScript, PGF ("Portable Graphics Format"), Metapost, etc. Preparation of LaTeX pictures using any of these technologies require to learn related procedure steps, new syntax and relevant functions. It can be reasonably time consuming and not all scientists and users have enough time to do it.

The paper presents a web service that enables to automate generation of pictures that contain graphical dependencies of variables on the base of uploaded numerical values. Considering properties of several packages we decided to use two of them: Pgfplots and Gnuplottex based on Gnuplot. Both are wide spread, their syntax is easy to learn and commands for graphics generation can be written directly in the LaTeX source code.

The presented web service is developed using JSON-RPC. The service and the complementary web application enable to take into account user's preferences regarding layout and appearance of resulting pictures and facilitate the picture production.

Keywords—computer-aided design, web service, JSON-RPC, Latex.

I. INTRODUCTION

It is said that "it's always better to see once rather than to hear twice". Another Chinese proverb says that "a picture's meaning can express ten thousand words" [5]. The meaning of both sayings is more or less the same and it can be related not only to common everyday life but also to technical education. Measured experimental results or results from simulations are very often documented by means of graphical dependencies. They enable to evaluate the quality of achieved outputs much faster than e.g. tables or verbal description. Pictures with charts can be generated by various software applications, e.g. Matlab, Maple, Mathematica, Excel, Maxima, etc. We could list many of them. However, it is usually not so common that such pictures are generated directly in the word processor. LaTeX can be considered as one of such examples. This paper

This work was supported by the grant "Program for support of young researchers" of Slovak University of Technology. It has also been supported by the Slovak Grant Agency, Grant KEGA No. 032STU-4/2013 and APVV-0343-12.

P. Buzák, K. Žáková and Z. Janík are with the Faculty of Electrical Engineering and Information Technology, Slovak University of Technology, Bratislava, Slovakia (e-mail: katarina.zakova @ stuba.sk, zoltan.janik @ stuba.sk).

aims to show how this procedure can be done automatically and more user-friendly. In order to achieve this aim, we have designed a new web service for this purpose.

Different authors give different definitions to Web Services. Leidago Noabeb [7] introduces that "A Web service basically is a collection of open protocols that is used to exchange data between applications. The use of open protocols enables Web services to be platform independent. Software applications that are written in different programming languages and that run on different platforms can use Web services to exchange data over computer networks such as the Internet." He also states that since "different applications are written in different programming languages, they often cannot communicate with each other. A Web service enables this communication by using a combination of open protocols and standards, chiefly XML, SOAP and WSDL." In spite of the fact that there already exist other open technologies for building service-based applications, Noabeb's definition describes all main features of the web service.

II. LATEX AND GRAPHICS

As it is written on LaTeX web site (<http://latex-project.org/intro.html>), LaTeX is a document preparation system for high-quality typesetting. It is most commonly used for medium-to-large technical or scientific documents but it can be used for almost any form of publishing. However, it is to say that it is not a word processor, but it is a markup-based typesetting language.

LaTeX contains features mainly for typesetting journal articles, technical reports, books, and slide presentations. It is able to take control over large documents containing sectioning, cross-references, tables and figures. It enables to typeset complex mathematical formulas, generate bibliographies and indexes, etc. In addition, it can be also used to produce graphical objects.

LaTeX can be used together with PostScript (on which PDF is based). LaTeX's mathematical capability, its paragraph building, its hyphenation, and its programmable extensibility can cooperate with the graphical flexibility and font-handling capabilities of PostScript and PDF [1].

PostScript is object-oriented computer language enabling to describe the graphical appearance of a printed page. It was developed by Adobe Systems Incorporated. Its main advantage is that it is independent on device on which the document is printed. PostScript can be considered as a standard for

desktop publishing. It is supported by the most of high-resolution printers to produce camera-ready copy. There exist several packages for generation LaTeX graphics that are based on PostScript:

- PSTricks, where the necessary PostScript code can be generated by TeX macros defined in the package. It is often used as a base for other LaTeX libraries.
- Pst-plot utilizes PSTricks macros for creation of vector graphics.
- Barddiag, Bchart – both of these packages are already deprecated. They can be used only for producing bar graphs.

Another possibility to generate LaTeX Graphics is offered by command line based Gnuplot program that is a portable command-line driven graphing utility for various platforms.

The set of programs PGF/TikZ also enables the creation of high quality drawings for LaTeX. PGF is the basic layer, providing a set of basic commands for producing graphics, and TikZ is the frontend layer with a special syntax, making the use of PGF easier.

PGFPLOTS is a package that is based on the combination of programs PGF/TikZ. It was directly developed to generate graphs for LaTeX.

Package Matlab2Tikz converts graphs from Matlab to LaTeX using PGFPLOTS library.

Metapost programming language enables to create vector graphics. It generates figures for technical documents where some aspects of a picture may be controlled by mathematical or geometrical constraints that are best expressed symbolically [2].

Similarly Asymptote is also language for generating vector graphics. However, it requires an external program for compilation of a resulting output document.

Finally, R language can be mentioned. It is a free software environment for statistical computing and graphics.

A brief comparison of all mentioned projects is listed in Table 1. Since we usually use MikTeX distribution of LaTeX, we were interested in the fact, whether the considered package is included in MikTeX repository or not. Subsequently, it is interesting to know whether the package includes functions for graphics generation directly. Since the final documentation is very often prepared in PDF format, it is important to know how demanding the preparation of PDF document is - whether it can be compiled directly from the LaTeX source code or whether the source code needs to be compiled to a postscript file first and only then it can be converted from the postscript file to the PDF format.

Considering all properties of mentioned packages, we decided to focus on two solutions: Pgfpplots and Gnuplotex based on Gnuplot. Both of them are wide-spread, their syntax

| Title | MikTeX repository | Integrated graph functions | pdf export | PostScript based | URL address |
|-------------|-------------------|----------------------------|------------|------------------|--|
| PSTricks | ✓ | | | ✓ | http://www.ctan.org/pkg/pstricks-base |
| Pst-plot | ✓ | ✓ | | ✓ | http://www.ctan.org/pkg/pst-plot |
| Barddiag | ✓ | | | ✓ | http://www.ctan.org/pkg/bardiag |
| Bchart | ✓ | | | ✓ | http://www.ctan.org/pkg/bchart |
| Barkom | ✓ | | | ✓ | http://www.ctan.org/pkg/barkom |
| Gnuplot | package only | ✓ | ✓ | | http://www.gnuplot.info/download.html http://www.ctan.org/pkg/gnuplotex |
| PGF/TikZ | ✓ | | ✓ | | http://sourceforge.net/projects/pgf/ |
| TikZ | ✓ | | ✓ | | http://sourceforge.net/projects/pgf/ |
| PGF Plots | ✓ | ✓ | ✓ | | http://pgfplots.sourceforge.net/ |
| Matlab2Tikz | ✓ | ✓ | ✓ | | http://www.mathworks.com/matlabcentral/fileexchange/22022-matlab2tikz |
| Metapost | ✓ | ✓ | | | |
| Asymptote | | ✓ | | | http://asymptote.sourceforge.net/ |
| R | | ✓ | ✓ | | http://cran.r-project.org/ |

Tab. 1 Packages for LaTeX graphics generation

is easy to learn and commands for graphics generation can be written directly in the LaTeX source code. Pgfplots enables to produce PDF format of document without a need to use external programs (using pdflatex). Gnuplot needs to prepare Gnuplot code that can be compiled to PDF format directly. Both of these packages were implemented into the presented solution.

III. REMOTE PROCEDURE CALL

Remote Procedure Call (RPC) is a protocol for requesting a service from a program located in a remote computer through network without having to understand the under layer network technologies [8].

RPC uses the client/server model. The requesting program is a client and the service-providing program is the server. First, the client sends a call message that includes the procedure parameters to the server process (Fig.1). After that, the caller process waits for a reply message. Next, a process on the server side, which is idle until the arrival of the call message, extracts the procedure parameters, computes the results, and sends a reply message. The server waits for the next call message. Finally, the caller's process receives the reply message, extracts the results of the procedure, and the caller resumes execution [8]. The server and the client application logic are kept independently, thus multiple clients may be written using the same server API.

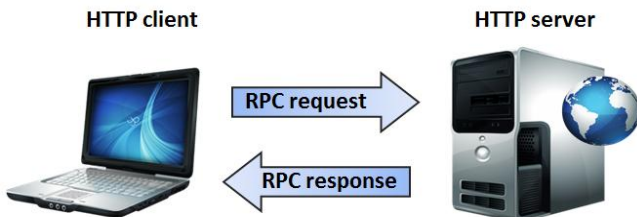


Fig. 1 Remote Procedure Call communication

According to the format of the sent messages, it is possible to consider XML-RPC or JSON-RPC. We decided to use JSON-RPC because JSON is not as verbose as XML and for humans, it is faster to write JSON. Despite that XML is used to describe structured data, it doesn't include arrays, while JSON does.

IV. REALIZATION

As it was already mentioned, the developed service allows to process requests in JSON-RPC. The server provides responses according to the used RPC request protocol.

A. Web Service Request

For API implementation JSON-RPC 2.0 specification was used [6]. In such a case, the request object can contain three properties:

- method - a string containing the name of the method to be invoked;
- params - an array of objects to pass as arguments to the method. This property can be omitted;

- id - the request ID that can be of any type. It is used to match the response with the request that it is replying to.

The created web service implements only single method – generate. Its task is to produce LaTeX code that is able to generate the picture presenting graphical dependencies with values specified in the input file.

Afterwards the generated code can be included to the LaTeX document and compiled to the final PS or PDF file. The created service enables to produce not only LaTeX code with the required graphics but also its PNG or PDF equivalent.

Fig.2 illustrates an example of the JSON-RPC request. As one can see, the request contains several parameters. Parameter user_input_data enables to specify input file with data that should be visualised by means of graphical dependence. In the picture, one or more graphical dependences can be presented. Parameter user_template allows to choose a LaTeX template that forms the environment for graphics included to the document source code. APIkey parameter specifies the alphanumerical code of the person that is allowed to use the presented service. Parameter pdf defines the format of the desired output. In similar way, one can define PNG or LaTeX format. The rest of parameters describe the graphical presentation and graphical layout of the resulting figure.

```

{
    "jsonrpc": "2.0",
    "method": "generate",
    "params": [
        {
            "APIkey": "xxxxx",
            "graph_type": 0,
            "user_template": "pgfplots.tex",
            "user_input_data": "input.dat",
            "font_size": 2,
            "pdf": 1,
            "show_grid": 1,
            "legend_show": 1,
            "x_tics": 1,
            "x_min": -10,
            "x_max": 10,
            "y_min": -1.2,
            "y_max": 1.2,
            "width": "15cm",
            "legend_position": "outer north east",
            "x_label_pos_x": 1.05,
            "x_label_pos_y": 0.5,
            "y_label_pos_x": 0.5,
            "y_label_pos_y": 1.1,
            "lines": [
                {
                    "file_index_x": 0,
                    "file_index_y": 1,
                    "legend": "sinus",
                    "file_index_x": 2,
                    "file_index_y": 3,
                    "legend": "kosinus",
                    "line_color": "green"
                }
            ],
            "id": 1
        }
    ]
}

```

Fig. 2 Example of JSON-RPC request

In Fig.3, one can see an example of LaTeX template that was used in the previous JSON-RPC request. As it is possible to see, the template is a standard LaTeX document that starts with the import of necessary packages and continues with setting of page style. The body of the document is created by the graphics that was completed using the presented service.

B. Web Service Response

The response object also has three properties:

- result - the object that was returned by the invoked method;
- error - an error object if there was an error invoking the method;
- id - the same id as the corresponding request id.

It is to say that in the JSON-RPC 2.0 specification, each response object can contain only one of the first two properties (either “result” or “error”).

```
\documentclass{article}

\usepackage{pgfplots}
\usepackage{fullpage}

\pagestyle{empty}
\begin{document}

%EXPORT_BEGIN%
\begin{tikzpicture}
\begin{axis}[axis x line=center, axis y line=center,
 xlabel={$x$}, ylabel={$y$},
 xlabel style={at={(1.05, 0.5)}},
 ylabel style={at={(0.5, 1.1)}},
 xmin=-10, xmax=10, ymin=-1.2, ymax=1.2,
 width=15cm, height=5cm,
 every axis/.append style={font=\small},
 xtick={-10,-9,...,10},
 grid, legend pos=outer north east]

\addplot[smooth, line width=1pt, color=red, style=solid]
    table[x index=0, y index=1] {input.dat};
\addplot[smooth, line width=1pt, color=green, style=solid]
    table[x index=2, y index=3] {input.dat};
\legend{$\sin x$, $\cos x$}

\end{axis}
\end{tikzpicture}
%EXPORT_END%

\end{document}
```

Fig. 3 LaTex template specified in JSON-RPC request (pgfplots.tex)

The successfully realized response to the request from the previous example is shown in Fig.4.

The response returns the URL address of the generated PDF file. In the case when the LaTe \backslash x code was requested, the result property contains the code that can be seen in Fig.3 between strings EXPORT_BEGIN and EXPORT_END.

If the request fails, the response will contain the error property as it is demonstrated e.g. in Fig.5.

```
{"jsonrpc": "2.0",
"result": "http://www.example.sk/latex/tmp/139357/pgfplots.pdf",
"id": 1}
```

Fig. 4 Example of successful JSON-RPC response

```
{"jsonrpc": "2.0",
"error": {"code": 1, "message": "Wrong API key."},
"id": 1}
```

Fig. 5 Example of failure JSON-RPC response

To extend the presented web service, we also developed the online web application. It enables to set all graph parameters via online form. Then, after uploading the file containing numerical data that should be visualized as graphical dependence/dependencies in the picture, choosing the preferred library and the output format, the generation of the required result can start. The created graphical user interface offers a comfortable way of the picture production.

V. CONCLUSION

The paper presents a service that can facilitate preparation of scientific documents written in LaTe \backslash x - the documents that include graphical dependencies of measured or calculated values. The required LaTe \backslash x code that describes the picture is generated automatically using one of two available LaTe \backslash x packages: Pgfplots and Gnuplottex. The introduced tool enables to take into account user's preferences regarding the layout and the appearance of produced pictures. In this way, it offers extension to the LaTe \backslash x usability for unskilled users, too. It can also be used by scientists, teachers and students during writing their final thesis.

REFERENCES

- [1] M. Goossens, F. Mittelbach, S. Rahtz, D. Roegel, H. Voß (2007). The LaTe \backslash x Graphics Companion. Second Edition. Addison-Wesley.
- [2] J. D. Hobby et al. (2013). METAPOST A user's manual v.: 1.503. [online] Available at <http://ftp.cvut.cz/tex-archive/graphics/metapost/base/manual/mpman.pdf> [Accessed 02 January 2014].
- [3] R. Koehler (2008). Simple is better: RPC / JSON-RPC. [online] Available at <http://www.simple-is-better.org/rpc/> [Accessed 27 February 2014].
- [4] E. Králiková, M. Kamenský, J. Červeňová (2013). E-Learning Support in Engineering Education of Robotics Specialists. In: Proc. of Int. Conf. Distance Learning, Simulation and Communication "DLSC", Brno, Czech Republic, IDET 2013, pp. 121-127.
- [5] P. M. Lester (2014). A Picture's Worth a Thousand Words? [online] Available at <http://commfaculty.fullerton.edu/lester/writings/letters.html> [Accessed 27 February 2014].
- [6] M. Morley (2013). JSON-RPC. [online] Available at <http://json-rpc.org/> [Accessed 10 May 2013].
- [7] L. Noabeb (2013). Anatomy of a Web Service: XML, SOAP and WSDL for Platform-independent Data Exchange. [online] Available at http://www.webrference.com/authoring/web_service/index.html [Accessed 09 May 2013].
- [8] RPC protocol. [online] Available at <http://www.javvin.com/protocolRPC.html> [Accessed 09 May 2013].
- [9] P. Slivka (2012). Design of API for CAS service. Diploma thesis, FEI STU Bratislava, in Slovak.
- [10] L. Stuchlíková, J. Benkovská, M. Donoval (2013). An Easy and Effective Creation of E-Learning Courses. In: Proc. of Int. Conf. Distance Learning, Simulation and Communication "DLSC", Brno, Czech Republic, IDET 2013, pp. 159 – 164.
- [11] A. J. Turgeon. Implications of Web-Based Technology for Engaging Students in a Learning Society", Journal of Public Service and Outreach 2(2): 32-37.
- [12] I. Zolotová, R. Mihaľ, R. Hošák (2013). Objects for Visualization of Process Data in Supervisory Control. Topics in Intelligent Engineering and Informatics 2: Aspects of Computational Intelligence: Theory and Applications. - Berlin Heidelberg: Springer-Verlag, pp. 51-61.

Entropy In Terms Of Vehicular Distance Under Driving Constraints

Caglar KOSUN

Department of City and Regional Planning
Izmir Institute of Technology
Izmir, TURKEY
cglrksn@gmail.com

Serhan OZDEMIR

Department of Mechanical Engineering
Izmir Institute of Technology
Izmir, TURKEY
serhanozdemir@iyte.edu.tr

Abstract—Car following models are typically concerned with the interaction between adjacent vehicles on roadways. Managing vehicular interaction is an important research topic in traffic engineering literature. In an entropy framework, the authors investigate the effect of vehicular safety distance between the two consecutive vehicles during a car-following process on the generated entropy. A general formulation is given. Then, as a case study, interactions of only one vehicle and its follower are considered to characterize the car following behavior. The concept of entropy in such a traffic scenario could be considered not simply as disorder but an indicator of possible choices in certain situations. The entropic form used is the conventional Boltzmann-Gibbs entropy (BGE). But when two cars start interacting, Boltzmann-Gibbs entropic concept seems to be violated. This paper intends to provide a relationship between the length of vehicular distances and entropy, and a particular distance when this BGE apparently violated. To this purpose, a hypothetical unidirectional multi-lane roadway lattice is created with discrete cells. The interaction and the distance between adjacent vehicles are analyzed and the results are discussed in the paper.

Keywords—*Boltzmann-Gibbs entropy; Tsallis entropy; traffic flow; nonextensivity; car following; vehicle; safety distance*

I. INTRODUCTION

Statistical mechanics concerns the microstates of a system and deals with statistical behaviors of its individual particles. Many possible state configurations can occur in such a system. In this paper, to specify such configurations and degree of disorder, the concept of entropy is considered.

The definition of the entropy for thermodynamics goes to the Clausius [2]. Moreover, there have been many attempts on the entropy formulations. For example, a logarithmic expression for the entropy has known as Boltzmann-Gibbs (BG) entropy for almost a century. Moreover, much more recent one is Tsallis entropy which is the generalization of BG entropy [3]. This paper dwells upon the extensive statistical mechanics called BG entropy and Tsallis statistical mechanics.

In literature, the BG entropy does not seem to be universal and its application is only limited to the extensive systems even though it has remarkable applications in variety of dynamical systems over one century. After the generalization of BG statistics by Tsallis [3], nonextensive systems have

been investigated in the new entropy domain. Furthermore, it is known that BG entropy belongs to only special cases where entropic index q equals to unity [4]. BG entropy is additive, whereas Tsallis entropy has nonadditive property unless $q=1$ [4]. There would be possible interactions among sub-systems of the given system to address the nonadditive property. Those subsystems especially involve long-range interactions. Investigation of such subsystems in the light of nonextensive domain would be more meaningful since it is universal and has generalized entropic form.

The main goal in this paper is the investigation of vehicular traffic flow via the entropy framework. Indeed, the vehicular traffic flow is composed of vehicle interactions and possible states. Their basic interactions are discussed in Tsallis entropy framework.

II. ENTROPY FORMULATIONS

The concept entropy is utilized in many fields of science and engineering. Entropy is basically a statistical measure of the amount of energy or uncertainty particularly of a thermodynamic system. In this paper, entropy is considered in the framework of the molecular disorder, molecular interaction and the number configurations in which a system arranges. Molecular means here vehicles in the traffic flow and the main aim is to build a relationship between the entropy formulations and vehicular traffic flow.

A. Boltzmann-Gibbs Entropy

BG entropy has an extensive property, and thus the total entropy of a system is equal to the sum of the entropies of the N parts of the system.

If a statistical system typically exhibits for example short-range interactions, short-term memory (Markovian process), ergodicity, Gaussian distributions, strong chaos (i.e. positive maximal Lyapunov exponents) and mixing, it refers to extensive statistical mechanics [5].

BG entropy formulation is given below:

$$S_{BG} = -k \sum_{i=1}^W p_i \ln p_i \quad (1)$$

where W is the total number of configurations whose probabilities are p_i , k is Boltzmann constant.

When W increases, the information starts to lose. If a system consists of equal probabilities, the maximum entropy occurs. The probability distribution would be uniform and this extremizes entropy. Thus, there is zero information. When equiprobability assumption exists, the entropy formulation is expressed as celebrated Boltzmann principle

$$S_{BG} = k \ln W \quad (2)$$

BG entropy maintains those mathematical properties such as non-negativity, maximal at equal probabilities, expansibility, additivity, concavity, Lesche-Stability or experimental robustness, Shannon uniqueness theorem, composability etc. [4].

B. Tsallis Entropy

Tsallis entropy (nonextensive statistical mechanics) is a generalization of standard BG entropy. The violation of the typical properties of BG statistical mechanics for example vanishing the largest Lyapunov exponent i.e. weak chaos, nonergodicity, long-term memory, q-Gaussian distributions i.e. asymptotic power-laws and long-range interactions in many body systems indicate nonextensive statistical mechanics [5]. The possible generalization of the BG entropy is based on the following entropy form

$$S_q = k \frac{1 - \sum_{i=1}^W p_i^q}{q-1} \quad (3)$$

where q is the entropic index.

For the generic probabilities for S_1 , the entropy form is obtained as

$$\lim_{q \rightarrow 1} S_q = S_1 = -k \sum_{i=1}^W p_i \ln p_i \quad (4)$$

Tsallis entropy can be expressed as nonadditive unless $q=1$, in which case it belongs to specific case i.e. BG statistical mechanics.

Reference [6] and [4] state that the statistical mechanics of microcanonical ensemble (isolated system) involves equally probable states, i.e. $p_i = 1/W$. Instead, in canonical ensemble i.e. a system in longstanding contact with a large thermostat at fixed temperature would necessitate energy constraints as well as the norm constraint. Thus, the optimization of the entropy can be obtained by a possible couple of the constraints

$$\sum_{i=1}^W p_i = 1 \quad (5)$$

$$\sum_{i=1}^W p_i E_i = U_q \quad (6)$$

where U_q is the mean energy, and E_i is the eigenvalues of the Hamiltonian of the system.

The extremization of S_q with the two constraints provides

$$p_i \propto [1 - (q-1)\beta E_i]^{1/(q-1)} \quad (7)$$

where β is Lagrange parameter.

III. CASE STUDY

In this study a simple traffic flow example is chosen. There are three lanes and the lanes are divided into cells. Vehicles follow each other towards north. For the left figure, the following vehicle approaches the slower vehicle and it has three equal possible choices. However, when there is a vehicular distance constraint assumption in which the following vehicle cannot move to the cell behind the slower vehicle. Thus, the faster vehicle has two equal possible choices i.e. states or configurations. This second case generates less entropy.

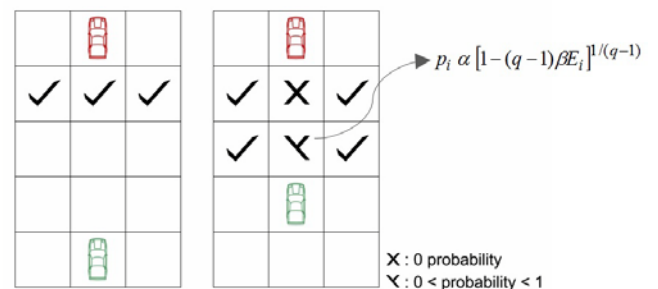


Fig.1 Schematic view of the traffic flow.

IV. CONCLUSIONS

As in the work [1], there is a certain distance considered by drivers where cars are thought to be independent moving objects. This certain distance changes from one driver to the other. Personal preferences and psychology of the drivers, vehicle speeds, road conditions all affect this psychological personal space. This personal space is intended to explained in terms of entropy. In Fig. 1, the figure on the left depicts the case where vehicles are separated by a distance so that these two vehicles are not interacting. The choices of the following driver are formulated by BG entropy, where interactions are either zero or negligible. But when the gap between the cars has come to a nonnegligible spacing, the application of the BG is not appropriate. Here, the Tsallis entropic framework is in use. Initial choices are three, all given by an equal probability of 1/3. When the chasing car is quite close, some of the previously allowable state or states are now forbidden for safety concerns, and available the choices are now reduced to 2, giving 1/2 probability each. This obviously amounts to a drop in entropy.

References

- [1] M. Krbálek and K. Kittanová, "Lattice thermodynamic model for vehicular congestions," *Procedia Soc. Behav. Sci.*, vol. 20, pp. 398-405, 2011.
- [2] C. Tsallis and U. Tirnakli, "Nonadditive Entropy and Nonextensive Statistical Mechanics--Some Central Concepts and Recent Applications," *J. Phys. Conf. Ser.*, vol. 201, (1), 2010.
- [3] C. Tsallis, "Possible generalization of Boltzmann-Gibbs statistics," *J. Stat. Phys.* vol. 52, (1-2), pp. 479-487, 1988.
- [4] C. Tsallis, *Introduction to Nonextensive Statistical Mechanics: Approaching a Complex World*. Springer, New York: 2009.
- [5] C. Tsallis, "Entropy: A unifying path for understanding complexity in natural, artificial and social systems," *Information, Knowledge, Systems Management*, vol.10, (1-4), pp. 291-311, 2011.
- [6] C. Tsallis, R.S. Mendes, and A.R. Plastino. "The role of constraints within generalized nonextensive statistics," *Phys A*, vol. 261, (3-4), pp. 534-554, 1998.

Governance and Adaptation to Innovative Modes of Higher Education Provision

Silvia, Florea, Lucian Blaga University of Sibiu, Romania, silvia.florea@ulbsibiu.ro
Cecile, Hoareau McGrath, University of Maastricht, The Netherlands,
cecile.hoareau@empowereu.org
On behalf of the GAIHE consortium

Abstract: In the context of the ever growing use of technology through e-learning and open-courseware, our paper describes a project that is being carried out by a consortium of twelve university partners and is coordinated by the University of Maastricht and RAND Europe (Cambridge). This project sets out to examine the evolution and sustainability of the innovative modes of higher education provision in teaching and learning across Europe, the motivations for their emergence as well as the ways in which higher education management and governance have responded and adapted to such new modes of provision. In the highly competitive sector of higher education (HE), while attempting to enhance the quality of teaching and learning, the increasing range of teaching and learning providers (encouraging both new delivery models and the ‘unbundling of delivery’ through partnerships, spin-out organisations, franchising, etc.), has challenged the ‘traditional’ model of university and stimulated changes in the provision and management of higher education.

Our paper outlines the project and discusses the first preliminary results obtained from a survey administered to 47 European higher education institutions (HEIs) based in 9 countries against the background of a literature review of more than 180 bibliographic sources, critically reviewed for the purposes of the GAIHE project.

Keywords: technology, higher education, MOOCs, governance

Acknowledgment: The Project (Reference number: 539628-LLP-1-2013-1-NL-ERASMUS-EIGF) is entitled: *Governance and Adaptation to Innovative Modes of Higher Education Provision* (GAIHE), it is funded by the Education, Audiovisual and Culture Executive Agency (EACEA) through the Lifelong Learning Programme and it is run by a consortium of 11 partner Universities: Ecole Normale Supérieure de Lyon (France), University of Strasbourg (France), Lucian Blaga University of Sibiu (Romania), the Higher Education Policy Research Unit of Dublin Institute of Technology (Ireland), Academic Unit of the University of Latvia, Comenius University and the University of Ss. Cyril

and Methodius (Slovak Republic) the University of Maribor (Slovenia), the University of Salamanca and the University of Alicante (Spain) and RAND Europe (Cambridge). The consortium partners are coordinated by the School of Governance (SoG) of the University of Maastricht, Netherlands. Project Duration is 36 months (01.10. 2013 to 31.03.2016).

Project Background

This project aims to study governance and management changes of higher education institutions that have become increasingly fragmented ('unbundled') as a result of new technological advances and globalisation. It sets out to identify the resulting innovations, analyse their motivations, drivers, barriers and impact on the management and governance of higher education, as well as investigate the role of the university governance and management in innovative provision.

In its assessment and for clear project purposes and reference, the project reviews significances of such terms as: *innovation*, *governance*, *management* and *unbundling* and places them in the current HE European space. Hence, an *innovation* is taken to mean the implementation of a new or significantly improved product (good or service), a process, a new marketing method, or a new organisational method in business practices, workplace organisation or external relations, according to UNESCO [1]. In addition, this project assumes that innovations have an increased added value, for example, in terms of how learning takes place and how it is organised.

A broad debate already admittedly exists around identifying educational innovations and their origins, however for the purpose and practical matters of this project, educational innovation is considered to be a trend that has expanded over the past five years and has attracted considerable attention, having admittedly the potential to provide fundamental alterations to the higher education offer. The *governance* of universities is responsible for overseeing its activities, determining its direction and monitoring the process whereas the *management* of universities is in charge of its operational running. In what regards *unbundling*, it represents “the process of breaking down a recently stable

product unit size into component parts, forcing margin reduction and lower prices for consumers” [2] and, in higher education, various educational innovations are modifying this traditional model, making it possible to segment the educational offer by providing separate alternatives online offers.

Indeed, online offers have revolutionised the ability to unbundle the traditional educational offer, which typically merges content, learning & teaching, assessment & credentialing, research & development, and business management [3]. Massive Online Open Courses (MOOCs) constitute an example of this trend toward the unbundling of content delivery [4]. With the rising new generation of tablet-toting, hyper-connected youth, the university will continue to extend its reach to students around the world, unbounded by geography and time zones, at a fast pace and at a fraction of the cost of a traditional college education. “MOOCs are best viewed as higher education’s version of TV networks offering individual shows (i.e., parts of the bundle) online for free” [5]; they provide access to recorded lectures, online tests and digital documents as alternatives to traditional classroom instructions. Instead of attending a face-to-face course, students may attend one course online, typically free of charge. Various MOOC initiatives, including Coursera or the Kahn academy, have been very much talked about in the US and beyond. Although the number of MOOCs has tripled since March 2013 [6], there are still twice fewer MOOCs than non-European MOOCs. But ‘unbundling’ of higher education includes not only MOOCs but franchising as well. Apple’s online university, Wikipedia, or YouTube also provide additional learning channels. In addition, franchising represents the right to ‘brand’ products (deliver assessment and credits) so long as the franchisee adheres to strict standards and policies. As a result, branch campuses have multiplied [7] and have occurred wherever such extensions were possible, albeit such new developments are not being adopted uniformly, nor, one might add, without controversy [8]. Just to quote an example, the UK had 400 franchise arrangements in 2008. Likewise, currently there are seventy eight branch campuses registered worldwide, including thirty seven in the UAE, 18 in Singapore, 10 in Qatar, seven in Malaysia, two in Botswana and four in Hong Kong [9].

Research Questions

Such ‘unbundling of delivery’, through partnerships, spin-out organisations, franchising and the fragmentation of knowledge and information provision [10] as well as the growing range of providers, encouraging new delivery models (for example providing IT or e-based services) are apt to pose many and significant managerial challenges. In this context, ‘traditional’ higher education institutions have to rethink their governance models in order to adapt to these changes and domestic reforms.

Being able to understand how higher education adapt to these changes is important because modern history contains many examples of industries that failed to see the signs of

major disruption early enough to avoid painful consequences to their businesses [11].

‘Traditional’ higher education provision typically includes a concentration of activities in the institution, a reliance on public grants and state control through *a priori* command and control rather than a *posteriori* evaluation, which does not necessarily match the new forms of management described above, based, for example, on unbundling and fragmentation. New managerial types are emerging, including the ‘Amazon university’, (based on e-learning and sharing content), the *on-demand university*, where students tailor their courses and credits over a period of time, the *learning hotel*, which continually changes flows of collaboration and interchanges between academic scholars and corporate, government or professional practitioners, as well as the *umbrella university*, which sees the university as a cooperative rather than a self-contained entity with fragmented activities, the university becoming a ‘holding structure with a conglomerate of separately managed businesses’[12]. Further models include the ‘Corporate University’ [13], arguably said to represent a “paradigm shift in the development of organisational human capital” [14] which is strategically oriented toward integrating the development of people as individuals with their performance as teams and ultimately as an entire organisation.

Against this background of changes in the landscape of higher education provision that have challenged the ‘traditional’ model of university and its future, the project aims to provide answers to several emerging key questions:

- How do/can higher education institutions innovate their modes of provision, all the while respecting the quality of higher education?
- How is higher education management adapting to these new modes of provision?
- Do higher education institutions innovate through a distributed leadership, which facilitates the adoption of bottom-up initiatives [15] or given a strong core, with a clear top-down innovation strategy [16]?

The project rests on a comparative analysis resulting in a final report including policy recommendations, survey results and case study reports. It is intended to inform and support the exchange of best practices among higher education management, national ministries and the international higher community regarding innovative modes of higher education provision. The desk research involved ENS and DIT, the survey DIT, Maribor and Comenius University whereas the case study analysis was led by the University of Latvia, the University of St Cyril, University of Alicante, University of Salamanca and ENS Lyon. The final report elaboration is to be shared between the University of Maastricht, the University of Latvia and Comenius University of Bratislava.

Preliminary Research Results; the Literature Review

The basic purpose of the literature review (LR) was to prepare a starting point for the survey and case studies design. So far, the LR has been completed and focused mainly on:

1. Description and analysis of innovations related to the modes of higher education provision as well as the governance and management of higher education institutions in a global framework.
2. Identification of the drivers and outcomes of innovation in higher education in Europe.
3. Making new connections between existing research on the challenges facing higher education and possible solutions offered by innovative modes of provision and innovative institutional governance or management implemented elsewhere.

Furthermore, the LR reviewed classification, benefits, and disadvantages of distributed leadership as well as leadership types resulting from a failed implementation of distributive leadership. The main outcomes were built on the works of Bolden et al (2009), Bennett et al (2003), Simkins (2005), Creanor (2011), and Jones et al (2012)[17].

The LR discussed also how selected actors like: a) university personnel (both academics and administrative staff), b) students and even the c) institutions themselves can potentially either facilitate or impede the introduction of innovation in higher education.

As change agents, certain trends may impact students' expectations of higher education and attitudes toward learning. The current cohort of students is variously described as "digital natives", "new millennium learners" or the "net generation". They are characterized by non-linear thinking, multitasking, and interactivity, and their heavy reliance on technology and more specifically the internet that are also likely to push for structural and organizational innovations. The teaching staff plays perhaps the most active role in independently implementing innovation from the bottom up. Academic entrepreneurs could be viewed as those higher education actors who innovatively leverage internal and external opportunities to not only generate economic resources for their own profit or in support of their academic units and institutions, but also to create within the academy social and political change platforms. Despite of the fact, that academic institutions are many times described as possessing a culture of resistance to change, one of the key changes that can be made in order that institutions might benefit from both approaches and engender adaptive but sustainable innovation is by introducing flexible approaches that contribute to an institutional culture of creativity and openness. In essence, this entails combining elements of negative and positive liberty; i.e. on the one hand adopting a position of non-interference and removing barriers where they exist, and, on the other, providing the appropriate support and resources where required.

As change barriers, it has been found that many students are uncomfortable with unfamiliar techniques and scenarios. Certain departures from traditional pedagogical methods can leave students, at least in the short term, disoriented. As for the academic staff, ongoing refinement of adaptive technologies that can provide tailored feedback, and

the rise of team-based learning and peer-review style assessment, as well as the diminishing role of the academic as the 'gatekeeper' of knowledge can appear to undermine the skills of the teacher. With regards to more structural changes related to the introduction of the entrepreneurial university model, Jacob et al. (2003) identified the deficiency of entrepreneurial champions and leaders amongst the staff as the staff related barriers to the entrepreneurial turn, and the reasons for the absence of an entrepreneurial culture within the university [18]. As for the organizational obstacles, apart from institutional resistance to innovations in the area of education provision, there is also evidence in the literature that institutions can act as barriers to the implementation of different structural and governance modes in higher education institutions.

Besides the analyses and their basic results described above, the LR raised several questions and tested the validity of the hypotheses related to the linkages between the various innovations introduced by higher education institutions. In doing this the focus was on correlations between innovative modes of higher education provision and changes in institutional governance and management. The posed questions were: 1. Do universities with a centralised leadership and a traditional core have more traditional educational provisions de facto? And conversely, do institutions with a decentralised leadership automatically have an entrepreneurial strategy with innovative modes of education provision? How relevant are organisational structures in comparison to teaching professionals in the adoption of innovations? What is the sequencing of change events? Do changes in the organisational structure of institutions arise before educational innovation or can the latter create broader changes? Finally, what are the benefits of these educational innovations, if at all?

In conclusion, the LR highlighted that the higher education institutions are nowadays facing numerous challenges resulting from various global shifts and trends. The factors driving innovation were identified under five headings: the knowledge-economy, accessibility (or the appearance of mass education), financial pressures (due to primarily declines in public funding), the changing role of universities (i.e. increased pressures for universities to enhance development and boost innovation on a regional and national level) and disruptive innovation. Furthermore, universities are also increasingly pressured to adopt a third role (alongside teaching and research) and act as agents of innovation and development on both the regional and national levels.

These drivers of innovation have led universities, among others, to introduce more innovative modes of provision (e.g. online learning and the use of different social media) as well as to challenge their traditional structures and innovate in the areas of higher education governance and management (which have been conceptualized in literature by the theories of Entrepreneurial University or Distributed Leadership). Further, the LR found it useful to distinguish these drivers of innovation from what are here referred to as agents of change – students, teaching staff, and higher education institutes. Interestingly, these agents of change also emerge in the literature as barriers to innovation,

demonstrating the wide variation in attitudes to, motivations for and results of higher education innovation.

In the LR it was assumed that the higher education institutions have responded to those challenges by introducing various innovations in their systems and structures. Those have led to the introduction of more innovative modes of provision which include, among others, online learning and the use of different social media. Furthermore, universities have also challenged their traditional structures and introduced various innovations in the areas of higher education governance and management. Many of the changes introduced by universities have been conceptualized in literature by the theories of Entrepreneurial University or Distributed Leadership, with the former evolving around the ideas of tightening relationships with the private sector, promoting universities as innovation hubs, emphasizing the developmental role of universities and many more while the latter (which in fact is to an extent embodied within the former) underlines the need for diffusion of responsibilities and control within the institutions. It is also worthwhile mentioning that success or failure of the implementation of innovations in higher education is largely dependent on the individuals and institutions related to it.

The changes in modes of provision as well as institutional management and governance can potentially be correlated and impact one another. However, an analysis of the relationship of the aspects is very challenging due to rather limited empirical data available on the matter. To illustrate, although there appears to be a wealth of literature on innovative modes of higher education provision, much of it consists of descriptions of and extrapolations from small-scale case-studies; surveys on the implementation of very specific innovations; or policy recommendations prescribed as largely untested remedies to identified ailments. The selection of empirical research on technological and pedagogical innovations reviewed also broadly suggested ways in which institutional governance could provide support, but these again remain in the realm of recommendation rather than data on adaptations already implemented. The apparent sluggishness of institutions to respond to innovation is perhaps due to the fact that those surveyed, although diverse, can generally be characterised by their student-centred, distributed and flexible approach to education provision, which has been found to be difficult to cater for in the context of higher education institutions' typical hierarchical and bureaucratic structures. Thus, a thorough empirical investigation into the consequences of the innovations is needed to draw more concrete conclusions regarding their impacts on each other and on the higher education landscape as a whole.

Preliminary Research Results; the Survey

Below are the initial findings and observations based on the 21 responses so far received to the 'Survey on the Governance and Adaptation to Innovative Modes of Higher Education Provision' (the survey). The survey was circulated on April 1st, April 8th, April 22nd, and April 29th 2014 to potential respondents that had been identified in 47 European higher

education institutions (HEIs) based in 9 countries. Based on the responses a number of trends are clearly discernible:

It is generally accepted by respondents that significant innovation has taken place throughout the HEIs surveyed since 2008. In terms of the 'level' of innovation, there is evidence that 'module' level innovations dominate over 'programme' or 'institution'. Unsurprisingly, the use of 'new technologies' is seen as an emerging trend in response to crisis, however their use has not always been considered successful. Similarly there is evidence of varying degrees of participation between institutions, with some institutions having merged, and many more (90% of respondents) describing the establishment of 'partnership(s) with other institution(s)' since 2008. However, the success or effectiveness of these moves is also questioned by participants.

Other measures such as a focusing on research-based study and real-life experiences have also been used as a way of innovating. A range of other factors were posited by respondents in terms of innovations since 2008, including the need to respond to 'societal/economic needs and regional accessibility', and the need for 'efficiency and better use of resources'. Furthermore, unsurprising measures including increases in 'progressive internationalisation' as well as improvements in 'learning outcomes' and 'graduation rates' are also mentioned.

The question of leadership of innovation is interesting. Top management/rector-level and university teaching staff are regarded as significant for innovation/change leadership, while students, admin staff, and library staff are regarded as relatively less significant, as are the media, and general public was relatively low.

An interesting area is the varying significance of government and local authorities, and institutional autonomy, which may reflect different traditions in different parts of Europe. A range of factors are seen to inhibit innovation such as: insufficient financial resources, insufficient skilled personnel, absent/insufficient control mechanisms, lack of leadership to support/understand change, and related to this, 'Insufficient vision for innovativeness'. Measures that emerge as relatively important in this context included the decentralization /transfer of greater responsibility for decisions and budgets to faculty or school level, and changes to HEI mission statements. This may indicate an institutional commitment to innovation, without necessarily recording any significant change. Noticeably, a greater focus on quality assurance has not been seen as an important factor in the institutions surveyed.

The survey recorded an increase in the demands made on academic staff as well as (a relatively smaller) increase in demands of flexibility from academic staff. Related to this, there is greater emphasis on information sharing and cooperation within institutions. In terms of future challenges, it is clear that respondents see the next years and decades as challenging for HEIs. Improvements in technology, increased use of blended learning, improved teaching methods, internationalisation and search for funding and resources will be central to successful change. Academic staff are seen by the

respondents as central to this change, and appropriate support for them will be essential.

Conclusions

The ongoing project has so far completed two of its most important stages: the LR and Survey. The governance of higher education institutions has been shown to be key to the diffusion of innovative practices for teaching and learning, but it is still not yet clear how these will evolve. There are two more set milestones before successful completion: the case studies of particular, small-scale implementations of technological, pedagogical and/or organisational innovations and the policy recommendations (in the form of a report) produced for relevant national bodies or (supra) governmental and multilateral organisations.

With all results so far obtained, the GAIHE research project represents *the first European-wide analysis of these innovative modes of provision in Europe*, leading to opportunities for enhanced quality teaching and learning. It is apt to fill a gap in our current knowledge and understanding by investigating the evolution of new modes of provision in teaching and learning across Europe, the motivations for the emergence of these new modes as well as how higher education management and governance have adapted to these new modes of provision. Its added value is represented by its significant contribution to decision-makers, higher education institutional managers, educators and importantly learners, providing them with an up-to-date assessment on new modes of provision and relevant policy recommendations. Nonetheless, the project is more than just a mere evaluative exercise. Its strong informative component is an added value and, as a useful education tool, it is practical to use, sustainable and effective, providing an argumentation for policy-makers to support innovation.

REFERENCES

- [1] UNESCO *Oslo Manual - Guidelines for collecting and interpreting innovation data*, p. 46, Paris: 2005, UNESCO URL: <http://www.oecdilibrary.org/docserver/download/920511e.pdf?Expires=1384342823&id=id&accname=ocid56013842&checksum=E1E7DA3E2312AB5F66F892C5734C9B0A>
- [2] Ferreira, J., "The Unbundling of Higher Education", in Knewton Blog, 26 February, 2014. Available: <http://www.knewton.com/blog/ceo-jose-ferreira/unbundling-higher-education/>
- [3] Sheets, R.G., Crawford, S., (2012), "Harnessing the Power of Information Technology: Open Business Models in Higher Education", EDUCAUSE Review 47, no. 2, March/April 2012, accessed 17 July 2012, <<http://www.educause.edu/ero/article/harnessing-power-information-technology-open-business-models-higher-education>>.
- [4] Fowler, G. 'An Early report card on MOOCs', in *Wall Street Journal*, R; and *Wall street journal*, 'The Opportunities and risks in the MOOC business model', 15th of October 2013.
- [5] University Ventures 'The Great unbundling – popping bundles, not bubbles', UV Letter - Volume II, #17, 2012, Available: <http://universityventuresfund.com/publications.php?title=the-great-unbundling>
- [6] Open Education Europa, EC. Available: http://www.openeducationeuropa.eu/en/european_scoreboard_moocs
- [7] Altbach, P. 'Franchising: the McDonaldisation of higher education', in *International Higher Education*, 66 Winter, 2012. Available: https://htmldbprod.bc.edu/prd/f?p=2290:4:0::NO:RP:4:P0_CONTENT_ID:116549
- [8] Wilkins, S. and Huisman, J., 'The International branch campus as transnational strategy in higher education', in *Higher Education*, 64:628, 2012.
- [9] Ibid.
- [10] Universities UK, *Futures for higher education: analyzing trends*, London: U.K, 2012.
- [11] Squires, L., Husmann, E., (2012), "Closing the gap between perception and reality for Open Education", European Foundation for Management Development (EFMD), EFMD Global Focus, January 2012.
- [12] P.A. Consulting group Escaping the red queen effect, *Escaping the Red Queen Effect; Re-thinking the University in the New Economics of HE*, London: P.A. Consulting Group, 2008.
- [13] Prince, C. and Beaver, G. 'The Rise and rise of corporate university: the emerging corporate learning agenda', in *The International Journal of Management*, 1(3), 17-26.
- [14] Holland, P. and Pyman, A. "Corporate Universities: A Catalyst for Strategic Human Resource Development" in Department of Management Working Papers Series, Working Paper 39/05, May 2005.
- [15] Jones, S., Lefoe, G., Harvey, M., & Ryland, K. (2012). Distributed Leadership: A Collaborative Framework for Academics, Executives and Professionals in Higher Education. *Journal of Higher Education Policy and Management*, 34(1), 67-78.
- [16] Clark, Burton (1998), *Creating Entrepreneurial Universities: organizational pathways of transformation*, Bingley: Emerald Group
- [17] Smith, K. 'Lessons learnt from the literature on the diffusion of innovative learning and teaching practices in higher education', in *Innovation in higher education and teaching international*, 49(2): 173-82, 2012.
- [18] See Bolden, R., Petrov, G., & Gosling, J. (2009). *Distributed leadership in higher education rhetoric and reality*. Educational Management Administration & Leadership, 37(2), 257-277; Bennett, N., Wise, C., Woods, P. A. & Janet, A. H. (2003). *Distributed Leadership: A Review of Literature*. National College for School Leadership; Simkins, T. (2005) *Leadership in Education 'What Works' or 'What Makes Sense'*? Educational Management Administration & Leadership, 33(1), 9-26; Creanor, L. (2011) *Scholarship, leadership and technology: a case study of embedding evidence-based practice*. Conference: Asilite 2011- Changing Demands, Changing Directions. West Point, Hobart, Tasmania, Australia, 4-7 December 2011; Jones S., Lefoe G., Harvey M. & Ryland, K. (2012). *Distributed leadership: a collaborative framework for academics, executives and professionals in higher education*. Journal of Higher Education Policy and Management, 34(1), 67-78.
- [19] Jacob M, Lundqvist M, Hellmark H (2003) Entrepreneurial transformations in the Swedish University system: the case of Chalmers University of Technology. Research Policy 32(2003):1555–1568

Development and Analyses of “M-LearnSys” Mobile Learning Course Management System

Bekim Fetaji¹

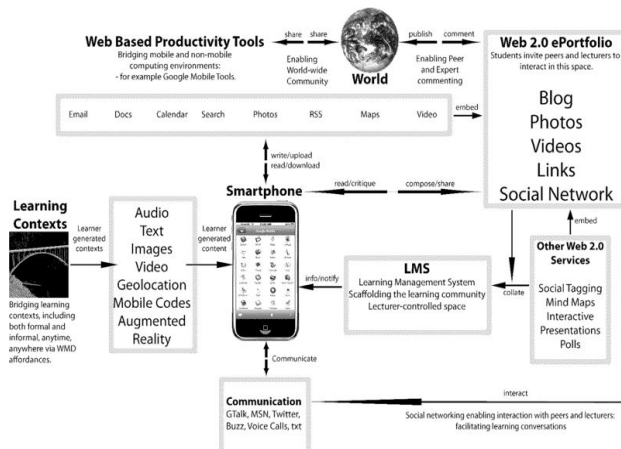
South East European University,
Contemporary Sciences and Technologies, Computer
Science
Ilindenbska bb, 1200 Tetovo, Republic of Macedonia
b.fetaji@seeu.edu.mk

Abstract - The research study investigates the development approach and analyses of m-learning course management system developed as case study. The contribution of the research study is the analyses of the task based instructional strategy and conceptual definition of the assessment methods regarding the level of mobile learning outcomes while assessing different software engineering aspects of development mobile application for Windows phone 8. The analysis also covers the development with primary focus on mobile learning using ASP.NET MVC 5 technology, and design issues for responsive techniques. Finally insights are stated, results of the analyses are provided and recommendations and discussions of the approach are described.

Keywords— Mobile Learning Course Management System, M-learning analyses, conceptual development

I. INTRODUCTION

Because the constant changing of the technologies, how the learners learn and interact, their demands are constantly growing for different types of learning materials [2], [3]. For example we might say that a professor has shared youtube.com video URL and the professor demands of the student to know the context of the particular video. The older management system did not allow the users to share easily video URL's [9]. Then the students had to copy the link and transfer it to a web browser, and the content can be easily accessed by a single click, and be opened by a mobile browser quickly and from anywhere at any time.



Majlinda Fetaji², Jovica Saveski², Mirlinda Ebibi²

South East European University,
Contemporary Sciences and Technologies, Computer
Science
Ilindenbska bb, 1200 Tetovo, Republic of Macedonia
m.fetaji@seeu.edu.mk, js17035@seeu.edu.mk,
m.ebibi@ibu.edu.mk

Figure 1. Mobile Web 2.0 Concept Map[2]

This interoperability has inflicted the need to create new and improved learning systems, that not only could assist the learning of contents but also speed up the process of interaction, allow different ways of conducting it, and allow for it to be accessed literally from any device or any place.

II. ANALYSES OF M-LEARNING PROJECTS AND TRENDS

An example of mobile learning system called GoLearn from the initial Merrill Lynch pilot is given by ADL Mobile Learning Team [9]. Standards for delivery on the BlackBerry were established in design, technology, security and privacy. The goals of the pilot included proving the access, usage and the effectiveness of learning delivered via the BlackBerry to the global population. Additionally they sought to:

- Deliver training with no degradation to learning effectiveness
- Achieve 25% of eligible participation
- Achieve a comparable average score to the control groups, and
- Obtain a 10% higher completion rate in 10% less time

Over a seven-week period, the learning materials were wirelessly pushed to over 2,100 investment bankers and select support staff.

The outcomes exceeded the goals. Higher scores were obtained in half the time. Bankers who completed the training did so in 54 less minutes and tested higher on the final assessment tests than the remainder of the firm. Mobile users also completed their training twenty days earlier than those who trained via MLU.

According to [8] VPs and higher leveraged the mobile materials the most. Of the 2100 eligible employees, 61% launched the content at least once. 317 people completed 704 courses. Overall the mobile learners obtained a 12% higher completion rate in 30% less time than the control group.

170 employees responded to a survey indicating:

- 99% felt the format and presentation supported the learning
- 100% would complete more training in this format
- More than 75% praised the benefits of convenience, time management and training with no distractions

With this successful pilot, Merrill Lynch moved into the next phase with additional training topics such as onboarding for new hires, ethical decisionmaking, performance management, market abuse, and sexual harassment.

According to [4] there is an increasing number of colleges and universities who are adopting mobile wireless technologies as teaching and learning tools. More than 90% of public universities and 80% of private universities in the US have some level of mobile wireless technologies, such as mobile wireless devices and networks.

According to [4] Task based learning as instructional strategy has been shown as the most appropriate for mobile learning compared with inquiry, project and problem based learning. The user filling the 4 task defined each semester week out of 15 weeks is guided and not left alone but instructed and forced to work regularly and in exact time periods.

An important advantage of the handheld computer and mobile devices in general is that can be accessed from anywhere at any certain time, providing learning resources to be articulated in the learning and other actions [4]. There are advantages in using a mobile device offering individual, private and learning at own pace and learning within specific contexts which can provide ‘reliable cultural and environmental indications for understanding the uses of information which may enhance encoding and recall and enable learners to access relevant information when and where it is needed’. The learners and institutions that consume m-learning systems because of the changing dynamics and can benefit from it.

III. RESEARCH METHODOLOGY

The study focused on fundamental research on m-learning, current projects and trends, exploratory research regarding the conceptual design and afterwards action research to build a software solution to test the insights gained from previous phase. In order to evaluate the results the solution was evaluated from different participants. Participants were students, teaching and administrative staff of the Contemporary Sciences and Technologies Faculty of the South East European University.

IV. CONCEPTUAL DESIGN

The main purpose of the web application is to provide learning system to students, professors and educational institutions with option to be accessed from anywhere at any time. In this regards the web application is available for any internet capable device such as mobile phone devices, mobile touch devices (tablets and slates) and

television sets with internet connection through a browser. This application at this first version primarily focuses on knowledge assessment for students with given administration rights to the professors following the guidelines from [11].

The M- Learning aspect of this application gives it a huge importance in today’s dynamic world where distance learning and constant connectivity to internet are a regular state. On the other side the usage of the ASP.NET MVC 5 framework gives it a huge advantage because it is the latest technology and the easiest framework available to maintain in regards of updating the business logic or the design.

Primarily the idea was to make just a quiz generating application, but during the research I realized that what this world lacks of is more learning assessment systems based on mobile learning and using latest and best technologies. Learning assessment systems now are hugely needed not only to evaluate the knowledge of the final user, but also to specify the direction in which the learning process should go and declare where the final user did not pay attention.

This application also has a big advantage in the aspect of scalability, and for development, testing and presentational purposes, will be hosted on the Cloud, a cloud hosted by Microsoft called Windows Azure [13].

In essence the main research questions is: “how to develop a good and easily changeable and maintainable m-learning web application accessible from any device?”

Below is given the Activity diagram in which are represented the activities in a general form for the web application. Represented is the flow of the application. At first the client needs to access the website where he has only access to data that is available to all users. If he wishes to interact with the web application he needs to verify his credentials. He sends his credentials information’s to the ASP.NET identity membership provider [10]. He is then verified by the application using the Azure MS SQL Server.

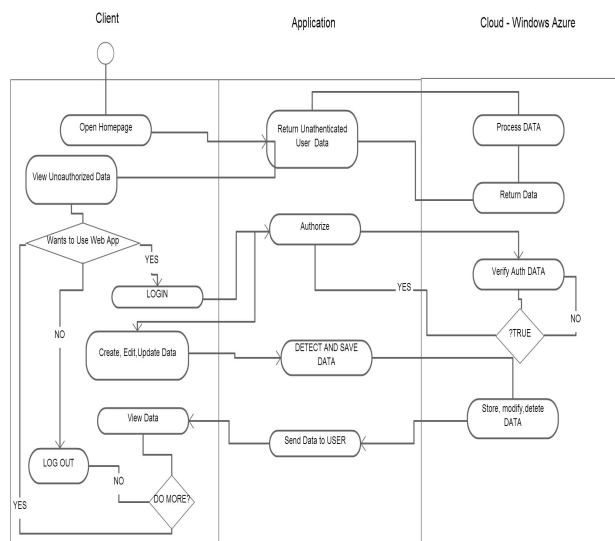


Figure 2. Activity diagram of the developed solution

If the user gets verified correctly he has access to the web application. If the user wishes to interact with the application, according to his role in the system the user gets different options. In general the user can create, edit and update data on the web application. For example, if the user has a role of administrator he has access to every functionality of the web application except for solving quizzes which is a functionality of the web application only accessible to users with the role student [1].

The data is stored on Microsoft SQL Server on Windows Azure Cloud [5], [6], [7], [10], [12]. When the user is finished, if he wants to delete his session, cookies and exit the application he can easily log out.

On figure below is shown the sequence diagram for an example scenario when an administrator is creating a course. Here we have four objects which literally present the Model View Controller software architecture [13]. When the user first demands a website resource he is firstly encountered in the background of http process with the routing rules of the application. In MVC the paths, URL's or routes are defined in the routing module [12]. The application decides where it will send the request to, to which controller it will be directing the user. The controller gets the data from the model which takes the data from within itself connecting to the database and applies its methods and presents the data to the end user using the view [5].

Sequence Diagram Create Course

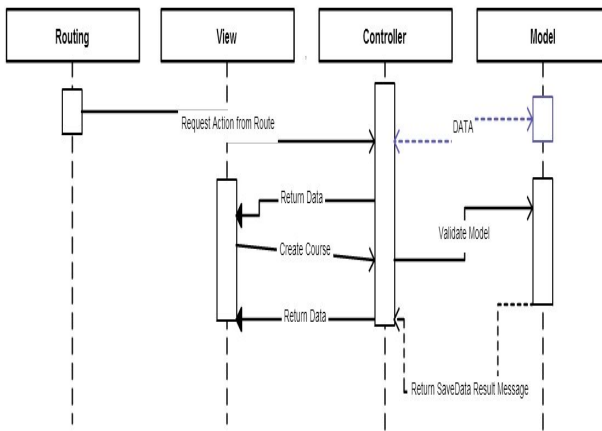


Figure 3. Sequence diagram of the developed solution

Created the following classes: Course, Enroll, Quiz, Question, Answer, StudentQuizTake and studentAnswers. We are using these classes in order to organize my web application in a way that the system has courses which have students enrolled.

In each course created quizzes with questions and answers. Afterwards when the student goes's to solve a quiz he creates a new instance of the StudentQuizTake class as an object.

The user fills the StudentAnswers class with his answers to the appropriate questions in the quiz. In order to differentiate users from one another will be using the new ASP.NET identity membership provider.

The ASP.NET identity uses the following classes: UserRole class, ExternalLogin class, LoginViewModel class, User class, UserSecret class, RegisterViewModel class, Role class, UserLogin class and ManageUserViewModel class.

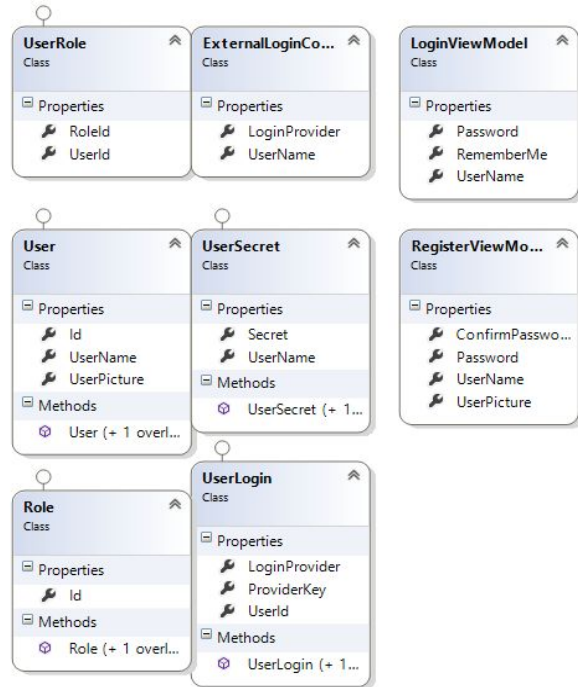


Figure 4. Class diagram identity

V. DEVELOPMENT ASPECTS AND APPROACH

The name of the developed solution is M-LearnSys, and it is developed in ASP.NET MVC 5.

We have used Microsoft Visual Studio Ultimate 2013 Preview, .NET Framework 4.5 folowing the guideliness from [11] and [13].



Figure 5. The screenshot of the developed solution

According to [13] Microsoft defines the ASP.NET MVC framework as follows: The Model-View-Controller (MVC) architectural pattern separates an application into three main components: the model, the view, and the controller. The ASP.NET MVC framework provides an alternative to the ASP.NET Web Forms pattern for creating Web applications. The ASP.NET MVC framework is a lightweight, highly testable presentation framework that (as with Web Forms-based applications) is integrated with existing ASP.NET features, such as master pages and membership-based authentication. The MVC framework is defined in the System.Web.Mvc assembly.

The developed solution is a cloud application; it is being hosted on Windows Azure Cloud platform by Microsoft. It is using a SQL Server on the cloud. This feature of the web application gives it enormous advantage because it is scalable, flexible and cost friendly. In one in a million case it could happen that the page in its first month of being published online to get thousands of users. Having the web application on the cloud allows me to scale the servers up and get new processors for serving the website, expand database space or the other way around.

Another of its best features is that the security of the application is being provided by a cloud service. Also if the server fails the cloud system transfers the applications to another server and in seconds time it is up.

In order to differentiate the web application users we have created a filter that is used just as an attribute in a declaration of controller classes. The code for the authorization filter follows:

```
namespace Mvc5website1.Filters
{
    [AttributeUsage(AttributeTargets.Class |
    AttributeTargets.Method)]
    public class AuthorizeRedirection : AuthorizeAttribute
    {
        private const string IS_AUTHORIZED =
        "isAuthorized";
        public string RedirectUrl =
        "~/Error/UnauthorizedUser";
        protected override bool
        AuthorizeCore(System.Web.HttpContextBase
        httpContext)
```

This filter allows us to easily restrict access or allow access to a particular role in the controllers. So just by using “[AuthorizeRedirection(Roles = “student”)]” The code communicates with the ASP.NET MVC Framework that will only allow access to the particular action or controller to the users which have a role of “student”.

Also listed all of these classes in the DbContext class called MyDbContext. The DbContext class is used by Entity Framework to reference the already declared classes in the project, in order to allow Entity Framework to understand what the developer wants its business logic/model work like. Upon starting the application, if the DbContext classes in instantiated the referenced classes or DbSet's in DbContext are created as entities in a database which connection string have declared in Web.config.

Entity Framework analyses the defined classes and looks at the data types, the relationships declared between the class properties of different classes. If the class contains Data Annotations, Entity Framework uses them to constraint the values, define foreign keys or just change the display name [12].

We have enabled Entity Framework Migrations in the web application project. With the enabling of Entity Framework Migrations allowed automatic migrations, and allowed Entity Framework to update the database model automatically based on the changes made in the classes declared as DbSet's in my DbContext class. So in the case when wanted to add user pictures to the user class and save that information to the database Entity Framework upon calling detects the changes in the model and applies the changes to the database.

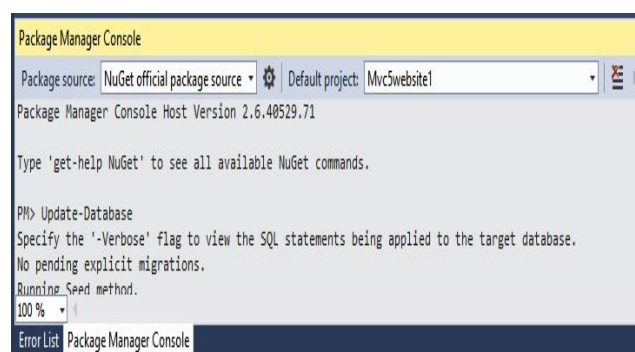


Figure 6. Database migration

The “Update-Database” shown in figure above tries to detect the changes in the model and finds out there is no pending explicit migrations, and finally executes the Seed method. I have created a Seed method that populates the database with startup users and roles as seen in the use case diagram I have three user roles and those are administrator, professor and student. For each role I assigned one startup user.

On the screenshot below is shown the management panel where the administrator of the web application can change the roles of the users registered to the web application.

| Profile | Sys Engine | About | Contact | Dashboard | Courses Panel | Hello administrator! | Log off |
|---------------|------------|-------|---------|-----------|-----------------------------|----------------------|---------|
| jovica | | | | | ChangeRoles | | |
| admin2 | | | | | ChangeRoles | | |
| studenttest | | | | | ChangeRoles | | |
| administrator | | | | | ChangeRoles | | |
| professormain | | | | | ChangeRoles | | |
| BekimFetaji | | | | | ChangeRoles | | |

Figure 7. Administrator options available

The following screenshot displays the view for creation of a course. Only the administrator has the right to create courses. Also only he has the privilege to edit or delete them. Professors who are owners of a course, can only edit the information about the course they own, and if they try to change a course that they do not own, the Course Controller in the web application will redirect them to an error “Unauthorized”.

Only the administrator has the right to delete a Course from the web application.

Upon Creating a Quiz, the Professor or Administrator will declare the duration of the Quiz. So if a Quiz is declared by the professor with 20 minute mark, the student will only get results for the answers he gave in that period.

Course

Course Title: New Course

Course Code: New Course Description...

Course IsActive:

User: professormain

Create

Figure 8. Course creation functionality

The only place, that only a student has access to, it is the student controller which is used to display his quiz data and direct the user to solve the quiz. When a student starts to solve a quiz this system notes the time when the user has started solving the quiz. In the meantime for each answers submissions the application stores the student's answers. After the student finishes the quiz, the result is given to him.

VI. NATIVE MOBILE CLIENT ON WINDOWS PHONE 8

The project also includes a native mobile client on Windows Phone 8. This native mobile application gives the user who in this case is the student the options to check in the system in which courses he is currently enrolled in, the option to view the quizzes that he needs to solve (he has not solved them yet) and view the names of the quizzes he has already solved. In the case if the user decides to solve another quiz or just visit the web application he can use the button to go to the web application, in which case he is transferred to default browser.

Used a Microsoft HTTP client libraries in order to bring the common functionality of the HttpClient class.

```
c1 = new HttpClient();
c1.BaseAddress = new Uri("{URL}/api1/");
```



Figure 9. Native mobile application for Windows Phone 8

VII. TESTING

In order to check if the existing and planned functionality of the application is all right, conducted tests on four kinds of display.

First and foremost tested the functionality, usability and design on a Windows 8 (15" display monitor). Afterwards tested it on a 10" android tablet. After summarizing the results of the previous two devices conducted another two tests. One on a 4" Windows phone HTC 8s and finally tested the application on a 42 display using a television set.

The results were satisfying in the means of that in every device the user could access the needed data, functionality and resources. The front end of the web application was equally responsive to the display size and type on every devise.

Engaged and had the help of 10 collaborating testers, who tested the web application and gave me feedback. All of the feedback that was received was positive, and helpful. The beta testers during the time of testing and feedback giving gave advice on some other features that might be implemented in the future.

They successfully managed to access to web application, also it was easy for them to create courses and manage them. They used the panels to create quizzes, and even made a small competition among them taking the quiz.

Five advanced users were among the beta testers which had some kind of knowledge of the process of creating applications. And five of them were regular users which interests were not developing applications, but using it for their own needs and for sharing an expanding the knowledge among people.

Different beta testers got different users roles, some of them were students, some of them were professors and some were administrators.

VIII. CONLUSION

The study tried to contribute with analyses of the conceptual design and development aspects of an M-learning Course Management System. As development platform used ASP.NET MVC 5 and although at the time of its development it is a relatively new framework it has flawlessly worked during the creation, testing debugging and publishing the project. The web application works in the defined parameters and specs and is equally functional and tested its responsive on a Windows 8 laptop (Asus k52jt), on Android Tablet (10" Quart QP1070), and on HTC 8s Windows Phone (4" mobile phone).

The web application after the testing is evaluated a useful to the students as it is for the professors; it allows interaction between the standing parties. The best feature of the web application is that it is available equally among all capable devices. It saves the precious time of the professors, giving immediate results to the student, without the need for the professor to check each and every one of the quiz takes, if the professor needed to check all of the quiz results by hand. That is another advantage, if the student base expands, the professors cannot manually manage the learning assessment in the same time as they did before.

A great feature is that it can be easily changed, in a way that the market demands. The web application can easily be upgraded to become a big learning management system, with features like no other. Feedback from users can quickly be heard and implemented, thanks to the MVC software architecture pattern.

In the future we can implement a fully grown API, for all kinds of developers, and make it more available to even more devices, such as Raspberry PI, Windows Kinect, and even an electronic news feeder tool.

If this web application is implemented in another institution, it can quickly adapt it to its needs. For example

if this web application is implemented as an assistance tool for conferences guests' lottery, we can add this functionality fast using Entity Framework Migrations.

For the future work intended is to add more common functionality, such as course based real time chat, messaging, file sharing, library and wiki panel.

REFERENCES

- [1] Christian Gross (2008), Beginning C#: From Novice to Professional, 2008
- [2] Dominic Betts, Alex Homer, Alejandro Jezierski, Masashi Narumoto, Hanz Zhang (2012), Moving Applications to the Cloud 3rd Edition, 2012
- [3] Dominic Betts,Alex Homer, Alejandro Jezierski,Masashi Narumoto,Hanz Zhang (2012), Developing Multi-tenant Applications for the Cloud 3rd Edition, 2012
- [4] Fetaji Majlinda., and Fetaji, Bekim., (2008) "Universities go mobile: Case study experiment in using mobile devices" – ITI IEEE conference, Dubrovnik, Croatia, 2008
- [5] Jeffrey Palermo, Jimmy Bogard, Eric Hexter, Matthew Hinze, and Jeremy Skinner (2012), ASP.NET MVC 4 in Action, 2012
- [6] Jess Chadwick, Todd Snyder, and Hrusikesh Panda (2012), Programming ASP.NET MVC 4, 2012
- [7] Jon Galloway , Phil Haack, Brad Wilson, K. Scott Allen (2012), Professional ASP.NET MVC 4, 2012
- [8] Judy Brown and Jason Haag (2011), Mobile Learning Handbook, 2011
- [9] Kim, S.H., Mims, C., & Holmes, K.P. , 'An introduction to current trends and benefits of mobile wireless technology use in higher education'. AACE Journal, 14(1), 2006
- [10] Mahesh Chand, (2002) A Programmer's Guide to ADO.NET in C#, 2002
- [11] O'Malley, UoN , G. Vavoula, UoB, J.P. Glew, UoB, J. Taylor (2003) OÜ,M. Sharples, UoB,P. Lefrere, OU, WP 4 – Guidelines For Learning/Teaching/Tutoring In A Mobile Environment, 2003
- [12] Simon Robinson,Christian Nagel,Jay Glynn,Morgan Skinner,Karli Watson,Bill Evjen (2004) Professional C# Third Edition, 2004
- [13] Tom Dykstra (2012), Getting Started with the Entity Framework 4.1 Using ASP.NET MVC, 2012

A Survey on Mobile Augmented Reality Based Interactive, Collaborative and Location based Storytelling

P. Sagaya Aurelia

Department of Computer Science
Faculty of Education
Beniwalid, Libya
Sagaya.aurelia@gmail.com

Durai Raj

Department of Computer Science
Bharathidasan University, Tiruchirappalli,
Tamilnadu, India.
durairaj.bdu@gmail.com

Omer Saleh

Department of Computer Science
Faculty of Education
Beniwalid, Libya
immer.jomah@gmail.com

Abstract--Mobile technology improvements in built-in camera, sensors, computational resources and power of cloud sourced information have made AR possible on mobile devices. This paper surveys the field of mobile augmented reality and how it is used as interactive, collaborative and location based story telling medium. This survey provides a starting point for anyone interested in researching or using Mobile Augmented Reality and interactive storytelling irrespective of the application.

Keywords-- *Digital storytelling, Human Computer Interaction, Immersive environment, Interactive storytelling, Mobile Augmented reality, Mixed reality,*

I. INTRODUCTION

This paper surveys the current state-of-the-art in Mobile Augmented Reality and how it is used as a medium for Interactive, Collaborative and location based storytelling.

A survey paper does not present new research results. The contribution comes from consolidating existing information from many sources and publishing an extensive bibliography of papers in this field. This paper provides a good starting point for anyone interested in beginning research in this area[2].

Section 1 describes what MAR is, and Interactive storytelling. Section 2 explains the related works based on interactive book. Multimodal, Multi-User and Adaptive Interaction for Interactive Storytelling, Location based storytelling, Storytelling in Collaborative Augmented Reality Environments. Finally, Section 3 draws reviews and conclusions.

II. DEFINITION

1. Augmented Reality:

Extend Azuma's [Azuma et al. 2001] definition of AR to MAR in a more general way as follows:

- Combine real and virtual objects in a real environment.
- Interactive in real time.
- Register (align) real and virtual objects with each other.
- Run and/or display on a mobile device.

We do not restrict any specified technology to implement a MAR system. Any system with all above characteristics can be regarded as a MAR system. A successful MAR system should

enable users to focus on application rather than its implementation [Papagiannakis et al. 2008].

MAR is the special implementation of AR on mobile devices. Due to specific mobile platform requirements, MAR suffers from additional problems such as computational power and energy limitations. It is usually required to be self-contained so as to work in unknown environments. AR and MAR supplement real [1].

III. INTERACTIVE STORYTELLING

Interactive storytelling is a form of digital entertainment where authors, public, and virtual agents participate in a collaborative experience. Crawford [2004] defines interactive storytelling as a form of interactive entertainment in which the player plays the role of the protagonist in a dramatically rich environment. The experience offered to the public by an interactive story differs substantially from a linear story. An interactive story offers a universe of dramatic possibilities to the spectator. In this form of entertainment, the audience can explore an entire set of storylines, make their own decisions, and change the course of the narrative.

Typically, the way viewers interact with a storytelling system is directly linked to the story generation model: character or plot-based model. Character-based approaches [Cavazza et al. 2002][Young 2001][Aylett et al. 2006] give to the system great freedom of interaction. Usually, the story is generated based on the interactions between the viewer and the virtual characters. In some cases, the viewer can act as an active character in the story. In plot-based approaches [Grasbon and Braun 2001][Ciarlini et al. 2005], the interaction options are quite limited. The users can perform only subtle interferences to guide the progress of the narrative plot[3].

1. Interactive Augmented reality storybook:

Listening to stories draws attention to the sounds of language and helps children develop a sensitivity to the way language works'', said by Isbell [14]. She stated that children tend to learn more while they are listening to stories because stories are fiction which most of it are fairytales that will not happen in the reality. It challenged children's imagination, hearing and seeing while listening to stories. Therefore, AR was brought in to build a system which include audio and graphics

which allows children not only to read aloud with but interact with the system at the same time [4].

1.1 Multimedia Interactive Book (*miBook*)

Compared to previous AR book setup which needed some initial setup before usage, this mobile AR book concept can be used directly as a normal user reading a normal book. Thus, it will reduce the learning hassle as well as increasing the interactivity between user and book. This so called playbook is mainly focused on two parts which consist of physical book and mobile application. Mini Interactive Book is a new tool providing a responsive environment and an interactive learning, which handles with different type of content.

miBook is the combination of a printed book (or its digital format) with the respective audiobook and its 3D models (as well as the 2D graphics). Technologically, *miBook* environment consists of a handheld camera, a personal computer (to generate user's individual scene views), and a physical book. *miBooks* uses "normal books" with text and pictures on each page and have an additional audio content – the correspondent audiobook.

By supporting a real-time AR texture-tracking algorithm, which uses the novel feature detection technique from Bastos and Dias (2007) (see Figure 1), the enhancement of global algorithm performance allows the support of different hardware profiles, both in desktop and mobile setups. It also includes the possibility of tracking several images/textures at the same time and it supports several 3D standard formats (3DS, VRML, OBJ, DXF, Cal3D, among others). As we can see on Figure 1, there is no need to have the black borders as tracking marks. The first picture on Figure 1 (left side) is the 2D sheet of a book and the right side one shows a 3D object registration where someone is interacting in real time with *miBook*. As for interactivity enhancement, *miBook* features provide a physic engine to enable scientific simulations. It will also enable audio storytelling with virtual elements interaction (Script) and both artificial intelligence and speech recognition algorithms for user guidance. All features may be available both in desktop and mobile (PDA or Smartphones) setups, being one of the biggest breakthroughs for the AR community [5].



Fig. 1 – Example of virtual object registration in a real scene in *miBook9* (texture image and registered scene) [5]

The application of the *miBook* solution to new forms of learning can be naturally and fully under control of users (both students and educators). The new interactive way of linking traditional pedagogical approaches (such as reading printed books), common devices capabilities (like handheld devices with camera) and the potential of multimedia technologies

(audiovisual interpretation technologies) can provide a better understanding, knowledge acquisition and enhanced learning experience[5].

1.2 An Interactive Mobile Augmented Reality Magical Playbook:



Fig. 2 General structure of the magical playbook [6]

The prototype concept of AR book presented in this paper is shown in Figure 2. The overall book design divided into story page and marker page. Story page covered the story line and illustration that illustrated the story within that current page. Marker page consists of marker that representing each 3D character with animation within that current page. This prototype is using handheld display (mobile device) for viewing the augmentation of the book because handheld display will help user to experience the AR concept while maintaining the context of reading normal book.

Natural interaction between user and the physical book should be included in AR book to maintain the context of normal user reading normal book. As AR book, it is aimed to enhance the traditional book, but not to replace the entire book [4]. Thus, the normal interaction with the book such as pointing will be presence in AR book. Tangible User Interface (TUI) in AR is the interaction that uses a physical environment to be tangible while interacting with the AR system [19]. In this prototype, finger can be used to interact with the AR book. Figure 3 shows the interaction with the AR book using Fig [6].



Fig 3 The interaction with the AR book using finger [6]

1.2.1 Mobile Application

Mobile AR application has gaining popularity nowadays due to mobile technology advancement. As mention early, mobile devices advanced in computing power and also in 3D graphic processing. This mobile application developed in Android platform. Figure 4 shows the mobile application installed in Android device.



Fig. 4 Mobile application for AR book installed in Android device [6]



Fig. 5 The user uses the mobile application via mobile device to augment the character of the book[6]

The mobile application included with the ability to augment the 3D character and animation (the crow) with audio onto the marker page of the book. Figure 5 shows the user using the mobile application with the book. This application is not only augmenting the 3D character, animation and audio, but it also provides the users with narrator. The narrator is aimed to help children as guidance for them to read throughout the storyline. The learning number part is shown in figure 6.



Fig 6 Learning number part[6]

Based on figure 6, learning number part is highly interactive designed for children. The user will interact with the book using their finger to count together with animation of the augmented 3D character on the book, leaving the natural means interaction between the user and the book. From here, the concept of engaging the student within learning environment in the learning process is fully applied[6].

1.3 Augmented Reality Children Storybook (ARCS)

The system will provide read aloud function so that children can listen and read along at the same time because much of the language children learn reflects the language and behaviour of the adult models they interact with and listen to [8]. Figure 7 shows the system architectural of the project [4]

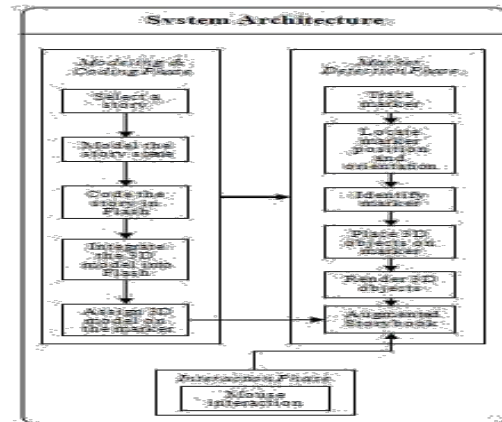


Fig. 7: System architecture graph for Augmented Reality Children Storybook (ARCS)[4]

As the targeting audience are the young learners who aged from 4 to 12 in Malaysia, the application have to be engaging and enjoyable so that it will motivate them. Hence, fun and attractive interface will help to capture the children's interest. However, every child has different learning skills and levels. Therefore, various stories will be included in the application for different categories of interest. The stories will include categories such as picture books, fiction, traditional literature which includes myths, legends and fairy tales and so on [4].

1.4 Children 's Interaction with Augmented Reality Storybooks

The story used for the prototype of the AR storybook was written in collaboration with two friends. The artefact in this study is a prototype of an AR storybook and the target group is eight-to ten-year-old Norwegian children. The AR book will be augmented using virtual 3D models, sound and interactive tasks. Sketching up a use case diagram as shown in figure 8, where user activities as well as system responses are the main focus [9].

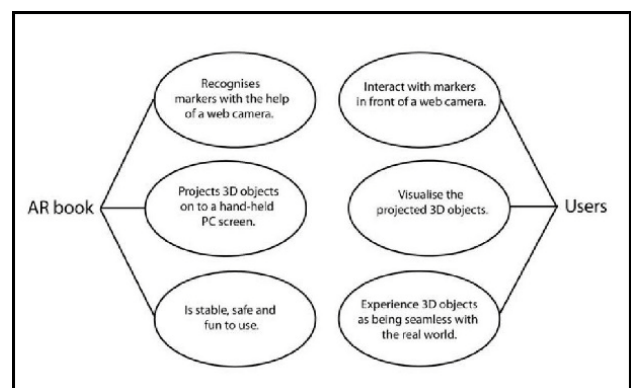


Fig. 8: Use case diagram of Children 's Interaction with Augmented Reality Storybooks [9].

BuildAR Pro tracks and identifies markers in order to overlay the real world with virtual content. While writing the story, it had been decided that animals would be used for augmentation. Therefore, it was only natural that the pattern on the markers would also be animals, and markers were designed using more or less the same degree of detail [9].

1.5 Interactive Playspaces for Object Assembly and Digital Storytelling

A. Playspace

A playspace is an interactive system that aims to combine the advantages of doing a task physically and virtually. Figure 9 shows the novel active systems for virtual 3D content design applications – Block model assembly, Digital storytelling and 3D Scene design. In this setup, the user works on a planar work surface. The surface is divided into two parts – Play Area and Control Boxes. Any physical objects in the Play Area are tracked in real-time using the Kinect R color+depth camera.

The Play Area is exactly mapped to a part of the virtual world which is rendered on the display screen in front of the user.

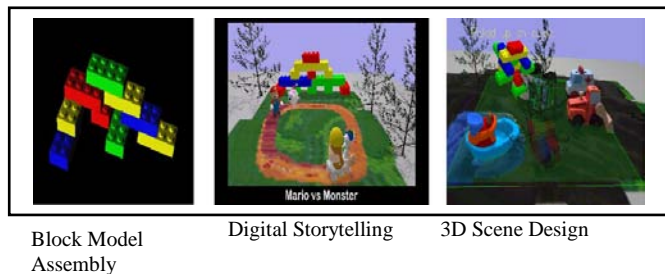


Fig. 9: The novel interactive systems for virtual 3D content design applications – Block model assembly, Digital storytelling and 3D Scene design [7].

The tracked motion of physical objects is reflected in the virtual world in real-time. The Control Boxes can be used for gesture-based inputs [7]. Software framework of a playspace is shown in figure 10. The streams from the input modalities are given as input to the playspace algorithms – RGBD Processing module (for camera feed), Voice Recognition module (for microphone feed) and Event handlers for keyboard and mouse. The outputs of these algorithms are given as controls to the application running on the playspace. The application renders the virtual world and provide context-specific visual feedback on the display screen.

B. Assembly of Block Models.

Building block models with Lego R or Duplo R blocks is a popular hobby across adults and children. The block sets usually come with a set of instructions to put together a preconfigured model.

A system named DuploTrack is introduced, where a user works in a playspace with physical Duplo R blocks to build a pre-defined model. The system uses a novel 3D-tracking based guidance method to present instructions to the user. It also tracks the assembly process in real-time, points out any mistakes and helps correct them. The capability to track the assembly process also enables the system to learn how a new block model is assembled by a user. This learned representation can be used to share the model with other users via automatically generated representations like virtual 3D mesh models, static instructions, instruction videos or by bootstrapping it back into the system for guiding a new user [7].

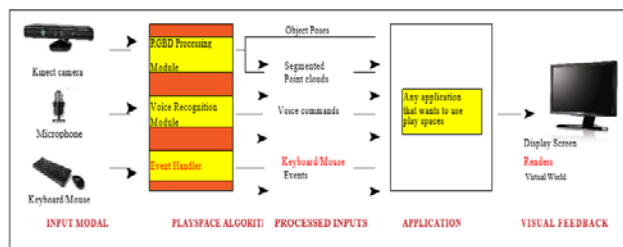


Figure 10: Software framework of a playspace

C. Digital storytelling:

The system allows a user to act out a story using rigid puppets and automatically converts that into an animation. Further, it also allows the user to record multiple takes for the same story and merge them automatically after the user has roughly annotated them based on his liking. This is helpful when the user wants to try out different styles and later merge them [7].



Fig. 11(a) Toys for storytelling. Fig. 11(b) 3D-Puppetry system for story telling

Figure 11: Natural and intuitive interfaces for storytelling. (a) Toys and puppets are the traditional ways of natural story telling. (b) The 3D-Puppetry system tracks the moving physical objects using a Kinect R camera and renders their tracked virtual replicas

An intuitive interface to tell a visual story for novice users is through physical puppets and toys (Figure 11.a). Hence we can develop systems which automatically track and transfer the acted out motion to virtual characters and hence record an animation.

The 3D-Puppetry system uses the framework of a playspace. Figure 11.b shows a user using the system. As is the case with playspace framework, the user first scans in the physical objects that he intends to use in the story. Then he acts out the story using objects in the Play Area which the system tracks in real time and renders replicas in a pre-selected virtual environments on the display screen in front of the user. This rendering is also recorded as a video which is the resulting animation. This system allows user to use some keyboard and mouse-based controls to edit the animation later by changing light positions, camera viewpoint etc [7].

II. Multimodal, Multi-User and Adaptive Interaction for Interactive Storytelling

The design of multimodal, multi-user, and adaptive interaction model follows some requisites for the design of multimodal interfaces described by Reeves et al. [2004]. Adapting some of these concepts to the interactive storytelling domain, defines the following requisites to the interaction system [8]:

Natural Interaction: The multimodal interaction must be natural. The viewers must feel comfortable interacting with the system;

Adaptable Interaction: The multimodal interface must adapt itself to the needs and abilities of different viewers;

Consistent Interaction: The result of an input shared by different interaction modalities must be the same;

Error Handling: The system must prevent and handle possible mistakes in the interaction, as well allowing the viewers to easily undo their actions;

Feedback: The system always must give a feedback to the viewer's when some action resultant from a multimodal interaction be executed;

Equal Interaction: In a multi-user scenario, the interaction system must offer equal possibilities of interaction to all viewers [8].

The multimodal interaction interface is based on gestures and speech. The choice of these interaction modalities was made due to the need of natural interaction modalities in a multi-user setting. Gestures and speech provide a natural interaction interface and allow the interaction of several users by using computer vision and speech recognition technique. The viewers are free to use both interaction modalities[8].

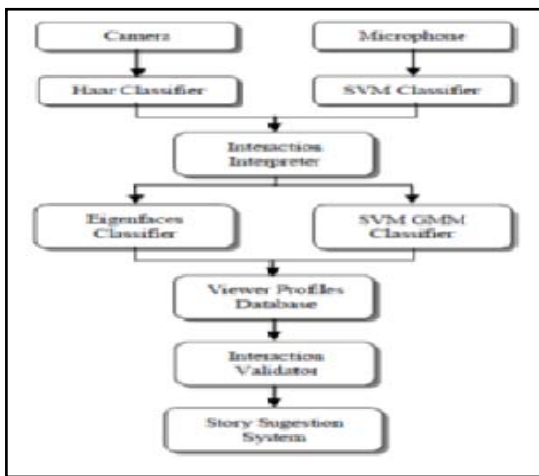


Fig. 12 Multimodal, Multi-User and Adaptive Interaction architecture [8]

The architecture of the interaction system presented in this paper as show in figure 12. The system uses a conventional camera and a microphone to capture the input of the system. The vieweres are located on the video input by the Haar Clasifier alogrithm, and the viewer's speech is recognized by the SVM Classifier based on the audio input. The interaction Interpreter module analyses and interprets and the viewer's gestures and speech commands. Next, the Eigenface Classifier and the SVM GMM Classifier identify the viewer based on the profile of the viewers (which is stored in the Viewers Profiles Database). Each interaction is the recorded in the appropriated viewer's profile. The profile management updates the viewer's profile based on the viewer's interactions and the atmosphere traits associated to the events as modeled in the Atmosphere

Database. Before the viewer's interaction affects the system, the Interaction Validator module checks if the viewer is not interacting for the second time in the same option (for example to avoid a viewer voting more than one time in the same option). Finally, the user interaction is sent to the Story Suggestion System [8].

III. Location-based Storytelling in the Urban Environment

The user experience and user interaction with the system was designed using sketching, mockups, and paper prototypes in parallel with the story writing activity. We wanted to combine the digital elements of the story with tangible interactions with real-world locations and objects such as inscriptions and symbols on buildings, paper maps, and physical props similar to what might be found in a theatre production of the story.

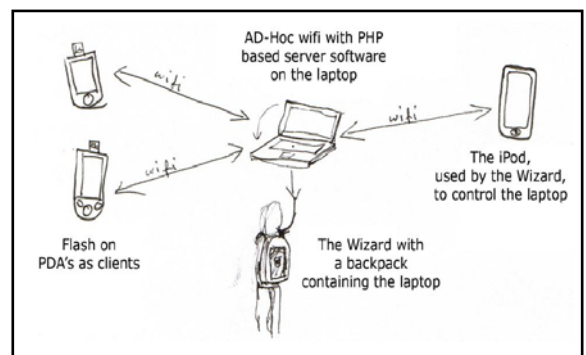


Fig. 13 Technical set-up of the prototype.[10] Proceeding from one scene to the next

Other props explored included marked envelopes with physical evidence or clues to be opened at particular points of the story, and to be passed between the users. Another approach explored to tie the digital experience closely to the physical surroundings was the use of printed photographs of actual locations in the user's current surroundings overlaid with fictional characters and objects from the storyline [10]. Technical set-up of the prototype is shown in figure 13.

Once the two detectives have gathered enough pieces of information at a particular location they are prompted to move on to the next scene at a different place. Rather than providing way-finding information on the PDAs for this purpose, the users are provided with a physical map of the city with key locations of the story highlighted. However, in order to keep the path through the city flexible and secret, each location is annotated with a unique symbol rather than numbers or letters, making it impossible for the detectives to know where to go next. Increasing the challenge, the correct symbol can only be obtained through collaboration. Based on the information gathered from individual interrogations, each detective will at some point in time be provided with half the symbol needed to move on. Only when both halves have been obtained is it possible for the two participants to work out go to next by locating the corresponding composite symbol on the physical map (figure 14) [10].

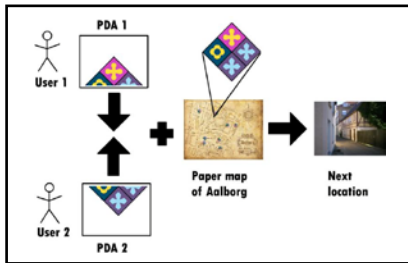


Figure 14. Finding the next location of the story from a composite symbol and a physical map [10].

IV. Storytelling in Collaborative Augmented Reality Environments

Figure 15 shows the architecture of the system in regard to the several modules and layers used. Every layer is parted in several AI sub-modules to improve the possible evolution of the systems abilities, as we wanted to design a reusable software system with the possibility to replace modules in regard to project specifications and scientific research ideas [11].

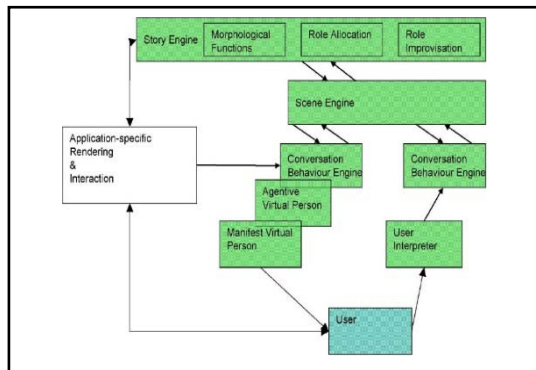


Fig. 15: Architecture of CSCIS system[11]

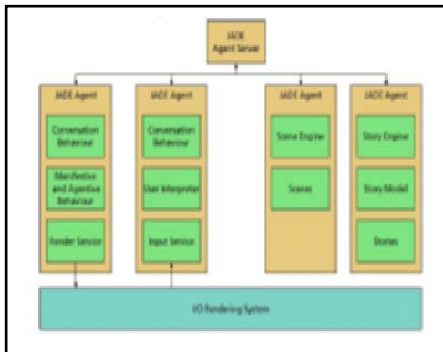


Fig. 16: Development of the CSCIS System[11]

Figure 16 provides a sketch of the implementation of the system. We used several AI-related software packages to develop the story engine (done with Prolog), as well as the conversational behavior, agentive and manifest modules of the several agents, with these agents playing roles (virtual characters) in AR story environment (done with Jess, the Java Expert System shell [Fri01]). Communication between the several modules is done using the JADE Agent Platform [Bel01].

The authoring process of Interactive Stories is supported in regard to the definition of scenes for the AR environment and the relation of scenes to the morphological story model

(functions and roles), as well as to improvisational features: see Schnieder [Sch 02] [11].

D. Digilog book for temple bell tolling experience based on interactive augmented reality

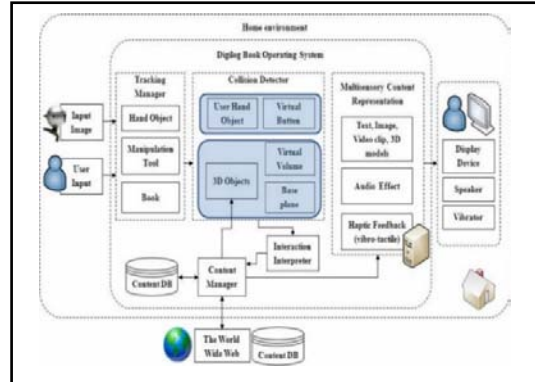


Fig. 17 Dialog Book system architecture[12]

Fig. 17 shows the Dialog Book system architecture based on the proposed interactive AR system. Based on input images from a camera, a computer vision based tracking manager recognizes and tracks a paper book, a manipulation tool, and a hand object. The collision detector then inspects penetrations between a virtual line created by the manipulation tool and a bounding volume of the augmented 3D objects that are based on the book. The detector also checks an occluded area between the virtual buttons and the user's hand objects. At this point, the interaction interpreter conducts examinations like 3D object pointing and hitting, movement interactions or hand interactions for pushing virtual buttons[12].

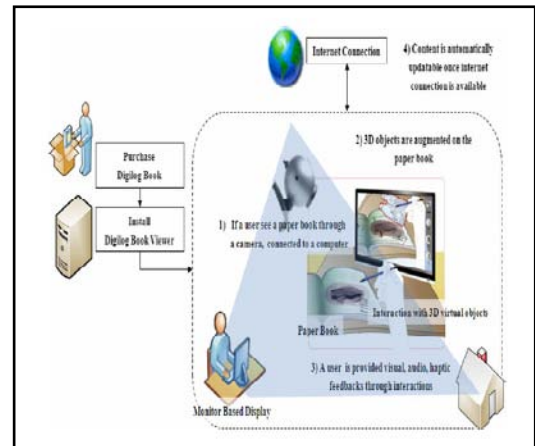


Fig. 18 Conceptual figure of Dialog book usage[12]

Next, the content manager composes proper multisensory content in order to react to the user input. The multisensory content consists of visual feedback (text, images, background sounds) and haptic feedback (vibro-tactile interactions). Finally, a display device, a speaker, and a vibrator of the manipulation tool represents the multisensory content. Additionally, if AR content in a remote database is updated, then the AR content of a Dialog Book will be updatable through an Internet connection [12]. Fig 18 shows conceptual figure of Dialog book usage.

V. User Interaction in Mixed Reality Interactive Storytelling

The approach used in [13] is character-based, which means that the narrative is driven by the individual roles of each of the virtual actors, rather than by an explicit plot representation. The actors' roles are formalised as plans, which are executed in real time using a modified Hierarchical-Task Network planning algorithm. During execution, the planner selects the next action for a character, this action being played in the virtual environment, which is also updated to take into account its consequences. When an action fails (i.e. its intended outcome is not achieved), another course of action is generated through replanning. The real-time selection of action supports interactivity, as the user can interfere with the environment, changing the executability conditions of potential actions[13]. The system overview of user interaction is shown in figure 19.

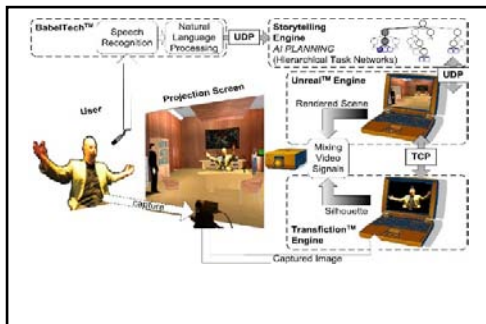


Fig. 19 System overview of User Interaction in Mixed Reality Interactive Storytelling [13].

III. REVIEW AND CONCLUSIONS

The combination of mobile augmented reality and interactive storytelling can be used in various applications. The Interactive augmented reality storybooks surveyed in this paper are available both as physical book and AR book[5][6]. It can also be used in Mobile phones (PDA and smart phones)[4][6] and [5] can be used in desktop and mobile phones. With reference to markers, [4] author as used visible, black bordered markers whereas, work [5][6] uses invisible markers which is one of the added advantage to the application. The basic difference between all the surveyed paper lies in the different user interaction. [4] uses mouse interaction, [6] uses tangible user interface (finger), [8] uses multimodal interactions (gesture and speech), [12] uses hitting, movement interaction or hand interaction. The real- time selection of action supports interactivity, as the user can interfere with the environment changing the executable condition of potential actions [13]. Considering the story engine, several AI related software package are used to develop the story engine in [11]. Some of the other features are multi modal (gesture and speech), multi-user, Adaptive Interaction (based on viewer's option), location based, Collaborative and Interactive options. Education can be much more interesting and interactive by applying computer technologies such as multimedia into in. In order to promote the reading habit to the children nowadays, the Interactive AR Storybooks not only provides knowledge but entertainment at the same time. With so many successful examples of how computer technologies were applied in education, this Interactive Storybooks based on Mobile augmented reality will be one of it as well. The Augmented reality storybooks are used

to learn either English, learning numbers using an old folklore literature or any other subject. Since the children prefer audio and graphics, the Augmented Reality Storybook will provide not only these but allow interaction so that children can learn and play a role in the story at the same time.

IV. REFERENCE:

- [1] Zhanpeng huang, pan hui, christoph peylo, dimitris chatzopoulos
- [2] "Mobile augmented reality survey: a bottom-up approach", arxiv:1309.4413v2 [cs.gr] 18 sep 2013
- [3] Veronica teichrieb, joao paulo silva do monte lima, eduardo lourenç,o apolinario, thiago souto maior cordeiro de farias marcio augusto silva bueno, judith kelner, and ismael h. F. Santos, "A survey of online monocular markerless augmented reality", International journal of modeling and simulation for the petroleum industry, vol. 1, no. 1, august 2007
- [4] Edirlei soares de lima, bruno feijó, simone barbos , fabio guilherme da silva, antonio l. Furtado, cesar t. Pozzer , angelo e. M. Ciarlini , "multimodal, multi-user and adaptive interaction for interactive storytelling applications", sbc - proceedings of sbgames 2011"
- [5] Behrang parhizkar, tan yi shin, arash habibi lashkari, yap sing nian, "Augmented reality children storybook (ARCS) ", 2011 international conference on future information technology ipcsit vol.13 (2011) © (2011) iacsit press, singapore
- [6] Albertina dias, "Technology enhanced learning and augmented reality: An application on multimedia interactive books",International business & economics review, vol.1, n.1 issn 1647-1989
- [7] [6] Azfar bin tomi, dayang rohaya awang rambli,"An interactive mobile augmented reality magical playbook: learning number with the thirsty crow", 2013 international conference on virtual and augmented reality in education doi:10.1016/j.procs.2013.11.015
- [9] [7]Ankit gupta , "Interactive playspaces for object assembly and digital storytelling", university of washington 2013
- [10] [8]Edirlei soares de lima, bruno feijó simone barbosa ,fabio guilherme da silva, antonio l. Furtado, cesar t. Pozzer,angelo e. M. Ciarlini, "multimodal, multi-user and adaptive interaction for interactive storytelling applications", sbc - proceedings of sbgames 2011
- [11] [9]Olaug eiksund, "children's interaction with augmented reality storybooks -a human-computer interaction study", spring 2012
- [12] [10] Jeni paay and jesper kjeldskov , anders christensen, andreas ibsen, dan
- [13] jensen, glen nielsen and rené vutborg, " location-based storytelling in the urban environment", OZCHI 2008 Proceedings ISBN: 0-9803063-4-5
- [15] [11]Norbert braun, "storytelling in collaborative augmented reality environments", WSCG'2003,Februry 3-7, 2003, Plzen Czech Republic
- [16] [12] Taejin Ha, Youngho Lee, Woontack Woo,"Digilog book for temple bell tolling experience based on interactive augmented reality", Virtual Reality (2011) 15:295–309 DOI 10.1007/s10055-010-0164-8
- [17] [13] Cavazza, M. O. et. al. (2003) 'User interaction in mixed reality interactive storytelling', 2nd IEEE/ACM international symposium on mixed and augmented reality in Proceedings of the 2nd IEEE/ACM international symposium on mixed and augmented reality. Washington: IEEE, p.304.
- [18] [14] Isbell, R., " Telling and retelling stories – learning language and literacy", Young Children, 2002, 57(2), 26–30.

Crowdsourcing implementation platform as methodology in process management –BPM- of services information system in health

- Case study collaborative online work Colombian Caribbean Islands system –

Fernando Prieto Bustamante, Yaneth P.Caviativa, Yoan Manuel Guzman, Victor Manuel Castro Rodríguez

Abstract—To give answer to necessities that nowadays presents the object (health), it is required to update its management processes, allowing to be at vanguard of technological advances. Taking into account the above, the proposal is to design an implementation platform, process management and crowdsourcing as an information system of services in health for the Colombian Caribbean Islands system, which includes Secretary of Health of San Andrés Archipelago Department, Providencia and Santa Catalina. The execution of this proposal will allow to evaluate crowdsourcing methodologies of participative online activities, from data collection for the generation of indicators related to: risk management, promotion and prevention programs, and disease control, implementing the application of Integral Care Guides and prevalence of diseases of interest in public health of mandatory for its adscription and relation in a interoperable way with the information integrated system of health of the islands, and Business Process Management (BPM) while evaluating the mechanisms of Vigilance and Control Inspection (VCI), from Health and Social Protection Ministry through the Integrated System of Information of Social Protection (SISPRO in Spanish).

Keywords—business process management, collaborative online work, Crowdsourcing methodology, processes management, promotion and prevention, public health, Vigilance and Control Inspection.

F. Prieto is with Universidad Santo Tomás, Bogotá, Colombia. Phone number: +57 310 572 24 86 (e-mail: fernando.prieto@usantotomas.edu.co)

Y. Caviativais with Universidad Manuela Beltrán, Bogotá, Colombia. Phone Number: +57 1 546 06 00 ext. 1151 (e-mail: janeth.caviativa@docentes.umb.edu.co)

Y. Guzmán is with Universidad Manuela Beltrán, Bogotá, Colombia..Phone Number: +57 1 546 06 00 ext. 1151 (e-mail: yoan.guzman@docentes.umb.edu.co)

V. Castro is with Universidad Santo Tomás, Bogotá, Colombia. Phone Number: +57 3118535005 (e-mail: victor.castro@usantotomas.edu.co)

I. INTRODUCTION

THE necessity of using technology and health areas represents nowadays and increment measured by the adequate use of technological gadgets that increase access factor, which implies to relate access capacity of health system to which to population has granted access. This project searches to implement Process Management in health adequate from the online participative methodology Crowdsourcing which will allow managing all the organization of Information Integrated System in health based in processes, understanding these as a sequence of activities oriented to generate an added value about an input to achieve a result. For which an output that at the same time satisfy the requirements of the information integrated system of Colombian Caribbean islands (case study) allowing to respond to users complaints and necessities, as more and more, citizens, organizations and companies claim to the health sector quality in their services. Critic in health sector management refers to inefficiency of big hierarchical structures of the Administration when trying to adapt to a world in full technological and economic transformation. The development of this management system will allow achieving a system of processes management (health), dealing with important challenges. Between the main challenges that will have to be overcome are: low quality, automatic processes, management and communication heterogeneity of the process at national level; the widespread perception of lack of use of emergent technologies, the deficient and unreliable information, as well as attention time in the service of information from online collaborative participation. Meanwhile, Colombian Caribbean islands Administration system (Case study Secretary of Health of San Andrés Archipelago Department, Providencia and Santa Catalina), will improve its perception about health processes quality with reliable information, granting access to promotion and prevention programs, and disease control implementing the application of Integral Care Guides and prevalence of diseases

of interest in Colombian Caribbean islands public health system.

This methodology allows managing from evaluation and qualification, health territorial direction, and health promoter entities and health services institutions of the Colombian caribbean islands system, San Andrés department, Providencia y Santa Catalina. Crowdsourcing will get and use for its benefit the user contribution, looking for indicators related to Risk Management, disease prevention and control programs, and prevalence of diseases of interest in public health for the department. Thus, through the implementation of this new technology, will be evaluated the Vigilance and Control Inspection mechanisms, access and consult of the information, information quality control, date and certification of health services and effectiveness of components, processes and standards of Guarantee Quality Assurance System and its impact on health services provision to users in an accessible and equitable way.

All the above establish the advantages of crowdsourcing methodology that supports in being a tool of collaborative online type, in which a person, institution, nonprofit organization or company, proposes to a group of individuals, through an open flexible call, the free and willingly fulfillment of a task. The fulfillment of the task, of variable complexity and modularity, and in which the crowd must participate providing their work, money, knowledge and/or experience, implies always a mutual benefit.

II. THEORETICAL APPROACH

A. Problem description

For the Colombian Caribbean islands system from the administration of San Andrés Archipelago Department, Providencia and Santa Catalina, one of the main factors for the tracing, planning and control lies in the management of programs related to Public Health, being this a point of interest from the necessity of the country in this area and particularly in Caribbean region. The mentioned necessity is aligned with Health and Social Protection Ministry politic that considerate in Article 111 of Law 1438 of 2011 a development of an evaluation and qualification system of Health Territorial Directions, of and health promoter entities and health services institutions, as a result of the application of indicators related to: risk Management, disease promotion and control programs, and prevalence of diseases of interest in public health. Similarly in the article 112 of Law 1438 de 2011 commands the Health and Social Protection Ministry to articulate the management and administration of information through the Integrated System of Social Protection Information [1].

Evaluation of attention quality in health establishments in the San Andrés Archipelago Department, Providencia and Santa Catalina, at present, is based on user satisfaction. There are different tools to measure the perception of this satisfaction, not being there any processes nor standardized methodologies for the collection of data in health or evaluation of quality in the Situational Analysis that is not systematized either, likewise the compilation of the consults observations

and clients and providers interviews, are done in an inconstant way or are not even registered nor there is assumption of implantation of any quality system.

For all the above the present research raises the question:

Will the information system for process management and crowdsourcing, using the ICT services, Case study Colombian Caribbean islands system Secretary of Health of San Andrés Archipelago Department, Providencia and Santa Catalina serve for the management of governmental processes in the object of Health?

B. Justification

The implantation of processes management, as politic to incorporate, ingrain quality and continuous improvement in organizational culture of San Andrés Archipelago, Providencia and Santa Catalina Governorship (Case study Secretary of Health of San Andrés Archipelago Department, Providencia and Santa Catalina), as a more decentralized and participative system, that will help achieving resolution 4505 of December 28th of 2012 of Health and Social Protection Ministry, by health services institutions, companies administrators of benefits plans, and for this particular case, departmental direction, where with their work, besides of reducing substantially heterogeneity in the quality level amongst the different types of public health services, will accomplish an information system for process management with the functional administration, assigning "owners" to key processes, making possible an international management generator of value for the user and that, therefore, seeks their satisfaction. In order to do the above, it will be determined which processes need to be improved or redesign in contrast to the ones the governorship has at the present, establishing so priorities and a context to initiate and maintain improvement plans which allow to fulfill established objectives. In this way it is possible the comprehension of the mode that business processes are configured, as well as their strengths and weaknesses.

Against the above article 111 of Law 1438 of 2011, suggests orientate the fulfillment of the development of an evaluation and qualification system of Health Territorial Directions, of Health Promote Entities and Health Service Institutions, as a result of the application of indicators related with: risk management, disease prevention and control programs, and prevalence of diseases of interest in public health. All of this can be executed in adequate way with tools such as Business Process Management (BPM) and processes layout languages such as BPMN (Business Process Management Notation) and crowdsourcing, which purpose is to consolidate all the efforts that would make a government administration system in order to achieve its objectives. BPM and BPMN are presented as a new tendency to increase efficiency in business and generate competitive advantages that market demands. Reason why now is important to have in count that the key elements to achieve objectives are processes and their good administration, since processes occupy a transcendent place in technological initiatives, but are important too because they constitute the way organization can generate value for the client [1].

Therefore, departmental directions, must obey articles 43.1.2; 43.1.3; 43.1.6 and 46 of Law 715 of 2001 and 114 of Law 1438 of 2011; Departmental Directions will be responsible of: a) Recollect and consolidate the registry per person of activities of Specific Protection, Early Detection and the application of Integral Care Guides to the diseases of interest in public health of mandatory, remitted by Health Municipal Directions or Health Services Institutions (IPS as in Spanish) of their services net. b) Report to the Health and Social Protection Ministry, the register per person of activities of Specific Protection, Early Detection and the application of Integral Care Guides to the diseases of interest in public health of mandatory according to Technical Annexed that is part of the Resolution. c) Respond for fitting, coverage and quality of the information reported. d) Carry out technical assistance, training, monitoring and feedback to the Health Municipal Direction, Administrators Company of Benefits Plans including the ones in health exception regime and Health Services Institutions (IPS), which have in their charge the care of people who are not affiliated to the Social Security General System in Health. e) Carry out the verification of the reliability of reported information to Health Municipal Directions or Health Services Institutions (IPS) of their services net.

Besides, it is necessary to find a methodology that eases the use of tools which help to achieve the wished strategy. Business processes management is a sequence of activities that are carried out in series or parallel by two or more individuals or informatics applications, with the goal of finding a common objective. BPM helps to propose a strategy and transform it in measurable objectives. Processes approach allows examining the object (health), through a sequence that goes from macro processes, to procedures and their contribution to the objectives fulfillment, and primarily the relation between what is said, done and obtained.

To achieve the purposes and give answer to necessities that nowadays presents the object (health), it is required to update its management processes, allowing to be at vanguard of technological advances. Taking into account the above, it will be design a system that manages all the processes related to Early Detection and the application of Integral Care Guides for diseases of interest in public health of mandatory, implemented in health services, for their integration into the Integrated System of Information of Social Protection (SISPRO).

It would be of great importance that the Colombian Caribbean island system, from governorship of San Andrés islands, Providencia and Santa Catalina (Study case Secretary of Health of San Andrés Archipelago Department, Providencia and Santa Catalina), count, for their processes management, with a methodological tool which performs all the operations of handling information, related with responsibilities of health department secretary.

III. CONCEPTUAL FRAMEWORK

A. Legal framework

HEALTH AND SOCIAL PROTECTION MINISTRY RESOLUTION NUMBER 0004505 OF 2012 (28 DEC 2012)

By which is established the report related to the register of activities of Specific Protection, Early Detection and the application of Integral Care Guides for diseases of interest in public health of mandatory [1].

B. Theoretical framework

Here are exposed the necessary themes to establish a clear context about the topics or issues related with the crowdsourcing implementation project.

- Process management

Process management implies 'reorder workflows so they add value directed to increase satisfaction of clients and to ease tasks to the professionals'. In this sense, a care process should have a clearly definable mission (what, what for, for whom), demarcated borders with concrete inputs and outputs, clearly integrated sequences of stages, and should be measurable (quantity, quality, cost).

But not every process that is carried out in organizations has the same characteristics, motive by which they can be classified, according to the more or less direct impact on the final user, in the following criteria:

-Strategic processes: they adequate the organization to the necessities and expectations of users. Definitely, they lead the organization to increase quality in services that are offered to its clients. They are oriented to strategic activities in the company.

-Operative processes: those that are in direct contact with the user. They include all activities that generate more added value y have more impact on the satisfaction of users. All clinic-care processes can be considered included in this category [2].

-Support processes: they generate resources that other processes need.

Table. 1 Types of processes. Taken of Xavier Badía

| Strategic or management processes | Operative or key processes | Support processes |
|---|--|---|
| Needed for maintenance and progress of the organization | Direct relation with clients, and the impact on their satisfaction | Support operative processes so they can be fulfilled |
| Strategic plan, Satisfaction surveys, Quality plans, Investigation plans, Self evaluation | Clinic-care process | Patient management, Storage, Hostel, Maintenance, Pharmacy. |

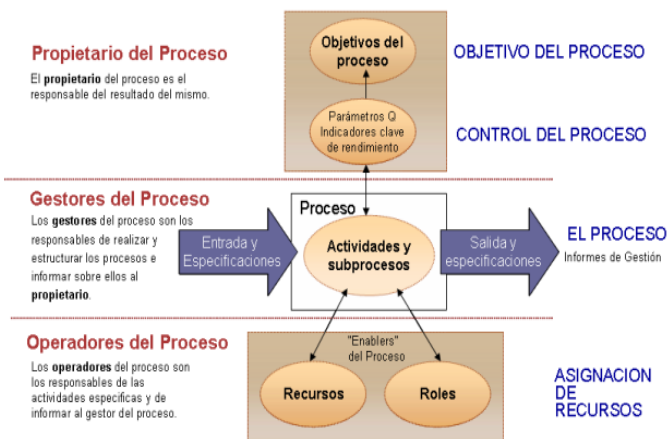


Fig. 1 Process structure [1].

As much as total quality concerns, traditional approval methods are not enough. It is necessary to ensure not only of some determined characteristics of the product or service. It is about certifying that the organization or institution is in position of truly offer, and keep offering in the future, the products/services on demand with the characteristics that are specified, with the fulfillment of deadlines, with attention that user expects, etc, ergo, total quality [3].

Processes Management is based on the assignment of a responsibility directive in each process of the organization. In its most radical form, the departmental organization is *substitute*. In other forms, perhaps transitional ones, departmental structure is maintained, but the responsible of one process has its responsibility, and to what that process refers to, he/she can have authority over functional responsible [4] [5].

- BPM: Business Process Management and its implementation in health sector

BPM emerged as a successfully concept of total quality management (TQM) in the decade of 1980 (Crosby, 1979; Powell, 1995) and business process reengineer (BPR) in the decade of 1990 (Hammer, 1990; Hammer & Champy, 1993; Davenport, 1993). After BPR, various systems of Information Technology (IT), such as Enterprises Resources Management (ERP) and Client Relations Management (CRM) gained organizational approach (Jeston&Nelis, 2008a). The decision to improve business processes as a path to obtain higher performance in the results of organizations is not a new theme. Since beginnings of century, processes have been being approached with different methodologies with the goal of increase financial results of firms. Nonetheless, overtime these initiatives have approached to the improvement problem from perspectives that do not integrate the variables that affect directly in the results of organizational activities [9].

Overtime, vision about processes and organizational improvement initiatives were changing and there was evidence of efforts to make changes in business activities, which were perceived with a higher importance due to the impact in financial performance. From this view were originated systems known as ERP (Enterprise Resource Plannin), which participated as storage elements and consult of information of

process, and did not counted with robust mechanisms to control business process management in integral way [9].

In context of processes improvement, BPM constitutes one of the tendencies in management, which allows in a deliberate and collaborative form to systematically manage all business processes of an enterprise. The benefits of BPM to organizations are extensive: it gives visibility to the directives about processes dynamics carried out in unconscious way by human resources of organization, and makes possible its quick modification to accelerate the adoption of change in operations companies [10] [11].

To Khan Rashid, business process management is a discipline for shaping, automation, management and optimization of a business process through its life cycle with the goal of obtaining higher profits.

Howard Smith on the other hand, defines BPM as a new approach to address and manage innovation processes in companies, which constructs improvement, from the actual state of a process in a determinate time and that raises a radical difference in front of reengineering; which constructs improvement from total redefinition of process. In this view, BPM becomes an answer to the operative chaos that presents companies nowadays [13] [14].

After the impact of Workflow in the nineties, BPM is considerate its evolution, for this reason is interesting to take into account the concepts and terminology of workflow. In fact, the organism Workflow Management Coalition (WfMC) defines it as: "the automation of a business process, totally or partly, during which documents, pass information or tasks from one participant to another for the action, according to a group of procedure normative". [6] [11] [15] [16].

BPM is based on information technology to automate tasks and to give agility to required changes for the enterprise. The technology that makes possible the implantation and adoption of BPM constitutes a new category of informatics systems called Bussines Process Management System (BPMS). Unlike traditional information systems based in data management, these systems specialize in business process management [17].

Generally and integrally, BPM can be defined as an improvement in business processes management of an organization from beginning to the end, from the deliberate, collaborative and increasing definition of technology, so in that sense attain clarity in strategic direction, alignment of resources of the organization and continuous improvement discipline, all of which are necessities and critical to fulfill the expectations of clients. The role of business processes modeling is to allow vision of processes in different levels (strategic, tactic and operational) as well as identification of processes optimization necessities in those levels.

At present, a question might surge and is how can the organization execute adequately and optimize processes? Organizations only count with two forms of implementing strategy: projects and processes. A project is "a temporal effort that is carried out to create a single product or service", while a process can be define as "a group of activities that transform inputs in products of value for a client" (Hammer & Champy). It is important to note that projects themselves are formed by processes and that 80% of failure or success in projects is related to good administration [20] [21] [22].

In this context, surges with strength the initiative called Business Process Management (BPM) that can help to consolidate all the previous efforts. In year 2000, Gartner (Lawrence, 1997) predicted that BPM would be the next grand phenomenon; and later commented that “BPM wins the triple crown for saving money, saving time and adding value”. Another study executed by BPM Institute showed that 96% of respondents indicated that a processes centered approach was critical for success in their company [11].

- Crowdsourcing

The term crowdsourcing was proposed by Jeff Howe in year 2006 on Wired magazine. Its etymological meaning, separating the two terms that conforms it -crowd and sourcing- means sourcing or supplying from a crowd or multitude.

When defining the term, Howe argues that crowdsourcing is –the fact of taking the job that usually was done by an employee and externalize it to a undefined and generally group of people through an open call.

Obviously, this term, as Howe defines it, is possible thanks to Internet and associated information technologies. Before the era of Internet, the fact that there were a crowd in determined moment depended on the physical proximity of people conformed it. Now, thanks to Internet and the rest of related technologies, it is relatively simple to have virtual crowds, which physical distance can be of thousand kilometers.

Attending to the definition, we can adapt crowdsourcing to health thanks to a net of specialized contacts, each of one in their own matter, on which consults are carried out by an “open call” that has information and wants to share it with the user easing very much the work. Teamwork sensation is wide, and a highly recommended experience, since feeling part of a community is one of the inherent characteristic of human being.

Crowdsourcing methodology helps to center in the patient so that collaboratively, new designs are established, problems are solved, or solutions are given to patients with not so frequent diseases, and that are applied in collaboration between actors for the resolution of problems in health sector. Patients who live with their illness know much more and can provide useful and relevant information to other patient in the same conditions about personal a necessary cares, and also difficulties that the sickness brings, sometimes more than what the doctor might explain or say. Patients provide support and many advices because they provide the experience that the medic lacks of. Nowadays instead of being consumers of sanity services, they are becoming providers of the own sanity cares [23] [24].

IV. RESULTS

With the development of this proposal, users of Caribbean islands system from the Health Departmental Direction of archipelago San Andrés, Providencia y Santa Catalina, will get benefit from the agility of processes and document search, since it will be more efficient in the provision of their services,

they will be able to communicate quicker and will have more easiness in information management that is required from Healt and Social Protection Ministry through the Integrated System of Information of Social Protection (SISPRO). Finally government will also see benefits since it will be able to have control over Departmental Directions or Health Districts.

Governorship as a future user of the information system will be able to perceive a substantial saving in processes generation as well as in acquisition of an ICT system for this kind of processes, achieving an efficient system which will avoid time expenses to execute procedures since by technology contremps will be avoid.

Users of health system will have a better attention care because the entity will have a more efficient management system being interoperable, which will avoid contremps and will make different procedures to be carried out in organize and agile way.

Design, development and implementation of this proposal will generate a success case, for the implementation of BPM, that will ease an efficient communication and management, which will allow in the future to carry out the implementation of this type of information systems in others departments as well as in different secretaries such as environment, education and planning of the same department.

V. CONCLUSIONS

The design of an Information System pro the Colombian Caribbean island system within the framework of Governorship of archipelago San Andrés, Providencia y Santa Catalina by processes management and ICT services, is established from the own necessity of health integrated system that guides online collaborative processes that allow to bring closer the user and health system to vanguard, and implements technological tools of information to automate tasks and bring agility to changes required by the state enterprise.

Colombian Caribbean islands system, under this information analysis, can make possible the implantation and adoption of BPM constructing a new category of informatics systems denominated Business Process Management System (BPMS), that for service processes interest, uses better systems of governmental support associated to advance process from online government.

An implementation of a crowdsourcing platform as a proposal for the islands system of Governorship of archipelago San Andrés, Providencia y Santa Catalina, is possible through the insertion of a previous knowledge about its collaborative development, the use of techniques of information update and the environment in which will be carried out, are the main base for its implementation, thus the developer group of the tool will get knowledge based on academic activities since pedagogical engineer that makes stronger and potentiates fundamental dimensions in promotion and prevention systems development; promotion and prevention programs, and disease control implementing the application of Integral Care Guides and prevalence of diseases of interest in public health of mandatory in politics of recent health administration.

The execution of this proposal will allow evaluating crowdsourcing methodologies, by recollection of data for the generation of indicator related to: risk management, disease prevention and control programs, and prevalence of diseases of interest in public health, in the Colombian caribbean islands system, San Andrés department, Providencia y Santa Catalina, relating it in interoperable way with the integrated system of health information of the islands and management itself from the Health and Social Protection Ministry through the Integrated System of Information of Social Protection (SISPRO).

2010, a partir de
<http://www.informaworld.com/smpp/content~content=a921783560~db=all~jumptype=rss>

- [24] » La Larga Estela – El fin de Pareto Babalum. (s.d.). Recuperado Noviembre 10, 2010, a partir de <http://babalum.com/2006/10/12/la-larga-estela-el-fin-de-pareto/>

REFERENCES

- [1] Resolución 4505 de 28 de diciembre de 2012. Ministerio de Salud y Protección Social.
- [2] H.J: Harrington. 1994. *Mejoramiento de los proceso de la empresa*. Tomo 4. Cap. 1”¿Porque centrarse en los procesos de la empresa?”. Colombia: McGraw-Hill, Inc. Traducido de la primera edición en inglés. p. 1-28.
- [3] INSTITUTO COLOMBIANO DE NORMAS TÉCNICAS Y CERTIFICACIÓN.ICONTEC.2001. *ISO 9000:2000 Guía para las pequeñas empresas*. Bogotá Colombia. P 7-25.
- [4] H.J: Harrington. 1994. *Mejoramiento de los proceso...Ob. cit. P. 14-19.*
- [5] H.J: Harrington. 1994. *Mejoramiento de los proceso...Ob. cit. P. 14-19.*
- [6] Van der Aalst, W., ter Hofstede, A., & Weske, M. (2003). Business process management: A survey. *Business Process Management*, 1019–1019.
- [7] Harmon, Paul; Rosen, Michael y Gutman, Michael. (2001). *Developing e-Business Systems Architecture: A Manager's Guide*. San Francisco, Estados Unidos: Morgan Kaufmann Publishers.
- [8] Vom Brocke, J., & Sinnl, M. T. (2011). Culture in Business Process Management: A Literature Review. *Business Process Management Journal*, 17(2), 8–8.
- [9] Sanchez Maldonado, L.F. (2005). Business Process Management (BPM): articulando estrategia, procesos y tecnología.
- [10] Weske, W.M.P. Van der Aalst, H.M.W. Verbeek. (2004). Advances in Business Process Management. *Data & Knowledge Engineering* 50 (2004) 1–8.
- [11] Van der Aalst W.M.P. (2004). Business Process Management: A personal view. Eindhoven (Netherlands).
- [12] Rashid Khan. (2003). Evaluating BPM Software, *Business Integration Journal*. www.bijonline.com (Accedido 20/07/10)
- [13] Smith, Howard & Fingar, Peter. (2003). Business Process Management: the third wave. The breakthrough that redefines competitive advantage for the next fifty years. *Meghan-KifferPress*. Florida (United States of America)
- [14] Lee, R.G. and Dale B.G. (1998). Business process management: a review and evaluation. Manchester (United Kingdom).
- [15] Lawrence Peter, editor. (1997). Workflow Handbook, Workflow Management Coalition. *John Wiley and Sons*, New York.
- [16] Ryan K.L. Ko, Stephen S.G. Lee, EngWah Lee. (2009). Business process management (BPM) standards: a survey. Singapur.
- [17] Havey, M. (2005). Essential Business Process Modeling. *O'Reilly Media, Inc. Introduction to Business Process Modeling*, capítulo 1.
- [18] Zolghadar, M. (2004). Business Process Management and the Need for Measurements. *Appian*. (2008). *On Demand – Business Process Management*.
- [19] Leymann, F. R., D.; Schmid, M.-T. (2002). Web services and business process management, *IBM Systems Journal*, vol. 41, no. 2, p. 8.
- [20] Joyce William, NoriaNitin, Robertson Bruce. (2003). What Really Works. *Harvard Business Review*.
- [21] Sinur Jim, Thompson Jess. (2003). The Business Process Management Scenario. *Gartner Research*.
- [22] Thompson, Michael. (2003). Requirements for effective BPM, *Butler Group*.
- [23] 'New-wave' global firms: Web 2.0 and SME internationalisation - Journal of Marketing Management. (s.d.). Recuperado Octubre 29,

Free Software for the Modelling and Simulation of a mini-UAV

An Analysis

Tomáš Vogeltanz, Roman Jašek

Department of Informatics and Artificial Intelligence
Tomas Bata University in Zlín, Faculty of Applied Informatics
nám. T.G. Masaryka 5555, 760 01 Zlín, CZECH REPUBLIC
vogeltanz@fai.utb.cz, jasek@fai.utb.cz

Abstract—This paper presents an analysis of free software which can be used for the modelling and simulation of a mini-UAV (Unmanned Aerial Vehicle). Every UAV design, construction, implementation and test is unique and presents different challenges to engineers. Modelling and simulation software can decrease the time and costs needed to development of any UAV. First part of paper is about general information of the UAV. The fundamentals of airplane flight mechanics are mentioned. The following section briefly describes the modelling and simulation of the UAV and a flight dynamics model. The main section summarizes free software for the modelling and simulation of the UAV. There is described the following software: Digital Datcom, JSBSim, FlightGear, and OpenEagles. Other software is mentioned only. Finally, the results of the analysis are discussed in conclusion.

Keywords—aircraft; airplane; analysis; flight dynamics model; free software; modelling; simulation; UAV

I. INTRODUCTION

Mini-UAVs are a relatively inexpensive alternative to manned aircraft for a variety of applications, including aerial reconnaissance, environmental monitoring, agriculture, surveying, and safety. [1] [2] [3]

The research community does not clearly define the term mini-UAV (or small-UAV). [2] Instead of creation new definition about weight and proportions of the mini-UAV, we can simply say, a UAV is mini (or small) if the strength of an average man suffice for lifting and moving the UAV without any trouble. For the remainder of this paper, the term mini-UAV is implied.

The flight-testing of an aircraft is a well-documented engineering procedure. However, every aircraft design, construction, implementation and test is unique and presents different challenges to engineers, pilots, and test team. The same can be said about UAVs, but the criteria for UAVs can be different from manned aircraft. [2] [4] [5]

This work was supported by the Internal Grant Agency at Tomas Bata University in Zlín, project No. IGA/FAI/2014/006.

Current standards for handling qualities apply to only piloted aircraft and there are no specific standards for UAV handling qualities. Relevant article discussing dynamic stability and handling qualities for small UAVs is [4]. [2]

Any UAV system depends on its mission and range, however, most UAV systems include: airframe and propulsion systems, control systems and sensors to fly the UAV, sensors to collect information, launch and recovery systems, data links to get collected information from the UAV and send commands to it, and a ground control station. [3] [5]

UAVs promise greater precision, but the auto-pilot system which keeps the vehicle in the air and in control is critical to the success of UAV systems. The ability to test autopilot systems in a virtual environment is significant for development. A reliable UAV simulation process which can be adapted for different aircraft would provide a platform for developing autopilot systems with reduced dependence on expensive field trials. In many cases, testing newly developed autopilot systems in a virtual environment is the only way to guarantee absolute safety. Additionally the model allows better repeatability in testing. [1] [2] [4]

II. FUNDAMENTALS OF AIRPLANE FLIGHT MECHANICS

The basic aeronautical concepts and definitions required to be understood in order to deal with the flight dynamics model. Flight mechanics is the application of Newton's laws (1) and (2) to the study of vehicle trajectories (performance), stability, and aerodynamic control. [3] [6]

$$F = m \cdot a \quad (1)$$

$$M = I \cdot \alpha \quad (2)$$

The equations of motion are composed of translational (force) equations (1) and rotational (moment) equations (2) and are called the six degree of freedom (6DOF) equations of motion. The aircraft can move in three dimensions in space and can rotate about three axes. Motion caused by gravity, propulsion, and aerodynamic forces contribute to the forces

and moments which act upon the body of the airplane. Fig. 1 shows the three axes and the forces and moments acting on an aircraft. The center of gravity of the aircraft is at the intersection of the axes. [1] [2] [3] [6] [7]

For trajectory analysis (performance), the translational equations are uncoupled from the rotational equations by assuming that the airplane rotational rates are small and that control surface deflections do not affect forces. The translational equations are referred to as the three degree of freedom (3DOF) equations of motion. [6] [7]

The forces of lift, weight, drag, thrust, and side force act along the axes, forcing the aircraft to move in the axes direction. On the other hand, the three moments, yaw, roll, and pitch force the aircraft to turn around the axes. [1] [2] [3]

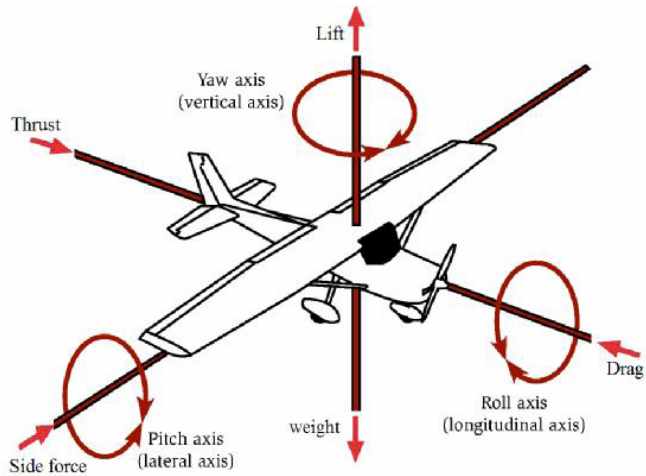


Fig. 1. The forces and moments acting on an aircraft

Table I. defines each of the state variables. Although the forces and moments are relative to the atmosphere, the state variables are defined relative to the earth. [2]

TABLE I. FLIGHT PATH COMPONENTS VARIABLE DEFINITION

| Variable | Symbol |
|-------------------------|----------|
| Roll Rate (rad / sec) | P |
| Pitch Rate (rad / sec) | Q |
| Yaw Rate (rad / sec) | R |
| Velocity (m / sec) | V |
| Sideslip Angle (rad) | β |
| Angle of Attack (rad) | α |
| Bank Angle (rad) | μ |
| Flight-Path Angle (rad) | γ |
| Heading Angle (rad) | χ |
| North Position (m) | ξ |
| East Position (m) | η |
| Altitude (m) | h |

V , χ , and γ represent the magnitude of the velocity vector, heading angle, and flight path angle respectively. P , Q , and R represent the components of angular velocity; roll, pitch, and yaw. The position of the aircraft relative to the earth in Cartesian coordinates is ξ , η , and h . Body attitude relative to the velocity vector are μ , β , and α . [2]

All longitudinal motion occurs in the xz -plane of the aircraft. Stability along the longitudinal axis is both static and dynamic. Longitudinal static stability is the tendency of the airplane to return to pitch equilibrium following an angle of attack disturbance. Static stability is the aircraft's initial response to an input command. In the case of flight test, aircraft considered statically stable immediately tend to return to its steady level flight condition. The airplane is statically stable if the center of gravity is located at the wing aerodynamic center. When viewed over time, the aircraft is dynamically stable if it tends to return to steady level flight condition. [2] [6] [7]

III. THE MODELLING AND SIMULATION OF A UAV

The modelling and simulating of a UAV accurately is not an easy task, due to the need to calculate many parameters either by physical measurements, experiments, or estimation from available data of similar UAV or by software tools. One of the big challenges is calculating aerodynamic coefficients. Aerodynamic coefficients characterize the response of the proposed vehicle based on its geometry. [1] [3]

Several major assumptions are often made for the modelling and simulation of the aircraft. First, the aircraft is rigid. Although aircraft are truly elastic in nature, modelling the flexibility of the UAV should not contribute significantly to the research. Second, the earth is an inertial reference frame. Third, aircraft mass properties are constant throughout the simulation. For UAV modelling, it can be assumed the aircraft has constant mass over a flight. Finally, the aircraft has a plane of symmetry. The first and third assumptions allow for the treatment of the aircraft as a point mass. This assumption is a satisfactory approximation for UAV models. [1] [2]

For the modelling and simulation of a UAV the following items must be created: [3]

- A complete Flight Dynamics Model (FDM)
- A 3D graphical model (only if 3D visualization of the UAV is needed)
- An effective autopilot
- A way to identify flight route
- Autonomous flight simulation

The FDM is the physics/math model which defines the movement of an aircraft under the forces and moments applied to it using the various control mechanisms and from the forces of nature. The FDM includes development of a physical, inertial, and aerodynamic model representing the UAV. The FDM processes parameters from all input information. By manipulating input variables mathematically, an FDM predicts the future states of an aircraft. [1] [2] [3]

The best equations to use to completely and accurately model an aircraft's true motion are nonlinear fully coupled ordinary differential equations. With these equations of motion, UAV response to any commanded inputs or wind disturbances is accurately modeled. [2]

However, a software model developed from first principles has unknown accuracy. For the model which is supposed to be used for real simulation, it is necessary to include implementation, verification and validation into its development process. [1]

The 3D graphical model is necessary only if 3D visualization of the UAV is needed. 3D Visualization can give us a better view of the simulation than numbers and graphs alone. [3]

The effective autopilot is very important for the good control of the UAV. Autonomous flight and stability of the UAV depend on the autopilot. If the autopilot is designed and implemented wrongly, the UAV can crash very easily. Every crash can increase distrust of the UAV and of its using in cities. [1] [2] [4] [7]

The way to identify flight route means to simulate system similar to the GPS or the GPS itself. [3]

Autonomous flight simulation depends on all things above. Additionally, use cases and activity diagrams of simulation have to be designed to define what should be found and how it should be found. Next, the settings of simulation parameters (e.g. density, gravity, airspeed, and altitude) must be defined and then the simulation itself can be run with or without visualization. [2] [3]

IV. FREE SOFTWARE

There is a lot of free software for the modelling and simulation of the aircraft on the Internet. Most of it can be also used for the modelling and simulation of the UAV. This paper cannot include and analyze all free software and therefore the most interesting free software only is described in detail. Other software is mentioned only.

A. Public Domain Aeronautical Software (PDAS)

For many years the Air Force, Navy, NASA and educational institutions have sponsored the development of computer software that is useful to aeronautical engineers, airplane designers, and aviation technicians. [8]

Public Domain Aeronautical Software (PDAS) was founded to make this valuable software available to the aeronautical community for use on desktop computers. These programs include descriptions and complete public domain source code. The source code is not copyrighted and may be used in whole or in part in any of aeronautical studies. Many programs have sample cases (both input and output). Some of the programs on the website are noted as work-in-progress, indicating that they are lacking in instructions or documentation or do not run properly. [8] [9]

There are many interesting applications, e.g. Atmosphere which characterizes the 1976 standard atmosphere to 1000 km altitude, including nonstandard atmosphere routines (hot, cold,

polar, tropical), Aeroelastic Analysis which estimates the planform and aero-elastic effect on stability derivatives and induced drag, Flutter Analysis by Strip Theory which has been developed for rapidly predicting flutter of finite-span, swept or unswept wings at subsonic to hypersonic speeds, Induced Drag from Span Load Distribution which is a popular algorithm for computing the span load distribution on a planar wing when only a few sparse values of the loading are known, NACA Airfoils in which the coordinates of 4-digit, 4-digit-modified, 5-digit, 6-series, and 16-series airfoils may be accurately calculated, PANAIR which is a state of the art computer program developed to predict inviscid subsonic and supersonic flows about an arbitrary configuration by means of a higher order panel method, and more. [9]

There is no space to describe all applications in detail. Only Digital Datcom is described more because it has been used many times to real development of aircraft. [1] [2] [9]

1) Digital Datcom

The Stability and Control Data Compendium, Datcom for short, provides a systematic summary of methods for estimating basic stability and control derivatives. Datcom is over 1500 pages of detailed methodology to determine stability and control characteristics of a wide variety of aircraft and aircraft configurations. For any given flight condition and configuration the complete set of derivatives can be determined without resort to outside information. [2] [10]

Primarily intended for preliminary use, ahead of test data, it is designed to give an initial look at the stability performance of an aircraft design. In 1979, the Datcom was rewritten in FORTRAN IV computer language. Renamed the USAF Stability and Control Digital Datcom, it became an efficient, user-oriented computer program. However, it is not intended for use instead of wind tunnel or flight test data. [2]

In [1], the wind tunnel testing was performed in a low speed wind tunnel so accuracy was slightly compromised. There also has been said: "The results were sufficient to show that the aerodynamics coefficients determined by Datcom do not accurately represent the actual values. The experimental drag coefficients are higher than those predicted by the software model and this has a large effect on the accuracy of the flight dynamic model."

By interfacing Datcom with the FDM in the frontend, an aircraft model for any fix wing UAVs can be rapidly developed without wind tunnel testing. This feature significantly increases the repeatability of flight simulation and is found very useful for UAV preliminary designs where only a rough estimate of the vehicle's stability is required. [1]

Digital Datcom is used to calculate aerodynamic coefficients from first principles. By writing an input file containing all essential geometries of an aircraft, Datcom produces an output file with aerodynamic coefficients. The coefficients in the six degrees of freedom are drag, lift, side, pitching moment, rolling moment, and yawing moment coefficient. [1] [10]

Inputs to Datcom include desired flight conditions, aircraft attitudes, physical geometry, and desired outputs. Datcom treats inputs which represent a traditional wing-body-tail

configuration and any control or high lift devices. Some nonstandard geometry can be treated as well. Datcom inputs were assumed for a straight-tapered or nonstraight-tapered wing. For the longitudinal characteristics, the program assumes a mid-wing configuration. [2] [10] [11]

B. JSBSim Flight Dynamics Model

JSBSim is open source software which allows users to access the internal of the models. JSBSim is a 6-DOF nonlinear flight dynamics model. JSBSim is generally considered as a very accurate FDM. It is the default FDM for the FlightGear flight simulator and for the OpenEagles Simulation Framework. [1] [3] [12] [13] [14]

The open source feature of JSBsim has gained a lot of attention from researchers. A full 6-DOF simulator for flight simulation and pilot training was constructed at the University of Naples using JSBSim as its physics engine. JSBSim is also used to drive the motion-based research simulators in the Institute of Flight System Dynamics and Institute of Aeronautics and Astronautics at RWTH Aachen University in Germany. [1] [3] [12]

JSBSim is written in the C++ programming language. The use of an object-orientated approach makes JSBSim a generic simulator, and allows the modelling of any aircraft, missile, or rotorcraft. Particular aircraft flight control systems, propulsion, aerodynamics, landing gears, and autopilot are defined in eXtensible Markup Language (XML) format configuration files. [3] [12]

JSBSim can be run as a stand-alone application, or it can be run as an integrated part of the flight simulator which provides visual output. JSBSim models the rotational earth effects on the equation of motion and supports many data output formats such as to screen, socket, and file. [3]

The first step of the use of JSBSim to model and simulate a small autonomous UAV is to create the required JSBSim aircraft configuration files by using the Aeromatic. Aeromatic is a free web application and it is also included in source code of JSBSim. The next step is to make educated guesses to refine important sections in the created configuration files with the assistance of available data of similar UAV. [3] [13]

The Aeromatic takes inputs from the user such as system of measurements used, the aircraft name, type of aircraft, maximum take-off weight, wing span, length, wing area, landing gear layout, number of engines, engine type, and engine layout. Some values can be estimated, e.g. wing chord, wing area, inertia, and more. By clicking on the generate button, the main JSBSim configuration file will be generated in another window. The next step is to save the generated file by using save as, and giving the file a name. [3] [13]

The aircraft's metrics, the aircraft's airframe geometry, mass and inertia properties, landing gear positions and their ground reactions, flight control system, and aerodynamic characteristics are specified in the main aircraft configuration file. [3]

JSBSim can model different types of engines, for instance electric, piston, rocket and turbine engines. The aircraft's

propulsion system is specified in two files, one for the engine, and the other for the thruster. These files are referred to in the propulsion section in the main aircraft specification file which allows the researcher to assign different kinds of engines and thrusters to the aircraft. The propulsion section specifies information about engine, thruster, and fuel tank. Aeromatic takes the engine power, maximum engine RPM, pitch condition, and propeller diameter from the user. [3] [13]

JSBSim provides components which can be connected together to model a flight control system for an aircraft. The flight control surfaces are elevator, right and left ailerons, and rudder. [3]

C. FlightGear Flight Simulator

FlightGear is an open-source flight simulator, written in the C++ programming language, to model and simulate an aircraft. Data visualization is another aspect considered while building the flight dynamics model. FlightGear supports many 3D formats. The common format used in FlightGear has “ac” extension. The FlightGear can produce a 3D graphic animation in real time and is connected to a FDM. The animation facility allows the UAV to be viewed from any angles, and provides absolute visual information on the UAV attitude and stability. Moreover, it models real world instrument behavior, and system failures. [1] [3] [14] [15]

FlightGear allows the user to access the internal properties and monitor any of its internal state variables. By editing configuration files it is possible to create sound effects, model animations, instrument animations and network protocols for approximately any situation. [3] [15]

FlightGear can communicate with external flight dynamics models, GPS receivers, external autopilot, control modules, other instances of FlightGear, and other software. [3] [15]

It is possible to choose between two primary FDMs: JSBSim and YASim. Actually, there is a third FDM named UIUC and based on LaRCsim originally written by the NASA but UIUC is no longer supported by default FlightGear builds. It is possible to add new dynamics models or even interface to external “proprietary” flight dynamics models. [15] [16]

YASim is an integrated part of FlightGear and uses a different approach than JSBSim by simulating the effect of the airflow on the different parts of an aircraft. The advantage of this approach is that it is possible to perform the simulation based on geometry and mass information combined with more commonly available performance numbers for an aircraft. This allows for quickly constructing a plausibly behaving aircraft that matches published performance numbers without requiring all the traditional aerodynamic test data. [15]

Except of FDM configuration files, other files are required for use with FlightGear flight simulator which include the electric system file, autopilot file, and 3D graphical model specification file. The final file required is a file to tie the previous files together in order to perform complete simulation using FlightGear. [3]

The electrical system file specifies the battery characteristics, and the lights and other parameters. [3]

To fly the modelled UAV autonomously, a tuning process have to be made for the built-in generic PID (proportional, integral, and derivative) autopilot of FlightGear which has the ability to hold aircraft velocity, vertical aircraft speed, altitude, pitch angle, angle of attack, bank angle, and true heading. [3]

FlightGear implements a PID algorithm in a flexible way which makes it reusable with similar aircraft. Any number of PID controllers can be defined in the autopilot configuration file. A process value, reference point, any number of output values, and other tuning constants can be assigned to each controller. Cascading controllers can be implemented by specifying multiple PID controllers in which the output of the current stage is used as the input to the next stage. [3]

A flight path which contains a number of waypoints chosen over a selected area using Google Earth map can be constructed. In order to use the chosen waypoints with FlightGear navigation system, a unique ID can be assigned to each waypoint, and the FlightGear database can be altered to include the new waypoints with their IDs. [3]

The fixed waypoints are determined by latitude and longitude. When a waypoint is entered in the aircraft route during the simulation time, FlightGear checks the database to see if it is a valid fixed point or not. This data is stored in the compressed file called fix.dat which can be found in the directory FG_ROOT\FlightGear\data\NavAids. [3]

D. OpenEaagles Simulation Framework

OpenEaagles is an open source multi-platform simulation framework targeted to help simulation engineers and software developers rapidly prototype and build robust, scalable, virtual, constructive, stand-alone, and distributed simulation applications. OpenEaagles is written in the C++ programming language and it has been used extensively to build applications that demand deterministic real-time performance or simply execute as fast as possible. This includes applications used to conduct human factor studies, operator training, or the development of complete distributed virtual simulation systems. OpenEaagles has also been used to build stand-alone and distributed constructive applications oriented at system performance analysis. Constructive-only simulation applications that do not need to meet time-critical deadlines can use models with even higher levels of fidelity. [17] [18]

It should be emphasized that OpenEaagles is a cycle or frame-based system, not a discrete-event simulator. This approach satisfies the requirements for which it is designed; namely, support for models of varying levels of fidelity including higher level “physics based” models, digital signal processing models and the ability to meet real-time performance requirements. Model state can be captured with state machines and state transitions can use the message passing mechanisms provided by the framework. [19] [20]

The framework embraces the Model-View-Controller (MVC) software design pattern by partitioning functional components into packages (see Fig.2 - packages with white/clear background indicate the use of a third party open source tool.). This concept is taken a step further by providing an abstract network interface so custom protocols can be

implemented without affecting system models. Framework utilizes a number of other third party open source tools such as FLTK, Fox and wxWidgets for cross-platform GUI applications, and JSBSim as a high quality flight dynamics model. [18] [19] [20]

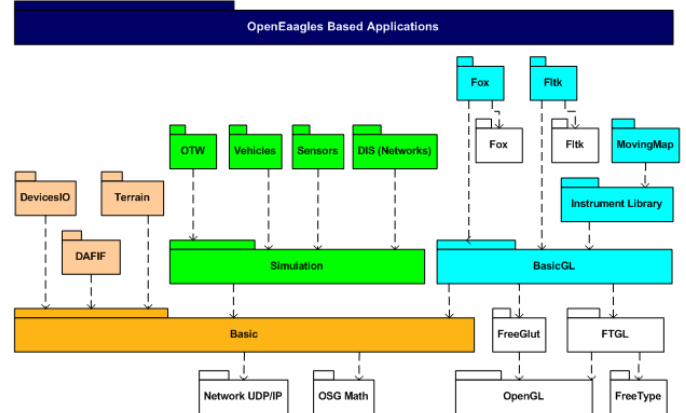


Fig. 2. OpenEaagles Package Hierarchy

The simulation side provides a wealth of capabilities including abstract classes for representing a variety of entity types such as aircraft, ships, tanks, ground vehicles, space vehicles and even lifeforms. A complete radar modeling environment is also included in the simulation hierarchy. [20]

The graphics hierarchy provides a mature collection of classes that can be used to render instruments that are commonly used in operator-vehicle interface displays. A sampling of the instrument objects available include: analog dials for altimeters, dials for direction finders, speedometer dials, and even landing gear indicators. [20]

Distributed applications can interoperate with other systems and simulations through Distributed Interactive Simulation (DIS) and/or High Level Architecture (HLA) interfaces. Numerous DIS compliant distributed simulation applications have been built using this framework as the foundation. [17] [18] [19]

Specific applications using the framework to support simulation activities include representative F-16 cockpits, an Unmanned Aerial Vehicle (UAV) ground control station (Predator MQ-9), Integrated Air Defense Systems (IADS) and a futuristic battle manager. [19]

The framework is routinely compiled with Microsoft Visual Studio for the Windows environment and GCC for Linux. [19]

Project files for Codelite and Codeblocks development environments can be generated by OE_source_ROOT\build\premake\make.bat file. For the Codelite project files generation, "%Premake% codelite" have to be added to the end of make.bat file.

E. Other Software

XFOIL is an interactive program for the design and analysis of subsonic isolated airfoils. It consists of a collection of menu-driven routines which perform various useful functions. [21]

Tornado for Octave is a Vortex Lattice Method for linear aerodynamic wing design applications in conceptual aircraft design or in aeronautical education. By modelling all lifting surfaces as thin plates, Tornado can solve for most aerodynamic derivatives for a wide range of aircraft geometries. [22]

Aerospace blockset for the Scilab/XCos is an external module providing aerospace palette. It is based on CelestLab aerospace library. Although Scilab/XCos and aerospace blockset are very interesting compensation for Matlab/Simulink, aerospace blockset is designed rather for satellites than aircraft nowadays. [23]

V. CONCLUSION

This paper has described the most interesting free software for the modelling and simulation of any UAV. The fundamentals of airplane flight mechanics and the basics of the modelling and simulation of a UAV have also been mentioned.

UAVs can be used in civilian operations such as searching for missing people, aerial photography, monitoring of illegal activities, traffic control, and monitoring of pollution. The future of any UAV program is open to a wide range of research topics: collision avoidance, autonomous formation flight, navigation without the use of GPS, autonomous detection of the potential criminal etc.

It has been explained that FDM and Flight Simulators are used in the development process of a UAV to test its design and control systems. In any FDM, the coefficients of lift, drag, and side forces and roll, pitch, and yaw moments have to be estimated in order to calculate the forces and moments acting on the UAV.

Public Domain Aeronautical Software contains many interesting applications. Especially Digital Datcom has been used in real projects many times. Digital Datcom gives very good way how to calculate aerodynamic coefficients from first principles but the creation of an input file may be complicated.

The combination of JSBSim Flight Dynamic Model and FlightGear Flight Simulator provide an excellent base for building the simulation environment. To model the UAV in JSBSim Flight Dynamic Model and simulate it with FlightGear Flight Simulator, essential configuration files have to be constructed. These files include main UAV configuration, engine configuration, propeller configuration, electric system configuration, 3D model configuration, and an autonomous flight autopilot configuration file. All these files are tied together in the top level configuration file.

OpenEaagles framework is designed for the simulation application developer; it is not an application itself. OpenEaagles is a cycle-based system, not a discrete-event simulator. OpenEaagles utilizes a number of other third party open source tools, e.g. JSBSim. OpenEaagles has been used extensively to build applications that demand deterministic real-time performance. This includes applications used to conduct human factor studies, operator training, or the

development of complete distributed virtual simulation systems.

REFERENCES

- [1] X.Q. Chen, Y.Q. Chen and J.G. Chase, Mobile Robots - State of the Art in Land, Sea, Air, and Collaborative Missions. Croatia: In-Teh, May 2009, pp.177-201.
- [2] N. M. Jodeh, Development of Autonomous Unmanned Aerial Vehicle. Ohio, USA: Wright-Patterson Air Force Base, March 2006, 185 p.
- [3] T. Abdunabi, Modelling and Autonomous Flight Simulation of a Small Unmanned Aerial Vehicle. Sheffield, UK: The University of Sheffield, August 2006, 61 p.
- [4] T. M. Foster, Dynamic Stability and Handling Qualities of Small Unmanned-Aerial-Vehicles. Brigham, USA: Brigham Young University, April 2005, 125 p.
- [5] R. Austin, Unmanned Air Systems: UAVs Design, Development and Deployment. Wiltshire, UK: Wiley, 2010, 332 p.
- [6] D. G. Hull, Fundamentals of Airplane Flight Mechanics. Springer, 2007, 298 p.
- [7] T.V. Chelaru, V. Pana, A. Chelaru, "Dynamics and flight control of the UAV formations," WSEAS Transactions on Systems and Control, vol. 4 no. 4, pp. 198-210, April 2009.
- [8] R. Carmichael. (2013, January 31). Public Domain Aeronautical Software. [Online]. Available: <http://www.pdas.com>
- [9] R. Carmichael. (2013, March 28). Public Domain Aeronautical Software: Contents. [Online]. Available: <http://www.pdas.com/contents15.html>
- [10] R. Carmichael. (2013, April 21). Description of Digital Datcom. [Online]. Available: <http://www.pdas.com/datcomDescription.html>
- [11] R. Carmichael. (2013, February 7). Addressable Configurations in Digital Datcom. [Online]. Available: <http://www.pdas.com/datcomTable1.html>
- [12] JSBSim contributors. JSBSim Open Source Flight Dynamics Model. [Online]. Available: <http://jsbsim.sourceforge.net/>
- [13] JSBSim contributors. (2005, December 31). Aeromatic. [Online]. Available: <http://jsbsim.sourceforge.net/aeromatic2.html>
- [14] FlightGear contributors. FlightGear Flight Simulator: Introduction. [Online]. Available: <http://www.flightgear.org/about/>
- [15] FlightGear contributors. FlightGear Flight Simulator: Features. [Online]. Available: <http://www.flightgear.org/about/features/>
- [16] FlightGear contributors. (2014, May 12). FlightGear Wiki - UIUC. [Online]. Available: <http://wiki.flightgear.org/UIUC>
- [17] D. Hodson. (2014, January 10). OpenEaagles Simulation Framework. [Online]. Available: <http://www.openeaagles.org>
- [18] D. Hodson. (2012, December 03). OpenEaagles Simulation Framework: Overview. [Online]. Available: <http://www.openeaagles.org/wiki/doku.php?id=overview:overview>
- [19] D. Hodson, D. Gehl and R. Baldwin, "Building Distributed Simulations Utilizing the EAAGLES Framework," Interservice/Industry Training, Simulation, and Education Conference (I/ITSEC), vol. 5, no. 2, May 2006.
- [20] D. Hodson, "OPENEAGLES, An Open Source Simulation Framework," A Publication of the AIAA Modeling and Simulation Technical Committee, vol. 1, no. 1, January 2008.
- [21] M. Drela. (2013, December 23). XFOIL: Subsonic Airfoil Development System. [Online]. Available: <http://web.mit.edu/drela/Public/web/xfoil/>
- [22] Redhammer Consulting Ltd. (2010). TORNADO. [Online]. Available: <http://www.redhammer.se/tornado/index.html>
- [23] P. Zagórski and C. David. (2013). Aerospace Blockset for Xcos. [Online]. Available: <http://forge.scilab.org/index.php/p/aerospace-blockset/>

Algorithmic Analysis of the Marketing Mix in Metallic Materials Industry

Adrian IOANA

Engineering and Management of Metallic Materials'
Making Department
University Politehnica of Bucharest (UPB)
Bucharest, Romania
adyioana@gmail.com

Augustin SEMENESCU

Engineering and Management of Metallic Materials'
Making Department
University Politehnica of Bucharest (UPB)
Bucharest, Romania

Abstract— This paper presents an algorithmic analysis of the marketing mix in metallurgy. It also analyzes the main correlations and their optimizing possibilities through an efficient management. Thus, both the effect and the importance of the marketing mix, for components (the four “P-s”) are analyzed in the materials’ industry, but their correlations as well, with the goal to optimize the specific management.

Keywords—Management, Marketing Mix, Correlations, Metallic Materials Industry.

component; formatting; style; styling; insert (key words)

I. INTRODUCTION

The four components of the marketing mix (the four “P-s”):

- Product (P1);
- Price (P2);
- Promoting (P3);
- Placement-Distribution (P4).

and their correlation is very important for an efficient management in materials’ industry. The analysis of the correlations between the 4 “P-s” (the four components of the marketing mix) and their management in metallurgy are also very important.

II. THE MAIN CORRELATION BETWEEN THE MARKETING MIX COMPONENTS IN METALLIC MATERIALS INDUSTRY

In figure no. 1 there are briefly presented the main correlations between the 4 marketing mix components (the 4 “P-s”) for a product within the metallic materials’ industry.

Aspects regarding management:

- (1) – The biunivocal correlation Product (P1) - Promoting (P2) is based on assuring the quality of the product.
- (2) – An important role in optimizing the correlation (1) is held by advertising directly correlated with the product’s quality level.

(3) – The Product (P1) needs and determines technological development for assuring the quality technical requirements.

(4) – The biunivocal correlation Product (P1) – and Price (P2) is based on cutting of production costs.

(5) – The level of technological optimization is directly correlated with the product’s quality [1,2].

(6) – A good (low) price of the product assures good placement condition of it.

(7) – A good placement of the product can lead to a good price (optimal in direct correlation with the sales level).

The lower the price (P2) is (which is facilitated by a high level of technological optimization), the higher the profit (benefit) is, which allows investing it in research-development.

The analysis of the main correlation between the 4 marketing mix components in a case of a product from the materials’ industry (presented in figure no.1) highlights the importance of management in order to optimize that product.

Figure 2 presents the main correlations between the functional and constructive betterments regarding a product from the metallic materials’ industry [3].

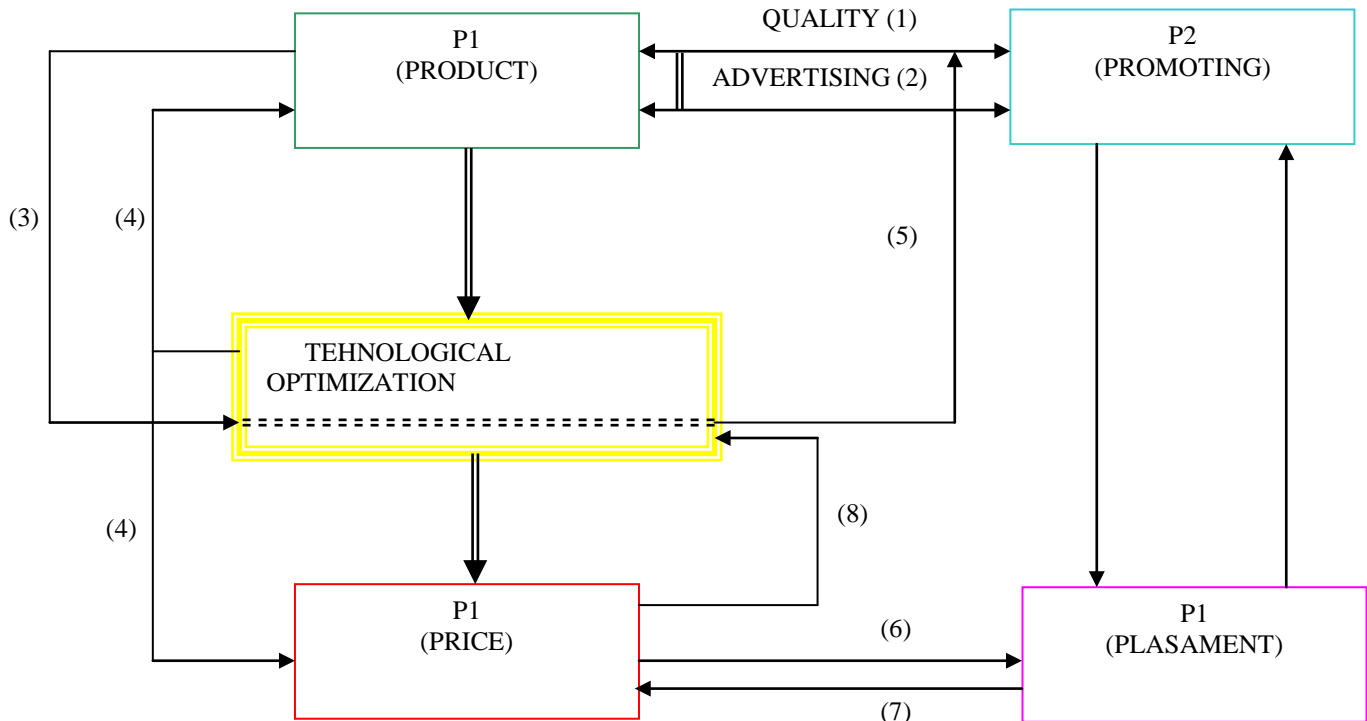


Figure 1. The main correlations between the four marketing mix components for a product with the metallic materials' industry

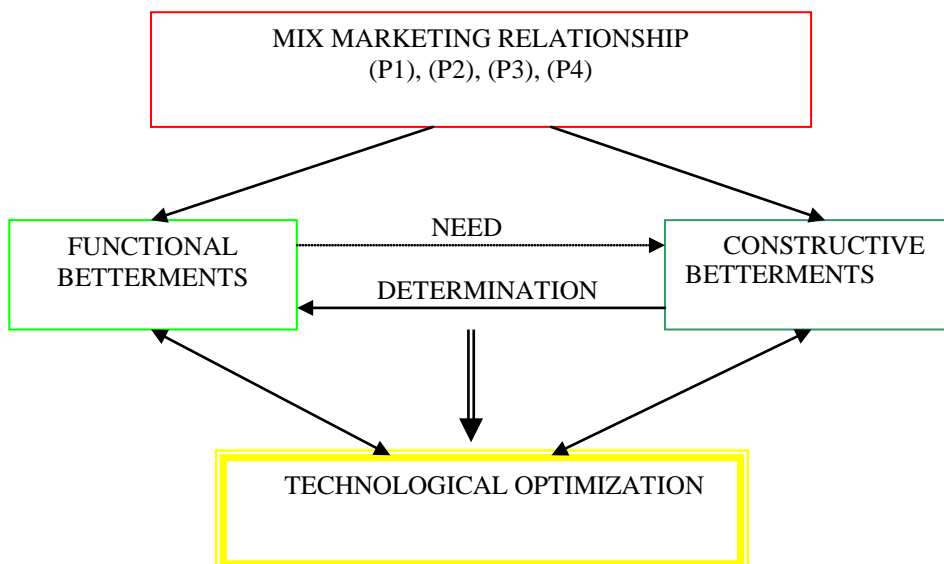


Fig. 2. The main correlation between the functional and constructive betterments in the technology of a product from the metallic materials' industry, needed in order to assure an optimal marketing mix.

It is to be noticed that, in order to obtain an optimal marketing mix for a product from the materials' industry, the technological optimization management must focus on both functional and constructive betterments.

The functional betterments need constructive betterments and constructive betterments generate functional betterments.

An important component of the marketing mix for a product in the metallurgical industry is the quality and the cost control activity [4,5].

The main steps (and their correlations) of the quality and cost control activity management for product in the metallic materials industry are briefly presented in figure no. 3.

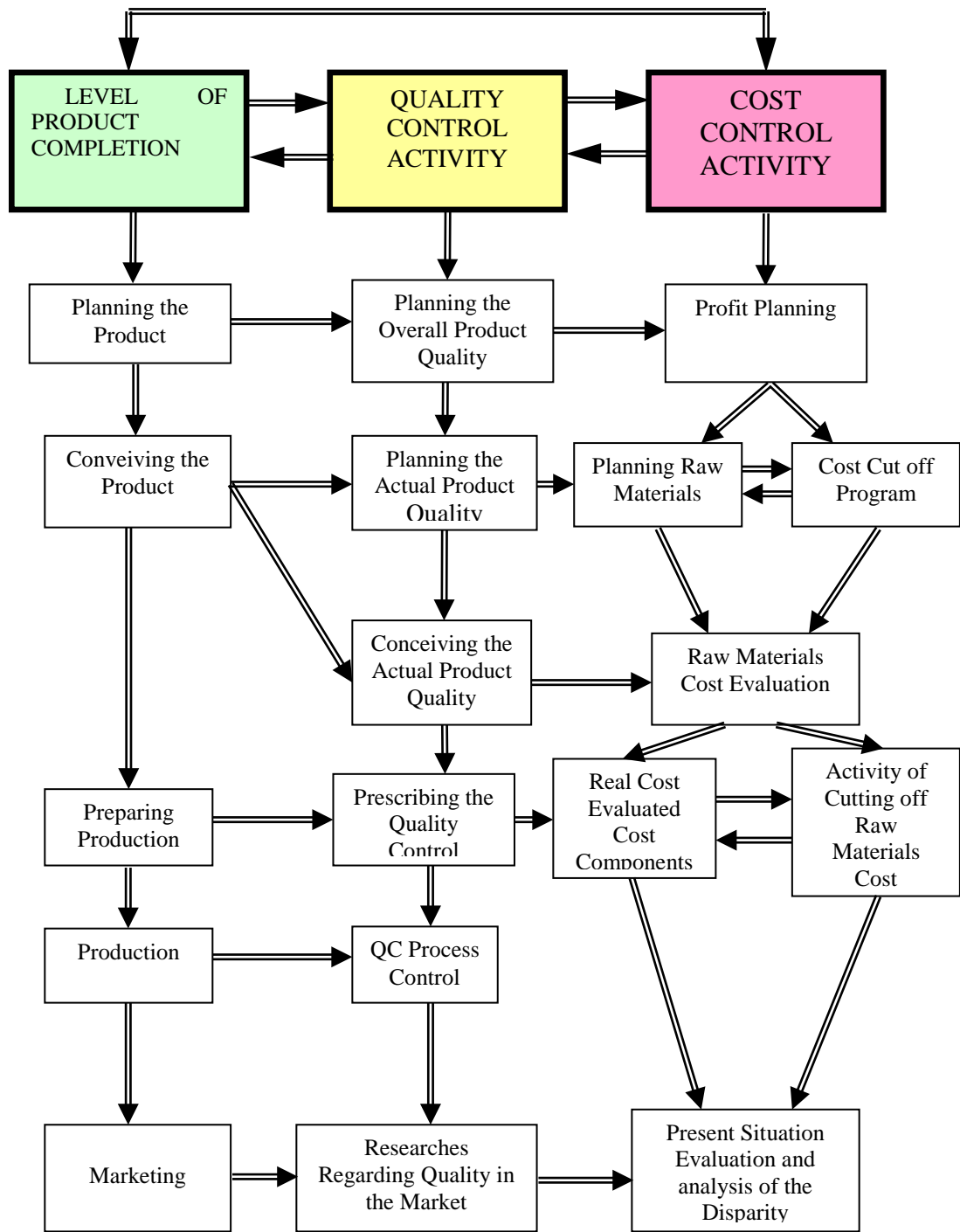


Fig. 3. The management of the quality and cost control activities for a product from the metallic material industry

The level of the product's completion is to be noticed. This based on the following activities: planning the product, conceiving the product, preparing production and marketing [6,7].

III. CONCLUSION

The marketing mix analysis for products in the metallurgical industry highlights the importance of the technological optimization in order to obtain an optimum in the field.

The technological optimization in the metallurgical industry is based on functional and constructive betterments. The optimization of the biunivocal correlation between them (need-determination) assures the efficiency of the marketing mix of that product.

REFERENCES

- [1] A. Ioana, A. Semenescu, "Technological, Economic, and Environmental Optimization of Aluminum Recycling", Journal of the Minerals, Metals & Materials Society, JOM: Volume 65, Issue 8 (2013), ISSN 1047-4838 (ISI-Web of Science/Science Citation Index Expanded), pp. 951-957, WOS: 000322136400007
- [2] A. Ioana, V. Mirea, C. Bălescu, "Analysis of Service Quality Management in the Materials Industry Using the BCG Matrix Method", Amfiteatru Economic Review, Vol. XI, Nr. 26, June 2009, pp 270-276, [ISSN 1582-9146, ISI-Web of Science/Science Citation Index Expanded], București, 2009, WOS: 000267351800004
- [3] A. Ioana, "Metallurgy's Impact on Public Health", Review of Research and Social Intervention, Vol. 43/2013, ISSN: 1583-3410, (ISI-Web of Social Science/Social Science Citation Index Expanded), pg. 169-179, Iași, 2013.
- [4] A. Ioana, A. Nicolae, et al., "Optimal Managing of Electric Arc Furnaces", Ed. Fairs Partners, Bucharest, 2002.
- [5] A. Ioana, "The Electric Arc Furnaces (EAF) Functional and Technological Performances with the Preheating of the Load and Powder Blowing Optimization for the High Quality Steel Processing", PhD Thesis, University "Politehnica" of Bucharest, 1998.
- [6] A. Ioana, "Optimum Operation and Automation of Electric Arc Furnace Instalations", Review of Installations Technique. 5(46)/2007, 12-14.
- [7] A. Ioana, "Production Management in Metallic Materials Industry. Theory and Applications", Ed. PRINTECH, Bucharest, 2007.

Particle Shape Effect on Extraction in Vibration Screening: ellipsoidal vs spherical particle approximation

IVANOV Kirill Sergeevitch

REC "Mekhanobr-tehnika"

V.O. 22nd Line,3, St. Petersburg 199106, Russia

ivanoff.k.s@gmail.com

VAISBERG Leonid Abramovitch

REC "Mekhanobr-tehnika"

V.O. 22nd Line,3, St. Petersburg 199106, Russia

ivanoff.k.s@gmail.com

Abstract— Mathematical formalization is critical for the development of numerical models of technical processes. Rational utilization of computing resources requires consideration of only those parameters that have a significant impact on system behavior. Despite the long history of vibration screening, these essential factors still represent relevant subjects of research. This paper studies the influence of particle shape on the efficiency of sieve classification using a simplified process model and image analysis methods. It is demonstrated that the influence of particle shape may be an important factor in these calculations. Additionally, an improved probability formula is suggested for screen separation of material particles as approximated by ellipsoids.

Keywords— vibration screening, particle shape, probability, mathematical modeling.

I. INTRODUCTION

Identification of the extent of influence of various factors on the screening process has long been a subject to numerous studies [1, 2, 3]. For example, paper [1] studies the effects of vibration mode on the screening process. This research was performed using the universal discrete element method that ensures realistic results, but involves considerable computing resources. The present paper uses so much as a specially developed simplified model of the vibration screening process, the basics of which are given in [4]. This model was adapted for the simplest case: classification in a thin layer of material.

II. BASIC MODEL

The model assumes that material particles are transported along the screening surface and may pass through the screen into the through product at each toss caused by surface oscillations. The probability of single particle passing through a screen opening was determined using the Gaudin formula recorded for the spherical shape of particles, while the clear area of the screen was recalculated with account of its hole shielding by the material flow. If the material is seen as a granulation of N size grades D_i ($i=1..N$), with specified concentration in the initial

product C_i , the expected recovery to through product may be calculated for each of these grades for a screen with square holes and side length d_0 as follows:

$$\varepsilon_i = 1 - (1 - (1 - S)\varphi P_i)^{N_p}, \quad (1)$$

where S – shielding factor (an experiment showed that for sufficiently dense monolayer material flows this may be considered equal to oversize concentration $S \approx \sum_{D_i < d_0} C_i$), φ – clear area, P_i – penetration probability determined using the Gaudin formula ($P_i = \left(1 - \frac{d_i}{d_0}\right)^2$), N_p – maximum expected number of particle presentations on the screening surface. The maximum number of presentations depends on screen vibration parameters and the particle exposure time determined, in turn, by the vibration displacement rate, and hence by friction and elasticity characteristics of material particles [5]:

$$N_p = \frac{\omega l}{2\pi\nu}, \quad (2)$$

where $\omega/2\pi$ – screen vibration frequency, ν – vibration displacement rate, and l – screen length.

III. EXPERIMENTAL STUDY

Three materials were selected for the study: complex polymetallic ore from Kondyor deposit, copper-nickel ore from Pechenga deposit and granitic rock from Semiozersk deposit. Below is a table of grain-size distribution of these materials and their basic mechanical parameters.

TABLE 1

| | Granulation | | Frict coeff | Density [kg/m ³] | | Rest coeff | |
|---|-------------|--------|----------------|---------------------------------|------|---------------|-------|
| | D [mm] | Cont | | mat | bulk | | |
| G R A N I T E | 10,000 | ... | 0,197 | 0,6 | 2630 | 1830 | 0,045 |
| | 5,000 | 10,000 | 0,291 | | | | |
| | 2,500 | 5,000 | 0,172 | | | | |
| | 1,400 | 2,500 | 0,024 | | | | |
| | 0,630 | 1,400 | 0,098 | | | | |
| | 0,315 | 0,630 | 0,065 | | | | |
| | 0,000 | 0,315 | 0,153 | | | | |
| P O L Y M E T A L | 10,000 | ... | 0,226 | 0,61 | 2960 | 1900 | 0,035 |
| | 5,000 | 10,000 | 0,361 | | | | |
| | 2,500 | 5,000 | 0,130 | | | | |
| | 1,400 | 2,500 | 0,013 | | | | |
| | 0,630 | 1,400 | 0,067 | | | | |
| | 0,315 | 0,630 | 0,059 | | | | |
| | 0,000 | 0,315 | 0,144 | | | | |
| C O P P N I C K | 10,000 | ... | 0,082 | 0,54 | 3220 | 1880 | 0,040 |
| | 5,000 | 10,000 | 0,440 | | | | |
| | 2,500 | 5,000 | 0,181 | | | | |
| | 1,400 | 2,500 | 0,020 | | | | |
| | 0,630 | 1,400 | 0,092 | | | | |
| | 0,315 | 0,630 | 0,049 | | | | |
| | 0,000 | 0,315 | 0,136 | | | | |

Figure 1 shows calculation results for material particles recovery to the through product, using the previously described method. Analytical recovery curves are provided with bold dots indicating averaged experimental data for a series of screening operations.

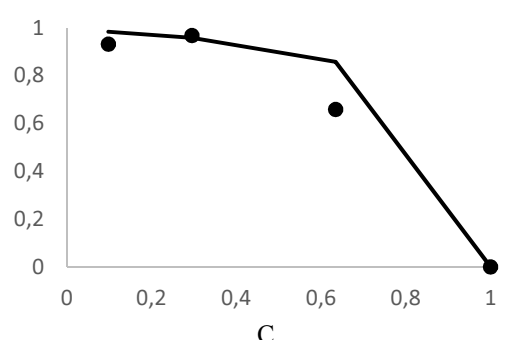
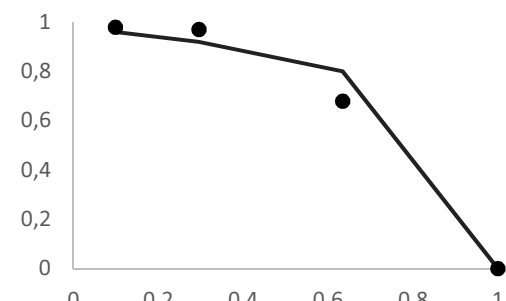
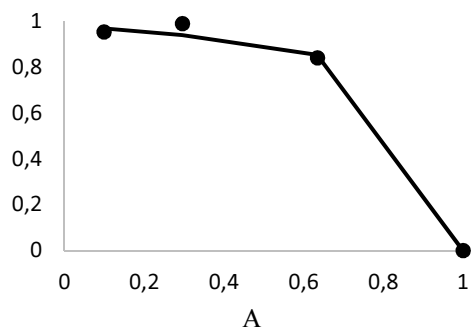


Fig. 1 Theoretical extraction curves and experimental points for A granite, B polymetal ore, C copper-nickel ore

It may be seen that the copper-nickel ores had relatively smaller shielding coefficient than polymetal ore, which naturally preconditioned better extraction. However, it should be noted that the experimental data showed consistently lower recovery rates than were expected. Below is a comparative analysis of these two materials.Units

IV. EFFECTS OF PARTICLE SHAPE, A REFINED MODEL

A detailed study using image analysis methods demonstrated that the deviation of experimental points from theoretical curves may be due to the differences in particle shapes. This suggested that particles of copper-nickel ore are somewhat more elongated than other samples. Fig. 2 shows photographs of particles of materials studied. Table 2 below presents the respective data on average aspect ratios of the smallest parallelepipeds these particles could be inscribed into.

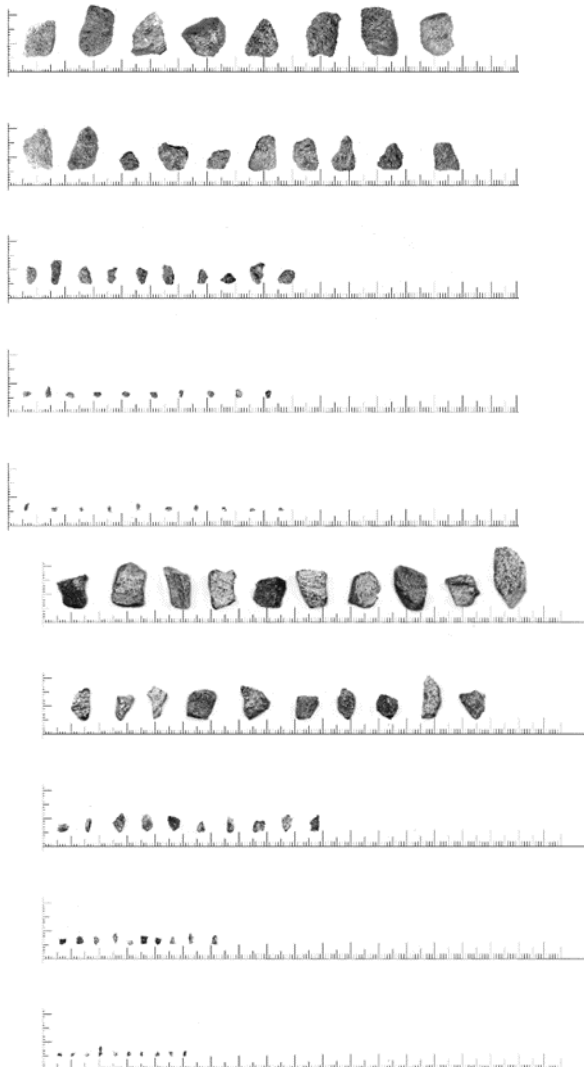


Fig. 2 Particles of the materials under consideration
Polymetal ore the first and copper-nickel ore the second
Table 2 describes the average proportions of the particles/
TABLE 2

| | a | b | c |
|-------------------|------|---|------|
| Polymetal ore | 0,65 | 1 | 1,55 |
| Copper-nickel ore | 0,63 | 1 | 1,64 |

As a result, it was suggested to recalculate the penetration probability for single particles approximated by ellipsoids using the specified semi-axes ratio. Assuming that particle orientation at the time of the fall is determined by Euler angles $(\varphi, \psi, \vartheta)$ and its semi-axes have sizes of a, b and c , its projections on the sides of a square screen hole may be calculated as follows (see Fig. 3):

$$L_x = a(\sin \varphi \cos \psi \cos \vartheta - \cos \varphi \cos \psi), M_x = b(\cos \varphi \sin \psi \cos \vartheta - \sin \varphi \cos \psi)$$

$$\begin{aligned} N_x &= c \sin \psi \sin \vartheta \\ d_A &= \sqrt{L_x^2 + M_x^2 + N_x^2} \end{aligned} \quad (3)$$

A similar method may be used to calculate d_B projections.

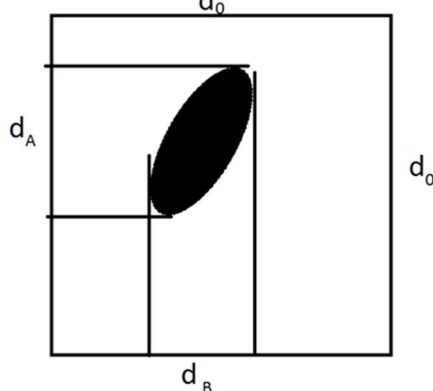


Fig. 3 Particle projection

In this case, using the same logic applied when deriving the Gaudin formula, the penetration probability for a particle in such a position may be recorded and averaged over all rotations as follows:

$$\tilde{P}_l = \left\langle \left(1 - \frac{d_A}{d_0}\right) \left(1 - \frac{d_B}{d_0}\right) \right\rangle_{\varphi, \psi, \vartheta} \quad (4)$$

The resulting formula may be easily generalized for rectangular and slot openings in the screening surface.

The recovery curves, as updated using the new probability formula, are shown in Figure 4. Dashed lines indicate the new theoretical data.

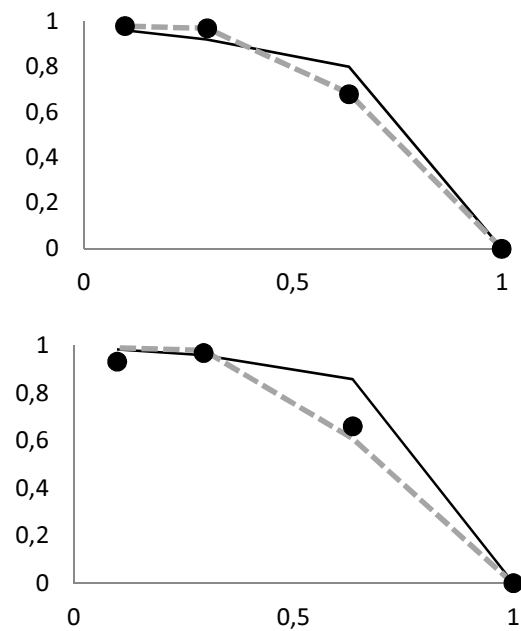


Fig. 4 Updated extraction curves

As can be seen, the resulting probability formulas for single particle penetration through a screen opening significantly increase the accuracy of data obtained.

CONCLUSION

It was established that consideration of particle shapes may play an important role in vibration screening simulations. The improved probability equation for individual particle penetration into the through product may be used to increase the accuracy of calculations made by traditional methods, in particular in conjunction with the presented original screening mathematical model for thin material layers. The above computational models may also be used for optimization of process and design parameters of vibrating screens in order to separate materials by specified parameters.

ACKNOWLEDGMENT

The work was supported by the Russian Government grant #14.579.21.0023.

REFERENCES

- [1] H. Donga, C. Liua, Y. Zhaob, L. Zhaoa, Influence of vibration mode on the screening process, International Journal of Mining Science and Technology, V. 23 I.1, (2013) 95-98.
- [2] H.M. Pang, K. Ridgway, Mechanism of sieving: effect of particle size and shape, Powtech '83 Particle Technology (280 of the EFCE, 1983) 163-169
- [3] K.S. Liu, Some factors affecting sieving performance and efficiency, Powder Technology, 193 (2, 2009) 208-213.
- [4] K.S. Ivanov, Optimization of Vibrational Screening Process, Proc. int. conf. ICOVP 2011 (2011) 174-179.
- [5] T. Dyr, P. Wodqinski, Model particle velocity on a vibrating surface, Physicochemical Problems of Mineral Processing, 36 (2002), 147-157.

Subdiffusive Dynamics Of Istanbul Highway Traffic Flow

Caglar KOSUN

Department of City and Regional Planning
Izmir Institute of Technology
Izmir, TURKEY
cglrksn@gmail.com

Tunc BILGINCAN and Serhan OZDEMIR

Department of Mechanical Engineering
Izmir Institute of Technology
Izmir, TURKEY
{tuncbilgincan & serhanozdemir}@iyte.edu.tr

Abstract—In this study, the authors investigate traffic dynamics at Istanbul Highway. The average vehicle speeds are the main concern to identify the traffic dynamics. It is found that two distinct speed regimes exist in the phase space for the fast lane, and there are transitions between those regimes during the traffic flow. The traffic dynamics of the slow and the fast lanes are investigated with R/S, phase space and autocorrelation analyses. Hurst values in the neighborhood of 0.3 for both lanes, a memory effect in the autocorrelation graphics, and the phase diagrams all point at an introverted traffic characteristic. Based on these findings, it is hypothesized that the vehicle speed fluctuations reveal subdiffusive behavior. The results are discussed.

Keywords—Vehicle speed; diffusion; Levy flights; traffic dynamics; highway traffic flow

I. INTRODUCTION

In different-dimensional spaces, a random walk can be basically defined as a path that composed of consecutive random steps. It can provide a mathematical model for stochastic processes. The random walk is considered in various disciplines such as ecology, biology, physics, chemistry, finance and computer sciences and it can have different forms of motions depending on observed phenomenon in those disciplines. Levy flights are comprised of step-lengths which have heavy-tailed probability distribution. The application of Levy flight is still an active area. In different disciplines, evidence of Levy flight motion can be investigated. For example, it may exist to define statistical mathematic models in physics [1] and finance [2].

In biology, evidence of Levy motion is investigated by many researchers. Reference [3] investigated Brownian and Levy motion in animals. Another study then investigated foraging trajectories of albatrosses with Global Positioning System [4]. Reference [5] has also studied the food searching of wandering albatrosses by considering Levy flights. The study [6] observed a species of African jackal and investigated the existence of Levy flights in the foraging patterns. Reference [7] presents wide survey about the random searches in various types of animals and discussed it from different aspects.

Brownian motion and Levy flights are also presented in mathematical models for the motion of particles in physics. Levy flights over the quantum paths are studied by [8]. The authors [9] presented a model in celestial mechanics stating that Levy flight behavior exists there. A study on financial application of Levy flight is conducted by [10]. The authors [10] suggested autocorrelation as a source of Levy flights for exchange rates. The long term correlations and behavior of Levy flights are tested in Indian Market Indices by the study [11].

The topic of Levy flights attracts interest of some geophysical researches. The study [12] investigates the earthquake behavior via Levy flights. The universal laws of the Levy flight distributions provide many other applications in varying research areas. Reference [13] formulated an algorithm called Cuckoo Search optimization algorithm. It is based on the nature of Levy motion and behavior of cuckoo species.

In this study, the traffic speed data obtained at Istanbul Highway is analyzed and the traffic flow is characterized. The long term memory effects are examined and the presence of Levy motions is investigated.

II. HURST EXPONENT

Hurst exponent measures the smoothness of time series. Hurst exponent (H) must lie between 0 and 1. When the process is persistent (positive correlation), H would be greater than 0.5 (Levy flight or superdiffusion). When it is anti-persistent (negative-correlation), the H would be less than 0.5 (subdiffusion), and Brownian motion for $H = 0.5$. One of the techniques of computing H is the rescaled range analysis (R/S) to measure Hurst exponent. The basic steps of this technique are as follows [14]:

First, compute the average of the time series data

$\chi_1, \chi_2, \chi_3, \dots, \chi_T$ over the time period T ,

$$\langle \chi \rangle_T = \frac{1}{T} \sum_{t=1}^T \chi_t \quad (1)$$

Compute $X(t, T)$ cumulative deviation from the mean,

$$X(t, T) = \sum_{j=1}^t (\chi_j - \langle \chi \rangle_T) \quad (2)$$

Calculate the difference between maximum and minimum that gives the range,

$$R(T) = \max X(t, T) - \min X(t, T) \quad (3)$$

Calculate the standard deviation of χ_t over the same time period,

$$SD = \sqrt{\frac{1}{T} \sum_{t=1}^T (\chi_t - \langle \chi \rangle_T)^2} \quad (4)$$

Compute $(\frac{R}{S})_t$ rescaled range series.

To obtain Hurst exponent (H), log (R/S) is plotted against $\log T$ and the slope would provide H.

In this study, the computed Hurst exponent values of the slow and fast lanes are 0.288 and 0.315, respectively.

III. DATA ANALYSES AND RESULTS

The authors investigate the speed data obtained from a traffic observation point at Istanbul Highway. The speed data from slow and fast lanes for six consecutive days are considered and the data over 24 hour period at two-minute intervals are used in the analyses. The different dynamics of slow and fast lanes are investigated. The data is analyzed with autocorrelation function, generalized Hurst exponent and phase space diagrams.

The autocorrelation of a time series data describes the correlation between values of the variable at different times in the system. The autocorrelation functions of slow lane and fast lane are shown respectively in Fig.1a. and Fig.1b.. As it is seen in the figures below the autocorrelation of the slow lane is more persistent, suggesting that the long term memory effects and predictability of the slow lane-flow are stronger than the fast lane.

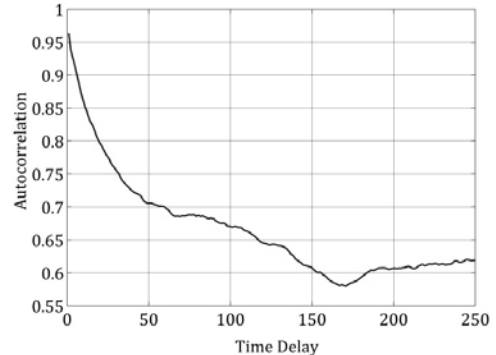


Fig. 1a. Autocorrelation function of slow lane.

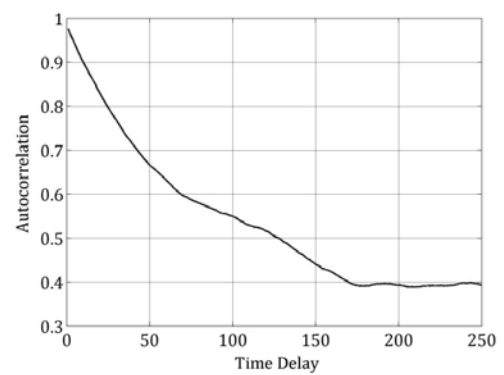


Fig. 1b. Autocorrelation function of fast lane.

Phase space diagrams (Fig. 2a., Fig. 2b.) are well-known indicators for the orientation of the data free from temporal variations. The phase space diagrams of slow and fast lanes are shown below:

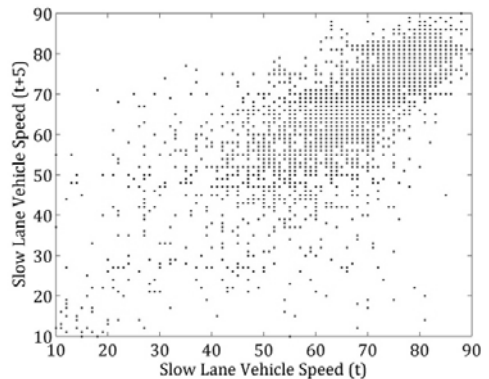


Fig. 2a. Phase space diagram of slow lane for $(x=t)$, $(y=t+5)$.

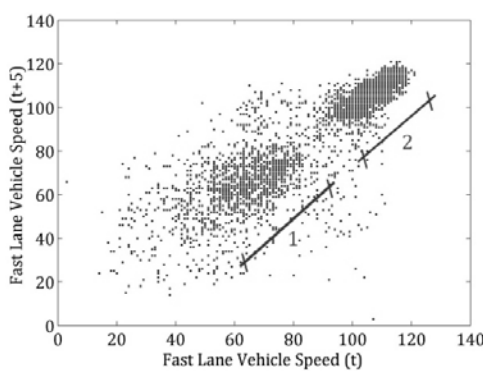


Fig. 2b. Phase space diagram of fast lane for ($x=t$), ($y=t+5$).

As it is seen in Fig. 2a and Fig. 2b, the traffic is concentrated between 50 km/h and 85 km/h, and tend to stay within this speed span. On the other hand, the phase space of fast lane is seen to have two distinct regimes and transitions between those regimes exist in the time series. Even though not provided here, a vectoral flow simulation clearly shows a transition from the region 1 to region 2 in Fig. 2b.. Region 2 represents a fast flowing traffic, or a free-flow around 110 km/h. When the traffic tends to get congested, traffic slows down to 60-65 km/h levels. Each regime has a distinct subdiffusive characteristic on the basis that the traffic tries to get back to these attractor speeds at all times.

IV. CONCLUSIONS

A segment of the Istanbul traffic flow was recorded on a daily basis in two minute intervals and then analyzed. Each lane of the three-lane highway is analyzed separately. On account of the fact that the mid lane resembled the fast lane in terms of the flow nature, the analyses of the mid lane were omitted. The fast and the slow lane data were subjected to R/S analysis which provides a Hurst value, as well as phase space and autocorrelation analyses. A Hurst value of 0.288 for the slow lane as opposed to the fast one with 0.315 implies that the fast lane is more fluid than the slow lane. Relatively higher Hurst value of the fast lane hints at a less subdiffusive nature. Authors believe that the autocorrelation graphs of both lanes are suggestive of this claim in that there are stronger long term connections with the slow lane. What the phase space

diagrams provide us is that the fast flowing traffic has two distinct attractors and the traffic is being attracted to either of these two based on the driving dynamics at any instant. Considering the Hurst values and the phase space diagrams, it is shown that the general behavior of the traffic flow at that highway segment is a subdiffusive one.

References

- [1] N. Mercadier, W. Guerin, M. Chevrollier, and R. Kaiser, "Lévy flights of photons in hot atomic vapours," *Nat Phys*, vol. 5, (8), pp. 602-605, 2009.
- [2] R.N. Mantegna and H.E. Stanley, "Scaling behaviour in the dynamics of an economic index," *Nat*, vol. 376, (6535), pp. 46-49, 1995.
- [3] N.E. Humphries et al., "Environmental context explains Lévy and Brownian movement patterns of marine predators," *Nat*, vol. 465, (7301), pp. 1066-1069, 2010.
- [4] N.E. Humphries, H. Weimerskirch, N. Queiroz, E.J. Southall, D.W. Sims, "Foraging success of biological Lévy flights recorded in situ," *Proc of the Natl Acad Sci*, vol. 109, (19), pp. 7169-7174, 2012.
- [5] G.M. Viswanathan et al., "Lévy flight search patterns of wandering albatrosses," *Nat*, vol. 381, (30), pp. 413-415, 1996.
- [6] R.P.D. Atkinson, C.J. Rhodes, D.W. Macdonald, and R.M. Anderson, "Scale-free dynamics in the movement patterns of jackals," *Oikos*, vol. 98, (1), pp. 134-140, 2002.
- [7] G.M. Viswanathan, E.P. Raposo, and M.G.E. Da Luz, "Lévy flights and superdiffusion in the context of biological encounters and random searches," *Phys of Life Rev*, vol. 5, (3), pp. 133-150, 2008.
- [8] N. Laskin, "Lévy flights over quantum paths," *Commun in Nonlinear Sci and Numerical Simul*, vol. 12, (1), pp. 2-18, 2007.
- [9] J.L. Zhou and Y.S. Sun, "Lévy flights in comet motion and related chaotic systems," *Phys Lett A*, vol. 287, (3), pp. 217-222, 2001.
- [10] A. Figueiredo, I. Gleria, R. Matsushita, and S. Da Silva, "Autocorrelation as a source of truncated Lévy flights in foreign exchange rates," *Phys A*, vol. 323, pp. 601-625, 2003.
- [11] M.C. Mariani et al., "Long correlations and normalized truncated Levy models applied to the study of Indian market indices in comparison with other emerging markets," *Phys A*, vol. 387, (5), pp. 1273-1282, 2008.
- [12] O. Sotolongo-Costa, J.C. Antoranz, A. Posadas, F. Vidal, and A. Vazquez, "Lévy flights and earthquakes," *Geophys Res Lett*, vol. 27, (13), pp. 1965-1968, 2000.
- [13] X.S. Yang and S. Deb, "Cuckoo search via Lévy flights," In *World Congress on Nature & Biologically Inspired Computing, NaBIC, IEEE*, pp. 210-214, 2009.
- [14] J.M.O. Matos, E.P. de Moura, S.E. Krüger, and J.M.A. Rebello, "Rescaled range analysis and detrended fluctuation analysis study of cast irons ultrasonic backscattered signals," *Chaos, Solitons Fract*, vol. 19, (1), pp. 55-60, 2004.

Investigating factors that influence e-school management in high schools in Macedonia

Majlinda Fetaji¹

South East European University,
Contemporary Sciences and Technologies, Computer
Science
Ilindenska bb, 1200 Tetovo, Republic of Macedonia
m.fetaji@seeu.edu.mk

Bekim Fetaji² Mirlinda Ebibi³

South East European University,
Contemporary Sciences and Technologies, Computer
Science
Ilindenska bb, 1200 Tetovo, Republic of Macedonia
m.fetaji@seeu.edu.mk m.ebibi@ibu.edu.mk

Abstract— The focus of this research study is on investigating concepts, analyses and development of e-school management system. High schools in Macedonia still utilize the manual classical paper-based administration and school management. Therefore, e-School Management System (e-SMS) is developed to facilitate teaching and administration staffs to manage school activities in high schools and parents to have in-time information about the performance of their child. As a result, users found that they are willing to use e-SMS which also showed to have improved the quality of the management process in schools and improved information and communication among teachers, parents, students and the general public and. Empirical research is conducted to evaluate the satisfaction of e-SM and the attitude towards using this system in the future. Furthermore, the factors that influence the usage and the positive and satisfactory level of attitude towards electronic school management will be identified. Findings are presented and recommendations are provided.

Keywords— e-SM, e-SMS, e-school management, e-school management system, web services, Regression Model of Statistical Significance of Results

I. INTRODUCTION

In Macedonia, the classical method of management and administration of learning and school activities is practiced in all secondary schools. The fact is that this classical approach of management is not appropriate and contains various deficiencies such as keeping records on paper, face-to-face miscommunication, misuse of a position, not-in-timely information and communication, inadequate communication and information among school staff itself, students and parents and other deficiencies. Therefore, e-School Management System (e-SMS) is developed to facilitate teaching and administration staff to manage school activities in high schools and parents to have in-time information about the performance of their student/child. This school management e-Model will offer tasks such as registering students, teachers, forming classes, keeping track of teachers' and students' status and profiles; generating reports, official transcript, etc.

II. HYPOTHESIS

Formulated are the following hypotheses which this paper should give answers to:

H0: The electronic school management will improve the quality of school management processes and information and communication between the school staff, students, parents and the general public.

H1: The experience in using e-applications previously and the confidence on e- applications influence and increase the satisfactory level of attitude towards e-school management.

III. RESEARCH METHODOLOGY

The study is conducted through qualitative testing method using a questionnaire consisted of 20 questions about the profilization, academic background, computer skills; usage and attitude towards different features of electronic school management activities and have they used and do they believe e-applications. Participants were students, teaching and administrative staff and parents of 3 high schools in Kumanovo, RM. 15 teachers, 41 parents and 5 administrators filled-in an online questionnaire that contained multiple-choice questions. For some of the questions students had to denote their own attitude. The questionnaire was alienated into four sections: "General information", "Computer skills", "Attitude towards different features of electronic school management", „Attitude towards reliability and quality of management in e-school management“ and „have they used and believe e-applications“.

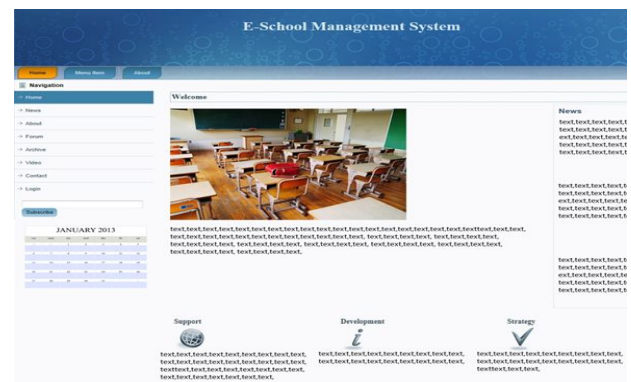


Fig 1. A screen shot of welcome screen

The results are presented in tables of percentages, graphics and diagrams. Screen shots of the welcome screen is shown in the given figure 1.

IV. RESULTS AND FINDINGS

Precondition for successful utilizing an e- management application is having a computer and internet access at home/neighbor cafeteria. It is evident that the percentage of owned computers in high schools in deployed countries in the world increases every day. In our target high schools, the results shown in the figure 3 and 4, we found that the lack of computer and/or internet access is not an obstacle. We can see that 95% of users have a computer at home, while 87% have an internet access.

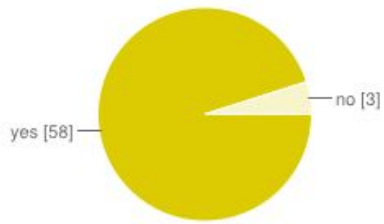


Fig 2. Percentage of owned computers (100%)

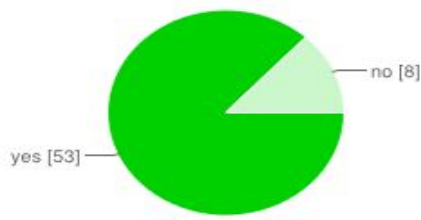


Fig 3. Percentage of having internet access (89%)

The results about the question Q12: Is the school management administered this way improved compared to the classical manual method; and Q14: Does the approach of using e-SMS offer better quality management, which are shown in the figure 4 and figure 5.

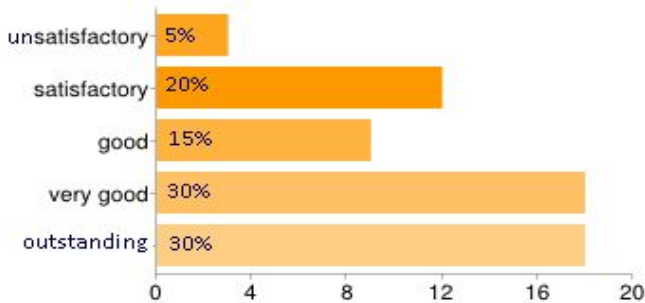


Fig 4. The e-SMS management improvement compared to the classical manual method.

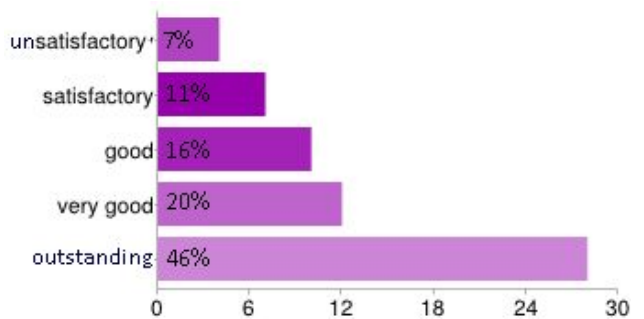


Fig 5. The e-SMS management offers better quality management

60% of users claim there is improvement in the school management using e-SMS, 15% claim it is good while 25% do not see any improvement in e-SMS management vs. manual management. 66% of users claim that e-SMS offers better quality management, 10% say the e-management is good while 18% are not satisfied with the quality of the e-management. These results indicate that the electronic school management is outstanding in aspect of improvement and better quality of management compared to the classical manual management which is expected, but still there are a percentage of users that are not satisfied.

These results verified our hypothesis H0 is true.

Furthermore, we are interested in the usage and positive attitude of users towards electronic school management. This is investigated by the survey question Q15: Are you satisfied the way school management is organized vs. classical way?; and Q16: Do you like using this school management application, shown in the figure 6 and figure 7. The answers of the question Q17: If you do not like the electronic school management, what is the reason?, tell us some of main reasons why users do not like e-school management, which are shown in figure 8.

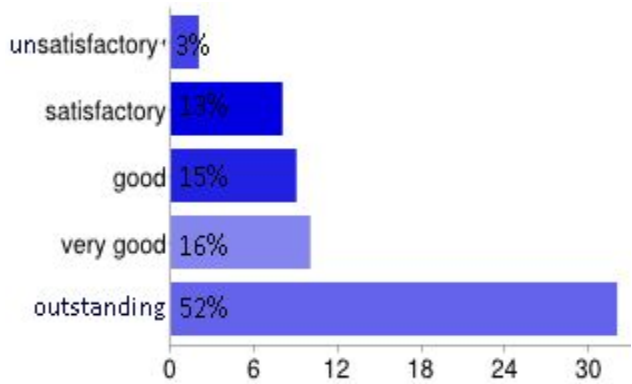


Figure 6. Satisfaction of the way e-school management is organized vs. classical manual method

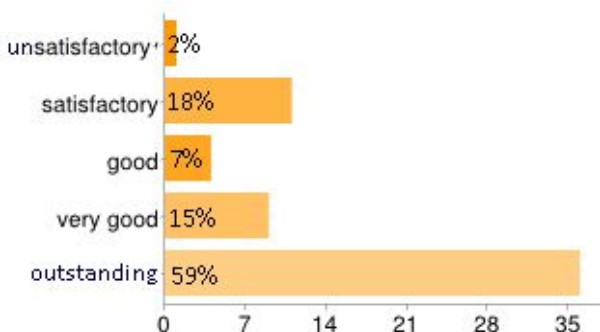


Figure 7. Satisfaction of performing e- school management (e-SM)

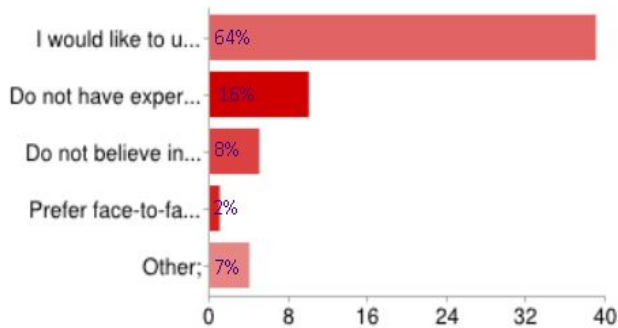


Figure 8. Reasons users do not like to use e- school management system

From the results we see that users' satisfaction how the school management is organized vs. classical manual way is in high percentage 68% outstanding and very good, while 16% are not satisfied with the electronic management, 15% think it is good. About 74% of users are outstanding and very good satisfied using the e-SMS for school management, 20% are not satisfied, while 7% say it is good. From the question if the users would not like to perform e-school management, 64% answered they would like to use the e-SM, while 45% of those who would not like to use stated the reason that they do not have experience in using e-applications, 23% stated that they do not believe in the security of e-applications, just 5.5% prefer face-to-face communication, and 19.5% stated other reason. The highest percentage of users who do not like electronic school management stated their experience in using e-applications as a reason. The next higher percentage is of those that do not believe e-applications. Also, the percentage of users that would not like to use e-management is very high 45%. That is a good reason to look for what influences the still high percentage of unwillingness to use e-management, even though the percentage of users with very good and outstanding attitude is very high 64%. Therefore, we want to investigate the influence of previous experience in using e-applications and the users' confidence in e-applications in the increase of the satisfactory level of attitude towards electronic school management. Also, we want to investigate how does the role of the user in the education process influence the satisfactory level of attitude towards electronic school management. The

main independent variables of our investigation are the previous experience in using e-applications and confidence towards e-applications, where the initial questions to which the students had to answer was "The level of previous use of e-applications", "The level of confidence towards e-applications" and "Are they satisfied the way school management is organized using e-management". They were given five options to answer: Unsatisfactory (1); Satisfactory (2); Good (3); Very Good(4) and Outstanding(5). The results about dependency of satisfactory level of attitude towards electronic school management on the previous experience in using e-applications and confidence in e-applications and the role of the user in the education process are shown in the following table 2, table 3 and table 1 and fig 10, fig 11 and fig 12.

Table 1. Satisfactory level of attitude towards electronic school management on the role of the user

| Level of satisfaction of e-school management | Role in the education process | | |
|--|-------------------------------|--------|------------------------|
| | Teacher | Parent | Administration Officer |
| Unsatisfactory | 2% | 2% | |
| Satisfactory | | 13% | |
| Good | 2% | 3% | 2% |
| Very good | 10% | 3% | 3% |
| Outstanding | 11% | 46% | 2% |

Table 2. Dependency of satisfactory level of attitude towards electronic school management on the previous use of e-applications

| Level of satisfaction of e-school management | Level of previously used e-applications | | | | |
|--|---|-----------|--------------|------------|--------|
| | Never | Sometimes | Intermediate | Frequently | Always |
| Unsatisfactory | 3% | | | | |
| Satisfactory | 3% | 8% | 7% | | |
| Good | 2% | 2% | 2% | 2% | |
| Very good | 5% | 3% | 2% | 5% | 2% |
| Outstanding | 3% | 2% | 3% | 40% | 11% |

Table 3. Dependency of satisfactory level of attitude towards electronic school management on the level of confidence on e-applications

| Level of satisfaction of e-school management | Level of confidence towards e-applications | | | | |
|--|--|--------------|------|-----------|-------------|
| | Unsatisfactory | Satisfactory | Good | Very Good | Outstanding |
| Unsatisfactory | 3% | | | | |

| y | | | | | |
|--------------|----|----|----|-----|-----|
| Satisfactory | 5% | 8% | | | |
| Good | 2% | 2% | 2% | 2% | |
| Very good | 7% | 3% | | 2% | 5% |
| Outstanding | 3% | 2% | 2% | 36% | 16% |

According to the results shown in tables 2 and 3, we can see that 50% / 33% of users which **have never/ sometimes** used e-applications have an outstanding and very good level of satisfaction on attitude towards electronic school management, while 38% / 54% are not satisfied with the e-management, 13% / 13% think it is good. The satisfactory level of attitude towards **electronic school management** resulted to be outstanding and very good with the highest percentage of 96%/100% of users which level of previously used e-applications is outstanding and very good, while 4% / 0% think it is good and there are no unsatisfied users. We have similar results from the influence of the confidence towards e-applications in satisfaction towards e-management. 50% / 33% of users which **have unsatisfactory/satisfactory level** of confidence towards e-applications have an outstanding and very good level of satisfaction on attitude towards electronic school management, while 40% / 54% are not satisfied with the e-management, 10% / 13% think it is good. 96% / 100% of users which **have outstanding/very good level** of confidence towards e-applications have an outstanding and very good level of satisfaction on attitude towards electronic school management, while 4% / 0% think it is good and there are no unsatisfied users. We can conclude that previous use of e-applications and level of confidence on e-applications directly influence the level of satisfaction on attitude towards electronic school management. Even the users that have not previously used e-apps and have no confidence in e-apps have a positive attitude towards electronic school management. Those that have an experience in using e-apps and confidence in e-apps have a strongly positive and a high level of satisfaction on attitude towards electronic school management. From the results presented in table 1 and fig 13, only 8% of teachers are not satisfied and do not have positive attitude towards electronic management, while 84% have outstanding and very good satisfactory level on attitude towards e-management. 73% of parents have outstanding and very good satisfactory level on attitude towards e-management while just 23% are unsatisfied with e-management. Administration officers have declared themselves as highly satisfied with the e-management.

Moreover, after investigating their correlation, it was found that there is a strong correlation among satisfactory level of attitude towards e-school management with the 2 indicators, shown in the following fig 9, which is strong enough (closer to 1 – stronger) to say that by increasing the level of use of e-apps and level of confidence towards e-apps, the satisfactory level of attitude towards electronic school management increases. Hereby, the hypothesis H1 is proved.

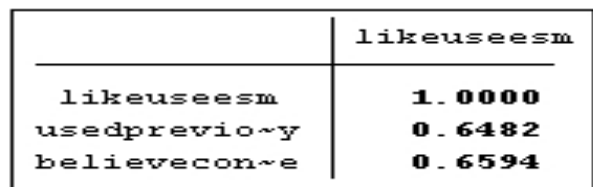


Figure 9. Correlation of the level of satisfaction towards e-SM with the used previously e-apps and confidence on e-apps

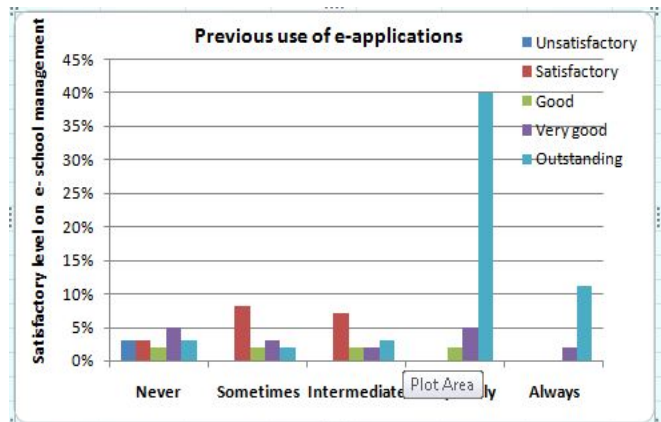


Figure 10. Satisfaction level towards e-SM vs. previous use of e-applications

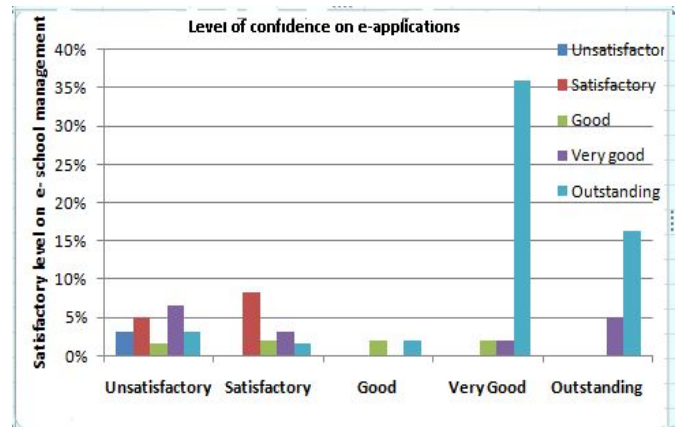


Figure 11. Satisfaction level towards e-SM vs. confidence on e-applications

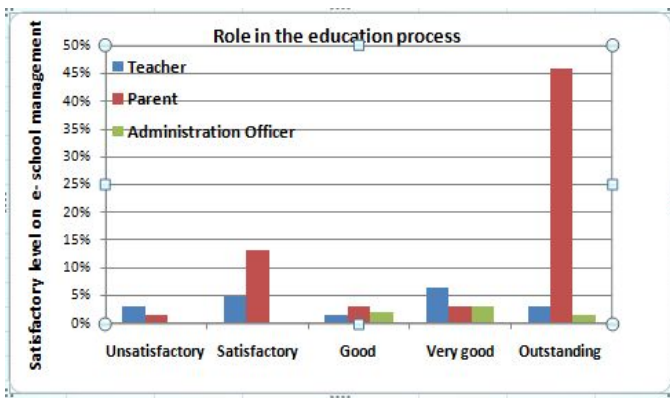


Figure 12. Satisfaction level towards e-SM vs. role in the education process

Moreover, we want to prove the significance of the obtained results using regression model of statistical significance.

V. THE REGRESSION MODEL OF STATISTICAL SIGNIFICANCE OF RESULTS

Regression analysis is a statistical tool to investigate the relationships between variables and to develop a model that is useful for predicting the value of the dependent variable for given values of the independent variable. We want to prove the statistical significance of the proof of hypothesis. Actually we want to determine the fundamental effect of the independent variable(s) upon dependent variable—"satisfactory level of attitude towards electronic school management". To explore these issues we gathered data on the variables of interest and use regression to estimate the quantitative effect of the fundamental variables upon the variable that they influence. We also evaluate the "statistical significance" of the estimated relationships, that is, the degree of self-reliance that the true relationship is close to the estimated relationship.

First we define the research hypothesis that is H_1 ="higher levels of previous experience in using e-applications and higher levels of confidence on e- applications influence and increase the satisfactory level of attitude towards e-school management", H_0 ="There is no relationship between levels of previous experience in using e-applications and higher levels of confidence on e- applications and the satisfactory level of attitude towards e-school management".

To investigate this hypothesis, we have gathered set of measured values on levels of previous use of e-applications and levels of confidence on e-applications. Let x symbolize levels of previous use of e-applications and let y symbolize satisfactory level of electronic school management. We suppose that factors other from x which are being unobserved (noise) influence it. Accordingly, we suppose that: i) users from the group which level of previous use of e-apps is "never and sometimes" might show higher satisfactory level on attitude towards e-SM (we had such results, see figures 10-figure 12.) and ii) satisfactory level on attitude towards e-SM increases above this baseline (called intercept parameter b_0

[10]). Our hypothesis may be written as a regression equation as follows: $y = b_0 + b_1 * x + e$, where b_1 is slope parameter, b_0 is intercept parameter and e is disturbance in the relationship between y and X .

VI. CONCLUSIONS

Now we have to test how good this regression equation predicts values of y , for given values of X_i , $i=1, \dots, 5$. We use stata_9. The results of regression are shown in the following Tables 4-5. Results are presented in the following regression equations:

$$Y = 2.2 + 0.59 * X,$$

Coefficients (slope) $b_1=0.59$ is positive which means that for each increase level in use of e-applications, the satisfactory level of attitude towards e-SM increases respectively by $b_1=0.59$. The constants b_0 is the initial position: the satisfactory level of attitude towards e-SM would be about $b_0=2.2$, (meaning would be mostly good and— among level 2 and 3) for users that have never used e-applications.

Table 5. Regression of satisfactory level of attitude towards e-SM vs. level of previous use of e-apps

| Source | SS | df | MS | Number of obs | = 60 |
|----------|------------|----|------------|---------------|----------|
| Model | 37.1140143 | 1 | 37.1140143 | F(1, 58) | = 42.03 |
| Residual | 51.2193191 | 58 | .883091708 | Prob > F | = 0.0000 |
| Total | 88.3333333 | 59 | 1.49717514 | R-squared | = 0.4202 |
| | | | | Adj R-squared | = 0.4102 |
| | | | | Root MSE | = .93973 |

| likeuseesms | Coef. | Std. Err. | t | P> t | [95% Conf. Interval] |
|----------------|----------|-----------|------|-------|----------------------|
| usedpreviously | .5938242 | .0915992 | 6.48 | 0.000 | .4104684 .77718 |
| _cons | 2.236738 | .3214685 | 6.96 | 0.000 | 1.593249 2.880227 |

Table 6. Regression of satisfactory level of attitude towards e-SM vs. level of confidence on e-apps

| Source | SS | df | MS | Number of obs | = 60 |
|----------|------------|----|------------|---------------|----------|
| Model | 38.4087462 | 1 | 38.4087462 | F(1, 58) | = 44.62 |
| Residual | 49.9245872 | 58 | .860768744 | Prob > F | = 0.0000 |
| Total | 88.3333333 | 59 | 1.49717514 | R-squared | = 0.4348 |
| | | | | Adj R-squared | = 0.4251 |
| | | | | Root MSE | = .92778 |

| likeuseesms | Coef. | Std. Err. | t | P> t | [95% Conf. Interval] |
|-------------------|----------|-----------|------|-------|----------------------|
| believeconfidence | .5473931 | .0819459 | 6.68 | 0.000 | .3833604 .7114257 |
| _cons | 2.369393 | .2945118 | 8.05 | 0.000 | 1.779863 2.958922 |

The probability of the F statistic, the test for statistical significance of the regression equation (an F-value > 4.0 is usually statistically significant), for which we got the values of $F=42$, means that the regression equations help us to understand the relationship between level of previous use of e-apps X and y . The probability of the F statistic for the overall regression relationship, the p value describes the statistical

significance of the test: it is significant at 99% level, because the p value is 0.000. The values of r-squared, $r^2=0.42$, which is the measure of relationship and indicates that with the known value of X (the level of previous use of e-apps), we can explain 42% of the variance in y (the satisfactory level towards e-SM). We reject the null hypothesis that there is no relationship. The standard error is very small, approximately Std. Err.=0.09. A t-test that indicates statistical significance of the coefficient b_1 (a t-value > 2.0 is usually statistically significant) which is large in our case $t=6.48$, and we can conclude that there is a statistically significant relationship. This means that the independent variable or X, (level of previous use of e-apps) should be kept in the regression equation, since it has a statistically significant relationship with the dependent variable or y (satisfactory level of attitude towards e-SM).

We got similar results when investigating the second independent variable “level of confidence on e-apps”. The regression equation is formulated as: $Y=2.3 + 0.54 * X$,

Coefficients (slope) $b_1=0.53$ is positive which means that for each increase level in confidence in e-applications, the satisfactory level of attitude towards e-SM increases respectively by $b_1=0.54$. The constants $b_0=2.3$ meaning the satisfactory level of attitude towards e-SM would be about $b_0=2.3$, (meaning would be mostly good and– among level 2 and 3) for users that have no confidence on e-applications. The F value $F=42$, means that the regression equations help us to understand the relationship between level of confidence on e-apps X and y. The p value describes the statistical significance of the test: it is significant at 99% level, because the p value is 0.000. The values of r-squared, $r^2=0.43$, indicates that with the known value of X (the level of confidence on e-apps), we can

explain 43% of the variance in y (the satisfactory level towards e-SM). We reject the null hypothesis that there is no relationship. We support the research hypothesis that there is a statistically significant relationship between the level of confidence on e-apps and the satisfactory level of attitude towards e-SM. A t-test is $t=6.48$, we can conclude that there is a statistically significant relationship. This means that the level confidence on e-apps has a statistically significant relationship with the dependent variable (satisfactory level of attitude towards e-SM). We have verified the statistical significance of data and conclusions. Level of previous use of e-apps and level of confidence on e-apps are highly significant. We recommend giving effort to increase the user experience on e-applications and also increase the confidence towards e-applications by organizing trainings and by presenting users (teachers, parents and administration officers) the real advantages of e-management.

REFERENCES

- [1] [1] Douglas C. Montgomery, Elizabeth A. Peck (2006) “Introduction to Linear Regression Analysis”, John Wiley & Sons Inc, Wiley-Interscience, ISBN: 0471754951, New York.
- [2] [2] Chong, G., & Jun, Ch., (2005) “Performance of some variable selection methods when multicollinearity is present”, Chemometrics and Intelligent Laboratory Systems, Elsevier B.V, Volume 78, Issues 1-2, 28 July 2005, Pages 103-112 (doi:10.1016/j.chemolab.2004.12.011)
- [3] Curtis, B. (1980). Measurement and experimentation in software engineering. Proceedings of the IEEE, vol. 68, no. 9, (pp. 1144-1157).
- [4] Van Vliet, H. (2000). Software Engineering: Principles and Practices, 2nd Edition. West Sussex, England: John Wiley & Sons.

Automatic paint mixing process using LabView

Mohamed A. Muftah, Abdulgani M. Albagul, and Abdullah M. Faraj

Abstract—The paint industry is one kind of process that depends on the automatic control techniques. The paint composition is the most important issue in paint industry. Therefore, many techniques have been developed to overcome this problem. In the past, paint composition has been done manually where sometimes does not meet the required color. For this reason, the automatic paint preparation techniques take place to solve the manual paint composition. In this research, an automatic color machine depends on the LabVIEW techniques as a control algorithm is designed and fabricated. The proposed control technique is one kind of graphical control techniques that uses a block diagram and icons as a control algorithm. The LabVIEW program is divided in two parts. The first is the front panel (user interface) and the second is Block diagram (algorithm code). The LabVIEW provided the user with user interface panel which will help the user to feed the quantity of the desired new color. The precision of the output color was acceptable compared to the original color. The outcome of the project will help researchers and those interested in the area of paint industry to explore the features of LabVIEW and its usage.

Keywords—Paint mixing, control algorithm, LabView, software tools.

I. INTRODUCTION

PAINT is one of the oldest synthetic substances known, with a history stretching back into prehistoric times. It was made more than 3500 years ago by prehistoric man as they mixed clays and chalks with animal fats and used these paints to depict their hunts on cave walls. By 2500 BC the Egyptians had improved this technology considerably. They had developed a clear blue pigment by grinding azurite, and instead of animal fats they used gums, wax and maybe also albumen (egg white) as binders and solvents for their paints. The technology improved still further during the first millennium BC as the Greeks learnt to blend paints with hot wax, rather than water, making a paint that was both thicker and easier to spread and thus making it possible to blend colors. By this time many colors were available from both natural and synthetic sources, one of the most interesting being a purple pigment made from heating yellow earth till it turned red and then plunging it into vinegar. The technology then lapsed for many years, with techniques being passed down from generation to generation by travelling craftsmen. This continued until the eighteenth century, when paint

A. M. Albagul is a professor with Control engineering Department, Faculty of Electronic Technology, Baniwalid, Libya (phone: 218 -535242335; fax: 218-535243134; e-mail: albagoul@yahoo.com).

M. N. Muftah is with Control engineering Department, Faculty of Electronic Technology, Baniwalid, Libya (e-mail: eshlipta@yahoo.com).

A. M. Faraj is with Control engineering Department, Faculty of Electronic Technology, Baniwalid, Libya (e-mail: abdalla_milad@yahoo.com).

factories began to be opened in Europe and America, and by the nineteenth century this mass production had brought prices down to such an extent that houses began to be painted. Color is the visual perceptual property corresponding in humans to the categories called red, blue, yellow, green and others. Color derives from the spectrum of light (distribution of light power versus wavelength) interacting in the eye with the spectral sensitivities of the light receptors. Color categories and physical specifications of color are also associated with objects or materials based on their physical properties such as light absorption, reflection, or emission spectra. By defining a color space, colors can be identified numerically by their coordinates. Now, in the twentieth century, the chemistry of many aspects of paint manufacture and function is understood, meaning that paint manufacture has finally moved from being an art to being a science. The science of color is sometimes called chromatics, chromatography, colorimetry, or simply color science. It includes the perception of color by the human eye and brain, the origin of color in materials, color theory in art, and the physics of electromagnetic radiation in the visible range (that is, what we commonly refer to simply as light).

II. HISTORICAL BACKGROUND

Color theory was originally formulated in terms of three "primary" or "primitive" colors red, yellow and blue (RYB) because these colors were believed capable of mixing all other colors. This color mixing behavior had long been known to printers, dyers and painters, but these trades preferred pure pigments to primary color mixtures, because the mixtures were too dull (unsaturated). The RYB primary colors became the foundation of 18th century theories of color vision, as the fundamental sensory qualities that are blended in the perception of all physical colors and equally in the physical mixture of pigments or dyes. These theories were enhanced by 18th-century investigations of a variety of purely psychological color effects, in particular the contrast between "complementary" or opposing hues that are produced by color afterimages and in the contrasting shadows in colored light. These ideas and many personal color observations were summarized in two founding documents in color theory: the Theory of Colors (1810) by the German poet and government minister Johann Wolfgang von Goethe, and The Law of Simultaneous Color Contrast (1839) by the French industrial chemist Michel Eugène Chevreul. Subsequently, German and English scientists established in the late 19th century that color perception is best described in terms of a different set of primary colors red, green and blue violet (RGB) modeled through the additive mixture of three monochromatic lights. Subsequent research anchored these primary colors in the differing responses to light by three types of color receptors or

cones in the retina (trichromacy). On this basis the quantitative description of color mixture or colorimetry developed in the early 20th century, along with a series of increasingly sophisticated models of color space and color perception, such as the opponent process theory.

A. Primary Color Models

Primary colors are sets of colors that can be combined to make a useful range of colors. For human applications, three primary colors are usually used, since human color vision is trichromatic. For additive combination of colors, as in overlapping projected lights or in CRT displays, the primary colors normally used are red, green, and blue. For subtractive combination of colors, as in mixing of pigments or dyes, such as in printing, the primaries normally used are cyan, magenta, and yellow, though the set of red, yellow, blue is popular among artists. See RGB color model, CMYK color model, and RYB color model for more on these popular sets of primary colors. Any particular choice for a given set of primary colors is derived from the spectral sensitivity of each of the human cone photoreceptors; three colors that fall within each of the sensitivity ranges of each of the human cone cells are red, green, and blue. Other sets of colors can be used, though not all will well approximate the full range of color perception. The combination of any two primary colors creates a secondary color. The most commonly used additive color primaries are the secondary colors of the most commonly used subtractive color primaries, and vice versa.

B. RGB Color Model

The RGB color model, shown in figure 1, is an additive color model in which red, green, and blue light are added together in various ways to reproduce a broad array of colors. The name of the model comes from the initials of the three additive primary colors, red, green, and blue.

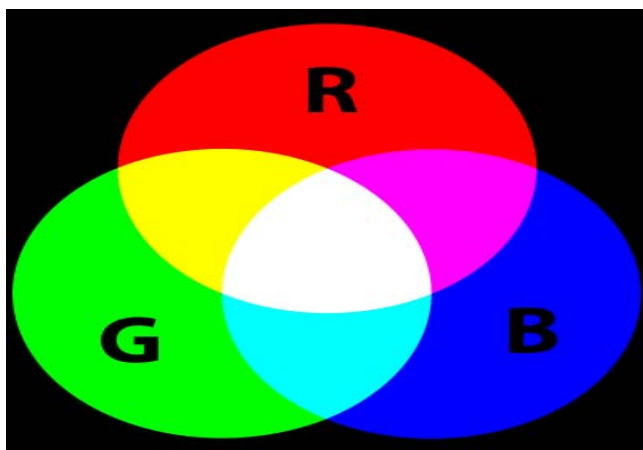


Fig. 1 RGB color model

The main purpose of the RGB color model is for the sensing, representation, and display of images in electronic systems, such as televisions and computers, though it has also been used in conventional photography. Before the electronic age, the RGB color model already had a solid theory behind it, based in human perception of colors. Typical RGB input devices are color TV and video cameras, image scanners, and

digital cameras. Typical RGB output devices are TV sets of various technologies (CRT, LCD, plasma, etc.), computer and mobile phone displays, video projectors, multicolor LED displays, and large screens such as Jumbo Tron. Color printers, on the other hand, are not RGB devices, but subtractive color devices (typically CMYK color model).

C. CMYK Color Model

The CMYK color model (process color, four color) is a subtractive color model, used in color printing, and is also used to describe the printing process itself. CMYK refers to the four inks used in some color printing: cyan, magenta, yellow, and key (black). Though it varies by print house, press operator, press manufacturer, and press run, ink is typically applied in the order of the abbreviation. The "K" in CMYK stands for key because in four-color printing, cyan, magenta, and yellow printing plates are carefully keyed, or aligned, with the key of the black key plate. Some sources suggest that the "K" in CMYK comes from the last letter in "black" and was chosen because B already means blue. However, this explanation, although useful as a mnemonic, is incorrect. The CMYK model works by partially or entirely masking colors on a lighter, usually white, background. The ink reduces the light that would otherwise be reflected. Such a model is called subtractive because inks "subtract" brightness from white. In additive color models such as RGB, white is the "additive" combination of all primary colored lights, while black is the absence of light. In the CMYK model, it is the opposite: white is the natural color of the paper or other background, while black results from a full combination of colored inks. To save money on ink, and to produce deeper black tones, unsaturated and dark colors are produced by using black ink instead of the combination of cyan, magenta and yellow.

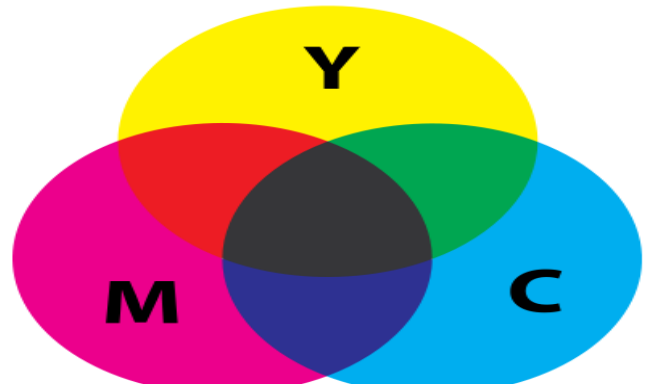


Fig. 2 CMYK color model

D. RYB Color Model

RYB (an abbreviation of red-yellow-blue) is a historical set of colors used in subtractive color mixing, and is one commonly used set of primary colors. It is primarily used in art and design education, particularly painting. RYB predates modern scientific color theory, which argues that magenta, yellow, and cyan are the best set of three colorants to combine, for the widest range of high-chroma colors. Red can be produced by mixing magenta and yellow, blue can be produced by mixing cyan and magenta, and green can be

produced by mixing yellow and cyan. In the RYB model, red takes the place of magenta, and blue takes the place of cyan. However, reproducing the entire range of human color vision with three primaries either in an additive or subtractive fashion is generally not possible; see gamut for more information.

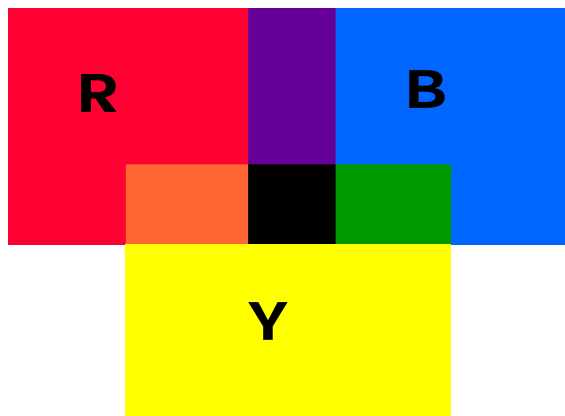


Fig. 3 RYB color model

E. Secondary Color

A secondary color is a color made by mixing two primary colors in a given color space. Examples include the following:
 1) Additive secondaries (Light RGB); For the human eye, the best primary colors of light are red, green, and blue. Combining the wavelengths of light we see as these colors produces the greatest range of visible color. Since color is defined as the wavelengths of the emitted light, combining RGB colors means adding light (thus the term "additive color"), and the combinations are brighter. When all three primaries (or for that matter all three secondaries) are combined in equal amounts, the result is white. The RGB secondary colors produced by the addition of light turn out to be the best primary colors for pigments, the mixing of which subtracts light.

- 1) Additive secondaries (Light RGB); For the human eye, the best primary colors of light are red, green, and blue. Combining the wavelengths of light we see as these colors produces the greatest range of visible color. Since color is defined as the wavelengths of the emitted light, combining RGB colors means adding light (thus the term "additive color"), and the combinations are brighter. When all three primaries (or for that matter all three secondaries) are combined in equal amounts, the result is white. The RGB secondary colors produced by the addition of light turn out to be the best primary colors for pigments, the mixing of which subtracts light.
- 2) Subtractive Secondaries, Pigments, such as inks and paint, display color by absorbing some wavelengths of light and reflecting the remainder. When pigments are combined, they absorb the combination of their colors, and reflect less. Thus, combining pigments results in a darker color. This is called subtractive color-mixing, as mixing pigments subtracts wavelengths from the light that is reflected.

i) Printing (CMY), The mixture of equal amounts of these colors produce the secondary colors red, blue, and "lime" green (the RGB primary colors of light). That is, the primary and secondary CMY colors (with secondary colors in boldface) Ideally, combining three perfect primary colors in equal amounts would produce black, but this is impossible to achieve in practice. Therefore a "key" pigment, usually black, is added to printing to produce dark shades more efficiently. This combination is referred to as CMYK, where K stands for Key.

ii) Traditional painting (RYB) Before the discovery of CMY, at least as far back as Goethe, the best primary colors were thought to be red, yellow, and blue. These are used even today in painting. Mixing these pigments in equal amounts produces orange, green, and purple. That is, the primary and secondary RYB colors (with secondary colors in boldface)

F. Tertiary Color

A tertiary color is a color made by mixing either one primary color with one secondary color, or two secondary colors, in a given color space such as RGB (more modern) or RYB (traditional). Tertiary colors are a combination of full saturation of one primary color plus half saturation of another primary color and none of a third primary color. Tertiary colors have specific names, one set of names for the RGB color wheel and a different set of names and colors for the RYB color wheel. These names are shown below. Brown and grey colors can be made by mixing complementary colors.

- 1) **RGB or CMY primary, secondary, and tertiary colors;** The primary colors in an RGB color wheel are red, green, and blue, because these are the three additive colors—the primary colors of light. The secondary colors in an RGB color wheel are cyan, magenta, and yellow because these are the three subtractive colors—the primary colors of pigment.
- 2) **Traditional painting (RYB);** The primary colors in an RYB color wheel are red, yellow, and blue. The secondary colors in an RYB color wheel are made by combining the primary colors orange, green, and violet. In the red-yellow-blue system as used in traditional painting, and interior design, tertiary colors are typically named by combining the names of the adjacent primary and secondary.
- 3) **Tertiary-and quaternary-color terms;** The terms for the RYB tertiary colors are not set. For the six RYB hues intermediate between the RYB primary and secondary colors, the names amber (yellow-orange), vermillion/cinnabar (red-orange), magenta (red-purple), violet (blue-purple), viridian (blue-green), and chartreuse (yellow-green) are commonly found. The names for the twelve quaternary colors are more variable, if they exist at all, though indigo and scarlet are standard for (blue-violet) and (red-vermilion).

III. LABVIEW FOR COLOR MIXING PROCESS

In this section, the LabView software is used to control the paint mixing process in the system. The overall structure of the Automatic mixer paint machine is illustrated in figure 4. The control strategy of this machine can be summarized as follows; firstly, the desired or specified quantity of raw material (white paint) can be controlled by adjusting the wait time of the opening (SVRM), where SVRM is a solenoid valve, and then the new color can be prepared by adjusting the duration of the opening of the three valves SVR, SVG, SVB for the three tinctures. After this feeding, the mixer will turn ON to mix and to achieve good construction of the new color. Then SVO will be opened to take the new color. After that, the cleaner liquid in tank tank will be pumped to the mixer tank to clean the inner surface of the mixing tank.

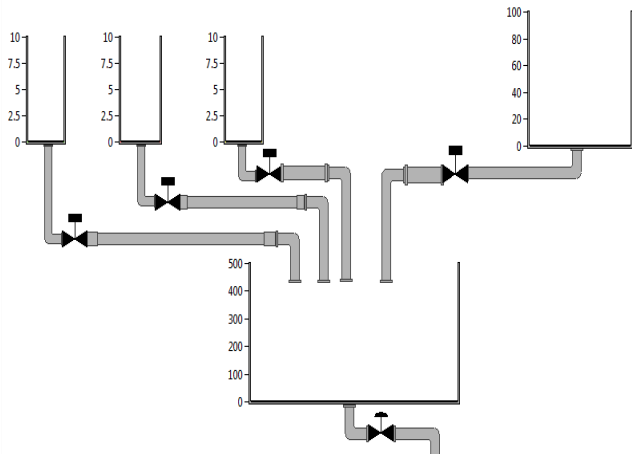


Fig. 4 Paint mixing machine

A. LabView Program Configuration

From the introduction of LabVIEW program in the chapter three, the code will be written in this chapter. The new VI will be opened by clicking on the Blank VI. After opening the new VI, two windows will be emerged, the block diagram and the front panel. They are the main components of the LabVIEW. While the front panel consists of the input and the output, which is seen by the user. Since, the block diagram is code window, where the functions are connected graphically. The following sections will illustrate the block diagram and front panel respectively. In block diagram, the flat sequence will be added by clicking on the right mouse button the function palette will be emerged, click the structure and then the flat sequence will appear. The other frame will be added to the flat sequence automatically. With the same way, another frame will be added to the flat sequence, which is the main window in the program, consists of three frames. Frame 2 will not execute till the frame 1 executes and the frame 3 will not execute till the frame 1 and frame 2 executes and so on.

B. Frame 1 (white paint quantity control)

The first frame has an input which is the quantity of the paint that need to be mixed. The quantity of the white paint raw can be controlled by using time delay (wait) in this frame, the value of wait in (ms) determine the duration of valve

opening, which is connected between the tank 1 and the mixed tank. Figure 5 illustrates frame 1.

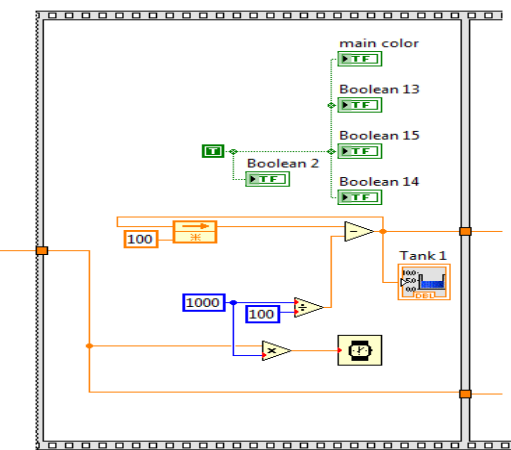


Fig. 5 Frame 1

C. Frame 2

Frame 2 have two inputs, first input is the same input as the frame 1. The second input, represent the code of the required paint from data base. Figure 6 shows the frame 2 and the container case structure, each case devoted to one paint color, and the data of the case are presented from the color data base. In addition the control of each valve of the three tinctures is depends on the value of wait (ms), which is calculated from the data base of each color. The number of case in frame 2 depends on the number of required color paints. This mean, every color paint has one case structure. In this project, three color have been selected which are (RGB1, RGB7, and RGB10). Every case has three tinctures, which are needed to be added to the main color to get the needed paint. The input to the case structure is Enum consists of 3 options, which are the needed colors. The required color is chosen from the front panel, every color has a unique number to distinguish between them. In addition to the case structure, there are three flat sequence, every one consists of two frames responsible on opening and closing the valves for the tanks, which are consists of the colors. The frame 2 has the value of the quantity of the mixed color in addition to the tinctures.

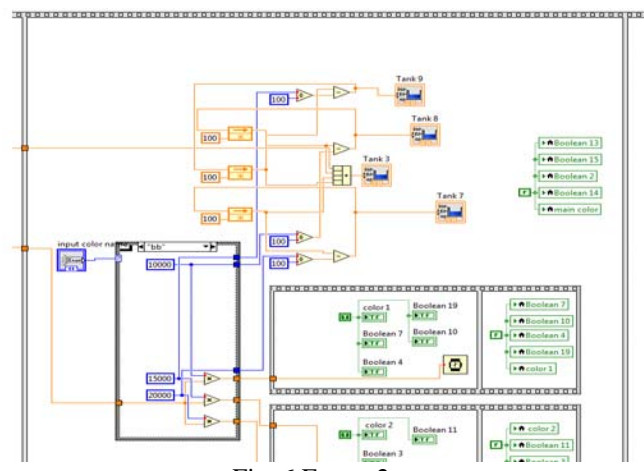


Fig. 6 Frame 2

D. Frame 3

Frame 3 as shown in figure 5.9, consists of the flat sequence which is consists of three frames. The first frame responsible on turn ON the mixer with the specific time delay. The second frame consists of time delay which is responsible on the opening of the output valve (required paint), also responsible on the turning off the mixer. The third frame responsible on the turning off the output valve, also responsible on the reset of the value of the main tank

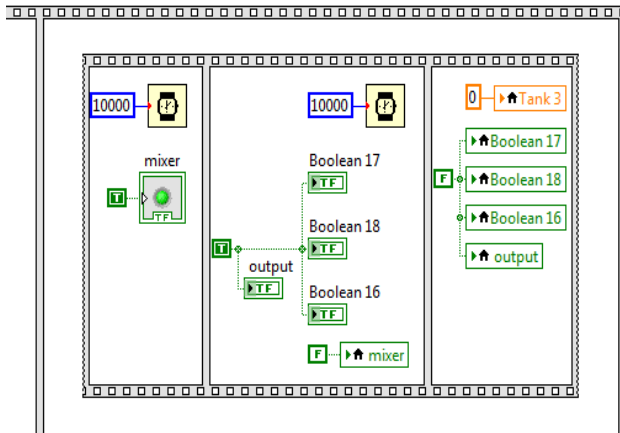


Fig. 7 Frame 3

E. Front Panel Programming

The second part of the LabVIEW program is called front panel which consists of the 'Tab control', which is consist of two pages. The page 1 , as shown in figure 8, consists of two parts, part one devoted to the user input data, which is include the value of paint quantity (each quantity equal to one litter), also include the code of required paint. Part two devoted to equipment states, which include several LEDs indicators for the states of valves, mixer, and cleaner pump.

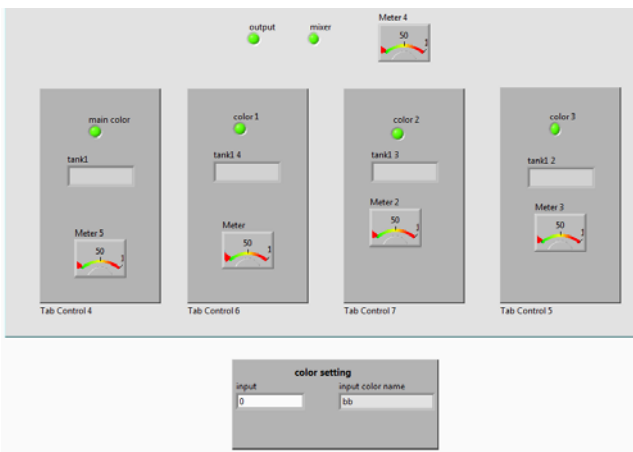


Fig. 8 Front panel page 1

The page 2, as shown in figure 8, illustrates the whole system. It consists of three tanks for tinctures, white color raw tank, the mixer tank, and the cleaner trainer tank. The new color is prepared by mixing the raw with the three tinctures by using the mixer tank and the laboratory color database.

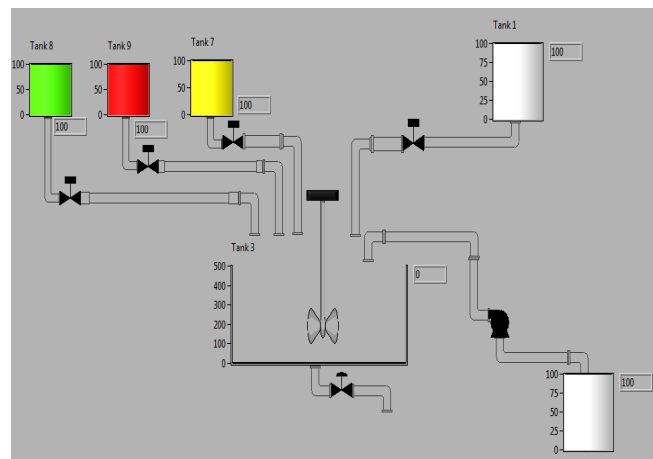


Fig. 9 Front panel page 2

IV. DATA LOGGING AND SUPERVISORY CONTROL MODULE

The DSC Module extends the LabVIEW graphical development environment with additional functionality for the rapid development of distributed measurement, control, and high-channel-count monitoring applications. The DSC technique is used to give a good animation of the virtual implementation of the real project. This technique will show the flow rate of the three tinctures, and the white paint, also show the level of the paint and tinctures in the tanks. Also, it will show the state of all equipments in the project. The DSC module can be added by using the front panal of (VI), this can be done by selecting the controls menue in the front panal, and by select the DSC module menu from the controls menue, then 2D controls and vessels will be appeared as shown in figure 10.

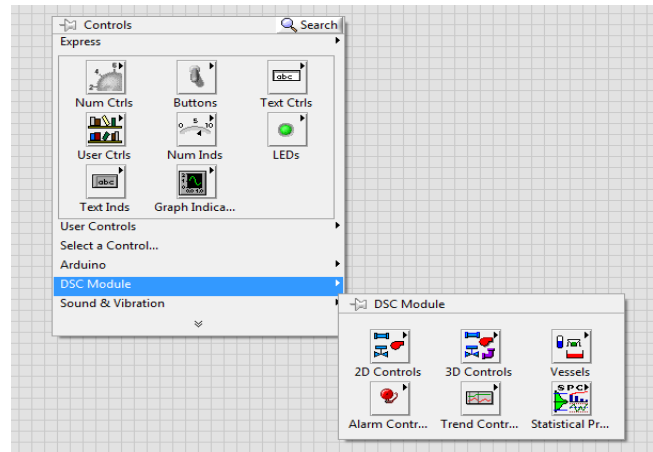


Fig. 10 2D controls and vessels

If (2D controls) are chosen, the other menu will be appeared which has (2D pipes) application. The pipes and connectors are chosen from this menu. Also the valves can be selected from the (2D valves) from (2D controls) menu. The cleaner liquid pump can be selected from (2D pumps) in the same control window. Figure 11 shows these selections. The tanks are chosen from (vessels) in the (2D controls) menu.

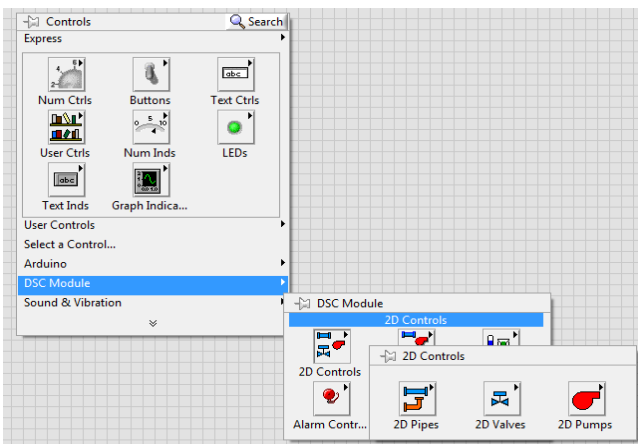


Fig. 11 2D pipes, valves and pumps

Figure 12 shows the suitable form for tanks which can be chosen from (open tank) in (vessels) menu, as shown in. After these selections, the overall implementation of this project can be done by connect the tanks, valves, and pump by using the suitable virtual pipes.

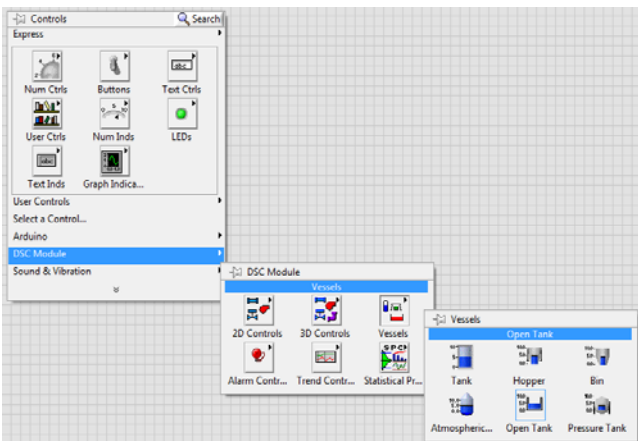


Fig. 12 The overall implementation of the process

The block diagram of the implemented system is built by using suitable blocks in (VI) and their connections for the front panel of the overall implementation, shown in figure 9, is shown in figure 13.

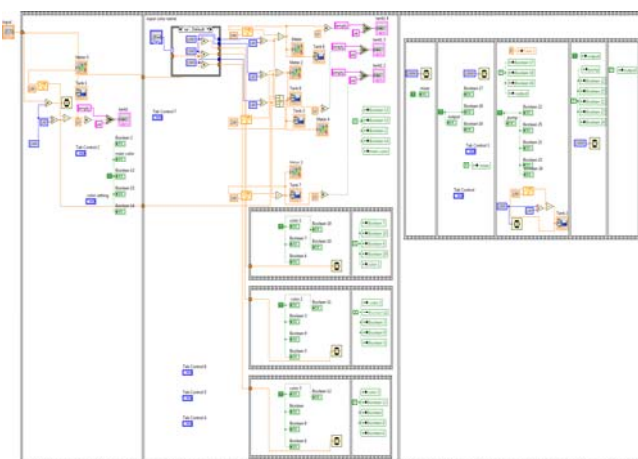


Fig. 13

V. CONCLUSION

The automatic paint mixing machine has been designed and implemented successfully in the LabVIEW environment. The main goal for this work has been achieved to overcome problems related to manual paint mixing. LabVIEW technique has offered a powerful tool to design and implement a complete operation to automate the color mixing machine. This has been archived through the virtual screen on the computer to monitor and control the mixing process. The LabVIEW software made the PC controls the fabricated machine through the data acquisition interface and required programming. The data base which encompasses all colors has been fed to the LabVIEW to control the amount of tinctures for each color. The amount of tinctures, which necessary to produce the desired color, has been controlled by adjusting the time interval of the valve opening. A front panel (graphic user interface GUI) has been designed to assist the user in how to feed the required amount of tincture to produce the specified color. It also provides the user with information about the state of tincture control valves and the availability of the tinctures in the tanks as well as the raw material tanks. It also informs the user by sending a message whether if the tinctures and raw material tanks are empty (Empty) or full (OK).

REFERENCES

- [1] Matthew Luckiesh (1915). Color and Its Applications. D. Van Nostrand company.
- [2] Chris Grimley and Mimi Love (2007). Color, space, and style: all the details interior designers need to know but can never find. Rockport Publishers.
- [3] James Gurney (2010). Color and Light: A Guide for the Realist Painter. Andrews McMeel Publishing.
- [4] Kathleen Lochen Staiger (2006). The Oil Painting Course You've Always Wanted: Guided Lessons for Beginners and Experienced Artists. Watson-Guptill. ISBN 0-8230-3259-0.
- [5] William J. Miskella, 1928, Practical Color Simplified: A Handbook on Lacquering, Enameling, Coloring And Painting.
- [6] Jennings, Simon (2003). Artist's Color Manual: The Complete Guide to Working with Color. Chronicle Books LLC.
- [7] Gatter, Mark (2004). Getting It Right in Print: Digital Pre-press for Graphic Designers. Laurence King Publishing.
- [8] Marcus Weise and Diana Weynand (2007). How Video Works. Focal Press. ISBN 0-240-80933-5.
- [9] Stan Place and Bobbi Ray Madry (1990). The Art and Science of Professional Makeup. Thomson Delmar Learning. ISBN 0-87350-361-9.
- [10] Adrienne L. Zihlman (2001). The Human Evolution Coloring Book. HarperCollins. ISBN 0-06-273717-1.
- [11] Jeffrey Travis, Jim Kring: LabVIEW for Everyone: Graphical Programming Made Easy and Fun, 3rd Edition, July 27, 2006, Prentice Hall. Part of the National Instruments Virtual Instrumentation Series. ISBN 0-13-185672-3.
- [12] Peter A. Blume: The LabVIEW Style Book, February 27, 2007, Prentice Hall. Part of the National Instruments Virtual Instrumentation Series series. ISBN 0-13-145835-3.
- [13] Drew SM, Steven M. (December 1996). "Integration of National Instruments' LabVIEW software into the chemistry curriculum". Journal of Chemical Education (ACS) **73** (12): 1107–111.
- [14] Moriarty PJ, Gallagher BL, Mellor CJ, Baines RR, P. J.; Gallagher, B. L.; Mellor, C. J.; Baines, R. R. (October 2003). "Graphical computing in the undergraduate laboratory: Teaching and interfacing with LabVIEW". American Journal of Physics (AAPT) **71** (10): 1062–1074.

Approach for automated person identification from any type of Identification Document

Krasimir Diyanov Dimitrov

Computer sciences and technologies

Technical university of Varna

Varna, Bulgaria

kr.dimitrov93@gmail.com

Sivo Vladimirov Daskalov

Computer sciences and technologies

Technical university of Varna

Varna, Bulgaria

sivodaskalov@gmail.com

Assoc. Prof. Mariana Tsvetanova

Stoeva

Computer sciences and technologies

Technical university of Varna

Varna, Bulgaria

mariana_stoeva@abv.bg

The aim of this paper is to research many of the widely used filtering techniques in image processing and state what would be the most optimal manipulation of the original image in order to perform text recognition. Furthermore, it develops the idea of automatic adjustment of the chosen optimal filter with no human aid, as well as a user aided educational process for the software.

Keywords—*Computer aided vision; Text recognition; Image processing*

I. INTRODUCTION

The idea of minimizing human labor and possibility of a mistake has always been of great importance to our society. With the rapid development of both hardware and software, opportunities to optimize labor emerge in nearly all spheres of human activity. One of the less popular uses of the technology we have developed is that of text recognition in computer aided vision. However, a series of transformations needs to be applied to the original image in order to enable the use of recognition software. Furthermore, these modifications of the image are not universal, thus requiring the development of software to automatically adjust its filters in relation to the given task.

II. THEORETICAL BASE

A. Optical character recognition

Optical Character Recognition (OCR), is the mechanical or electronic conversion of scanned or photographed images of typewritten or printed text into machine-encoded/computer-readable text. It is widely used as a form of data entry from a paper data source. It is a common method of digitizing printed texts so that they can be electronically edited, searched, stored more compactly, displayed on-line, and used in machine processes such as machine translation, text-to-speech, key data extraction and text mining. OCR is a field of research in pattern recognition, artificial intelligence and computer vision.

B. Digital image processing

Digital image processing offers a wide variety of algorithms, of which a collection of filters will be used to remove impulse, white and Gaussian noise [1]. Among those are the Median, Adaptive Threshold and Bilateral filters. To

optimize performance speed the filter parameters will be selected by processing a sample group of images along with their text data and storing the sets of parameters that lead to a correct reading of all sample images in a database.

III. APPROACH FOR ID TEXT RECOGNITION

The method consists of the following major phases:

A. Forming of the initial filter database

A sample group of images is chosen including a wide variety of noise and contrast differences and their string data is manually input by the operator. The filter database initially includes all possible sets of filter parameters for the chosen filters. Every sample image is processed by all each of the parameter sets in the database and then OCR is performed for all cases. If the results from the reading differ from the manually input data for the original image, the parameter set leading to such a reading is removed from the database “Fig. 1.”. This preparation stage of the approach is time consuming but improves significantly the performance of the processing.

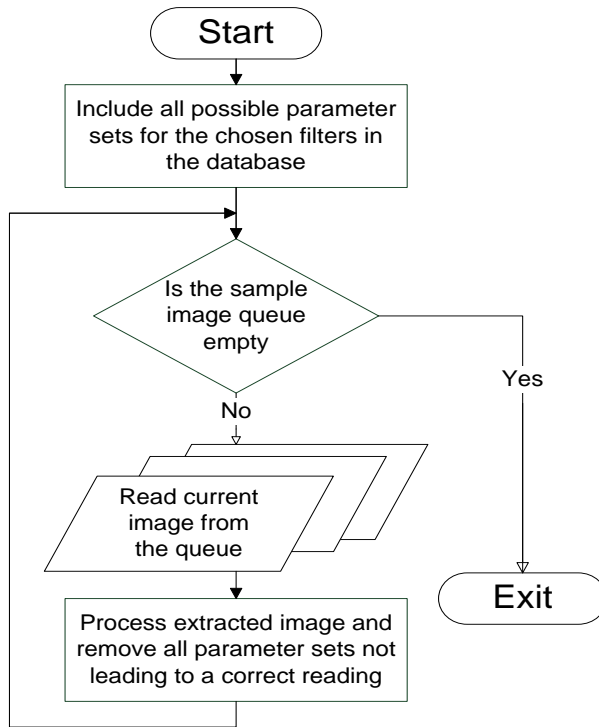


Fig. 1. Block diagram of the initial filter database creation

B. Main cycle of ID processing

The processes performed by the algorithm are depicted in "Fig. 2.". The input image is rotated so that the borders of the identification document (ID) are parallel to both axes of the coordinate system. Any remaining whitespace around the document is removed leaving only useful data on the image. Each of the sets in the parameter database is used to process the image and OCR is performed for each result. If the readings match an entry in the person database, the image is considered successfully read. However, if this is not the case identification is redirected to an operator and the data input by him along with the ID is stored in a queue for future parameter database optimization.

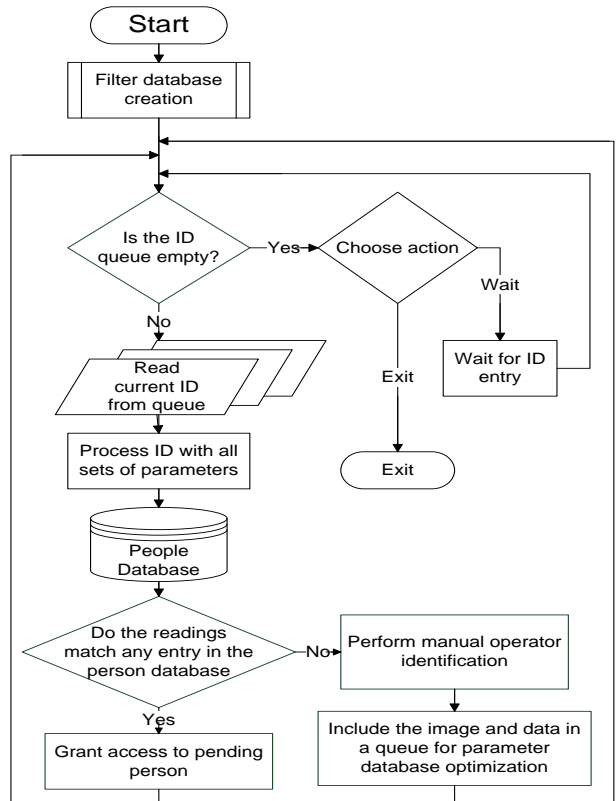


Fig. 2. Block diagram of the main cycle of person identification

C. Parameter database optimization (PDO)

When the ID queue is empty or on demand, the process of parameter database optimization can be performed. Images and data from the PDO queue are processed with all possible sets of parameters and filters until the data is correctly read from the image. When that occurs, the parameter set leading to the correct reading is added to the parameter database for future reference. This process is tedious and should be performed during the inactive hours of the day.

D. Correction function

Common inconsistencies could be observed, resulting from the various fonts and ID specifics. In order to reach a correct reading, the resulting collection of strings read by the OCR system needs to be passed to a correction function.

IV. EXPERIMENTAL DATA

A. Experimental setup



Fig. 3. Example of a Bulgarian ID card

The experiments have been conducted on Bulgarian ID cards "Fig. 3.". For image processing we've used OpenCV [2], an open source C++ library, which contains powerful tools for digital image editing. For optical character recognition we've used Tesseract OCR [3], also an open source C++ library. The images used are scanned with resolution of 300 dpi. The experimental software was executed on a PC with the following characteristics:

- CPU - Intel Core i5 3570 @ 3.40GHz
- RAM - 8.00GB Dual-Channel DDR3 @ 1.33GHz
- GPU - NVIDIA GeForce GTX 770

B. Filter usage

The three filters of our choice are the median, adaptive threshold and bilateral filter [4,5].



Fig. 4. Example results of applying the median filter

The example results of applying Median filter with size of matrix = 3 are shown on "Fig. 4." and are unreadable by Tesseract OCR.



Fig. 5. Example results of applying the bilateral filter

The results of Fig. 2 : bilateral filter with parameters diameter of each pixel neighborhood that is used during filtering = 15, filter sigma in the color space= 60 and filter sigma in the coordinate space = 60 is shown on "Fig.5." and is readable by Tesseract OCR.

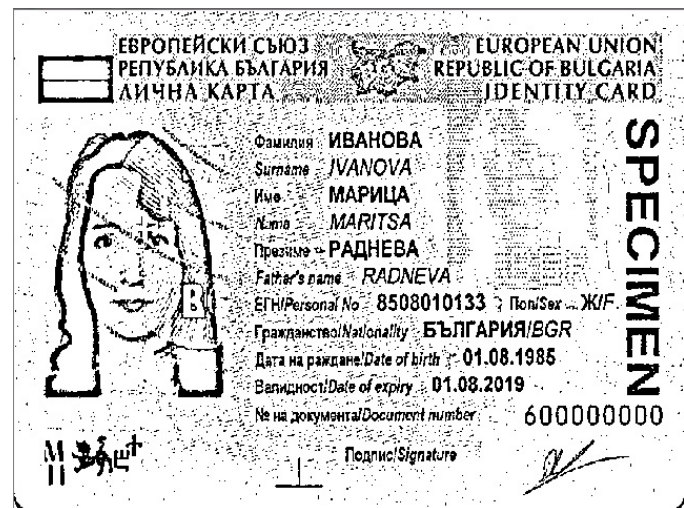


Fig. 6. Example results of applying adaptive threshold with unsuitable parameters

The results of applying Adaptive Threshold Filter with size of matrix = 21 and calculation constant = 10 are shown on "Fig.6." and are unreadable by Tesseract OCR.

The results of applying Adaptive Threshold Filter with size of matrix = 149 and calculation constant = 18 are shown on "Fig.7." and are readable by Tesseract OCR. Best results for Bulgarian ID are reached by using the adaptive threshold and therefore it is the main focus of the majority of our experiments. The initial parameter database consists of all pairs of values for size of matrix (Size) and calculation constant (C) where Size is an odd number and between 1 and 255 and C is between 1 and 64.

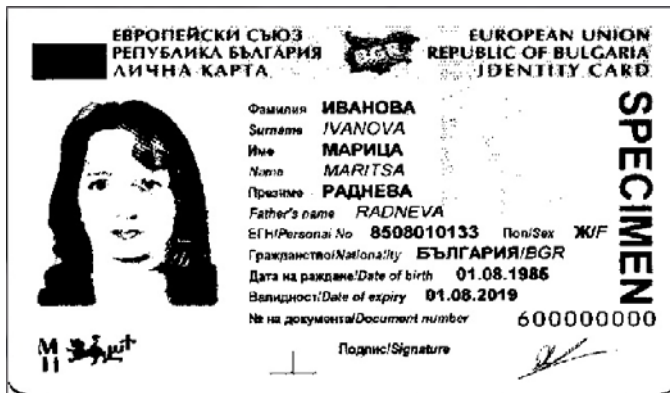


Fig. 7. Example results of applying adaptive threshold with suitable parameters

C. Optimization of the filter database

A collection of 5 sample Bulgarian ID images has been chosen for the parameter database optimization. The initial count of the parameter sets was reduced from 16320 to 21 after processing all of the sample images. The time required to process each subsequent image was reduced significantly as depicted in "Fig. 8." and "Table 1."

Table 1. Reduction in the number of entries in the parameter database

| Image № | Number of parameter sets | Time elapsed (min) |
|---------|--------------------------|--------------------|
| Start | 16320 | X |
| 1 | 698 | 48 |
| 2 | 312 | 20 |
| 3 | 140 | 9 |
| 4 | 56 | 3 |
| 5 | 21 | 1 |

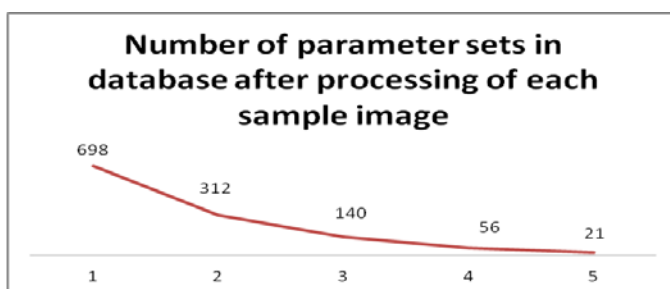


Fig. 8. Reduction in the number of entries in the parameter database

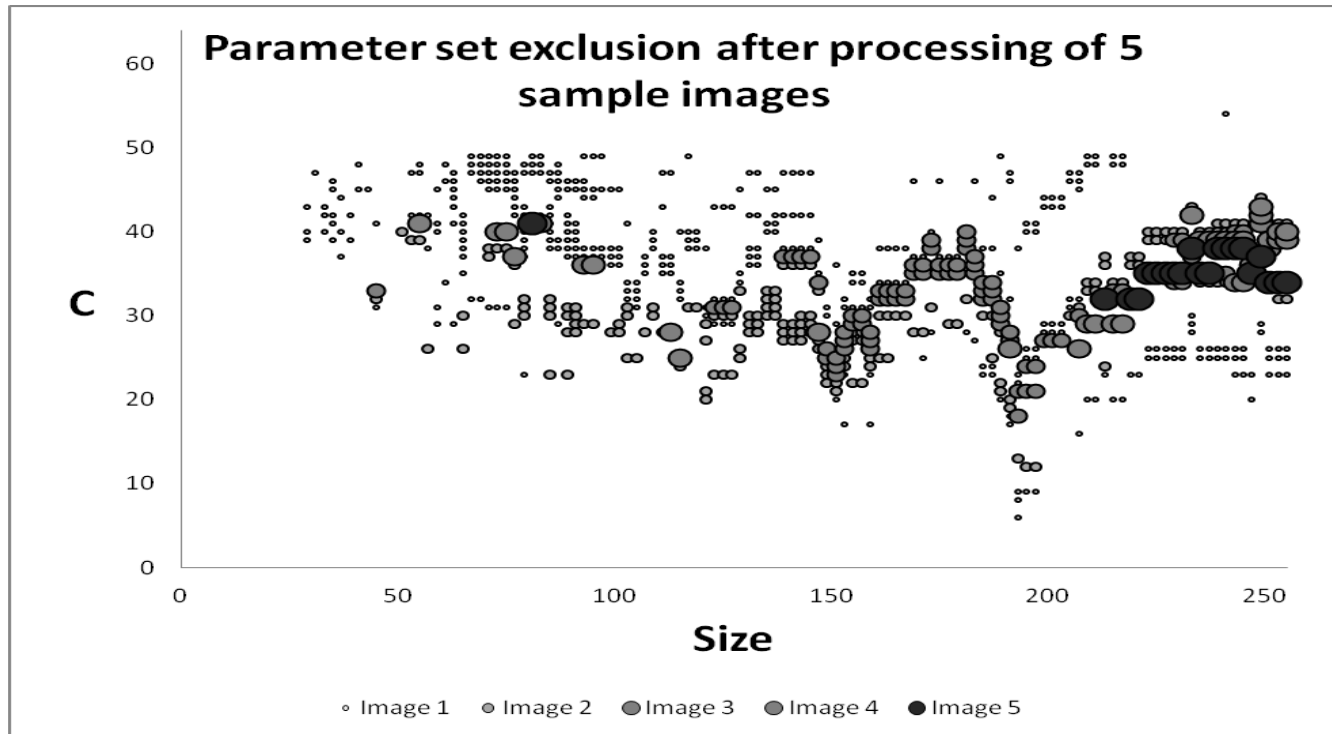


Fig. 9. Distribution of the remaining parameter sets after processing of each sample image

On “Fig. 9.” is shown the distribution of the parameter sets in the database for every round of optimization. The remaining values after the processing of each subsequent sample image are shown with a larger and darker circle.

V. CONCLUSIONS

A well defined filter parameter database significantly reduces the time needed to process a random image from the ID queue for correct readability.

Adaptive threshold seems to be most suitable for filtering the design specifics of Bulgarian ID. However, this is not necessarily the case for other types of ID.

The aforementioned approach can be modified in order to be applied to various types of objects apart from ID.

The approach is adaptive, which lowers the possibility of a misreading when working with bad quality or damaged images.

VI. FUTURE RESEARCH

One of the aims towards improvement of readability is to create a custom filter in order to reach optimal results when manipulating a certain type of ID.

The way parameter sets are added to or removed from the database can also be improved in the future. Each

parameter set could be evaluated in a way as to secure or deny its position in the database.

The expectations towards the approach need to be either confirmed or disproved by observation of the behavior of the created software when processing large amounts of data.

Acknowledgment

The authors would like to thank the Computer sciences and technologies department of the Technical university of Varna for the much needed resources both theoretical and physical.

References

- [1] http://en.wikipedia.org/wiki/Filter_%28signal_processing%29
- [2] <http://docs.opencv.org/>
- [3] <https://code.google.com/p/tesseract-ocr/wiki/Documentation>
- [4] http://docs.opencv.org/modules/imgproc/doc/miscellaneous_transformations.html
- [5] http://docs.opencv.org/doc/tutorials/imgproc/gaussian_median_bilateral_filter/gaussian_median_bilateral_filter.html

Advantages of the implementation of Service Desk based on ITIL framework in telecommunication industry

Anel Tanovic, Fahrudin Orucevic, Asmir Butkovic

Department of Computer Science and Informatics University of Sarajevo, Faculty of Electrical Engineering

Zmaja od Bosne bb, Sarajevo 71000, Bosnia and Herzegovina

atanovic@etf.unsa.ba, forucevic@etf.unsa.ba, abutkovic@hotmail.com

Abstract: - This paper describes the significance of the implementation of Service Desk based on ITIL framework. For the reference model is taken a Service Desk in Telecom operator which solves hundreds of users incidents, problems and requests during a one day. The aim of the paper is to compare the results of normal working a Service Desk before the implementation of ITIL and after the implementation of ITIL. The result of this comparison should show that a Service Desk with the implemented ITIL processes has achieved a better results than a Service Desk which doesn't contain processes from ITIL. For the implementation of ITIL Service Desk are chosen all processes which are dealing with users: Service Level Management, Supplier Management, Change Management, Event Management, Incident Management, Request Fulfillment and Problem Management. This paper gives a focus to the implementation of Service Desk solutions based on ITIL framework in any business environment in order to increase the business productivity.

Key-Words: - ITIL, Service Desk, Service Level Management, Supplier Management, Change Management, Event Management, Incident Management, Request Fulfillment, Problem Management.

1 Introduction

Service Desk plays an important role for the normal work of each organization. Today every organization must have some Service Desk solution which is responsible for solving users requests, incidents and problems. Service Desk software solutions take key activities for the implementation of its processes from various number of IT Service Management (ITSM) frameworks which include: CobiT, eTOM, ITIL, ISO/IEC 20000 etc. All these ITSM frameworks contain processes which are responsible for dealing and solving users requests, incidents and problems. By implementing all these solutions organizations get recommendations from these ITSM frameworks how to implement these strategic processes.

For this paper and the implementation of Service Desk is taken ITIL 2011 framework. ITIL is the most popular framework for the management of IT services. It contains five phases in which are placed 26 processes. For each process ITIL gives a set of key activities which are important for the implementation and a set of key performance indicators which are important for the measurement of processes. This paper is divided in two parts: the first one is just the measurement of key performance indicators in the old model of Service Desk. The second one is the description of the implementation of ITIL Service Desk by describing key activities for seven ITIL processes which are used for this

model and by the measurement of the same key performance indicators as in the first part of the paper. For the implementation of this ITIL Service Desk model are taken seven processes which are also the part of any sophisticated ITSM solution: Service Level Management, Supplier Management, Change Management, Event Management, Incident Management, Request Fulfillment, Problem Management.

This paper is divided in six chapters. The second chapter describes a test environment and a methodology used for this research. The third chapter shows results of the measurement of the old model of Service Desk solution. The fourth chapter shows the implementation of a ITIL Service Desk model by describing the realisation of key activities for seven ITIL processes. The fifth chapter shows results of the measurement of the new model of Service Desk solution. The sixth chapter of the paper is the conclusion of the paper which shows the advantage of the new model of Service Desk which is based on ITIL 2011 framework.

2 Reference model and research methodology

For the reference model is taken Service Desk in one Telecom operator in Bosnia and Herzegovina. Telecom operator contains all main services which include: fixed telephony, mobile telephony, IPTV,

VoIP, Internet, Hosting and E-mail. Before the implementation of this project, Telecom operator has the old software Service Desk solution which was not compatible with any of IT Service Management frameworks and standards. The process of solving users incidents and problems was too slow especially on services connected to the IP network: IPTV, VoIP, Internet, Hosting and E-mail. Some everyday users requests and problems which appear on Service Desk are: termination of telephone device, the loss of TV picture, stop working of internet on cell phones, stop working of cell phones, changing password for internet, changing PIN for IPTV, excessive bills for services, inability to purchase video content on Video on Demand service, inability to record content on TV channels, the request for the replacement of terminal equipment, creating of new e-mail addresses, creating a new domain on hosting service, loss of codes for mobile phones, long time for solving problems between departments within Telecom operators etc. Figure 1. shows Service Desk and departments inside a Telecom operator which all have installed a Service Desk application.

The methodology of this paper contains two basic steps. The first step are measurements of the implemented Service Desk by using a predefined set of key performance indicators. The second step is the implementation of Service Desk by using ITIL recommendations for seven processes and finally making measurements for all seven ITIL processes. For the measurement of results is taken a technique called Gap Analysis.

Gap analysis is a business assessment tool enabling an organization to compare where it is currently and where it wants to go in the future. This provides the organization with insight to areas that have room for improvement. The process involves determining, documenting and approving the variance between business requirements and current capabilities. Gap analysis naturally flows from benchmarking or other assessments such as service or process maturity assessments. This comparison becomes the gap analysis, which can be performed at the strategic, tactical or operational level of an organization. Gap analysis provides a foundation for how much effort in time, money and human resources is required to achieve a particular goal.

3 Measurement results on Service Desk before the implementation of ITIL processes

Table I. shows the result of the implementation for each key performance indicator for Service

Level Management process, the value of critical success factor and the percentage of the successful implemented key performance indicators. The final result of the successful implemented key performance indicators for this process is 74%.

Table II. shows the result of the implementation for each key performance indicator for Supplier Management process, the value of critical success factor and the percentage of the successful implemented key performance indicators. The final result of the successful implemented key performance indicators for this process is 69.60%.

Table III. shows the result of the implementation for each key performance indicator for Change Management process, the value of critical success factor and the percentage of the successful implemented key performance indicators. The final result of the successful implemented key performance indicators for this process is 71.80%.

Table IV. shows the result of the implementation for each key performance indicator for Event Management process, the value of critical success factor and the percentage of the successful implemented key performance indicators. The final result of the successful implemented key performance indicators for this process is 77%.

Table V. shows the result of the implementation for each key performance indicator for Incident Management process, the value of critical success factor and the percentage of the successful implemented key performance indicators. The final result of the successful implemented key performance indicators for this process is 78.40%.

Table VI. shows the result of the implementation for each key performance indicator for Request Fulfillment process, the value of critical success factor and the percentage of the successful implemented key performance indicators. The final result of the successful implemented key performance indicators for this process is 81%.

Table VII. shows the result of the implementation for each key performance indicator for Problem Management process, the value of critical success factor and the percentage of the successful implemented key performance indicators. The final result of the successful implemented key performance indicators for this process is 77.80%.

Table VIII. shows a brief summary of results of the implementation for each ITIL process before the implementation of ITIL Service Desk solution. The final result of the successful implemented key performance indicators for all ITIL processes before the implementation of these processes is 75.65%.

4 Implementation of Service Desk based on ITIL framework

Service Desk based on ITIL has been developed on University on Sarajevo (Faculty of Electrical Engineering) in laboratory for IT Service Management. This Service Desk contains seven processes which are all connected with suppliers, clients and internal processes. This developed Service Desk is user friendly and adaptive for learning to all employees in company. ITIL processes which are integrated in this solution are: Service Level Management, Supplier Management, Change Management, Event Management, Incident Management, Request Fulfillment and Problem Management. For all these processes will be shown key activities which are used for the implementation of this software solution. Figure 2. shows user interface of the developed Service Desk solution.

Key activities with Service Level Management process should include:

- Determining, negotiating and documenting requirements for new and changed services in SLA contracts, and managing and reviewing them through the service lifecycle
- Monitoring and measuring service performance achievements of all operational services against targets in SLAs
- Producing service reports
- Conducting service reviews, identifying improvement opportunities for inclusion
- Collating, measuring and improving customer satisfaction in cooperation with business relationship management
- Reviewing and revising SLAs and OLAs
- Developing and documenting contacts and relationships with the business, customers and stakeholders in cooperation with business relationship management process
- Logging and managing complaints and compliments in cooperation with business relationship management.

Key activities for Supplier Management process should include:

- Definition of new supplier and contract requirements: identify business need and prepare of the business case
- Evaluation of new supplier and contracts: identify method of purchase and procurement, establish evaluation criteria and negotiate contracts and targets

- Categorization of suppliers and contracts: assess and reassess the supplier and contract, ensure changes progressed and categorization of suppliers
- Establishment of new suppliers and contracts: setting the supplier service and contract, transitioning the service and establishing contacts and relationships
- Supplier, contract and performance management: manage and control the operation and delivery of service, monitor and report and manage the supplier and the relationship.

Key activities for Change Management process include:

- Planning and controlling changes
- Change and release scheduling
- Communications
- Making change decisions and authorization of change
- Ensuring that remediation plans are in place
- Measurement and control
- Management reporting
- Understanding the impact of the change
- Continual improvement.

Key activities for Event Management process include:

- Event occurs – Everybody involved in designing, developing, managing and supporting IT services understand what type of event need to be detected
- Event notification – A general principle of event notification is that the more meaningful data it contains and the more targeted the audience, the easier is to make decisions about the event.
- Event detection – Once an event notification has been generated, it will be detected by an agent running on the same system, or transmitted directly to a management tool specifically designed to read and interpret the meaning of the event.
- Event logged – The event can be logged as an event record in the event management tool.
- First level event correlation and filtering – The purpose is to decide whether to communicate the event to a management tool or to ignore it. In that case the event will be usually recorded in a log file on the

- device and no further action will be taken.
- Significance of events – Every organization will have its own organization of the significance of an event but it is suggested that at least these three broad categories be represented.
- Second level event correlation – If it is a warning event, a decision has to be made about exactly what the significance is and what actions need to be taken to deal with it. A correlation engine is programmed according to the performance standards created during service design.
- Further action needed – If the second level correlation activity recognizes the event, a response will be required. There are many different types of responses, each designed specifically for the task it has to initiate.
- Response selection – At this type of the process, there are a number of response options available. Response options can be taken in any combination. There are lots of options like: auto response, alert and human intervention, incident, problem, or change, open an request for change, open an incident record and open or a link to a problem record.
- Review actions – It is important to check that any significant events or exceptions have been handled and to track trends or event types. In many cases it can be done automatically. In cases where events have initiated an incident, problem or change, the action review should not duplicate any reviews that have been done as part of those processes.
- Close event – Some events will remain open until a certain action takes place, for example an event that is linked to an open incident. It is sometimes very difficult to relate open and closed events if they are in different formats.

Key activities for Incident Management process include:

- Incident identification – All key components should be monitored so that failures are detected early. This means that this process can be started quickly.
- Incident logging – All incidents must be fully logged regardless it is raised through a telephone call, automatically detected or from other source.
- Incident categorization – It is needed to

allocate suitable incident categorization so that the exact type of incident is recorded. This is very important because of incident types.

- Incident prioritization – Prioritization can be normally determined by taking into account the urgency of the incident and the level of business impact it is causing. An indication of impact is very often the number of users affected.
- Initial diagnosis – If the incident has been routed via the service desk, the service desk analyst must carry out initial diagnosis, typically while the user is on telephone and to try to discover the full symptoms of the incident and to determine exactly what has gone wrong and how to correct it.
- Incident escalation – If the staff of Service Desk is unable to resolve the incident, it must be immediately escalated for further support. Some incidents may require multiple support groups to resolve. Support groups may be internal and they may be third parties like software suppliers or hardware manufacturers.
- Investigation and diagnosis – All support groups involved with the incident handling will investigate and diagnose potential problems and make the full documentation about it. The valuable time can often be lost if investigation or diagnostic action is performed serially. Such actions should be performed in parallel to reduce overall timescales.
- Resolution and recovery – Any potential resolution should be applied and tested. The specific actions need to be undertaken. Even when some resolution of incident is found, sufficient testing must be performed to ensure that recovery action is complete and that normal state service has been restored.
- Incident closure – The service desk should check that the incident is fully resolved and that users are satisfied and agree that some incident can be closed.
- Rules for reopening incidents – There will be occasions when incidents recur even though they have been formally closed. Because of such cases, it is wise to have predefined rules about if and when an incident can be reopened. It is very undesirable situation when some incidents are solved in one working day after re-opening of them. The exact time may vary between

individual organizations but clear rules should be agreed and documented and guidance given to all service desk staff so that uniformity is applied.

Key activities for Request Fulfillment process include:

- Receiving a request – Fulfilment work on service requests should not begin until a formalized request has been received. Service requests should mostly come from the Service Desk.
- Request logging and validation – All service requests should be fully logged and timely stamped, regardless is service request from service desk, telephone call or e-mail.
- Request categorization – Part of the initial logging it is needed to allocate request categorization so that the exact type of the request is recorded.
- Request prioritization – Another very important step is to allocate an appropriate prioritization code, and to determine how the service request is handled by the Service Desk staff.
- Request authorization – All service requests need to be properly authorized. Simple authorizations can take place via Service Desk. Service requests that can not be properly authorized should be returned to the requestor with the reason for the rejection.
- Request review – The request is reviewed to determine the function that will fulfil it. As requests are reviewed, the request records should be updated to reflect the current request status.
- Request model execution – A request model should be used that documents a standard process flow, roles and responsibilities to fulfill it. The appropriate request model should be chosen based on the type of service request. All service requests in the real environment should also be authorized through Change Management process.
- Request closure – When service request activities have been completed, the service desk should be notified of the completion status. The Service Desk should check that the request has been fulfilled and that users are satisfied and agree to close the service request.

Key activities for Problem Management process include:

- Problem detection – There are multiple ways of detecting problems that will exist in all organizations. These can include triggers for reactive and proactive problem management.
- Problem logging – All the relevant details of the problem must be recorded so that a full historic record exists. This must be date and time stamped to allow suitable control and escalation.
- Problem categorization – Problems should be categorized in the same way as incidents so that the nature of the problem can be easily traced in the future and meaningful management information can be obtained.
- Problem prioritization – Problems should be prioritized in the same way as incidents. The frequency and the impact of related incidents should be also taken into account. For the problem prioritization it is very important the severity of the problems. Severity explains how serious is the problem from a service or customer perspective.
- Problem investigation and diagnosis – An investigation should be conducted to try to diagnose the root cause of the problem. The speed and the nature of the investigation will depend on the impact, severity and urgency of the problem. There are a lot of useful techniques that can be used to diagnose and resolve problems.
- Raising a known error record – This is defined as a problem with a documented root cause and workaround. The known error record should identify the problem and a status of document which status is important for resolving the problem. In some cases it may be advantageous to raise a known error record even earlier in some processes, even though a diagnosis it may not be complete. This might be used for information purposes or to identify some workaround that appears to address the problem that has not been fully completed.
- Problem resolution – When a root cause has been found and a solution to remove it has been developed, it should be applied to resolve the problem. If the problem is very serious and some urgent fix is needed because of business reasons, than an emergency request for change should be

raised.

- Problem closure – When a final resolution has been applied, the problem record should be formally closed. A check should be performed at this time to ensure that a record contains a full historical description of all events.
- Major problem review – After every major problem, a review should be conducted to learn any lessons for the future. Such reviews can be used as part of the training and awareness activities for support staff.

5 Measurement results on Service Desk after the implementation of ITIL processes

Table IX. shows the result of the implementation for each key performance indicator for Service Level Management process, the value of critical success factor and the percentage of the successful implemented key performance indicators after the implementation of ITIL Service Desk. The final result of the successful implemented key performance indicators for this process is 88.80%.

Table X. shows the result of the implementation for each key performance indicator for Supplier Management process, the value of critical success factor and the percentage of the successful implemented key performance indicators after the implementation of ITIL Service Desk. The final result of the successful implemented key performance indicators for this process is 86.80%.

Table XI. shows the result of the implementation for each key performance indicator for Change Management process, the value of critical success factor and the percentage of the successful implemented key performance indicators after the implementation of ITIL Service Desk. The final result of the successful implemented key performance indicators for this process is 82%.

Table XII. shows the result of the implementation for each key performance indicator for Event Management process, the value of critical success factor and the percentage of the successful implemented key performance indicators after the implementation of ITIL Service Desk. The final result of the successful implemented key performance indicators for this process is 85.20%.

Table XIII. shows the result of the implementation for each key performance indicator for Incident Management process, the value of critical success factor and the percentage of the successful implemented key performance indicators after the implementation of ITIL Service Desk. The

final result of the successful implemented key performance indicators for this process is 90.20%.

Table XIV. shows the result of the implementation for each key performance indicator for Request Fulfillment process, the value of critical success factor and the percentage of the successful implemented key performance indicators after the implementation of ITIL Service Desk. The final result of the successful implemented key performance indicators for this process is 87.60%.

Table XV. shows the result of the implementation for each key performance indicator for Problem Management process, the value of critical success factor and the percentage of the successful implemented key performance indicators after the implementation of ITIL Service Desk. The final result of the successful implemented key performance indicators for this process is 88.80%.

Table XVI. shows a brief summary of results of the implementation for each ITIL process after the implementation of ITIL Service Desk solution. The final result of the successful implemented key performance indicators for all ITIL processes after the implementation of these processes is 87.05%.

6 Conclusion

Service Desk based on ITIL has achieved better results of the implementation than the first model of Service Desk. This new model has achieved a better result for 11.40% than the previous model of Service Desk. All seven processes from the Service Desk based on ITIL have achieved better results of the implementation: Service Level Management (14.80%), Supplier Management (17.20%), Change Management (10.20%), Event Management (8.20%), Incident Management (11.80%), Request Fulfillment (6.60%) and Problem Management (11%).

Service Desk based on ITIL has performed all processes in Telecom operator which are connected to end users. This means that this Service Desk even improves internal business processes inside the organization and automatize some internal processes. What's the most important is that a new Service Desk can be implemented in any business organization and that this Service Desk contains even seven processes responsible for solving user's requests, incidents and problems.

Future research is connected to the improvement of the implemented Service Desk solution based on ITIL. The aim is to improve it by adding some new processes from ITIL which will include Service Catalogue Management and Access Management. Service Catalogue Management should be responsible for providing and maintaining a single

source of consistent information of all operational services. Access Management will be responsible for providing the right for users to be able to use one service or group of services.

References:

- [1] J. van Bon, A. de Jong, A. Kolthof, M. Pieper, R. Tjassing, A. van der Veen, and T. Verheijen, "Foundations of IT Service Management Based on ITIL 2011", The Office of Government Commerce, September 2007.
- [2] B. Orand and J. Villarreal, "Foundations of IT Service Management: The ITIL Foundations Course in a Book", CreateSpace, June 2011.
- [3] R. A. Steinberg, "Measuring ITIL: Measuring, Reporting and Modeling – the IT Service Management Metrics That Matter Most to IT Senior Executives", Trafford Publishing, January 2001.
- [4] R. A. Steinberg, "Servicing ITIL: A Handbook of IT Services for ITIL Managers and Practitioners", Trafford Publishing, September 2007.
- [5] R. A. Steinberg, "Architecting ITIL", Trafford Publishing, October 2008.
- [6] R. A. Steinberg, "Implementing ITIL: Adapting Your IT Organization to the Coming Revolution in IT Service Management", Trafford Publishing, October 2005.
- [7] G. Blokdijk and I. Menken, "Help Desk, Service Desk Best Practice Handbook: Building, Running and Managing Effective Support - Ready to use supporting documents bringing ITIL Theory into Practise", Emereo Publishing, August 2008.
- [8] A. Tanovic, I. Androulidakis, and F. Orucevic, "Development of a new improved model of the ITIL V3 framework for the information system of Telecom operator", 11th WSEAS International Conference on Data Networks, Communications, Computers (DNCOCO '12), pp. 209-215, September 2012.
- [9] A. Keller and T. Midboe, "Implementing a Service Desk: A practitioner's perspective", IEEE Network Operations and Management Symposium (NOMS 2010), pp. 685-696, April 2010.
- [10] A. Lahtela, M. Jantti, and J. Kaukola, "Implementing an ITIL-Based IT Service Management Measurement System", 4th International Conference on Digital Society (ICDS'10), pp. 249-254, February 2010.
- [11] A. Tanovic and F. Orucevic, "Proposal of the improvement of Actual ITIL Version based on Comparative IT Service Management Methodologies and Standards – The Improved Model of ITIL 2011 Framework", 13th WSEAS International Conference on Applied Informatics and Communications (AIC'13), Valencia, August 2013.
- [12] M. Spremici and H. Spremici, "Measuring IT Governance Maturity – Evidences from using regulation framework in the Republic Croatia", Proceedings of the European Computing Conference (ECC '11), pp. 98-104, April 2011.
- [13] J. J. Cusick and G. Ma, "Creating an ITIL inspired Incident Management approach: Roots, response, and results", IEEE/IFIP Network Operations and Management Symposium Workshops (NOMS Wksps), pp. 142-148, April 2010.
- [14] M. Jantti and A. Suhonen, "Improving Service Level Management Practices: A Case Study in an IT Service Provider Organization", International Conference on Advanced Applied Informatics, pp. 139-144, September 2012.
- [15] S. Heikkinen and M. Jantti, "Identifying IT Service Management Challenges: A Case Study in Two IT Service Provider Companies", 23rd International Workshop on Database and Expert Systems Applications (DEXA 2012), pp. 60-64, September 2012.
- [16] L. Ruile, "Research on IT Service Management of college or university campus network", 7th International Conference on Computer Science & Education (ICCSE 2012), pp. 320-324, July 2012.

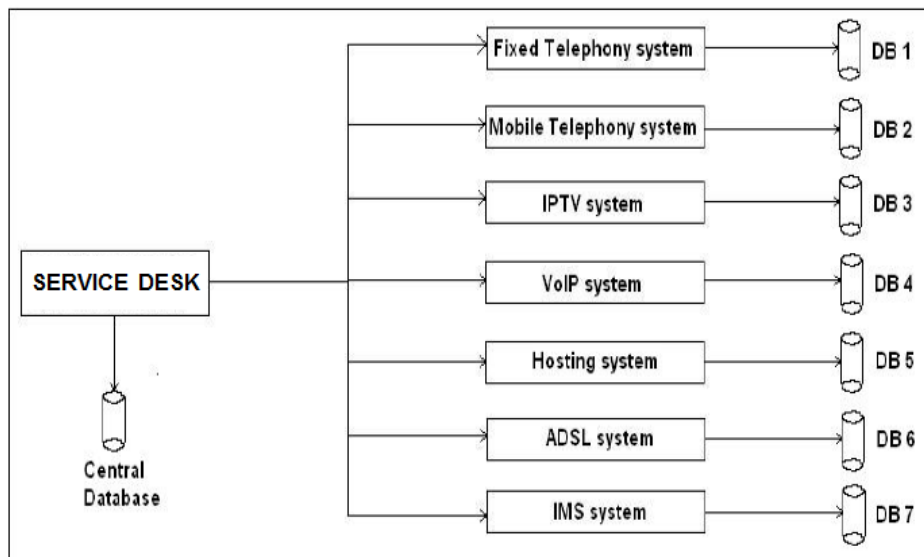


Figure 1. Service Desk and departments inside a Telecom operator

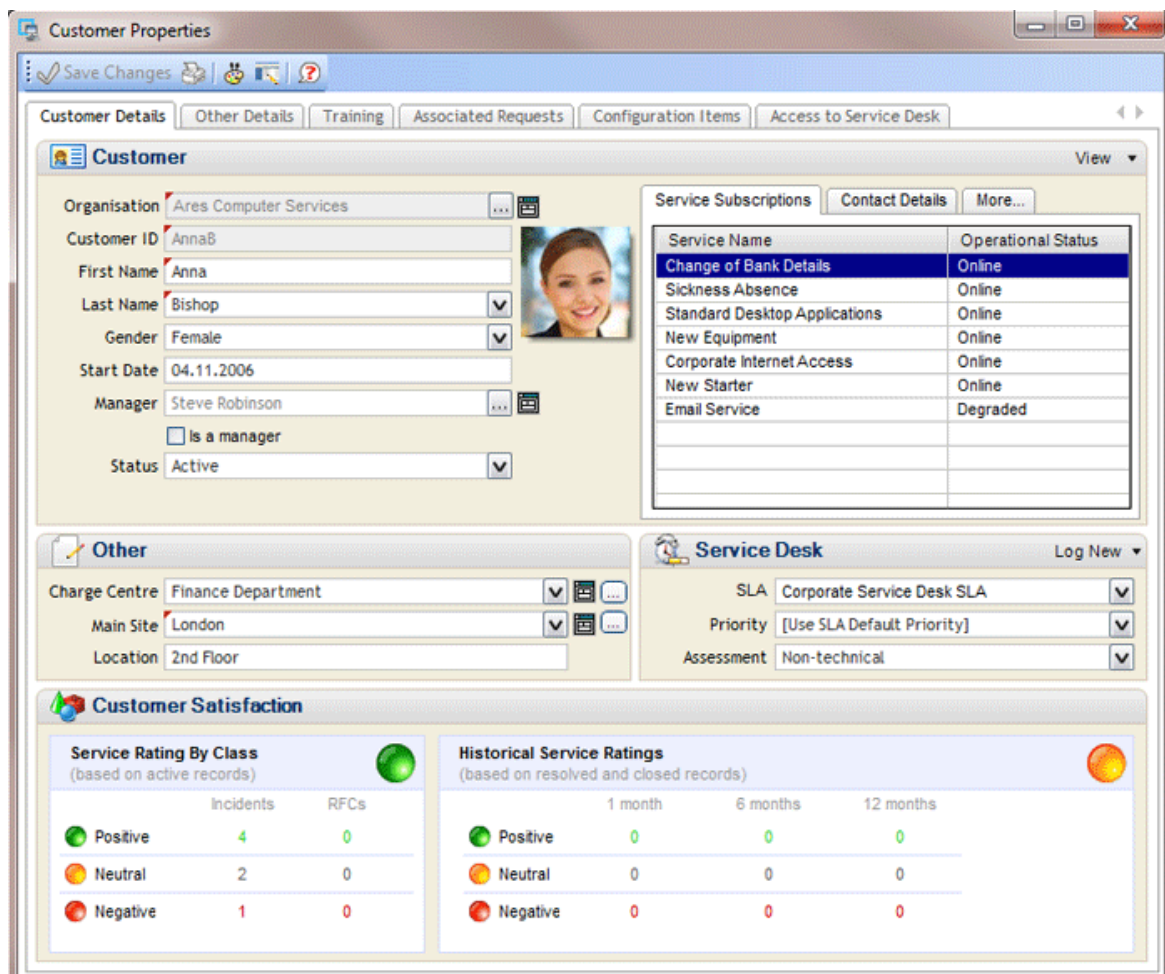


Figure 2. User interface for the developed Service Desk solution

TABLE I. MEASUREMENTS FOR SERVICE LEVEL MANAGEMENT PROCESS

| Key performance indicator for Service Level Management process | The measured value of key performance indicator | The value of critical success factor | The percentage of the successful implemented key performance indicators |
|--|--|---|--|
| The percentage of services which are covered under SLA | 82% | 100% | 82% |
| The percentage of users with SLAs contract which submitted a complaint | 12% | 10% | 80% |
| The percentage of suppliers with contract which submitted a complaint | 25% | 20% | 75% |
| The maximum allowed time for defining SLA, OLA or contract | 22 days | 15 days | 53% |
| The maximum allowed reduction in time taken to respond to and implement SLA requests | 6 days | 5 days | 80% |

TABLE II. MEASUREMENTS FOR SUPPLIER MANAGEMENT PROCESS

| Key performance indicator for Supplier Management process | The measured value of key performance indicator | The value of critical success factor | The percentage of the successful implemented key performance indicators |
|---|--|---|--|
| The number of suppliers meeting the targets within the contract | 8 | 10 | 80% |
| The number of service and contractual reviews held with suppliers | 12 | 16 | 75% |
| The number of service breaches caused by suppliers | 6 | 4 | 50% |
| The number of suppliers with nominated supplier managers | 5 | 8 | 63% |
| The number of contracts with nominated contract managers | 12 | 15 | 80% |

TABLE III. MEASUREMENTS FOR CHANGE MANAGEMENT PROCESS

| Key performance indicator for Change Management process | The measured value of key performance indicator | The value of critical success factor | The percentage of the successful implemented key performance indicators |
|--|--|---|--|
| The percentage of changes that meet the customer's agreed requirements | 85% | 95% | 89% |
| The percentage of reduction in the number of incidents attributed to | 20% | 30% | 67% |

| changes | | | |
|--|-----|-----|-----|
| The percentage of reduction in the number of unauthorized changes identified | 15% | 25% | 60% |
| The percentage of reduction in the number of changes with incomplete change specifications | 18% | 25% | 72% |
| The percentage of reduction in the number of changes with incomplete impact assessments | 12% | 17% | 71% |

TABLE IV. MEASUREMENTS FOR EVENT MANAGEMENT PROCESS

| Key performance indicator for Event Management process | The measured value of key performance indicator | The value of critical success factor | The percentage of the successful implemented key performance indicators |
|---|---|--------------------------------------|---|
| The number of incidents that occurred and which are triggered without a corresponding event | 18 | 26 | 69% |
| The percentage of events compared with the number of incidents | 60% | 75% | 80% |
| The percentage of events caused by existing problems or known errors | 70% | 85% | 82% |
| The percentage of events that resulted in incidents or changes | 65% | 90% | 72% |
| The percentage of events indicating performance issues | 72% | 88% | 82% |

TABLE V. MEASUREMENTS FOR INCIDENT MANAGEMENT PROCESS

| Key performance indicator for Incident Management process | The measured value of key performance indicator | The value of critical success factor | The percentage of the successful implemented key performance indicators |
|---|---|--------------------------------------|---|
| The percentage of incidents closed by the service desk without reference to other levels of support | 65% | 82% | 79% |
| The percentage of incidents solved remotely without the need for a visit | 43% | 55% | 78% |
| The maximum allowed time for solving every type of incident | 30 hours | 24 hours | 75% |
| The average number of service desk calls during one day | 147 | 120 | 78% |

| | | | |
|---|-----|------|-----|
| The percentage of incidents handled within agreed response time | 82% | 100% | 82% |
|---|-----|------|-----|

TABLE VI. MEASUREMENTS FOR REQUEST FULFILLMENT PROCESS

| Key performance indicator for Request Fulfillment process | The measured value of key performance indicator | The value of critical success factor | The percentage of the successful implemented key performance indicators |
|--|---|--------------------------------------|---|
| The percentage of service requests which are completed in agreed target times | 72% | 85% | 85% |
| The percentage of service requests closed by the service desk without reference to other levels of support | 74% | 92% | 80% |
| The percentage of service requests solved remotely without the need for a visit | 41% | 60% | 68% |
| The percentage of the total number of calls on Service Desk connected to service requests | 32% | 30% | 93% |
| The percentage of problems handled within agreed response time | 79% | 100% | 79% |

TABLE VII. MEASUREMENTS FOR PROBLEM MANAGEMENT PROCESS

| Key performance indicator for Problem Management process | The measured value of key performance indicator | The value of critical success factor | The percentage of the successful implemented key performance indicators |
|--|---|--------------------------------------|---|
| The percentage of problems closed by the service desk without reference to other levels of support | 75% | 85% | 88% |
| The percentage of problems solved remotely without the need for a visit | 42% | 55% | 76% |
| The maximum allowed time for solving every type of problem | 7 days | 10 days | 70% |
| The average number of service desk calls during one day | 12 | 10 | 80% |
| The percentage of problems handled within agreed response time | 75% | 100% | 75% |

TABLE VIII. THE RESULTS OF THE IMPLEMENTATION OF ITIL PROCESSES BEFORE THE IMPLEMENTATION OF ITIL SERVICE DESK

| ITIL process name | The result of implementation for each ITIL process |
|--------------------------|---|
| Service Level Management | 74.00% |
| Supplier Management | 69.60% |
| Change Management | 71.80% |
| Event Management | 77.00% |
| Incident Management | 78.40% |
| Request Fulfillment | 81.00% |
| Problem Management | 77.80% |

TABLE IX. MEASUREMENTS FOR SERVICE LEVEL MANAGEMENT PROCESS AFTER THE IMPLEMENTATION OF ITIL SERVICE DESK

| Key performance indicator for Service Level Management process | The measured value of key performance indicator | The value of critical success factor | The percentage of the successful implemented key performance indicators |
|--|--|---|--|
| The percentage of services which are covered under SLA | 94% | 100% | 94% |
| The percentage of users with SLAs contract which submitted a complaint | 10% | 10% | 100% |
| The percentage of suppliers with contract which submitted a complaint | 22% | 20% | 90% |
| The maximum allowed time for defining SLA, OLA or contract | 18 days | 15 days | 80% |
| The maximum allowed reduction in time taken to respond to and implement SLA requests | 6 days | 5 days | 80% |

TABLE X. MEASUREMENTS FOR SUPPLIER MANAGEMENT PROCESS AFTER THE IMPLEMENTATION OF ITIL SERVICE DESK

| Key performance indicator for Supplier Management process | The measured value of key performance indicator | The value of critical success factor | The percentage of the successful implemented key performance indicators |
|---|--|---|--|
| The number of suppliers meeting the targets within the contract | 9 | 10 | 90% |
| The number of service and contractual reviews held with suppliers | 14 | 16 | 88% |
| The number of service breaches caused by suppliers | 5 | 4 | 75% |
| The number of suppliers with nominated supplier managers | 7 | 8 | 88% |
| The number of contracts with nominated contract managers | 14 | 15 | 93% |

TABLE XI. MEASUREMENTS FOR CHANGE MANAGEMENT PROCESS AFTER THE IMPLEMENTATION OF ITIL SERVICE DESK

| Key performance indicator for Change Management process | The measured value of key performance indicator | The value of critical success factor | The percentage of the successful implemented key performance indicators |
|--|--|---|--|
| The percentage of changes that meet the customer's agreed requirements | 88% | 95% | 93% |
| The percentage of reduction in the number of incidents attributed to changes | 23% | 30% | 77% |
| The percentage of reduction in the number of unauthorized changes identified | 17% | 25% | 68% |
| The percentage of reduction in the number of changes with incomplete change specifications | 21% | 25% | 84% |
| The percentage of reduction in the number of changes with incomplete impact assessments | 15% | 17% | 88% |

TABLE XII. MEASUREMENTS FOR EVENT MANAGEMENT PROCESS AFTER THE IMPLEMENTATION OF ITIL SERVICE DESK

| Key performance indicator for Event Management process | The measured value of key performance indicator | The value of critical success factor | The percentage of the successful implemented key performance indicators |
|---|--|---|--|
| The number of incidents that occurred and which are triggered without a corresponding event | 24 | 26 | 92% |
| The percentage of events compared with the number of incidents | 63% | 75% | 84% |
| The percentage of events caused by existing problems or known errors | 68% | 85% | 80% |
| The percentage of events that resulted in incidents or changes | 74% | 90% | 82% |
| The percentage of events indicating performance issues | 77% | 88% | 88% |

TABLE XIII. MEASUREMENTS FOR INCIDENT MANAGEMENT PROCESS AFTER THE IMPLEMENTATION OF ITIL SERVICE DESK

| Key performance indicator for Incident Management process | The measured value of key performance indicator | The value of critical success factor | The percentage of the successful implemented key performance indicators |
|---|--|---|--|
| The percentage of incidents closed by the service desk without reference to other levels of support | 69% | 82% | 84% |
| The percentage of incidents solved remotely without the need for a visit | 46% | 55% | 84% |
| The maximum allowed time for solving every type of incident | 27 hours | 24 hours | 88% |
| The average number of service desk calls during one day | 108 | 120 | 100% |
| The percentage of incidents handled within agreed response time | 95% | 100% | 95% |

TABLE XIV. MEASUREMENTS FOR REQUEST FULFILLMENT PROCESS AFTER THE IMPLEMENTATION OF ITIL SERVICE DESK

| Key performance indicator for Request Fulfillment process | The measured value of key performance indicator | The value of critical success factor | The percentage of the successful implemented key performance indicators |
|--|--|---|--|
| The percentage of service requests which are completed in agreed target times | 79% | 85% | 93% |
| The percentage of service requests closed by the service desk without reference to other levels of support | 81% | 92% | 88% |
| The percentage of service requests solved remotely without the need for a visit | 47% | 60% | 78% |
| The percentage of the total number of calls on Service Desk connected to service requests | 32% | 30% | 93% |
| The percentage of problems handled within agreed response time | 86% | 100% | 86% |

TABLE XV. MEASUREMENTS FOR PROBLEM MANAGEMENT PROCESS AFTER THE IMPLEMENTATION OF ITIL SERVICE DESK

| Key performance indicator for Problem Management process | The measured value of key performance indicator | The value of critical success factor | The percentage of the successful implemented key performance indicators |
|--|--|---|--|
| The percentage of problems closed by the service desk without reference to other levels of support | 80% | 85% | 94% |
| The percentage of problems solved remotely without the need for a visit | 48% | 55% | 87% |
| The maximum allowed time for solving every type of problem | 9 days | 10 days | 90% |
| The average number of service desk calls during one day | 11 | 10 | 90% |
| The percentage of problems handled within agreed response time | 83% | 100% | 83% |

TABLE XVI. THE RESULTS OF THE IMPLEMENTATION OF ITIL PROCESSES AFTER THE IMPLEMENTATION OF ITIL SERVICE DESK

| ITIL process name | The result of implementation for each ITIL process |
|--------------------------|---|
| Service Level Management | 88.80% |
| Supplier Management | 86.80% |
| Change Management | 82.00% |
| Event Management | 85.20% |
| Incident Management | 90.20% |
| Request Fulfillment | 87.60% |
| Problem Management | 88.80% |

An Improved Hybrid Distributed Image Compression Model

Sherin M. Youssef
 College of Engineering
 Arab Academy for Science and
 Technology
 Alexandria, Egypt
sherin@aast.edu

Ahmed Abou Elfarag
 College of Engineering
 Arab Academy for Science and
 Technology
 Alexandria, Egypt
abouelfarag@aast.edu

Noura S. Khalil
 College of Engineering
 Arab Academy for Science and
 Technology
 Alexandria, Egypt
nourasamirkh@gmail.com

Abstract— Due to resource-constrained in wireless sensor network (WSNs), efficient compression and transmission of images have gained wide attention. Distributed image compression and transmission is proposed as a solution in order to overcome the computation energy limitation of individual nodes through sharing processing of tasks and to extend the overall network lifetime through the distribution of the computational load among otherwise idle processors [6]. In this paper to address the above mentioned goals the image is splitting into a group of equal sliced in size then distributed it on multiple nodes to compress and transmit it which will reduce image size and less effect of noise. The proposed model integrated algorithms such as Discrete Wavelet Transform, encoding technique called set partitioning in hierarchical trees (SPIHT), binary Code Book (CB) and clustering technique. Image quality, network lifetime and energy consumption are the three performance parameters should be considered during the image compression and transmission. Simulation results are presented and show that the proposed scheme optimizes peak signal to noise ratio, compression ratio, and network lifetime and reduces significantly the energy consumption.

Keywords- Wireless sensor networks (WSNs), set partitioning in hierarchical trees (SPIHT), Code Book (CB), Distributed Wavelet Transform and System lifetime.

I. INTRODUCTION

Recently wireless sensor network (WSN) have drawn the attention of the research community in the last few years since, it reduces costs (installation, time and maintenance costs), increase efficiency and monitor anywhere. A wireless sensor network (WSN) is built of distributed autonomous sensors which composed of few to several hundreds or even thousands of nodes to monitor physical or environmental conditions, such as temperature, sound and pressure and to cooperatively pass their data through the network to a main location. The more modern networks are bi-directional, also enabling control of sensor activity [1]. Unfortunately, nodes suffer problems such as memory limitations, restricted computational power, energy supplied and narrow bandwidth. These resource constraints form serious difficulties for the design wireless sensor networks [2]. For image-based applications, images have to compress to reduce the size of data (the number of transmitted bits) by removing redundant information such as spatial, temporal and spectral redundancies to save communication energy (power of nodes) because visual data such as still pictures, stream video

and monitoring data requires a large amount of information which leads to severe of resource [3]. Distributed image compressing and transmission in a WSN is presented as the solution for the above mention problem and evaluate their performance in terms of energy consumption and image quality in a wireless sensor network.

The advantages of using distributed image compression and transmission in WSNs can be clarified in the following two cases. In the first one, nodes have extremely constrained computation power. Hence, a node does not have sufficient computation power to completely compress a large raw image. In this case, a distributed method to share the processing task is required to overcome the computation power limitation of each single node. In the second one, even if nodes are not extremely computation power constrained, but are battery operated, distributing the computation load of processing every raw image among otherwise idle processors of other nodes extends the overall lifetime of the network [4].

The mechanism proposed in [5] uses a scheme for error robust and energy efficient image transmission over wireless sensor networks. The innovations of proposed scheme are two folds: multiple bit stream images encoding to achieve error robust transmission and small fragment burst transmission to achieve efficient transmission. By uses a scheme based in SPIHT coding of data blocks generated from parent-child relation chips of wavelet coefficients. This parent-child relationship is performed in order to reinforce SPIHT fragilities in bit error transmission cases. The proposed algorithm achieve energy efficient transmission by saving energy consumed on control overhead and device switching from sleep to active. In [6] The proposed algorithm achieve energy efficient compression and transmission of images in a resource-constrained multihop wireless network by distributing wavelet transform processing workload over several groups of nodes along the path from the source to the destination in order to overcome the computation and/or energy limitation of individual nodes and to extend the overall lifetime of the network by distributing the computational load among otherwise idle processors with respect to image quality. Two methods were proposed for exchanging data, the first one is parallel wavelet transform (Divide by rows/columns) and the second one is tilling method.

Simulation results show that scheme prolongs the system lifetime and has total energy consumption comparable to the centralized algorithm.

This paper is organized as follows. Section II represents the architecture of distributed image compression over a wireless sensor node; section III represents the experimental results; finally section IV represents conclusion.

II. DISTRIBUTED IMAGE COMPRESSION

Before explaining the proposed model there are some terminologies and background needed to be described of image compression as it related to this paper.

A. Background and Terminologies of Image Compression

A common characteristic of most images is that the neighboring pixels are correlated and therefore contain redundant information. Image compression is an application of data compression that aims to encode and reduce the original image with few bits to represent an image by removing the spatial, temporal and spectral redundancies as much as possible to store or transmit data in an efficient form. [16].

As mention before image compression techniques used to compress visual data which requires a large amount of information which leads to severe of resource, since WSNs has a limitations in resources, distributed image compressing and transmission used to save resources of WSNs by distributing the workload of task to many groups of nodes along the route from the source to the destination which achieve our goal.

B. The Proposed Model Architecture for Distributed Image Compression Over a Wireless Sensor Node

Figure 1 shows the proposed model architecture which has different phases including image splitting phase, sub-region multi level wavelet, encoding using set partitioning in hierarchical trees (SPIHT), generating binary codebook and transmitting data using clustering technique.

Our contribution in this paper includes the using of hierarchical trees (SPIHT) in encoding with the advantage of good image quality, high PSNR, especially for color images, it is optimized for progressive image transmission, produces a fully embedded coded file, simple quantization algorithm, fast coding/decoding (nearly symmetric), has

wide applications, completely adaptive, can be used for lossless compression; can code to exact bit rate or distortion and efficient combination with error protection [12]. Then integrated with binary codebook generation with the advantage of minimize the average distortion between a given training set.

The embedding of Wavelet Transform in distributed image compression is due to its advantage of being more robust under transmission and decoding errors, and also facilitates progressive transmission of images. Because of their inherent multi-resolution nature [7], the benefit from wavelet coding schemes are especially suitable for applications just as scalability, orthogonality, compact support, linear phase and high approximation/vanishing moments of the basis function, efficient multi-resolution representation and embedded coding with progressive transmission [8] and [9].

1) Image Splitting Phase

From source images (512x512), at first, the data is partitioned into n slices R_1, R_2, \dots, R_n where each slice consists of one or more rows. Second, each node runs one decomposition (1D) wavelet transforms on R_i ($i = 1, 2, 3, \dots, n$). Once the 1D wavelet transform is completed on all rows, one node collects the intermediate results Q_1, Q_2, \dots, Q_n and divides the results into m blocks I_1, I_2, \dots, I_m . Then each node applies 1D wavelet transform on I_i ($i = 1, 2, 3, \dots, m$). Finally, a node gathers the 2D wavelet transform results J_1, J_2, \dots, J_m . This data exchange scheme does not result in any image quality loss compared to the traditional centralized scheme [7].

2) Lifting Scheme for Wavelet Transform (Sub-band Coding)

In recent, wavelet transform has gained widespread acceptance in signal processing in general and in particular in image compression research. The main idea behind wavelet transform is to split up the frequency band of a signal (image in this paper) and then to code each sub-band using octave-band decomposition in our case.

The octave-band decomposition procedure can be described as follows. A Low Pass Filter (LPF) and a High Pass Filter (HPF) are chosen, such that they exactly halve the frequency range of the input signal. First, the LPF is applied for each row of data, thereby getting the low frequency components of the row [2].

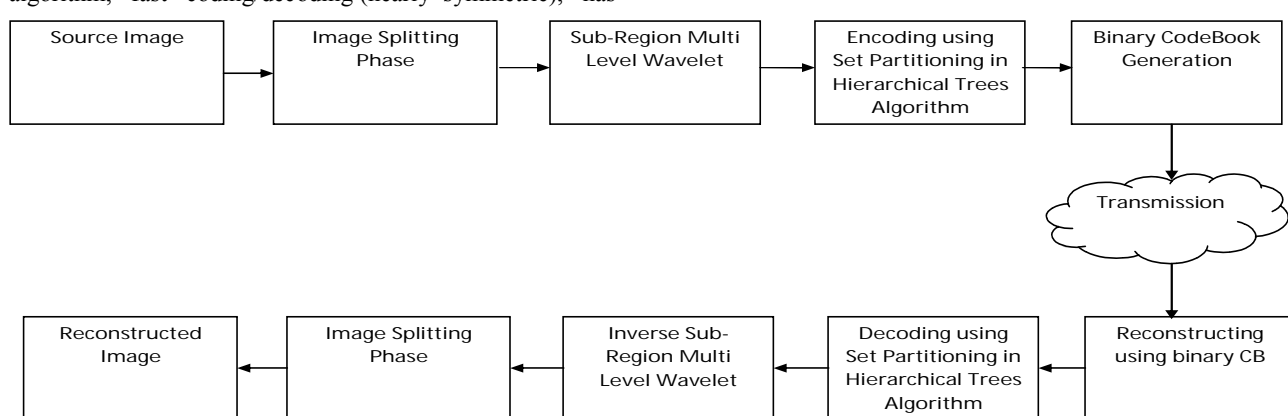


Fig. 1. Functional block diagram of architecture of distributed image compression

The output data contains frequencies only in the first half of the original frequency range because the LPF is a half-band filter. Then, the HPF is applied for the same row of data, and similarly the high pass components are separated. The low and high pass components are arranged into a row of output data.

This row operation is known as one decomposition (1D) wavelet transforms. Next, the filtering is done for each column of the intermediate output data. This whole procedure including both row and column operations is called a two decomposition (2D) wavelet transform. The resulting 2D array of coefficients contains four bands of data such as LL (low-low), HL (high-low), LH (low-high) and HH (high-high). The LL band can be further decomposed in the same manner, thereby producing even more sub-bands. This can be repeated up to any level, thereby resulting in a pyramidal decomposition [2].

3) Set Partitioning in Hierarchical Trees (SPIHT) Encoding

Set Partitioning in Hierarchical Trees (SPIHT) Encoding is primarily a wavelet-based image compression scheme which encodes the decomposed image to a bit stream. In SPIHT, the wavelet coefficients are fed to the encoder after converted the image into its wavelet transform. SPIHT has been selected because SPIHT and its predecessor achieved better quality when compared to vector quantization and other algorithms. [11] and [17].

SPIHT coding operates by exploiting the relationships among the wavelet coefficients across the different scales at the same spatial location in the wavelet sub-bands. Generally, SPIHT coding involves the coding of the position of zero-trees in the wavelet sub-bands and the coding of the position of significant wavelet coefficients [13]. The SPIHT coder exploits the following image characteristics:

a) The majority of an image's energy is concentrated in the low frequency components and a decrease in variance is observed as moving from the highest to the lowest levels of the sub-band pyramid

b) It has been observed that there is a spatial self-similarity among the sub-bands, and the coefficients are likely to be better magnitude-ordered if moving downward in the pyramid along the same spatial orientation [13].

To describe the spatial relationship on the hierarchical pyramid, a tree structure, termed spatial orientation tree shown in Fig. 2 shows how the spatial orientation tree is defined in a pyramid constructed with recursive four-sub-band splitting. Every pixel in the image signifies a node in the tree and is determined by its corresponding pixel coordinate. Its direct descendants (offspring) symbolize the pixels of the same spatial orientation in the next level of the pyramid. The tree is defined in such a manner that each node has either no offspring (the leaves) or four offspring's, which at all times form a group of 2 x 2 adjacent pixels. In Fig. 2, the arrows are directed from the parent node to its four offspring's. The pixels in the highest level of the pyramid are the tree roots and are also grouped in 2 x 2 adjacent pixels. Nevertheless, their offspring branching rule is different, and in each group, one of them (indicated by the star in Fig. 2) has no descendants [14].

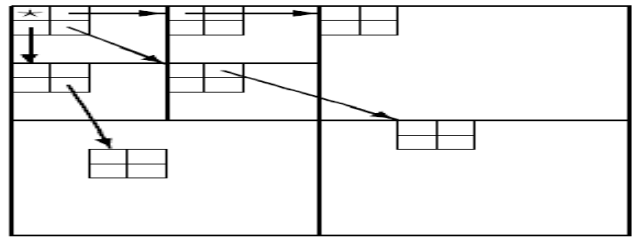


Fig. 2. Spatial-orientation trees

4) Codebook (CB) Generation

Before explaining binary codebook generation there are some terminologies and background needed to be described of recent algorithms that used to generate codebook such as vector quantization.

a) Vector Quantization (VQ)

Vector Quantization (VQ) is efficient and simple approach for data compression, because it is simple and easy to implement, VQ used to generate a good codebook such that the distortion between the original image and the reconstructed image is the minimum. In the past years, many improved algorithms of VQ codebook generation approaches have been developed.

VQ is a mapping function which maps k-dimensional vector space to a finite set CB = {C₁, C₂, C₃... C_N}. The set CB is called as codebook consisting of N number of codevectors and each codevector C_i = {c_{i1}, c_{i2}, c_{i3}... c_{ik}} is of dimension k. Good codebook should be designed to reduced distortion in reconstructed image. For encoding, image is split in blocks and each block is then converted to the training vector X_i = (x_{i1}, x_{i2}... x_{ik}). The codebook is looked for the nearest codevector C_{min} by computing squared Euclidean distance [10].

b) Binary CodeBook (CB) Generation

Due to the output of SPHIT is a stream of bits so binary codebook (CB) could generated by dividing the output matrix from SPHIT into n*n blocks to generate training vectors matrix then generate binary CB (truth-table) with size 2ⁿ then match between training vectors and CB to get indexed matrix, suppose n = 2 so CB size will be 4, so instead of sending CB with size 128 or 512 or 1024 CB with size 4 will be sent as shown in TABLE I.

TABLE I. CODEBOOK WITH SIZE n = 2

| CodeBook | | |
|----------|------------|---|
| Indexed | Codeword's | |
| 1 | 0 | 0 |
| 2 | 0 | 1 |
| 3 | 1 | 0 |
| 4 | 1 | 1 |

III. EXPERIMENTAL RESULTS

The proposed model has been carried out on several experiments to test the efficiency of the model. The model has been tested using different benchmark images. Moreover, different results from the scheme have been compared with results of other algorithms in [10], [13], and [15].

In this section the performance indicators used to evaluate the proposed model is illustrated.

A. Performance measures

In order to properly evaluate the performance of image compression schemes and to allow a fair comparison between different schemes, a benchmark suite must include a set of tests and a way of measuring the results of the tests using controlled conditions.

In compression, the tests are oriented to measure the requirements of an application. So, the robustness, the fidelity and the capacity are commonly measured.

1) Mean-Square-Error (MSE):

MSE is the cumulative squared error between the original and watermarked image as shown in (1)

$$MSE = \frac{1}{M \times N} \sum_{x=1}^M \sum_{y=1}^N [I(x, y) - I'(x, y)]^2 \quad (1)$$

Where M, N is the dimension of Image, I(x, y) is the original image, I' is the watermarked image.

2) Peak-Signal-To-Noise-Ratio (PSNR):

PSNR as shown in (2) is one of the most common measures of distortion in the image field. PSNR is a useful tool to measure perceptibly level, it not always accurate to human eyes adjustment.

$$PSNR = 10 \log_{10} (255^2 / MSE) \quad (2)$$

3) Compression Ratio(CR):

CR, as shown in (3) is the ratio of the original (uncompressed) image to the compressed image.

$$CR = \frac{\text{Uncompressed Image Size}}{\text{Compressed Image Size}} = \frac{Usize}{Csize} \quad (3)$$

Where Usize = M x N x K and Csize = size of compressed image file stored in a disk, where M, N is the dimension of Image, K is 8 bit image.

B. Results

Different experiments have been carried out to test and validate the proposed model using the different data sets. The performance indicators described above were used to provide statistical evaluation of performance without effect of noise. Examples of the tested images are shown in Fig. 3.

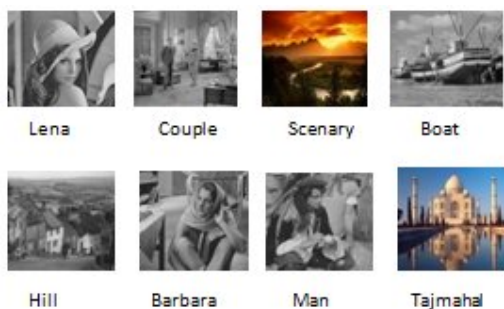


Fig.3. Examples of the tested images

The PSNR and MSE were calculated for different images using different algorithms as shown in TABLE II which clarify that PSNR and MSE of proposed algorithm is better than PSNR and MSE of other algorithms in [10], [13] and [15].

TABLE II. VALUES OF THE PSNR AND MSE FOR DIFFERENT IMAGES UNDER DIFFERENT ALGORITHMS

| Test Images | CB-Size | LBG | | REV | | Proposed Algo. | |
|-------------|---------|------|-------|------|-------|----------------|------|
| | | PSNR | MSE | PSNR | MSE | MSE | PSNR |
| Tiger | 128 | 21.2 | 491.4 | 22.8 | 340.0 | 11.9 | 37.4 |
| | 256 | 21.3 | 487.7 | 23.5 | 288.7 | | |
| | 512 | 21.3 | 480.5 | 24.4 | 235.5 | | |
| | 1024 | 21.5 | 465.7 | 25.2 | 195.2 | | |
| Strawberry | 128 | 18.4 | 933.5 | 23.9 | 266.8 | 21.6 | 34.8 |
| | 256 | 18.5 | 925.9 | 24.6 | 228.2 | | |
| | 512 | 18.5 | 912.8 | 25.4 | 186.7 | | |
| | 1024 | 18.7 | 885 | 26.3 | 152.9 | | |
| Tajma-hal | 128 | 18.5 | 910.2 | 23.3 | 301.2 | 11.5 | 37.6 |
| | 256 | 18.6 | 902.7 | 24.3 | 241.3 | | |
| | 512 | 18.6 | 889.4 | 25.6 | 179.1 | | |
| | 1024 | 18.8 | 862 | 26.7 | 137.6 | | |
| Gan-esh | 128 | 20 | 650.9 | 21.3 | 481.6 | 42.4 | 31.9 |
| | 256 | 20 | 645.6 | 21.9 | 421.7 | | |
| | 512 | 20.1 | 635.2 | 22.6 | 354.7 | | |
| | 1024 | 20.3 | 613.3 | 23.3 | 307.9 | | |
| Scen-ary | 128 | 22.6 | 356 | 25.3 | 191.3 | 1.46 | 46.4 |
| | 256 | 22.7 | 353 | 26.3 | 153.1 | | |
| | 512 | 22.7 | 346.5 | 27.4 | 119.1 | | |
| | 1024 | 22.9 | 333.8 | 28.6 | 90.2 | | |

Compared with LBG and REV the proposed model in Fig. 4 shown an outstanding improves in performance.

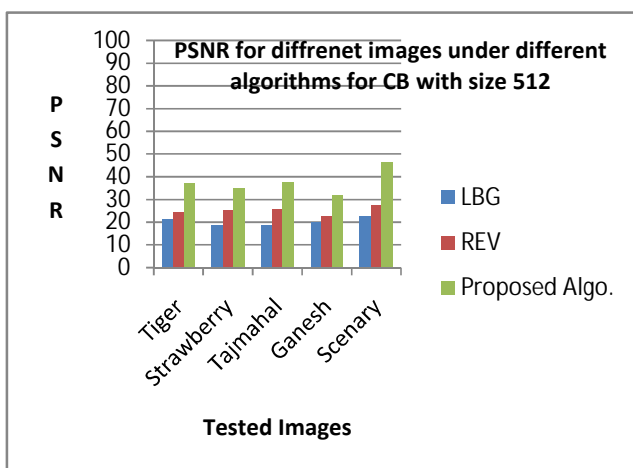


Fig.4. PSNR for different images under different algorithms for CB with size 512

The dataset images have applied under different algorithms (Two-Level KPE, KPE and proposed algorithm). TABLE III demonstrates changing of the PSNR and MSE for different images under different algorithms.

TABLE III. VALUES OF THE PSNR AND MSE FOR DIFFERENT IMAGES FOR DIFFERENT ALGORITHMS

| Test Images 512x512 | CB Size | Two-Level KPE | | KPE | | Proposed Algorithm | |
|------------------------|---------|---------------|------|-------|-------|--------------------|------|
| | | MSE | PSNR | PSNR | MSE | MSE | PSNR |
| Tiger | 256 | 267 | 23.9 | 21.47 | 463.8 | 11.9 | 37.4 |
| | 512 | 131 | 26.9 | 21.77 | 432.2 | | |
| | 1024 | 68.5 | 29.8 | 22.74 | 345.7 | | |
| Straw - berry | 256 | 168 | 25.9 | 22.84 | 338.1 | 21.6 | 34.8 |
| | 512 | 87.1 | 28.7 | 23.70 | 277.3 | | |
| | 1024 | 49.9 | 31.2 | 24.45 | 233.6 | | |
| Tajmahal | 256 | 159 | 26.1 | 22.51 | 364.6 | 11.4 | 37.6 |
| | 512 | 77.7 | 29.2 | 23.67 | 279 | | |
| | 1024 | 46.3 | 31.5 | 24.51 | 230.3 | | |
| Ganesh | 256 | 307 | 23.3 | 20.03 | 610.6 | 42.4 | 31.9 |
| | 512 | 204 | 25 | 19.97 | 533.1 | | |
| | 1024 | 125 | 27.2 | 20.77 | 449.1 | | |
| Scen- ary | 256 | 117 | 27.5 | 22.04 | 406.4 | 1.5 | 46.5 |
| | 512 | 73.1 | 29.5 | 23.41 | 296.8 | | |
| | 1024 | 34.4 | 32.8 | 25.36 | 189.2 | | |

As shown in Fig. 5, the PSNR of our proposed model remains high compared to Two-Level KPE and KPE for all tested images

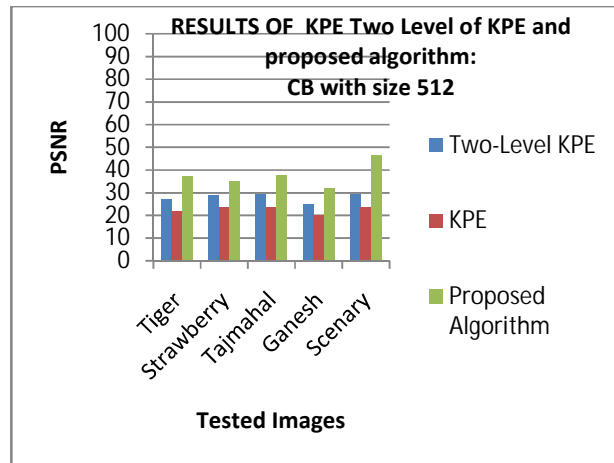


Fig. 5 PSNR of different algorithms for CB with size 512

The PSNR were calculated for different images under different algorithms shown in TABLE IV. In TABLE IV the values of the PSNR are illustrated that shows that the PSNR of proposed algorithm is high for all tested images.

TABLE IV. COMPARISON OF PSNR OF (A) SPIHT + SOFM BASED COMPRESSION SCHEME (B) PROPOSED ALGORITHM (SPHIT + BINARY CB BASED COMPRESSION SCHEME)

| Test Images 512x512 | SPHIT + SOFM Based Compression Scheme | Proposed Algorithm (SPHIT + Binary CB Based Compression Scheme) |
|------------------------|---------------------------------------|---|
| Lena | 32.14 | 39.26 |
| Barbara | 30.39 | 34.17 |
| Boat | 30.97 | 34.99 |
| Man | 31.90 | 36.01 |
| Couple | 30.64 | 35.28 |
| Hill | 30.98 | 35.08 |

Fig. 6 illustrate the change in the peak-signal-to-noise-ratio for (a) SPIHT + SOFM based compression scheme (b) Proposed Algorithm (SPHIT + Binary CB Based Compression Scheme). As shown from the chart, the PSNR remains high for all test images.

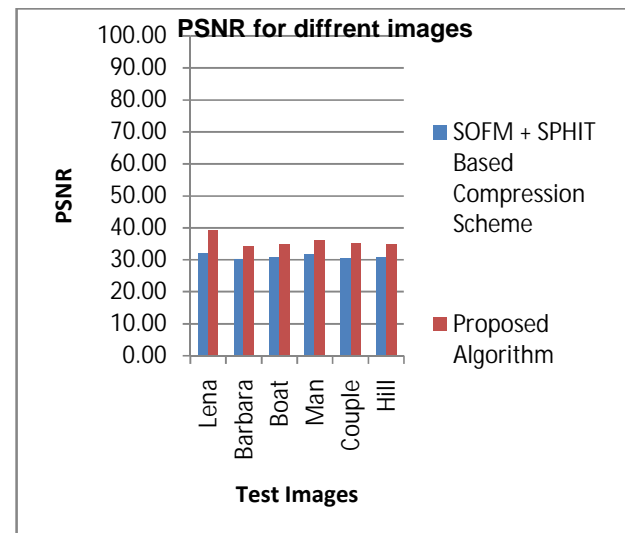


Fig. 6 Comparison of PSNR of (a) SPIHT + SOFM based compression scheme (b) Proposed Algorithm (SPHIT + Binary CB Based Compression Scheme)

The CR were calculated for different images for (a) SPIHT + SOFM based compression scheme (b) Proposed Algorithm (SPHIT + Binary CB Based Compression Scheme) as illustrate in TABL V. In TABL V the values of the CR are illustrated that shows that the CR for proposed algorithm is less than SPIHT + SOFM based compression scheme.

TABL V. Comparison of CR between (a) SPIHT + SOFM based compression scheme (b) Proposed Algorithm

| Test Images 512x512 | SOFM + SPHIT Based Compression Scheme | Proposed Algorithm |
|------------------------|---------------------------------------|--------------------|
| Lena | 14:01 | 8:01 |
| Barbara | 14:01 | 8:01 |
| Boat | 13:01 | 8:01 |
| Man | 16:01 | 8:01 |
| Couple | 15:01 | 8:01 |
| Hill | 22:01 | 8:01 |

As for Fig. 7 illustrate Comparison of CR between (a) SPIHT and SOFM based compression scheme (b) Proposed Algorithm (SPHIT + Binary CB Based Compression Scheme).

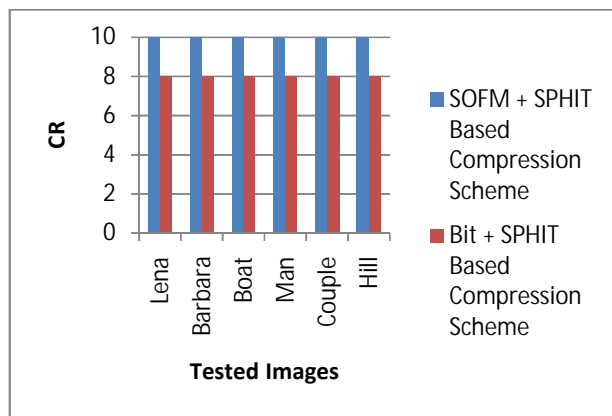


Fig.7 Comparison of CR of (a) SPIHT + SOFM based compression scheme
(b) Proposed Algorithm

IV. CONCLUSION

In this paper, an improved image compression model has been introduced. The proposed scheme has been integrated with set partitioning in hierarchical trees (SPHIT) encoding to provide high PSNR. The embedded wavelet transform with SPHIT and binary codebook achieve efficient and high quality of reconstruction images comparing with other algorithms as shown in experimental results.

REFERENCES

- [1] A.karthikeyan, T.shankar, V.srividhya, Suryalok.sarkar, Akanksha gupte,"energy efficient distributed image compression using jpeg2000 in wireless sensor networks (wsns)," journal of theoretical and applied information technology, vol. 47, no.3, pp 875 -883. january 2013
- [2] Yang Xiaobo, Sun Lijuan, Wang Ruchuan, 2010, Distributed Image Compression Algorithm in Wireless Multimedia Sensor Networks, <http://wwwen.zte.com.cn/en/>. [Online]. Available at http://wwwen.zte.com.cn/endata/magazine/ztecommunications/2010Year/no1/articles/201003/t20100321_181536.html [Accessed 26th Oct. 2013]
- [3] Mohammad Hossein, Yaghmaee, Donald A. Adjeroh, "Priority-based rate control for service differentiation and congestion control in wireless multimedia sensor networks", Computer Networks, vol. 53, no. 11,pp. 1798–1811, July 2009.
- [4] Wu, H.; Abouzeid, A.A., "Energy efficient distributed JPEG2000 image compression in multihop wireless networks," Applications and Services in Wireless Networks, 2004. ASWN 2004. 2004 4th Workshop, pp.152-160, 9-11 Aug. 2004, doi 10.1109/ASWN.2004.185166.
- [5] Min Wu; Chang Wen Chen, "Multiple bitstream image transmission over wireless sensor networks," Sensors, 2003. Proceedings of IEEE, vol.2, pp.727-731, Vol.2, 22-24 Oct. 2003, doi 10.1109/ICSENS.2003.1279037.
- [6] Huaming Wu, Alhussein A. Abouzeid," Energy efficient distributed image compression in resource-constrained multihop wireless networks," Computer Communications, vol. 28, no 14, pp 1658-1668, Sept. 2005.
- [7] Andreopoulos, I.; Karayannidis, Y.A.; Stouraitis, T., "A hybrid image compression algorithm based on fractal coding and wavelet transform," Circuits and Systems, 2000. Proceedings. ISCAS 2000 Geneva. The 2000 IEEE International Symposium on , vol. 3, pp. 37- 40 , 2000, doi: 10.1109/ISCAS.2000.855990
- [8] S. Esakkirajan, T. Veerakumar, V. Senthil Murugan and P. Navaneethan "Image Compression using Multiwavelet and Multi-stage Vector Quantization," International Journal of Signal Processing (IJSP), vol. 4, no.4, pp. 246-253, 2008.
- [9] Antonini, M.; Barlaud, M.; Mathieu, P.; Daubechies, I., "Image coding using wavelet transform," Image Processing, IEEE Transactions on , vol. 1, no. 2, pp. 205-220, Apr 1992, doi: 10.1109/83.136597.
- [10] H. B. Kekre, Tanuja K. Sarode , "New Clustering Algorithm for Vector Quantization using Rotation of Error Vector,"(IJCSIS) International Journal of Computer Science and Information Security, vol. 7, no. 3, 2010.
- [11] Fry, T.W.; Hauck, S.A., "SPIHT image compression on FPGAs," Circuits and Systems for Video Technology, IEEE Transactions on , vol. 15, no. 9, pp. 1138-1147, Sept. 2005, doi: 10.1109/TCSVT.2005.852625
- [12] A. Said, W. A. Pearlman, "SPIHT Image Compression: Properties of the Method", <http://www.cipr.rpi.edu/research/SPIHT/spiht1.html>[accessed 29/10/2013].
- [13] Chandan Singh D. Rawat, Sukadev Meher,"A Hybrid Coding Scheme Combining SPIHT and SOFM Based Vector Quantization for Effectual Image Compression," European Journal of Scientific Research, vol. 38, no. 3, pp. 425-440, 2009.
- [14] Said, A.; Pearlman, W.A., "A new, fast, and efficient image codec based on set partitioning in hierarchical trees," Circuits and Systems for Video Technology, IEEE Transactions on , vol. 6, no. 3, pp. 243,250, Jun 1996, doi: 10.1109/76.499834
- [15] H. B. Kekre, Tanuja K. Sarode,"Two-level Vector Quantization Method for Codebook Generation using Kekre's Proportionate Error Algorithm ,International Journal of Image Processing, vol. 4, no. 1, pp. 1-10 , 2010.
- [16] Vidhi Dubey, N.K.Mittal, S.G.kerhalkar,"A Review on Wavelet-Based Image Compression Techniques,"International Journal of Scientific Engineering and Technology, vol. 2, no. 8, pp. 783-788, Aug. 2013.
- [17] Waltenegus Dargie. Digital Signal Processing. [Online].Available: <http://wwwpub.zih.tu-dresden.de/~dargie/wsn/slides/students/2009/dsp.pdf>, [Accessed 21th Jan. 2014]

Comparison of cryptographic methods based on the arithmetic of elliptic curves (ECC) with symmetric cryptography methods on the Android platform

Milan Oulehla

Faculty of Applied Informatics
Tomas Bata University in Zlín
nám. T. G. Masaryka 5555, 760 01 Zlín
oulehla@fai.utb.cz

David Malaník

Faculty of Applied Informatics
Tomas Bata University in Zlín
nám. T. G. Masaryka 5555, 760 01 Zlín
dmalanik@fai.utb.cz

Abstract—the paper describes a systematic comparison of cryptographic methods based on the arithmetic of elliptic curves with symmetric cryptographic methods Triple DES and AES. The cryptographic tests were performed by using special cryptographic benchmark. The benchmark was created by the author of this paper for the cryptographic research needs. The comparison was performed on the physical hardware including smartphones and a tablet (The tests performed by the emulator would be considerably misleading.)

Keywords—*arithmetic of elliptic curves, Android, cryptographic benchmark, symmetric cryptography.*

I. INTRODUCTION

The cryptographic methods based on the arithmetic of elliptic curves are the modern cryptographic methods that could be suitable for mobile devices which have limited hardware performance. The ECC method was compared with the methods of symmetric cryptography AES and TripleDES. The operating system Android has specific management of RAM memory so there are two file sizes: Heap ready size - File size which is allowed to be encrypted in RAM all at once. Heap not ready size - File size which is not allowed to be encrypted in RAM all at once. These files must use buffer for encryption. And they must be encrypted part by part.

Performance of the cryptographic methods was tested on heap ready files. Data which was measured was statistically processed.

II. CREATION OF CRYPTOGRAPHIC TESTS AND DATA SELECTION

We created cryptographic tests with emphasis on real conditions. Thus we selected these types of files:

- *.mp3 files - Users can record their voice notes. Audio notes can be recorded for example by "Hi-Q MP3 Voice Recorder" application. [1]
- *.jpg files - Users can take pictures with their smartphones. Android has native support for taking

This work was supported by the European Regional Development Fund under the Project CEBIA-Tech No. CZ.1.05/2.1.00/03.0089.

photographs.

- *.mp4 files - Video files can be recorded by mobile device. Android has native support for video recording.
- *.txt files - Short text notes can be made by using many Android applications, e.g. Simple Notepad [2].

All of these files can contain sensitive information and users may wish to encrypt them. Android mobile devices are often used for viewing the content. Files which a user creates in mobile devices are very small. The files typically have size about several megabytes. This fact was reflected in the structure of the test files:

- files up to 250 KB.
- files up to 500 KB.
- files up to 1 MB.
- files up to 3 MB.
- files up to 5 MB.

The most of Android devices are able to encrypt at once files which have this size by using method doFinal. Method doFinal is provided by class Cipher (Encrypts data in a single-part operation [3]). The result of encryption can be written at once to a file on a SD card or to internal, persistent memory of a mobile device.

Since the encryption using the doFinal method is relatively quick, it is practically usable even on inexpensive or older devices. For example: LG P500 Optimus One which has CPU ARM 11 performs AES encryption of 1 058 496 B file with 256-bit key in 1.72 s. The time includes both encryption and writing of encrypted file to a SD card. This CPU works on low frequency 600 MHz [4]. Data encryption in a single-part operation is fast but it also has some risks. The main risk is OutOfMemoryError. There is a danger when the Java Virtual Machine cannot allocate an object because it is out of memory, and no more memory could be made available by the garbage

collector [5]. And the exact heap size limit varies between devices based on how much RAM the device has available overall. If your app has reached the heap capacity and tries to allocate more memory, it will receive an OutOfMemoryError [6].

For example, if we try to encrypt a file of 10 583 904 bytes by using phone LG P500 Optimus One and doFinal method, the Android operating system terminates the encryption. After then we can read the following message in logcat: “dalvikvm-heap:Out of memory on a 10583936-byte allocation”. On the other hand, the encryption of the same file on your Samsung i9505 Galaxy S4 will be fine. This means that the application programmer who wants to use for encryption fast doFinal method must first call getMemoryClass () to determine whether the application has enough space in memory for the encryption of a particular file. The encryption application needs space in memory for:

- unencrypted file
- encrypted file
- all other objects which an application needs for work.

If there is not enough space in memory, it must be done by using Buffer encryption. In this case instances of Cipher class have to use some variant of the update method. The encryption using the update method is slower, but there is no OutOfMemoryError. The size of encrypted files is not limited by the size of available space in RAM which the system is able to allocate to the application. Using update method has some problems in Android operating system. For more information [7].

The differences between ‘At once encryption’ (As it was written above, it uses doFinal method.) and ‘Buffer encryption’ are shown in Figure 1.

The encryption methods which were used for testing:

- Triple DES (DESEde/ECB/PKCS5Padding), provider: AndroidOpenSSL, length of the key: 168 bits. Note: DESEde is alias of TripleDES method. This alias is usually used with Cipher class.
- AES (AES/ECB/PKCS5Padding), provider: AndroidOpenSSL, length of the key: 256 bits.
- ECC (ECIES, FlexiEC), provider: FlexiProvider, 160-bit elliptic curve.

Isolated observation of encryption process running in the RAM does not have relevant results. We need more complex view for detection of the specific character of the encryption on the Android platform. Comprehensive encryption process is a sequence of all operations that end by storing encrypted file on a user device. Sequence of the operations is following:

- loading data from a file stored on the SD card or in persistent memory to the operating memory,
- creation of a randomly generated key,
- encryption of a file by using a randomly generated key.

If we want real-life results of measuring, none of these steps can be omitted. Same conditions for all tests were ensured by using same microSD card for all tested device. Passwords were not used for the encryption but we used randomly generated encryption keys (as mentioned earlier). Key lengths were chosen by the used method, safety and time demands. Some Android mobile devices have no SD card slot, for example Nexus 5. Therefore, encryption tests were performed both on the SD card and in internal memory of the mobile device.

III. CREATION OF A CRYPTOGRAPHIC BENCHMARK

The principle of measuring the performance of the application:

- The application stores the start time.
- The application starts the code whose performance is measured.
- The application stores the end time.
- The application calculates the elapsed time. Elapsed time is the difference between end time and start time.

Although the principle of measuring the performance of the application is very simple, its practical implementation is very difficult. There are many pitfalls that can distort the results of measurement. Correct cryptographic benchmark has to avoid them. The following is the list of the biggest problems and actions which were done to prevent the distortion problems:

No. 1: The measurement is not performed in a separate thread. If the encryption task shares the main thread with operation of GUI, it may cause that the measured time will be extended by time needed for the GUI operations. Also, the time may be extended by time of other operations from the main thread. These operations from the main thread have nothing to do with the test encryption method and they can distort the results of measurement too.

Solution of the problem No. 1: The application will create a special thread only for encryption testing. This thread will create instance of cipher class of a particular encryption method. Then, constructor of the cipher class will create everything what is needed for the encryption. The start time will be saved and testing thread will call encrypt () method. Encrypt() will perform encryption. After the encryption is finished, the end time will be saved. In the end, the elapsed time as difference between end time and start time will be calculated.

Problem No. 2: One file is encrypted with a particular cryptographic method only once. During the first encryption a lot of activities are performed. But those activities aren't directly connected with the encryption. It is more about the behavior of the JVM. Thus, it needs more iteration. It is called as a warmup code.

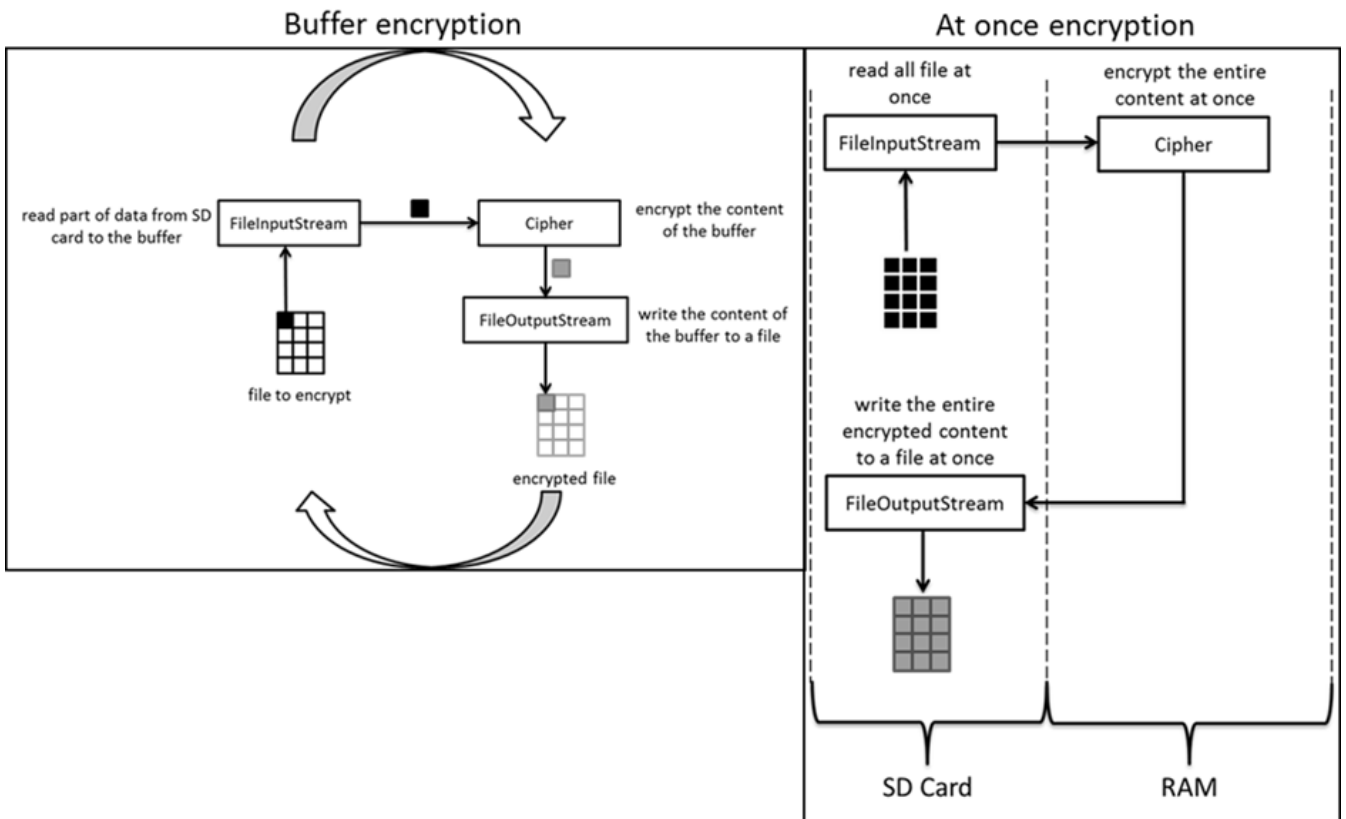


Fig. 1. The differences between At once encryption and Buffer encryption

Solution of problem No. 2: The tests which were conducted in our research showed that the first iteration almost always lasted longer than the other iterations. The situation is shown in Figure 2. Also, it rarely happened that the latest iteration lasted a shorter or longer period than the other iterations. For this reason first and last iteration were removed from the results.

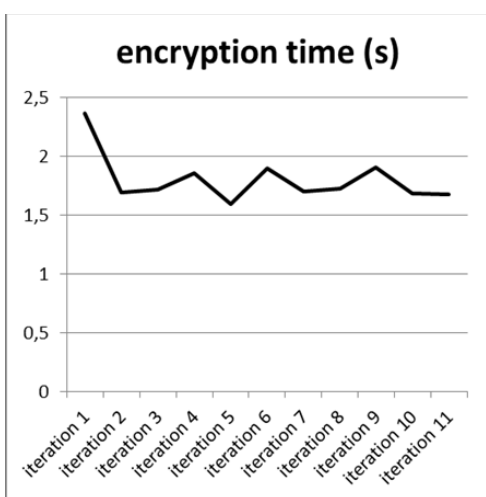


Fig. 2. The iterations AES encryption of 1 058 496 B file using phone LG P500

Problem No. 3: Theoretically `System.currentTimeMillis()` cannot be used for cryptographic tasks which have the encryption times shorter than 200 ms. Practically, the measurement accuracy may be 10 times to 100 times worse. That means that the measurements which use `System.currentTimeMillis()` should not be used for encryption tasks that are performed in less than 10 s [8].

Problem No. 4: `System.currentTimeMillis()` reflects the "wall clock time". If the system synchronizes time via NTP (Network Time Protocol) during the measuring, then this synchronization distorts the measurement result. The distortion affects all cryptographic tasks; it is not important that their execution takes less or more than 10 s [8].

Solutions of the problem No. 3 and No. 4: For this reason, all measurements were made using the API `System.nanoTime`. It can be used for shorter tasks than 10 s and "wall clock time" does not affect the benchmark results.

Problem No. 5: If the benchmark application uses huge GUI, for example `ProgressDialog` (for displaying the test status) or something similar, it can also distort the measurement accuracy.

Solution of the problem No. 5: Our cryptographic benchmark has only a minimal GUI, which consists of a single button. This button has only one function: It triggers the test. Any other visualization and interaction with the user was not built into the application. Benchmark sets all parameters of the test including the selection of files for testing, the number of

iterations and all necessary paths. [8] The test results are automatically saved to the *.csv file after completion of the test.

IV. TEST EVALUATION

In total, 6660 test files were encrypted. These devices were used for testing:

- LG P500 OptimusOne (phone).
- Samsung Galaxy S4 i9505 (phone).
- Acer IconiaTab A511 (tablet).

As mentioned earlier, both SD card and internal memory were used for saving encrypted files to the tested device.

Dependence of the encryption time and the file size is for all encryption methods approximately linear. Therefore, the regression lines were put over the dot plots.

A. Interpretation of the regression coefficient

The regression coefficient determines the speed of the encryption method. The value of the regression coefficient can be interpreted like this: increase in the file size by one megabyte causes increase in the encryption time value by regression coefficient (in seconds). The speed of methods ECC, AES and Triple DES on particular devices can be compared by using the values of the regression coefficients.

B. Interpretation of the regression constant

The values of the regression constant represent the time for preparation before the encryption itself.

The essential difference between the ECC method and the other two methods is that the former has a non-zero constant but constants of the other two methods can be considered to be a zero. In practice it means that the time of the ECC encryption is not insignificant even for files which have size close to a zero. These files have encryption time approximately equal to the value of regression constant. It is caused by the fact that the ECC method needs significant preparation time. Before the encryption process, ECC method has to create a finite field, an elliptic curve, etc. Only after that, the ECC method can start with encryption. The measured results show that the ECC method is not suitable for small size files. On the other hand, the encryption time dependence on file size of the other two methods can be considered directly proportional. (The files which are insignificantly smaller have insignificantly shorter encryption time.)

C. Results of the encryption on Acer Iconia Tab A511 device

The AES method has the lowest regression coefficient and has insignificant regression constant. Therefore, the AES can be considered as the fastest method on this device. The comparison of the two other methods is not so clear. ECC method has a lower regression coefficient than TripleDES. Since the method ECC does not have insignificant time of preparation (internal persistent memory: 0.81 second, SD card: 0.78, see the values of the regression constants in Figure 3 and Figure 4), the ECC is not suitable for small size files. The Figures 3 and 4 show the intersections of the regression lines. This means that the encryption of the files up to 2.2 megabytes

size is ECC method slower than the TripleDES method. For files which have larger size than 2.2 megabytes is the opposite situation. There the ECC method is faster than the TripleDES.

Both internal persistent memory and SD card have very similar encryption speed.

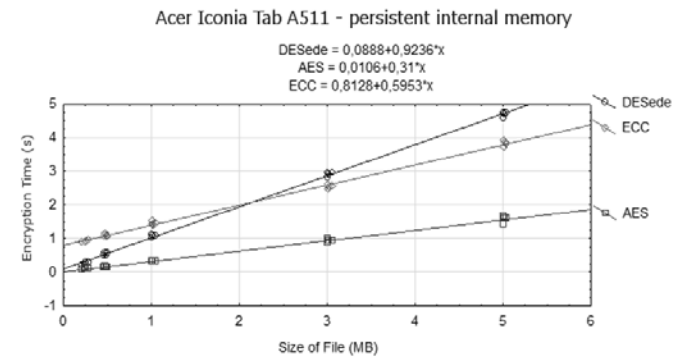


Fig. 3. The results of measurements on Acer Iconia Tab A511 device - persistent internal memory

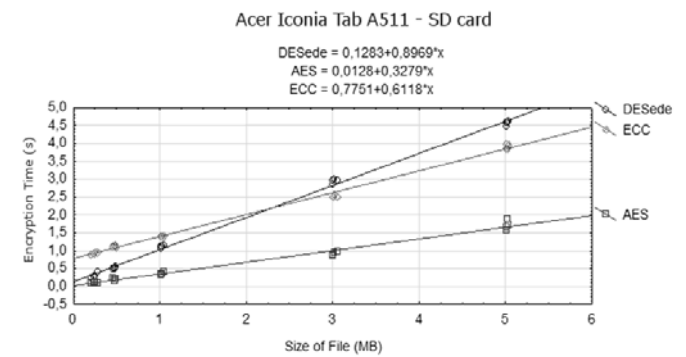


Fig. 4. The results of measurements on Acer Iconia Tab A511 device - SD card

D. Results of the encryption on LG P500 Optimus One device

The AES method has the lowest regression coefficient and has insignificant regression constant. Therefore, the AES can be considered as the fastest method on this device. The comparison of the two other methods is not so clear again. The ECC method has once again regression coefficient lower than the TripleDES. The ECC method takes a long preparation time - in this case the preparation time is 2.7 s.

Low computing power (CPU frequency, RAM frequency etc.) causes that the ECC method has a long preparation time. But effectiveness of ECC causes that the intersection of the regression lines is already at 0.8 megabytes. Therefore TripleDES is more suitable for files which have size up to 0.8 megabytes and ECC is more suitable for larger files.

The tests show that LG P500 Optimus One has much higher values of the regression coefficients compared to Acer Iconia Tab A511. Therefore the encryption speed of LG P500 Optimus One device is generally slower than the speed of Acer Iconia Tab A511.

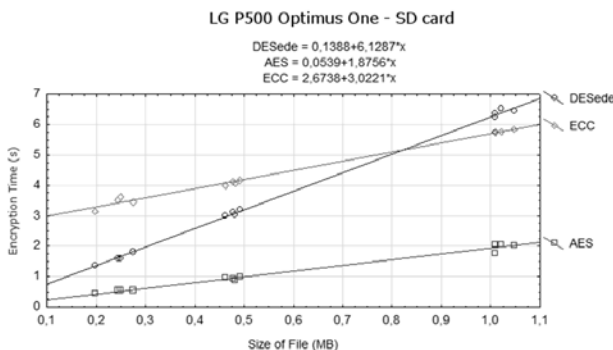


Fig. 5. The results of measurements on LG P500 Optimus One device - SD card

E. Results of the encryption on Samsung Galaxy S4 i9505 device

The test results which were made on Samsung i9505 Galaxy S4 were surprising. While AES and TripleDES methods significantly accelerated the encryption, the ECC method was decelerated. The ECC encryption on this device is slower in comparison with the Acer Iconia Tab A511. The values of regression coefficients 0.6 x (Acer Iconia Tab A511 - persistent internal memory) and 1.13 x (Samsung i9505 Galaxy S4) are not connected with the computing power of those devices. Because, according to benchmark performance [9], the device Samsung i9505 Galaxy S4 has more computing power than the Acer Iconia Tab A511.

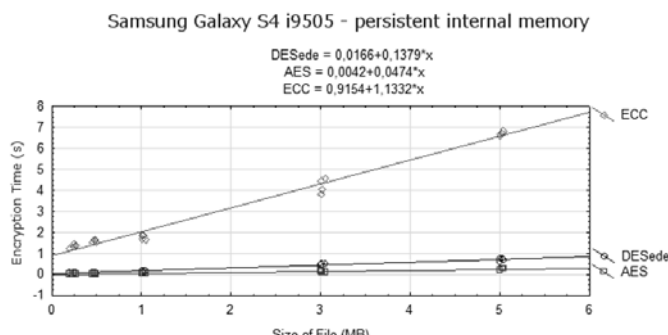


Fig. 6. The results of measurements on Samsung Galaxy S4 i9505 device - internal persistent memory

Hardware specs:

- Acer Iconia Tab A511 Chipset: NvidiaTegra 3, CPU Quad-core 1.3 GHz Cortex-A9, GPU ULP GeForce.
- Samsung Galaxy S4 i9505, Chipset, Qualcomm APQ8064T Snapdragon 600, CPU Quad-core 1.9 GHz Krait 300, GPU Adreno 320.

There may be a lot of reasons for the bad ECC method results, i.e. TouchWiz or a different hardware architecture. It will be necessary to create special tests for resolving this problem. These tests will be developed as part of the research at the Faculty of Applied Informatics [10].

V. CONCLUSION

The test results show that the AES method with a 256-bit key has the best encryption times for all files and on all devices. The AES method has good performance on Android mobile devices and at the same time AES is considered to be safe enough. For this reason, we recommend to application programmers to use the AES method for the encryption in their applications. The length of the key should never be less than 256 bits.

Occasional time anomalies occurred during the tests. They provide interesting information about the operating system and devices. Detailed information about the time anomalies we will publish.

REFERENCES

- [1] Hi-Q MP3 Voice Recorder. *Google Play* [online]. ©2014 [cit. 2014-01-20]. Available: https://play.google.com/store/apps/details?id=yuku.mp3_recorder.lite&hl=en
- [2] Simple Notepad. *Google Play* [online]. ©2014 [cit. 2014-01-20]. Available: <https://play.google.com/store/apps/details?id=org.mightyfrog.android.simplenotepad&hl=en>
- [3] Java™ Platform Standard Ed. 6. Class Cipher. *Docs.oracle.com* [online]. © 1993-2011 [cit. 2013-01-25]. Available: <http://docs.oracle.com/javase/6/docs/api/java/crypto/Cipher.html>
- [4] LG Optimus One P500. *GSMARENA* [online]. ©2000-2014 [cit. 2013-01-30]. Available: www.gsmarena.com/lg_optimus_one_p500-3516.php
- [5] Java™ Platform Standard Ed. 7. Class OutOfMemoryError. *Docs.oracle.com* [online]. © 1993- 2014 [cit. 2013-01-30]. Available: <http://docs.oracle.com/javase/7/docs/api/java/lang/OutOfMemoryError.html>
- [6] Managing Your App's Memory. *Android Developers* [online]. [cit. 2013-01-30]. Available: <http://developer.android.com/training/articles/memory.html>
- [7] Ouleha, M. *Šifrování dat na mobilních zařízeních Android*. Zlín: Univerzita Tomáše Bati ve Zlíně, Fakulta aplikované informatiky. Diplomová práce, 177 p. Available: <http://dspace.k.utb.cz/handle/10563/24705>.
- [8] Boyer, B. *Robust Java benchmarking, Part 1: Issues. Understand the pitfalls of benchmarking Java code*. 2008, 18p. Available: <http://www.ibm.com/developerworks/library/j-benchmark1/j-benchmark1-pdf.pdf>
- [9] Qualcomm Snapdragon S4 Pro (APQ8064) vs Nvidia Tegra 3 (T30). *CPUBoss* [online]. [cit. 2013-01-30]. Available: [http://cpuboss.com/cpus/Qualcomm-Snapdragon-S4-Pro-\(APQ8064\)-vs-Nvidia-Tegra-3-\(T30\)](http://cpuboss.com/cpus/Qualcomm-Snapdragon-S4-Pro-(APQ8064)-vs-Nvidia-Tegra-3-(T30))
- [10] Tomas Bata University in Zlín. The Faculty of Applied Informatics. Available: <http://www.utb.cz/fai-en>

Analysis Of The Triple Correlation: Commerce – Sustainable Development – Risk Management

Adrian IOANA

Engineering and Management of Metallic Materials'
Making Department
University Politehnica of Bucharest (UPB)
Bucharest, Romania
adyioana@gmail.com

Augustin SEMENESCU

Engineering and Management of Metallic Materials'
Making Department
University Politehnica of Bucharest (UPB)
Bucharest, Romania

Abstract— The paper presents the main types of the triple correlation: Commerce – Sustainable Development – Risk Management. This triple correlation highlights the Sustainable Development priority. In this correlation the commerce must to realize a balance between the Sustainable Development and the Risk Management. The concept of Sustainable Development would include a critical analysis of a quantitative measure of the Gross Domestic Product (GDP), and a different vision of the qualitative transformation. The goals of sustainable development goals include the harmonization of the economic, social and environmental targets.

Keywords—Commerce, Sustainable Development, Risk Management

I. INTRODUCTION

Sustainable Development involves achieving this need without compromising the ability of future generations to meet their own needs.

In the standard theory of economic development involves both quantitative change (increase in Gross Domestic Product) and qualitative change (the transformation from pre-capitalist economy based on agriculture to industrial capitalist economy) [1, 3].

Theory of sustainable development involves both a critique of quantitative measure of GDP and a different vision of qualitative transformation. The goals of sustainable development goals include the harmonization of the economic, social and environmental targets.

The concept of sustainable development was born 37 years ago, in response to the emergence of environmental and natural resource crisis, in particular those related to energy. Practical, Conference on the Environment in Stockholm in 1972 is when you recognize that human activities contribute to environmental deterioration, which put the future of the planet-threatening [7].

Sustainable development has become an objective of the European Union since 1997, when it was included in the Maastricht Treaty, and in 2001, the Summit at Goetheborg was adopted Strategy for Sustainable Development of the European

Union, which was added an external dimension to Barcelona in 2002.

Risk management in banking designates the entire set of risk management processes and models allowing banks to implement risk based policies and practices. They cover all techniques and management tools required for measuring, monitoring and controlling risks. The spectrum of models and processes extends to all risks: credit risk, market risk, interest rate risk, liquidity risk, operational risk and country risk.

II. THE COMMERCE, NONPERFORMING LOANS AND THE RISK MANAGEMENT ELEMENTS

The nonperforming loans (NPL) are those loans for which principal or interest is due and left unpaid for 90 days or more (this period may vary by jurisdiction). The NPL portfolio, along with the bank's collection ratio and the level of provisions record [1, 2, 4].

There are various reasons why the quality of bank loan portfolios deteriorates and research reveals that most reasons relate to the nature of the bank's credit culture. Below are listed the most usual drivers of loan portfolio deterioration:

- Self – dealing refers to an overextension of credits to directors and large shareholders, while compromising sound credit principles under the pressure from related parties.
- Compromise of credit principles refer to the granting with full knowledge of loans under unsatisfactory risk terms.
- Anxiety over income outweighs the soundness of lending decisions, underscored by the hope that the risk will materialize.
- Incomplete credit information concerns loans granted without proper appraisal or borrower creditworthiness.
- Complacency is typically manifested in a lack of adequate supervision of old, familiar borrowers, based on an optimistic interpretation of known credit weaknesses because of survival in distressed situations in the past.

- Technical incompetence and poor selection of risks include a lack of ability among credit officers to analyze financial statements and obtain and evaluate pertinent credit information.

Measures to counteract credit risks normally comprise clearly defined policies that express the bank's credit risk management philosophy and the parameters within which credit risk is to be controlled.

Among the policies targeted at limiting the credit risk can be mentioned: policies on concentration and large exposures, adequate diversification, lending to connected parties or over-exposures.

Bank regulators have paid close attention to risk concentration by banks, the objective being to prevent banks from relying excessively on a large borrower or group of borrowers. Modern prudential regulations usually stipulate that a bank should not make investments, grant large loans, or extend other credit facilities to any individual entity or related group of entities in excess of an amount that represents a prescribed percentage of the bank's capital and reserves.

According to international practice, a single client is an individual, a legal person or a connected group to which a bank is exposed. Single clients are mutually associated or control (directly or indirectly) other clients, usually through a voting right of at least 15-20 percent, a dominant shareholding or the capacity to exercise a controlling influence on policy making and management. These clients' cumulative exposure may represent a singular risk to a bank if financial interdependence exists and their expected source of repayment is the same.

The second set of credit risk policies consist of the asset classification method, which employs a periodic evaluation of the collectibility of the loan portfolio. The general rule is that all assets for which a bank is taking a risk should be classified, including loans and advances, accounts receivable, investments, equity participations and contingent liabilities.

Asset classification, by means of which assets are classified at the time of origination and then reviewed and reclassified as necessary (according to the degree of credit risk) a few times per year, is a key risk management tool. The periodical review considers loan service performance and the borrower's financial condition. Assets classified as "standard" or "specially mentioned" are typically reviewed twice per year, while critical assets are reviewed at least each quarter.

Banks determine classifications by themselves, but follow standards that are normally set by regulatory authorities. Standard rules for asset classification that are currently used are listed below:

- Standard (pass) are loans for which the debt service capacity is considered to be beyond any doubt. In general, fully secured loans by cash or cash substitutes (bank deposits, certificates, treasury bills etc) are usually classified in this category.
- Specially mentioned (watch) are assets with potential weaknesses that may, if not checked or corrected, to weaken the asset as a whole or

jeopardize the borrower's repayment capacity in the future. In this category are included, for example, credits given through inadequate loan agreements, lack of control over the collateral, lack of proper documentation. Loans to borrowers operating under economic or market conditions that may negatively affect the borrower in the future are also included in this category.

- Substandard regard well defined credit weaknesses that jeopardize debt service capacity, in particular when the primary sources for repayment are insufficient and the bank must look to secondary sources for repayment, such as collateral, the sale of a fixed asset or refinancing. In this category can be included term credits to borrowers whose cash flow may not be enough to meet currently maturing debts, as well as short term loans and advances to borrowers for which the inventory-to-cash cycle is insufficient to repay the debt at maturity.
- Doubtful are assets having the same weaknesses as substandard assets, but their collection in full is questionable on the basis of existing facts. The possibility of loss is present, but certain factors that may strengthen the asset exist as well.
- Loss regard assets that are considered uncollectible and of such little value that the continued definition as bankable assets is not warranted. The inclusion in this category does not mean that the asset has absolutely no recovery or salvage value, but rather that it is neither practical nor desirable to defer the process of writing it off, even though partial recovery may be possible in the future.

The third set of credit risk management policies are policies regarding loss provisioning, by means of which allowances are set up at an adequate level as to absorb anticipated loss.

Asset classification is the one providing a basis for determining an adequate level of provisions for possible loan losses. The aggregate level of provisions, together with general loss reserves, indicates the capacity of a bank to effectively accommodate credit risk.

In determining an adequate reserve, all significant factors that affect the collectibility of the loan portfolio should be considered. These factors include the quality of credit policies and procedures, prior loss experiences loan growth, quality of management in the lending area, loan collection and recovery practices, changes in national and local economic and business conditions, and general economic trends. Assessments of asset value should be performed systematically, consistently over time and in conformity with objective criteria.

Policies on loan-loss provisioning range from mandated to discretionary, depending on the banking system. In many countries, in particular those with fragile economies, regulators have established mandatory levels of provisions which are related to asset classification.

III. TRIPLE CORRELATION: COMMERCE - SUSTAINABLE DEVELOPMENT - RISK MANAGEMENT

Trade, Sustainable Development and Risk Management are (and should be) always correlated. Optimization of this triple correlation must be performed by any good manager [5, 6].

The main types of the correlations Commerce (C) - Sustainable Development (SD) - Risk Management (RM) are presented below (figure no. 1).

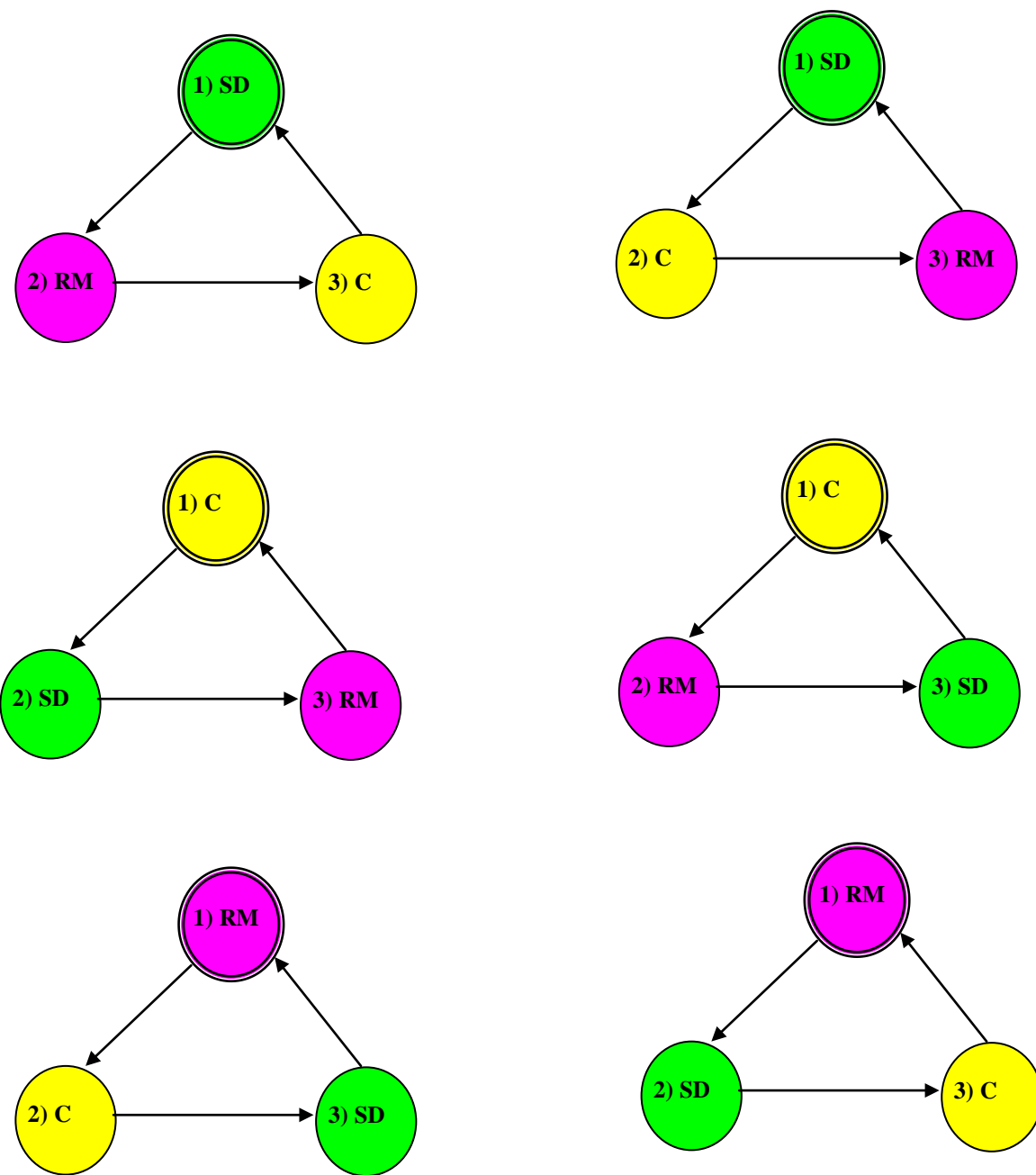


Figure no. 1. The types of the correlations Commerce - Sustainable Development - Risk Management

SD – Sustainable Development; C – Commerce; RM – Risk Management

Review of the correlations Commerce - Sustainable Development - Risk Management involves three successive levels:

- a) The level a), where the Sustainable Development (SD) occupies the priority position; it has two subcomponent, a1) and a2);
- b) The level b), where the Commerce (C) occupies the priority position; it has two subcomponent, b1) and b2);
- c) The level c), where the Risk Management (RM) occupies the priority position; it has two subcomponent too, c1) and c2);

Of the 3 levels of correlation (a, b, c) and 6 subcomponent (a1, a2, b1, b2, c1, c2) is notable correlation a1) which includes:

- Putting the concept of Sustainable Development (SD) on the priority position.
- Direct correlation between Commerce (C) and Sustainable Development (DD), for the purposes of developing of an “organic” commerce, to ensure that the concept of Sustainable Development.
- Putting Risk Management (RM) as a liaison between balance and Sustainable Development (SD) and Trade (C).

IV. CONCLUSION

The satisfaction of human needs and aspirations in the major objective of development. The essential needs of vast numbers of people in developing countries for food, clothing, shelter, jobs - are not being met, and beyond their basic needs these people have legitimate aspirations for an improved quality of life. A world in which poverty and inequity are endemic will always be prone to ecological and other crises. Sustainable development requires meeting the basic needs of all and extending to all the opportunity to satisfy their aspirations for a better life.

The level of the commerce is dependent by the specific credit resource. There are three sets of policies specific to credit risk management: policies aimed at limiting or reducing the credit risk, policies of asset classification and policies concerning loss provisioning.

In determining an adequate reserve, all significant factors that affect the collectibility of the loan portfolio should be considered. These factors include the quality of credit policies and procedures, prior loss experiences loan growth, quality of management in the lending area, loan collection and recovery practices, changes in national and local economic and business conditions, and general economic trends. Assessments of asset value should be performed systematically, consistently over time and in conformity with objective criteria.

The main types of the triple correlation Commerce – Sustainable Development – Risk Management reflect the priority of the Sustainable Development concept. In this context, the commerce must to realize a balance between the requirements of Sustainable Development and the Risk Management.

REFERENCES

- [1] M. Ammann, Credit Risk Valuation: methods, models and application, Springer Publishing House, Berlin, 2002.
- [2] A. Ioana, A. Semenescu, “Technological, Economic, and Environmental Optimization of Aluminum Recycling”, Journal of the Minerals, Metals & Materials Society, JOM: Volume 65, Issue 8 (2013), ISSN 1047-4838 (ISI-Web of Science/Science Citation Index Expanded), pp. 951-957, WOS: 000322136400007
- [3] A. Ioana, V. Mirea, C. Bălescu, “Analysis of Service Quality Management in the Materials Industry Using the BCG Matrix Method”, Anfiteatru Economic Review, Vol. XI, Nr. 26, June 2009, pp 270-276, [ISSN 1582-9146, ISI-Web of Science/Science Citation Index Expanded], Bucureşti, 2009, WOS: 000267351800004
- [4] A. Ioana, “Production Management in Metallic Materials Industry. Theory and Applications”, Ed. PRINTECH, Bucharest, 2007.
- [5] A. Ioana, “Metallurgy’s Impact on Public Health”, Review of Research and Social Intervention, Vol. 43/2013, ISSN: 1583-3410, (ISI-Web of Social Science/Social Science Citation Index Expanded), pg. 169-179, Iaşi, 2013.
- [6] A. Ioana, A. Nicolae, et al., “Optimal Managing of Electric Arc Furnaces”, Ed. Fairs Partners, Bucharest, 2002.
- [7] A. Ioana, “The Electric Arc Furnaces (EAF) Functional and Technological Performances with the Preheating of the Load and Powder Blowing Optimization for the High Quality Steel Processing”, PhD Thesis, University “Politehnica” of Bucharest, 1998.

Adaptive Risk-Based Assessment of Security Investments

M'hamed Chammem

Institut Supérieur des Etudes Technologiques en Communications de Tunis
ISET'Com
Tunisia

Mohamed Hamdi

Ecole Supérieure des Communications des Tunis
Sup'Com
University of Carthage
Tunisia

Abstract—The rapid proliferation of information systems and technology during the last decades has motivated important investments in online and distributed services. However, these services have been the target of various attacks that considerably affected the corresponding income. This has motivated the development and implementation of security solutions at a large scale. The importance of security is well-acknowledged by the key stakeholders in most organizations but the cost-efficiency of the hardware and software tools deployed to protect networked assets against network threats is still questionable.

This paper investigates the techniques that have been proposed in the literature to study the tradeoff between the cost associated with security investments and the benefit stemming from the reduction of the risk level. A particular interest is given to the approaches based on the Return on Security Investment (RoSI), which has been widely referred to as a valuable metric that leads to the selection of cost-efficient security controls. The limitations of the existing approaches are accurately discussed and analyzed. To cover these shortcomings, a new adaptive risk-based approach to estimate the RoSI is proposed. The major advantage of our approach is that it allows adapting the security investments to the dynamic context where modern security systems operate. Unlike the existing techniques, our approach considers an engine that collects information from the context and updates the investment plan accordingly.

Keywords—Security cost estimation, Return on Security Investment (RoSI), adaptive risk management.

I. INTRODUCTION

The dramatic increase of network attacks (in number and outcome) has motivated the deployment of advanced security mechanisms at different scales. The security systems available in the market allow not only the protection of private and public organizations but also the preservation of national sovereignty. In fact, the existing defense mechanisms allow protecting Communication and Information Systems (CISs) against various attacks whose objectives vary from industrial espionage to cyber terrorism. Recent security surveys show that antivirus firewalls, and Intrusions Prevention Systems (IPSs), to cite only a few, are nearly omnipresent in modern CISs. Nonetheless, statistics also reveal that the losses resulting from the occurrence of security incidents have also increased significantly during the last years. Figure 1, in which

the typical evolution of the amount of security investment and loss stemming from security incidents are depicted, illustrates the trade-off between the efficiency of the deployed security solutions and their cost. It can be noticed that rather than being based on accurate cost-benefit analyses, security solutions should be implemented while taking into account their economic convenience in order to reach the optimum where the security investment is proportional to the value of the protected assets.

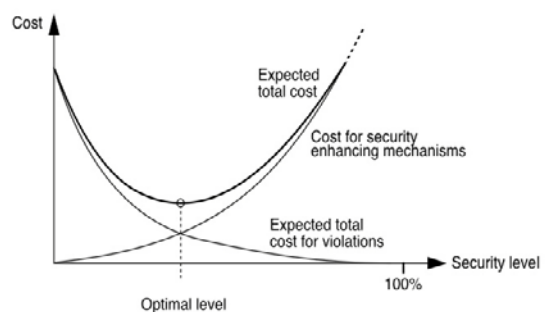


Fig. 1. Cost and performance of security countermeasures.

A plethora of techniques have been proposed in the literature to deal with the adequacy of the amount of investment made in security controls and the quantitative benefit provided by these controls. Most of these techniques are based on the estimation of the Return on Security Investment (RoSI), which slightly differs from the traditional concept of Return on Security Investment (RoI), in the sense that it measures the gap between the impacts of incident occurrences without the implementation of security solutions and with implemented security solutions, respectively. Indeed, the gain resulting from the deployment of security solutions is, in general, not direct since it comes from the reduction of the potential loss associated with the existence of security threats. In spite of the advantages of the RoSI-based security decision-making strategies, multiple drawbacks make them inefficient in a dynamic context where the factors leading to the selection of the security controls rapidly change. This paper analyzes these shortcomings and proposes a new framework to make the Security Investment Plan (SIP) flask enough to adapt to the dynamicity of the information system under protection. In

fact, the SIP is often affected by several changes that might occur during its deployment. These changes are related to the evolution of the technology, the legal framework, the standards, the environment, and the deployment team, to cite just a few. Our framework takes such changes into consideration so as to provide more accurate indicators to the stakeholders in order to assist them in the elaboration of the SIP.

The key contributions of the paper are listed in the following:

1. We discuss the efficiency of the existing security investment models and their applicability in new service architectures including cloud computing and the Internet of Things.
2. We underline the need to develop adaptive approaches to estimate and assess security investments. This allows adapting to the rapid changes occurring in the environments where security solutions are being deployed.
3. We propose a new architecture to evaluate the RoSI and highlight the key challenges that should be tackled to improve the cost-effectiveness of security policies.

The rest of the paper is organized as follows. Section II reviews the existing approaches that addressed the cost-efficiency of security policies. In section III, we describe the Annual Loss Expectancy (ALE) model, which is widely used to estimate the risks characterizing CISs. The shortcomings of the existing techniques are highlighted in Section IV. A new adaptive approach to optimize the SIP is presented in Section V. Finally, Section VI concludes the paper.

II. RELATED WORK

This section reviews the approaches that have been proposed in the literature to evaluate the cost-effectiveness of security projects. A particular emphasis is done on the study of quantitative risk analysis as a tool to achieve this objective.

In [1], Boehme and Felegyhazi review and compare existing security investment models and discuss the relation between security management and security metrics. The high-level security production function is decomposed into two steps: cost of security is mapped to a security level, which is then mapped to benefits. This allows to structure data sources and metrics, to rethink the notion of security productivity, and to distinguish sources of indeterminacy as measurement error and attacker behavior. It is further argued that recently proposed investment models, which try to capture more features specific to information security, should be used for all strategic SIPs beneath defining the overall security budget.

Sonnenreich et al. [12] explore a number of techniques that can be used to measure security within an organization. They propose a benchmarking methodology and underline the importance of the corresponding results to both decision makers and technology practitioners. The tasks of the methodology constitute a combination of practical experience and high-level design to determine a meaningful return on

security investment for security expenditures. The authors develop a model for estimating this return on investment and show how the underlying factors can be computed.

The importance of a business approach of security was underlined in [16]. Such approach should demonstrate how the security investments can enable measurable business value and determine which security investments will create value. One of the most significant obstacles to the deployment of such approaches is that most organizations conduct risk management process periodically (often annually or bi-annually) rather than continuously. This considerably affects the efficiency of the security solutions that are being deployed in spite of the increase of the related investment cost. The paper also reviews a set of potential techniques that can be used to cope with these issues such as optimization models, risk analysis, and RoSI. However, the potential links between these techniques have not been explored.

In [17], Pontes et al. investigate several Risk Management (RM) standards and good practices and propose an extension so as to integrate the estimation of the return on investment as a final phase in the RM process. The authors suggest experimental techniques to compute the ROSI based on metrics extracted from the IT environment. The use of forecasting techniques also allows knowing the behavior and the volume of the security attacks, thus helping to verify if the SIP done for the ROSI will be confirmed before or after the defined deadline. Finally, the paper recommends the preparation of a formal proposal for the implementation of RaSI taking into account the life cycle of CISs.

Bojanc et al. [5] present a mathematical model for an optimal security-technology investment evaluation and decision-making processes based on a quantitative analysis of the security risks and a digital-assets assessment in an organization. The model is based on a quantitative analysis of different security measures that counteract individual risks by identifying the information-system processes in an enterprise and the potential threats. The basic parameters of the model include the target security levels for all the identified core business processes and the probability of the security incidents together with the possible losses resulting from the occurrence of these incidents. In addition, the model allows in-depth analyses and computations providing quantitative assessments of different investments options. The output of the model is a set of recommendations that facilitate the selection of the best security solutions and the associated strategic planning.

It comes from this brief literature review that most of the approaches that have been proposed to analyze security investments are tightly related to risk management. In fact, IT security investments have always been based on three parameters:

1. The value of the potential assets
2. The impact of the potential security threats
3. The cost of the security solutions

Generally, the assessment and evaluation of IT security risks involve some degree of quantification of these risks. This

provides a more accurate view to the security analyst about the importance of the risks in order to prioritize the tasks of the SIP in a manner that fits with the available budget. In the following section, we provide a detailed analysis of how risk assessment is related to the evaluation of security investments. To this end, we review the methodologies that are being used to compute the risk parameters and explore their usage in the calculation of various security indexes.

III. QUANTIFYING THREAT RISK EXPOSURE AND MITIGATION

Most of the approaches that addressed risk analysis in CISs refer to the Annual Loss Expectancy (ALE). It results from a simple analytical model of computing the risk by multiplying the impact of a security incident (Single Loss Expectancy) by its estimated Annual Rate of Occurrence (ARO). The SLE typically depend on the nature of the threat and the value of the protect asset whereas the ARO varies according to the existing security mechanisms. Therefore, given a threat T and an asset A , and supposing that a set of security mechanisms denoted by S is deployed to protect A , the risk exposure of A to T is denoted by $\text{ALE}_{T,A,S}$ and computed as follows.

$$\text{ALE}_{T,A,S} = \text{SLE}_{T,A} \times \text{ARO}_{T,S}. \quad (1)$$

In addition, $\text{SLE}_{T,A}$ is derived using the percentage of loss that the realization of T could have on an asset (EF_T – Exposure Factor of the threat T) by the value of the asset A , denoted by V_A .

$$\text{SLE}_{T,A,S} = \text{EF}_T \times V_A. \quad (2)$$

In order to use this notion of risk exposure to assess SIPs, multiple indexes and metrics have been proposed. In addition to RoI and RoSI, the most popular indexes are the Return on Attack (RoA) and the Return on Response Investment (RoRI). In the following, we review these indexes and highlight the differences between them. We also review the definitions of two traditional metrics: the Net Present Value (NPV) and the Internal Rate of Return (IRR).

The simplest and mostly used approach to assess the cost-efficiency of business investments in general is the RoI, where the benefits and the cost resulting from a specific investment are used [3,6,15]. In other terms, the RoI of a security control S is defined as follows:

$$\text{RoI}_{T,A,S} = (B_S - C_S)/C_S, \quad (3)$$

where B_S and C_S are the benefit and the cost of the countermeasure S , respectively.

The NPV is a financial metric allowing the comparison of costs and benefits over a period of time. It is generally used to analyze long-term investments. The main idea behind the NPV is to discount all expected costs and benefits from an investment to its present value, therefore the time value of money is taken into consideration. The NPV concept is then used to compare the discounted income generated in the future with its initial investment. When a period of n years is considered, the NPV is computed as follows.

$$\text{NPV}_{T,A,S} = (B_{S,0} - C_{S,0}) + (B_{S,1} - C_{S,1})(1+r)^{-1} + \dots + (B_{S,n-1} - C_{S,n-1})(1+r)^{n-1}, \quad (4)$$

where $B_{S,i}$ and $C_{S,i}$ denote the benefit and the cost of countermeasure S at year i , respectively. In addition, r represents the internal rate of discount.

From Equations 3 and 4, one can easily remark that the major advantage of NPV with respect to RoSI is that supports the study of long-term investments.

Another metric that is often used in financial analysis is the $\text{IRR}_{T,A,S}$, which is equal for the value of r for which the following condition holds.

$$\text{NPV}_{T,A,S} = 0. \quad (5)$$

In other terms, the IRR is the rate at which the total present value of the anticipated income is the same as the initially required investment. Although the IRR has the advantage of being less responsive to the time value of many than the NPV, it relies on the questionable assumption that the rate of return is constant during the period of the analysis.

Security surveys have often referred to the Return on Security Investment (RoSI) to assess the cost-efficiency of security solutions. This concept was defined in the seminal work of Sonnenreich [4] to compare the difference between the damages resulting from security incidents (with and without security solutions) to the costs of these solutions. Supposing that one wants to decide whether to implement or not a countermeasure S given that a set S of countermeasures is already implemented, the RoSI is computed as follows:

$$\text{RoSI}_{T,A,S,S} = (\text{ALE}_{T,A,S} - \text{ALE}_{T,A,S \cup \{S\}} - C_S)/C_S. \quad (6)$$

Other security-oriented techniques have been introduced to cover these shortcomings. In [18], the Return on Attack has been defined as the gain expected by the attacker from a harmful action over the cost that he sustains due to the implementation of security solutions on the victim system. The formal definition of the RoA is given below.

$$\text{RoA}_{T,A,S,S} = G_T/C_{T,S \cup \{S\}}, \quad (7)$$

where G_T is the expected gain from the realization of T and $C_{T,S}$ is the cost of realizing T when the set of countermeasures S is implemented. Unlike the RoI index, RoA captures the various impacts of the security solutions on the attack process.

More recently, the Return on Response Investments (RoRI) has been introduced in [1] to conduct a financial comparison between potential security solutions.

$$\text{RoRI}_{T,A,S,S} = 100 \cdot (\text{ALE}_{T,A,S \cup \{S\}} \cdot E_{S,T} - C_S)/(V_A + C_S), \quad (8)$$

where $E_{S,T}$ is the efficiency of countermeasure S in mitigating the threat T .

The RoRI is useful in practice to rank a set of countermeasures based on their ability to thwart the identified threats and on their costs. One major disadvantage of the model is that does not take into consideration the depreciation of the initial investment. Moreover, the parameter $E_{S,T}$ is difficult to estimate.

Tables 1 and 2 provide a summary of the indexes and metrics reviewed in this section and underline their major features.

Table 1: Traditional models for evaluating financial investments.

| | Method | Definition | Main parameters | Optimality | Limitations |
|------------|-------------------------|--|---|-----------------------------|--|
| ROI | Return On Investment | Security Solution Cost, Effectiveness | - Net benefits over a certain time period - Initial costs of investment | Highest ROI value | Useless for long-term Investments ; Time value of money is not considered ; Operational costs are not considered; False positives and false negatives are not considered |
| NPV | Net Present Value | NPV is a capital budgeting tool used in corporate finance and is designed to help firms assess the financial feasibility of various capital expenditures | - Benefits at the period t - Costs at the period t - Internal rate of discount - Number of years T | NPV > 0 | Useful if combined with other metrics ; Operational costs are not considered ; False positives and false negatives are not considered |
| IRR | Internal Rate of Return | IRR is frequently used by corporations to compare and decide between capital projects. | - Net annual cash inflow - Investment required | IRR > Project discount rate | Same rate of return for the whole investment period; Operational costs are not considered; False positives and false negatives are not considered |

Table 2: Security-focused models for evaluating financial investments.

| | Method | Definition | Parameter's | Optimality | Limitations |
|-------------|-------------------------------|--|---|--------------------|---|
| ROSI | Return On Security Investment | ROSI is a relative metric that compares the differences between the damages originated by attacks against the cost of the countermeasure. | - Risk Exposure - Risk Mitigated - Solution Cost | Highest ROSI index | Useless for long-term investments ; Time value of money is not considered; Operational costs are not considered; False positives and false negatives are not considered |
| RORI | Return On Response Investment | RORI is used as a quantitative approach to evaluate and rank a set of countermeasures, which allows selecting the one that best mitigates the effects of a given attack. | - ALE: Annual Loss Expectancy - RM: Risk Mitigation level - ARC: Annual Response Cost - AIV: Annual Infrastructure Value | Highest RORI index | Useless for long-term investments; Time value of money is not considered. |
| ROA | Return On Attack | Measure convenience of an attack by considering the impact of a security solution on the attacker's behavior. | - Gain from successful attack - Cost before Security Measure - Loss caused by Security Measure | Lowest ROA value | Not accurate while predicting attacker's behavior ; Useless for long-term investments; Operational costs are not considered; False positives and false negatives are not considered |

IV. LIMITATIONS OF THE EXISTING APPROACHES

Multiple comparative studies have been published to highlight the advantages, limitations, and differences between the indexes referred to in the previous section. For instance,

Boehme [7] highlighted that the evaluation of security investment is impeded by many factors, notably the difficulties of estimating the risk parameters. He noticed that the probability of a threat is difficult to estimate because the behavior of the malicious user is often not controlled by known probability distributions. In addition, when the events corresponding to a threat are rare, it is not statistically possible to compute a good estimate of the probability of occurrence of this threat.

Nonetheless, none of these studies did consider the way these indexes are used within a security risk management approach. In order to understand how the assessment of security investment can be integrated in a risk management process, we consider the ISO31000 standard for Risk Management depicted in Figure 2. For the sake of parsimony; the steps of the approach are not discussed in this paper. Our interest is focused on how security investment indexes can be used in this process. At first glance, it appears that the cost-efficiency of security solutions is considered in **RE** (Risk Evaluation). In fact, once the security risks are estimated in **RA** (Risk Analysis), the objective is to select the appropriate treatment for each of these risks in **RT** (Risk Treatment). Therefore, Step **RE** selects the most cost-effective security solutions based on one of the security indexes mentioned above.

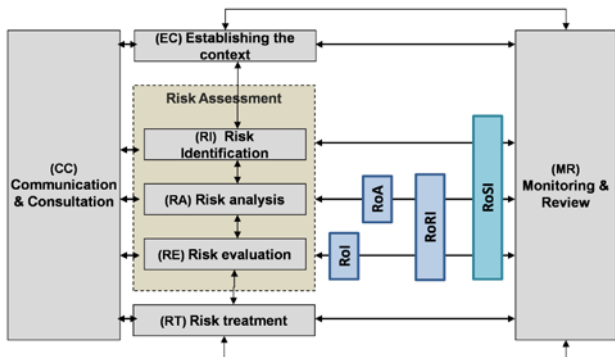


Fig. 2. ISO 31000.

The first criterion we use to compare the potential brought by each of these indexes is their ability to capture the links existing between the steps of the ISO31000 process. As depicted in Figure 2, we notice that the RoI is limited to step **RE** because it only considers the benefit and the cost of security solutions, which are intrinsic parameters. In addition, since RoA captures information of the impact of security solutions on the security risks, input from Step **RA** is also used to this purpose. Finally, computing the RoSI encompasses the estimation of the damages resulting from the occurrence of the threats, which requires information on the value of the victim assets (Step **RI**). Consequently, we conclude that the **RoSI** index better adapts to the structure of the risk management process.

We also compare the security indexes based on the way they interface with the risk management process, and more specifically to the **RT** step, which consists in selecting the

appropriate risk reduction strategy knowing the threats that are applicable to the context of the analysis. Basically, four strategies can be thought of to mitigate security risks:

1. Acceptance: This is the choice to do nothing against a risk of having threat exploiting a specific vulnerability and considers the damaging consequence as a cost of doing business. Risk acceptance can be a reasonable strategy where the cost of mitigation or transference the risk is greater than the total losses resulting from the existence of the threat.
 2. Transference: This strategy consists in transferring the risk to other assets, therefore reducing the impact (SLE). The cost of transference is often hard to estimate because it encompasses revising the deployment models and re-engineering the protection infrastructure.
 3. Avoidance: This alternative consists in thwarting the risk through the reduction of its source or consequences. For instance, the deactivation of some vulnerable services can be fit to this reasoning. This strategy is preferably applied when the risk impact is higher than the benefit from that asset.
 4. Mitigation: This strategy consists in implementing security controls including access control, authorization, intrusion detection, and logging policies. Generally, it has the highest cost compared to the other alternatives.

We notice that ROI and RoA do not take into consideration risk acceptance because they only focus on the parameters of the security solutions and the security attacks, respectively. Therefore, these indexes hide to the security analyst the residual risk corresponding to the threats that have been purposely left uncovered by the security solutions due to budget limitations. This serious shortcut has also been overlooked in the existing analyses.

Another important disadvantage of the existing RoSI-based approaches is that they do not adapt to the variations of the environment of the protected system. The RoSI calculation is based on the ALE, which is an annual index. In other terms, the underlying parameters (mainly the probability and the impact of the threats of interest) are approximated under the assumption that they will not vary before the following year. Obviously, this considerably affects the accuracy of the RoSI. Therefore, we recommend the use of a variable index that can adapt to the changes that occur in the context where the security solutions are deployed. In fact, many of the hardware/software security solutions available on the market integrate self-configuration abilities that are often under-exploited. In the following section we provide more details on how such adaptive security indexes can be computed.

V. TOWARDS AN ADAPTIVE FRAMEWORK FOR THE EVALUATION OF SECURITY INVESTMENTS

The limitations highlighted in the foregoing section can be covered through the development of adaptive analysis of security investments, which enables the introduction of

dynamic changes on varying inputs. This involves gathering contextual information both from the building blocks of the framework and from the environment, measuring the security metrics, pre-processing the collected data, and adapting the analysis to the changes occurring in the environment. In our context, this adaptation is made by:

1. Modifying the structure of the analysis framework.
2. Adjusting the internal parameters of the analysis.

In this section, we introduce a new approach for improving security management based on a thorough analysis of the risks affecting the IT infrastructure and an optimization of the expenditures spent to protect against these risks. We focus on the capability to adapt and learn the risk factors affecting the key processes of the CIS, which enables security managers to dynamically reallocate resources to ensure a better outcome given the updated risk profile.

We propose an adaptive framework for the analysis of security investments. Our approach has the interesting property to acquire data from multiple contextual sources and to process these data so as to generate accurate estimates of the probability and outcome of the potential threats. Our model includes four main phases:

1. Data collection: Multiple sources are investigated to capture information about the security state in which the system of interest operates. These sources include international enterprise surveys (e.g., CSI/FBI, CLUSIF, McAfee, Symantec ...), internal and external questionnaires (e.g., ISO 2700x, COBIT), and real-time monitoring systems (e.g., SIEM).
2. Data pre-processing: The raw data captured in the previous phase is subjected to parsing and fusion in

order to identify the relevant components and to minimize the redundancy between the various sources. Two data repositories are devised to this purpose: one to store raw data and the other to store pre-processed data.

3. Adaptive risk-based analysis of security investments: Given the threats identified in the collection phase and refined in the pre-processing phase, a set of processes are executed to estimate the probability and the impact of these threats. An adaptive engine is developed to adapt these values to the dynamic context in which the security infrastructure operates. This provides a continuously updated view on the cost-efficiency of the security system.
4. Updating the environment: Once the security indexes are estimated, adaptive decision making is needed to update the interaction between the security system and its environment based on the results of the previous step. The system has to: (a) dynamically determine whether changes and adaptation should be made, (b) to select the optimal adaptive security model for a given situation, and (c) to apply the identified changes by guaranteeing the highest likelihood of achieving the greatest benefit at the lowest cost (provided that the residual risk is minimized). This building block requires flexible learning and decision making processes for structural and parametric adaptive that help in providing the best estimates for the security indexes, and mainly the RoSI.

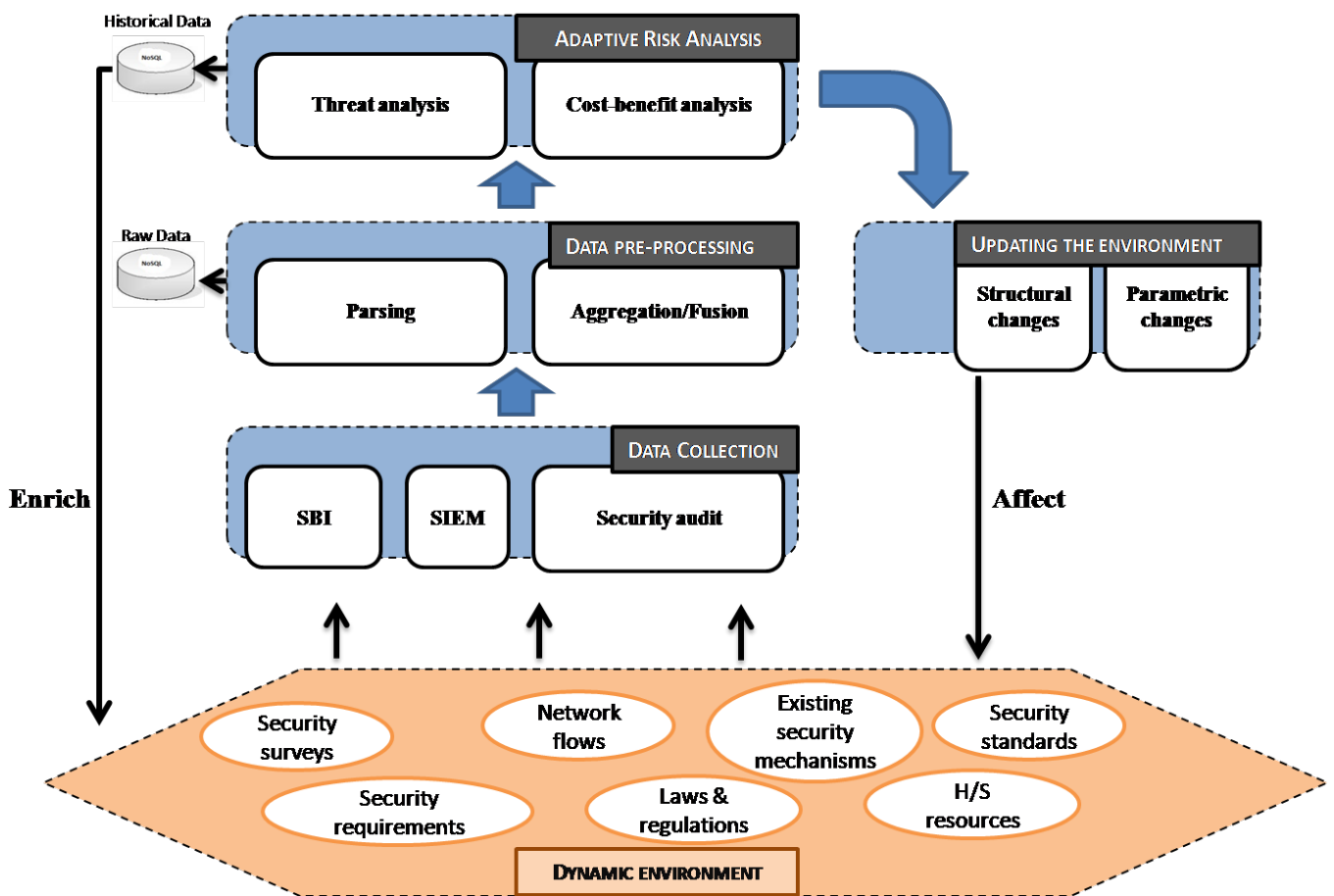


Fig. 3. Adaptive risk-based analysis of security investments.

The cornerstone of the framework illustrated in Figure 2 is the adaptive risk-based analysis of security investments. Our model distinguishes itself from the existing models in that it reacts and changes the security system based on varying inputs. The adaptation mechanisms introduced at this level must consider two sets of requirements:

- Security requirements: Novel adaptive security and privacy mechanisms and methods are required that adapt to the dynamic context where the CIS operates and changing threats to them. Thus, the scenarios should be generic enough to capture the security needs for the data processed and exchanged within the components of the CIS. This is particularly challenging because this system encompasses multiple networking technologies, data, users, and applications, addressing varying processing capabilities and resource use.
 - Quality of service requirements: Unlike traditional applications and services relying on communication networks, modern applications accessible through wireless networks have stringent QoS requirements. Items such as the communication delay, the quality of the communication channels, and the lifetime of the self-powered mobile terminals are crucial context parameters that have significant impact on the safety of the patient. The scenarios should highlight the needs in

terms of QoS and illustrate the dynamic interplay between these needs and the security requirements.

The importance of the learning mechanisms must also be underlined at this level. For instance, Intel [12] developed a model to measure the RoSI in its manufacturing environments with a better level of accuracy compared to other studies. The model allows decision making activities on safety programs, resulting in huge savings. By analyzing historical incident cyber-attack trends data in similar environments and extrapolating, it is possible to predict the intermediate trends security incident occurrence for the financial impact of the adoption of the technology programs security. The methodology is scalable, manageable, and can be automated, is a valuable tool for calculating the ROSI, decisions, justifying IT security spending, resource allocation, and implement a level of optimal security.

VI. CONCLUSION AND FURTHER WORK

In this paper, we addressed the assessment of security investment from a risk analysis perspective. We studied the indexes that have been previously proposed to tackle this challenge and found out that RoSI is the most appropriate. Then, we identified the shortcomings that affect the efficiency of RoSI-based evaluation of the efficiency of security solutions. Many of these shortcomings constitute a serious obstacle that prevent the use of RoSI in contexts where the

protected CIS integrates new technologies such as cloud computing or IoT. To overcome this limitation, we proposed a new adaptive framework that enhances the accuracy of RoSI estimation and therefore provides a better view on the landscape where the CIS is deployed.

Currently, we are working on the design of a game-based framework that will implement the adaptive framework proposed in this paper. This strategy will model the dynamic interaction between the security system and its environment so as to allow real-time update of the RoSI index.

REFERENCES

- [1] G.G. Granadillo, M. Belhaouane, H. Debar, and G. Jacob, "RORI-based countermeasure selection using the OrBAC formalism," International Journal of Information Security, pp. 1-17, 2013.
- [2] R. Böhme and T. Moore, "Security Metrics and Security Investment," September 9, 2013. Available: <http://lyle.smu.edu/~tylern/courses/econsec/reading/lnse-secinv2.pdf>
- [3] M. Al-Humaigani, and D. Dunn, "A model of return on investment for information systems security," *argument*, Vol. 4, p.9, 2003.
- [4] W. Sonnenreich, J. Albanese, and B. Stout, "Return On Security Investment (ROSI)--A Practical Quantitative Model," Journal of Research & Practice in Information Technology, 38(1), 2006.
- [5] E. Pontes, A.E. Guelfi, A.A. Silva and S.T. Kofuji, "A Comprehensive RiskManagement Framework for Approaching the Return on Security Investment (ROSI)," In: Dr. Matteo Savino, Dept. of Engineering, University of Sannio, Benevento, Italy. (Org.). Risk Management. 1ed.Rijeka: Intech, 2011, v. 2, p. 20-46.
- [6] R. Böhme, "Security metrics and security investment models," In *Proceedings of the 5th international conference on Advances in information and computer security (IWSEC'10)*, Isao Echizen, Noboru Kunihiro, and Ryochi Sasaki (Eds.). Springer-Verlag, Berlin, Heidelberg, 10-24, 2010.
- [7] R. Böhme, and M. Félegyházi, M., "Optimal information security investment with penetration testing," In *Decision and Game Theory for Security* (pp. 21-37). Springer Berlin Heidelberg, 2010
- [8] T. Tsakris, "Information security expenditures: a techno-economic analysis," International Journal of Computer Science and Network Security (IJCSNS), 10(4), 7-11, 2010
- [9] W. Sonnenreich, J. Albanese, and B. Stout. "Return On Security Investment (ROSI): A practical quantitative model," In Proc. 3rd Int. Workshop on Security in Information Systems, WOSIS 2005, In conjunction with ICEIS2005, pages 239– 252. INSTICC Press, 2005.
- [10] S. Poslad, M. Hamdi, and H. Abie, "Adaptive security and privacy management for the internet of things," (ASPI 2013). In Proceedings of the 2013 ACM conference on Pervasive and ubiquitous computing adjunct publication (UbiComp '13 Adjunct). ACM, New York, NY, USA, 373-378, 2013.
- [11] W. Leister, M. Hamdi, H. Abie, and S. Poslad, "An evaluation scenario for Adaptive Security in eHealth," In PESARO 2014, February 23 - 27, 2014.
- [12] M. Rosenquist, "Measuring the Return on IT Security Investments," White Paper Intel Information Technology, December 2007, <https://communities.intel.com/docs/DOC-1279>
- [13] V. Kanhere, "Driving Value From Information Security: A Governance Perspective," ISACA Journal Vol. 2, 2009.
- [14] S.H. Kim, M. W. Park, J.H. Eom and T.M. Chung, "An Approach for Security Management Cost Optimization through Security Value Lifecycle," In Proceedings of the 7th International Conference on Information Security and Assurance, Cebu, Philippines (pp. 26-28), 2013.
- [15] H. Cavusoglu, B. Mishra, and S. Raghunathan, "A model for evaluating IT security investments," Commun. ACM 47 (7), pp. 87-92, July 2004
- [16] S.M. Huang, C.L. Lee and A.C. Kao, "Balancing performance measures for information security management: A balancedscorecard framework," Industrial Management & Data Systems, Vol. 106 Iss: 2, pp.242 – 255, 2006.
- [17] T. K. Tsakris and G. D. Pekos, "Analysing and determining Return on Investment for Information Security," In International Conference on Applied Economics–ICOAE, pp. 879-883, 2008.
- [18] M. Cremonini, and P. Martini, "Evaluating Information Security Investments from Attackers Perspective: the Return-On-Attack (ROA)," in WEIS, June 2005.
- [19] G.G. Granadillo, "Optimization of cost-based threat response for Security Information and Event Management (SIEM) systems," Doctoral dissertation, Institut National des Télécommunications, France, 2013.
- [20] W. De Bruijn, M.R. Spruit, and M. Van Den Heuvel, "Identifying the Cost of Security," Journal of Information Assurance and Security, Vol.5(1), 2010.

Knowledge Modelling of Electric Arc Furnace (EAF)

Adrian IOANA

Engineering and Management of Metallic Materials' Making" Department
University Politehnica of Bucharest (UPB)
Bucharest, Romania
adyioana@gmail.com

Augustin SEMENESCU

Engineering and Management of Metallic Materials' Making" Department
University Politehnica of Bucharest (UPB)
Bucharest, Romania

Abstract— The paper presents the main principles for the optimization of the functional and technological performances by mathematical modelling of the Electric Arc Furnace's Processes (EAFP). These principles are based on the classification of the functional and constructive options for the electric arc furnace's charge preheating plants. The classification's most important criterion is the proceeding's technical-economical efficiency. The main scope of the paper is to validate an original mathematical model for the electric arc furnace (EAF) functioning optimization.

Keywords—modelling; EAF; management

I. INTRODUCTION

The original optimization mathematical model [1, 7] of the electric arc furnace's charge preheating process mainly takes into consideration two thermo-technological aspects:

- The heat transfer between fluids and particles and
- The heat transfer between the fizz layer and an exchange surface.

According to the energetic balance at the gaseous environment level, the conductive transfer model is also analyzed through the finished elements method.

Mathematical modelling of the electric arc furnace's processes (EAFP) for the optimization of the functional and technological performances of this complex unit is based on the next principles [2, 3]:

A. The principle of analogy – consists of observing and competently analyzing the modeled reality, using both analogy with other fields of research and logical homology. According to this principle, for mathematical models making the following steps were used:

- The modeled subject definition – represents the first phase of the modelling analysis. This step must satisfy both the purpose and the simultaneous system's aims, assuring their compatibility;
- The efficiency criteria's definition – is a step imposed on the correct definition of the system's aims and allows the optimization of the modelling solutions;

- Providing the options – based on accessing some realistic, original and efficient solutions;
- Choices evaluating – depending on the established efficiency criteria;
- Choosing the final solution – based on the analysis between the different solutions of the modelling.

B. The principle of concepts is based on the systems' theory, including the feedback concept.

C. The principle of hierarchisation consists of making a hierarchical models system, for structuring the decision and coordinating the interactive subsystems.

II. THE CONCEPT OF THE BLOCK DIAGRAM FOR THE MODELLING SYSTEM

The modelling system's central element of the EAF processes conceived consists of the system's criteria function. Knowing that the technological processes study for EAF is subordinated to high quality steel obtaining [4], the modelling system's criteria function (CF) is the ratio between quality and price:

$$CF = \left(\frac{QUALITY}{PRICE} \right)_{max} \quad (1)$$

The maximum of the criteria function is assured by the mathematical model of prescribing the criteria function (M.P.C.F.)

The mathematical model of prescribing the criteria function concept consists of transforming the criteria function (CF) in a quality-economical matrix MQE, as in the scheme presented in figure 1.

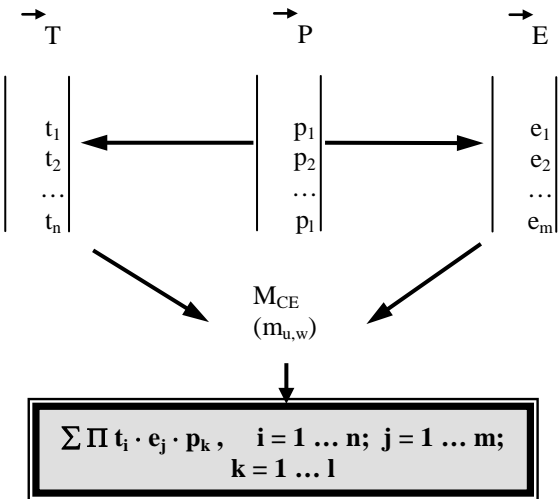


Figure 1. The modelling system's criteria function's evaluation

The levels of prescribing the criteria function could be obtained by using a composition algorithm for three vectors [5, 6]:

- vector – technical parameters' vector (t_i);
- vector – economic parameters' vector (e_j);
- vector – weight vector (p_k).

In figure 2 there is presented the general logical scheme used for the EAF's charge preheating.

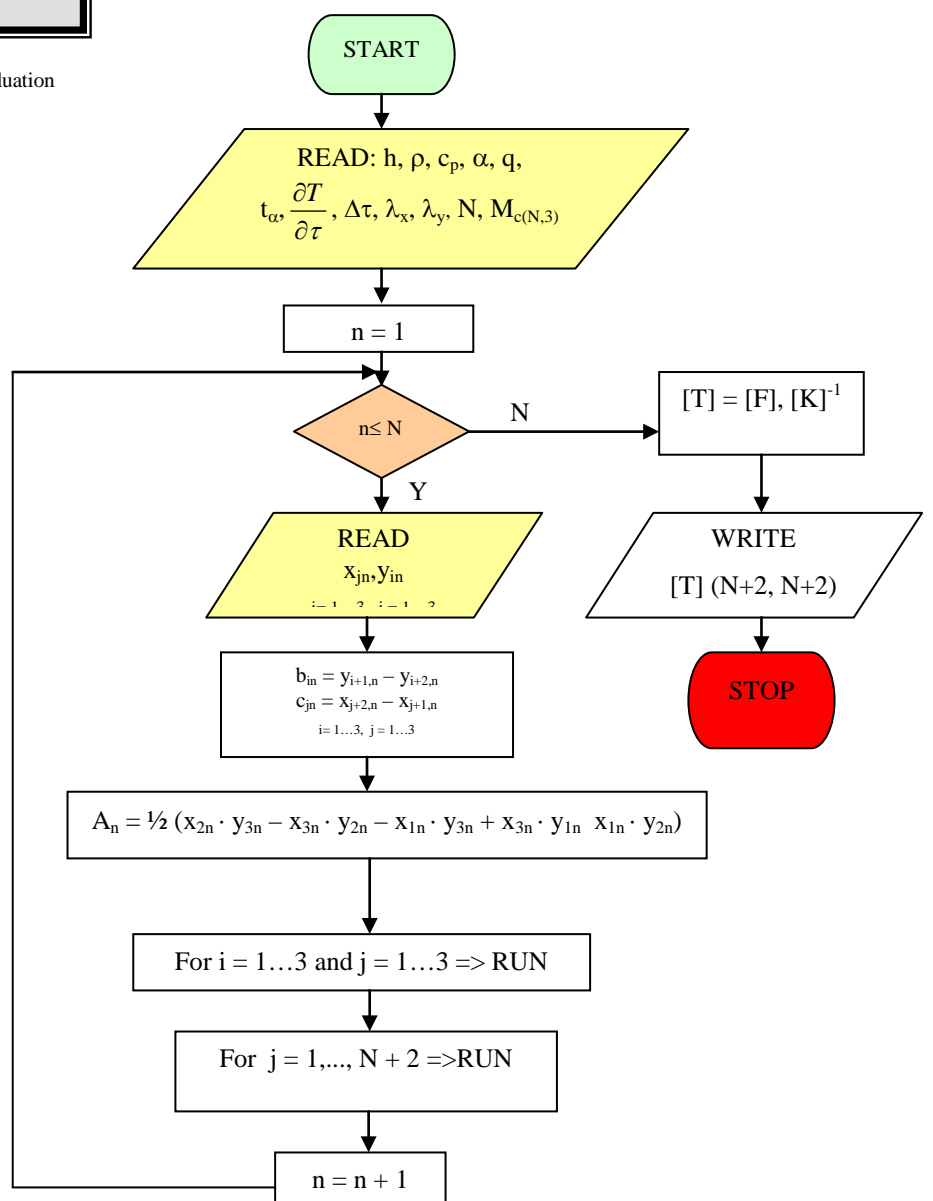


Figure 2. The general logical scheme

III. RESULTS AND CONCLUSION

The correlation between the criteria function's (C.F.) prescribed levels and the vector's components' variation is presented in figure 3.

In figure 4 there is presented the scheme of the grid used for the EAF's charge preheating modelling.

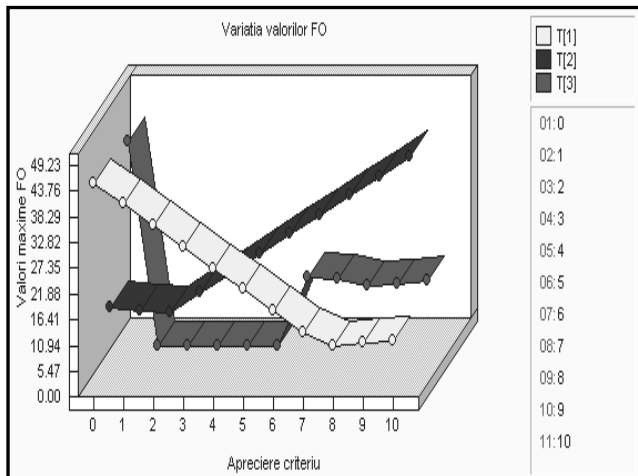


Figure 3. The correlation between the criteria function's (CF) prescribed levels and the vector's components' variation (1, 2, 3)

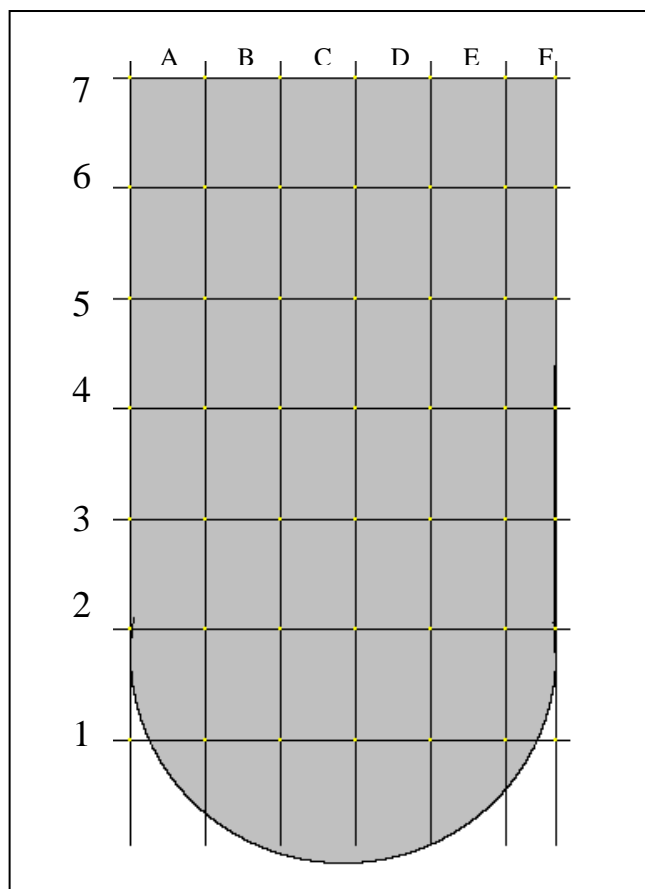


Figure 4. The grid scheme

The executions of the EAF's Charge Preheating Modelling (CPM) were made both for a 10t EAF (figure 5 a, b, c) and for a 50t EAF (figure 5d). It was considered to be a load with medium permeability $\varepsilon = 0.45$.

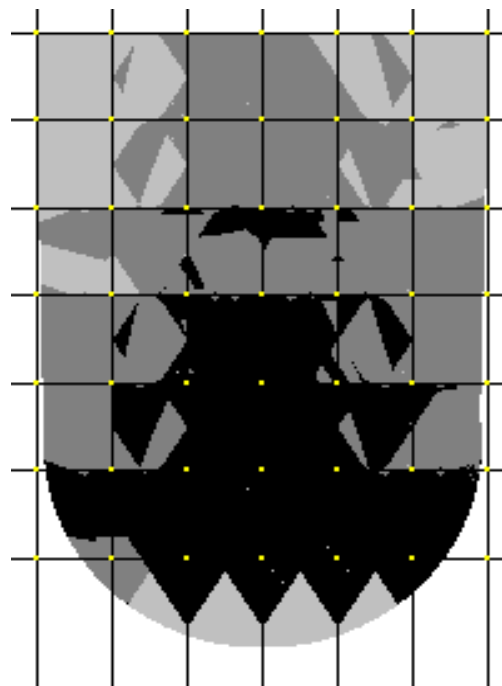


Figure 5a. CPM's results - 10t EAF ($t_1 = 10$ min)

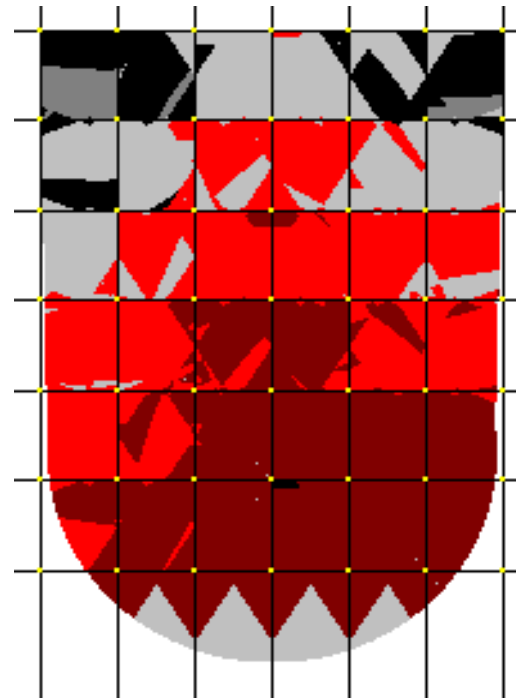
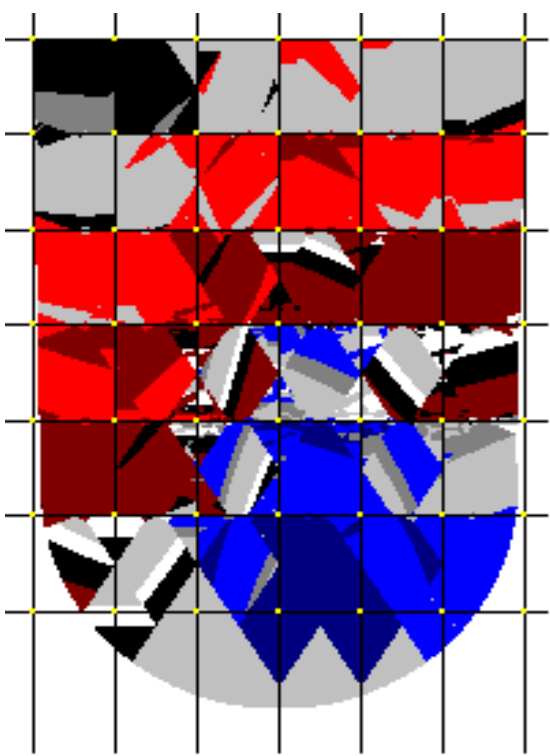
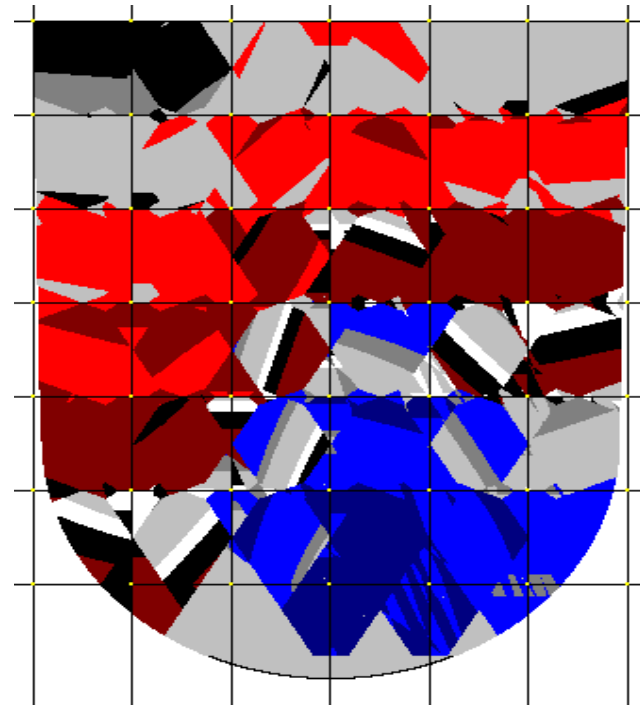


Figure 5b. CPM's results - 10t EAF ($t_2 = 20$ min)

Figure 5c. CPM's results - 10t EAF ($t_3 = 30$ min)Figure 5d. CPM's results - 50t EAF ($t_3 = 30$ min)

The thoroughly analysed preheating (including from the descriptive point of view) process's steps were established at the moments: $t_1 = 10$ min; $t_2 = 20$ min; $t_3 = 30$ min; reported to the process's start ($t_0 = 0$).

At the moment $t_1 = 10$ min, the CPM execution's results show the load's temperature gradient minimum – maximum of $145^{\circ}\text{C} – 330^{\circ}\text{C}$, which corresponds to a preheating speed between the $580^{\circ}\text{C/h}-1320^{\circ}\text{C/h}$ limits. The temperature's distribution in the longitudinal section shows a superior temperature zone.

REFERENCES

- [1] A. Ioana, "Metallurgy's Impact on Public Health", Review of Research and Social Intervention, Vol. 43/2013, ISSN: 1583-3410, (ISI-Web of Social Science/Social Science Citation Index Expanded), pg. 169-179, Iași, 2013.
- [2] A. Ioana, A. Semenescu, "Technological, Economic, and Environmental Optimization of Aluminum Recycling", Journal of the Minerals, Metals & Materials Society, JOM: Volume 65, Issue 8 (2013), ISSN 1047-4838 (ISI-Web of Science/Science Citation Index Expanded), pp. 951-957, WOS: 000322136400007
- [3] A. Ioana, V. Mirea, C. Bălescu, "Analysis of Service Quality Management in the Materials Industry Using the BCG Matrix Method", Amfiteatru Economic Review, Vol. XI, Nr. 26, June 2009, pp 270-276, [ISSN 1582-9146, ISI-Web of Science/Science Citation Index Expanded], București, 2009, WOS: 000267351800004
- [4] A. Ioana, "The Electric Arc Furnaces (EAF) Functional and Technological Performances with the Preheating of the Load and Powder Blowing Optimization for the High Quality Steel Processing", PhD Thesis, University "Politehnica" of Bucharest, 1998.
- [5] A. Ioana, A. Nicolae, et al., "Optimal Managing of Electric Arc Furnaces", Ed. Fairs Partners, Bucharest, 2002.
- [6] A. Ioana, "Production Management in Metallic Materials Industry. Theory and Applications", Ed. PRINTECH, Bucharest, 2007.
- [7] A. Ioana, "Optimum Operation and Automation of Electric Arc Furnace Installations", Review of Installations Technique. 5(46)/2007, 12-14.

Videogame design as strengthening in communicational and cognitive processes.

Yaneth P.Caviativa, María Inés Mantilla Pastrana, Yoan M.Guzmán, Adán Beltrán, Valentino Jaramillo, Ana Milena Rincón

Abstract— The objective of the research is to design a videogame as a technological tool to favor communicational and cognitive processes of children whose ages are between 5 and 6 years, in preschool stage. The methodology corresponds to a descriptive type investigation with instructional design modeling which considers: analysis of learning necessities, formation objectives, adequate recollections to the purposes of learning processes and development of activities and contents, all of which favors operational functions by which the child organizes, associates, improves concentration, orientation and spatial notion capacity.

The previous, are elements applied in videogame design, and that in a future, are expected to be implemented under a detailed analysis for the strengthening of communicational and cognitive abilities, fading significantly phonological processes such as omission and substitution of phonemes that improve the structure of more elaborated and intelligible sentences, that are required to perform their social interaction in the context towards the recognition of objects, figures and colors from the abstraction of the linguistic symbology. It is recommended to continue the investigation including bigger samples, and so, objective proofs for the evaluation of the communicative and cognitive pattern, increasing the quantity of videogame sessions in order to determine the effects of the playful in virtual reality learning.

Keywords— Communicative processes, education, videogame.

I. INTRODUCTION

THE technological progress in which actual world is immerse, requires that different disciplines optimize learning processes during early ages where communicative and linguistic abilities favor integral development of the human being.

This work was supported in part by the department of investigation of Universidad Manuela Beltrán, Bogotá, Colombia.

Y. Caviativa is with Universidad Manuela Beltrán, Bogotá, Colombia. Phone Number: +57 1 546 06 00 ext. 1151 (e-mail: janeth.caviativa@docentes.umb.edu.co)

M. Mantilla is with Universidad Manuela Beltrán, Bogotá, Colombia..Phone Number: +57 1 546 06 00 ext. 1151 (e-mail: mariaines.mantilla@docentes.umb.edu.co).

Y. Guzmán is with Universidad Manuela Beltrán, Bogotá, Colombia..Phone Number: +57 1 546 06 00 ext. 1151 (e-mail: yoan.guzman@docentes.umb.edu.co)

A. Beltran is with Universidad Manuela Beltrán, Bogotá, Colombia..Phone Number: +57 1 546 06 00 ext. 1151 (e-mail: Adan.Beltran@docentes.umb.edu.co)

V. Jaramillo is with Universidad Sabana, Bogotá, Colombia..Phone Number: +57 1 3167471874 (e-mail: ValentinoJaramilloG@yahoo.es)

A. Rincon is with Universidad Manuela Beltrán, Bogotá, Colombia.. Phone Number: +57 1 546 06 00 ext. 1151 (e-mail: ana.rincon@docentes.umb.edu.co)

In the same sense, it is required to potentiate the mentioned abilities towards their social interaction during the development of 5-6 years old children, in a playful way and incorporating the new information and communication technologies, among which is the videogame, since these abilities affect social interaction as it is affirmed “A range of psychosocial and emotional disorders has been associated to language disorders” [1]. Those disorders show difficulties such as: omissions, phonemes substitutions, poor structure sentences, fluctuating instruction following or with an exaggerated support by the adult.

Thus, the development of the research is done from the themes about videogame as a didactic strategy, the communicational processes and their influence in the integral development of human being since early childhood, and the cognitive areas that favors the fulfillment of social abilities, in the constructivism pedagogical frame. Despite the coordination limitations, the kinet, and laterality of children in these early ages, videogames generate integration patterns where they achieve communicational abilities strengthening the emission and reception of concepts, interpreting messages, decoding different sounds and expressing them in coherent ways.

There are benefits that promote the creation and implementation of videogames in educational field for the development of cognitive and communicative abilities, taken in account from the constructivist pedagogical model, where children learn by association and meanings of constructions, since their knowledge is based according to the context, explanations given by adults and their own lived experiences; for which they need to recognize linguistic signs as part of language development, which in turn promotes mental processes more structured by the videogame as a technological tool in didactics.

THEORETICAL DISCUSSION

Videogames and using of virtual reality have extended to different human activities in populations of all ages [2]. Beside of technological development, one of the reasons why the use of these games has increased, are familiar dynamics where parents occupy their time in work activities and children spent their free time in videogames, internet and television, since time to share with family outdoors has been reduced. This has contributed to the increment of digital culture in different countries.

Information and Communication Technologies (ICT or TICs in Spanish), as well as virtual reality games, have turned into strategically allies in learning processes since interactivity increases motivation, a process that underlies learning. In the same way, the mentioned games have been used as methods of cognitive rehabilitation.

A videogame is an informatic interactive program destined to entertainment that can work on different devices: computer, consoles, mobile phones, etcetera; it integrates audio and video, and allows enjoying experiences that, in many cases, would be very difficult to live in reality. Within the features of videogames are found [3], graphics quality (in the beginning in two dimensions, nowadays in three), the control of the game must be easy and intuitive, and sound (from speaker to surround).

There exist different types of videogames, amongst them it can be named the games of adventure (intelligence tests or resolution of puzzles for advancing), arcade (skills activities), sports, strategy (coordinating actions), role (the player controls a character, and keeps evolving during the game according to the user decisions) and simulation (it simulates some type of action such as flying a plane). The mentioned benefits are attributed in different ages to improve learning, attention, concentration and meanings constructions.

The selected actions for each videogame are the reflect of the pupil concern to use the best learning strategy through the playful, situation that is based on the ***Constructivist Pedagogical Model*** which not only observes how to teach but how to learn [4]. This model has various implications: 1. Knowledge is constructed from action, 2. It recognizes the existence of previous knowledge, 3. Acquired knowledge constitutes the repertoire in which the subject handles and interprets the world, and 4. Concepts, that are the ideas about things, constitute the base of a net from the action.

In the same sense, it is required the articulation of playful benefits of videogames, with the constructivist model, and the communication and cognitive processes. Communicative processes are based in the interpretation of linguistic signs, which consists of three principal components, not necessarily of the same relevance: form, content and use [5]. Form contents morphosyntax and phonology. These components connect sound or symbols in a determine order. Content constitutes semantic, which allows giving meaning to the words. The use contents the pragmatic, which establish language into a social context.

II. METHODOLOGY

In this research, methodologies for development and design of educative software are articulated, using from these tools the process of the software construction. This vision is considered from the traditional model [6], that determines necessity and after the requirements to subsequently obtain the application design, develop it, implement it, and test it. In this regard and following the parameters of the mentioned model, that on the whole is part of the software elaboration process; it is summarize the following step order: 1. Obtain software requirements. 2. Do the preliminary design and the detailed design. 3. Do the implementation. 4. Do the tests. 5. Carry out the installation. 6. Execute and update software tasks.

For the construction of the videogame design, it is used levels of difficulty established since the foundation of constructivist processes, by using abstraction processes of communicational type: listening and projection of sounds; linguistic: description of objects and their use; cognitive: spatial location, classification of different objects, shape and figures recognition from the interaction with the scholar. Application software: the objective action of the design is aimed to evaluate learning in the strengthening of communicational and cognitive processes since the first stages of school formation.

In the creative phase, it was recognized the capacity of graphic library according to preschool ages (colors, figures and adequate context spaces). Thereof, the header and display menu are developed with a symbolic language which is accessible to the preschool child.

III. RESULTS

The design of a videogame with educative features allows from the pedagogical engineer to strengthen and potentiate four fundamental dimensions in human development, which are motor, intellectual, affective and social development.

Despite of non having definitive investigations, this type of descriptive work about preschooler population allows to give a beginning to the development of skills that are favored by the use of videogames from the fundamental characteristics in the encouragement and development of abilities such as relation, classification, categorization, interpretation, identification, description and information decoding presented in a symbolic way and in language of association to the scholar context, structured so that they must be included in the process of designing a videogame under levels of low, medium and high difficulty structured for this type of population.

Hence, abilities of communicational, linguistic and cognitive type, can be evidenced in the design of increasing and progressive levels of difficulties inside the videogame for the scholar, which is adaptable to the interest and rhythm of the child, with the possibility of expanding the capacity of hearing before the oriented activities, since experiences in videogame design have shown difficulty in searching elements that connect the outside world to the school, with the adequate and motivating language. Therefore, the use of this type of videogame utilizes phrases such as:

Did you hear that? – Go in and find out what is going on! – Oh my ... The kitchen is enchanted – You see, it is magic...things are floating around...help me put them in the right place – Hoy many spoons are in the table?

In this way, it is allowed the development of interactional processes in the classroom, as well as increase abilities in instructional comprehension of two or three commands, lowering the presence of phonological processes such as omissions, phonemes and assimilations substitutions, being more adequate the structure of the sentences, thus the oral productions will be more intelligible.

During the process of videogame development, various changes were made because of findings in the design of motivational type to the scholar, in a way that language is accessible with a playful component accord to the targeted age. In this way, there were made changes of:

- Association activities (silhouettes and masked figures) which allow the size and organization differentiation of objects.
- Elaboration of low and medium structure questions with an adequate pronunciation.
- Showing the username that load the board.

The software consists in three levels and nine games in total, each level with three games. Each one of the games is associated with basic, medium and moderate levels of difficulty. They are founded in series as a logic operation from the social context of the scholar. (House –introduction-, Living room – Level 1 -, Room –Level 2-, Kitchen –Level 3-). The games 1, 2 and 3 of level 1, present comparison systems between each one of them in which objects can be develop and organize in increasing or decreasing way according to the difference of the objects.

In the same way, activities of the games 1, 2 of levels 2 and 3 allow to identify geometrical figures, colors and associate sounds while dragging figures to objects of storage (baskets or the wall). This condition allows identification by association of elements that are known.

As a condition of attractive design alternatives, the use of visual-motor coordination elements is allowed by following a “guardian” under the simulated walking movement in the place; not leaving aside that components of motor development can be developed, such as concentration and basic spatial concentration and notion, that allow the orientation in the videogame (up, down, close, far).

Finally, association of objects in the kitchen as game 3 in levels 2 and 3, allows to regroup physical common properties, being this an element of establishment of similarities and differences between objects.

One of the features of educative design software consists in develop and promote abilities about symbolic linguistics and cognitive processes associated to the use of spatial notion, that is allowed through informs (Fig. 1) enabling the register of strengthening about communicational and cognitive processes of children while using the videogame.

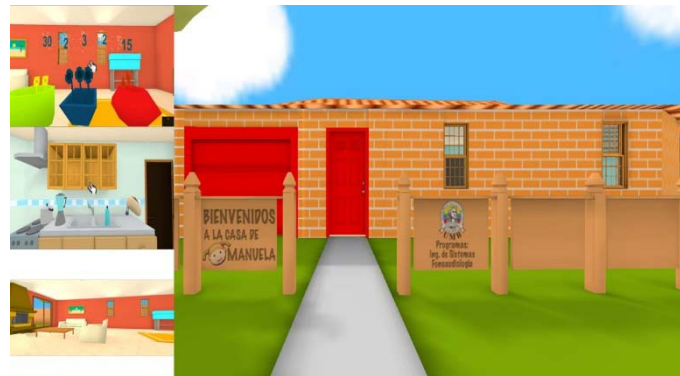


Fig. 1. Game interface and access

This type of strategy of videogame design from pedagogical engineer allows to base learning processes in which, from the constructivism as a model of design, makes more complex the different levels of effort to which children of 5-6 years old have to face. In the same way, the direction of the accompanying adult as a tutor is necessary in this process, as well as indications funded in each level, projections of indications and sounds allow an interactive learning with the environment in which is presented. Thus, this position has an influence with processes of trial and error, which implies abilities of the subject (boy/girl) to interpret past and present experiences, and actualize therefore their content [7]. This condition implies major processes of abstraction, internalization and elaboration of learning processes associated to language development and particular processes.

IV. CONCLUSION

Videogame design allows, from pedagogy, to strengthen and potentiate four fundamental dimensions in human development, which are motor, intellectual, affective and social development. After the obtained results, it can be concluded that the use of technological tools strengthen abilities of communicational processes in children. On the other hand, it also strengthen the possibility of expanding the capacity of listening before the oriented activities, since experiences in videogame design have shown difficulty in searching elements that connect the outside world to the school, with the adequate language.

Additionally, it is necessary to keep creating technological tools and this research initiates a path in which other investigations can be done including bigger samples, with more objective proofs that can be useful in process of therapeutic support and other related contexts, such as scholar and familiar.

ACKNOWLEDGMENT

The authors would like to thank Richard Jose De Sousa Da Silva for his translating collaboration and adjustment of the text to the corresponding and required format.

REFERENCES

- [1] Cohen. Available in: <http://www.encyclopedia-infantes.com/documents/CohenESPx.pdf>
- [2] Gómez, M. (2013). Aplicación de realidad virtual en la rehabilitación cognitiva. *Revista Vínculos. Ciencia, Tecnología y Sociedad*, 10(1), 130-135.
- [3] Galeon. (2012). Historia de los Video juegos, [en línea]. Available in: www.historia-videojuegos.galeon.com [cited on June 25th of 2012].
- [4] Serrano, J. & Pons, R. (2008). La concepción constructivista de la instrucción. *Revista Mexicana de Investigación En Educación*, 13(38), 681–712.
- [5] Bloom, L. & Lahey, M. (1978). Language development and language disorders. New York, Wiley.
- [6] Calvo P., Cataldi Z. & Lage F. (2007). Evaluación sistematizada de software educativo: estudio de un caso aplicación de grafos. *Revista Iberoamericana de Tecnología en educación y educación en tecnología*, (2).
- [7] Patrick, F. (2009). Video Juegos en el aula. Edición European Schoolnet.

Characterisation of High Carbon Ash from Captive Power Plant for Potential Utilisation

Ruma Rano, A. Sarkar

Abstract: High carbon ash (LOI > 47.4 %) from mechanical hoppers of a local captive Power Station using stoker fired combustor has been thoroughly characterized in respect of their physico-chemical, mineralogical and morphological features. Various size classified fractions of each ash along with their magnetic and non-magnetic components have also been characterized. Coarser fractions contain a substantial amount of unburnt/char materials. The particles are irregular, macroporous as well as contain significant percentage of micropores. X-ray diffraction (XRD) analysis reveals that the carbon present is mostly turbostratic in nature which have high calorific value content and may be used as fuel substitute, adsorbent for phenolic effluents, support for chemicals to sequester carbon dioxide etc. Morphological analysis of the magnetic components reveals presence of various types of Fe-bearing phase with less porous and more regular shape as compared with their non-magnetic components. The geometrical patterns of the crystallites widely vary in nature ranging from dendritic, pine-tree type to blister types. EDX-analysis reveals high surface enrichment of Fe bearing crystallites, these materials can be used for coal floatation.

Key words: High carbon ash, Stoker fired combustor, Morphological analysis, Turbostratic, Fuel substitute and sequestering carbon dioxide.

I. Introduction

Fly ash generated at thermal power plants (TPPs) in India are of three types [1] (a) low/ultra low carbon ash (b) moderately high carbon ash (c) very high carbon ash. Small captive power plants working on stoker-fired combustors generally produce very high carbon ash. One of the major deterrent in the path for proper utilization of FA in India, is that these ashes have a substantial amount of unburnt carbon/ char [1]. If LOI can be considered as rough estimate of the carbon content [2], then the FAs generated at various TPPs in India may be considered as useless for utilization in cement and concrete industry, except as fuel [3]. The allowable limit of LOI *albeit* carbon content being 6% [4]. LOI restriction has been made because unburnt carbon present in ash is responsible for adsorbing the air entrainment admixtures (AEAs) which are added to cement so that crack formation is minimized [5].

Reasons suggested [6-9] for presence of high percentages of unburnt carbon in FAs is the development of

low NO_x burners and their subsequent application in TPPs. However, other factors may be suggested as well. These are (a) improper maintenance of the boiler (b) non-adherence to the limiting size of the feed coal (c) not using quality coal [10]. Some of the captive power stations in India (other than those of National Thermal Power Corporation) are not so alert in this matter, resulting in formation of high carbon ashes. While it will not be prudent to suggest ways and means in improving the carbon burn out, the present investigations were undertaken to identify channels for utilization of the high carbon ash, after a thorough and extensive characterization which involved physico-chemical, mineralogical, morphological and other relevant features.

.It has been observed by the present investigators that there are substantial differences between high carbon ash obtained from TPP using stoker fired combustor and the studied one – which is obtained from a TPP that uses PFC [11], the data for various physico-chemical, mineralogical and morphological analyses have been assessed and various utilization potentials of the size fractions/magnetic materials have been suggested [6,7].

The FA collected from Mechanical Hopper (MH) of DPSC presumably had a very high percentage of unburnt carbon. In the present work, size classified fractions were obtained by sieving the bulk FA so that a thorough examination can be made. The size classified fractions were further subjected to magnetic separation, so that magnetic and non-magnetic components can be obtained. Subsequently, based on the data obtained from various analyses, suitable suggestions regarding the utilities of various size fractions have been made. While some of the well known utilities of high carbon ash like, use as fuel [12], fillers [13], catalyst support [14], production of activated carbon as adsorbent for trace elements, organic and organometallic compounds [15-17] can be the channels of utilization for the presently discussed ash, an innovative application has also been investigated.

II. Material and methods

The TPS namely Dishergarh Power Supply Corporation (DPSC) from which FA has been collected from the mechanical hopper, which is generating 30 MW /day. It uses stoker -fired combustors. The relevant combustion data are: combustion temperature 900-1000°C, air flow 68.54 t/h, the excess oxygen being 7-8 %.

In order to obtain a true representative picture of the various physico-chemical and morphological features of the ash, a representative sample was prepared by mixing the FA samples (1Kg/day) collected over a month. The homogenized ash sample was sieved (30 mins.) using sieves No. B.S 150, 250, 300 and 350.

Accordingly, five size-classified ash fractions namely A, B, C, D and E were obtained. Thereafter, magnetic concentrates were isolated from each of the fractions using Davis tube. Two sets of fractions (a) non - magnetic and (b) magnetic were obtained. For convenience of discussion, the terms $A_{11}, B_{11}, C_{11}, D_{11}$, and E_{11} have been assigned to the non-magnetic components of each fraction. The terms $A_{12}, B_{12}, C_{12}, D_{12}$, and E_{12} correspond to the magnetic components.

Various physico-chemical, morphological and mineralogical characteristics of the size classified fractions as well as magnetic /non-magnetic components were determined. These are (a) weight percentage size distribution (b) loss on ignition (LOI), [ASTM C 311-04 method] (c) chemical composition (XRF model: PW 2404 X-ray spectrometer) (d) particle size analysis using Laser based particle size analyser: Model, Fritsch Particle Sizer Analysette 22 (e) mineralogical compositions (X-ray diffractrometer Model PW-1710 with $CuK\alpha$ radiation) (f) morphological and surface composition analysis (Scanning Electron Microscope [SEM] Model S-440, LEO Electron Microscopy equipped with an Oxford link-Isis Energy Dispersive X-ray analyser). Calorific values of various size-classified fractions were determined on a Isoperibal Bomb Calorimeter– Model AC –350, using Benzoic acid as internal standard. The nature of the carbon (graphitic/turbostratically disordered) for some fractions were determined by first demineralising the samples (boiling with HF) and then obtaining X-Ray diffractograms.

Ash samples, which float in water (char particles of larger dimension having macropores) were also isolated. Such experiments were necessitated by the fact that these ash particles may be suitable candidates for use as fillers in particle board preparation (for absorbing sound and heat), domestic fuel substitute, absorbing chemicals/fertilizer for slow release etc.

III. Results and discussion

A. General physical characteristics

The weight percentage size distribution of the ash in various size-classified fractions reflects (Table-1) that the coarsest fraction (A) has the greatest contribution (59%) to the as received ash followed by fraction C and E. LOI values are very high for the first two coarser fractions namely A & B and gradually decrease as size decreases (C, D, and E). However, the very high abundance of the coarsest fraction coupled with its high LOI value gives a primary indication regarding the abundance of unburnt carbon in the as received ash. The apparent density and bulk density values for the various size

classified fractions can also be correlated with the LOI values *albeit* the unburnt carbon content. It is quite well known [18] that with decrease in the carbonaceous matter content, the density increases.

B. Particle size distribution

Particle size distribution reveals that in general the particles are larger. D_{10} , which denotes that 10% of the particles are below this diameter, is quite low for the as received ash. D_{90} may be as high as 602.71 μm (Table-2). Size classification using sieves No.150, 250, 300 and 350 leads to significant changes in such values. Thus, the coarsest fraction (A) has D_{10} of 103.07 μm and the finest one (E) 9.55 μm . D_{90} for the corresponding fractions are 581.75 and 35.27 μm . In general, it may be concluded that the ash has an abundance of large sized particles. This is particularly true for coarser fractions specially A&B. Coupled with relevant LOI values and weight percentage distribution pattern of fraction A, it may be inferred that the ash has a very high percentage of unburnt carbon which speaks of the inefficiency of the combustion process.

C. Chemical Composition

The chemical composition of the various size-classified fractions of fly ash is presented in Table-3.

It is observed that for the coarser fractions namely A & B, the Si and Al content are appreciably lower than the other fractions (C, D, E). This observation is quite in consonance with the LOI values obtained for the fractions, where a similar appreciable drop has been observed for the finer fractions. Thus, it can be mentioned that LOI and Si/Al concentrations are complimentary to each other. CaO, which plays a very important role in pozzolanic activity of an ash is not present to that extent. However, it is observed that with decrease in particle size, there is an increase in the concentration (almost threefold increase from fraction A to E). Similar trend is observed for the element Fe.

Trace elements (Table-4) are present in various size-classified fractions of fly ash. However their concentrations are low. Very low abundance of various trace elements, particularly those of toxic or potentially toxic elements like Cr, Co, Pb, Ni, Mn etc in the various fractions of the ash makes these ashes harmless as far as possible environmental pollution is concerned.

D. Mineralogical features

X- ray diffractograms of the size classified fractions of fly ash (A, B, C, D, E) reveal that the quartz is the main mineral phase, it is observed that the peak intensities (100 for quartz $2\theta = 26.6^\circ$) generally increase with decrease in particle size. The non-magnetic fractions ($A_{11}, B_{11}, C_{11}, D_{11}, E_{11}$) have very strong peak intensities for quartz [Fig.1]. Peaks for mullite (100) as well as for refractory mullite are not that

significant. The XRD diffractogram of the magnetite components (A_{12} , B_{12} , C_{12} , D_{12} , E_{12}) [Fig.2] have in general stronger peaks for magnetite, though hematite is also observed. Similar observation has been made elsewhere [19,20]. However, the peak intensities are not as strong as those observed in case of the fly ashes with lesser carbon content [21]. This is probably due to buttressing effect of the carbonaceous matters present.

Another interesting observation was, the X-ray diffractogram for the coarsest non-magnetic fraction A_{11} , revealed that between $20^0 - 30^0$ (20), there is a hump along with sharp intense peak for quartz (100). The humps flatten out from the coarser to finer fractions (A_{11} to E_{11}). Possibly this was due to turbostratic nature of the carbon present. Subsequently, this fractions A_{11} , B_{11} and E_{11} were demineralised to remove the crystalline phases and X-ray diffractogram were obtained. It was observed that demineralisation has removed most of the quartz particles and no sign of graphitic carbon is observed (absence of peak at $\theta = 44.7^0$) for the coarser fraction. Moreover, the hump between $\theta = 40 - 50^0$ is also observed. Hence, the nature of the carbon present is „turbostratic” [12].

E. Morphological Characteristics:

(I) Non-magnetic components:

SEM analysis of the non-magnetic components reveals that the particles in general are irregular in shape [Fig.4]. The coarser fractions contain large pores which appear to be mostly chars. EDX analysis reveals that in general the particles have very high surface enrichment of carbon with moderate „O”, Al and Si enrichment. Some alumino-siliceous glassy spheroids along with Cinder like carbonaceous particles are observed with high enrichment of „C” and low O, Al, etc. Large alumino-siliceous spheroidal particles probably cenospheres and some particles in a state of fusion are also observed. EDX analysis reveals that the finer particles still have a significant enrichment of carbon matter along with Al, Si. This observation is quite different from that of fraction A_{11}/B_{11} in which particles with high surface enrichment of carbon and almost insignificant amount of Si/Al are observed. It may be therefore inferred that most probably amorphous carbon has been included in the alumino-siliceous glassy phase.

(II) Magnetic component:

SEM image of the magnetic components reveals the particles are less porous than non-magnetic ones [Fig.5]. One of the microphotographs reveals some interesting features, appears to be a hollow ferrosphere in which smaller particles are embedded [Fig.5(f)]. It is quite probable that a melt comprising of Al, Si, Fe, bearing material has encapsulated smaller particles during mineral matter transformation. Another particle is observed with high enrichment of „C”, moderate „O”, Al, Si and low Fe. It is highly porous in nature.

High carbon enrichment at the surface probably indicates that these contain high percentage of carbonaceous

material. This is inspite of the particles being iron bearing in nature. With decrease in particle size the spheroidal character increases. One of the SEM image reveals that the particles have blister like surface pointing towards an apparent expansion of entrained gases when the particle is being formed during melting of alumino-siliceous material . One of the particles appears to be a ferrosphere with crystallite formation like pine tree [22]. The observation that there are two distinctly different types of arrangement (in rows) of the crystallites which, point towards two different axis of rotation of the basic alumino-siliceous spheres during turbulent motion in the combustor [23]. Surface enrichment of Fe is extremely high. One of the particles, although appears to be glassy melt like material has extremely high surface enrichment of Fe, which probably indicates the formation of glassy Fe-oxide containing material [21,24]. SEM image gives some interesting hint regarding the formation of „Cenosphere”.

F. Potential Utilisation Channels based on analysis:

A careful examination of the various results has revealed that the ash is highly carbonaceous in nature. The immediate reaction to such revelation was whether these can be used as fuel substitute. Some of the water floatable components (F_1 and F_2) have substantially high calorific value (6276.4 Cal/g and 6442.3 Cal/g), which may be compared with „A” grade coal. Out of the five sizes classified fractions, fraction A & B appear to have some significant amount of calorific values. Thus fraction F_1 , F_2 , A and B can be conveniently combined with some binder to form fuel cakes.

Phenol adsorption study, which was carried out in view of the porous nature of the ash particles, revealed that while the as received ash had an adsorption capacity of 4.04 mg/g of ash, the size classified fractions showed greater adsorption capacity.

In order to exploit the macroporous character of the ash, particularly the coarser fractions, experiments were designed to develop suitable materials that can absorb sound and heat. The highly carbonaceous chars having „pockets” could be ideal candidates for entrapping air when mixed with suitable liquid polymers. Uniform light weight particle boards were prepared which showed the promise of sound dampness / shock absorbers. This aspect is being thoroughly investigated.

The other possible uses as envisaged are as follows
(a) template for slow release fertilizer (b) template for hazardous radio active waste (c) template for aminoalcohols / diethylene glycol for carbon dioxide sequestration (d) templates for regioselective /stereoselective synthesis of organic compounds.

IV. Conclusions

A review of the various results obtained in respect of physico-chemical, mineralogical, morphological properties of the various size fractions as well as the magnetic and non-

magnetic components leads to the following conclusions: (a) the ash obtained is highly carbonaceous and contains large size char particles which are essentially macroporous (though containing some amount of micropores) (b) the mineralogical analysis leads to the conclusion that the carbon matter present is mostly having „turbostratic” order (c) the magnetic components are associated with carbon matters through having high Fe enrichment (d) some of the coarser fractions may effectively be used as fuel substitute, adsorbent for organic effluents and support for adsorbing chemicals which can sequester carbon dioxide.

References

- [1] P.S. M. Tripathy and S.N. Mukherjee; Perspective on Bulk use of Fly ash: CFRI Golden Jubilee Monograph: Allied Publishers, 1997.
- [2] T. Gurupira, C.L. Jones, A. Howard, C. Lockert, T. Wandell, J.M. Stancel; New products from coal combustion ash: selective extraction of particles with density > 2, 2001 International Ash Utilisation Symposium, Center for Applied Energy Research, University of Kentucky. <http://www.flyash.info>
- [3] S. Maitra; Utilisation of solid wastes from Power, Steel and Aluminium Industries for the Development of value Added Ceramics and Construction Materials: Perspectives and Prospects, Proceedings of International Symposium on Beneficiation, Agglomeration and Environment, Bhubaneswar, Jan 20-22, (1999) 426-433
- [4] I. Kualots, R. H. Hurt, E.M. Suuberg , Fuel, 83 (2004) 223-230
- [5] P.K. Mehta; Role of Fly ash in Sustainable Development. Concrete, Flyash and the Environment –Proceeding, 8th Dec., (1998), <http://www.buildinggreen.com/features/flyash/mehta.cfm>
- [6] S. S. Tyson; Proceedings of the Third Annual Conference on Unburned Carbon on Utility Fly ash, US Department of Energy, FETC, May (1997) 3
- [7] J. Makansi ; Power, 37 (1994) 114-123
- [8] J.C. Hower, R.F. Rathbone, T.L. Robl, G. A. Thomas, B.O. Haeberlin, A.S. Trimble, Waste Management, 17 (1997) 219
- [9] J.Y. Hwang, X. Huang, J.M. Gillis, A.M. Hein, D.C. Popko, R.E. Tieder, M.C. Mc Kimpson; Utilisation of Low NO_x coal Combustion By- Products
- [10] A. Sarkar, Ruma Rano, G. Udaybhanu, A.K. Basu, Fuel Processing Technology; 87(2006) 259-277
- [11] “Characterisation of High Carbon Ash from Thermal Power Station using Pulverised Fuel Combustor” A. Sarkar, R. Rano, A. Kumar, Energy Sources, Part A, vol. 32, pp 607 - 619, 2010.
- [12] R. Hurt, K. Davis, N. Yang , T. Headley, G. Mitchell, Fuel, 74 (1995) 1297-1306
- [13] T. Sakulpitakphon, J. Hower, A. Trimble, W. Schram, G.Thomas, Energy Fuels, 14 (2000) 727-733
- [14] S.V. Vassilev, R. Menendz, A. G. Borrego, M. Diaz-Somaano, M.R. Martinez-Tarazona, Fuel 83 (2004) 1563-1583
- [15] J. Baltrus. A.Wells , D. Fauth , J.Diehl , C. White , Energy Fuels, 15 (2001) 455-462
- [16] M. Maroto-Valer, D. Taublee, J. Hower; Fuel, 80 (2001) 795-800
- [17] Y. Soong, M. Schoffstall , T. Link, Fuel, 80 (2001) 879-889
- [18] Y. Zhang, Z. Lu, Maroto-Valer M, Anderson J., Schobert H., Energy, Fuels 17 (2003) 369-377
- [19] S.V. Vassilev, R. Menendez ; Fuel 84 (2005), 973-991
- [20] O. Ozdemir, B. Ersoy, M.S. Celik; Separation of Pozzolanic Material from Lignite Fly Ash, Fly ash Utilisation Symposium, Lexington, Kentucky, USA, 22-24 Oct. 2001.
- [21] R. Giere, L.E.Carleton , and G.R. Lumpkin, American Mineralogist 88 (2003) 1853-1865
- [22] E.V. Sokol, V.M. Kalugin , E. N. Nigmatulina , N. I. Volkova , A. E. Frenkel, N.V Maksimova , Fuel, 81 (2002) 867-876
- [23] S. Torrey, Coal Ash Utilization: Fly ash, Bottom ash and slag, Noyes Data, Ridge, NJ, USA, 1978 Park
- [24] A. Sarkar, Ruma Rano, K.K. Mishra, I.N. Sinha, Fuel Processing Technology, 86(2005) 1221-1238

TABLE -1

WEIGHT PERCENTAGE SIZE DISTRIBUTION, LOI %, APPARENT / BULK DENSITIES OF THE VARIOUS SIZE CLASSIFIED FRACTIONS OF FLY ASH

| TPS | Collection Point | Size Classified Fraction | | | | |
|-------------------------------------|-------------------|---------------------------------------|----------------|-----------------|----------------|-----------------|
| | | A | B | C | D | E |
| | | Weight % & LOI % | | | | |
| Dishergarh Power Supply Corporation | Mechanical Hopper | 59.02 (58.2) | 4.06 (46.5) | 21.03 (28.0) | 1.26 (24.3) | 23.03 (21.5) |
| | | Apparent density (g/cm ³) | | | | |
| | | 1.19 | 1.31 | 1.42 | 1.55 | 1.78 |
| | | Bulk density (g/cm ³) | | | | |
| | | 0.24 | 0.32 | 0.44 | 0.56 | 0.62 |
| | | (Values in parentheses reflect LOI%) | | | | |

Where,

- A= Fraction retained by Sieve No. 150 B.S (+ 104µm)
- B= Fraction retained by Sieve No. 250 B.S (-104µm to + 66µm)
- C= Fraction retained by Sieve No. 300 B.S (-66µm to +53µm)
- D= Fraction retained by Sieve No. 350 B.S (-53µm to +45µm)
- E= Fraction passed through Sieve No. 350 B.S (-45µm)

**TABLE-2
PARTICLE SIZE DISTRIBUTION PROFILES OF AS RECEIVED AND SIZE CLASSIFIED ASH**

| TPS / Collection Point | Fraction | Undersize (%) | | | D ₁₀ | D ₅₀ | D ₉₀ | AMD (µm) | SPAN (D ₉₀ - D ₁₀) / (D ₅₀) |
|---|-------------|---------------|-------|--------|-----------------|-----------------|-----------------|----------|--|
| | | <10µm | <50µm | <100µm | | | | | |
| Dishergarh Power Supply Corporation (Mechanical Hopper) | As received | 6.43 | 34.44 | 52.45 | 14.68 | 91.56 | 602.71 | 200.16 | 6.42 |
| | A | 0.82 | 3.62 | 9.25 | 103.07 | 229.83 | 581.75 | 292.41 | 2.08 |
| | B | 1.54 | 7.75 | 42.67 | 58.95 | 107.05 | 173.11 | 114.45 | 1.06 |
| | C | 1.64 | 20.69 | 85.68 | 32.19 | 64.38 | 108.60 | 71.67 | 1.10 |
| | D | 3.62 | 51.33 | 98.11 | 20.4 | 49.31 | 76.88 | 48.99 | 1.14 |
| | E | 10.95 | 97.79 | 100.0 | 9.55 | 22.15 | 35.27 | 22.68 | 1.16 |

Where,

- D₁₀: 10% of the particles is smaller than this diameter (µm)
- D₅₀: 50% of the particles is smaller than this diameter (µm)
- D₉₀: 90% of the particles is smaller than this diameter (µm)
- AMD: Average Mean Diameter
- SPAN: (D₉₀ - D₁₀) / D₅₀

TABLE-3

CHEMICAL COMPOSITION OF DIFFERENT SIZE CLASSIFIED FRACTION (% W/W) OF FLY ASHES USING PW 2404 XRF

| Size Fraction | SiO ₂ | Al ₂ O ₃ | Fe ₂ O ₃ | CaO | MgO | P ₂ O ₅ | K ₂ O | Na ₂ O | TiO ₂ | SO ₃ |
|---------------|------------------|--------------------------------|--------------------------------|------|------|-------------------------------|------------------|-------------------|------------------|-----------------|
| A | 21.4 | 10.63 | 2.05 | 1.06 | 0.65 | 0.001 | 0.75 | 0.21 | 0.53 | 0.23 |
| B | 28.1 | 13.92 | 3.53 | 1.62 | 0.70 | 0.004 | 1.02 | 0.42 | 0.72 | 0.32 |
| C | 40.3 | 21.05 | 3.42 | 2.41 | 1.15 | 0.067 | 1.41 | 0.29 | 1.19 | 0.31 |
| D | 41.8 | 22.0 | 3.47 | 2.26 | 1.15 | 0.29 | 1.46 | 0.29 | 1.19 | 0.27 |
| E | 43.9 | 22.4 | 4.08 | 2.86 | 0.94 | 0.64 | 1.57 | 0.27 | 1.42 | 0.20 |

TABLE-4

TRACE ELEMENT CONTENTS IN DIFFERENT SIZE-CLASSIFIED FRACTIONS OF FLY ASHES (ppm)

| Size Fraction | Cr | Mn | Co | Ni | Cu | Zn | Y | Zr | Rb | Sr | Ba | Pb | Nb |
|---------------|----|-----|----|-----|-----|-----|----|-----|----|-----|-----|-----|----|
| A | 30 | 410 | 30 | 30 | 40 | ND* | 8 | 70 | 30 | 170 | 329 | ND | 6 |
| B | 33 | 500 | ND | 60 | 100 | ND | 9 | 86 | 30 | 250 | 325 | ND | 6 |
| C | 70 | 370 | 40 | 80 | 200 | 150 | 11 | 97 | 40 | 200 | 310 | 110 | 7 |
| D | 60 | 500 | 40 | 100 | 150 | 90 | 17 | 155 | 90 | 280 | 550 | 140 | 15 |
| E | 80 | 400 | 50 | 80 | 190 | 210 | 21 | 263 | 60 | 360 | 650 | 175 | 21 |

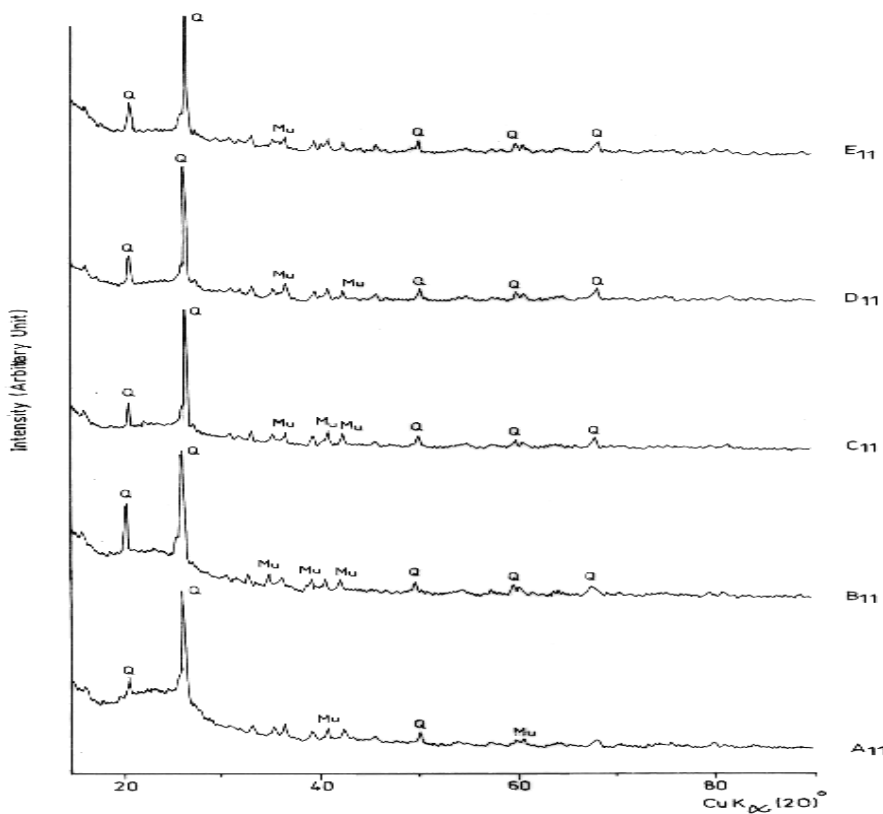


Fig.1: XRD patterns of non-magnetic fractions (A₁₁, B₁₁, C₁₁, D₁₁, E₁₁) of Dishergarh fly ash.
Mineral abbreviations: Q-quartz; Mu- mullite

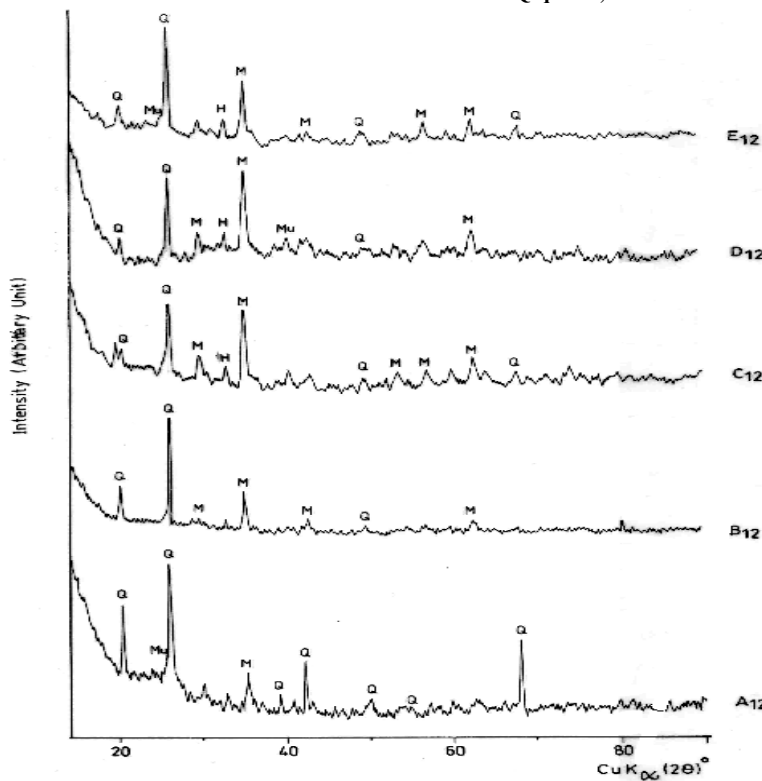


Fig.2: XRD patterns of magnetic fractions (A₁₂, B₁₂, C₁₂, D₁₂, E₁₂) of Dishergarh fly ash.
Mineral abbreviations: Q-quartz; Mu- mullite ; M-magnetite ; H- hematite

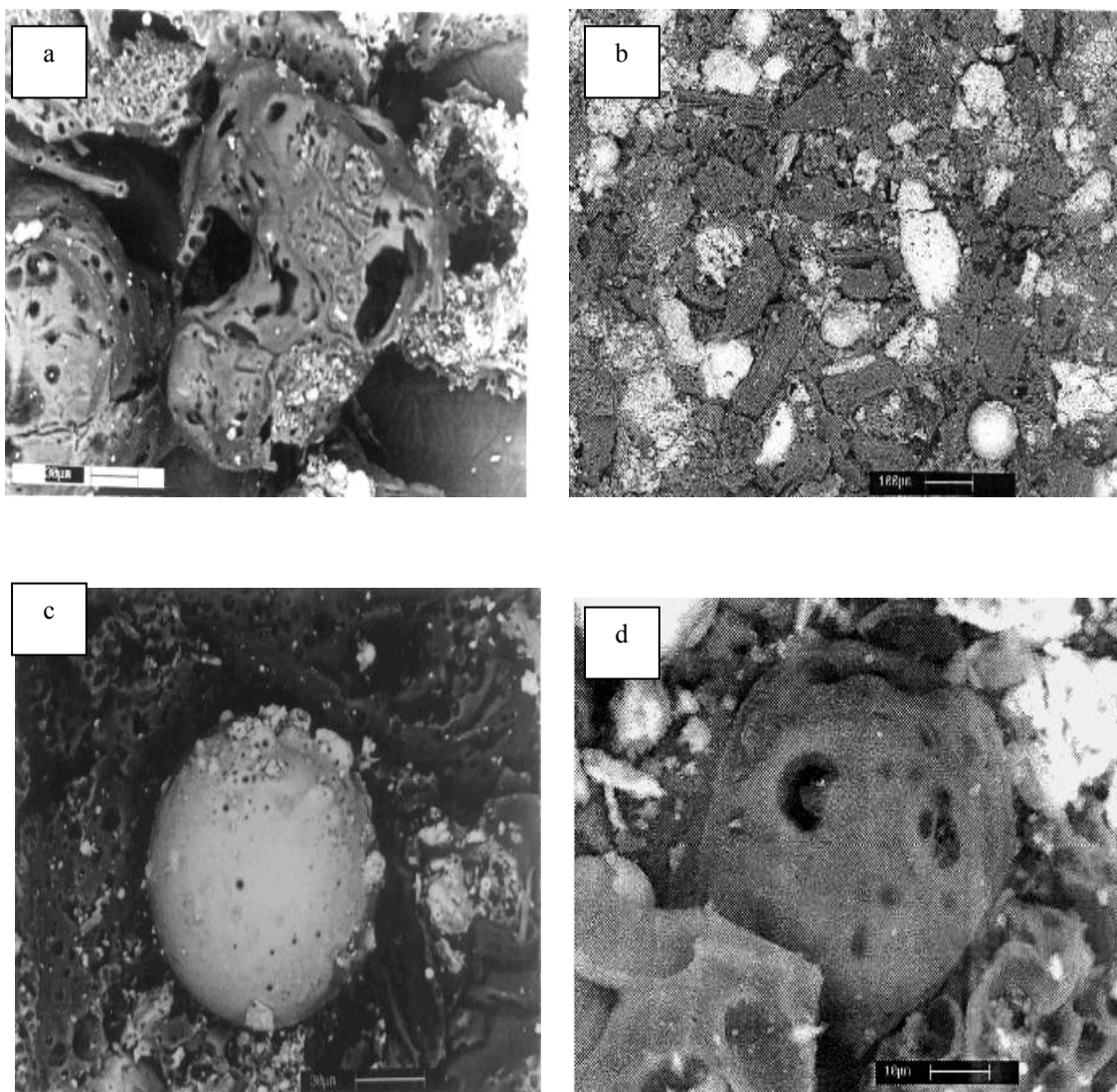


Fig.4: (A) SEM image of highly porous char from fraction A₁₁ (b) SEM image of a general view –non-magnetic component coarser fraction- A₁₁. Shale like particles can be observed (c) A cenosphere(open pore)from B₁₁ (d) Highly porous chars with interspersed alumino-siliceous particles can be observed from D₁₁.

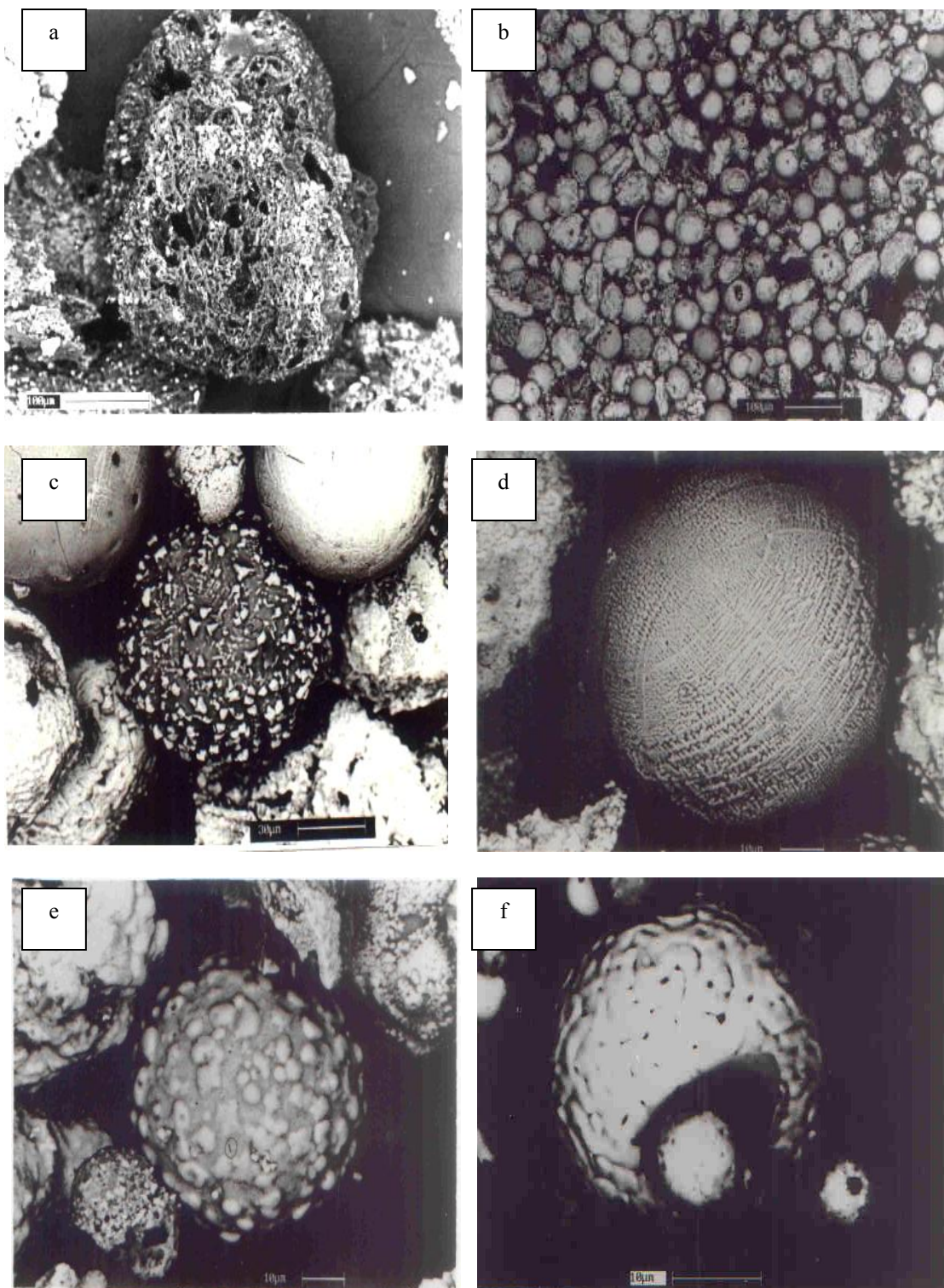


Fig.5: (a) SEM image of a general view –magnetic component coarser fraction (A₁₂). Particles are irregular in shape and size (b) A particle from A₁₂-highly porous sponge like surface is observed (c) SEM image of particles from B₁₂-smaller iron bearing crystallites are observed to be embedded on the surface. (d) A ferrospee from C₁₂-crystallite deposition has taken place in two different orientation, clearly signifying two different direction of rotatory motion during the formation stage. ‘Pine tree’ type of deposition of crystallites (e) A particle from C₁₂. Surface morphology indicates swelling of the surface material due to an attempt by the entrapped gas to expand (f) A big sphere embedded with a smaller sphere

Palm Vein Recognition and Verification System Using Local Average of Vein Direction

Asmaa M.J. Abbas and Loay.E. George

During the last years, hand vein patterns recognition is one of the most recent biometric technologies used for the identification/verification of individuals. The vein trace is hard to damaged, changed or falsified since veins are internal to the human body. In this paper a novel palm vein recognition and verification system is presented. The first step in the proposed system is image enhancement and localization of veins grid which is a major challenge due to poor quality of veins images. The second challenging task is the palm vein feature extraction. In this research the spatial distribution of local averages of veins direction is introduced and used as feature vector.

The system was tested over a database collected from 250 volunteers, where 24 images for the 2 palms are collected for each person. In total, a database contains 6,000 images belong to 500 different palms. The attained identification result is encouraging (99.95%). The verification tests indicated the achieved minimum equal error rate (EER) is 0.24%.

1. INTRODUCTION

The prime responsibility of any technological development, concerned with access control issue, is to provide a unique and secure identity for citizens, customers or stake holders, and it is a major challenge for organizations. There is an increasing interest for biometric in the research community since the traditional verification methods (such as passwords, personal identification numbers (PINS), magnetic swipe cards, keys and smart cards) offer limited security and are unreliable [Rao10].

Biometrics means "life measurement". A biometric system either makes identification or verifies an identity. It is based on the use of unique and measurable physiological or behavioral characteristics. Physiological characteristics include, but are not limited to, a person's vein patterns, facial structures, ocular characteristics, hand geometry, or fingerprint [Wil10].

Each kind of physical biometrics has merits and demerits. In the case of fingerprints, direct contact of the finger with the fingerprint-image-extracting sensor causes degradation in performance, where good-quality fingerprints are

hard to obtain due to oil from the finger, moisture, dirt,...etc. For retina scanning users must place their eye close to the scanner, causing an uncomfortable feeling and concerns of privacy. With hand-shape recognition devices, problems may arise with users who suffer from arthritis or rheumatism, leading to poor performance.

Compared with the other physical characteristics, vein pattern recognition is one of the newest biometric techniques were developed to resolve many problems facing the traditional biometric systems. The main reasons for adopting vein palm biometric techniques are:

1. The acquisition process of palm vein image needs no direct contact with the vein pattern-extracting sensor. Since contactless models are more hygienic than all forms of contact biometrics, so the user comfort is improved with use of vein imaging technology [Lee12].
2. Vein pattern does not change over time [Wan11b], and they can represent the liveness of a person [Zha07], so the cognition performance can be improved with use of vein imaging technology, and a stable operation is expected [Lee12].

3. Vein recognition technology is notably less costly than many of other biometric technologies (like, iris scanning technology) [Lee12]. In fact, the only biometric solution less expensive than palm-vein is fingerprint recognition but it has its own overheads on security feature [Rao10].
4. For the case of veins imaging, in addition the blood vessels are hidden underneath the skin and are mostly invisible to the human eye; the vein patterns are much harder for intruders to copy, and extremely difficult to steal/misuse compared to other biometric features [Hee09].

Hand veins biometric are robust and steady human authentication more than other biometric technologies so it is considered to be one of the most reliable biometrics for personal identification [Wan11b].

2.LITERATURE REVIEW

Many recognition and verification technologies using biometric features of hand veins have been developed over the few last years.

Heenaye and Ali [Hee09] introduced a veins recognition method based on quadratic inference function to extract the dorsal hand vein features. For matching task they used the Euclidean distance measure.

Wang and et al [Wan10] presented a new method based on Partition Local Binary Pattern (PLBP). After preprocessing, the image is divided into sub-images. A set of LBP uniform pattern features is extracted from each sub-image. Then, these sets are combined to form the feature vector for token vein texture features. Wang and et al [Wan11a] proposed a novel approach to extract multi-scale LBP features of hand vein images using wavelet decomposition. Wang and Chen [Wan11b] setup a creatively vein-image capturing system and presented a novel framework. It is composed of image enhancement, feature extraction, noise removal, thinning, skeletonization, and pruning for vein pattern extraction.

Liu and Zhang [Liu11] presented a new method palm recognition based on Two-Dimensional FLD (2DFLD). They applied PCA, PCA+FLD and 2DFLD algorithms to extract the palm-dorsa vein feature subspace.

Wang and et al [Wan12] introduced a novel method for hand vein recognition based on fusing multiple sets of key points extracted from the scale-invariant feature transform (SIFT).

Tang and et al [Tan12] proposed a novel approach for hand dorsa vein recognition; it makes use of multi-level key point detection and SIFT feature based local matching. Prabu and Sivanandam [Pra13] attempted to improve the performance of palm vein based verification system with the help of energy feature based on wavelet transform.

3.PALMVEINRECOGNITIONANDVERIFICATION SYSTEM

The layout of the proposed system is shown in Figure(1). It consists of three main modules: preprocessing, feature extraction and matching. Detail descriptions of the system modules are given in the following sections.

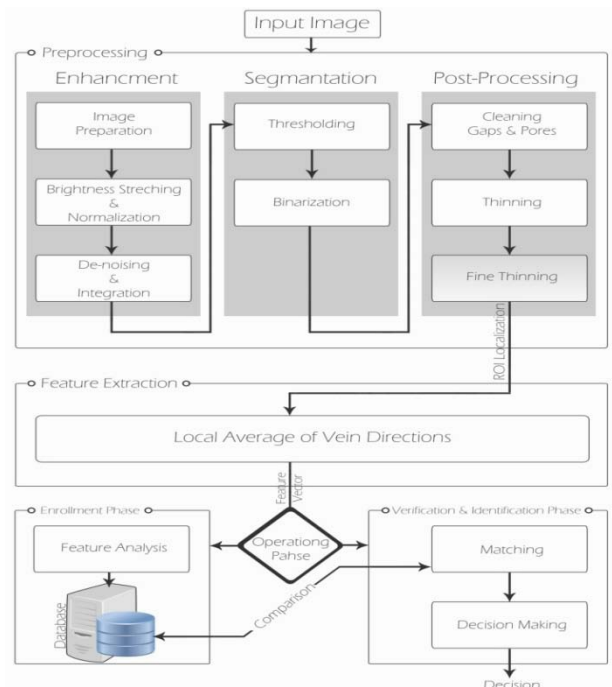


Fig.(3) The general structure of the proposed system

3.1 Preprocessing Stage

The performance of feature extraction algorithm relies heavily on the quality of the input images. In practice, the quality of the obtained raw images is very low because the images are blurred and noisy due to variations in environmental conditions, skin conditions, and acquisition devices, etc. A set of tasks are applied; they are necessary to improve the clarity of the vein pattern structure and localize the veins grid.

A. Image Enhancement

The purpose of this stage is to improve the imaging quality so that vein patterns can be more easily detected during the segmentation. This stage implies the following steps:

1. Image Preparation: The input image is converted to be 8-bit gray image. Then, it is converted to the negative which make the ROI as bright region.
2. Brightness Stretching & Normalization: A simple linear type of contrast stretching is applied to enhance the visual appearance of the image details. The dynamic range of pixels values is adjusted to be [0,1]. This process is done using the following equation [Nix12]:

$$N(x, y) = \frac{N_{\max} - N_{\min}}{O_{\max} - O_{\min}} (O(x, y) - O_{\min}) + N_{\min}$$

3. De-Noising & Integration: Despite the image is blurred, a simple mean smoothing filter is used to reduce the noise and to integrate the white ROI. Mean filter can lead to good result, when applying it in a specific way. The size of the applied mean filter is 7x7, and is applied four times to obtain an acceptable result, denoted $I_s()$.

B. Segmentation

Once the noise is reduced and the contrast enhanced, segmentation permits to separate the vein pattern from the background, it consists of the following tasks:

1. Thresholding: Because the images contain considerable background noise, and there is variation in contrast and illumination gradient.

So, the local thresholding mechanism is more suitable to be used than the global thresholding. In this project, the applied local thresholding process implies the following steps:

- Partition the image, $I_s()$, into small non-overlapped blocks, each has size (kxk).
- For each block, make a scanning window (with area nxn) covers the block area and extends to the surrounding area (i.e., n>k), see figure (2).
- Determine the mean (m) and standard deviation (σ) of the pixels values located inside the window (nxn).
- Then for each pixel belong to the scanned block (mxm) apply the following thresholding criterion:

$$I_{thr}(x, y) = \begin{cases} I_s(x, y) & \text{if } I_s(x, y) \geq m - \alpha\sigma \\ 0 & \text{otherwise} \end{cases}$$

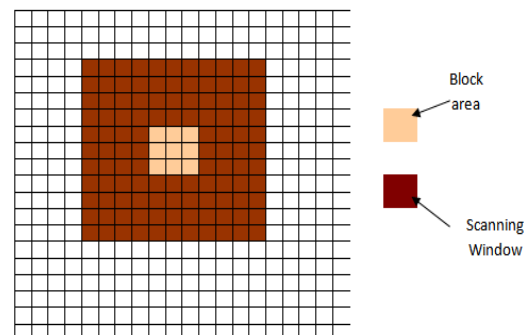


Fig.(2) The Scanning Block and Window Areas

In this project, the test results indicated that the setting (block size= 2x2, window size= 18x18 & multiplication factor $\alpha = 0.025$) led to best thresholding results.

2. Binarization: After applying local thresholding the produced vein image will have better background brightness, and in such case global thresholding becomes more suitable to do binarization. In our proposed system the following steps are adopted to do image binarization:

- Get the highest pixel value (Max) found in the threshold image.
- Map each pixel belong to threshold image using the following:

$$I'(x, y) = I_{thr}(x, y) \times \frac{255}{Max}$$

- Binarize the pixels values using the following criterion

$$I_{bin}(x, y) = \begin{cases} 0 & \text{if } I'(x, y) < T \\ 1 & \text{otherwise} \end{cases}$$

The test results indicated that the best value for T is 100.

C. Post-Processing

This stage was used to process the image after the segmentation, in order to reduce the effect of undesired elements such as noise, and improve the shape of the vein grid. It consists of the following steps:

A. Cleaning the Gaps and Pores: In this stage we need to reconstruct the vein image in order to improve the shape of the veins; this was accomplished by: (1) eliminating the small objects in the image; these objects are noise and parts of the background, they were classified as veins due to misclassification, (2) eliminating protrusions, (3) smoothing the contour of the objects (veins), (4) solving the problem of existence of regions containing mixed white and black pixels, (5) removing small holes, and (6) conserving the necks and slim parts of veins from breakage. When applying closing morphological operation on the veins images several defects may appear in the resulting images, like: (1) the small objects are kept and strengthened instead of removing them from the image, (2) when two veins are too close to each other they may linked, (3) misclassification may occur for the regions containing mixed white and black pixels, because such regions are always considered as veins. Because of the above reasons, the closing operation is not useful to improve the studied images.

The opening morphological operation gives more acceptable results than the closing operation for allocating the shape of veins in the image. It is used to remove small objects from the image without altering the overall shape and size of the large objects (veins

object). Also, its smooth the contours of the existing large objects. But when the traditional opening operation is applied on the veins images several defects appeared, like: (1) the vein in some places appears too skinny, or it may be narrow (like a neck) and due to traditional opening operation this part will disappear, (2) there are many regions in the vein image are mixture of white and black pixels; these regions may be parts of veins, parts of the background, or noise; they appear due to converting the image from gray to the binary. The traditional opening operation deletes all these regions without any consideration to the probability of being veins, (3) the holes are not removed from the veins regions. These defects significantly affect shape of veins grid.

For these reasons, a new algorithm is proposed to allocate and improve the shape of veins grid by cleaning the appeared gaps and pores from the image. This algorithm works to:

- Remove the small objects from the image.
- Smooth the boundary of veins (contour).
- Remove the small holes.
- Conserve the necks and slim veins regions from breakage defect.
- Take into consideration that the mixed regions could be part of the veins or not.

In the proposed algorithm the treatment of each pixel depends on its location. The applied steps of the introduced algorithm are:

1. For each corner pixel the algorithm counts the number of all the adjacent white pixels; then the pixel is treated depending on this number. There are two possible cases: For black pixel (i.e., 0): if the number is more than one, then the pixel is considered as gap and converted to the white pixel, otherwise it kept black. For white pixel (i.e., 1): if the number is zero then pixel is considered as pore point and converted to black, otherwise it is kept white.

2. For each pixel on the edge line the algorithm counts the number of all adjacent white pixels, then, the pixel is treated depending on this number. The number of white pixels. There are two cases: For black pixel (=0): if the number is higher than two, then the pixel is considered as gap point and converted to white, otherwise it is left black. For white pixel (=1): if the number is less than two, then the pixel is considered as pore point and converted to black, otherwise is left white.
3. For each pixel in the inner region: the algorithm counts the number of all the adjacent white pixels then the pixel is treated depending on this count value. The result depend on the value of the selected pixel, there are two cases: For black pixel (0): if the number is more than four, then the pixel is considered as gap point and converted to white, otherwise it is left black. For white pixel (1): if the number is less than four, the pixel is considered as pore point and converted to black, otherwise is left white.

B. Thining: The vein patterns could have different thicknesses due to physiological status of a person (for example, fatigue or non-fatigue) or it may due to the preprocessing operations. Therefore, vein thickness is not a stable pattern for recognition. So, the thinning operation is needed to ensure representation of veins objects that can correctly describe the main features like shape and connectivity.

A new thinning method is developed for more control to make thinning up to a certain width. The proposed thinning algorithm is designed to reduce the width of the pattern to five pixels width line. It will solve the problem of hand shift when taking its IR image. The algorithm tests only the white pixels in the image, either it decides to leave the pixel or convert it to black pixel (white pixels indicate vein and black pixels refer to background).

The introduced algorithm consists of the following steps:

1. Apply the mask, $M()$,on the selected pixel in order to find if the pixel is inside the vein area or not, this implies counting the number of the white pixels surrounding the tested white pixel; this is done by applying the following equation:

$$F_{out}(x, y) = \sum_{j=-2}^2 \sum_{i=-2}^2 I(x + i, y + j) M(i + 2, j + 2)$$

Where, $I()$ is the input image array, $M()$ is the used mask (in our system a 5x5 mask is used because the required vein width is five pixels), F_{out} is the number of the adjacent white pixels. All the mask's element values are "1", except the corner pixels they set "0". This mask is designed to make the output vein as smooth as the natural veins. If the value of F_{out} is more than 20 then the tested white pixel is considered as part of vein and left as it is; otherwise the algorithm applies the multi-directional checks on that pixel.

2. In this step, the thinning operation starts after applying the full area test and knowing that the specific pixel is not inside the vein. A set of multi-directional checks are applied on the tested white pixel to decide if the pixel has to be removed (i.e., convert the white pixel to black) in order to thin the vein segment. The multi-directional checking operations imply checking along the horizontal extent: for each tested pixel the algorithm scans the four neighbor pixels on both sides horizontally to check the existence of the four successive white pixels. Now, if the algorithm found these successive white pixels on one side or both sides it will start the vertical checking. Otherwise, the pixel is left as white pixel and considered as a part of vein skeleton. This task is repeated for other directions (i.e., vertical, main diagonal, and second diagonal).

3. Apply the gaps and pores algorithm twice.

4. The algorithm repeats its steps until the required thinning achieved. The proposed algorithm rounds are stopped when the following conditions satisfied:

$$\beta > \frac{M_2}{M_1} > \alpha$$

Where,

$$M_1 = \sum_{\forall y} \sum_{\forall x} I(x, y), \quad M_2 = \sum_{\forall y} \sum_{\forall x} I'(x, y)$$

5. Where, $I()$ is the input image array, $I'()$ is the image array after processing. In this project, the parameters values ($\alpha=0.985$ and $\beta=1.015$) led to the best skeleton result.

C. Fine Thining: The purpose of this stage is making better thinning for the veins body. More thinning can be achieved by applying the following steps:

1. Integration: In this stage, the integration process is applied to make veins thinner; this is done by increasing the brightness of vein's center, and reducing the brightness of the vein's sides. This step will give more characterization for the center of the veins.

The integration process works by opening a window (nxn) around each pixel and calculate the new value by applying the following equation:

$$I'(x, y) = \sum_{j=-r}^r \sum_{i=-r}^r I(x+i, y+j)$$

$$r = \frac{1}{2} (n-1)$$

Where, $I'()$ is the resulted integrated image, $I()$ is the input image and n is the window length.

2. Edge Normalization: now, the normalization process is applied to improve the intensity contrast between the center of veins and its sides. In this project, the applied normalization process consists of the following steps:

- For each non zero pixel, open a window (nxn) to determine the mean value (m) for all the pixels located inside the window. Then, the following thresholding criterion is applied:

$$I_{th}(x, y) = \begin{cases} I(x, y) & \text{if } I(x, y) \geq \alpha m \\ 0 & \text{otherwise} \end{cases}$$

In our applied system, when the window size is taken (3x3) and the multiplication factor α is set 0.25; it was found that the attained normalization is the best.

- Determine the new value using the following equation:

$$I_R(x, y) = \frac{1}{m} I_{th}(x, y)$$

Then find the global maximum pixel value (I_{max}).

- Calculate the normalization value for each pixel by applying the following equations:

$$I_{norm}(x, y) = Slp \times I_R(x, y)$$

$$Slp = \frac{I'_{max}}{I_{max} \times \alpha}$$

Where, $I_R()$ is the final process image array, $I_{norm}()$ is the edge normalized image array, I'_{max} is set 255, I_{max} is the maximum found pixel value, and ($\alpha=0.9$).

3. Binarization with Thinning: This stage aims to allocate the center of vein. In this stage, the gray image is converted to binary image to keep only the object of interest. Several global and local adaptive thresholding methods were investigated, and founded that these methods lead to lose some parts of the veins.

In the proposed method each non-zero pixel in the image is compared twice with its four adjacent pixels. In the first check, the pixel is compared with the left and right pixels; and in the second check, it is compared with the up and down pixels, then by applying the following criteria the pixel is binarized:

$$I_{bin}(x, y) = \begin{cases} 1 & \text{if } (I(x-1, y) \leq I(x, y) \geq I(x+1, y)) \\ & \quad \text{or } (I(x, y-1) \leq I(x, y) \geq I(x, y+1)) \\ 0 & \text{otherwise} \end{cases}$$

Where $I()$ is the input gray image after normalization and $I_{bin}()$ is the output binary

image. Figure (3) presents an illustration for the preprocessing stage.

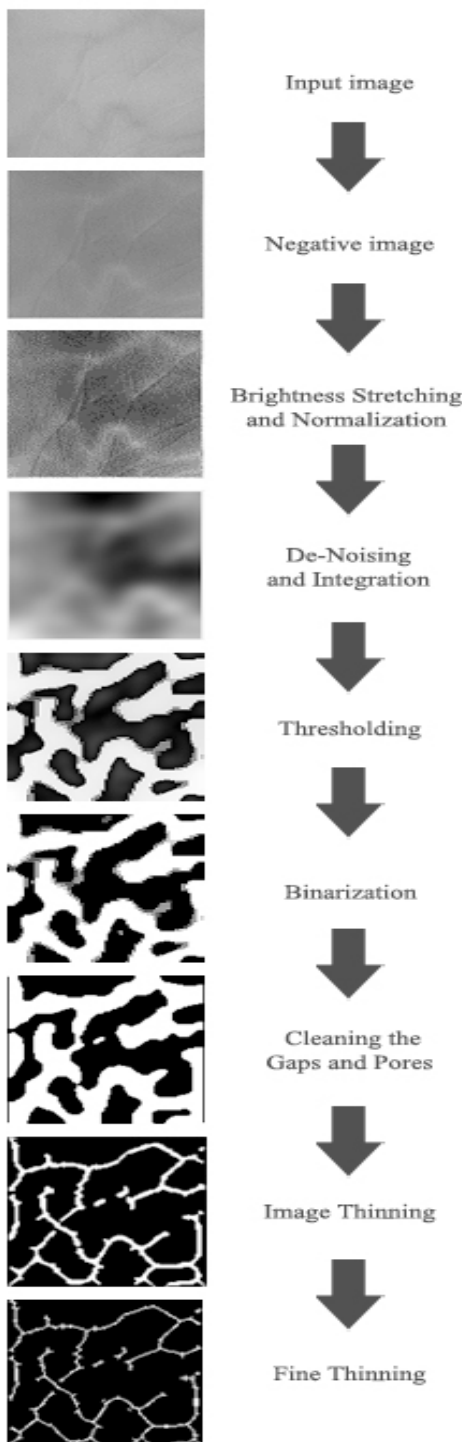


Fig (3) Illustration for the outcomes of preprocessing stage

required features to distinguish between persons. The local average of veins directions method is proposed as discriminating veins grid features.

The benefits of this method are: (1) it is applicable in spatial domain and reflects the directionality of veins tracks, and (2) it is indirect measure to the distribution of veins density in each parts of image. So, this set of features depends mainly on the distribution of vein's directions at different parts of the image.

The following steps have been applied to extract the features vector:

1. Determine the direction of each vein pixel in the image; that is by checking if the pixel is located in the vein body along the horizontal, vertical, main diagonal or second diagonal direction. This is done by checking all the connected pixels, surrounding the tested pixel, along the four directions and to count the extent of these pixels. Then, the longest extent is taken as the local direction of the vein at the tested pixel location.
2. The resulting 2D-array of vein direction is divided into blocks.
- 3.

The average of local directions is determined for each block, separately; and the determined average values for all blocks are assembled as a feature vector. Four features extracted from each block, that is the densities of the (i) vertical, (ii) horizontal, (iii) main diagonal, and (iv) second diagonal veins direction. Each of these direction features is calculated by counting the number of pixels which have that direction, and then dividing it by the total number of veins pixels. Figure (4) presents an example of pixel with second diagonal feature.

3.3 Feature Extraction

In this stage, a set of key information is extracted from the final processed vein's image. The extracted information represents the set of

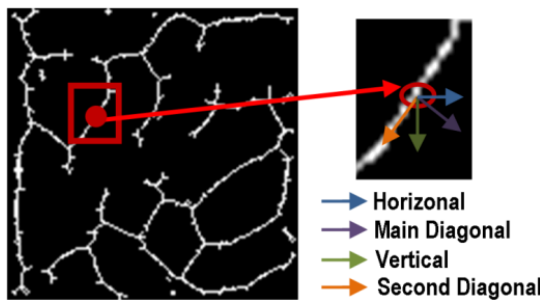


Fig. (4) Example of pixel with second diagonal feature

3.4 Matching Stage

This stage calculates the degree of matching between two vein patterns. The extracted vein patterns of the input image can directly be compared with the stored templates. A similarity measure should be used to evaluate the similarity degree between a template and an input pattern.

In this work the two Euclidean similarity measures (i.e., mean square difference and the mean absolute difference; called city block distance) have tested to evaluate their suitability for matching the veins feature vectors.

4. EXPERIMENTAL RESULTS

The performance of the proposed system was tested using a database collected from 250 volunteers, including 195 males and 55 females. The age distribution of volunteers is from 17 to 60 years. The samples are collected in two separate sessions. In each session, the subject was asked to provide 6 images for each palm. Therefore, 24 images of each volunteer are collected, 12 of them for each of his/her 2 palms. In total, the database consists of 6,000 images taken from 500 different palms. The average time interval between the first and the second sessions was about 9 days. The proposed method have used the near-infrared (NIR) illuminations images of PolyU multi-spectral palm print database[PolyU].

The results of the conducted tests are described in details in the following subsections.

4.1

veins Localization Results

To achieve an efficient performance for vein recognition and verification, veins grid must be

extracted correctly. The localization of vein can be subjectively evaluated by matching the extracted vein grid with the veins network that can be seen in the original image. Figure (5) presents the final vein localization image for one person and his image after projecting the vein localization on the enhanced original images (note: the original images have been modified for the purposes of assisting the subjective comparison task).

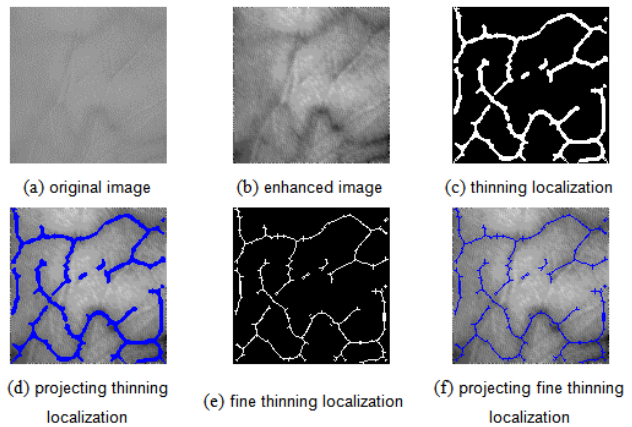


Fig.(5) Final vein localization image for one person

4.2 Identification (Recognition) Results

In the identification mode, the system performance is measured using the parameter correct recognition rate (CRR); it is the ratio of the number of samples being correctly classified to the total number of tested samples.

There is a set of system parameters that affect the recognition performance behavior, the main affecting ones are :

- Number of blocks (ROI divided into NxN block).
- The ratio of the overlapped blocks.

The recognition rate is determined for the two cases: (i) apply thinning only, and (ii) apply fine thinning. The Euclidean distance and City Block distance are used to measure the similarity between features vector. Table (1) lists the attained recognition values for different number of blocks.

Table (1) Recognition rate versus the number of blocks

| No. of Blocks | Recognition Rate | | | |
|---------------|------------------|---------------|--------------------|---------------|
| | With Thinning | | With Fine Thinning | |
| | Seq. Distance | Abs. Distance | Seq. Distance | Abs. Distance |
| 4x4 | 85.65% | 85.65% | 95.25% | 95.90% |
| 5x5 | 95.35% | 95% | 98.15% | 98.65% |
| 6x6 | 98.55% | 98.35% | 99.30% | 99.60% |
| 7x7 | 99.35% | 99.30% | 99.60% | 99.80% |
| 8x8 | 99.75% | 99.70% | 99.80% | 99.80% |
| 9x9 | 99.75% | 99.80% | 99.90% | 99.95 |
| 10x10 | 99.65% | 99.55% | 99.75% | 99.85% |

The table shows that the recognition rate is improved when adding the fine thinning stage. Also, according to the blocks number parameter, the best recognition rate is achieved when dividing the image into 9x9 blocks, while the second best result came when dividing the image into 8x8 Blocks.

4.3 Verification (Authentication)

The performance of verification system is evaluated by the Receiver Operating Characteristic (ROC) curve, which illustrates the False Rejection Rate (FRR) against the False Acceptance Rate (FAR) at different thresholds on the matching score[Zha10]. The performance is also evaluated by the Equal Error Rate (EER), which is defined as the error rate where the FAR and the FRR are equal. The EER indicate the minimum verification error. So, the threshold value is selected according to the minimum error.

The FAR and FRR are defined, respectively, as[Mer13]:

$$\text{FRR} = \frac{\text{Number of rejection genuine}}{\text{Total number of genuine access}} \times 100\%$$

$$\text{FAR} = \frac{\text{Number of accepted imposter}}{\text{Total number of imposter access}} \times 100\%$$

Also the performance of biometric systems can be measured by accuracy; i.e., the proportion of correct predictions, without considering what is positive (P) and what is negative (N) [Pol11].

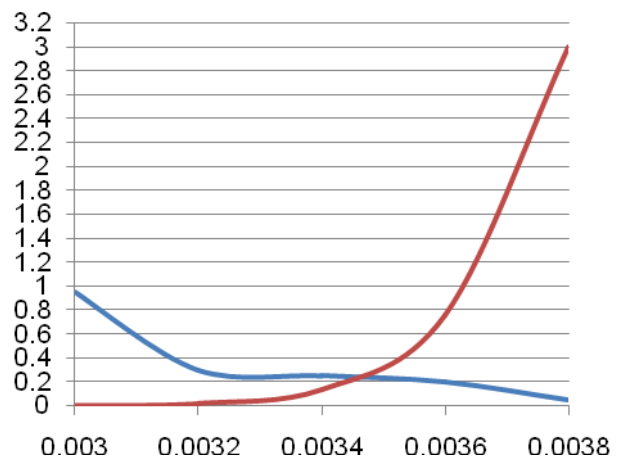
$$\text{Accuracy} = (\text{TP} + \text{TN}) / (\text{P} + \text{N})$$

Table (2) shows FAR, FRR and Accuracy values with different threshold.

Table (2) FAR,FRR and accuracy versus different threshold

| Threshold | FRR% | FAR% | Accuracy% |
|-----------|------|---------|-----------|
| 0.003 | 0.95 | 0.00125 | 99.997 |
| 0.0032 | 0.3 | 0.01688 | 99.982 |
| 0.0034 | 0.25 | 0.1366 | 99.863 |
| 0.0036 | 0.2 | 0.7622 | 99.238 |
| 0.0038 | 0.05 | 2.9963 | 97.006 |

The ROC curve between the FAR and FRR with various thresholds is shown in Figure (6). Equal error rate (EER) is the point where FRR is equal to FAR. Our ROC curve shows that the EER point equals to 0.24% at the threshold value equals to 0.00348.

**Fig.(6) The ROC curve for the local average of Veins Directions**

4.4 Time Results

Another performance parameter in the recognition system is the time. The time details of the best achieved recognition rate are shown in table (3).

Table (3) Execution time

| Stage | Time (msec) |
|--------------------|-------------|
| Preprocessing | 1.704 |
| Feature Extraction | 170.14 |
| Matching | 158.415 |
| Total | 330.25 |

4.5 Comparison with Published Results

Many vein recognition methods have developed and published. Here, we give a comparison between the performance of our

proposed method and some the published methods.

Table (4) presents the recognition(CRR)and verification(EER) results. These results demonstrate that the proposed method outperforms the other methods.

Table (4) Performance comparison of several methods

| Method | Dataset | Performance | | Time |
|-----------------|--|--------------------|------------|-------------|
| | | CRR | EER | |
| [Wan10] | 2040 images 102 individuals | 98.14% | NA | NA |
| [Wan11a] | 2040 hand images, 102 individuals | 99.02% | 2.067 % | 0.368s |
| [Wan11b] | 10 images for left, and for right hand, 25 persons | 93.4% average | NA | NA |
| [Liu11] | 500 images. 50 persons | 98.44% | NA | 0.4s |
| [Wan12] | 2040 images with 10 for each hand, 102 person | 97.95% | NA | NA |
| [Tan12] | Both 10 right and left hand 102 subjects | 98.04% | NA | NA |
| [Pra13] | NA | 96.66% | 0.73% | 0.121s |
| Proposed method | 6,000 images from 500 palms, 250 persons | 99.95% | 0.2% | |

5.CONCLUSIONS AND FUTURE WORK

In this work, we have proposed a reliable palm vein recognition and verification system. The proposed method to enhance the image and veins localization shows a high performance to extract the veins network, even though the vein images have poor-quality and suffer from many problem (blurry, noisy, etc..). Also, anew algorithm for

feature extraction is proposed; it depends on the local average of veins direction.

The experimental results show that our system achieved high recognition rate 99.95%, and EER =0.24% which indicate high performance in verification. The total recognition time is around 0.33ms; which is fast enough for real time applications.

At present, the proposed system can be applied to various parts of the human body where the veins are accessible (like: Finger, wrist, and etc). The quality of image data is vital for the application; hence more work is needed in the data preprocessing stage. So, the current image enhancement methods can be improved to provide better enhancement results with lower complexity and time. Finally, attempts shall be made to integrate the vein pattern biometrics with other types of biometrics to become a multi-modal biometric system. And the candidate biometric technologies under current research include hand geometry and palm-print recognition.

REFERENCES

- [Hee09] Heenaye- Mamode, M., Mamode, N. Ali., “A New Method to Extract Dorsal Hand Vein Patternusing Quadratic Inference Function”, International Journal of Computer Science and Information Security, Vol. 6, No. 3, 2009.
- [Liu11] Liu, J., Zhang, Y., “Palm-Dorsa Vein Recognition Based on Two-Dimensional Fisher Linear Discriminant”, IEEE, 2011.
- [Lee12] Lee, J.-C., “A novel biometric system based on palm vein image“, “Pattern Recognition Letters”, Elsevier B.V., Pp. 1520–1528, 2012.
- [Mer13] Merouane, A., Benziane, S., Boulet, P., Benyamina, A. E.- H., Loukil, L., “Hybridization of Discrete Binary Particle Swarm Optimization and Invariant Moments for Dorsal Hand Vein Feature Selection”, IEEE, 2013.
- [Nix12] Nixon, M., and Aguado, A., “Feature Extraction & Image Processing for Computer Vision”, Third Edition, Academic Press,2012.
- [Pol11] Polli, R. M., Maran, A. V., Jouglas, A. T. Z, Silva E., Brandi, P. S., Hass D. I., “A

- proposal for the Hand Palm Identification, using Local Binary Pattern”, International Journal of Advanced Engineering Sciences and Technology (IJAEST), Vol. 9, Issue 2, Pp. 302 – 309, 2011.
- [Pra13] Prabu, S.M., Sivanandam, S.N., “A Novel Biometric system for Person Recognition Using Palm vein Images”, International Journal on Computer Science and Engineering (IJCSE), Vol. 5, No. 08, Aug 2013.
- [PolyU] Multispectral PolyU database,
ww4.comp.polyu.edu.hk/~biometrics/.
- [Rao10] Rao, T. V., Preethi, K., “Future of Human Security Based on Computational Intelligence Using Palm Vein Technology”, Global Journal of Computer Science and Technology, Vol. 10, Issue 10, Pp. 68-73, 2010.
- [Rao10] Rao, T. V., Preethi, K., “Future Of Human Security Based On Computational Intelligence Using Palm Vein Technology”, Global Journal of Computer Science and Technology, Vol. 10, Issue 10, Pp. 68-73, 2010.
- [Tan12] Tang, Y., Huang, D., and Wang Y., “Hand-dorsa Vein Recognition based on Multi-level Keypoint Detection and Local Feature Matching”, 21st International Conference on Pattern Recognition (ICPR),pp. 2837-2840, 2012.
- [Wan10] Wang, Y., Li, K., Cui, J., ”Hand-dorsa Vein Recognition Based on Partition Local Binary Pattern”, IEEE, 2010.
- [Wil10] Wilson,C.,”Vein Pattern Recognition”, Taylor and Francis Group, 2010.
- [Wan11a] Wang, Y.-D., Yan, Q.-Y., Li, K.-F., “Hand Vein Recognition Based on Multi-Scale LBP and Wavelet”, IEEE, 2011.
- [Wan11b] Wang, J.-W., Chen, T.-H., ‘Building Palm Vein Capturing System for Extraction”, IEEE 21st International Conference on Systems Engineering, 2011.
- [Wan12] Wang, Y., Fan Y., Liao, W., Li, K., Shark, L.-K., Varley, M. R., “Hand Vein Recognition Based On Multiple Keypoints Sets”, IEEE, 2012.
- [Zha07] Zhang, Y.-B., Li, Q., You, J., and Bhattacharya, P., “Palm Vein Extraction and Matching for Personal Authentication”, Springer-Verlag Berlin Heidelberg, Pp. 154-164, 2007.
- [Zha10] Zhang, H., Hu, D., “A Palm Vein Recognition System”, IEEE, 2010.

Inter comparison of classification techniques for vowel speech imagery using EEG Sensors.

Anaum Riaz
 National University Of Sciences and Technology (SEECS) Islamabad, Pakistan
anaumriaz@yahoo.com

Sana Akhtar
 National University Of Sciences and Technology (SEECS) Islamabad, Pakistan
sanakhtar02@gmail.com

Shanza iftikhar
 National University Of Sciences and Technology (SEECS) Islamabad, Pakistan
09beesiftikhar@seecs.edu.pk

Amir Ali Khan
 National University Of Sciences and Technology (SEECS) Islamabad, Pakistan
amir.ali@seecs.edu.pk

Ahmad Salman
 National University Of Sciences and Technology (SEECS) Islamabad, Pakistan
ahmad.salman@seecs.edu.pk

Abstract: The use of Electroencephalography (EEG) in the domain of Brain Computer Interface is a now common place. EEG for imagined speech reproduction and observation of brain response to audio stimuli are active areas of research. In this paper, we consider the case of imagined and mouthed non-audible speech recorded with EEG electrodes. We analyze different feature extraction techniques such as Mel Frequency Cepstral Coefficients (MFCCs), log variance Auto Regressive (AR) coefficients. Based on these extracted features, we perform a pairwise classification of vowels using three different classification models based on Support Vector Machine (SVM), Hidden Markov Models (HMM) and k-nn classifier. The proposed methodology is applied on four different data sets with some preprocessing techniques such as Common Spatial Pattern (CSP) filtering. The data sets principally comprised of either mouthing or solely imagining 5 vowel sounds without speaking or making any muscle movement. The goal of this study is to perform an intercomparison of different classification models and associated features for pairwise vowel imagery. The proposed approach is validated on different data sets and offer reasonable accuracies for pairwise classification.

Index terms—Speech imagery, HMM, SVM, k-nn, MFCC, AR

I. INTRODUCTION

Speech processing has long been an area of central importance in the signal processing community. Likewise, lot of attention and resources are being focused in biomedical signal and image processing domain. The current work falls into the category of speech processing for biomedical applications. Speech is one of the most vital communication tools of a human and partial or complete loss of audible speech may be an impediment to effective communication. Some of the major causes of this impairment include cerebral palsy, laryngeal cancer, Laryngectomy and hyper laryngeal cancer. The net result is the loss of interconnectivity between the brain and the speech production unit or the damage/removal of the unit

itself. Patients suffering from the speech production disorder are rehabilitated through different methods which include esophageal, tracheoesophageal and electromechanical speech [1]. While these methods are common and prefer for certain cases, they are not always very effective and may require invasive medical procedures. New and improved technologies are needed to provide a more efficient communication alternative for the speech impaired individuals. Silent speech interfaces offer one such alternative, whereby a speech signal is produced from an unintelligible signal by processing different non-audible speech attributes such as murmur, facial movement, and imagined speech.

While the idea of silent speech interface existed since the seventies, the first commercial systems started to appear in the late eighties such as the one developed in Japan [1]. A very concise historical background appears in Denby et al.[3]. Several types of sensing mechanisms have been developed to capture pertinent attributes for non-audible acoustic signal. Some of the concurrent systems include: ultrasound and optical imaging, non-audible murmur microphone based speech reproduction, interpretation of signals from brain using electro-encephalographic (EEG) sensors, Electromagnetic Articulography (EMA) sensors and larynx or muscular articulation using surface mounted Electromyography (sEMG) sensors [3].

The current work focuses on EEG recordings where different experiments are conducted using imagined and mouthed vowels. EEG has seen tremendous development in the areas of Brain Computer Interface (BCI) as well as epileptic seizures [4]-[5]. Most of the focus of EEG has been on the applications requiring external stimulus. The current work falls in the domain of speech synthesis through thinking procedure only. In this work, we perform imagination and mouthing tasks for vowels without producing audible speech signal. Different experimental setups were used in this study, details of which will be discussed in the next section.

II. EXPERIMENTAL SETUP

The main target of this work is speech imagery (imagined speech) but we started our work with mouthing of words to

facilitate the process understanding and analysis. In this context, we will present the results for both imagined and mouthed speech. Overall, we will consider four data sets in this study with two each for imagination and mouthing tasks.

Data Set I is the free source data set made available by DaSalla et al [6]. The data were acquired with 64+8 active Ag-AgCl electrodes and a sampling rate of 2048 Hz. The three tasks considered were the imagination of the vowels /a/, /u/ or control state. The experimental protocol is illustrated in Figure 1. At the start of the experiment, visual cues appeared on a screen placed at a distance of approximately 1 m from the subject. An audible beep along with the fixation cross marked the start of each trial which was followed by imagination of one of either /a/, /u/ or control state. The control state here refers to a state of no thinking whose time was empirically chosen to be from 2-3 seconds. The purpose of this was to remove the influence of any evoked potential before starting the tasks.

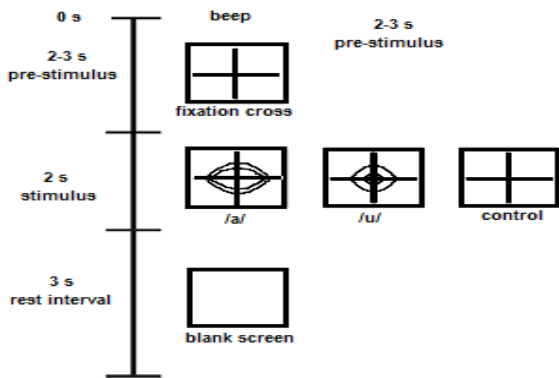


Figure 1: Experiment Paradigm used by DaSalla et al [6].

The second experiment was carried out by the authors using a Nihon Kohden EEG-1100 system with 20 electrodes at a sampling rate of 500Hz. Data were recorded for two subjects (one male and one female) with the recording starting once the subjects are well settled. Five tasks were performed for each subject which included: vowel [a]: mouthing of the sound of vowel (/a/); vowel [i:] : mouthing of the pronunciation ‘ee’; vowel [ai] : mouthing of ‘I’ as in ‘ice’; vowel [o]: mouthing of vowel o (/o/) as in sold and vowel [u:]: mouthing of vowel u (/u/) as in ‘blue’. The subjects were briefed before the experiment on how to mouth the words and about movement restrictions. The timing of different events for the experimental protocol is demonstrated in Figure 2

Visual cues appeared on a PC placed at a distance of a meter from the subject. An audible beep appeared along with the fixation cross which is followed by mouthing of one of the tasks, i.e., a, e, i, o or u. The initial fixation cross allowed the user to blink and to gather concentration. Fifty trials were performed for each task per subject, resulting in a total of 100 trials per task. This data set is here after referred to as DataSet 2.

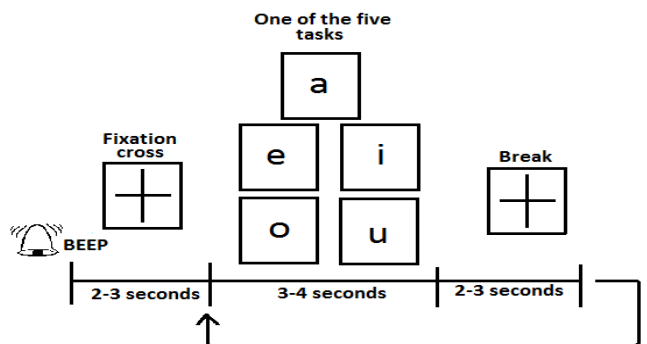


Figure 2: Experimental protocol for EEG signal acquisition for the Data Set II.

A third dataset was recorded by considering only the electrodes that carry significant information. For this experiment, a cascade of four 2-channel ML4856 PowerLab 26T system was used to obtain 8 channels simultaneously. The purpose of this experiment was to study if reasonable results could be obtained with limited number of electrodes. However, the positioning of these electrodes was carefully chosen to tap the most active brain areas for the tasks at hand. The experience with the Dataset 2, where we had 20 electrodes, became handy in this regard. Recordings were done on two female subjects as they performed one of the five tasks similar to the DataSet 2 (see Figure 2). Same experimental protocol as Data Set 2 was used for this experiment.

A total of fifty trials were performed for each task per subject, resulting in a total of 100 trials per task. Figure 3 shows the top view of the brain and the possible electrode placement. The eight electrodes that were used for this experiment are marked with the solid rectangular boxes. The left mastoids were used as reference and the sampling frequency was 400 Hz. The positioning of the electrodes was done using head cap with 10-20 international system. The data acquired during this experiment is hereafter referred as DataSet 3.

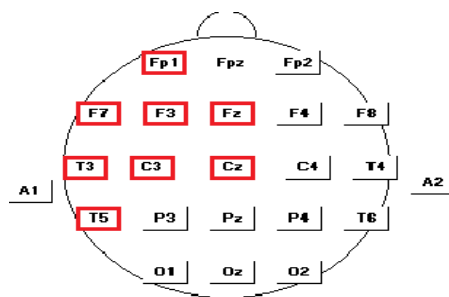


Figure 3: The top view of the electrode placement on the scalp. The eight electrodes used in this experiment are marked with solid rectangles.

As a final experiment, the same experimental protocol as for DataSet 3, in terms of the event timings and the electrode placement, was used. However, instead of

mouthing the vowels, this experiment was based completely on imagination. This dataset will be mentioned as Dataset 4 in this text.

III. PROPOSED METHODOLOGY

Brain signals acquired through EEG are categorized as alpha, beta, delta, theta and gamma waves [7]. These waves are divided into different frequency bands and are linked to behavioral state of the subject. The frequencies of our interest lie in alpha and beta waves (8-40 Hz), which correspond to awake, relaxed and attentive states. The proposed methodology is described by the block diagram of Figure 4. The raw recorded data is influenced by the power line frequency and its harmonics. The very first stage, thus, involves filtering of the raw data by a band pass filter (8-40 Hz). The filtering removes the noise and allows selection of only the desired frequency band. The selection of this frequency band is important for the feature extraction and modeling blocks that follow in the processing chain.

The filtered data for each subject and each trial is a multi-dimensional time series, $\Re^{N_t \times N_x}$, where N_t corresponds to the total number of samples (time), and N_x to the total number of channels (electrodes). In order to extract information from the most relevant channels only, the channel selection is applied. The purpose is to achieve a reduction in dimensionality before feature extraction. The principal channel selection technique deployed is Common Spatial Pattern (CSP) filtering [6]. Common spatial pattern filtering is a matrix filtering technique which maps a multi-channel high dimensional EEG data into a low-dimensional subspace. The variances of the resulting time series across different channels are maximally discriminative. The algorithm is based on simultaneous diagonalization of the covariance matrices for pairwise classification tasks. The details of the algorithms are presented in [6]. For each pair of tasks, we have two $N_t \times N_x$ data matrices for each trial. The overall computations involve calculation of a composite covariance matrix as the sum of average (across all trials) covariance matrix for each task in the pair. The whitening transformation is then applied to this composite matrix for decorrelation purposes followed by selection of 4 most significant filters (on the basis of Eigen values. It should be mentioned that channel selection can be an optional module as some of the models used in this work such as Hidden Markov Model (HMM), discussed later, works well without this channel reduction.



Figure 4: Proposed methodology for characterization of the vowel speech imagery.

The direct processing of raw data through models and classifiers does not reveal interesting results. This is because the attributes that we are looking for are not well characterized in the raw time series. Some transformation to the data is usually applied to extract the most relevant attributes (features) for a given application. Speech processing being a widely researched area, different features exists in literature [4]. For our application, we tested the popular features such as signal energy (rms value), variance, Short Time Fourier transform, entropy, Mel Frequency Cepstral Coefficients (MFCCs) and Auto regressive (AR) features. The best performing features for our data sets were MFCCs. MFCCs are widely used in the speech processing community [8]-[9] and have been deployed for numerous applications. Nguyen et al. [4] demonstrated that EEG signals can be considered stationery for relatively small time windows [9]. Since we are representing the speech imagery problem through EEG data acquisition, similar features can be used for our application [4]. The MFCC algorithm also computes the Cepstral coefficients, delta and delta-delta coefficients. The results were optimized for 12 MFCC coefficients. Once the relevant features have been extracted from the data set, we pass these features to a classifier. Different approaches exist in signal processing and machine learning community for achieving this classification, both supervised and unsupervised. In this work, we used three different supervised classification approaches with a goal to compare their relative accuracies for our application. The tested approaches include classifiers based on the Support Vector Machine (SVM), the Hidden Markov Model (HMM) and the k-nearest neighborhood (k-nn) classifier.

their relative accuracies for our application. The tested approaches include classifiers based on the Support Vector Machine (SVM), the Hidden Markov Model (HMM) and the k-nearest neighborhood (k-nn) classifier. The supervised classification was utilized because we had a relatively significant number of trials for each task. Support Vector Machine is one of the most widely used tool in supervised classification[10]. It models the decision boundary for class separation as a hyper plane. It involves mapping into a high dimensional feature space based on a kernel. The two popular kernels are the linear basis and the radial basis functions. We experimented with both the radial and the linear basis functions. The linear basis function allowed a better separation because of the pre-processing by CSP and the nature of the features used, i.e. MFCCs. Hidden Markov Model (HMM) is a very popular tool for pattern matching and speech processing applications [11]. As a mixture model, it involves modeling the system in terms of latent variables which are related through the Markov processes. The main parameters of the model are the number of the hidden states, the state transition probabilities, the number of possible output observations and the output probabilities. The specific parameters used in this study will be discussed in the results section. The third model that we use for this study is the k-nearest neighborhood (k-nn) classifier, based

on the calculation of centroids for the k classes during the training and subsequent association of a test data set to one of these classes. A comparative analysis of the three models for four different data sets is performed in the next section with an aim to characterize the best possible model.

IV. RESULTS AND DISCUSSION

In this section, we present the results achieved with different models for the four datasets discussed earlier. SVM was used with the prior application of CSP for channel dimensionality reduction. k-nn was used with CSP as initial pre-processing for channel reduction. The feature extraction step in this case is followed by Principal Component Analysis (PCA)/Linear Discriminant Analysis (LDA) for avoiding the curse of dimensionality in the case when the size of training data set is small [11]. Hidden Markov Model in left-right configuration was used with different number of HMM states (5, 6, 7, 8, 9, 10) and number of Gaussians per states (16, 32, 64). The optimum parameters depend on the pair of words and the type of equipment from which we acquired data. Model for each vowel was estimated using Baum-Welch algorithm. For testing of the tasks, Viterbi Algorithm was used to trace the most probable state sequence. The most significant results were obtained using the MFCC as feature vectors and we restrict ourselves to the presentation of these results here. In all the cases, 40% of the available data set was used for training purposes and 60% for the testing purposes.

The Dataset I was made available by DeSalla et. al. after pre-processing by CSP [6]. They had used variance in the recorded time series as their principal feature and SVM as their classification tool with a reported average accuracy of around 68% to 78%. Table I presents the results obtained through the proposed methodology using different models. While, the results of all the models represent an improvement over the reported results, the k-nn classifier seems to be outperforming the other two especially for subjects 2 and 3. Although, SVM appears to be the best candidate for subject I, k-nn runs very close.

Table I: Comparison of pairwise classification results for the DataSet 1 using MFCC as feature vectors.

| Subject | Classifier | A /Rest | U/Rest | A/U |
|-----------|------------|-------------|-------------|-----------|
| Subject 1 | SVM | 95 | 82.5 | 80 |
| | HMM | 72.5 | 90 | 75 |
| | k-nn | 90 | 92.5 | 77.5 |
| Subject 2 | SVM | 77.5 | 72.5 | 65 |
| | HMM | 70 | 65 | 67.5 |
| | k-nn | 72.5 | 90 | 99 |
| Subject 3 | SVM | 70 | 65 | 75 |
| | HMM | 70 | 62.5 | 62.5 |
| | k-nn | 62.5 | 99 | 99 |

The results for the DataSets 2-4 are demonstrated in Table II-Table IV.

Table II, which represents the mouthed data, reveals HMM as best performing model because of its probabilistic nature and its complexity. Reasonable accuracies for the pairwise classification of vowels are obtained in each case with the best separation between the vowels /A and /I and /E and /U. The average accuracy for this dataset is around 75% for Subject I and around 68% for the Subject II. It is difficult to ascertain this variance among the two subjects but initial investigation points to the concentration levels of the two subjects. SVM fails miserably in this case, with accuracies at times even falling below the chance probability. The results of the DataSet 3 (Table III), again using the mouthing protocol, gives mixed results in terms of the best classifier for the task and an average accuracy of around 75% is obtained. However, the classification variance across different pairs is relatively very high. Although, the current work focused on pairwise classification, we are working for extending it beyond a binary classification problem. Finally, Table IV presents the results for the completely imagined set of vowels. The tasks were performed across a single subject in this study, where HMM and k-nn show reasonably good performance. Average accuracies of around 75% are obtained across different pairs for HMM and k-nn models. SVM does not give encouraging results in this case.

We also tested the Autoregressive (AR) features and obtained reasonable results with the HMM. However, their accuracy was slightly lower than the MFCC based feature extraction discussed in this paper.

I. CONCLUSION

Through this research, we sought to expand the research in the domain of speech imagery through EEG signals with the interest of testing different feature extraction and classification models. We proposed the use of three classifiers SVM, k-nn and HMM for the supervised pairwise classification of vowels. The principal features used were the MFCC coefficients. The proposed methodology was validated on 4 different data sets, with a free source reported data set used for comparison purposes. This study also allowed us to test different speech imagery protocols such as the mouthed and the imagined speech. Overall, we achieved accuracies around 75% for pairwise classification with certain pairs giving even better accuracies. We also tried to identify the principal electrodes and their physical significance. The detailed results will be shared elsewhere. In brief, we found that out of the 20 channels (electrodes), six or seven were enough to give good classification results. These prominent electrode positions were Cz, F3, C3, F7, T3 and T5 which are placed on the left side of the brain and cover areas close to motor cortex, Broca and Wernicke's area (area 22). We aim to extend this work beyond pairwise classification to move a step closer to practically efficient systems in the domain of BCI for speech imagery.

Table II: Comparison of pairwise classification results for the DataSet 2 using MFCC as feature vectors.

| Subject | Classifier | A/E | A/I | A/O | A/U | E/I | E/O | E/U | I/O | I/U | O/U |
|-----------|------------|-------------|-----------|-------------|-------------|-------------|-----------|-------------|-------------|-------------|-------------|
| Subject 1 | SVM | 54 | 52.4 | 51.7 | 70.1 | 54.7 | 43.9 | 74.1 | 59.3 | 66.6 | 73.3 |
| | HMM | 69 | 83 | 65 | 73 | 69 | 83 | 73 | 61 | 77 | 78 |
| | k-nn | 70 | 62.7 | 62.4 | 67.1 | 70.2 | 62.8 | 76.3 | 63.8 | 63.9 | 64.1 |
| Subject 2 | SVM | 57.1 | 50 | 52.6 | 52.6 | 57.1 | 45 | 35 | 52.6 | 47.3 | 50 |
| | HMM | 68.5 | 80 | 58.5 | 70.5 | 68 | 64.5 | 79.5 | 67.5 | 67.5 | 61.5 |
| | k-nn | 66.6 | 58.3 | 55 | 66.7 | 41.6 | 65 | 75 | 55 | 58.3 | 61.7 |

Table III: Comparison of pairwise classification results for the DataSet 3 using MFCC as feature vectors.

| Subject | Classifier | A/E | A/I | A/O | A/U | E/I | E/O | E/U | I/O | I/U | O/U |
|-----------|------------|-------------|-------------|-------------|-------------|-----------|-------------|-------------|-------------|------------|------------|
| Subject 1 | SVM | 74.2 | 66.7 | 67.15 | 71.8 | 53.3 | 60.7 | 75.8 | 36.7 | 54.8 | 62 |
| | HMM | 57 | 62 | 69 | 63 | 75 | 78 | 68 | 79 | 77 | 75 |
| | k-nn | 71.1 | 57.9 | 73.9 | 59 | 59.4 | 65 | 75 | 55 | 58.3 | 61.6 |
| Subject 2 | SVM | 46.8 | 61.7 | 43.7 | 80 | 56.3 | 56.6 | 84.8 | 56.2 | 91.4 | 90.9 |
| | HMM | 71 | 67 | 57 | 62 | 71 | 79 | 63 | 61 | 67 | 75 |
| | k-nn | 67.2 | 67 | 57.5 | 100 | 51.1 | 83.3 | 100 | 88.9 | 100 | 100 |

Table IV: Comparison of pairwise classification results for the DataSet 4 using MFCC as feature vectors.

| Subject | Classifier | A/E | A/I | A/O | A/U | E/I | E/O | E/U | I/O | I/U | O/U |
|-----------|------------|-----------|-------------|-------------|-----------|-------------|-----------|-----------|-----------|-----------|-----------|
| Subject 1 | SVM | 44.2 | 55.6 | 62.5 | 45.4 | 64.7 | 40 | 51.6 | 53.1 | 44.4 | 62 |
| | HMM | 84 | 62.5 | 70.5 | 74 | 77.5 | 76 | 81 | 91 | 75 | 65 |
| | k-nn | 75.5 | 72.7 | 65.9 | 70.7 | 90.5 | 65 | 74.5 | 40 | 74 | 75 |

REFERENCES

- [1] Prades, J. M., "Extended and standard supraglottic laryngectomies: a review of 110 patients," European Archives of Oto-Rhino-Laryngology and Head & Neck, 2005.
- [2] Yoshihisa Nakamura, Hiroaki Matsubara (1988), Publication number: US6801894 B2
- [3] Denby, B., Schultz, T., Honda, K., Hueber, T., Gilbert, J.M., and Brumberg, J.S., "Silent speech interfaces", Speech Communication, 52, pp. 270-287, 2009
- [4] B.R. Greene, S. Faul, W.P. Marnane, G. Lightbody, I. Korotchikova, G.B. Boylan, "A comparison of quantitative EEG features for neonatal seizure detection". Clinical Neurophysiology, 119 (2008), pp. 1248–1261
- [5] Wolpaw, J. R. N. Birbaumer, DJ. McFarland, et al, "Brain-computer interfaces for communication and control," Clin. Neurophysiol. vol. 113, pp. 767-791, 2002.
- [6] DaSalla, Charles S.; Kambara, Hiroyuki; Sato, Makoto; Koike, Yasuharu, "Single-trial classification of vowel speech imagery using common spatial patterns", Neural Networks, Vol 22(9), pg. 1334-1339, 2009
- [7] iworx psychology Lab experiment, experiment 32
- [8] Chazan, Dan, et al. "Speech reconstruction from mel frequency cepstral coefficients and pitch frequency." Acoustics, Speech, and Signal Processing, 2000. ICASSP'00. Proceedings. 2000 IEEE International Conference on. Vol. 3. IEEE, 2000.
- [9] Nguyen, P., Tran, D., Huang, X., & Sharma, D, "A Proposed Feature Extraction Method for EEG-based Person Identification"
- [10] Burges J. C., "A Tutorial on Support Vector Machines for Pattern Recognition," Data Mining and Knowledge Discovery, 2, pp. 121-167, Kluwer Academic Publications, 1998.
- [11] Lawrence R. Rabiner et al, "A Tutorial on Hidden Markov Model and Selected Application in Speech Recognition", Proceedings of IEEE, vol. 77, No. 2, 1989.
- [12] M. Wand, C. Schulte, M. Janke, and T. Schultz, "Array based electromyographic silent speech interface." Submitted to Biosignals 2013, International Conference on Bio-Inspired Systems and Signal Processing, 2013.

Offline Detection of P300 in BCI Speller Systems

Mandeep Kaur^{#1}

^{#1}School of Computer Science & Engg., Sharda University, Greater Noida, U.P., India
¹mandeepanzra@gmail.com

Abstract— The paper presents a framework for offline analysis of P300 speller system using seeded k-means based ensemble SVM. Due to the use of small-data sets for the training of the classifier, the performance deteriorates. The Proposed framework emphases on semi-supervised clustering approach to training the SVM classifier with large amount of data. The normalized mutual information (NMI) has used for cluster validation that gives maximum 88 clusters of 10 fold cross-validation data set with NMI approx equals to 1. The proposed framework has been applied to the EEG data acquired from two subjects and provided by the Wadsworth center for brain-computer interface (BCI) competition III. The experimental results show the increase in SNR value and obtain better accuracy results than linear, polynomial or rbf kernel SVM.

Index Terms— P300 signal, Wavelet Transform, semi-supervised clustering, ensemble, support vector machines (SVMs).

I. INTRODUCTION

The P300 is a positive wave with a latency of about 300–350 ms, was first reported by Sutton and colleagues in 1965 and P300 based Brain Computer Interface system was first introduced by Farwell and Donchin in 1988 [1] [2]. This paradigm also called *P300 Speller* System that latter improved by Donchin et.al. in 2000, to be used for disabled subjects [3]. In this paradigm, the subject presented a matrix of symbols where each row and column intensifies in random order with predefined interval. The P300 is an event related potential, elicited when the subject pays attention to only that row and column intensifications that contain the desired symbol. With P300 occurrence, the target row-column assumed and the desired symbol inferred [4]. For the offline analysis, BCI competition data sets have been widely used to measure the performance of BCI systems. This is the main reason for testing the novel seeded k-means based ensemble algorithm for predicting the occurrence of P300 in the ongoing EEG on the BCI competition data, so that the results can be directly compared to other available algorithms and their comparative differences explored. Within BCI, the P300 signal plays a significant role of detecting human's intention for controlling external devices [5]. The major concern is to classify the P300 signal from the ongoing EEG (the background noise) in P300 based BCI systems. As EEG is the process of recording brain activities from cerebral but it also records some electrical activities arising from sites other than the

brain. Therefore, during acquisition, the P300 (ERPs) is contaminated with a lot of noise, also known as artifacts in EEG. The unwanted electrical activities arising from some different source rather than from cerebral origin are termed as artifacts. The noise can be electrode noise called extra-physiologic artifacts or may be generated from subject body called physiologic artifacts. The Extra-physiologic artifacts are the noises arises from equipment, environment, etc., whereas the physiologic artifacts generated from the patient's body rather than the brain. The various types of extra-physiologic artifacts are like Inherent Noise, generated from electronic equipment; Chemical Noise, generated due to changes in humidity; Ambient Noise, generated from electromagnetic devices, etc. Thermal or Johnson noise (voltage to 60 Hz), caused by thermal agitation of electrons and other charge carriers in electronic devices, e.g. resistors, capacitors, transistors, wires, connections, etc. (this noise is independent of frequency, also called white noise because present at all frequencies in a constant amount). Shot noise, arises due to semiconductor holes and diffusions, another type of white noise that is uniform across all frequencies; Flicker noise is inversely proportional to frequency i.e. $1/f$, also called $1/f$ noise. The cause of this noise is due to contact pins [6]. The various types of physiologic artifacts are like activities of the eye (electrooculogram, EOG), muscles (electromyogram, EMG), Cardiac (electrocardiogram, ECG), Sweating, swallowing, breathing, etc. Due to this, the amplitude of the P300 (ERP) signal becomes much lower than the amplitude of the noise; causes P300 signal presets a very low signal-to-noise ratio (SNR). Therefore, to detect P300 signal from ongoing EEG, the signal-to-noise ratio (SNR) must be enhanced. Coherent Averaging is the most common method to achieve this goal. The artifacts can remove using various techniques like filtering, independent component analysis, principal component analysis, wavelet transform etc. The approximate coefficients of Daubechies4 (db4) have considered as a feature vector for further analysis. As the P300 detection is the primary task of this research, a number of features are required for training the classifier. The P300 based BCI systems have reported the requirement of bigger search space as the number of features increases, the training of the classifier is very time consuming; number of channels increases the cost of the system. To overcome these limitations, this research emphasis on implementing semi-supervised cluster classification using seeded k-means and ensemble SVM classifier for P300 based BCI Speller paradigm [7]. The paper is organized as follows: Section II discusses the material and methods used in the work. Then detailed

methodology is given in Section III. The Result analysis has discussed in Section IV. And Section V gives the conclusion.

II. MATERIAL AND METHODS

A. BCI PARADIGM

The subject was presented a screen with 36 symbols arranged in a 6 by 6 character matrix. The rows and columns of the matrix were intensified randomly at a rate of 5.7Hz. The user's task was to focus attention on letter of the word, prescribed by the investigator (i.e., one character at a time). Twelve intensifications (six row and six columns) were made out of which only two (one row and one column) intensifications contained the desired character. Each row and column in the matrix were randomly intensified for 100ms and after intensification of a row/column the matrix was blank for 75ms. For each character, 12 intensifications were repeated 15 times and thus total 180 intensifications for each character epoch. Each character epoch was followed by a 2.5 s period, and during this time the matrix was blank [8].

B. DATA ACQUISITION

The EEG dataset used is acquired from Wadsworth BCI competition 2004 Data set IIb (P300 speller paradigm). The data acquired using BCI 2000 system. The dataset is still available on the competition webpage [9], recorded from two subjects A and B in 5 sessions each. Each session consisted of a number of runs and in each run, the subject focused attention on a series of characters i.e. a word. The data set was made up of 85 training characters and 100 testing characters, each composed of 15 trials. The data set was recorded from 64 electrodes that are first band-pass filtered from 0.1-60 Hz and then sampled at 240 Hz.

C. DATA PRE-PROCESSING

Only 10 channels are used for P300 detection in ongoing EEG. The data were latter low-pass filtered at 30 Hz and high-pass filtered at 0.1 Hz using an 8th order butter-worth filter [10].

D. COHERENCE AVERAGING

The data set was further pre processed to detect the P300 signal via increasing the signal-to-noise ratio using coherent averaging. Coherent Averaging is the most common method to average the potential registered synchronized with the application of the stimulus. The following equation (2.1) represents coherence averaging:

$$y_K[n] = \frac{1}{K} \sum_{k=1}^K x_k[n] = s[n] + \frac{1}{K} \sum_{k=1}^K r_k[n] \quad (2.1)$$

Where $x_k[n]$ is the k-nth epoch of potential registered, $s[n]$ is the signal P300 with length $1 \leq n \leq N$, $r_k[n]$ is the k-nth signal with noise variance σ^2 and K is the total number of epochs. For each time instant n, consider noise as an estimator of the average value of a sample of K data. This averaging results in a new random variable, having same average value and a variance σ equals to σ^2/K . This also results in signal-to-noise ratio (SNR)

improvement, but also contaminated with white noise and other artifacts [10].

E. INDEPENDENT COMPONENT ANALYSIS (ICA)

Due to the contamination of artifacts, the EEG signal is described as $x(t) = a(t) + s(t)$ where $x(t)$ is the EEG signal, $a(t)$ is an artifact and $s(t)$ is the signal of interest. Using vector-matrix notation ICA is defined by equation (2.2) [11, 12], $x = As$. ICA algorithm applied to the filtered EEG data to remove the artifacts from EEG signal and separate independent sources for each trial.

$$x_i(t) = a_{i1} * s_1(t) + a_{i2} * s_2(t) + a_{i3} * s_3(t) + a_{i4} * s_4(t) \quad (2.2)$$

ICA algorithm assume that the sources are non-Gaussian or non-white (i.e., the activity at each time point does not correlate with the activity at any other time point), because if the sources are white Gaussian, then there are an infinite number of unmixing matrices that will make the unmixed data independent and the problem is under-constrained [13, 14]. ICA Algorithm to remove artifacts from EEG

1. ICA starts with EEG signals recorded from 10 channels $X(t) = \{x_1(t) \dots x_{10}(t)\}$
2. As these signals are mixed with ($n \leq 10$) unknown independent components (sources) $S(t) = \{s_1(t), s_2(t), \dots, s_N(t)\}$ containing artifacts say A.
3. Centering the input observation signal x
4. Whitening the centered signal x
5. Initializing weight matrix w, Consider A as unknown mixing matrix defining weights at which each source is present in the EEG signals recorded at the scalp.
6. The number of independent components S(t) is determined by the number of EEG channels recorded and considered.
7. Components were selected using a-priori knowledge that the P300 evoked potential reaches a peak around 300 ms after the stimuli. Therefore, only those ICs with a peak in amplitude between 250 and 400 ms were retained.
8. Remove artifact components and re-compute data $X = SW^{-1}$ where X=cleaned data, S=components, with artifact components set to zero [14] [15] [16].

ICA applied to de-noising the EEG signal in order to enhance the signal to noise ratio of the P300, and separating the evoked potential from some artifacts, like signals obtained from eye-blinking, breathing, or head motion, cardiac etc. Evoked Related Potential and electroencephalogram analysis are one of the practical applications of ICA [14-19].

F. PRINCIPLE COMPONENT ANALYSIS (PCA)

With ICA, it is possible to reduce the dimension of the data by discarding the eigenvalues of the covariance matrix, obtained during whitening, and using principal component analysis also. PCA assumes that the most of the information is contained in the directions along which the variations are the largest. PCA based on Eigen analysis technique.

PCA Algorithm to remove artifacts from EEG:

1. Acquire the EEG signal after ICA
2. Obtain mean of the input signal
3. Subtract the mean from each of the input data dimensions

4. Calculate the covariance matrix and thus represent EEG as covariance matrix of the vectors.
5. Determine Eigen values and Eigen vectors of the above data on covariance matrix. Consider Eigen values and Eigen vectors of a square symmetric matrix with sums of squares and cross products. The eigenvector related with the largest Eigenvalue has the same direction as the first principal component. The eigenvector associated with the second largest Eigenvalue determines the direction of the second principal component. Note: The sum of the Eigenvalues equals the trace of the square matrix and the maximum number of eigenvectors equals the number of rows (or columns) of this matrix.
6. For each Eigenvector low pass filtering is done using a filter of cutoff frequency 50 Hz and the energy of filtered data is calculated.
7. The energy, calculated corresponding to Eigenvalue, is compared with a threshold. If this energy is greater than that of threshold, then marked these for reconstruction, else discard the vector. (Compute the number of eigenvalues that greater than zero (select any threshold)).
8. Reconstruct only on those Eigenvectors, which are marked for reconstruction.

PCA able to remove ocular artifacts, but not completely clean EEG as few artifacts like ECG, EMG have almost same amplitudes [20] [21].

G. WAVELET TRANSFORM: DAUBECHIES (db4)

It has been discussed that the EEG signals are non-stationary in nature and do not allow the accurate retrieval of the signal frequency information. Therefore, to extract frequency information, signal transformations like Fourier Transform (FT), Short-Time-Fourier Transform (STFT), Wavelet Transform (WT); Continuous Wavelet Transform (CWT) and Discrete Wavelet Transform (DWT) are required. It has discussed in [22] that Wavelet transform (WT) is the best signal analysis tool. Daubechies wavelet was discovered in 1988 as a useful class of filter coefficients. The most common type of Daubechies that has only 4 coefficients. The simplest set has only 4 coefficients (DAUB4), and will serve as a useful illustration. The 4th order Daubechies is applied to each extracted PCA component to decompose the signal to the required band for the approximated coefficients. Daubechies (Db4) wavelet used as the mother wavelet and the approximated coefficients used as the features for the next step and concatenated into feature vectors [23].

H. SEMI-SUPERVISED CLUSTERING

Semi-supervised clustering, involves some labeled class data or pairwise constraints along with the unlabeled data to obtain better clustering. Due to the consideration of noise seeds in the dataset, the proposed method employs generative, flat partitioning, distance-based Seed K-means semi-supervised clustering. Apply Seeded KMeans semi-supervised clustering on the obtained features [24].

G. ENSEMBLE SUPPORT VECTOR MACHINE (SVM)

Support vector machines (SVM) algorithm is originally designed by Vladimir Vapnik et.al. in 1979 for

binary or two-class classification [25]. To perform binary classification, SVM finds a hyperplane that divides the data sets into two classes with the largest margin. However, the data of real problems are also non-separable that requires mapping into high dimensional feature space, where the training is separable [26]. This leads to non-linear SVM that is dividing the non-separable data linearly in a higher dimensional space. This can achieve using a kernel function. The proposed framework uses the polynomial and Gaussian kernel functions [27]. However, it has reported that using these kernels, the number of support vectors increases [28]. A way to decrease these numbers of support vectors for the training of support vector machine (SVM), k-means clustering algorithm has used [29].

III. METHODOLOGY

Data recorded from 64 channels; instead of all the datasets from only 10 channels have selected. A pre-processing module used to filter and normalize the data. Then, the wavelet features have extracted and projected to Seeded K-Means [30-33] where the training of bagging based ensemble SVM performed. The Fig 3.1 depicts methodology and Fig 3.2 shows a complete framework for the proposed system. At last, the pre-processed unknown data have fed to the classifier for classification.

1. Load the training dataset: Size of the whole signal 85x7794x64. Two sets each A and B

2. Pre-processing

2.1 Select the specific channel in which P300 signals are present: Out of 64 channels of each A and B, 10 channels have selected. Now size of A and B is 85x7794x10

2.2 Low-pass and high-pass Butterworth filtering: 0.1 Hz – 30 Hz using an 8th order Butterworth filter: size of A and B after filtering is 85x3897x10

2.3 Coherence averaging: size of A and B after coherence averaging is 85x3897x10

2.4 Independent Component Analysis includes De-correlation approach: estimate independent component one by one like in projection pursuit. A number of independent components to be estimated: equals the dimension of data step size: 1 Stopping criterion: 0.0001 Max number of iterations: 1000 Max number of iterations in fine tuning: 100 Percentage of samples used in one iteration: all Initial guess for the corresponding mixing matrix: random After ICA, dimension of A and B is 85x3897x10

2.5 Apply Principal Component Analysis, dimension of A and B is 3897x84x10

3. Apply wavelet filtering to extract the features to be trained using db4 wavelet. Now we have 2 outputs from PCA (A, B). Both are 2D. Apply 2D wavelet transform on each using 'db4' wavelets. We get 4

outputs: approx sig A, approx sig B, detail signal A, detail sig B, each of dimension 1952x45x10.

4. Apply Seeded K-Means semi-supervised clustering on the obtained features. Consider the random number of features from the feature set to label the cluster. Assume that k=2 is known. On getting seed information, k-means will label the rest of the unlabeled features. A generalization of k-means clustering has developed for the problems where class labels are known [30]. Let x_i , and x'_i be the observations from a data set with p features, and x_{ij} represents the value of the jth feature for observation I.

Suppose further there exist subsets S_1, S_2, \dots, S_K of the x_i 's such that $x_i \in S_k$ implies that observation i is known to belong to cluster k. (Here K denotes the number of clusters, which is also assumed to be known in this case.) Let $|S_k|$ denote the number of x_i 's in S_k . Also, let $S = U^K \sum_{k=1}^K S_k$. The algorithm proceeds as follows:

1. For each feature j and cluster k, calculate the initial cluster means as:

$$\bar{x}_{kj} = \frac{1}{|S_k|} \sum_{x_i \in S_k} x_{ij}$$

2. For each feature j and cluster k, calculate $|x_{kj}|$, the mean of feature j in cluster k.

3. Repeat steps 2 and 3 until the algorithm converges [30, 31].

5. The clusters are fed to Bagging based SVM Ensemble for training. Two types of kernel have used polynomial, and RBF.

6. The unknown feature vectors, then classified using trained Ensemble SVM.

The system uses two-class non-linear Support vector machine with seeded k-means clustering, that requires three parameters: kernel parameter, γ , the penalty factor C and the number of clusters, C_n to detect whether a specified signal contains P300 or not. The framework uses bagging technique in which each individual SVM has trained using randomly chosen training samples via a bootstrap method. The output of individual trained SVMs has averaged via an appropriate aggregating strategy known as majority voting. The result shows that the ensemble SVM using bagging (majority voting) method procures better accuracy than the independent type of SVMs.

The proposed seeded k-means based ensemble SVM illustrated as:

Inputs:
 D_1 : Training set
 D_2 : Testing Set
 y : Labels
 P : SVM Parameters
 k : kernel parameters, C : penalty factor, C_n : number of clusters
For each SVM
{ Initial Phase

```

Select parameters k, C and  $C_n$  for each SVM
Bootstrapping Phase and Training Phase
For each SVM parameter, DO
{ Run Seeded k-means algorithm and all cluster centers
are
Regarded as input to the classifier
{  $S = \text{Train}(D_1, y_{D1}, P)$ ; }
}
Save the best parameters  $P_{\text{best}}$ 
For  $I = 1$  to 3 (linear, polynomial and rbs SVM)
{  $S^{(i)} = \text{Train}(D_1, y_T, P_{\text{best}})$ ; }
Testing Phase
For testing set  $D_2$ 
{  $\hat{y}^{(i)}_{D2} = \text{Test}(S^{(i)}, D_2, y_{D2})$ ; }

```

Decision Phase
{ Majority vote = $\hat{y}^{(i)}_{D2} \rightarrow \hat{y}_{D2}$ }
}
Return Accuracy of D_2

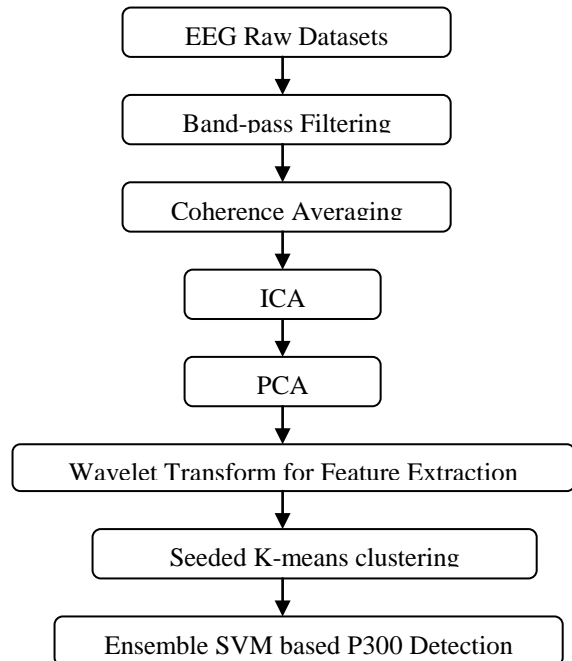


Fig 1. Methodology

IV. RESULT ANALYSIS

The performance of the proposed framework for P300 speller explained in various following ways:

1. SNR Comparison: The analysis of P300 waveform in the ongoing EEG performed using Signal-to-noise Ratio (SNR) until pre-processing phase has discussed in [7].

The algorithm applied to BCI Competition 2004 dataset II and obtained the average SNR of 4.7501 dB for Subject A and 4.7339 dB Subject B. In addition, we reported the average SNR of 4.5338 dB with respect to average trial (20 trials).

2. Cluster Validation: The Normalized mutual information (NMI) used as the cluster validation for proposed framework. The NMI estimates the cluster quality based on the given true labels of the data sets. It is an external validation metric that have a range of NMI values 0 to 1. The NMI value 1 means best clustering

quality. The NMI is a type of information entropy measure that is defined as

$$NMI(\mathcal{C}, \mathcal{B}) = \frac{I(\mathcal{C}; \mathcal{B})}{\sqrt{H(\mathcal{C})H(\mathcal{B})}} = \frac{\sum_{i=1}^k \sum_{j=1}^k n_{ij} \log \frac{n_{ij}}{n_i n_j'}}{\sqrt{\sum_{i=1}^k n_i \log \frac{n_i}{n} \sum_{j=1}^k n'_j \log \frac{n'_j}{n}}} W$$

here H means the entropy, and I mean the mutual information, n_i means data points in the i^{th} cluster, n'_j denotes the data point in the j^{th} cluster and n_{ij} denotes the data point included in i^{th} and j^{th} cluster. The proposed framework used maximum 10-fold cross-validation for each data set with a number of clusters varies from 20 to 88 shown in Table 1. It is not essential that when the number of clusters increases, the value of NMI increase, as with other external clustering validation measures like purity and entropy [34, 35].

Table 1: Cluster Evaluation uses NMI for Subject A and Subject B

| Subject A | | | Subject B | | |
|----------------------------------|------|--------------------|----------------------------------|------|--------------------|
| Seed Fraction (cross validation) | NMI | Number of Clusters | Seed Fraction (cross validation) | NMI | Number of Clusters |
| 0.2 | 0.45 | 67 | 0.2 | 0.33 | 70 |
| 0.4 | 0.56 | 74 | 0.4 | 0.49 | 81 |
| 0.6 | 0.60 | 82 | 0.6 | 0.57 | 68 |
| 0.8 | 0.74 | 80 | 0.8 | 0.66 | 79 |
| 1.0 | 0.8 | 88 | 1.0 | 0.79 | 82 |

3. Accuracy: The accuracy is determined in terms of whether the P300 exists in a cluster or not i.e. the detection of P300 in a Cluster using ensemble SVM. Suppose C is the clustering result, i.e. clusters and B define the predefined class (cluster) then the accuracy is defined as one to one association between the clusters and the classes:

$$Acc(\mathcal{C}, \mathcal{B}) = \frac{\max \left(\sum_{i=1}^k n_{i, \text{Map}(i)} \right)}{n}$$

Where n refers to the number of data points in the dataset, i refer to the cluster index, Map(i) is the class index corresponding to cluster index i and $n_{i, \text{Map}(i)}$ is the number of data points not only belonging to cluster i, but to class Map(i) [34, 35]. The Table 2 shows the accuracy of different types of SVM with optimal values of C and γ , in 10-fold cross-validation training data set. It concluded that ensemble SVM (using the majority voting method) outperforms better than linear, polynomial or rbf SVM.

Table 2: Accuracy of Proposed Framework

| Subject A | |
|------------------------|----------|
| Type of SVM | Accuracy |
| Linear SVM | 72.4% |
| Polynomial SVM | 84.1% |
| RBF SVM | 87% |
| Ensemble SVM (Bagging) | 97.2% |

| Subject B | |
|------------------------|----------|
| Type of SVM | Accuracy |
| Linear SVM | 77.3% |
| Polynomial SVM | 82.9% |
| RBF SVM | 84.4% |
| Ensemble SVM (Bagging) | 96.5% |

V. CONCLUSION

The aim of this work is to present a novel way of discovering the knowledge embedded in EEG signals. This knowledge is then used to classify an unknown signal into a discovered signal class that the said system will interpret into a device control signal. The purpose of this research is to explore the process of developing a novel P300 based BCI systems for disabled people. The work suggests a new framework of extracting the features using wavelet transform and discovering the knowledge (classes) from brain activity patterns using semi-supervised clustering and then classifying these using Classifier Ensemble in EEG based BCI system. The Seeded K-means based semi-supervised cluster classification using Ensemble SVM classifier has used as the basis of the framework. The ensemble SVM has trained from initial pre-defined cluster known as seed and then extends for large datasets to detect the presence of P300 signal. The system used two-class linear Support vector machine for non-linear high dimensional data. The complete illustration of the proposed framework depicted in Section III. The result shows that the ensemble SVM using bagging (majority voting) method procures better accuracy than the independent type of SVMs. The future work focuses on applying this approach for online P300 data analysis for more number of subjects.

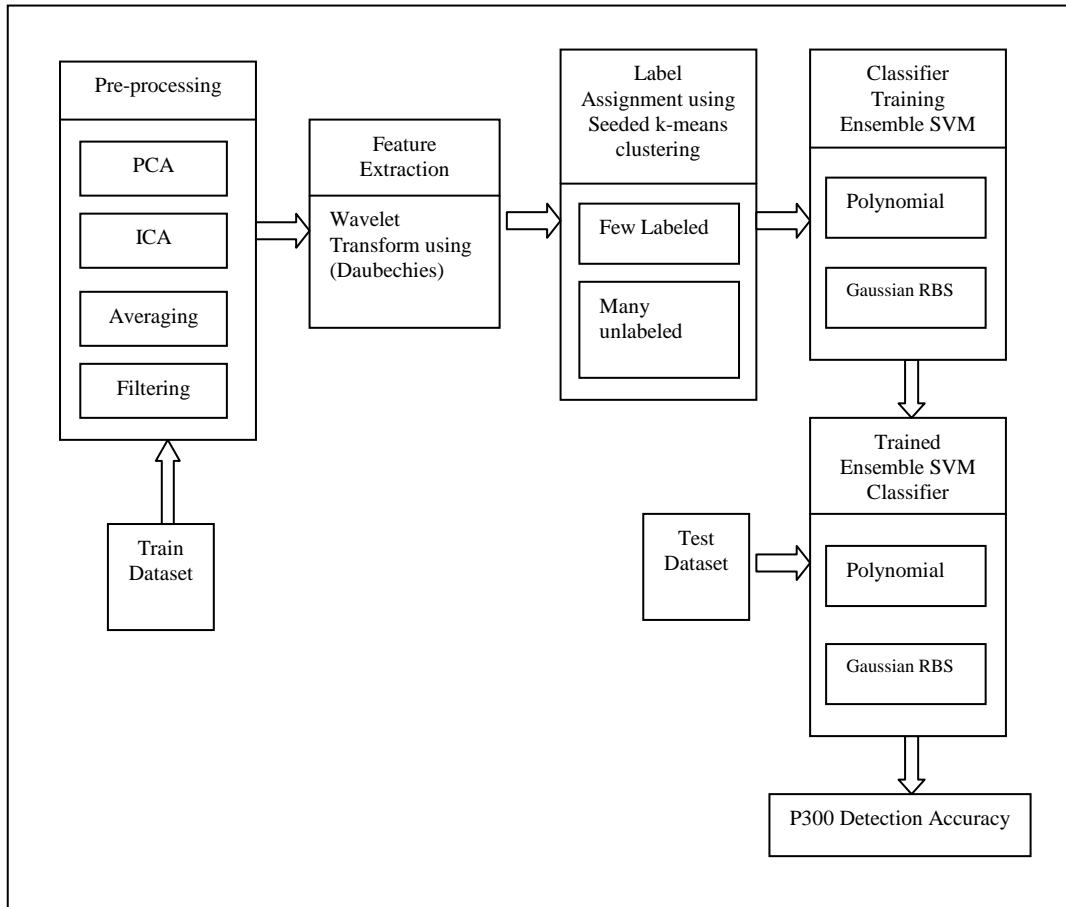


Fig 2: Illustration of Seeded k-means based Ensemble SVM Framework

References

- [1] Polich, J. (2010). Neuropsychology of P300. In S.J. Luck & E.S. Kappenman, Handbook of event-related potential components, Oxford University Press, in press.
- [2] Z Vahabi, R Amirfattahi, and AR Mirzaei, "Enhancing P300 Wave of BCI Systems Via Negentropy in Adaptive Wavelet Denoising", Journal of Medical Signals & Sensors, Vol 1, no. 3, pp. 165-176, Sep-Dec 2011 Jul-Sep.
- [3] Matthias Kaper, "P300 based brain computer interfacing", Thesis, pp. 1-149, Bielefeld University 2006.
- [4] Mathew Salvaris and Francisco Sepulveda, Wavelets and Ensemble of FLDs for P300 Classification, Proceedings of the 4th International IEEE EMBS Conference on Neural Engineering Antalya, Turkey, April 29 - May 2, 2009
- [5] Andrea Finke, Alexander Lenhardt, Helge Ritter, "The Mind Game: A P300-based Brain Computer Interface Game", Neural Networks, vol. 22, no.9, pp. 1329-1333, 2009.
- [6] <https://www.bhsu.edu/Portals/91/InstrumentalAnalysis/StudHelp/LectureNotes/Chapter5.pdf>
- [7] Mandeep Kaur et.al., Semi-supervised Clustering Approach for P300 based BCI Speller Systems", accepted for publication in Fifth International Conference on Recent Trends in Information, Telecommunication and Computing – ITC 2014, will be held during Mar 21-22, 2014, Chandigarh.
- [8] Hend El Dabbagh and Waleed Fakhr, "Multiple classification algorithms for the BCI P300 speller diagram using an ensemble of SVMs", IEEE Conference and Exhibition (GCC), Dubai, United Arab Emirates, February 19-22, 2011.
- [9] <http://bbci.de/competition/iii/#datasets>
- [10] Ricardo Espinosa, "Increased Signal to Noise Ratio in P300 Potentials by the Method of Coherent Self-Averaging in BCI Systems", World Academy of Science, Engineering and Technology, International Journal of Medical, Pharmaceutical Science and Engineering, pp. 106-110, vol. 7 (11), 2013.
- [11] Espinosa Ricardo: Increased Signal to Noise Ratio in P300 Potentials by the Method of Coherent Self-Averaging in BCI Systems, World Academy of Science, Engineering and Technology, International Journal of Medical, Pharmaceutical Science and Engineering, Vol. 7, No. 11, 2013, pp 106-110.
- [12] Rosas-Cholula Gerardo et.al.: On signal P-300 detection for BCI applications based on Wavelet analysis and ICA Preprocessing, Electronics, Robotics and Automotive Mechanics Conference, Sept. 28 -Oct. 1, 2010, pp 360 – 365. ISBN: 978-1-4244-8149-1
- [13] Presentation by Ata Kaban, "Independent Component Analysis & Blind Source Separation", The University of Birmingham.
- [14] Paul CRISTEA, "Independent Component Analysis (ICA) for Genetic Signals", SPIE's International Symposium, San Jose Convention Center, San Jose, California USA, 20–26 January 2001.
- [15] Aapo Hyvärinen and Erkki Oja , "Independent Component Analysis: A Tutorial", in Neural Networks, Helsinki University of Technology, Laboratory of Computer and Information Science, Espoo, Finlandpp, 411-430, vol. 13(4-5), 2000.
- [16] A. Srinivasulu, M. Sreenath Reddy, "Artifacts Removing From EEG Signals by ICA Algorithms", IOSR Journal of Electrical and Electronics Engineering (IOSRJEEE), pp. 11-16, vol 2, no. 4, Sep-Oct. 2012, ISSN: 2278-1676.
- [17] Paul H. Schimpf and Hesheng Liu, "Localizing Sources of the P300 using ICA, SSLOFO, and Latency Mapping", Journal of Biomechanics, Biomedical and Biophysical Engineering, pp. 1-11, vol. 2, no. 1, 2008.
- [18] Ganesh R. Naik and Dinesh K Kumar, "An Overview of Independent Component Analysis and Its Applications", Informatica, pp. 63–81, vol. 35, 2011.
- [19] Steven Lemm et.al, "Enhancing the Signal-to-Noise Ratio of ICA-Based Extracted ERPs", IEEE TRANSACTIONS ON BIOMEDICAL ENGINEERING, pp. 601-607, vol. 53, no. 4, April 2006.

- [20] Ashish Raj, Akanksha Deo, Manoj Kumar Bandil, "Canvassing Various Techniques for Removal of Biological Artifact in EEG", International Journal of Recent Technology and Engineering (IJRTE), pp. 149-154, vol 1, no. 3, August 2012, ISSN: 2277-3878.
- [21] Selin Aviyente et.al., ANALYSIS OF EVENT RELATED POTENTIALS USING PCA AND MATCHING PURSUIT ON THE TIME-FREQUENCY PLANE", IEEE Conference Proceedings on Med Biol Soc., 2006.
- [22] Mandeep Kaur, P. Ahmed, M. Qasim Rafiq, Analysis of Extracting Distinct Functional Components of P300 using Wavelet Transform, Proceedings of 4th International Conference on Mathematical Models for Engineering Science (MMES '13) and the 2nd International Conference on Computers, Digital Communications and Computing (ICDCC '13), Brasov, Romania, pp. 57-62, June 1-3, 2013, ISBN: 978-1-61804-194-4.
- [23] Priyanka Khatwani, Archana Tiwari, "A survey on different noise removal techniques of EEG signals", International Journal of Advanced Research in Computer and Communication Engineering pp. 1091- 1095, vol. 2, no. 2, February 2013.
- [24] Eric Bair, Semi-supervised clustering methods, Article first published online: 23 JUL 2013 DOI: 10.1002/wics. 1270 © 2013 Wiley Periodicals, Inc.
- [25] Boswell D.: Introduction to Support Vector Machines, August 6, 2002 [online] Available: <http://www.work.caltech.edu/boswell/IntroToSVM.pdf>
- [26] Moore Andrew W.: Professor School of Computer Science, Lecture Notes on Support Vector Machines, Carnegie Mellon University, Nov 23, 2001. <http://www.cs.cmu.edu/~cga/ai-course/svm.pdf>
- [27] Kaper Matthias: BCI Competition 2003—Data Set IIb: Support Vector Machines for the P300 Speller Paradigm, IEEE Transactions on Biomedical Engineering, Vol. 51, No. 6, June 2004, pp 1073-1076.
- [28] Morariu Daniel: Classification and Clustering using SVM, 2nd Ph.D Report, Thesis Title: Data Mining for Unstructured Data, University of Sibiu, 2005.
- [29] Xia Xiao-Lei et.al.: Methods of Decreasing the Number of Support Vectors via k -Mean Clustering, ICIC, Part I, LNCS, Springer-Verlag Berlin Heidelberg, 2005, pp 717 – 726.
- [30] Basu Sugato: Semi-supervised Clustering: Learning with Limited User Feedback, PhD Proposal, The University of Texas at Austin, Nov 2003 (Also Appears as Technical Report, UT-AI-TR-03-307)
- [31] Basu Sugato: Semi-supervised Clustering: Probabilistic Models, Algorithms and Experiments, Thesis, The University of Texas at Austin, August 2005.
- [32] Basu Sugato et.al.: Semi-supervised Clustering by Seeding, Proceedings of the 19th International Conference on Machine Learning (ICML-2002), Sydney, Australia, July 2002, pp 19-26.
- [33] Basu Sugato et.al.: A Probabilistic Framework for SemiSupervised Clustering, Proceedings of the Tenth ACM SIGKDD International Conference on Knowledge Discovery and Data Mining (KDD-2004), Seattle, WA, August 2004, pp 59-68.
- [34] Jinlong Wang, "AN EFFECTIVE SEMI-SUPERVISED CLUSTERING FRAMEWORK INTEGRATING PAIRWISE CONSTRAINTS AND ATTRIBUTE PREFERENCES", Computing and Informatics, pp. 597-612, vol. 31, 2012.
- [35] Wei Tang et.al, Enhancing Semi-Supervised Clustering: A Feature Projection Perspective", Proceedings of the 13th ACM SIGKDD international conference on Knowledge discovery and data mining, pp. 707- 716, ACM, 2007.

A Short Review of Location-Based Mobile Phone Emergency Systems: Current State and Future Guidelines

Anas Aloudat

Department of Management Information Systems
Faculty of Business, The University of Jordan

Amman, Jordan
a.aloudat@ju.edu.jo

Abstract—Location-based mobile phone emergency systems have the capacity to save lives. These systems, which are becoming vitally important in national emergency management arrangements in several countries around the world, have the ability to deliver customized safety information to an active mobile phone based on the geographic location on the phone before, during, or after a certain emergency, thus complementing the work of the traditional safety media channels such as sirens, television, or radio. A growing list of countries have already implemented or started to plan for implementing their national location-based emergency systems. In this paper the path forward for understanding the current state of these systems worldwide is given in a concise backdrop based on the review of related work from government, academia, and private sector studies, projects, and papers. Of particular relevance here are the administrative, legislative, and technical mechanisms governments are using or plan to use in order to deploy such kinds of systems. This paper also puts forwards a wide-ranging list of recommendations for future location-based emergency systems. These recommendations can be thought of as a set of guidelines to be taken into consideration if more successful and robust systems are to be deployed in a nation state.

Keywords—*location-based emergency system; location-based services; mobile phone; emergency management; implementation mechanism; short message service; cell broadcast service*

I. INTRODUCTION

Governments have long been exploring the utilization of different channels, including proprietary solutions and private infrastructures, for the purpose of communicating with the people during disasters and emergencies. In this sense, mobile telecommunications networks have been exploited over the past few years as a means to provide an additional flow of information to people during emergencies beside the conventional channels of emergency management, such as signage, sirens, door-knocking, speakers, radio, television, landline telephones and the Internet. Fortunately, there have been dramatic

advances in the mobile phone telecommunications networks to allow specific technologies and services within these networks to be effectively exploited for emergency management purposes. Amongst these, location-based services (LBS) have been suggested, trailed, and implemented by a number of governments for the goal of finding the almost exact geographic location of an active mobile handset after the user of the handset has initiated an emergency phone call or a short message request for help. The services are also suggested, currently trailed, and scarcely deployed by a few countries for the purpose of disseminating alerts, warnings, or relevant safety information to people who are located in the vicinity of a pre-defined geographic area(s) of an emergency via their active mobile handsets and across all phases of the emergency. Although LBS represent one of the most obvious and reasonable application areas where the deployment of location technology in emergency management not only makes sense [1] but can also be a life-sustaining tool the services are actually in their infancy stage of deployment as emergency services worldwide [2, 3]. Problems related to technical issues, including location determination mechanisms and accuracy standards, and issues related to legal, regulatory, and service level requirements still need to be determined or enhanced [2, 4, 5]. In addition, LBS as a special type of context-aware services have long raised social, ethical, and legal issues among users, such as the quality of the service information being provided, issues related to the privacy of the people and how, when, and for how long their locational information are collected and stored, and up to issues concerning the legal liability of a service failure or information disclosure inadvertently or deliberately [6-10].

In this paper, a review of the current state of play in the implementation and deployment of location-based emergency systems worldwide is presented and key recommendations for future LBS emergency management solutions are provided.

II. THE CURRENT STATE OF LOCATION-BASED EMERGENCY SYSTEMS

The implementation of location-based mobile phone systems, specifically for public alerting and warning purposes are for the most part has been carried out by telecommunications carriers with partial or full financial supported by governments through a variety of measures [11-13]. These measures include legislation, contractual or oral agreements, and compensation mechanisms. Table 1 summarizes these measures in several countries around the world. As presented in the table, the majority of the current implementations of LBS emergency systems worldwide are deployed using the short message service (SMS), the cell broadcast service (CBS), or a combination of the both. The two technologies actually fulfil most of the basic requirements of a warning message through a mobile phone and both technologies can be utilized for geo-specific

emergency purposes. But, a key factor in the selection of any or both of these two technologies is essentially in their ability to support most mobile handsets that are in use today, including legacy mobile phones that do not really support more advanced messaging functionalities. Taking the legacy handsets into account actually resulted in ruling out many of the promising and potential technologies available today from being exploited by governments. These include, for example, the 4G technologies such as the Long Term Evolution (LTE) or the Worldwide Interoperability for Microwave Access (WiMAX). This was a case of design and implementation issue for several countries, including Australia and Jordan, where their governments have ruled out most of the available technologies, even CBS, because these technologies are not supported by every handset still in use [14]. Table 1 is constructed based on the review of the following related literature [14-20].

TABLE 1. LOCATION-BASED EMERGENCY SYSTEMS IMPLEMENTATION [MECHANISMS

| Country | Instrument | Technology | Carrier Participation | Compensation |
|--------------------------|---|--|--------------------------|---|
| The United States | Legislation and contractual agreements | Cell broadcast + SMS | Proposed to be voluntary | Possibility of government financing |
| United Kingdom | Legislation and contractual agreements | Cell broadcast + SMS | Proposed to be voluntary | Possibility of government financing |
| Japan | Contractual agreements | Cell Broadcast + other technologies (e.g. Paging Channels) | Voluntary | No financial compensation |
| Australia | Yet to be determined | Yet to be determined | Voluntary | Possibility of government financing |
| New Zealand | Contractual agreements | Initially SMS | Voluntary | Financial compensation from the government |
| Finland | Legislation | Several technologies including SMS | Compulsory | Some financial compensation |
| The Netherlands | Contractual agreements | Cell broadcast | Voluntary | No financial compensation |
| Italy | Contractual agreements | SMS | Voluntary | No financial compensation |
| South Korea | Contractual agreements | Cell broadcast | Voluntary | No financial compensation |
| India | Oral agreements | SMS and cell broadcast simultaneously | Voluntary | No financial compensation |
| Malaysia | Oral agreements | Cell broadcast | Voluntary | No financial compensation |
| Jordan | Contractual agreement with the mobile telecommunications carriers | SMS | Voluntary | No financial compensation from the government |
| Maldives | Legislation and contractual agreements | Cell broadcast | Compulsory | No financial compensation |
| Sri Lanka | Legislation | Cell broadcast | Compulsory | No financial compensation |

III. REQUIREMENTS FOR FUTURE LOCATION-BASED EMERGENCY SYSTEMS

Several international standards organizations and a number of specialist researchers have undertaken extensive studies to identify and document different requirements for different emergency warning systems that should, in principle, allow support for all known or future unexpected types of emergency events. In these studies, many aspects were given attention, including legislative, regulatory, administrative, operational, technical, organizational, and

ethical requirements. Some of these contributions have been made by Miletic and Sorensen [21], the Cellular Emergency Alert Systems Association [22], Tsalgatidou et al. [23], The European Telecommunications Standards Institute [5, 24-26], The Federal Communications Commission [27], McGinley et al. [28], The International Telecommunications Union [29], The 3rd Generation Partnership Project [30, 31], Fernandes [32], Jagtman [33], Sanders [34], and Setten and Sanders [35] under the European Commission's CHORIST Project [36].

Defining the future requirements of a warning system serves several objectives including the establishing of a more standardized approach for designing, developing, and deploying the system, prioritizing the system's future functionalities while providing guidance on the system's expected performance levels, preventing duplicative reporting from the system's different stakeholders [37], and ensuring that the people who need access to the system during an emergency can be guaranteed that access in addition to any other mechanisms people have been traditionally using. However, with regard to the location-based mobile phone emergency systems, no explicit requirements, specifically legal or administrative requirements, currently exist anywhere in the world [4]. But, based on the concepts and principles outlined in the above-mentioned works about other kinds of warning systems, the following specific requirements have been drawn out from the literature. These include, but definitely are not limited to, the following:

- The location-based mobile phone emergency system should have the ability to be integrated or be used along with other existing alerting or warning systems.
- The system must be fully accessible only by the right authorities.
- Be flexible enough to allow support for different types or categories of emergency events and not to be designed to support only limited type(s).
- The system should allow the government the ability to operate it independent of a single or a specific telecommunications carrier network.
- The underlying technology should be supported by all telecommunications carriers in the country.
- The system should be flexible enough to allow for the accommodation of future technologies that can enable the enhanced message transfer modes (e.g. rich data content such as video, or an interactive GPS-based map showing safe areas or emergency help facilities).
- Provide mechanisms to ensure the protection of user's private locational information.
- Support both pre-planned and dynamic notifications and alerts.
- The system must be able to reach unrestricted number of people, ranging from hundreds in rural areas to millions in urban and metropolitan cities.
- The location-based mobile phone emergency system must be able to deliver its messages simultaneously to a large number of recipients.
- The delivery of the warning message should happen in almost real-time or within a planned specified time window.

- The system should have the ability to reach the appropriate recipients, as efficiently as possible, through the ability of its underlying technologies to segment the message recipients by the vicinity of their geographic location to the emergency.
- Allow the opportunity to send different messages to different groups of people (e.g. recommend different safety areas for different groups based on their locations or messages can be targeted at people in the immediate vicinity of an emergency to do one thing, and people travelling to an affected area to do another).
- Reach all kinds of existing mobile handsets, including legacy devices that are still largely in use.
- Support delivery of messages to those with special needs and unique devices, such as handsets for hearing and vision impaired persons.
- Reach the residents of remote areas, and people roaming from other mobile telecommunications networks, including visitors and tourists from other countries.
- Support the transmission of the warning message in languages beside the national language(s) of the country, to the extent where it is practical and feasible.
- Be able to deliver the message under network-congested conditions.
- Have a message re-delivery mechanism once the initial delivery of the message fails.
- Have a message reiteration mechanism for as long as the message is valid.

In addition to the above requirements for a location-based mobile phone emergency system, there are also requirements for the service/message that is conveyed via the system itself. These should also be taken into consideration, and include the following:

- The creation of the message should be driven by the country's specific characteristics and its own list of emergencies.
- The template of the message must be consistent across different warning sources from different emergency authorities.
- The message must be built on a standardized format for expressing and disseminating a consistent warning message simultaneously over different informative and media channels, including social media such as Twitter.
- The message should be specifically recognizable as being an emergency message that cannot be mistaken for an ordinary message.

- Should be credible, secure, and authentic.
- The message must be location-accurate to minimize social anxiety.
- It should be relevant, to ensure that the recipients realize that the warning relates to their personal situation or surroundings.
- Timely, to prevent wrong actions and to provide those at risk with enough time to take protective actions.
- Accurate, to indicate the level of severity, or the predicted severity degree, of the emergency event.
- Complete, to offer sufficient details for the recipient in one time about the situation.
- Concise, to avoid too much time in interpreting the message by the recipient.
- Provide adequate instructions to recipients regarding what should and should not be done to protect them before, during, or in the aftermath of an emergency.
- Fully clear and comprehensible to all people, including young and senior recipients.
- Positive, rather than negative to advocate people on what to do next.

IV. CONCLUSION

This paper briefly presented the current implementation state of location-based mobile phone emergency systems. It began with an overview of the use of LBS in mobile telecommunications networks for emergency calling/messaging and public warning purposes and then outlined the implementation mechanisms of the systems in a number of countries around the world. The paper also provided an overview of the requirements for future location-based emergency systems based on pertinent reports, studies, and projects. These requirements covered different aspects of the systems related to their design, deployment, and implementation. The requirements also covered some of the fundamental characteristics that should be considered in the provided warning service/message. Finally, this paper is expected to be particularly useful for governments where location-based services have been partially exploited as waring or safety services or for countries that are in the way to introduce these services within their national emergency management arrangements.

REFERENCES

- [1] A. Küpper, "Location-Based Services: Fundamentals and Operation". 1st ed, John Wiley & Sons Ltd.: Chichester, West Sussex, 2005.
- [2] A. Aloudat and K. Michael, "Toward the Regulation of Ubiquitous Mobile Government: A Case Study on Location-Based Emergency Services in Australia". *Electronic Commerce Research*, 2010. 10(4): p. 31-74.
- [3] A. Aloudat and K. Michael, "The Socio-Ethical Considerations Surrounding Government Mandated Location-Based Services during Emergencies: An Australian Case Study", in *Crisis Management: Concepts, Methodologies, Tools and Applications*, Information Resources Management Association (ed.), IGI Global: Hershey, Pennsylvania. p. 918-943, 2014.
- [4] R. Togt, et al., "Location Interoperability Services for Medical Emergency Operations during Disasters", in *Geo-information for Disaster Management*, P.v. Oosterom, S. Zlatanova, and E.M. Fendel (Eds), Springer Berlin Heidelberg. p. 1127-1141, 2005.
- [5] The European Telecommunications Standards Institute, *Study for Requirements for a Public Warning System (PWS) Service*. 2010: Sophia-Antipolis, France.
- [6] P.J. O'Connor and S.H. Godar, "We Know Where You Are: The Ethics of LBS Adversting", in *Mobile Commerce: Technology, Theory, and Applications*, B.E. Mennecke and T.J. Strader (Eds), Idea Group Publishing: Hershey, Pennsylvania. p. 211-222, 2003.
- [7] D. Tilson, K. Lyytinen, and R. Baxter. "A framework for selecting a location based service (LBS) strategy and service portfolio". in *37th Annual Hawaii International Conference on System Sciences*. Big Island, Hawaii. 2004.
- [8] L. Perusco, K. Michael, and M.G. Michael. "Location-Based Services and the Privacy-Security Dichotomy". in *Third International Conference on Mobile Computing and Ubiquitous Networking*. London. 2006.
- [9] L. Perusco and K. Michael 2007, "Control, trust, privacy, and security: Evaluating location-based services", *IEEE Technology and Society Magazine*, pp. 4-16.
- [10] A. Aloudat and K. Michael, "The Socio-Ethical Considerations Surrounding Government Mandated Location-Based Services during Emergencies: An Australian Case Study", in *ICT Ethics and Security in the 21st Century: New Developments and Applications*, M. Quigley (ed.), IGI Global: Hershey, Pennsylvania. p. 129-154, 2011.
- [11] A. Aloudat and K. Michael. "The Application of Location Based Services in National Emergency Warning Systems: SMS, Cell Broadcast Services and Beyond". in *National Security Science and Innovation*. Canberra, Australia: Australian Security Research Centre. 2010.
- [12] D. Coyle and P. Meier, *New Technologies in Emergencies and Conflicts: The Role of Information and Social Networks*. 2009, UN Foundation-Vodafone Foundation Partnership: Washington, D.C. and London, UK.
- [13] A. Aloudat, K. Michael, and Y. Jun. "Location-Based Services in Emergency Management- from Government to Citizens: Global Case Studies". in *Recent Advances in Security Technology*. Melbourne: Australian Homeland Security Research Centre. 2007.
- [14] M. Al-dalahmeh, et al., "Insights into Public Early Warning Systems in Developing Countries: A Case of Jordan". *Life Science Journal*, 2014. 11(3): p. 263-270.
- [15] N. Waidyanatha, G. Gow, and P. Anderson, *Community-Based Hazard Warnings in Rural Sri Lanka: Performance of Alerting and Notification in a Last-Mile Message Relay*, S.S.R. Network, Editor. 2007, Social Science Research Network.
- [16] A. Kidd, et al., *New Zealand Telecommunications Based Public Alerting Systems Technology Study*. 2008, New Zealand Centre for Advanced Engineering, University of Canterbury Campus: Christchurch, New Zealand.

- [17] The Victorian Bushfires Royal Commission, *Victorian Bushfires Royal Commission Interim Report*. 2009, Parliament of Victoria, Government State of Victoria: Melbourne, Australia.
- [18] G. Weiss, *The Right Information at the Right Time Saves Lives*. 2009, CHORIST Consortium: Istanbul, Turkey.
- [19] GSM- Disaster Response, *Mobile Network Public Warning Systems and the Rise of Cell-Broadcast*. 2013.
- [20] J. Miller, *Mobile phone emergency alert system to be tested in UK*, in *BBC News*. 2013.
- [21] D.S. Miletic and J.H. Sorensen, *Communication of Emergency Public Warnings: A Social Science Perspective and State-of-the-Art Assessment*. 1990, Oak Ridge National Laboratory: Oak Ridge, Tennessee.
- [22] The Cellular Emergency Alert Systems Association, *Handset Requirements Specification: Reaching Millions in a Matter of Seconds*. 2002, Cell Broadcast Forum: Berne, Switzerland.
- [23] A. Tsagatidou, et al. "Mobile E-Commerce and Location-Based Services: Technology and Requirements". in *The 9th Scandinavian Research Conference on Geographical Information Sciences*. Espoo, Finland. 2003.
- [24] The European Telecommunications Standards Institute, *Requirements for Communication of Citizens with Authorities/Organizations in Case of Distress (Emergency Call Handling)*. 2003: Sophia-Antipolis, France.
- [25] The European Telecommunications Standards Institute, *Analysis of the Short Message Service and Cell Broadcast Service for Emergency Messaging Applications; Emergency Messaging; SMS and CBS*. 2006: Sophia-Antipolis, France.
- [26] The European Telecommunications Standards Institute, *Emergency Communications (EMTEL): Requirements for Communications from Authorities/Organizations to Individuals, Groups or the General Public During Emergencies*. 2006: Sophia-Antipolis, France.
- [27] The Federal Communications Commission, *Review of the Emergency Alert System*. 2005: Washington, D.C.
- [28] M. McGinley, A. Turk, and D. Bennett. "Design Criteria for Public Emergency Warning Systems". in *The 3rd International Conference on Information Systems for Crisis Response and Management (ISCRAM)*. Newark, New Jersey. 2006.
- [29] The International Telecommunication Union, "Compendium of ITU'S Work on Emergency Telecommunications". 1st ed, The United Nations Agency for Information and Communication Technologies: Geneva, Switzerland, 2007.
- [30] The 3rd Generation Partnership Project, *Technical Specification Group Services and System Aspects: Study for Requirements for a Public Warning System (PWS) Service (Release 8)*. 2008: Valbonne, France.
- [31] The 3rd Generation Partnership Project, *Technical Specification Group Services and System Aspects; Functional Stage 2 Description of Location Services (LCS) (Release 9)*. 2009: Valbonne, France.
- [32] J.P. Fernandes, "Emergency Warnings with Short Message Service", in *Integration of Information for Environmental Security*, H.G. Coskun, H.K. Cigizoglu, and M.D. Maktav (Eds), Springer: Dordrecht, The Netherlands. p. 205-210, 2008.
- [33] E. Jagtman, *Reaching Citizens with CHORIST: Everything but Technology*. 2009, CHORIST Consortium: Istanbul, Turkey.
- [34] P. Sanders, *The CB Way Forward*. 2009, CHORIST Consortium: Istanbul, Turkey.
- [35] W.v. Setten and P. Sanders, *Citizen Alert with Cell Broadcasting:: The Technology, the Standards and the Way Forward*. 2009, CHORIST Consortium: Istanbul, Turkey.
- [36] The European Commission, *The CHORIST Project: Integrating Communications for Enhanced Environmental Risk Management and Citizens Safety*. 2009, CHORIST Consortium.
- [37] The United States Department of Homeland Security, *National Emergency Communications Plan*. 2008.

Relation and attribute fusion to detect communities of online social networks

Mohammad H. Nadimi, Member, IEEE

Faculty of Computer Engineering
Najafabad branch, Islamic Azad University
Esfahan, Iran
nadimi@iaun.ac.ir

Mehrafarin Adami

Faculty of Computer Engineering
Najafabad branch, Islamic Azad University
Esfahan, Iran
mehrafarina@sco.iaun.ac.ir

Abstract— Community detection is a vital research area for online social networks. Since there is no a formal context in users' profiles, a new data source of user's attributes is extracted from online social networks. In this paper a novel algorithm is proposed to use both attributes and relations of users; therefore communities can be detected through users' similar characteristics or users common relationships. The experimental results show that the accuracy of the algorithm is comparable to other well-known algorithms. Moreover, detected communities are self-described through the mode of each community members.

Keywords— Social networks; hybrid community detection; attributes and relations; self-descriptive communities

I. INTRODUCTION

In recent years, online social networks such as Facebook.com and LinkedIn.com become more popular. Since such social networks have millions of users, analyzing this amount of information is feasible through community detection where, users can be grouped according to their relations or their common attributes. Afterwards, by dividing the network to communities, more detailed analysis becomes possible. Social networks are usually represented as a graph, in which the nodes are users or individuals and their relations are represented by links. Users are often described by certain attributes, which are referred to as nodes content. For example, when it comes to the web pages, the contents are usually presented by histograms of keywords; furthermore, in the citation graph, the content of nodes is affiliation of researchers [1].

Previous studies on community detection methods focused on link analysis. Since those methods failed to extract semantic of the communities, hybrid methods are favored recently. These methods enhance the efficiency of community detection results [1-10]. Almost all of these methods use Bayesian models, and they combine two algorithms or two data sources. These data sources are often links and context. Using context as a data source has some limitations that are listed below. Handling context as a data source for community detection is a voluminous task that needs algorithms with high computational complexities; therefore, the majority of research studies extract

the most frequent words or keywords from the context, and then use these limited words as the content. Furthermore, Contexts are extracted from scientific papers written with correct grammatical instructions and formal vocabularies. In the case of online social networks comments and descriptions usually consist of informal words and phrases, which are particularly used in virtual environments. In addition, users' contexts are written in different languages. Because online social networks have users from all over the world; Hence, Extracting the context is not suitable in order to detect the communities in online social networks.

Resolving the above-mentioned limitations guides us to employ user's attributes as one of the data sources of hybrid community detection algorithm. These attributes can be extracted from users' profiles, which are available in almost all of the online social networks. These attributes are filled in by users; the information of this data source is often reliable and constant at least for a period. In other words, these attributes are not extracted from contexts of comments that are not clear if the writer is serious in his/her idea, or if his/her comment is just related to a transient emotion. In online social networks usually users make friendship relations with several users that sometimes do not communicate with them even once a year. On the other hand, there are some users that have similar interests and attributes, yet they do not have any connection with each other as they do not know each other. Through the proposed algorithm of this paper, discovered communities have members, which seem to be real members similar to those who we see in the society.

In this study, each node of the social networks is described by both attribute and link (relation) data sources, e.g. demographic information as attributes and relations or even a separate social network as links. Intuitively, in this paper a community is a connected subgraph of nodes, consisting of users who have the most similarity to each of the community members based on both of these sources. Relation data source form communities, when their users are connected to each other and at the same time, they have similar characteristics.

This paper is organized as follows. In section 2, the related works are reviewed. Then, the proposed algorithm is described

in section 3. Afterwards in section 4, the real data set from Facebook users and Soybean dataset are described, in order to demonstrate the accuracy of the algorithm. Finally, section 5 concludes the contribution and introduces some future research ideas.

II. RELATED WORK

A. Simple community detection approaches

The simple community approaches are graph partitioning, devise methods, spectral methods, Bayesian models, and clustering [11-17]. These approaches use one data source to construct the graph of social networks. This data source can show explicit links such as friendship relations or implicit relations that are gathered from the content of network. Two major content analyses are topic models and scientific authors' network, called citation graph. For detecting communities, each document is changed to some frequent keywords, and the document-word matrix is constructed for further analysis [5, 6]. This preprocessing is a costly step for community detection methods.

Citation graphs are social networks constructed from the references and used keyword in scientific papers. Experimental results show that the accuracy of community detection can be enhanced through this information [18]. In topic model studies, each community has one or more topics that its users are writing about that. Bayesian models are used for community detection algorithms; hence, most topic models are generative and vulnerable to words that are irrelevant to the target topic [1]. Furthermore, There are only a handful of scalable Bayesian approaches to community discovery in graph [10] that mostly extend Latent Dirichlet Allocation [19, 20].

B. Combinatorial community detection approach

Neither link information nor content information is sufficient to decide the community membership. Combining the link and content for community detection usually achieves better result. Two improvements of this approach is given following.

Combining different approaches covers drawbacks of every single algorithm. HCDF presented by Henderson et al, uses Latent Dirichlet Allocation on Graphs (LDA-G) as the core Bayesian method for community detection. A key aspect of HCDF is its effectiveness in incorporating hints from a number of other community detection algorithms and producing results that outperform the constituent parts. Furthermore, it produces algorithms that can predict links [10].

Complementary information used to propose new improved community detection methods. Influential nodes seem to be the centroids of communities. By this consideration, [21] proposed a new method that formed communities by influential nodes called leaders, and assigned other nodes to these leaders as followers. This complementary information is extracted from link sources but yields more accurate communities.

III. THE HYBRID COMMUNITY DETECTION ALGORITHM

Almost all the previous hybrid methods use context as content of social network. Context handling needs special models such as Bayesian models, but not all of them are scalable. Also preprocessing task is costly as related topic should be extracted. Furthermore, in some cases like online social networks, the context is not written in a proper grammatical and formal way; therefore, quality of community detection results will be decreased. In this paper the proposed algorithm utilizes two data sources of relations and attributes to detect communities. Therefore, the algorithm is able to detect communities of a social network without mentioned concerns. Using this algorithm, each node would be a member of a community if it has similar characteristics with others, or if it has common neighbors with other nodes of its community. This section is followed by describing how the nodes in each community are scored based on their relations or attributes, and then the way of fusing these two data sources is described. Finally the proposed algorithm shows how to detect communities.

A. Relations and the neighborhood score

Relationship data source is modeled by adjacency matrix; each element in the matrix is computed as follows [22]:

$$m_{ij} = 1 \text{ iff } \text{relation}(x_i, x_j) = \text{True} \quad (1)$$

The neighbors of each node are compared with all the cores' neighbors, then that node will be assigned to the community that has the maximum score of common neighbors with its core. The score of neighborhood is computed as follows, where N is the number of users in their community.

$$\text{score}_{ij}(\text{neighborhood}) = \frac{|\text{common_neighbors}(\text{node}_i, \text{core}_j)|}{N} \quad (2)$$

B. Users' attributes and the similarity score

Attribute data source can be represented as an $n*m$ user - attribute matrix, where n is the number of users or nodes, and m represents the number of attributes that each user has. The proposed algorithm uses categorical variables as attribute data source. Such as k-modes algorithm, each node should be assigned to a cluster/community with the most similar core. The dissimilarity between two nodes are computed by simple mismatching [23]. Simple mismatching between two nodes of (x_i, x_j) with d attributes is computed as follows:

$$D(x_i, x_j) = \sum_{l=1}^d \delta(x_{il}, x_{jl}) \quad (3)$$

$$\delta(x_{il}, x_{jl}) = \begin{cases} 0 & x_{il} \neq x_{jl} \\ 1 & x_{il} = x_{jl} \end{cases}$$

Recently, a new dissimilarity measurement parameter was introduced by Cao et.al that enhanced the accuracy of k-modes clustering algorithm [24]. This parameter for p attributes is computed as follows:

$$NDis_p(z_l, x_i) = \sum_{a \in p} NDis_a(z_l, x_i) \quad (4)$$

$$NDis_a(z_l, x_i) = 1 - Sim_a(z_l, x_i) \times m_a \quad \square$$

$$m_a = \frac{|x_i| |f(x_i, a) \equiv f(z_l, a), x_i \in c_l|}{|c_l|}$$

$$f(x, a) \equiv f(y, a) = \begin{cases} 1 & \text{if } f(x, a) \neq f(y, a) \\ 0 & \text{otherwise} \end{cases} \quad (5)$$

Finally, the similarity score is computed as follows:

$$score_{i,j}(\text{similarity}) = 1 - dissimilarity(\text{node}_i, \text{core}_j) \quad (6)$$

C. Detecting communities based on fusing two sources

The proposed algorithms need k representative nodes as cores of communities. Each node in the data set will be assigned to one of these cores which have the maximum score by that core. First communities are formed by attribute source. Next, an iterative process happens until communities undergo no change, refine the communities and update the best core of each community. The proposed algorithm, like other hill climbing algorithms such as k-modes, is sensitive to its initial nodes that the algorithm will be started by them. Moreover, the number of communities is another input parameter for this algorithm.

To detect communities based on similar attributes and relations, two scores should be considered. The way of fusing these scores is summation. If one of these sources has greater influence on the social network, the related score can be multiplied by an instant number as the weight of that source. In this study, we do not assign weight to sources. Before summation of two scores, scores should be normalized. By min-max normalization, both of the scores will be in the same range of values. Finally, total score will be:

$$\begin{aligned} \text{total score}_{i,j} = \\ \text{normalized score}_{i,j}(\text{neighborhood}) + \text{normalized score}_{i,j}(\text{similarity}) \end{aligned} \quad (7)$$

Algorithm 1 highlights the major steps of the hybrid community detection algorithm. The major steps are forming the communities and updating the cores. First assignments form first communities based on the similarity between nodes and cores, but for the iterative section, both the similarity and

neighborhood scores are considered. Experiments show that first formation will be refined by iterative section. That is why it only used the similarity score of attributes for the first discovering of communities. Iterative section considers both scores. Common neighbors between each node and the core should be computed through all of the native nodes. If the core or the considered node - has common neighbors with other communities, these neighbors should be ignored as they are not members of that community. Also the similarity will be compared to the nodes of each core's community.

Considering two data sources of attributes and relations for community detection make updating step more complex in comparison to one source used algorithms, such as k-modes. The next subsection focuses on selection of new cores after the new formation of each community.

Algorithm 1. The proposed algorithm

1. **INPUT:** dataset (attributes, adjacency matrix), k
 2. Selecting cores
 3. // first assignments
 4. **for** all nodes n \in dataset **do**
 5. assign n to the community which has minimum dissimilarity with its real centroid(core) and make first communities
 6. **end for**
 7. **for** all communities **do**
 8. Update the core of community // Algorithm 2
 9. **end for**
 10. // iterative section
 11. **Repeat**
 12. **for** all nodes n \in dataset **do**
 13. assign n to the community which has maximum total score with its core
 14. **end for**
 15. **for** all communities **do**
 16. Update the core of community// Algorithm 2
 17. **end for**
 18. **until** there is no change in communities
-

1) Updating cores

The core of a community is the most similar node to all the other nodes in its community. Since the attributes are categorical variables, the mode of each community is a good choice to show that core. Mode of a cluster or a community is a vector of attributes that can be not a node's attributes in the data set. That is why we do not use the mode to present the core. On the other hand, the node with the maximum influence in the community can also be an appropriate choice for selecting of cores. Influence can be measured by degree centrality, which is one of the best and simplest measurements [25]. It is computed using the following formula where N is the number of nodes and $deg(n, c)$ is the degree of node n in community of c:

$$DC(n) = \frac{deg(n, c)}{N - 1} \quad (8)$$

To update the core of each community, both similarity score and influence score will be computed for all nodes of that community. After the normalization of the scores, the node with maximum normalized score would be the new core of that community. Algorithm 2 depicts the updating process of each core in a community.

Algorithm 2. Core Updating

```

1. INPUT: community C
2. new_mode  $\leftarrow$  mode(C)
3. for all nodes  $c \in C$  do
4.   influence ( $c$ )  $\leftarrow$  Compute influence ( $c$ )
5.   similarity ( $c$ )  $\leftarrow$  Compute similarity ( $c$ , new_mode)
6.   Find min, max of both scores
7. end for
8. //normalization
9. for all nodes  $c \in C$  do
10.  Ninfluence( $c$ ) = [influence ( $c$ ) - min (influence)] / [max (influence) - min (influence)]
11.  Nsimilarity( $c$ ) = [similarity ( $c$ ) - min (similarity)] / [max (similarity) - min (similarity)]
12.  score( $c$ )= $Nsimilarity(c)+Ninfluence(c)$ 
13. end for
14. core(C)  $\leftarrow$  node  $c$  with maximum score

```

IV. EXPERIMENTAL STUDY

The proposed algorithms are coded in Matlab 7.10.0 programming language. Other related results and illustrations are using NodeXL 10.0.1.229. In this section first, data sets are introduced. Then, the accuracy of datasets will be computed and compared with a well-known community detection algorithm.

A. Data sets

1) Soybean network:

Since there is not a well-known data set to evaluate the proposed algorithm, Soybean disease data set which is frequently used for categorical clustering algorithms is selected. This data set has 47 instances, each being described by 35 attributes. Each instance is labeled as one of the four diseases. Except for the fourth disease which has 17 instances, all other diseases have 10 instances each. To make this data set as a social network, we added links to those instances that had the same disease. By adding this kind of relations to categorical attributes, communities can be found. Since the extracted information of these two sources is consistent, the accuracy of algorithm can be evaluated by comparing detected communities to instances with the same label of disease.

Fig. 1 shows the Soybean network. The visualization illustrates that there are four communities in this data set; similar to the number of diseases. For this data set, the number of communities is fixed to 4 and two sets of initial nodes are used.

2) Facebook Dataset:

Facebook is one of the most popular online social networks. Users in this website have their own profiles. To make a data set consistent with the proposed algorithm, we use 3 users as seeds. Two of these users are from Isfahan, Iran and they live in their hometown at the moment. They are single and their age is under 30. The third user is a 45 year old Iranian woman who has migrated and works in U.A.E. She is divorced. These users have 600 friends and all of the inter friendship relations are also considered. 2362 relations exist in the data set. The adjacencies of users are stored as a matrix.

Beside the relations data source, some attributes are gathered from user profiles. These attributes are: the city, state and country of hometown and current location of users. Gender, locale and relationship of each user are available too. For religion, about 97% of people left it blank, as it does not have a categorical value and a large amount of this attribute was null, this attribute is ignored.

In each profile, there are eight fields that users can write freely about their interests. We extracted two attributes from these context fields; the language of the writings and the number of filled fields. Table 1 describes these attributes and their domains. Domains are extracted from the available information in the dataset, not the whole feasible domains.

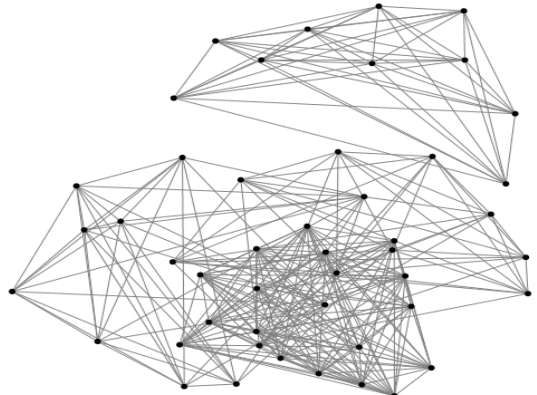


Fig. 1. Soybean network

TABLE I. ATTRIBUTES OF FACEBOOK DATASET

| Attribute | Categorical Domain | Some examples |
|--------------------------|--------------------|------------------------------|
| Gender | [1,2] | Female/male |
| Locale | [1,8] | fr_Fr, fa_Ir, en_US, en_UK |
| Relation | [1,11] | Single, married, complicated |
| Cities, states, Counties | [1,145] | - |
| Degree of nodes | [1,318] | |
| Language | [1,3] | English, Persian, others |
| Filled context fields | [1,8] | |
| Religion | - | - |

Fig. 2(a) illustrates the graph of Facebook link data source. Almost 27% of the nodes have just one friend in this data set. For this data set, the number of communities is set to 3 and initial cores are the seeds.

B. Accuracy evaluation

To evaluate the efficiency of proposed algorithm, the accuracy is employed in the experiments, where k is the number of communities which is known and a_i is the number of objects that are correctly assigned to their community.

$$\text{Accuracy} = \frac{\sum_{i=1}^k a_i}{n} \quad (9)$$

The accuracy of proposed algorithm is compared with two well-known algorithms; k -modes for attributes, and Newman-Girvan algorithm [26] to test the link data source. Finally, the accuracy of hybrid sources is computed. The dissimilarity parameter for Soybean data set is the simple mismatching parameter[23].

Our algorithm detects communities by two data sources of relations and attributes. Since there is not a prior algorithm to compare its results with our algorithm, it is necessary to compare the proposed algorithm with well-known algorithms that either use links or categorical attributes. therefore, for Facebook dataset we compared the accuracy results with Newman-Girvan's algorithm. Table 2 summarizes the number of members in each community. The accuracy of the proposed algorithm and Newman-Girvan algorithm were also computed. Fig. 2(b) illustrates these communities.

TABLE II. FACEBOOK MEMBERS OF EACH COMMUNITY AND ALGORITHM ACCURACY

| | 1st community | 2nd community | 3rd community | Accuracy |
|--------------------|---------------|---------------|---------------|---------------------------|
| Newman-Girvan | 318 | 220 | 65 | $\frac{601}{603} = 0.996$ |
| Proposed algorithm | 318 | 216 | 69 | $\frac{600}{603} = 0.995$ |
| Friends of seeds | 320 | 219 | 73 | - |

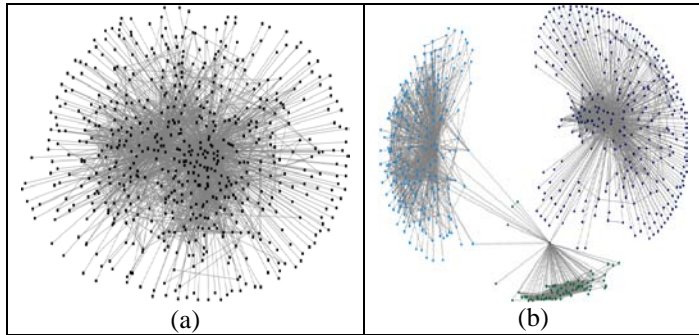


Fig. 2. Facebook social network (a) the random visualization of data set (b) detected communities of the data set

Since the ground truth of Facebook data set is not available, the attribute data source efficiency is just compared through the Soybean data set. Therefore, to reveal the accuracy of hybrid sources, the Soybean communities were compared to the kind of disease that each instance has. This study consisted of two set of initial nodes to start the algorithm. Similar to other hill climbing algorithms, initial nodes have effects on the accuracy. The experiment set was run for 10% of dataset nodes and the average results of accuracy on Soybean data set are summarized in table 3. In this test, number of links is not constant. For the first experiment, the adjacency matrix is null, then it has just 61 edges and the other experiments have full adjacency matrix. The last experiment did not select the first cores randomly; instead each core was an instant with one of the fourth kind of diseases. The increasing value of the accuracy shows that this source is really essential in this algorithm. As each core is a node with real influential score, accuracy for the link-based method is comparable to other methods; however, the core is not really the mode of that community; hence, we expect that the effect of links is greater, especially for Soybean data set.

V. CONCLUSION AND FUTURE WORK

The previous hybrid community detection methods were proposed based on the context and link sources. Since context processing is a voluminous task and online social networks contain informal vocabularies, a new source is introduced in this paper. Users have profiles with their information that yields to detect self-descriptive communities besides the link data source. Hence, the proposed algorithm is investigated to detect communities based on these two data sources. Experiments show the accuracy of the proposed algorithm; the results are comparable to well-known algorithms. The next extension is specifying a solution to extract the best first cores, and estimating the number of communities in the social network.

TABLE III. ACCURACY VS. LINK SOURCE COMPLETENESS

| Number of edges | First core selection method | Accuracy |
|-----------------|-----------------------------|----------|
| 0 | Randomly | 0.357 |
| 61 | Randomly | 0.6 |
| 271 | Randomly | 0.71 |
| 271 | Specified nodes | 0.893 |

REFERENCES

- [1] T. Yang, R. Jin, Y. Chi, and S. Zhu, "Combining link and content for community detection: a discriminative approach," in Proceedings of the 15th ACM SIGKDD international conference on Knowledge discovery and data mining, 2009, pp. 927-936.
- [2] K. Yang, "Combining Text-and Link-based Retrieval Methods for Web IR," in TREC, 2001.

- [3] Y. Wang and M. Kitsuregawa, "On combining link and contents information for web page clustering," in Database and expert systems applications, 2002, pp. 902-913.
- [4] J. Li and O. R. Zaïane, "Combining usage, content, and structure data to improve web site recommendation," in E-Commerce and Web Technologies, ed: Springer, 2004, pp. 305-315.
- [5] S. Zhu, K. Yu, Y. Chi, and Y. Gong, "Combining content and link for classification using matrix factorization," in Proceedings of the 30th annual international ACM SIGIR conference on Research and development in information retrieval, 2007, pp. 487-494.
- [6] N. F. Chikhi, B. Rothenburger, and N. Aussenac-Gilles, "Combining link and content information for scientific topics discovery," in Tools with Artificial Intelligence, 2008. ICTAI'08. 20th IEEE International Conference on, 2008, pp. 211-214.
- [7] F. Moser, R. Ge, and M. Ester, "Joint cluster analysis of attribute and relationship data without-a-priori specification of the number of clusters," in Proceedings of the 13th ACM SIGKDD international conference on Knowledge discovery and data mining, 2007, pp. 510-519.
- [8] C. Wang, Z.-y. Guan, C. Chen, J.-j. Bu, J.-f. Wang, and H.-z. Lin, "Online topical importance estimation: an effective focused crawling algorithm combining link and content analysis," Journal of Zhejiang University SCIENCE A, vol. 10, pp. 1114-1124, 2009.
- [9] Y.-M. Li and C.-W. Chen, "A synthetical approach for blog recommendation: Combining trust, social relation, and semantic analysis," Expert Systems with Applications, vol. 36, pp. 6536-6547, 2009.
- [10] K. Henderson, T. Eliassi-Rad, S. Papadimitriou, and C. Faloutsos, "HCDF: A Hybrid Community Discovery Framework," in SDM, 2010, pp. 754-765.
- [11] H.-W. Shen and X.-Q. Cheng, "Spectral methods for the detection of network community structure: a comparative analysis," Journal of Statistical Mechanics: Theory and Experiment, vol. 2010, p. P10020, 2010.
- [12] M. E. Newman, "Modularity and community structure in networks," Proceedings of the National Academy of Sciences, vol. 103, pp. 8577-8582, 2006.
- [13] B. Kernighan, Lin, S, " An efficient heuristic procedure for partitioning graphs," Bell system technical journal, vol. 49, pp. 291-307, 1970.
- [14] D. Zhou, E. Manavoglu, J. Li, C. L. Giles, and H. Zha, "Probabilistic models for discovering e-communities," in Proceedings of the 15th international conference on World Wide Web, 2006, pp. 173-182.
- [15] C. C. Aggarwal, An introduction to social network data analytics: Springer, 2011.
- [16] S. Fortunato, "Community detection in graphs," Physics Reports, vol. 486, pp. 75-174, 2010.
- [17] S. Parthasarathy, Y. Ruan, and V. Satuluri, "Community discovery in social networks: Applications, methods and emerging trends," in Social Network Data Analytics, ed: Springer, 2011, pp. 79-113.
- [18] D. Greene and P. Cunningham, "Multi-view clustering for mining heterogeneous social network data," presented at the 31st European Conference on Information Retrieval 2009.
- [19] T. Hofmann, "Probabilistic latent semantic indexing," in Proceedings of the 22nd annual international ACM SIGIR conference on Research and development in information retrieval, 1999, pp. 50-57.
- [20] S. Lacoste-Julien, F. Sha, and M. I. Jordan, "DiscLDA: Discriminative learning for dimensionality reduction and classification," in Advances in neural information processing systems, 2008, pp. 897-904.
- [21] R. R. Khorasgani, J. Chen, and O. R. Zaïane, "Top leaders community detection approach in information networks," in Proceedings of the 4th Workshop on Social Network Mining and Analysis, 2010.
- [22] S. Zhou, A. Zhou, W. Jin, Y. Fan, and W. Qian, "FDBSCAN: a fast DBSCAN algorithm," RUAN JIAN XUE BAO, vol. 11, pp. 735-744, 2000.
- [23] Z. Huang, "Extensions to the k-means algorithm for clustering large data sets with categorical values," Data Mining and Knowledge Discovery, vol. 2, pp. 283-304, 1998.
- [24] F. Cao, J. Liang, D. Li, L. Bai, and C. Dang, "A dissimilarity measure for the k -Modes clustering algorithm," Knowledge-Based Systems, vol. 26, pp. 120-127, 2012.
- [25] J. Sun and J. Tang, "A survey of models and algorithms for social influence analysis," in Social Network Data Analytics, ed: Springer, 2011, pp. 177-214.
- [26] M. Girvan and M. E. Newman, "Community structure in social and biological networks," Proceedings of the National Academy of Sciences, vol. 99, pp. 7821-7826, 2002.

Mobile Augmented Reality and Interactive Storytelling

Sagaya Aurelia
 Department of Computer Science
 Faculty of Education
 Beniwalid, Libya
 pSagaya.aurelia@gmail.com

Dr. Durai Raj
 Department of Computer Science
 Bharathidasan University,
 Tiruchirappalli, Tamilnadu, India.
 durairaj.bdu@gmail.com

Dr. Omer Saleh
 Department of Computer Science
 Faculty of Education
 Beniwalid, Libya
 immer.jomah@gmail.com

Abstract--Augmented reality (AR) is a technology that enhances user perception and experience, and allows users to see and experience the real world with virtual content embedded into it. This paper talks about the Mobile Augmented Reality (AR), its technological overview and architecture, Interactive storytelling and reasons how it can help to change the world when it is combined along with augmented reality are also stated. Thus, advantages and applications of MAR are highlighted to support the powerful technology with evidence.

Keywords: *Augmented Reality, Digital Storytelling, Interactive Storytelling, Immersive environment, Mobile Augmented Reality, Mixed Reality, Human Computer Interaction.*

I. INTRODUCTION

The ultimate goal of immersive environments that improve the process of understanding is to provide opportunities for the creation of spaces that are perfect displays for presenting seamless images, create the feeling of being there and present the content in the way that the medium (screen) is invisible. It also generates possibilities to access supplemental information. MAR systems integrate 3D virtual objects into a 3D real environment in real-time, enhancing user's perception of and interaction with the world. The paper proceeds as follows: In section 1 definition, Technological overview, architecture and applications of Mobile augmented reality are discussed. In section 2 we discuss about the Interactive storytelling and augmented reality based storytelling. Section 3 the limitations and future of augmented reality are discussed and how can this augmented reality be used as a storytelling medium is discussed in section 4. Finally conclusions are stated in section 5.

II. AUGMENTED REALITY

Azuma [16] defines AR as systems that have the following three characteristics:

1. Combine physical and virtual reality
2. Interactive in real time
3. Registered in 3-D

Let us note here that although this definition is very broad, most researchers have concentrated on visual augmentation

during the last years. Milgram [6] defines the Reality-Virtuality continuum as shown in figure 1. The real world and a totally virtual environment are at the two ends of this continuum with the middle region called Mixed Reality. Augmented reality lies near the real-world end of the spectrum with the predominant perception being the real world augmented by computer-generated data. Augmented Virtuality is a term created by Milgram to identify systems that are mostly synthetic with some real world imagery added, such as texture mapping video onto virtual objects [2].

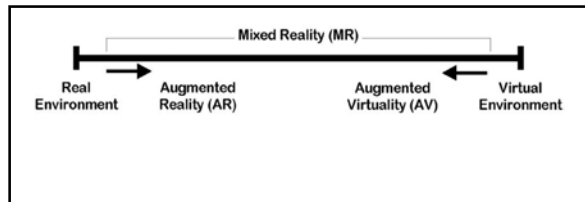


Fig. 1 Milgram's Reality – Virtuality continuum[2]

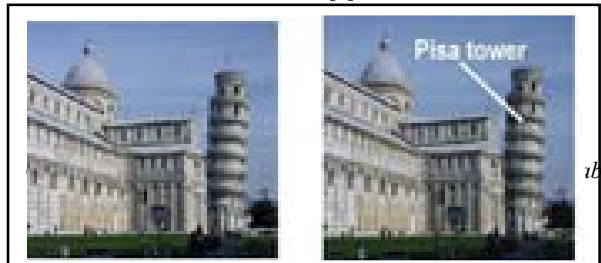


Fig. 1c.AV

Courtesy Ericsson Medialab

Fig. 1d. Virtual Environment Courtesy Ericsson Medialab



III. MOBILE AUGMENTED REALITY

We define MAR system which is: 1. what your eye can see through camera blends it with digital sources of information about what you are seeing; present both to you in a composite view, 2. Combination of reality and virtuality, 3. Execute in mobile mode real time. 4. Object which are real and virtual registers (aligns) each other as shown in figure 2. The fundamental components of mobile augmented reality are (1) Hardware computational platform, (2) software, (3) Wireless network, (4) Tracking, (5) Display, (6) Wearable input, (7) User interaction[3].

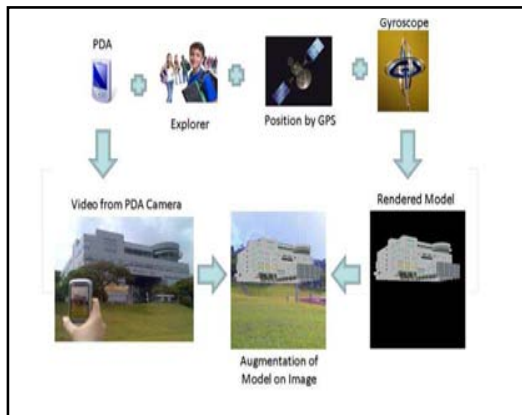


Fig. 2 Stages in Mobile augmented reality[3]

IV. TECHNOLOGY OVERVIEW OF MAR

Four key factors highlight the main reasons for this rapid adoption by mobile users:

Democratization of smartphones: The high penetration of these mini computers coupled with the unlimited data flat rates associated with them have led to a market explosion for applications and Internet access from mobile phones, leading to the proliferation of on-the-go services.

Maturity of the market: Users no longer demand mere mobile applications, they want to live experiences that are easy to use and that add value.

A boom in location-based services: The success of location solutions in recent years acts as an enabler for the takeoff of AR solutions.

Consolidation of Apps Stores: In a very short period of time, Apps Stores have managed to position themselves as the user's favorite distribution channel of mobile applications and have created a reliable ecosystem for the development of new services.

At the moment, there are different kinds of AR services on the market that allow interaction with the outside world. These fall into two broad categories depending on the technology required to identify objects: Location and Recognition [1].

A. Location

If an individual knows their exact position and what their mobile camera is focused on, they can represent information about any object in their field of vision in 3D. This exploits the capabilities of the numerous navigation sensors incorporated in the latest smartphone generation to help contextualize surrounding information:

A GPS to accurately locate the user's position using satellite triangulation.

A digital compass, also called a solid-state compass, to measure the relative position to the Earth's magnetic North Pole.

An accelerometer to detect changes in orientation and speed, and the variation of inertial motion, including falling and vibration shocks.

A gyroscope to support the accuracy of the accelerometer and correct variations in the conservation of angular momentum.

All these features, which were unthinkable in a mobile phone just a few years ago, are now the basis for the development of all kinds of AR services that impose virtual information on real space. One example is the award-winning application Star Walk (Figure 3), where the terminal becomes a window for the recognition of stars from any position. By the phone at the sky and watching the screen, the user can obtain information about any known object in the universe and become a smart astronomer, at least for a while! [1].

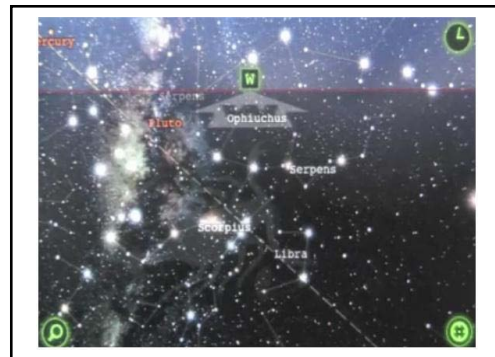


Fig. 3 Example of iPhone Star Walk Application[1]

B Recognition

The second method is more complex. It is based on the way that the phone is able to recognize the shapes and sounds that surround it by identifying digital patterns. Unlike the previous approach, this method can also work in indoor spaces because it does not depend on the user's GPS positioning. How does it work?

- *Using Markers:* Small images that allow the mobile device to recognize or translate content must be given. For example, when 2D barcodes (Figure 4), now ubiquitous in the market, are read by a terminal they are capable of generating an action: play a multimedia video, send an SMS, connect to a

mobile web device, etc. LLA Markers from Juniaio Company, can generate 3D content in real time from latitude, longitude and height as transmitted to the terminal that is then superimposed on the screen.

- *Marker-less indirect recognition*: the mobile device hears a song on the radio and is able to identify the album information to tell the user who the author is and simultaneously allow them to directly purchase the content. The sound is captured about for 20 seconds and is then sent in digital format to an Internet server, where it is compared with a database of songs to find similarities and return a result (title, album, singer, lyrics, etc.). A similar system, processing the data in the cloud and delivering a result, is used by the Google AR product known as Google goggles. Among its features is the ability to provide information about any monument, translate texts, read labels on wine bottles, download information from a picture in a museum, etc.

Marker-less direct recognition: This mode is by far the easiest to use as it is based on live image recognition in real time. Any image or object is susceptible to being digitized to provide a digital identity that permits it to be recognized. Once this has been done, a user simply approaches it with their mobile camera and an AR application can identify patterns that shape it and display information or media, or project an image of a 3D object to enrich it[1].



Fig. 4 Example of 2D code[1]

V. ARCHITECTURE OF MOBILE AUGMENTED REALITY IN LAYER

Layered approach architecture of mobile augment reality as shown in figure 5. As shown in layer 1 data generation capture the scene/object and the position using capturing device, supplementary details also adding by sensor. After that temporary data stored and forward in augmented unit. Data generation layer after mixing virtual and augmented environment sends data to augmentation layer .Finally display environment generated and display it [3]

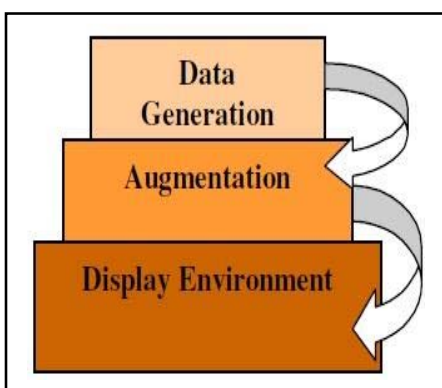


Fig. 5 Layered Architecture of MARS[3]

VI. HAND-HELD DISPLAYS FOR AUGMENTED REALITY

Hand-held displays as shown in figure 6 are tracked devices that can be held with the hand(s) and do not require precise alignment with the eyes (in fact the head is rarely tracked for hand-held displays). Hand-held augmented reality, also called indirect augmented reality, has recently become popular due to the ease of access to smartphones and tablets. In addition, system requirements are much less since viewing is indirect-rendering is independent of the user's head/eyes [7].



Fig. 6 Zoo-AR from GeoMedia and the iKat app from Zenitum are examples of hand-held augmented reality [7].

As the smartphone market continues to grow, consumers are using their devices to interact with all kinds of digital information. The experience of using your smartphone to connect the real and digital worlds is becoming more familiar for consumers, making them more likely than ever to engage with interactive experiences by scanning with their phone. Connecting meaningful and useful digital content to the real world isn't the future anymore, it's here today [8]. Figure 7 shows how mobile devices will rule the future world.

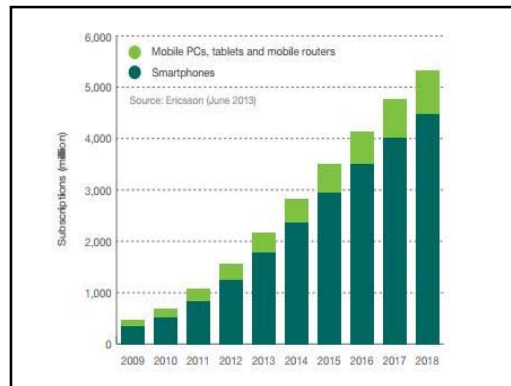


Fig. 7 Smartphone, PC, mobile routers and tablet subscriptions with cellular connections 2009-2018 [15]

VII. MOBILE AUGMENTED REALITY APPLICATIONS

MAR helps people make decisions in a simpler way from a few years ago, by:

- Showing the pharmacy that is closest and indicating how to get there.
- Drawing the virtual route of the road whilst a user drives on the real road.
- Guiding the user in the supermarket to a specific product.
- Indicating where and in what direction the nearest public service office is and checking opening times.



Fig 8: Indicating where the nearest city bike[1]

- Indicating where the nearest city bike can be found (Figure 8).
- Showing the way to the assigned gate when transferring at an unfamiliar airport [1].

VIII. WHAT IS DIGITAL STORYTELLING ?

Digital storytelling at its most basic core is the practice of using computer-based tools to tell stories. There are a wealth of other terms used to describe this practice, such as digital documentaries, computer-based narratives, digital essays, electronic memoirs, interactive storytelling, etc.; but in general, they all revolve around the idea of combining the art of telling stories with a variety of multimedia, including graphics, audio, video, and Web publishing[9].

The term "digital storytelling" can also cover a range of digital narratives (web-based stories, interactive stories, hypertexts, and narrative computer games) [10].

As with traditional storytelling, most digital stories focus on a specific topic and contain a particular point of view. However, as the name implies, digital stories usually contain some mixture of computer-based images, text, recorded audio narration, video clips, and/or music. The topics used in digital storytelling range from personal tales to the recounting of historical events, from exploring

IX. INTERACTIVE STORY TELLING

Interactive storytelling is a form of digital entertainment where authors, public, and virtual agents participate in a collaborative experience. [17] defines interactive storytelling as a form of interactive entertainment in which the player plays the role of the protagonist in a dramatically rich environment. The experience offered to the public by an interactive story differs substantially from a linear story. An interactive story offers a universe of dramatic possibilities to the spectator. In this form of entertainment, the audience can explore an entire set of storylines, make their own decisions, and change the course of the narrative.

Typically, the way viewers interact with a storytelling system is directly linked to the story generation model: character or plot-based model. Character-based approaches [18][19][20] give to the system great freedom of interaction. Usually, the story is generated based on the interactions between the viewer and the virtual characters. In some cases, the viewer can act as an active character in the story. In plot-based approaches [21][22], the interaction options are quite limited. The users can perform only subtle interferences to guide the progress of the narrative plot.

The level of interaction in storytelling must be carefully planned. Viewers should keep their attention on the narrative content and should not be distracted by the interaction interface. Another important aspect that must be considered during the design of an interaction model for an interactive storytelling system is the need of a multi-user interface. As in conventional TV and cinema, there may be more than one viewer watching the story at the same time. An interaction model must offer equal possibilities of interaction to all viewers. Another aspect that must be observed by an interaction system is the existence of several stereotypes of viewers. Some viewers like to interact actively with the story, others prefer to opine only on key points, while some prefer just to watch the story. The interaction system should adapt itself to the different types of viewers [13].

X. ARIS TOOL: AUGMENTED REALITY INTERACTIVE STORYTELLING

ARIS is a user-friendly, open-source platform for creating and playing mobile games, tours and interactive stories. Using GPS and QR Codes, ARIS players experience a hybrid world of virtual interactive characters, items, and media placed in physical space. As we contemplate open access and innovation, it is impossible to ignore the potential offered by ARIS (Augmented Reality Interactive Storytelling System). ARIS is not only a great tool, but a project that is gaining international notoriety. Here is a list of five reasons why the language learning community should pay attention [11]. Some features of ARIS are

1. Place-Based, Augmented Reality (AR) is Ideal for Many Areas of Language Learning

As language educators, the value of study abroad, service learning, and community interaction as beneficial for language learning are discussed. AR allows us to design interactive experiences, enhanced by mobile devices, to either create place-based interactions. The same way we might explore restaurants in a neighborhood using YELP, learners can explore (and hopefully expand) their surroundings via place-relevant resources.

2. The Notebook

Real time, geo-tagged, user-created data that can be made available to others within a public or restricted space and turned into game elements. Students can collect and share their language learning experiences (e.g., conversations, images, videos) for any number of reasons.

3. Potential for Student and Teacher Design and Building

The ARIS editor is designed for non-programmers and has an extensive documentation system and active discussion group always willing to offer help. This means your students can be up and running in a matter of a few hours. Design and creation have a great deal of potential as learning tools as well, which makes this feature great on multiple levels.

4. Innovative Funding Model

People contribute as they can to build different needed features, server space, etc. Also, the code is open to those wishing to work with it. ARIS success is a key model in terms of sustainable projects.

5. Free to Use

This is a key feature for many educational contexts [11].

XI. LIMITATIONS AND THE FUTURE OF AUGMENTED REALITY

Augmented reality still has some challenges to overcome. For example, GPS is only accurate to within 30 feet (9 meters) and doesn't work as well indoors, although improved image recognition technology may be able to help [23].

People may not want to rely on their cell phones, which have small screens on which to superimpose information. For that reason, wearable devices like SixthSense or augmented-reality capable contact lenses and glasses will provide users with more convenient, expansive views of the world around them. Screen real estate will no longer be an issue. In the near future, we may be able to play a real-time strategy game on our computer, or can invite a friend over, put on AR glasses, and play on the tabletop in front of us.

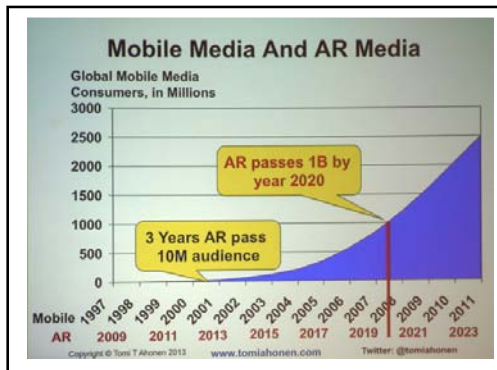


Fig 9. Future of Mobile media and AR media [15]

There are also privacy concerns. Image-recognition software coupled with AR will, quite soon, allow us to point our phones at people, even strangers, and instantly see information from their Facebook, Twitter, Amazon, LinkedIn or other online profiles. With most of these services people willingly put information about themselves online, but it may be an unwelcome shock to meet someone, only to have him instantly know so much about your life and background.

Despite these concerns, imagine the possibilities: we may learn things about the city we have lived in for years just by pointing your AR-enabled phone at a nearby park or building. In construction, you can save on materials by using virtual markers to designate where a beam should go or which structural support to inspect. Paleontologists working in shifts to assemble a dinosaur skeleton could leave virtual "notes" to team members on the bones themselves, artists could produce virtual graffiti and doctors could overlay a digital image of a patient's X-rays onto a mannequin for added realism.

The future of augmented reality as shown in figure 9 is clearly bright, even as it already has found its way into our cell phones and video game systems [12].

XII. HOW MAR CAN BE USED IN DIGITAL STORY TELLING

Using these six basic "ingredients," digital creators can cook up a great diversity of augmented reality experiences for people to participate in. They include [4]:

1. Playing games. There is an almost infinite variety of games users can play: trivia games; adventure games; mysteries; ball games; role-playing games; and so on.

2. Participating in a fictional narrative.

3. Exploring a virtual environment.

4. Controlling a simulated vehicle or device: a fighter jet, a submarine, a space ship, a machine gun.

5. Creating a character, including its physical appearance, personality traits, and skills.

6. Manipulating virtual objects: changing the color, shape, or size of an object; changing the notes on a piece of music; changing the physical appearance of a room.

7. Constructing virtual objects such as houses, clothing, tools, towns, machines, and vehicles.

8. Taking part in polls, surveys, voting, tests, and contests.

9. Interacting with smart physical objects: dolls, robotic pets, wireless devices, household appliances.

10. Learning about something. Interactive learning experiences include edutainment games for children, training programs for employees, and online courses for students.

11. Playing a role in a simulation, either for educational purposes or for entertainment.

12. Setting a virtual clock or calendar to change, compress, or expand time.

13. Socializing with others and participating in a virtual community.

14. Searching for various types of information or for clues in a game.

This is by no means an exhaustive list, though it does illustrate the great variety of experiences that augmented reality based interactivity can offer, and the uses to which it can be put.

XIII. CONCLUSION

Interactivity, as we have seen, profoundly changes the way we experience a work of entertainment. We go from being a member of the audience to becoming a participant. Instead of passively watching, listening, or reading, we take on an active role. Interactive works are immersive [4]. The 4 expected I's in storytelling such as Immersive, Interactive, Integration and Impact are fulfilled via augmented reality. Therefore, when immersive technology such as mobile augmented reality are used in interactive storytelling medium, the usability level increases and thereby the involvement and the level of understanding also increases.

REFERENCES:

- [1] Ascent white paper mobile augmented reality http://atos.net/content/dam/global/ascent-whitepapers/ascent-whitepaper-mobile_augmented_reality.pdf (accessed on 21/4/2014)
- [2] B J Ö R N E K E N G R E N ,Mobile Augmented Reality, Master of Science Thesis Stockholm, Sweden 2009
- [3] Mr.A.T.Vasaya , Mr.A.S.Gohil, A Survey of Mobile Augmentation for Mobile Augmented Reality System, INTERNATIONAL

- JOURNAL FOR RESEARCH IN APPLIED SCIENCE AND ENGINEERING TECHNOLOGY (IJRASET), Vol. 2 Issue II, February 2014, ISSN: 2321-9653
- [4] Carolyn Handler Miller, Digital Storytelling ,A Creator's Guide to Interactive Entertainment, Copyright 2004, Elsevier, ISBN : 0-240-80510-0
 - [5] Adiv G., "Determining Three-Dimensional Motion and Structure from Optical Flow Generated by Several Moving Objects", IEEE Transactions on Pattern Analysis and Machine Intelligence, vol 7, no. 4, July 1985 Page(s) 384-401
 - [6] Milgram, P., Kishino, F., "A Taxonomy of Mixed Reality Visual Displays", IEICE Transactions on Information Systems, Vol E77-D (12), pp 1321-1330 Dec. 1994.
 - [7] www.nextgeninteractions.com/what-we-do/virtual-and-augmented-reality/
 - [8] www.deloitte.com
 - [9] digitalstorytelling.coe.uh.edu/
 - [10] en.wikipedia.org/wiki/Digital_storytelling
 - [11] <https://blog.coerll.utexas.edu/augmented-reality-interactive-storytelling>
 - [12] <http://computer.howstuffworks.com/augmented-reality.htm/printable>
 - [13] Edirlei Soares de Lima, Bruno Feijó, Simone Barbos , Fabio Guilherme da Silva, Antonio L. Furtado, Cesar T. Pozzer , Angelo E. M. Ciarlini , "Multimodal, Multi-User and Adaptive Interaction for Interactive Storytelling Applications" , SBC - Proceedings of SBGames 2011
 - [14] www.realityaugmentedblog.com
 - [15] www.flickr.com
 - [16] Azuma R. T., "A Survey of Augmented Reality", Presence: Teleoperators and Virtual Environments vol 6, no 4 August 1997 Page(s) 355-385
 - [17] Crawford , C,2004 Chris Crawford on Interactive Storytelling, Estodos Unidos, New Riders
 - [18] CAVAZZA M CHARLES, F MEAD, S,2002 ,Character-based interactive storytelling.IEEE Intelligent System Volume 17, Issue 4, pp 17-24
 - [19] YOUNG, M., 2001. An Overview of the Mimesis Architecture: Integrating Intelligent Narrative Control into an Existing Gaming Environment. In: Working Notes of the AAAI Spring Symposium on Artificial Intelligence and Interactive Entertainment.
 - [20] AYLETT ,R, DIAS,J., PAIVA,A,2006. An affectively driven planner for synthetic characters, Proceedings of 16 th International Conference of Automated Planning and Scheduling, pp 2-10
 - [21] GRASBON D BRAUN,N,2001. A morphological approach to interactive storytelling, Proceedings of the 2001 Living in Mixed Realities,pp 337-340
 - [22] CLARLINI A.E.M,POZZER,C.T.FURTADO,A.L.FEIJO.B, A logical based tool for interactive generation and dramatization of stories,Proceedings of the International Conference on Advances in Computer Entertainment Technology, Valencia, Spain,pp 133-140
 - [23] www.metz-xs.com/augmented-reality.html

Concealing of Data Using Conjecturable Dissemination of Image

J.Hari

Department of Information Technology
 Vignan's Institute of Engineering for
 Women, Visakhapatnam
harijyothula@gmail.com

S.Kalyani

Department of Information Technology
 Vignan's Institute of Engineering for
 Women, Visakhapatnam

Abstract— Digital communication has become an essential part of infrastructure nowadays, a lot of applications are Internet-based and it is important that communication be made secret. As a result, the security of information passed over an open channel has become a fundamental issue and therefore, the confidentiality and data integrity are required to protect against unauthorized access and use. The main goal in this paper is to give new insights and directions on how to improve existing methods of hiding secret messages, possibly by combining steganography and cryptography. Data hiding techniques focus on methods of encrypting hidden data in which cryptographic algorithms are combined with the information hiding techniques to increase the security of transmitted data. This paper considers an unfolding approach for the above mentioned problem using encrypted information hiding based on RSA algorithm and Conjecturable Dissemination for encrypting digital images. Information embedding and host image embedding are done to increase the security of the transmitted data. Finally, the resultant image is found to be more secure.

Keywords- Encrypted Information Hiding, Conjecturable Dissemination, Digital Images, Host Image Embedding

I. INTRODUCTION

Information hiding techniques have recently gained great attention due to its importance for a large number of multimedia applications. Digital images are increasingly transmitted over non-secure channels such as the Internet. To protect the authenticity and confidentiality of multimedia images, several approaches have been proposed. These include conventional cryptography, steganography, digital signatures that are based on the image content. Adil Haouzia & Rita Noumeir present a survey and a comparison of emerging techniques for image authentication. Methods are classified according to the service they provide, that is strict or selective authentication, tamper detection, localization and reconstruction capabilities and robustness against different desired image processing operations[1]. Bin Li, Junhui He, Jiwu Huang, Yun Qing Shi present a survey on steganography and steganalysis for digital images, mainly covering the fundamental concepts, the progress of steganographic methods for images in spatial representation and in JPEG format, and the development of the corresponding steganalytic schemes. Some commonly used strategies for improving steganographic security and enhancing steganalytic capability are possible in

research trends[2]. Pratap Chandra Mandal state that how various steganographic techniques, its applications are different from cryptography. Steganography is important due to the exponential growth and secret communication of potential computer users on the internet. [3]. Shailender Gupta, Ankur Goyal, Bharat Bhushan state , how the two popular techniques Rivest, Shamir, Adleman (RSA) algorithm and Diffie Hellman algorithm encrypt the data. The result shows that the use of encryption in Steganalysis does not affect the time complexity if Diffie Hellman algorithm is used instead of RSA algorithm [4]. Mehdi Hussain and Mureed Hussain state that steganography means , not to alter the structure of the secret message, but hides it inside a cover-object (carrier object). After hiding process cover object and stego-object (carrying hidden information object) are similar. Due to invisibility or hidden factor it is difficult to recover information without known procedure in steganography. Detecting the procedure of steganography is known as Steganalysis[5]. There are also different techniques for Image Processing Using Cryptography and Steganography[6]-[10].

In this paper, the proposed model includes the encrypted information hiding concept to reduce the risk of using cryptographic algorithms alone. Data hiding techniques embed information into another medium making it imperceptible to others, except for those that are meant to receive the hidden information and are aware of its presence. It focuses on methods of encrypting hidden data in which cryptographic algorithms are combined with the information hiding techniques to increase the security of transmitted data. The remainder of this paper is organized as follows. Section II describes the proposed model; Section III describes the host image embedding. The implementation and results are given in Section IV, Conclusion is given in Section V.

II. PROPOSED MODEL

In this section, we describe the steps that are performed in the improved method for hiding information. This paper presents the encrypted information hiding concept to reduce the risk of using cryptographic algorithms alone. It focuses on methods of encrypting hidden data in which cryptographic algorithms are combined with the information hiding techniques to increase the security of transmitted data. In such schemes, the secret data is first encrypted, then embedded into cover image to generate ‘stego-image’, which

is then sent through a network or via the Internet. The unauthorized recovery of hidden encrypted data is very difficult because it needs the interceptor to first detect the existence of the hidden information, determine a way of extracting it from the host image and then decrypting it to recover the original information. The several well-defined stages, presented in Fig. 1.

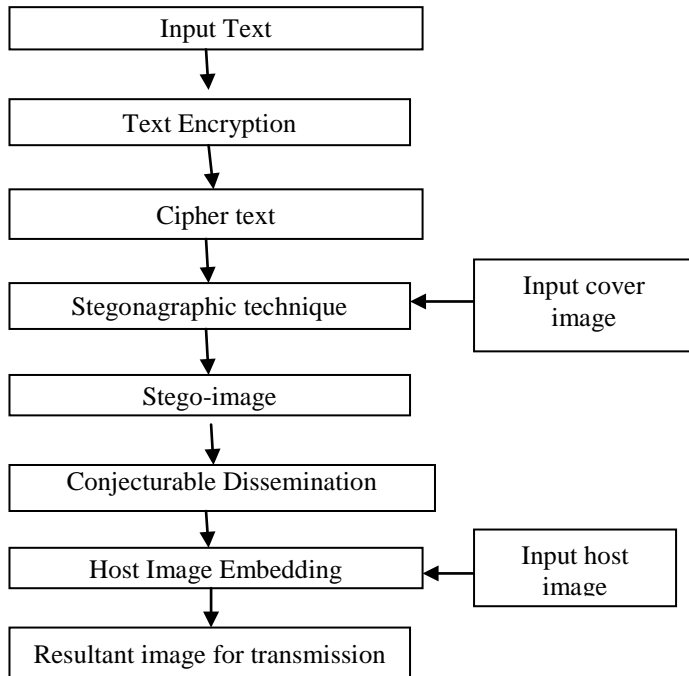


Fig .1. General Structure of Proposed method

Initially the plain text is encrypted using RSA algorithm. In the next step the encrypted text is embedded into the image. After that the embedded image is scrambled. Finally the scrambled image is embedded into another image.

A. Text Encryption:

The text encryption module concept is to reduce the risk of using cryptographic algorithms alone. In this the plain text is encrypted using RSA algorithm. RSA makes use of an expression with exponentials [11]. The plaintext is encrypted in blocks, with each block having a binary value less than some number n.

RSA algorithm:

Consider any two prime numbers p, q where p not equal to q. Now calculate $n=pq$ and also calculate $\phi(n)=(p-1)(q-1)$. Select an integer e such that $\gcd(\phi(n),e)=1(1 < e < \phi(n))$. Calculate d such that $d=e^{-1}(\text{mod } \phi(n))$. the public key is PU={e,n} and private key is PR={d,n}.

Consider the plaintext M ($M < n$) and the plaintext is encrypted to generate the cipher text by using the formula $C=M^e \text{ mod } n$, in the decryption side, consider the ciphertext C and from this the cipher text is decrypted to generate the plaintext using the formula $M=C^d \text{ mod } n$.

B. Encrypted Information Hiding:

In order to provide security, the encrypted data i.e., the ciphertext is hidden in the cover image to generate ‘stego-image’. In this module we read the cipher text that is to be embedded. To embed message into image we have to read the image from the folder of any format(*.jpg, *.jpeg, *.png, *.gif, *.tiff, *.bmp, *.dib, *.png, *.bmp). Calculate the image size and message length. We need to store the message length to know how many pixels to read to embed the message. Because the length of the message can't be predicted, 32 bits (for the first 32 pixels) are allocated. It stores message into least significant bit of R,G, and B. So, for the LSB of the R component, you want 8, for the G, 16 and for B, 24.



Fig .2. Organization of pixels under ARGB System

C. Conjecturable Dissemination:

The conjecturable dissemination process is used as cryptography method. In this module, the stego-image obtained from the encrypted information hiding module is scrambled. For scrambling the image, the pixel values and rgb value of every pixel of the image is calculated and from this maximum rgb value is considered. From this maximum rgb value the rgb value of every pixel is subtracted. Thus, new rgb values are generated at every pixel using which a new image is constructed .scrambling the stego image is achieved from the following steps.

Step1: calculate the pixel values and rgb value of every pixel of the image.

Step2: Determine the maximum rgb value.

Step3: Subtract the rgb value of every pixel from the maximum rgb value

Step4: New rgb values are generated at every pixel using which a new image is constructed.

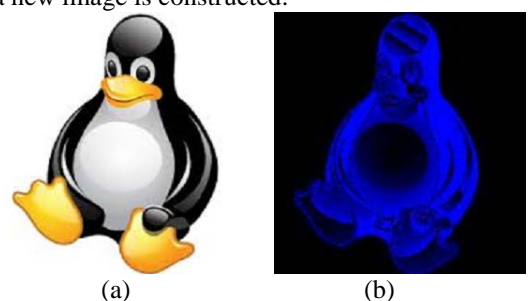


Fig .3. (a) Original image, (b) Scrambled Image.

III. HOST IMAGE EMBEDDING

To increase the security of the hidden data and improve the robustness of the cryptographic algorithms

discussed earlier, we consider a method of randomizing the cipher bits over multiple host image LSBs as well as randomizing the embedding bits order using different noise distribution (models) as hidden codes. The main advantage of this is however, modifying or destroying the host image will not cause full loss of the cipher bits because they are scattered along multiple bits which enables the intended receiver to recover the hidden data. In this the scramble image is taken as input. Another image with same dimensions like the scrambled is considered.

Step1: read the pixel values of both the images

Step2: calculate their respective rgb values.

Step3: add the rgb values of both the images

Step4: new rgb values are generated using which the new image is constructed.

From this the final host image is generated. The following figures show how the image embedded into another image.

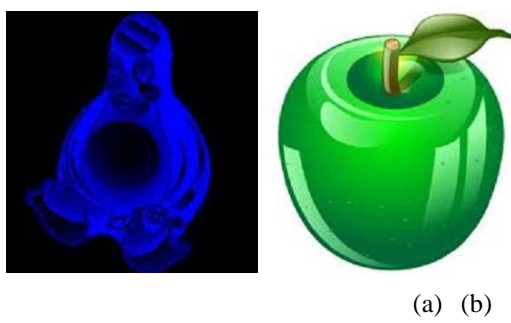


Fig .4. (a) shows Scrambled Image, (b) another Image (with same dimensions as scrambled image), (c) shows the Embedded Image

IV. RESULTS AND EXPERIMENTAL COMPARISION

The experimental results for the host image embedding is shown in Figure 4. The results so obtained are by adding the rgb values of the two images. In this paper, the concept of encrypted information hiding has been justified. The approaches that are discussed earlier i.e., conventional cryptography, steganography; digital signatures that are based on the image content have been justified. Compared to previous work our new system implemented an application for the collaborative management of encrypted data, called information hiding technique.

Steganography is the more conservative technology to hide any secret information within an image. Today steganography is mostly used on computers with digital data

being the carriers and networks being the high speed delivery channels.

V. CONCLUSION

In this paper, the concept of encrypted information hiding has been presented. The use of cryptographic algorithms together with steganography make it almost impossible for interceptor to recover the encrypted hidden data as this requires the interceptor to detect the existence of the information before attempting to decrypt it. To recover the original data, the attacker needs to first find a way to extract the hidden encrypted information from the stego-image, which requires knowledge of the data hiding codes and the appropriate algorithm/key(s). The exposure of the encryption key(s), the encryption algorithm and the embedding technique along with the hidden codes to those other than the intended receiver is practically impossible. We have considered the application of conjecturable dissemination for encrypting image data prior to embedding it into a host image.

However, this paper focuses on two key issues: (i) extending the application of conjecturable dissemination to hide 8-bit and 24-bit images into a full color image respectively to provide a high fidelity decrypt. Coupled with appropriate key-exchange protocols to initiate cryptographically strong ciphers, the approach provides a generic method of encrypting and hiding high fidelity digital image information. (ii) the use of the hidden ciphertext in the embedding process in two phases; the first phase is to scramble the pixel values order, while the second one is embedding one image into another image making it more secure and robust to certain attacks. However, modifying or destroying the host image will not cause full loss of the cipher bits because they are scattered along multiple bits which enables the intended receiver to recover the hidden data.

REFERENCES

- [1]. Adil Haouzia & Rita Noumeir, "Methods for image authentication: a survey". published online: 1 August 2007.
- [2]. Bin Li, Junhui He, Jiwu Huang, Yun Qing Shi, "A Survey on Image Steganography and Steganalysis", 2010, Journal of Information Hiding and Multimedia Signal Processing.
- [3]. Pratap Chandra Mandal, "Modern Steganographic technique: A survey" International Journal of Computer Science & Engineering Technology (IJCSET), 2012.
- [4]. Shailender Gupta, Ankur Goyal, Bharat Bhushan, "Information Hiding Using Least Significant Bit Steganography and Cryptography" I.J.Modern Education and Computer Science, 2012, 6, 27-34 Published Online June 2012 in MECS.
- [5]. Mehdi Hussain and Mureed Hussain, "A Survey of Image Steganography Techniques" International Journal of Advanced Science and Technology Vol. 54, May, 2013.

[6]. S.Dhanalakshmi, Dr.T.Ravichandran, “A New Level Of Image Processing Technique Using Cryptography And Steganography”: International Journal of Science, Engineering and Technology Research (IJSETR) Volume 2, Issue 3, March 2013.

[7]. Jonathan M Blackledge and AbdulRahman I Al-Rawi, “Steganography using Stochastic Diffusion for the Covert Communication of Digital Images; IAENG International Journal of Applied Mathematics, 41: 4, IJAM_41_4_02.

[8]. Che-Wei Lee and Wen-Hsiang Tsai, “A Data Hiding Method Based on Information Sharing via PNG Images for Applications of Color Image Authentication and Metadata Embedding”: Department of Computer Science and Information Engineering National Chiao Tung University, Hsinchu, Taiwan; Department of Information Communication Asia University, Taichung, Taiwan.

[9]. Abhinav Srivastava, “A survey report on Different Techniques of Image Encryption”; CSE Dept, IT-GGV, Bilaspur, India, International Journal of Emerging Technology and Advanced Engineering (ISSN 2250-2459,Volume 2,Issue 6, June 2012).

[10]A.Joseph Raphael,Dr.V Sundaram,” Cryptography and Steganography – A Survey” Department of Computer Applications, Karpagam University ,Coimbatore, India. International Journal of Computer Technology and applications, Vol 2 (3), 626-630

[11]. W.Stallings, “Cryptography and Network Security: Principles and Practice”, New Jersey : Prentice-Hall, 1999.

Remoulded Dredged Marine Clay: A Study of Time Factor on Strength Recovery

Chee-Ming Chan

Faculty of Engineering Technology
Universiti Tun Hussein Onn Malaysia
Batu Pahat, Johor, Malaysia
cheeming76@live.com

Abstract—Dredged marine soils, particularly clays and silts, are usually disposed of in open sea, inadvertently causing contamination and destruction of the marine ecosystem. Some of these adverse effects are long term, far-reaching and irreversible. However, if suitably assessed and managed, the dredged soil can be potentially reused as a backfill material with sufficient soundness and safety. Applications include reclamation and shoreline rehabilitation works, where artificial land is created using the dredged soil. Due to the very soft or slurry form of the material, significant subsidence is expected in a backfilled embankment, as the soil undergoes sedimentation and self-weight consolidation. This would be followed by time-dependent regain of strength, under constant water content or volume condition, also known as ‘thixotropic hardening’. It is imperative to know this time-dependent characteristic of the material for efficient reuse, where the time required for sufficient strength regain can be estimated. The present study simulates and examines the post-consolidation hardening of a couple of dredged marine clay samples, with the aim of shedding light on the ageing effect contributing to long term strength gain. The samples were retrieved from Malaysian waters, and remoulded in the laboratory to form a simulated backfilled soil bed. Measurements included the vane shear and cone penetration tests. The findings serve as a preliminary guide to the influence of time factor on strength recovery of reclaimed grounds backfilled with dredged marine clay left to settle by itself.

Keywords—dredged marine clay, time, remoulded, strength

I. INTRODUCTION

Dredging is carried out for the maintenance of navigation channels or the deepening of existing port facilities to cope with the docking vessels [1]. As dredging involves dislodging of the sediments, the process is inadvertently disruptive and causing temporary and long term effects on the surrounding marine environment. The large amount of dredged marine soils generated is commonly dumped in designated offshore disposal sites, consequently raising the risks of contamination and

Dredge-and-dispose is routinely carried out when the dredged soils contained mainly of fine grained materials, which constitute poor engineering properties with limited usage. Considering the adverse effects resulting from such practices, it is desirable to develop beneficial reuse of the

material, albeit not without some form of pre-treatment if necessary.

These fine-grained dredge sediments can be potentially reused as backfill material for reclamation works via strength and stiffness gain over time, or what is technically known as ‘thixotropic hardening’. Similar to the mechanism of secondary compression which is a post consolidation hardening process, the relocated material will regain strength and hardness under constant volume and water content with the rearrangement of the soil particles to a more stable state [3&4]. Nonetheless it is a time-dependent process and unless the rest period required can be precisely identified, practitioners would be reluctant to adopt the material due to financial concerns. Past reports on the successful improvement of dredged marine clays for potential reuse have been promising, e.g. [5]-[8], though most included solidification. Relatively fewer reports were presented on the remoulded strength recovery without the aid of admixtures.

The present study replicates and investigates the thixotropic hardening process of 2 remoulded dredged marine clay soils retrieved from Malaysian waters. Prepared at different water contents relative to the soil’s liquid limit, the strength and stiffness gain with time were monitored using the fall cone and vane shear tests. Taking into account the relatively small model of soil bed, the monitoring period was kept at 7 days only, with measurements taken at pre-determined intervals.

II. MATERIALS AND MEASUREMENTS

A. Dredged Marine Clay

The dredged marine samples examined in the present study came from 2 different dredging sites on the west coast of Peninsular Malaysia. Physical properties of the soils are given in Table 1. Note that the natural water content for both soils were far higher than the liquid limit, indicating a material saturated with water, soft and weak with negligible load resistance capacity. The soil samples were first semi-dried over a heated pan [9], so that test samples at various water contents could be prepared by addition of suitable amounts of water later. The amount of water added for remoulding of the soil samples were fixed at 0.75, 1.00 and 1.25 times the liquid limit. A separate set of samples were prepared at 1.25LL and

the addition of small quantities of cement (i.e. no more than 10 % per dry weight of the soil), for the purpose of examining possibilities of shortening the rest period before the soil was sufficiently strong and stiff for load bearing. The remoulded dredged marine soil samples were next placed in moulds of 9.5cm x 30 cm x 11 cm and lightly tapped to remove any entrapped air. The soil bed was thus ready for measurements with the fall cone and vane shear devices.

TABLE I. PHYSICAL PROPERTIES

| Properties | Samples | |
|-----------------------------|-------------------------------------|-------------------------------------|
| | Lumut (L) | Melaka (M) |
| Particle size distribution: | | |
| ▪ Sand (%) | 14 | 9 |
| ▪ Silt (%) | 8 | 18 |
| ▪ Clay (%) | 75 | 69 |
| Natural water content (%) | 165.7 | 166.16 |
| Atterberg limits: | | |
| ▪ Liquid limit (%) | 97.70 | 54.20 |
| ▪ Plastic limit (%) | 21.70 | 30.72 |
| ▪ Plasticity Index | 76.00 | 23.48 |
| Soil classification (USCS) | CH (C: clay; H: high plasticity) | CH (C: clay; H: high plasticity) |

B. Fall Cone Test (FCT)

The fall cone test is conventionally used to relate cone penetration with the liquid limit of soils, based on the reduced shearing resistance of the soil with increased water content [10]. However the test results can also be related to the undrained shear strength of the soil [11]. Hence in the present study, the test was adopted to gauge the increased shear resistance with time. The test procedure is simple: an 80 g cone with apex angle of 30° is released from the surface of the soil sample and left to penetrate by its self weight for 5 seconds, after which the penetration depth is measured. Note that the minimum centre-to-centre distance between the points of measurement was kept at 4 cm to avoid disturbance of the surrounding soil (Fig. 1). The similar distance was maintained for the vane shear test.

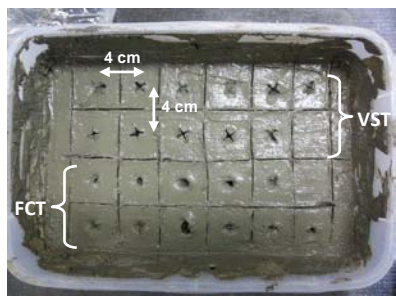


Fig. 1. Plan view of the soil bed.

C. Vane shear test (VST)

The increase in shear strength by thixotropic hardening, with or without induced solidification, was determined by the laboratory vane shear test. The test was considered the most

appropriate since the soils were classified as cohesive soil of fine grained type with very low strength, where other strength tests, such as unconfined compression test, would be impractical. A standard vane of 12.7 mm x 12.7 mm was used with the corresponding torsion spring for the measurements. The torsion spring was chosen based on the maximum stress it is expected to sustain while shearing the soil sample. Torque was applied to the soil via the vane by rotation at 10° per minute. Similar to FCT, disturbance of neighbouring points of measurement was minimized by maintaining a distance of 4 cm centre-to-centre (Fig. 1). The undrained shear strength (c_u) is derived from the vane shear test by Eq. (1):

$$c_u = 2T/\pi D^2[H+(D/3)] \quad (1)$$

where M = torque applied (Nmm), K = torsion spring constant (Nmm), D = overall width of the vane (mm) and H = the length of the vane (mm).

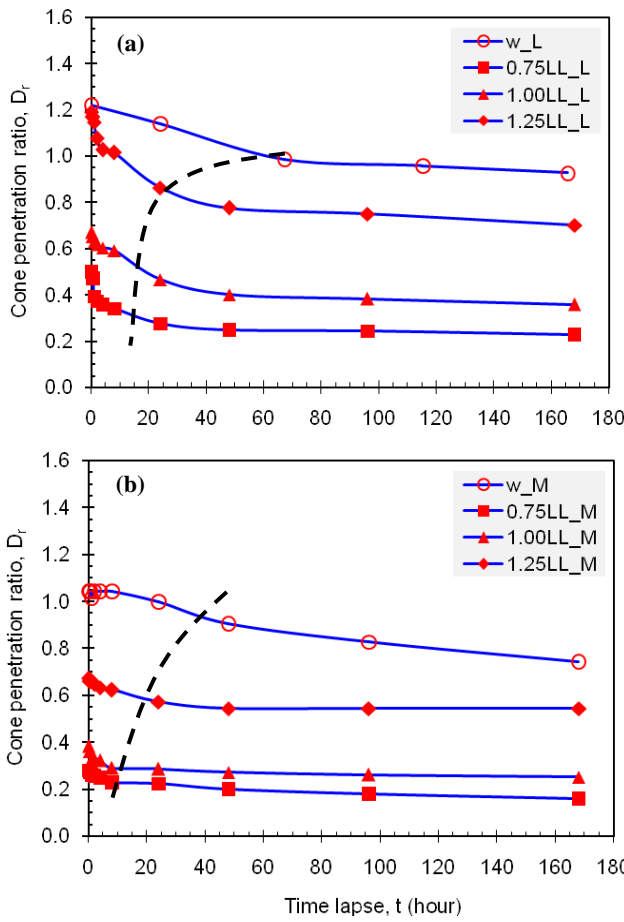
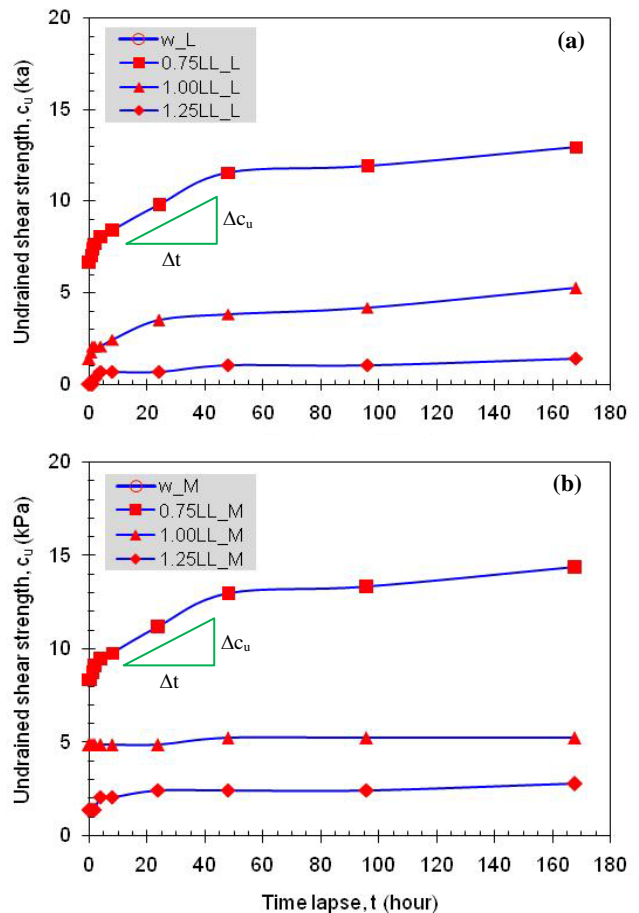
III. RESULTS AND DISCUSSIONS

A. Cone Penetration Ratio (D_r)

Fig. 2 shows the cone penetration ratio (D_r) plotted against the time lapse (t) for both soil samples. D_r is simply derived by normalizing the cone penetration depth with the cone's height, i.e. 35 mm. The normalization was mainly to give a quick and direct indicator of the soil's shear strength over time. Both soil samples show increased resistance against the cone weight with time, as represented by the gradually flattening out of the plots, though Sample M appeared to undergo less deformation compared to Sample L despite sharing the same initial water content. This could be attributed to the soil's physical properties, e.g. slightly lower clay content in Sample M. Samples at their natural water contents (w), which were greater than 1.25LL, clearly underwent the lowest stiffening effect. Nonetheless the deformation of Sample M stabilized approximately 10 hours sooner than Sample L. Indeed, the less water there was in the soil, the less initial deformation took place, followed by stiffness increase in lesser time.

Referring to Fig. 2, the deflection points (approximate intersection of the relatively linear sections of each plot) are joined with a dashed line to illustrate the time lapse between marked deformation caused by the cone drop and the subsequent plateau. While the deflection points could not always be readily distinguished (e.g. in Fig. 2b), the connecting plots emerged to be discernible. It can be noted that the rest period required for effective stiffness gain of the cement-treated samples was more subtle than the original samples.

The rest period required for the both soils at the natural water content was barely discernible, indicating the very gradual rearrangement of the soil particles in a flocculated matrix of excessive water in the pores (see Fig. 2). With dryer samples, i.e. less water content, the soil particles faced less resistance to come together and fill in the voids between them. The process results in a soil mass of fewer voids with more contact between the particles, hence enabling better resistance against the shearing force exerted by the falling cone. On site, some form of drainage path, such as a sand blanket, would be expedient in expulsion of the excess water.

Fig. 2 Cone penetration ratio (D_r) – time plots.Fig. 3 Undrained shear strength (c_u) – time plots.

B. Undrained Shear Strength (c_u)

The undrained shear strength (c_u) as derived from the vane shear test for both soil samples are shown in Fig. 3, as corresponding to Fig. 2. Note that the 1.25LL samples were too soft to be gauged even with the softest torsion spring, suggesting shear strengths of no larger than 10 kPa. Generally, shear strength of the soil increased with passing time, in conjunction with the decreased cone penetration depth as the soil's strength and stiffness improved. Referring to Fig. 3, both soils showed more significant strength increase with less initial water content, though the time lapse for the strength to stabilize appeared to be longer than the wetter samples, i.e. post 48 hours. This is notwithstanding the fact that the wetter samples underwent very minute strength gain overall. In 7 days, the 0.75LL samples for both soils recorded strengths of approximately 5 times those of the 1.25LL samples.

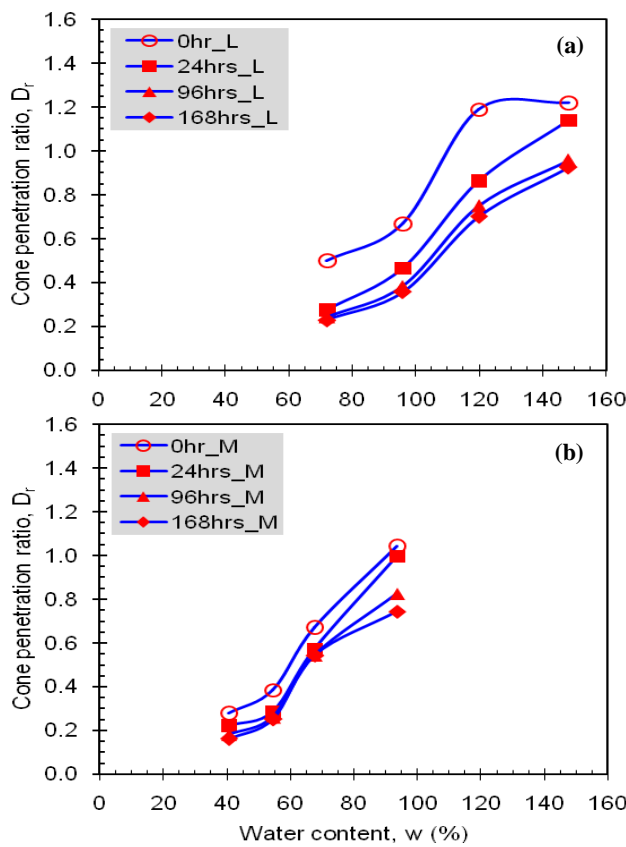
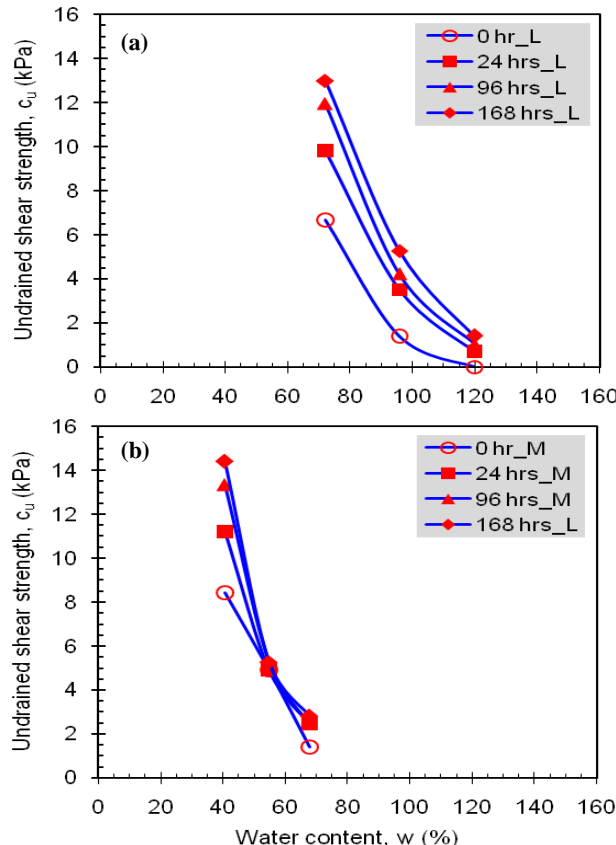
Overall the strength gain pattern is similar to that demonstrated by the cone penetration measurements, i.e. an increase in c_u corresponding with a decrease in D_r . At 0.75LL, both samples showed very similar strength gain rates, as indicated by the gradient triangle in Fig. 3. Indeed, the strength gain rate for both soils reached a peak at about the same time too, i.e. 48 hours. This was followed by a plateau of c_u over the next 120 hours, indicating negligible strength improvement with prolonged rest period. Sample M was found to have a slightly higher c_u after 168 hours, and this can again

be verified with the cone penetration results in Fig. 2. The soils do appear to gain strength at different rates despite the same water content at 1.00 and 1.25LL. Sample L appeared to undergo more significant strength gain in the initial stage upon placement of the soil bed compared to Sample M, and the slight continuous strength improvement beyond 24 hours were also more pronounced than Sample L. Nonetheless Sample M recorded a slightly higher c_u at 168 hours. This could be attributed to the different composition of soil particles (size-wise) in each sample, but further verifications are necessary.

C. Initial Water Content Effect

As discussed above, the initial water content has a marked influence on the strength recovery of the remoulded clay. Fig. 5 dan 6 show the compilation of the cone penetration ratio (D_r) and undrained shear strength (c_u) plotted against water content (w). Essentially the trend lines lie close to one another, with more overlapping observed in Sample M (Fig. 5b and 6b). This is consistent with earlier discussions on D_r and c_u (see Fig. 2 and 3), where the strength recovery rate was less obvious compared to Sample L.

Referring to Fig. 5, for both soils, the 0hr plot was slightly above the others, indicating the soil's susceptibility to shear failure with the fall cone. The strength recovery rate was effectively improved after 24-hour rest period, especially for Sample L. Generally, the distinct shift of the plots towards the

Fig. 5. Cone penetration ratio (D_r) – water content (w) plots.Fig. 6. Undrained shear strength (c_u) – water content (w) plots.

left-down in Fig. 5 and right-up in Fig. 6 clearly show better strength gain rate with less water in the soil initially. The fact that the plots for Sample L lie more rightwards (Fig. 5) suggests the soil's ability to attain similar strength recovery rate as Sample M, though with higher water contents. This seems counter-intuitive but as mentioned earlier, other factors such as the soil's particle size distribution, could play significant roles in the formation of the soil's damaged structure upon remoulding.

Similarly in Fig. 6b, the much narrower band of the c_u - w plots for Sample M corresponds with Fig. 5b. The similarly dramatic change in strength recovery rate within different range of water content for both samples require more in-depth investigations. For instance, if it is hypothesized that the higher clay content in Sample L facilitated better bonding of the soil mass (attraction of fine particles), the extent the particle size distribution influence on the strength gain pattern need to be ascertained. On the contrary, if it is perceived that the slightly higher silt and sand contents in Sample M enabled the reformation of a structured soil matrix (skeletal stiffening), the effect of coarse particle contents needs to be systematically examined.

D. Correlation between c_u and D_r

As D_r and c_u both demonstrated particular trends in relation with time, it is hypothesized that the 2 parameters can be correlated in some way. By plotting c_u against D_r according to the soil sample (Fig. 7a and 7b), there appears to be a distinct pattern where higher c_u corresponds with lower D_r . This indicates greater strength of the soil in resisting the falling cone, i.e. shear failure by the cone penetration. However, at the same strength range, it can be observed that Sample M underwent less cone penetration compared to Sample L. In fact, at $c_u < 3$ kPa, D_r for Sample M fell within the narrow band of 0.5–0.7, whereas for Sample L, D_r covered a wider range between 0.55 and 1.2. Elaboration on the possible reasons for this phenomenon can be found in the previous section.

In the combination plot of both samples as shown in Fig. 7c, the fairly good correlation of c_u and D_r is indicated by the R^2 -value of 0.917. As the cone penetration is a simple test to conduct with small amount of sample required, such a correlation chart could be useful for quick estimation of c_u in relation with time. For instance, a similar soil bed could be prepared and tested at predetermined intervals to gauge the strength recovered after a particular time lapse. Nonetheless it is necessary to verify if the correlation holds true for other dredged marine soils to make the correlation chart more versatile and reliable.

An area of concern worth more thorough investigation is the closely spaced data for Sample L at $D_r = 0.3$ –0.55 (Fig. 7c). Firstly, the data set seems to lie apart from the others along the regression line. Secondly, it encompasses a rather narrow strength range, i.e. 6–9 kPa. These could suggest either an over-estimation of c_u , or excessive resistance of the cone penetration, if the regression is assumed to be true. On the other hand, the data set which forms a plateau at about 5 kPa for Sample M in the same figure covers D_r of 0.25 to 0.4. It

appears as if the cone penetration test was incapable of detecting the small difference in the recovered shear strength within the range.

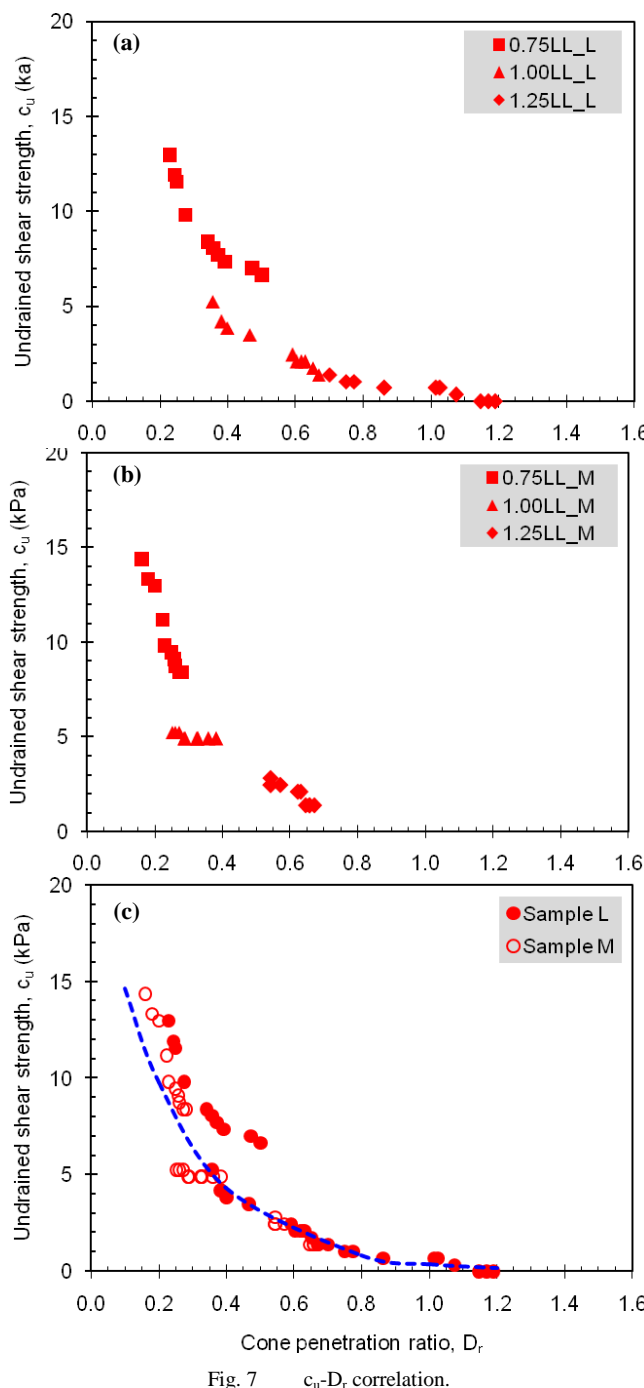


Fig. 7 c_u - D_r correlation.

Overall, the equation $c_u = 22e^{-4.1D_r}$ is applicable for the dredged marine clay with c_u up to 15 kPa. The discrepancies highlighted notwithstanding, the relationship between the measurements does seem plausible. Further investigation on the sensitivity of the cone penetration test in dredged marine soils would shed more light on the matter.

IV. CONCLUSIONS

The dislodged then relocated dredged marine clay undergoes the remoulding process, with destructureization of the original sediments' fabric. The fabric and hence strength loss due to the process can be regained with time though. The present study sheds some light on the possible responses and more importantly, the potential of reusing the otherwise waste geo-material with regard to the time factor.

Overall, the following conclusions can be made:

- The less water there is in the soil initially, the less time is required to attain thixotropic hardening, suggesting the benefits of pre-drying or pre-draining of the soil backfilled in an embankment to shorten the construction period.
- At 1.25LL, at least 5 % cement was necessary to induce hastened stiffening of the soil to that comparable with the soil at a much dryer state, i.e. water content of no more than 0.75LL. This would require pre-drainage of the excess pore water mentioned earlier.
- The different strength recovery rate of the remoulded dredged marine clays could be due to other factors, such as the inherent properties of the soil itself. As such, further verifications with carefully controlled / prepared samples are necessary to establish the strength recovery mechanism and behaviour of the dredged marine clay left to mature on its own.

Some recommended areas for further investigations include the following:

- The sensitivity of the cone penetration test to coarse particles in the soil sample, e.g. increased silt content effect on the cone resistance.
- The sensitivity of the cone penetration test to the coarse particle size present in the soil sample, e.g. the threshold particle size of the coarse fraction with significant effect on the measurement.
- Transition zones in the soil mass (e.g. different densities, coarse particle content, etc.), which could affect the measurements taken with the tests.
- The efficacy of incorporating sand blanket to facilitate some form of pre-consolidation prior to leaving the soil bed to regain its strength with time.
- The cost-benefit-time relationship for the various configurations examined above, which could be used by practitioners in selecting the most suitable approach.

In a nutshell, further work on the time-dependent performance of dredged marine soils reused for backfilling needs to be carried out, including measures to expedite the strength gain rate, and long term stability monitoring, from both the geotechnical and geo-environmental points of view.

Acknowledgment

The experimental work presented in the paper was conducted by the diligent HY Yong and CF Chu. Appreciation

is due to the Marine Department of Malaysia for access to the dredging site and permission for sampling. Financial support was made available via the RACE (KPM) and MDR grants (UTHM).

References

- [1] P. Bogers and J. Gardner, 2004, "Dredging near live corals," 17th World Dredging Congress, Hamburg, Germany, A31.
- [2] J.J. Cruz-Motta and J. Collins, 2004, "Impacts of dredged material disposal on a tropical soft-bottom benthic assemblage," *Mar Pollut Bull*, 48(3-4): 270-80.
- [3] H. Tanaka and S. Seng, 2012, "Properties of very soft clays: A study of thixotropic hardening and behaviour under low consolidation pressure," *Soils and Foundations*, 52(2), 335-345.
- [4] T. Takeda, M. Sugiyama, M. Akaishi and H.W. Chang, 2012, "Secondary compression behaviour in one-dimensional consolidation tests," *Journal of GeoEngineering*, 7(2), 53-58.
- [5] C-M. Chan, 2014, "Influence of mix uniformity on the induced solidification of dredged marine clay," *Environmental Earth Sciences*, 71(3), 1061-1071.
- [6] C-M. Chan, K-H. Pun and F. Ahmad, 2013, "A fundamental parametric study on the solidification of Malaysian dredged marine soils," *World Applied Sciences Journal*, 24(6), 784-793.
- [7] C-M. Chan, T. Mizutani and Y. Kikuchi, 2013, "Solidification of dredged marine clay for sustainable civil engineering applications: A laboratory study," International Conference on Eco-systems and Biological Sciences (ICEBS'2012), Penang, Malaysia, 27-33.
- [8] R.J. Zhang, A.M. Santoso, T.S. Tan and K.K. Phoon, 2013, "Strength of high water content marine clay stabilized by low amount of cement," *Journal of Geotechnical and Geoenvironmental Engineering*, 139, 2170-2181.
- [9] K.H. Head, 2006, "Manual on soil laboratory testing, 3rd. ed.," UK: Whittles Publishing.
- [10] British Standard Institution, 1990, "British Standard 1377 (BS1377): Methods of test for soils for civil engineering purposes, Part 2: Classification Tests."
- [11] S. Hansbo, 1957, "A new approach to the determination of the shear strength of clay by fall cone test," International Proceeding, Royal Swedish Geotechnical Society, 1-48.

A ROBUST HASH SCHEME FOR IMAGE AUTHENTICATION SYSTEM VIA SINGULAR VALUE DECOMPOSITION

Engr Faizullah¹ and Ayaz Hussain²

^{1,2} Department of Electrical Engineering,

Balochistan University of Engineering and Technology, Khuzdar, Pakistan

E-mail: ch_it2001@yahoo.com, engr_ayaz@yahoo.com.

Abstract. Popular multimedia has normally tried to present information in the form of digital images. Image authentication and integrity has been very important issues for multimedia application since digital images may be easily modified and absolutely reproduced. Image authentication provides a way to verify the originality of an image by detecting malicious non- malicious attacks, until and unless we have image authentication techniques, such image will be difficult to verify. Image hash function has found extensive applications to over come such difficulties in image authentications systems.

In this research paper, we will present a robust hash scheme for image authentication system by using singular value decomposition techniques. We plan the robustness of image hashing scheme as testing problem and evaluate the performance under various image processing operations. To access the performance, the proposed hash scheme has been tested by performing numerical experiments on image data base of more than one thousand images for the verification of image originality. The numerical experiments show that the proposed scheme is durable to show the authenticated results.

Key words: Robust, image authentication, hash function, SVD and matrices

Introduction

Nowadays, as a part of technology driven culture we are faced with several issues and one of them is user authentication. In recent years researchers have proposed diverse schemes and thoughts to over come this problem. Image authentication verifies the originality of an image by detecting by detecting manipulations (tapering, compression and enhancement) . By image authentication we mean to ensure the truthfulness of the image contents, a procedure able of ensure that image contents has not been tampered and are indicating there accurate origin. Main aim of image authentication is to prove the integrity of image i.e. provide assurance that image has not been tampered or modified [1]. More over if a modification has occurred; the location of the modified area(s) should be identified.

unauthorized manipulation of digital images and videos became an important issue. Which shows that a robust and secure image authentication and integrity are needed? Thus ensure trustworthiness, image authentication techniques have emerged to verify content integrity and prevent forgery; the attacker should not be able substitute false data for real data [2-6]. Image authentication plays a significant role in the digital era. Image editing software modifies images with ease and made it difficult to find any visible difference compared to the original image. This gives arise the need for researchers relating to image integrity verification to decide the image integrity [2, 22]. There have been two main approaches to verify the images: digital signature and water marking [4-7]. The digital signature approach encodes extracted data by using hash function and then transmits them to a receiver. Hash values are used to determine its integrity. By considering the robustness level of image authentication, based on digital signature the methods are classified as (a) complete Authentication and content Authentication (b) fragile and semi-fragile authentication and (c) content hashing, non-

In recent times the image authentication techniques have gained immense interest due to its significance for a large number of multimedia applications. Mostly transmission of the images has been carried out over channels which are not secure we quote the Internet. Therefore, quality control images must be protected against attempts to manipulate them; such manipulations could fiddle the decisions based on these images, therefore most of the existing image authentication techniques use both digital signature and digital water marking to achieve the goal [1, 2-4]. Thus, the requirement to protect multimedia contents from prohibited copying, tampering and manipulations has been made more critical by the coming on of recent digital technology [1, 5]. Digital information revolution has brought about many benefits along with new issues, the ease of editing and ideal duplicating, the production of ownership and prevention of hashing and crypto hashing [1, 2-7]. In this paper we will present a robust and authentic hash scheme which uses the singular value decomposition transform technique. The proposed scheme works by splitting original image into non-overlapping $n \times n$ blocks. We apply SVD transform technique on each of them to get singular values. We take three diagonal values to hash value. Typically, two types of hashing function are used in semi-fragile authentication: content hashing and crypto hashing. Semi fragile authentication refers to those methods that are robust to pre-defined content manipulations, it authenticate an abstracted version on the original image to get certain degree of robustness. In verification process, a specific threshold is used in order to compare the values if the distance between two hashed values is less than this threshold, the image is declared unaltered [8,9]. Specifically, we present a digital signature-based method for image authentication, which includes tampering detection, compression detection, high pass filtering and low pass filtering. Furthermore, we introduce the concept of image content hashing and discuss the most essential necessities for

an effective image authentication. We analyze the performance and feasibility of our proposed image authentication system, which relies on the use robust hash functions.

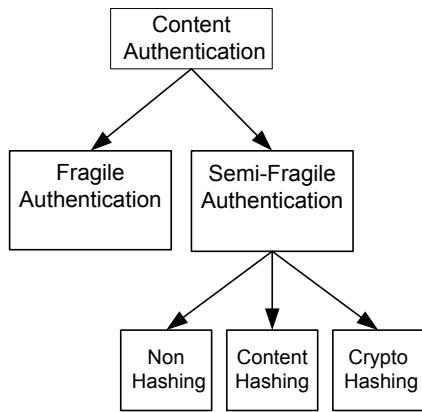


Figure 1: Categories of signature based Content Authentication (Source Ref. [2])

Our proposed image hashing scheme has the following promising features

- Robust in detecting tampering by showing manipulated area
- Robust against JPEG compression
- Discrimination between malicious and non malicious attacks.

Due to the popularity of digital technology, more and more images are being created and stored every day this introduces the problems in managing image databases.

The remainder of this paper is organized as follows: we introduce the general framework for image hashing in Section II, Section III presents a detailed overview of SVD transform, in section IV we describes the proposed image hashing scheme, next we offer experimental results to show the validity of our scheme in section V, section VI evaluate and analyze the authenticity for more than one thousand images and Finally, concluding remarks along future directions are given in section VII

II. General Frame work of image Hashing

Generally, an image hash provides a compressed representation of image that can be used for authenticating the image [1, 13]; image hash can be constructed by extracting and post-processing appropriate image features. The feature extraction step is mainly essential in order to achieve robustness. The robustness of image hashing largely relies on the robustness of image features. A robust image feature extraction scheme should hold up minor distortions to the image that do not alter the semantic content.

A number of the durable features employed in the literature include block-based histograms, image edge information, relative magnitudes of pairs of DCT coefficients, salient features based on local wavelet extrema, and Fourier features [12]. The sensitivity against minor distortion can be mitigated by preprocessing signals via low-pass filtering [1], applying quantization and clustering.

An image hash function change the visual domain produce hash value based on imaged visual appearance. A hash function is a transformation that takes an input and returns a fixed sized string; the values returned by hash function are called hash values, hash sums or simply hash. Image hash functions find extensive applications in content hashing authentication. Hash functions are usually used for image compression tasks, detecting duplication, tampering and so on. Feature extraction is special for dimension reduction. Transforming the input data into set of feature is called feature extraction. Hash code or traditional digital signature.

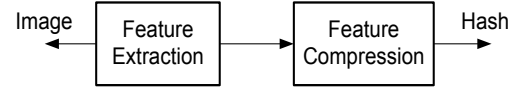


Figure 2: Block Diagram of general frame work for generating Image Hash

III. Singular Value Decomposition Transform

In electronics engineering any form of signal processing for which the input is an image. Most image processing techniques involves treating images as two dimensional signals and applying signal processing technique on it. An image is 2-D discrete time signal which is non zero over a finite region for example $m \times n$ square matrix. For such images m corresponding the row index while n corresponds the column index [13].

An Image can be created and stored as standard double precision floating point numbers (double) optionally , as 8-bit (unit -8) 16-bit (unit-16) unsigned integers. Thus a matrix of $m \times n$ dimension or $m \times n \times 3$ can contain double unit 8 or unit 16 data. Singular Value Decomposition is a prominent method for factorizing a rectangular matrix, real or complex, which has been widely employed in signal processing, like image compression and noise reduction etc. In recent times, the SVD transform are used to measure the image quality under different types of compression, tampering and distortions [8, 15]

Suppose we have an image represented as a real matrix A of size m rows by n columns, $A_{m \times n}$ applying the SVD on matrix

A will result in the three decomposition matrices $U_{m \times m}$ orthogonal matrix, $S_{m \times n}$ diagonal matrix and orthogonal matrix $V_{n \times n}$ as shown in equation (1)

SVD of

$$(A_{m \times n}) = [U_{m \times m} \quad S_{m \times n} \quad V_{n \times n}] \dots \dots \dots (1)$$

$$A_{m \times n} = U_{m \times m} \times S_{m \times n} \times V^T_{n \times n}$$

$$= \sum_{i=1}^{\text{Min}(m,n)} \sigma_i \times U_i \times V_i^T \dots \dots \dots (2)$$

$$\sigma_1 \geq \sigma_2 \geq \sigma_3 \geq \dots \geq \sigma_p \geq 0 \quad p = \min(m, n)$$

Where $\sigma_i \in \Re, i=1, \dots, \min(m, n)$ are singular values i.e. the available diagonal elements of matrix S stored in descending order. u_i are the left singular vectors, i.e., the columns of U , and v_i are the right singular vectors, i.e., the rows of V^T (or columns of V). U and V are unitary matrices, that means $U \times U^T = I_{m \times m}$, $V \times V^T = I_{n \times n}$ where $I_{m \times m}$ and $I_{n \times n}$ are the unit matrices [3, 15].

To calculate the SVD we need to compute the eigenvalues and eigenvectors of $A \times A^T$ and $A^T \times A$. The eigenvectors of $A \cdot A^T$ form the columns of U , whilst the eigenvectors of $A^T \cdot A$ form the columns of V . Moreover, the singular values in S are the square roots of the eigenvalues of $A^T \times A$ or $A \times A^T$. Singular values are usually arranged in descending order in magnitude [3, 6] as shown in equation (4).

Theorem 1:

The singular value decomposition, given any $m \times n$ real matrix A there is an $m \times m$ orthogonal matrix U and $n \times n$ orthogonal vector V such that

$$U^T A V = S = \begin{bmatrix} \text{diag}(\sigma_1, \dots, \sigma_r) & 0 \\ 0 & 0 \end{bmatrix} \quad (3)$$

Where $\sigma_1 \geq \sigma_2 \geq \dots \geq \sigma_r > 0$.

The σ 's are not eigenvalues of A . they are singular values [16].

Theorem 2:

Let $A \in \Re^{m \times n}$ there exists a unitary matrix

$$U = [u_1, u_2, \dots, u_m] \in \Re^{m \times m}$$

$$V = [v_1, v_2, \dots, v_n] \in \Re^{n \times n}$$

Such that

$$A = U \Sigma V^T = \Sigma = \begin{bmatrix} \Sigma_1 & 0 \\ 0 & 0 \end{bmatrix} \dots (4)$$

$$\text{Where } \Sigma_1 = \begin{bmatrix} \sigma_1 & 0 & 0 & 0 & 0 \\ 0 & \sigma_2 & 0 & 0 & 0 \\ 0 & 0 & \sigma_3 & 0 & 0 \\ 0 & 0 & 0 & \sigma_4 & 0 \\ 0 & 0 & 0 & 0 & \sigma_p \end{bmatrix}$$

Diagonal entries of Σ are known as singular values of A [6]

With increase in magnitude of singular values of matrix Σ will increase the image luminance, while with decrease in the magnitude will decrease the image luminance. Based on that motivation, it is right to state that S is in close relation with the image luminance, another interesting feature of the SVD techniques is the invariance of Singular values to common image processing operations. Due to these properties, the SVD techniques have been used in combination with other techniques (Discrete Fourier Transform, Discrete Cosine Transform, Zernike Moments Transform and Hadamard Transform) to devise robust image authentication systems.

From equation (2), we can examine that each singular value is multiplied by the corresponding left and right singular vectors. Hence, this creates different image layers, i.e., a sum of rank-one matrices, where the first image layer (generated multiplying the first singular value by the left and right singular vectors) represents the image shape, which concentrates a large amount of the energy contained into the final image [15]. Left and right singular vectors which correspond to the largest singular value represent the shape (i.e., strong edges) of the image, while the rest of singular vectors express edges and texture regions.

Theorem 3 : (perturbation)

Let $\tilde{A} = A + E \in \Re^{m \times n}$, be perturbation of A and let $\tilde{A} = \tilde{U} \tilde{\Sigma} \tilde{V}^T$ be SVD of \tilde{A} , then $|\lambda_i - \tilde{\lambda}_i| \leq \|E\|_2$ for $i = 1, \dots, p$ where $\|E\|_2$ is induced 2-norm of E

Since SVD is one of the renowned tools of control systems and linear algebra, we omitted to give detailed analysis of this subject and interested reader may find more details in [3, 6, and 8].

IV. Proposed hashing scheme for image authentication system

Image hash functions find extensive applications in contents authentication, database search. In this section, we present the image hashing scheme, the choice of the hashing function depends strongly on the nature of the input data and intended application. Our proposed image authentication scheme consists of two major algorithms one for generating of image hash and other for verification of image hash by comparing the hash values. Display the columns where the tempering has occurred.

Image blocks are useful representation of image contents, the original image is divided in $n \times n$ blocks. We represent images as matrices. The proposed scheme works by initially splitting the original image into non-overlapping blocks 16×16 , applying the SVD transform to each of them and subsequently into the singular vectors.

Essentially, MATLAB is the set of instructions that process the data stored in a workspace, which can be extended by user-written commands. The workspace stores the different lists of data and these data can be stored in a MAT file; the user-written commands are functions that are stored in M-files

(files with extension M). The procedure operates by instructions at the command line to process the workspace data using either one of MATLAB's own commands, or using your own commands. The results can be visualized as graphs, surfaces or as images [21].

A. Image hashing generation algorithm

The algorithm is used to generate robust hash function for image authentication. The basic step of the proposed algorithm includes. Select image as a row input and divide the image into 16×16 non- overlapping blocks and apply the Singular Value Decomposition technique to each block. By applying a SVD to each block, we view image as a two dimensional surface. And we will take first three diagonal elements from each block we will get hash value of each block

Step-1: select image as a row input, the original image A is a gray level image with $m \times n$ pixels. Let the $n \times n$ input image be $A \in \Re^{m \times n}$.

Step-2: divide input image into $3(16 \times 16)$ non overlapping blocks

Step-3: takes SVD of each block, the image is decomposed into three matrixes U S V

Step -4: take first three diagonal elements of each S block,

Step-5: save hash value.

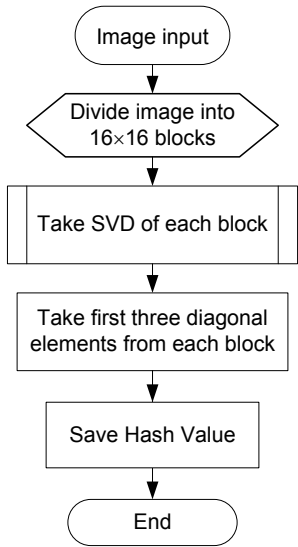


Figure 3: Basic Steps of the image hashing generation algorithm

B. Image Hash Verification Algorithm

Load old hash values, and generate hash report for new image compares the hash values and gives the maximum difference.

Step-1 load old hash value

Step-2 read tampered image

Step-3 saves hash value of the tampered image

Step-4 by comparing the original image hash values with tampered image hash value, generate maximum difference in hash values.

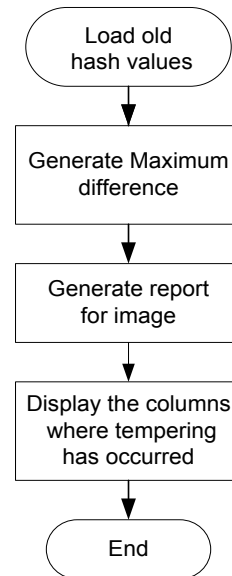


Figure 4: Basic Steps of the image hashing verification algorithm

V. Experimental Results on Robustness of Hash

In order to evaluate the proposed scheme, the original is shown in fig. In this section, we present experimental results concerning the image authentication robustness of our proposed scheme. To examine the robustness, we consider the performance of proposed hashing scheme preventing attacks such as filtering, image compression and image manipulations .An image hashing scheme should be robust against acceptable manipulations and at the same time be sensitive enough to detect malicious manipulations. The degree of robustness is really a tradeoff with respect to the amount of fragility required to detect malicious manipulations.

In verification process, a specified threshold is used in order to compare the values. If the distance between two hashed values is less than this threshold, the image is declared un altered. In our experiments, we have used images of size $256 \times 256 = 65536$ pixels and divided them into non-overlapping blocks of size 16×16 pixels. This gives a total of 1024 blocks. For each block, a random gray-level transformation has been applied

We studied the performance of our scheme by performing experiments. In our experiment we tested image data base of more than 1000 different images. Three kinds of attacks are considered compression; filtering and slight tempering on image contents and found that our approach is suitable for evaluating the image authentication.

To test the effectiveness of our scheme, four experiments have been made to validate the use of proposed scheme. If image A is tampered procedure is executed and damaged image is generated on original image. The following three experiments have been made in order to validate the use of our proposed scheme.

A. Experiment 1: Image Compression

We tested the proposed scheme on more than one thousand images under different JF Quality factor compression: 10, 20, 30, 40, 50, 60, 70, 80, 90 and 100. Computed the mean values at each compression factor results are shown in table -1

| JF Quality Factor | Mean value |
|-------------------|-----------------|
| 10 | 82.5893 |
| 20 | 74. 8122 |
| 30 | 67.9469 |
| 40 | 60.2401 |
| 50 | 53.0323 |
| 60 | 43.8958 |
| 70 | 38.6092 |
| 80 | 25.3001 |
| 90 | 11.9191 |
| 100 | 02.4528 |

Table: 1 JF Quality Factor of more than 1000 images and calculated mean value

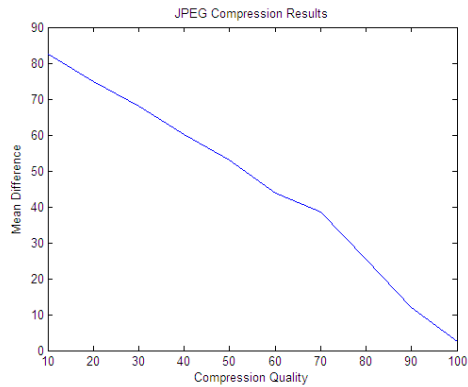


Figure 5: compression quality results

The baboon image is compressed with ratio 9:1; the authentication is generated based on original baboon image. The authenticated result is shown in figure

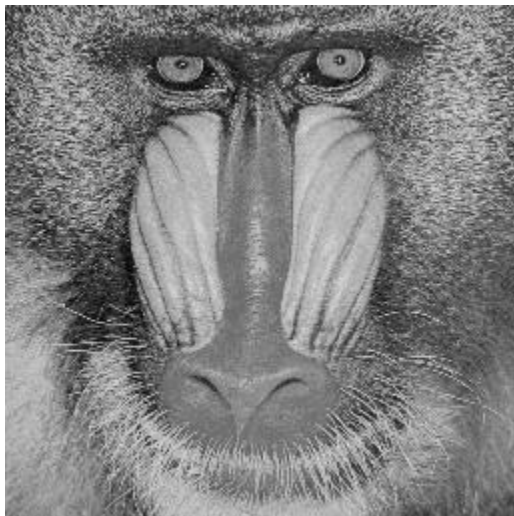


Figure 6: Original image of Baboon

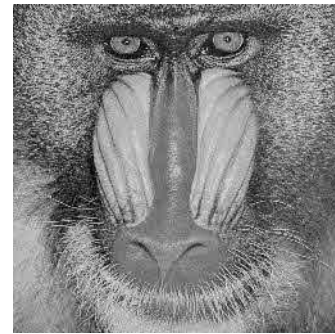


Figure 7: JPEG compressed image of Baboon

B. Experiment 2: Detection of Tampering

Image authentication technique verifies the originality of image by detecting manipulations. To detect the weather the image is tampered or not [22], the second experiment is made by manipulating the image by deleting the feather of parrot. This feather area (15×16 pixels) and cloned by its neighboring pixels this tampered image is shown in figure 8.authenticated results are shown in fig.9 the second experiment was made by manipulating the image by deleting the parrot (16×16) pixels area is removed. Figure 8 shows the tempered image, the labeled block of accurate location of tampered image in shown in figure 9; it is clearly shown that manipulated part has been detected as fake.

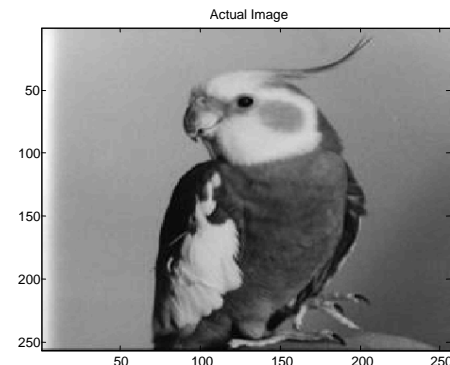


Figure 8 Original image: Parrot

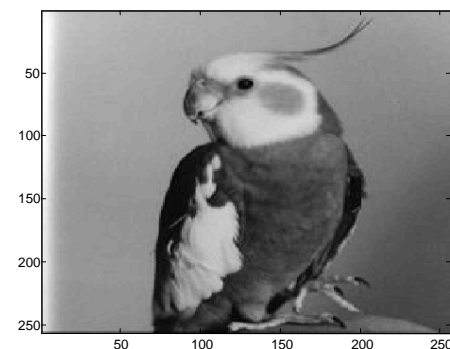


Figure 9: Tampered Image of Parrot

VI. Authenticity Evaluation Framework and Robustness Analysis

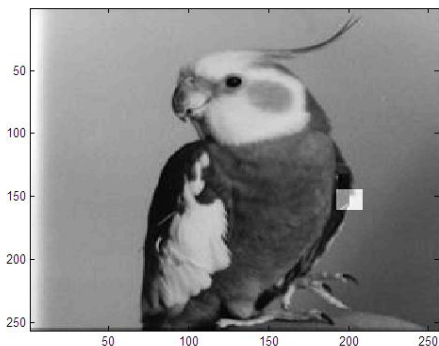


Figure 10: accurate location of tampered image (authenticated results of figure 9)

C. Experiment 3: low pass filter

Digital images can be processed in a variety of ways. The most universal one is called filtering and creates a new image as a result of processing the pixels of an existing image; each pixel in the output image is computed as a function of one or several pixels in the original image, usually located near the location of the output pixel

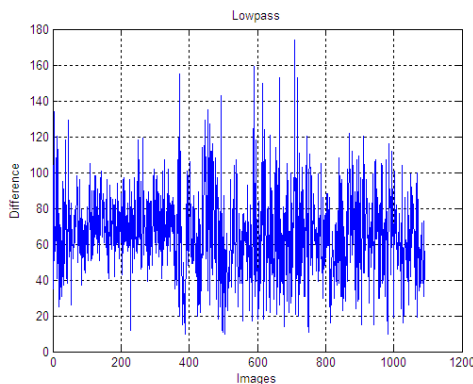


Figure 11: low pass filters

D. Experiment 4: High pass filter

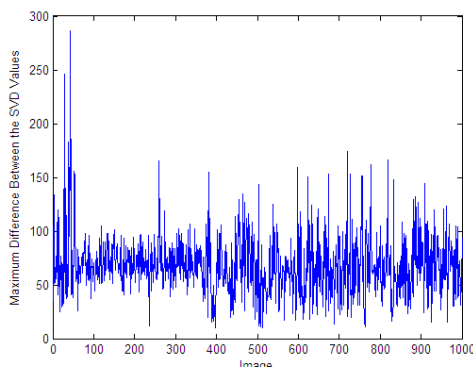


Figure 12: high pass filter

A hash function plays an important role in image authentication. Such a hash function would be useful in image authentication, in which the image possibly undergoes incidental changes, such as compression, tampering and format change etc. [23] A second significant application of an image hash could be for robust image authentication. In such cases, the hash must be invariant under perceptually insignificant modifications to the image but detect malicious tampering of source/input image [24].

Properties of an effective authentication

- Can determine whether an image has been altered or not
- Can locate any alteration made on the image
- Can integrate authentication data with host image rather than as a separate data file
- The embedded authentication data be invisible
- To allow the watermarked image be stored in lossy compression format

We show that the proposed hash function is resilient to content-preserving modifications; we introduce a general framework to study and evaluate the authenticity of image hashing systems.

Under this new framework, we model the hash values as random variables. Using this security framework, we analyze the security of the proposed schemes and several existing representative methods for image hashing. We then examine the security versus robustness tradeoff and show that the proposed hashing methods can provide excellent robustness

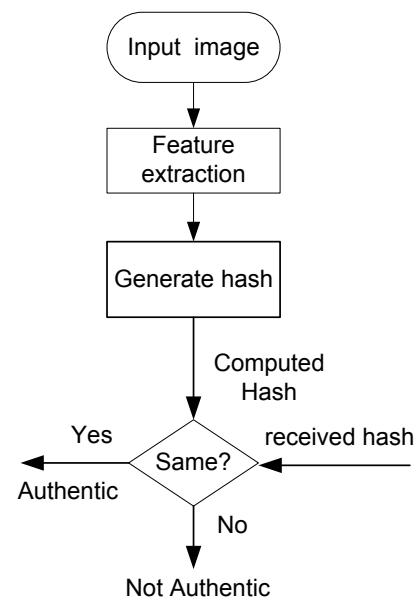


Figure 13: authentication process of proposed scheme

VII. Conclusion and future work

In this paper, we describe the needs of image authentication and integrity and propose a robust hash scheme for image authentication system. A hash function is based on singular value decomposition. A robust hash scheme has been developed and tested on more than one thousand images for verification and validation. The experimental test results show that the scheme is very efficient to show the authenticated results in the performance of robust image authentication helps to protect modification, like tampering, compression and filtering.

More over, a new image hashing algorithm is robust hashing scheme and it is also efficient against estimation and detection different attacks. Furthermore it can provide robust and safe representation of images for various applications

In order to make the scheme secure we include the security aspects as our future focus to generate a secrete key for secure image authentication and test our approach on larger image databases. Taking three singular values, this consideration would be part of our future work.

Reference

- 1) Fawad Ahmed and M Y Siyal "A Novel Hashing Scheme For Image Authentication" Innovations in Information Technology, 2006Volume , Issue , Nov. 2006 pp.1 - 5
- 2) Qibin Sun and Shih-FU Chang, Signature based media Authentication, CRC pressLCC 2005
- 3) Chi-Tsong Chen, linear system theory and design, Oxford University press 1999.
- 4) Chai-Hung LU, Hao Chai-Kuan TSO, Chyuan LOU and David Chien-TingTAI, 2007 "Image Authentication method by combining digital signature and watermarking", International journal of computer Science and Engineering systems, volume.1 No. 2 pp.77-83 (2007)
- 5) Romualdas Baušys, Artūras Kriukovas, A New Scheme For Image Authentication Framework Information Technology And Control, 2008, Vol.37, No.4 pp.294-300
- 6) Kemin Zhou and John C. Doyle "Essentials of robust control systems" Amazon Company UK 1998
- 7) Dekun Zou , Chai Wah Wu, GuorongXuan and , Yun Q. Shi A Content-Based Image Authentication System With Lossless Data Hiding, ICME 2003 pp.213-216
- 8) David C.Lay Linear Algebra and its Application , Pearson Education Singapore.2004
- 9) Madhurendra Kumar 2008. "Image Authentication Technique" School of Engineering Cochin University of Science & Technology, Kochi
- 10) Abdelkader Hassan Ahmed Oda; 2004. "Digital water marking techniques for image security and hidden communications" Ph.D thesis the University of Western Ontario London, Ontario, Canada (2004)
- 11) Ching-Yung Lin and Shih-Fu Chang "A Robust Image Authentication Method Distinguishing JPEG Compression from Malicious Manipulation
- 12) Jhon R.Buck,Michael M.Daniel and Andrew C.Singer " Computer Exploration in Signal and systems using MATLAB®, Prentice Hall , Upper Saddle River, NJ07458
- 13) Duane Hanselman and Bruce Littlefield "Mastering MATLAB® 7 Pear son Education Inc.
- 14) Alessandro Basso, Francesco Bergadano, Davide Cavagnino, Victor Pomponiu and AnnamariaVernone "A Novel Block-based Watermarking Scheme Using the SVD Transform" open Access algorithms",2009.
- 15) Rick L.Smith " the MATLAB Project Book for linear algebra" Prentice Hall , Upper Saddle River, NJ07458
- 16) Wenjun Zeng, Heather Yu and Ching-Yung Lin "Multimedia Security Technologies For Digital Rights Management" 2006, Elsevier Inc
- 17) Takeyuki Uehara "Contribution of image authentication and encryption" Ph.D thesis, university of Wollongong 2003.
- 18) Vishal Monga "Perceptually Based Methods for Robust Image Hashing" Ph.D Dissertation, University of Texas at Austin 2005.
- 19) Jeremy A. Hansen "A Four Component Cryptographic Hash Framework, Ph.D. Dissertation, University of Wisconsin-Milwaukee 2009
- 20) Mark S. Nixon Alberto S. Aguado "Feature Extraction and Image Processing" Oxford Auckland Boston Johannesburg Melbourne New Delhi 2002
- 21) Mi-Ae Kim, Geun-Sil Song, and Won-Hyung Lee, A Robust I mage Authentication surviving Acceptable modifications, Computational Science and its Applications, lecture notes on computer science ,2004
- 22) Image Processing Toolbox™ 6 The Math Works, Inc. User's Guide The Math Works, Inc.2008
- 23) R. Venkatesan, S.M. Koon, M. H. Jakubowski, and P. Moulin "Robust Image Hashing"
- 24) S.M. Rafizul Haque ,Singular Value Decomposition and Discrete Cosine Transform Based Image Watermarking Blekinge Institute of Technology, Sweden ,Master Thesis Computer Science 2008
- 25) R.Bausys, A.Kriukovas "digital signature Approach for image authentication, Electronics and Electrical Engineering ,2008, pp.65-83

Power-Line Communication-Revisited in the Context of Smart Grid

Saurabh Chaudhury

Sourav Bhattacharjee

Abstract— Power-line communication (PLC) is an integral part of Smart Grid today. This paper describes a novel analysis of a PLC channel for transmission and reception of analog signals namely, the voice/speech. It takes into consideration all possible noises that may get introduced into the channel. The noises that affect the performance of power line communications are mainly impulsive noise, narrow band noise and color background noise. In this paper, a model of power line communication channel, specifically, the SRC model is considered for analysis, however, the simulation results are also compared with echo model. Amplitude modulation/demodulation is used for signal transmission/reception and Weiner filter is used for noise suppression. It is seen that SRC model of PLC is the right candidate for analog transmission of speech signal if we compare the input and out signal in terms of SNR and the quality of the signal received.

Keywords— PLC, analog transmission, modulation, Weiner filter, signal quality

I. Introduction

The idea of sending communication signal over the same power lines (which is mainly used to distribute electrical power) is as old as telegraph itself. Power Line Communications uses the existing power cable infrastructure for communication purposes. It is becoming one of the strong competitors in the broadband communication market. However, it also faces its own set of obstacles and technical challenges. With the goal of providing operational telephone services and data communications across large geographical distances, the first power line communications (PLC) efforts were put in place by power utilities over HV power grid in the early 1920s. For some decades, the omnipresent power grid has been used for low-speed data communications [1]. Many different standardised or proprietary systems have been used for the transmission of control and management signals (e.g. remote meter reading) by

power supply companies. However, the power line has largely been dismissed as being too noisy and unpredictable to be useful as a practical high-speed communication channel.

A significant change occurred when the last telecommunication monopolies were ended by 1998. In the same time, major advances in the fields of modulation, coding and detection enabled the design of efficient broadband communication systems over power lines. The idea of exploiting the low-voltage (LV) power grid to provide broadband Internet access to residential customers has been proposed as an alternative to the other classical 'last-mile solutions' such as ADSL, cable modems, or wireless access systems. The ubiquitous presence of the low-voltage (LV), medium-voltage (MV), and high-voltage (HV) power grids is the key to developing an advanced smart grid power network. The deployment of broadband over power lines (BPL) networks through the entire grid forms a potentially convenient and inexpensive communication medium for delivering broadband last mile access in remote and/or underdeveloped areas [2]. Due to the upcoming Smart Grid adaption both in transmission and distribution power networks, the availability of a reliable communication network on the HV power grid side is important for the support of these significant changes [3 - 5]. Since overhead HV power lines are generally the lowest-cost method of transmission for large quantities of electric power, utilities employ primarily overhead HV transmission power grid for new urban, suburban, and rural installations [6 - 7].

LV power line communication (PLC) networks have a tree-like topology, with a PLC modem installed at the medium-voltage/low-voltage (MV/LV) transformer and providing connectivity to all premises in the neighbourhood. The architecture of the LV PLC network has to be optimized for the special characteristics of the distribution grid, which changes

from one geographic area to another, considering the number of households per transformer and the distance from the transformer to the customer premises. When larger distances are involved, intermediate repeaters are typically needed to regenerate the signal from the head-end and provide adequate coverage in every customer outlet.

There is also growing interest in the prospects of reusing in-building powerline cables to provide a broadband LAN within the home or office. Major advantage offered by power line based home networks is the availability of an existing infrastructure of wires and wall outlets, so new cable installation is not required. The user can employ home networking devices for connecting several computers, sharing printers, or sharing a broadband Internet connection. Channel characteristics of the power line show a typical behavior which is briefly described here. Impedance is highly varying with frequency and ranges from a few Ohm to few kilo Ohm. At some frequencies there are peaks in the impedance characteristics. At these peaks the network behaves like a parallel resonant circuit. However, in most of the frequency ranges the impedance shows inductive or capacitive behavior. Characteristic impedance of a power line cable is typically in the range of 90 Ohm. The overall impedance is not only influenced by characteristic impedance but also by network topology and connected loads which may have highly varying impedances as well. Moreover, the PLC channel is highly influenced by the noise spectrum.

The noise spectrum is highly varying with frequency and time. There is an overall decay of the noise level with increasing frequency. A typical example of a measured noise spectrum is shown in Fig. 1. Noise at the power line is influenced by a large number of different noise sources with different characteristics. Section 2 describes all such noises in detail.

We have limited our scope of work in this paper considering the following noises.

- Coloured background noise
- Narrow-band noise
- Impulsive noise (both periodic and aperiodic)

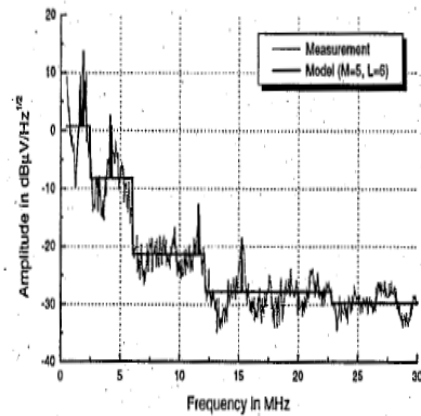


Figure 1: Example of Measured Noise Spectrum

Next section describes all these different kinds of noises, their characteristic behavior and models. Section 3 describes the PLC channel and the overall scheme for analog signal transmission-reception through PLC. Next, in section 4 results of simulation are presented and finally the paper concludes in section 5.

II. Power Line Noises

A. Coloured Background Noise- This type of noise is caused by overlaying of multiple sources of noise with relatively low power. Generally, power density of background noise is between -120 dB (V²/Hz) and -140 dB (V²/Hz) with an increasing power density towards lower frequencies (e.g. below 1 MHz) as in [8].

A typical measurement result of background noise with low power density is illustrated in Fig. 2 below

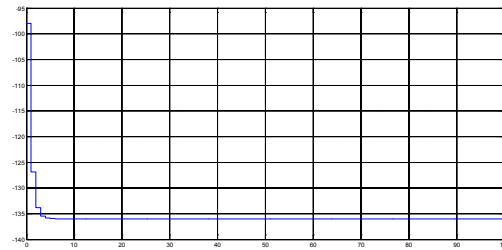


Figure 2: Colour background noise pattern

Results of multiple measurements of noise in [9] showed that decreasing power density with increasing frequency can be approximated by an exponential decaying curve in logarithmic scale.

$$A(f) = A_{\infty} + A_0 \exp(-f/f_0) \quad (1)$$

B. Narrow Band Noise- In general, noise scenarios in power line channels contain narrow-band noise, whose intensity and frequency varies over place and time. The main sources for narrow band noise are broadcasters in long, middle and short wave range as well as several radio services like amateur radio, so that almost the whole frequency range until 20 MHz is overlaid by narrow-band noise. A part of a noise spectrum with clearly visible narrow-band noise is shown Fig. 3 below as in [10].

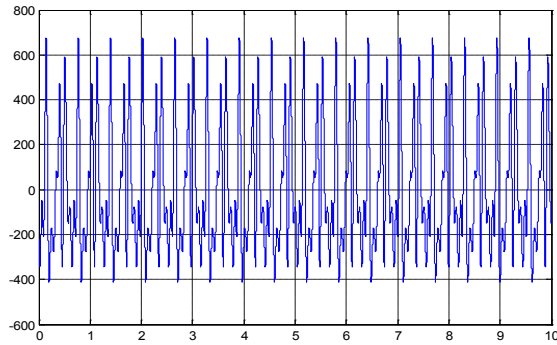


Fig. 3: Narrow-band noise pattern

Narrow-band noise can be modeled as a sum of multiple sine noises with different amplitudes. Using a deterministic model the signal results in the following equation

$$n_{\text{narrow-band}}(t) = \sum_{i=1}^N A_i(t) \cdot \sin(2\pi f_i t + \varphi) \quad (2)$$

C. Impulsive Noise- Net-synchronous impulsive noise occurs in 50 Hz-alternating voltage current network with frequencies of 50 Hz or 100 Hz. They are caused by synchronous power converters occurring in dimmers and by all kinds of rectifiers using diodes [10].

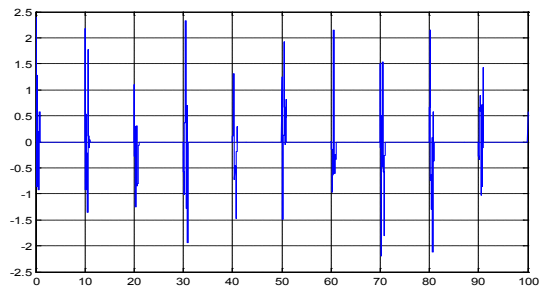


Figure 4: Periodic impulsive noise characteristics

Aperiodic impulsive noise is a signal which occurs time-randomly, is also known as “asynchronous impulsive noise”. However, since periodic impulsive

noise is also asynchronous to supply frequency, we will choose the clearer term “aperiodic impulsive noise”. This type of noise is caused by all kinds of switching operations, for example by household appliances, electric motors, or condenser discharge lamps. Aperiodic impulsive noise very often occurs in bunches (so called “burst noise”), which increases their disturbing impact. With many different sources this noise has very different properties regarding time response and spectral properties [11]. A typical example for such noise is given in Fig. 5.

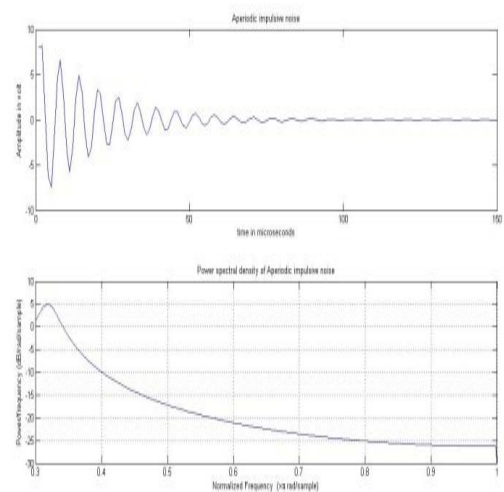


Figure 5: Time characteristics and spectral behavior of Impulsive noise

III. PLC channel and the Overall Scheme

Here we describe the power line channel models, the modulation /demodulation schemes and the filter to suppress noises which are inadvertently introduced into the channel. Basically there are two models for power lines to act as communication channel, namely, the echo model and the series resonant circuit (SRC) model. Echo model suffers from attenuation and phase lag while analog transmission and therefore the obvious choice is for SRC model.

A. SRC Model

Impedance measurements of electrical loads have shown that in many cases these loads can be described by one or a few series resonant circuits that consist of resistance R, capacitance C and inductance L.

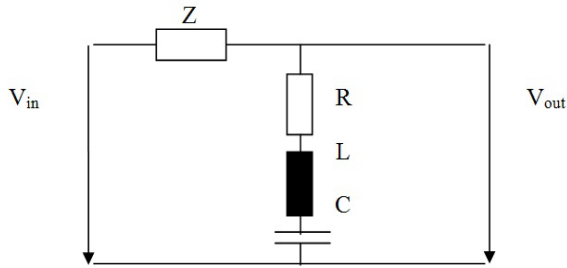


Figure 6: SRC model for PLC

As many appliances incorporate anti-interference capacitors at their input and possess a feeding line which has a resistive and an inductive portion of the impedance this approach is in close correspondence with reality. Since loads often are quite far apart from each other they do not influence each other. Hence, a power line channel can be described as a cascade of decoupled series resonant circuits (SRC). The impedance of the resonant circuit Z_s is frequency-dependent and can be described by:

$$Z_s(f) = R + j2\pi fL + 1/j2\pi fC \quad (3)$$

At resonance frequency f_{res} ,

$$f_{res} = 1/2\pi LC \quad (4)$$

The impedance is minimal with an imaginary part of the impedance equal to zero and a real part equal to R . The transfer function $H(f)$ is:

$$H(f) = 1/(1 + Z_s(f)) \quad (5)$$

A notch in the amplitude characteristics can be seen at resonant frequency. At lower and higher frequencies the transfer function is nearly 1. The depth of the notch depends on resistance R and impedance Z .

B. Modulation-Demodulation

The transmission of baseband signals, which have sizeable power at low frequencies, cannot be transmitted over a long distance without distortion. To avoid this type of distortion and faithful transmission of signals through a medium, it is customary to alter the frequency of the signal, from low frequency to high frequency. The technique used for this purpose is known as modulation. The purpose of modulation is usually to enable the carrier signal to transport the information in the modulation signal to some

destination. At the destination, a process of demodulation extracts the modulation signal from the modulated carrier. The three key parameters of a periodic waveform are its amplitude, phase and its frequency. Any of these properties can be modified in accordance with a low frequency signal to obtain the modulated signal. In our analysis we have used amplitude modulation technique for modulation purpose. Fig. 8 (b) and 9 (b) shows the results of amplitude modulated (demodulated) speech signal through PLC with a carrier frequency set to 100KHz.

C. Weiner Filter

Wiener filter is a filter proposed by Norbert Wiener during the 1940s. It is used to produce an estimate of a desired or target random process by filtering another random process through the filter. The discrete-time equivalent of Wiener's work was derived independently by Andrey Kolmogorov in 1941. Hence the theory is often called the Wiener-Kolmogorov Filtering Theory. A Wiener filter is not an adaptive filter because the theory behind this filter assumes that the inputs are stationary. The input to the Wiener filter is assumed to be a signal, $s(t)$, corrupted by additive noise, $n(t)$. The output, $\hat{s}(t)$, is calculated by means of a filter, $g(t)$, using the following convolution as shown in block diagram of Fig.7.

The error is defined as

$$e(t) = s(t + \alpha) - \hat{s}(t).$$

The goal is to minimize $E(e^2)$, the expected value of the squared error, by finding the optimal $g(\tau) / G(z)$, the Wiener filter impulse response function. The minimum may be found by calculating the first order incremental change in the least square resulting from an incremental change in g for positive time.

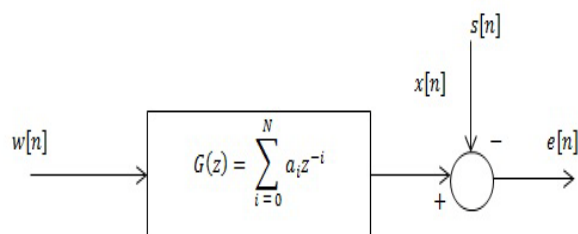


Figure 7: Block diagram view of the FIR Wiener filter for discrete series

Fig. 7 shows the block diagram representation of the FIR Wiener filter for discrete series. An input signal $w[n]$ is convolved with the Wiener filter $g[n]$ and the result is compared to a reference signal $s[n]$ to obtain the filtering error $e[n]$.

IV. Results and Discussions

A speech signal is taken as the input signal. It is modulated with a carrier by the procedure of Amplitude Modulation. The modulated signal is mixed with noise to account for real life scenario. This acts as the input to the transmission channel. Both SRC and Echo Models are tried as channel models. The transmitted signal is then passed through an Wiener filter to remove all the noises that inadvertently introduced into the channel. Then the filtered output is demodulated and compared with the original signal for qualitative analysis. The overall scheme is coded and realized in Matlab environment. For quantitative measurement of the received signal we have calculated the SNR ratios at different points in the process of communication. SNR ratio before modulation and transmission is 19.8445, whereas it is found to be 13.0046 after demodulation in case of Echo model. However, in case of SRC model, SNR before modulation and transmission through PLC is 18.3137 and after demodulation at the receiving end SNR is 17. 9222. Thus it is nearly the same signal which we receive at the receiver which is clear from Fig. 10, and is nearly the same as original speech signal. We have also observed the sound quality by hearing the out voice. Fig. 8 (a-c) shows the different states of the input speech signal-before modulation, after amplitude modulation, and after noisification. Fig. 9 (a-b) shows the same speech signal after denoising and demodulation, whereas, the final output signal through SRC model PLC channel and through echo model based PLC channel are shown in Fig. 9 (c) and (d) respectively which also show a comparison with original input signal. It is clear from the figure that SRC model is the most suitable model for PLC channel to transmit analog signal such as speech. Echo model suffers from distortion and phase

lag.

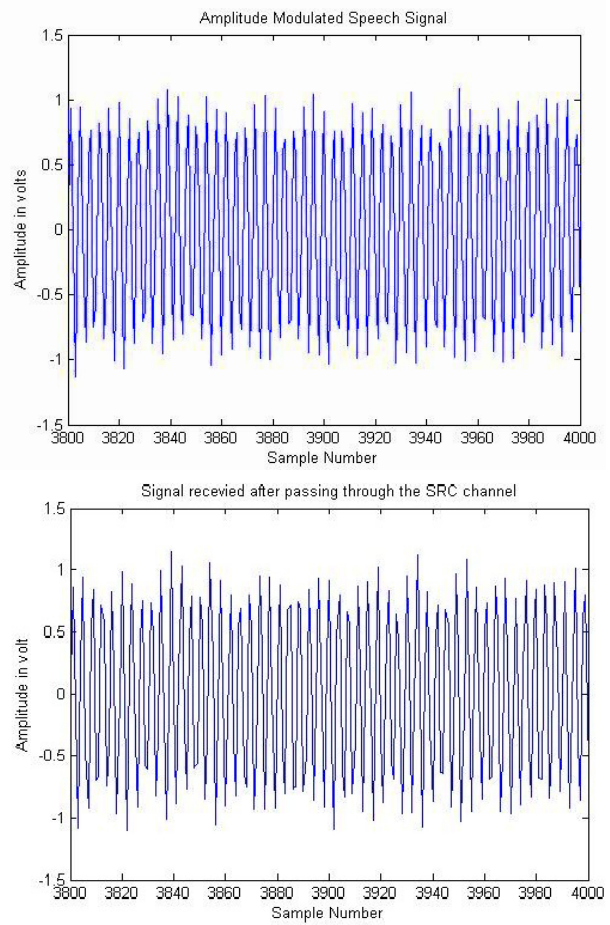
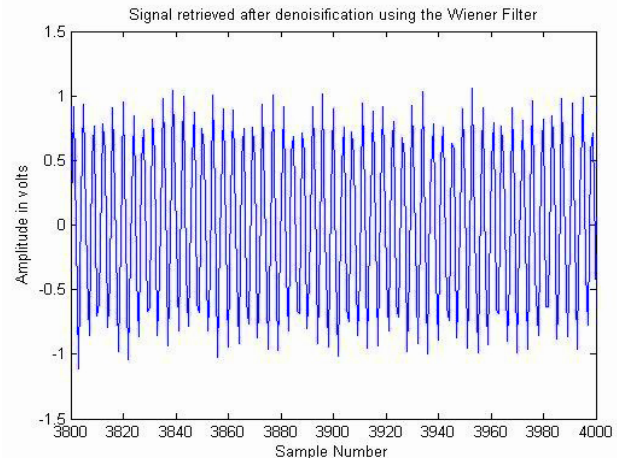


Figure. 8(a): Input Speech signal and (b) Modulated Speech signal
(c) input speech signal with noise



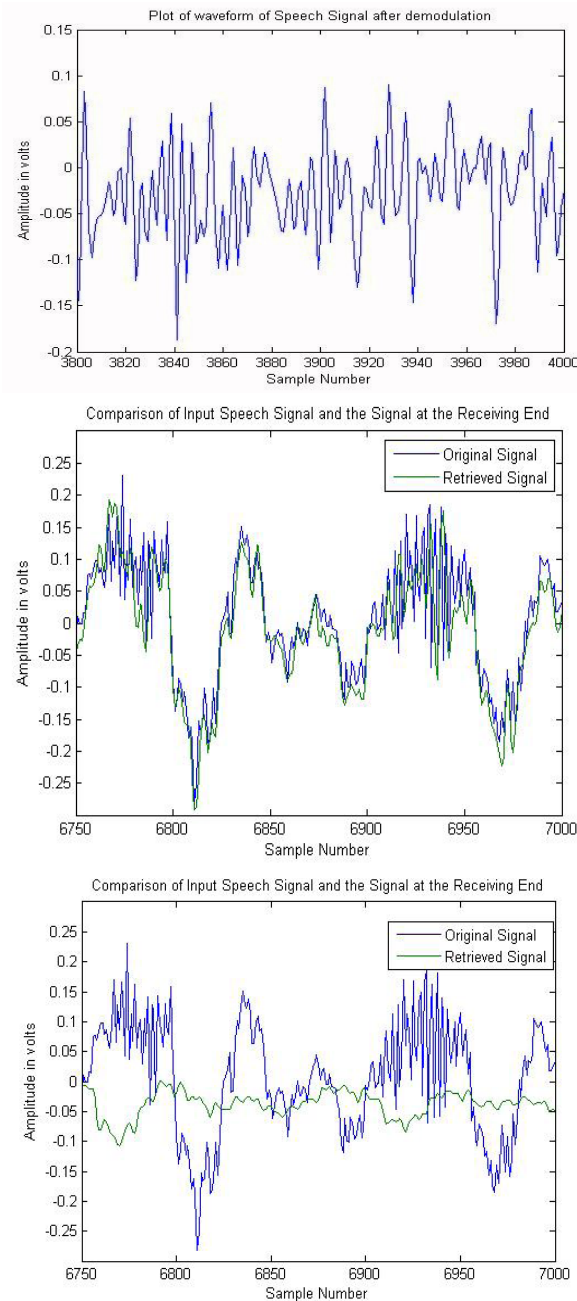


Figure 9: (a) Speech Signal after denoised by Weiner Filter (b) Signal after demodulation (c) Signal at the receiver for SRC channel (d) received signal in echo model

V. Conclusion

The main objective of this paper is to study and analyze a PLC channel for analog communication purposes, to check what are the challenges of such a communication and how to mitigate these problems. We have taken a realistic channel scenario by

incorporating different kinds of noises that may introduce in a PLC channel and devised a method to eliminate all these noises using an appropriate filter which we have taken as Weiner filter. We have compared qualitatively by listening the received speech signal and the input speech signal. Further, we have verified SNR values of the two signals and found to be almost equal in case of SRC model based PLC channel, whereas signal quality is largely deteriorated in case of echo model based PLC.

References

- [1] H. Ferreira, L. Lampe, J. Newbury, and T. G. Swart, 'Power Line Communications, Theory and Applications for Narrowband and Broadband Communications over Power Lines', John Wiley & Sons, New York, NY, USA, 2010.
- [2] H. K. Podszuek, 'Carrier Communication over Power Lines', 4th Edition, New York: Springer-Verlag, 1972.
- [3] IEEE Standard 643-1980, 'IEEE Guide for Power-Line Carrier Applications'.
- [4] OPERA1, 'D44: report presenting the architecture of PLC system, the electricity network topologies, the operating modes and the equipment over which PLC access system will be installed', IST Integr. Project No 507667, 2005.
- [5] NATO 'HF interference, procedures and tools (Interferences HF, procedures et outils) final report of NATO RTO information systems technology', RTO-TR-ISTR-050, 2007, [http://ftp.rta.nato.int/public/PubFullText/RTO/TR/RTO-TR-I-ST-050/\\$\\$TR-IST-050-ALL.pdf](http://ftp.rta.nato.int/public/PubFullText/RTO/TR/RTO-TR-I-ST-050/$$TR-IST-050-ALL.pdf).
- [6] O. Hooijen, 'On the relation between network-topology and power line signal attenuation', Proc. Int. Symp. Power Line Commun. and Its Appl., pp. 45 - 56, 1998.
- [7] N. Suljanović, A. Mujčić, M. Zajc, and J. F. Tasić, 'Corona noise characteristics in high voltage PLC channel', in Proceedings of the IEEE International Conference on Industrial Technology, vol. 2, pp. 10361039, Maribor, Slovenia, March 2003.
- [8] Yong-tao Ma, Kai-hua Liu, Zhi-jun Zhang, Jie-xiao Yu, Xiao-lin Gong, 'Modeling the Colored Background Noise of Power Line Communication Channel Based on Artificial Neural Network.' IEEE Trans on Consumer Electronics, 2007, 45(2): 345-348
- [9] H. Phillipps, 'Modeling of powerline communication channels', proc. 3rd Int.symp.power-line Communications and its applications, Lancaster, U.K., 1999,pp.14-21.
- [10] M. Zimmermann and K. Dostert, 'Analysis and modeling of impulsive noise in broad-band power-line communications,' *IEEE transactions on ELECTROMAGNETIC COMPATIBILITY*, Vol.44, pp.249-258, FEB 2002 .
- [11] H.J. Trussell, J.D. Wang 'Cancellation Of Harmonic Noise In Distribution Line Communications' *IEEE Transactions on Power Apparatus and Systems*, Vol. PAS-104, No. 12, December 1985

Using DSML in Moodle Configuration to Support PBL-Pedagogy

Khulood Khalil Al-Dous

Department of Computer Science and Engineering
Qatar University
Doha, Qatar
khuloodk@qu.edu.qa

Mohammed Samaka

Department of Computer Science and Engineering
Qatar University
Doha, Qatar
samaka.m@qu.edu.qa

Abstract—this study aim is to support teachers to design and deliver Problem-Based Learning (PBL) lesson plans in an easy, cost-effective, flexible, interoperable, and reusable manner. The aim is achieved by extending a pedagogy-generic Learning Management System (LMS) called Moodle to support PBL-pedagogy. That is, a PBL script editor and player were developed inside Moodle to facilitate teachers in designing and delivering PBL lesson plans to students. The facilitation provided according to an adopted PBL scripting language which is a domain specific modeling language (DSML). This study applied the Model Driven Approach (MDA) as the development method to transform a DSML into Moodle platform. The designed PBL lesson plans are delivered for both students and teachers through a developed Moodle's PBL player. Both Moodle's PBL script editor and Moodle's PBL player were evaluated and the results indicated the high usefulness of them.

Keywords—problem-based learning (PBL); learning management system (LMS); domain specific modeling language (DSML); PBL-pedagogy; moodle; model driven approach (MDA)

I. INTRODUCTION

Recently, a wide range of changes occurred in the economic and technological fields which lead the world to experience a huge transition from the post-industrial economy to knowledge economy. This transition transformed professional life and increased the number of skills that they need to master which includes dealing with increasing internationalization, using information technology, working within groups and mastering the required expertise. This affected highly the training programs of employee and high education expectations. Graduate students are expected to have convinced knowledge-basis beside the skills of solving problems, analyzing, synthesizing, coaching, leading, presenting and evaluating them. Hence, this is the expectation of the information community on the future [1].

Generally, the common way of teaching in Qatar and around the world is the traditional subject-based methodology. Hence, this methodology does not fit into the current expectations of students graduates and that raised the importance of integrating both knowledge and real-world problems together. The integrating can be done through developing and implementing instructional real-world practices. Normally, students gain huge amount of inert

knowledge from the traditional subject-based learning methodology, however students have to learn facts passively without linking them into the right real-world context. As a result, they are not able to use such knowledge in solving real-world problems, since they don't experience a real use of its context.

Many attempts have been made to address the integration of instructional models together with the traditional knowledge transmission models [Error! Bookmark not defined.]. One problem-driven approach that made inroads into different education fields, such as engineering and science, had been developed within the recent decade which is called problem-based learning (PBL). PBL is a learning-pedagogy that provides the students a guided experience in learning through solving complex, real-world problems [2].

Several definitions can be found to identify the process of PBL. One definition is “the learning which results from the process of working towards the understanding of, or resolution of, a problem” [3]. Another one is “the conception of knowledge, understanding and education that encourages open-minded, reflective, critical and active learning” [4]. Howard Barrows, one of the PBL inventors, defined PBL as “a total approach to education. In PBL there is a curriculum of carefully selected and designed problems. And there is a PBL process, which, among other things, replicates the commonly used systematic approach to resolve problems or meeting challenges. Students and teachers roles are redefined. Students assume the responsibility for learning and teachers become facilitators: stimulating and guiding students in their problem solving and self-directed learning” [5]. The common definition of PBL is using the problem to drive the learning process and assess the outcomes.

PBL has wide range of models with different specifications such as Wood's model [6], Maastricht “seven jump” model [7], and IMAS model [8]. A PBL model consists of steps that form a lesson plan for students to follow in order to solve a real-world problem. Applying PBL approach in learning environments raised the need for technical support that addresses the specification of PBL-pedagogy. According to this need the motivation of this study was to provide technical support for teachers to design and deliver PBL lesson plans for students. This study aims to investigate, design and develop an

innovative PBL online system that supports teachers in designing and delivering PBL lesson plans for students. Also, aims to facilitate the design and execution of wide range of PBL models with their variations in flexible and reusable manner. The scope and objectives of this study are as follows:

- Design and implement a PBL script editor to facilitate the design of PBL lesson plans for teachers.
- Design and implement a PBL player to simulate the execution of PBL lesson plans for students.
- Evaluating the usefulness of the PBL script editor for teachers.
- Evaluating the usefulness of the PBL player for students.

The Significance of this study is to support teachers to change their roles into facilitators instead of information source. At the same time, students who are used to passive listening, note taking, and memorization also need help in transitioning to activities that situate learning in the need to solve real-world problems.

II. BACKGROUND AND LITERATURE REVIEW

Problem-based learning was first developed for face-to-face learning environment. However, as the computer technologies are growing rapidly, many attempts have been conducted to combine PBL with computer supported collaborative learning (CSCL). Currently, the high availability of Internet makes it possible to implement PBL in online environment that can be used in hybrid with face-to-face environment.

Over the past decade researchers in the area of CSCL have developed numerous computer supported online PBL environments. Five of these environments were reviewed in this study including Socio-Technical Environment for Learning and Learning-Activity Research (STELLAR) [9,10], Computer Supported Intentional Learning Environments (CSILE)[11], Web-Scaffold Multi-user Integrated Learning Environment (Web-SMILE) [12], Collaborative Medical Tutor (COMET) [13], and electronic Problem-Based Learning (e-PBL) [14]. In summary, each of the reviewed online PBL environments relies on one specific PBL model. They support PBL processes by providing associated structures, resources, guidance, and tools. Using these PBL environments, teachers and students can easily generate, understand, and conduct PBL lessons. They all have a main common advantage for supporting a successful PBL process through providing proper and relatively complete environments. Nevertheless, such environments might be successful only in certain circumstances and might be inappropriate to other situations or domains. The practical problem of such environments is that they missed the support of interoperability and integration. That is users are limited to the functions and data structures provided in these environments. They can manually shift and transform data from one system/tool to another which is not easy for the users and is definitely a time-consuming task. Besides that, these PBL environments are built based on traditional software development methods where the cost of both time and effort is relatively high. Implementing such environments to change from one PBL model to another is not an easy task, hence the teachers have to follow the limited workflow in the software environment they are using. Consequently, teachers have less

flexibility to customize existing PBL models and to apply them in their own desired PBL lesson plans.

PBL scripting language is an Educational Modeling Language (EML) developed by Miao et al to support PBL-pedagogy where PBL scripts are used to structure and support technology-enhanced, problem-oriented, collaborative learning processes [15]. The PBL scripting language adopted a domain specific modeling language paradigm, which supports higher abstraction level, requires less effort and fewer low-level details to specify a given system than general-purpose modeling languages. It is designed for teachers to represent PBL models. Additionally, it was developed according to the best PBL practices and the well-known PBL models. A teacher can use this language to create a PBL process which is represented as a sequence of phases and within each phase there is a sequence of relevance activities, resources, artifacts and collaboration tools. A phase could be problem-engagement, problem-analysis, aim-and-plan, research, problem-resolution or evaluation. Some examples of activities are presenting, identifying, planning and investigating. A resource can be used as an input of an activity such as a problem source or real-world problem scenario. Artifacts are produced and used in activities, such as problem-statement and problem-solution. Furthermore, a collaboration tool could be chat room, wiki, or discussion-forum. In order to facilitate teachers in designing PBL lesson plans easily, a graphical PBL script editor was also developed based on the PBL scripting language[15].

A. State of the art Development

The formulation of PBL scripting language and the development of graphical PBL script editor addressed the limited aspects of the reviewed online PBL environments. However, using the graphical PBL script editor would require from teachers to first design the PBL process. Then to generate Unit of Learning (UoL) and use an IMS LD player to execute it, which is time and effort consuming. Eventually, a wide range of teachers are not familiar with IMS LD, as it is a research based specification.

Currently, the usage of Learning Management Systems (LMSs) is widespread over many colleges, universities and schools worldwide. Hence, most teachers and students are more familiar with such LMSs and they do not tend to experience or learn new systems. In this study, Moodle LMS was selected to be customized for implementing a PBL design and runtime environment. Moodle is an open source system that customizing it is much easier than other LMSs. The wide international usage of Moodle and its continued growth during the last six years have made it the leading open source LMS solution. Beside that Moodle provides a comfortable plugin mechanism for functional extension and customization. That raised up the challenge of adopting the PBL scripting language to extend Moodle LMS in which many teachers and students can benefit from it. The successfulness of e-PBL to extend Moodle towards the support of PBL-pedagogy and its limitation to support only the Woods' PBL model formed the basis of this study interest.

This study involves extending Moodle environment to dynamically instantiate a PBL lesson plan by adopting a PBL

scripting language. This would enable ordinary teachers to design and deliver online (and hybrid) PBL lesson plans in an easy, cost-effective, flexible, interoperable, and reusable manner.

III. METHODOLOGY OF BUILDING THE PBL SCRIPT EDITOR AND PBL PLAYER

This study adopted a Model-Driven Approach (MDA) as the software development method to extend Moodle platform in order to design and implement a PBL script editor based on PBL scripting language.

In this study, the MDA methodology supports customizing the design of PBL lesson plans for PBL teachers. For example, when they tend to create a new phase they will get a list of all possible phases and their associated activities, resources, and tools based on the PBL scripting language. In this way they can easily create PBL lesson plans with less time cost. The key challenge of adopting the MDA methodology is the transformation of both PBL meta-model and PBL script of PBL lesson plans into Moodle platform-specific configuration. By applying the MDA methodology to the development involved in this study, the system high-level architecture is designed as depicted in Figure 1. The system architecture consists of two main parts: design time environment and runtime environment. The design-time environment supports the design of PBL lesson plans where its core is a PBL script editor. The PBL runtime environment used to execute the PBL lesson plans by both teacher and students. The PBL runtime environment core component is called the PBL player.

A basic workflow of the system architecture starts by an ordinary teacher or by any PBL designer that has a desired PBL lesson plan. The teacher would use the PBL script editor to design the desired PBL lesson plan which is built based on a PBL scripting language. After the teacher completed the design of his/her desired PBL lesson plan, he/she can reuse and share it through a PBL script. Also, a PBL lesson plan can be automatically transformed into a PBL runtime environment using a PBL open source player. In this study Moodle open source was used to implement both the PBL script editor and the PBL player. Additionally, the teacher can instantiate multiple execution of a PBL lesson plan that can be used by both teachers and students.

IV. IMPLEMENTATION

This study involved the implementation of both Moodle's PBL script editor and Moodle's PBL player. The implementation of Moodle's PBL script editor first involved creating a new Moodle plugin according to the structure of Moodle plugins. Also, it required studying and analyzing the used PBL scripting language and being able to read and write PBL script files. Moodle's PBL script editor enables all the editing functions for teachers to design and create PBL lesson plans. Such editing functions including creating, editing and deleting a PBL lesson plan and all its elements. PBL lesson plan elements are phase, activity, tool, resource and artifact. A PBL lesson plan can have many phases and each phase consists of different activities. Resources and tools can be used by students in activity level to achieve the activity goals and submit artifacts as outputs. Figure 2 shows a simple PBL lesson plan created within the

developed Moodle's PBL script editor, which consists of three phases each phase has two activities with their associated resources, tools, and artifacts.

The second part of the targeted implementation in this study was implementing a simple PBL player by adopting the model driven approach and extending Moodle platform. Both teachers and students are supported within the PBL player to execute the designed PBL lesson plan. Moodle's PBL player manage the execution of the designed PBL lesson plans and make them ready for student to follow and for teacher to handle. One functional aspect was implemented for teachers to handle the execution of a PBL lesson plan and some functional aspects were implemented for students to follow a PBL lesson plan. The teacher can open/close and phase/activity at any time. The students can follow the PBL lesson plan phase by phase and use the available tools and resources. Also, students can submit artifacts within activities with editing functionality.

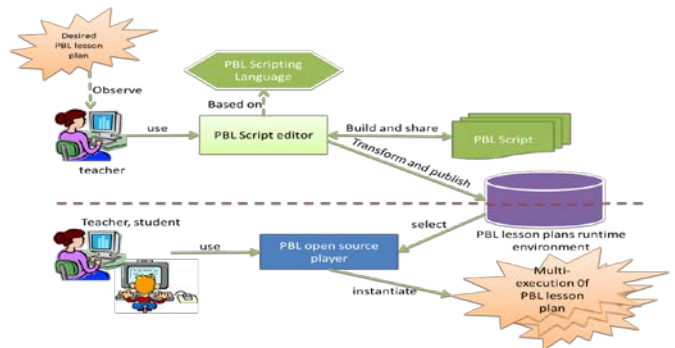


Figure 1: System architecture

| Import PBL plan Export PBL plan | | | | | |
|---------------------------------|--|---|---|-----------------------|-----------------|
| Add a new phase | | | | | |
| phase | Activities | Artifacts | Tools | Resources | |
| + Problem definition | + Create New activity + Present problem + Identify the problem | + Create New Artifact Problem tasks | + Create New Tool Online chat room Brainstorming tool | + Create New Resource | Problem trigger |
| phase | Activities | Artifacts | Tools | Resources | |
| + Gather and share information | + Create New activity + Gather information + Share information | + Create New Artifact | + Create New Tool Discussion forum | + Create New Resource | |
| phase | Activities | Artifacts | Tools | Resources | |
| + Problem resolution | + Create New activity + Develop the solution + Integrate Solutions | + Create New Artifact Problem Solution | + Create New Tool Wiki | + Create New Resource | |

Not opened yet Open Closed

Figure 2: A PBL lesson plan created within the developed PBL script editor in Moodle

V. EVALUATION

This section describes the evaluation methodology applied to evaluate the usefulness of both Moodle's PBL script editor and Moodle's PBL player.

A. Evaluation of Moodle's PBL script editor by teachers

This evaluation was applied to a PBL practical session conducted at Qatar University. The Moodle's PBL script editor evaluation comprised of eight ordinary teachers who participated in the session. They had been chosen to represent a wide range of subjects including computer science, computer engineering, Arabic, industrial engineering and civil engineering. Additionally, they also have come from different teaching levels such as teaching assistant, assistant professor and lecturer. The session was self-controlled, as the teachers started using the PBL script editor without any training. The target of this evaluation was to test the usefulness of the developed PBL script editor for teachers. The session lasting one hour was distributed in the following manner:

- The first ten minutes were used to give an introduction of the PBL learning methodology and the different models involved.
- The next 40 minutes were consumed to build a PBL lesson plan using Moodle's PBL script editor. A predefined PBL lesson plan was given to each of them which comprised of four phases. Each phase had two activities with some interconnected tools, resources, and artifacts. The participating teachers were asked to create the PBL lesson plan even though no prior training was given to them on how to use the PBL script editor.
- Following this, the teachers were given five minutes to fill a survey. The survey consisted of four sections to assess the teachers on; the background information, computer literacy, usefulness of the PBL scripting language and the PBL script editor, respectively. The last two sections of the survey evaluate the usefulness of the developed PBL script editor, while the first two sections used to analyze the relation between the teacher's evaluation and their prior background information and computer literacy. The last two sections consist of 17 statements, for each, the participant has to choose his/her level of agreement. (1: strongly disagree, 2: disagree, 3: no opinion/unsure, 4: agree, and 5: strongly agree).

The collected data was analyzed using descriptive statistics such as mean and standard deviation. Table 1 shows the mean and standard deviation values of the analyzed 17 statements. The mean represents the average agreement score (1: strongly disagree, 2: disagree, 3: no opinion/unsure, 4: agree, and 5: strongly agree) of the eight participated teachers for each survey statement. The mean scores of all seventeen statements are larger than 3.25 and most are near 4.0. The first five survey statements were related to the ease of use PBL scripting language, while the rest of the statements represented the ease of use PBL script editor. The PBL scripting language was part of the evaluation as it was used within the development of the PBL script editor. Obviously, most of the participated teachers responded positively on all aspects of the evaluation statements for both; the used PBL scripting language and the PBL script editor. Additionally, the Cronbach's alpha (α) value was calculated to measure the PBL script editor ease

of use scale. Hence, the PBL script editor ease of use α scale is 0.835. Nunnally [16], recommended that any instrument used in a basic research should has reliability of about 0.70 as a base or better. According to Nunnally, the resulted α scale of Moodle's PBL script editor demonstrates that the survey concerning ease of use is quite reliable comparing to the base value which is 0.70.

Table 1: Survey results for evaluating the PBL script editor ease of use

| | Survey statements | Mean | Std. Dev. |
|----|---|-------|-----------|
| 1 | The two levels (phase-level and activity-level) structure of the PBL script editor. | 3.875 | 0.35 |
| 2 | The terms or vocabularies used to define the PBL elements types. | 3.75 | 0.71 |
| 3 | Find an appropriate term or vocabulary to represent a PBL lesson plan. | 3.75 | 0.46 |
| 4 | The activity structure that includes tools, resources, artifacts and their interconnections | 4 | 0.00 |
| 5 | Represent a narrative into a PBL lesson plan. | 3.25 | 0.71 |
| 6 | Define students groups. | 4 | 0.53 |
| 7 | Create/delete a PBL lesson plan in a Moodle course. | 4.25 | 0.46 |
| 8 | Create/delete a phase. | 4.375 | 0.52 |
| 9 | Create/delete an activity. | 4.25 | 0.46 |
| 10 | Create/delete a tool (e.g. chat, forum). | 4.25 | 0.71 |
| 11 | Create/delete an artifact. | 4.25 | 0.71 |
| 12 | Create/delete a resource. | 4.25 | 0.89 |
| 13 | Interconnect tools to be used in an activity. | 4.25 | 0.71 |
| 14 | Specify activities and phases running sequence. | 4.125 | 0.35 |
| 15 | Define the detailed information of the PBL lesson plan such as description and goals. | 3.625 | 0.74 |
| 16 | Specify the completion condition (e.g. user control or time limit) of an activity or a phase. | 3.625 | 0.92 |
| 17 | Export a PBL lesson Plan into PBL script and then import it again. | 4 | 0.76 |

Additionally, the results of the first two sections of the survey were analyzed. The first section involved information about the participated teachers' prior PBL knowledge. Figure 3 shows the analysis of the prior PBL knowledge scale (1: Nothing, 2: a little, 3: basic knowledge, 4: knowledgeable, 5: expert) and the ease of use mean for each teacher where no significant difference was noticed regarding the different level of prior PBL knowledge. That is teachers with no strong prior PBL knowledge still thought that the Moodle's PBL script editor is easy to use.

Moreover, section two of the survey involved information about the teachers' computer literacy levels. In Figure 4, each point represents the relation between a teacher computer literacy level and his/her ease of use mean. The computer literacy level was calculated as the mean of different skills levels in different aspects significant for using Moodle's PBL script editor. The skills were regarding the teachers' use of generic computer tools (e.g. Word MS), communication tools (e.g. chat), teaching tools (e.g. digitalized whiteboards), and learning management systems (e.g. Moodle). On analyzing the collected data, we infer that there is slight positive influence of computer literacy level on the ease of use mean, though some deviations exist. Despite the fact, some participated teachers had little technical knowledge of computers; the majority of teachers still thought Moodle's PBL script editor is easy to use.

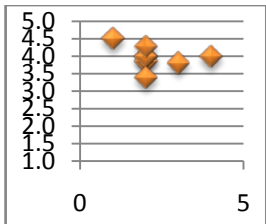


Figure 3: Scatter chart of teachers prior PBL knowledge(x-axis) and ease of use mean (y-axis)

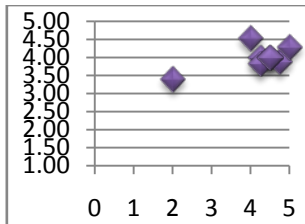


Figure 4: Scatter chart of teachers computer literacy mean(x-axis) and ease of use mean(y-axis)

B. Evaluation of Moodle's PBL Player by students

The evaluation of Moodle's PBL player was conducted through another practical session conducted at Qatar University. The PBL player evaluation covered a sample of ten students who participated in the session. The students have come from different education programs. One student from the master program, two students from secondary school, and the other seven students were from bachelor program. The conducted evaluation organized in term of self-controlled that is the students started using the PBL player without getting trained beforehand. This evaluation targeted testing the usefulness of the developed Moodle's PBL player for students.

A complete PBL lesson plan with details about a real PBL problem was created for students to solve. The PBL lesson plan consisted of four phases; problem definition, identification of learning issues, gathering and sharing information, and problem resolution. The PBL lesson plan was designed for group working mode, so the participating students were divided into three groups. The session lasting one hour was distributed in the following manner:

- The first ten minutes were used to give an introduction of the PBL learning methodology and the different models involved.
- The next 40 minutes, they worked in groups to solve a simple online PBL problem using Moodle's PBL player. They were asked to use Moodle's PBL player without prior training in how to use it.
- The last five minutes of the session they were asked to fill a survey according to their gained experience in using Moodle's PBL player. The survey consists of three sections; the first two sections are similar to the first two sections of the previously used survey in evaluating Moodle's PBL script editor. While the last section involved 12 ease of use statements that were created to measure the usefulness of the developed Moodle's PBL player by students.

The collected survey data for evaluating Moodle's PBL player was analyzed the same way it was done for evaluating the PBL script editor. Table 2 shows the twelve statements used in the survey together with their mean and standard deviation values for the ten participated students in the

evaluation session. Eventually, the mean score for the twelve statements is near 4.0 and most are greater. Noticeably, most of the participated students responded positively on all aspects of Moodle's PBL player evaluation statements. In addition, Moodle's PBL player ease of use Cronbach's alpha (α) value is 0.78 which also demonstrates that the surveys' ease of use is quite reliable.

Table 2: Results of evaluating the PBL player ease of use

| | Survey statements | Mean | Std. Dev. |
|----|---|------|-----------|
| 1 | Recognize the two-layer (phase-level and activity-level) structure of the PBL lesson plan | 4 | 0.47 |
| 2 | Recognize the activity structure that includes tools, resources, and artifacts. | 3.8 | 0.42 |
| 3 | Work in group while solving a PBL problem. | 4.7 | 0.48 |
| 4 | Navigate into an existing PBL problem in a course | 4.1 | 0.71 |
| 5 | View the PBL lesson plan details and its phases | 4.4 | 0.52 |
| 6 | Identify the current status, grade, and time of each phase and activity. | 4.4 | 0.52 |
| 7 | Use existing communication tool (e.g. chat, forum) in activity level | 4.1 | 0.32 |
| 8 | Submit/edit a required artifact within an activity. | 4.2 | 0.63 |
| 9 | Navigate into an available resource within an activity. | 4.2 | 0.42 |
| 10 | Know the execution sequence of the PBL lesson plan phases and their corresponding activities. | 3.8 | 0.63 |
| 11 | View detailed information (e.g. description and goals) of activities and their corresponding tools, resources, and artifacts. | 4.2 | 0.63 |
| 12 | Specify the completion condition of an activity (e.g. time limited) | 4.1 | 0.57 |

Furthermore, the results of the first two sections of the survey were analyzed the same way as described in evaluating Moodle's PBL script editor. This is because the first two sections are common between both used surveys. As shown in Figure 5 the analysis of the students' prior PBL knowledge level and the ease of use mean have no significant difference. This means that the evaluations of both Moodle's PBL script editor and PBL player were not affected by the level of prior PBL knowledge for the participated teachers and students. The scatter chart shown in Figure 6, presents the relation between each student computer literacy level and his/her ease of use mean. The computer literacy level was calculated the same way done previously in evaluating the PBL script editor. Though the computer literacy level showed a slight positive influence in evaluating the PBL script editor, a slight negative influence appeared in evaluating the PBL player with some deviations. That is some students with little computer literacy knowledge evaluated the PBL player more positively than students with higher computer literacy knowledge. However, the majority of the students still thought Moodle's PBL player is easy to use.

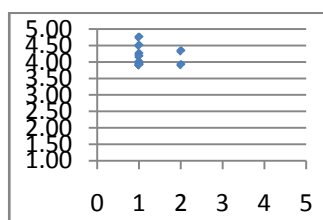


Figure 5:Scatter chart of students prior PBL knowledge (x-axis) and ease of use mean(y-axis)

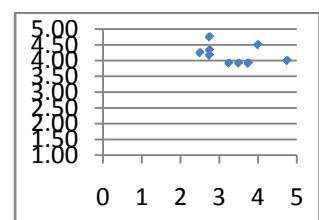


Figure6: Scatter chart of students computer literacy mean(x-axis) and ease of use mean(y-axis)

VI. CONCLUSION

In conclusion, this study provides a technical support for teachers to apply PBL learning methodology in their courses. A PBL online system was proposed for designing and delivering PBL lesson plans. The PBL online system consists of a PBL script editor to design PBL lesson plans and PBL player to simulate the execution of PBL lesson plans for students. Moodle's LMS was customized to implement both PBL script editor and PBL player. This study used an existing PBL scripting language to enable the design and delivery of a wide range of PBL models. The design and implementation of Moodle's PBL script editor facilitate teachers in building PBL lesson plans in flexible and reusable manner. Students would use Moodle's PBL player to follow a PBL lesson plan in order to solve a real world problem constructed by the teacher.

According to our evaluation of this study, both Moodle's PBL script editor and Moodle's PBL player are easy to use with Cronbach's alpha (α) value greater than 0.7. To the best of our knowledge, no other study has built a PBL script editor and PBL player within an existing LMS to support PBL-pedagogy which is making this study a unique international contribution. We believe that the developed Moodle's PBL script editor and PBL player would inroad the PBL learning methodology into education here in Qatar and around the world.

VII. FUTURE WORK

The future work of this study involves different aspects. One is that enhancing Moodle's PBL player to support different functional aspects for teachers, as within the scope of this study only one functional aspect was supported. Other functional aspects including feedback function to continually give feedback for students for each PBL lesson plan activity. Also, providing peer and rubric evaluation to evaluate the students work in solving a PBL problem. Another functional aspect is a notification function that would notify the teacher when the students submit PBL artifacts.

Additionally, build a repository of PBL lesson plans for the teacher within Moodle's PBL script editor to use and customize PBL lesson plans. Also, a search engine that aids the teacher to search the repository of PBL lesson plans for the best lesson plan that fit his/her needs from the repository. This would save the teacher's time and effort needed to design a new PBL lesson plan.

The interface of Moodle's PBL player will be improved in the future according to the students' feedback on the evaluation. Finally, this work inroads the development of PBL online system in other LMSs rather than Moodle.

ACKNOWLEDGMENT

This publication was made possible by NPRP grant # 5–051–1–015 from the Qatar National Research Fund (a member

of Qatar Foundation). The statements made herein are solely the responsibility of the author(s).

REFERENCES

- [1] Dochy, F., Segers, M., Van Den Bossche, P., & Struyven, K. (2005). Students' perceptions of a problem-based learning environment. *Learning environments research*, 8(1), 41-66.
- [2] Hmelo-Silver, C. E. (2004). Problem-based learning: What and how do students learn?. *Educational Psychology Review*, 16(3), 235-266.
- [3] Barrows, H. S. (1980). Problem-based learning: An approach to medical education. Springer Publishing Company.
- [4] Johnston, A. K., & Tinning, R. S. (2001). Meeting the challenge of problem-based learning: developing the facilitators. *Nurse Education Today*, 21(3), 161-169.
- [5] Barrows, H. S., & Kelson, A. M. (1993). Problem-based learning: A total approach to education. Monograph. Southern Illinois University School of Medicine, Springfield, Illinois.
- [6] Woods, D. R. (1994). Problem-based learning: How to gain the most from PBL. Waterdown, Ontario: DR Woods.
- [7] Wood, D. F. (2003). ABC of learning and teaching in medicine: Problem based learning. *BMJ: British Medical Journal*, 326(7384), 328.
- [8] IMSA's PBL teaching and learning Template. Retrieved March 15, 2014, from <http://pbln.imsa.edu/model/template/>
- [9] Derry, S. J., & Hmelo-Silver, C. E. (2005). Reconceptualizing teacher education: Supporting case-based instructional problem solving on the World Wide Web In L. PytlakZillig, M. Bodvarsson & R. Bruning (Eds.), *Technology-based education: Bringing researchers and practitioners together* (pp. 21-38). Greenwich, CT: Information Age Publishing.
- [10] Hmelo-Silver, C. E., Derry, S. J., Bitterman, A., & Hatrak, N. (2009). Targeting Transfer in a STELLAR PBL Course for Pre-Service Teachers. *Interdisciplinary Journal of Problem-based Learning*, 3(2).
- [11] Scardamalia, M., Bereiter, C., Mclean, R. S., Swallow, J., & Woodruff, E. (1989). Computer-supported intentional learning environments. *Journal of educational computing research*, 5(1), 51-68.
- [12] Guzdial, M., Hmelo, C., Hübscher, R., Nagel, K., Newstetter, W., Puntambekar, S., ... & Kolodner, J. L. (1997, December). Integrating and guiding collaboration: Lessons learned in computer-supported collaborative learning research at Georgia Tech. In *Proceedings of the 2nd international conference on Computer support for collaborative learning* (pp. 95-105). International Society of the Learning Sciences.
- [13] Suebnukarn, S., & Haddawy, P. (2007). COMET: A collaborative tutoring system for medical problem-based learning. *Intelligent Systems, IEEE*, 22(4), 70-77.
- [14] Ali, Z., & Samaka, M. (2013, March). ePBL: Design and implementation of a Problem-based Learning environment. In *Global Engineering Education Conference (EDUCON), 2013 IEEE* (pp. 1209-1216). IEEE.
- [15] Miao, Y., Samaka, M., Impagliazzo, J., Wang, Y., Wang, D., & Hoppe, U. (2013). A Model-driven Approach to the development of a PBL Script Editor. *Global Chinese Conference on Computers in Education (GCCCE)*.
- [16] Nunnally, J.C. (1978). *Psychometric Theory*, (2nd ed.). New York: McGraw-Hill.

Study of enzymatic hydrolysis and liquid glucose production by solid state fermentation from rice hull using Trichoderma Species

(Study of rice hull using Trichoderma Species)

Arezou Ghadi

Department of Chemical Engineering, Islamic Azad University, Ayatollah Amoli Branch, Amol, Iran
ghadi.arezoo@gmail.com

Azam Sinkakarmi

Department of Chemical Engineering, Applied Scientific University
Babol, Iran
azamsinkakarmi@yahoo.com

Abstract— This study investigates enzymatic hydrolysis of rice hull by *Trichoderma Reesei* to produce liquid glucose from cellulose under solid state fermentation. Medium fortifying effects on the rate of enzyme activity on (FPA, CMCASE) were studied and the optimum condition of main culture medium and optimization method for production of glucose were investigated. Results showed that in terms of activity of filter paper and activity of specific filter paper, medium containing pure rice hull moistened with liquid basal is optimum and then medium containing pure rice hull moistened with water has the highest level of activity. Therefore if the aim is to achieve the highest glucose concentration and highest concentration of filter paper, basal liquid medium must be used in this fermentation, and if the goal is to achieve the highest degree of carboxymethyl cellulase activity, it is enough to moisten substrate medium containing shell rice with tap water and monitor solid substrate fermentation for 4 days at 30 °C.

Keywords— Rice husk, *Trichoderma* species, solid substrate fermentation.

I. INTRODUCTION

In the last few decades, many efforts have been spent in the study of enzymes with cellulolytic activity as potential sources in obtaining energy from an abundant and renewable cellulose especially the cellulase system of the fungus *Trichoderma* sp. It has been known that cellulases from *Trichoderma* sp. can be effectively hydrolyze crystalline cellulose [1]. Lignocellulosic substrates, such as rice hull are the agricultural wastes and by-products of rice hulling plants. The major parts of them are cellulose polymerase, hemi cellulose and lignin which can be used to domesticate animals and birds as well as producing some of other microbial metabolites such as cellulolytic enzymes or ethanol [2-5].

In recent years, studies have been done to enhance the nutritional value of rice husk in some countries. Researches in Nigeria (2007) show that the fermentation of rice husk using *Trichoderma* fungi for 40 days can cause a significant increase in amount of crude protein, energy and

mineral content such as sodium and potassium and it can decrease the amount of crude fiber [6]. In Zaid et al., (2009) report, the amount of crude protein in the fermented rice husk increased about 97% and the amount of crude fiber has reduced about 45% [7]. In fermentation of rice husk, solid state fermentation (S.S.F) and liquid state fermentation (LSF) or submerged fermentation (SMF) can be used; each of which, due to the type of method, has its own advantages and disadvantages.

Solid state fermentation means control of growth of microorganism on wet solid substrate in absence of free water. This method is usually cheaper while equipment used in liquid state fermentation (L.S.F) is more expensive. Solid state fermentation (S.S.F) method does not need big space, so that operations can be done in a pan bioreactor or even in an Erlenmeyer. The greatest advantage of solid state fermentation is that this method does not need soluble substrate rather enough, just it is crucial to moisten the substrate a little, in fact we do not need to free water.

The desired product is concentrated so its purification is easier. Another advantage of SSF, due to the high concentration of microorganisms and low humidity of medium, is that it significantly reduces the microbial contamination. Also, the amount of material in SSF is less than SMF and enzymes show less susceptible to catabolic inhibition or stimulation. However, the SSF method is associated with some limitations, including limited use of microorganisms capable of growth in semi-humid environment and information about the increasing scale of production in this way is negligible [8,9].

II. MATERIAL AND METHODS

For this experimental research fungal strain *Trichoderma reesei* (PTCC 5142) as lyophilized ampoule was purchased from industrial scientific research organization and transferred to physiologic serum under

the sterile hood. Strains were cultured in steep medium of Malt extract Agar (MEA), and incubated at 4°C for long-term maintenance. Husk was used in this study as substrate and as carbon source.

A. Preparation of substrate

For preparation of substrate, husk has been incubated at 4°C and then grinded, the resulting rice husk particles size was less than 2 mm.

B. Preparation of pre culture

After elementary operation, 12.5 gr of rice husk powder was mixed with 17 cc water in the Erlenmeyer (500 ml). After preparation of solid bed, sterilization step 121°C and 15 psi in the autoclave is necessary. After that, the temperature of the contents of the flasks should be brought to room temperature.

C. Fermentation of culture

Spore suspension prepared from slants containing 3 strains that mentioned above with sterile distilled water, and using sterile pipet at near the flame, impregnation operation from slant to pre culture media took place and then, pre culture flasks were incubated 30°C for 5 days.

D. Preparation of main culture

After the flasks were placed in the autoclave and cooled at room temperature in the completely sterile conditions, impregnation from preculture to main culture took place. With sterile loop, a part of growth fungi colony on a solid bed was transferred to flask that contained main culture and was mixed and this process was repeated three or four times till 5% growth fungi colony was transferred. Then, after preparing fungi suspension with physiologic serum, amount of 10 micro liter of this suspension was put between lam and Lamel. Using optical microscope, the number of fungal spores in each square was counted and dilution factor that depends on the volume of physiological serum was applied. Number of spores was calculated. When the numbers of spores on a main culture reach to 8×10^5 wet weight¹, again cultures were incubated at at 30°C for 5-7 days. After the mentioned time finished, the culture was taken out from incubator.

E. Separation of enzymatic solution

For separation of raw enzymatic solution, first buffer citrate at pH= 4.8 was prepared, and then, about 5 fold of solid substrate weight, buffer citrate was added to flasks ($5 \times 12.5 = 125$ ml). Afterward, the flasks were put in the shaker for 15 mins, until the contents are equal. Then the solution was passed from Watman filter paper No.1. to assure of no presence of fungi spores, the passed solution from filter should be centrifuged at 4°C and 4000 rpm for 20 min. This prevents turbidity in the experiment. By this way, enzymatic solution that contains a lot of liquid sugar (glucose), can be separated. Indeed, during fermentation, oozed cellulose enzyme from Trichoderma fungi, hydrolyze the existed cellulose in the rice husk and convert it to glucose (lump sugar).

F. Measurement of glucose and protein concentration in raw enzymatic solution

For measurement of glucose concentration in raw enzymatic solution, kit of glucose oxidase (production of Man Company), which is an enzymatic method for lump sugar measurement was used. The produced glucose concentration in crud enzymatic solution (mg/dl), was calculated according to the existed direction in the kit. For the measurement of amount solute protein, Loury method has been used. Bovine Serum Albumin (BSA) solution is as a standard solution and at the end the amount of samples absorption read at 578 wave length and with using BSA standard curve, protein concentration in the unknown sample (mg/ml) was obtained.

G. Measurment of enzyme activity

This research is on the basis of calculation of filter paper activity and after that calculation of endoglucanase activity. With respect to the references in this field, experiments related to activity measurement done and at last, the amount of activity (unit/ml) was calculated.

Statistical analysis: To analyze the data and comparison the amount of produced glucose in cultural groups under different incubation times and temperatures, the statistical software SPSS and ANOVA were used and P<0.05 was considered significant

H. Optimize the assay of enzyme activity

For optimization of enzyme activity during 4 days at 30°C, during which *Trichoderma reesei* microorganism reaches its maximum growth [10], medium was considerd the effects on various substrates by adding some combination of mineral rich salts.

I. Calculation of filter paper

Since the sample is liquid enzyme and 0.5 ml of it is diluted with 1ml citrate buffer after that allowed to react for 1 hour in the oven and then according to the glucose oxidase kit. to measure the glucose level 10 ml or 0.01 µl of it was tested so calculation of filter paper is obtained following equation:

$$(U/ml)FPA = \frac{\left(\frac{mg}{ml} \times \frac{10^3}{180}\right)\left(\frac{\mu mol}{ml}\right) \times (1ml \text{ Buffer})}{0.5 \text{ ml} \times 0.01 \text{ ml} \times 1 \text{ h}} \quad (1)$$

J. Calculate the specific activity of filter paper

Specific activity (SP.A) is the ratio of the concentration of the enzyme on protein concentration and unit is defined as units / mg prot.

$$(SP.A) = \frac{\frac{U}{ml}}{\frac{mg \text{ prot}}{ml}} \quad (2)$$

K. Calculate the molecular activity of filter paper

Molecular activity is defined as units/ μmol . To calculate the molecular activity of filter paper, it is sufficient to divide the (u / ml)_{FPA} on ($\mu\text{mol} / \text{ml}$)_{FPA}.

• Methods of medium optimization

6 medium were numbered respectively and operated as follows:

1-11gr nolignin rice crust moist within 7.48 ml basal medium.

2- 11gr nolignin rice crust moist within 7.48 ml of tap water.

3- 11gr rice crust (pure culture) 7.48 ml

4-11gr purified rice crust moist within 7.48 ml of tap water.

5- 8.8 gr rice crust mixture with 2.2 gr wheat husk and moist within 7.48 ml basal medium.

6- 8.8 gr wheat crust mixture with 2.2 gr wheat husk (ratio of 8 to 2) and moist within 7.48 ml of tap water.

After preparing the cultures autoclave them for 20 min in 121°C. After cooling the cultures, from T.reseei pure culture under sterile conditions, fertilization operation is done to mediums and then to autoclave flasks containing medium cultures in optimum time and temperature (30°C temperature for 4 days)[10] then the media is removed from the incubator and 55 ml citrate buffer is given to them and placed on shaker and then the same operation is performed (filtration, centrifugation filter) finally what is achieved is raw enzymatic solution from 6 cultures. First optical absorption of sample obtained by glucose oxidase method in $\lambda=500$ nm then with Lowry method concentration of protein in the crude enzyme solution was measured and ultimately FPA and CMCase activity was obtained. Results of produced glucose concentration in the 5142 mediums to optimize fungal medium is shown in table 1.

III. RESULT AND DISCUSSION

A. Measuring of enzymatic soluble protein of 5142 species by lowry's method for optimization of fungal growth medium

Samples and dilutions is prepared according to the Lowry method. Bovine serum albumin standard samples adsorption standard is done in $\lambda=578$ nm wavelength so

that standard curve with equation $OD = 0.006 C_{\text{prot}} + 0.03$ is used. The protein concentration in the solution of 6 sample enzyme is shown in table 2.

TABLE II. THE PROTEIN CONCENTRATION IN THE SOLUTION OF 6 SAMPLE ENZYME

| Medium tested | protein concentration (mg/ml) |
|--|-------------------------------|
| No lignin in liquid basal medium containing rice crust | 0.044 |
| Medium containing no lignin rice crust with water | 0.04 |
| Liquid basal medium containing pure rice crust | 0.3 |
| Medium containing pure rice crust with water | 0.34 |
| Shell liquid basal medium containing wheat and rice husk | 0.22 |
| Mixed medium crust of wheat and rice flakes with water | 0.4 |

Rice husk is an organic source and has high percent of protein, after that medium containing pure wheat crust contains high protein concentration.

B. Calculation of filter paper activity, specific activity and molecular activities of filter paper

In terms of activity of filter paper and specific activity of filter paper, medium containing pure rice husk which soaked in liquid basal is optimum medium and then medium containing pure rice husk that has been moistened with water has the highest level of activity. Activity, specific activity, molecular activity and relative activity of tested media cultures are shown in table3.

C. Calculation of activity, specific activity and molecular activity of carboxymethyl cellulase

The filter paper activity and specific activity of filter paper medium containing pure rice husk which soaked in liquid basal is optimum medium and then medium containing pure rice husk that has been moistened with water has the highest level of activity. Activity, specific activity, molecular activity and relative activity of CMCase in tested media culture is shown in table4.

TABLE I. RESULTS OF PRODUCED GLUCOSE CONCENTRATION IN THE 5142 MEDIUMS TO OPTIMIZE FUNGAL MEDIUM

| Culture | Glucose concentration in the crude enzyme solution (mg/dl or mg/100cc) | Absorbance of standard solution (OD) $\lambda=500\text{nm}$ | Absorbance of sample (OD) $\lambda=500\text{nm}$ |
|---|--|---|--|
| No lignin wheat crust (Basal medium) | 12.35 | 0.34 | 0.042 |
| No lignin wheat crust (Free basal medium) | 14.7 | 0.34 | 0.05 |
| Pure wheat crust (Basal medium) | 50 | 0.34 | 0.17 |
| Pure wheat crust (Free basal medium) | 412 | 0.34 | 0.14 |
| Wheat flakes mixed with rice husk (Basal medium) | 48.5 | 0.34 | 0.165 |
| Wheat flakes mixed with rice husk (Free basal medium) | 23.5 | 0.34 | 0.08 |

TABLE III. ACTIVITY, SPECIFIC ACTIVITY, MOLECULAR ACTIVITY AND RELATIVE ACTIVITY OF CMCase IN TESTED MEDIA CULTURE

Standard solution OD_s= 0.34

| Number of tested culture medium | OD sample content CMCase | Activity CMCase (u/ml) | Activity of filter paper | Specific activity SP.A(units/mg _{prop}) | Molecular activity (units/μmol) | Relative activity |
|---------------------------------|--------------------------|------------------------|--------------------------|---|---------------------------------|-------------------|
| 1 | 0.09 | 288 | 17 | 6545.4 | 200 | 0.55 |
| 2 | 0.04 | 134 | 13 | 3350 | 200 | 0.26 |
| 3 | 0.13 | 422 | 120 | 1407 | 200 | 0.8 |
| 4 | 0.16 | 520 | 49 | 1529 | 200 | 1 |
| 5 | 0.14 | 460 | 26 | 2091 | 200 | 0.9 |
| 6 | 0.11 | 360 | 26 | 900 | 200 | 0.7 |

TABLE IV. ACTIVITY, SPECIFIC ACTIVITY, MOLECULAR ACTIVITY AND RELATIVE ACTIVITY OF CMCase IN TESTED MEDIA CULTURE

Standard solution OD_s= 0.34

| Number of tested culture medium | λ=500nm | λ=500nm | Activity of filter paper | Specific activity of filter paper | Molecular activity F.P | Relative activity |
|---------------------------------|---------|---------|--------------------------|-----------------------------------|------------------------|-------------------|
| 1 | 0.055 | 0.05 | 17 | 386 | 205 | 0.14 |
| 2 | 0.042 | 0.038 | 13 | 325 | 200 | 0.11 |
| 3 | 0.105 | 0.068 | 120 | 400 | 200 | 1 |
| 4 | 0.095 | 0.08 | 49 | 144 | 200 | 0.41 |
| 5 | 0.08 | 0.072 | 26 | 118.2 | 200 | 0.22 |
| 6 | 0.06 | 0.052 | 26 | 65 | 200 | 0.22 |

IV. CONCLUSION

Enzymatic hydrolysis of rice husk of production of glucose (sugar liquid) has been studied. 5142 T.reseei strain has maximum growth if incubated in optimum time and temperature (30°C in 4 days) on the pure rice husk substrate which didn't lignin formation and moist with liquid basal medium and has the highest enzymatic activity and glucose production. However highest glucose concentration obtained in the crude enzyme solution which substrate contains only pure rice husk that moisted with tap water. If to the rice husk medium add amount of wheat husk (ratio of 8 to 2) and the surface of substrate is wet with tap water glucose produced approximately 2-fold increase compared to before.

REFERENCES

- [1] Gaden, E.L., Mandels, M.H., Reese,E.T., Spano,L.A.Eds, 1976, "Enzymaticconversion of cellulosic maerials: Technology and Applications", Biothecnol. Bioeng. Symp.No.6, Jhon Wiley and sience, Newyork P.319.
- [2] I RR. Singhania, PK. Sukumaran, A. Pilli, et al. "Solid state fermentation of lignocellusic substrate for cellulase production by Trichoderma reesei", NRRL460. Indian J Biotech 2006, 5, 332-6.
- [3] LR. Lyud, PJ. Weimer, WH. Van Zyl, IS. Pretorius. Microbial cellulose utilization: Fundamentals and biotechnology", Microbial Mol Biol Rev 2002, 66, 506-77.
- [4] Y. Sun, J Cheng. "Hydrolysis of lignocellulosic materials for ethanol production: A review", Bioresour technol 2002, 83, 1-11.
- [5] J Zaldivar, J Nielson, L Olsson. "Fuel ethanol production from lignocelluloses: A challenge for metabolic engineering and process integration", APPL Microbiol Biotechnol 2001, 56, 17-34.
- [6] A Z Aderolu, A Iyaya, AA Onilude. "Changes in nutritional value of rice husk during Trichoderma viride degradation. Bulgarian J Agricultural Science, 2007, 13, 583-589.
- [7] AA Zaid , O Ganiyat. "Comparative utilization of biodegraded and undegraded rice husk in Clarias gariepinus diet", African J Biotechnol 2009, 8 (7): 1358-1362.
- [8] C Krishna. "Solid-state fermentation systems – An overview", Critical Rev Biotechnol, 2005, 25, 1-30.

- [9] CN Aguilar, G Gutiérrez-Sánchez, PA Rrado-Barragán, R Rodríguez-Herrera, JL Martínez-Hernandez, JC Contreras-Esquivel. "Perspectives of solid state fermentation for production of food enzymes". American J Biochem Biotechnol 2008, 4 (4): 354-366.
- [10] A.Ghadi , S. Mahjoub, R. Mehravar, "Management of Glucose Production Process from Rice Husk by Solid State Fermentation Method", 2011 International Conference on Biotechnology and Environment Management IPCBEE vol.18 (2011) © (2011)IACSIT Press, Singapoore

Comparative Analysis of Base Transceiver Station (BTS) and Power Transmission Lines Effects on the Human Body in Lagos Environs

Akinyemi, L.A, Makanjuola, N.T, Shoewu, O.

Department of Electronic & Computer Engineering, Faculty of Engineering,
Lagos State University, Epe Campus.

Edeko, F.O.

Department of Electrical & Electronic Engineering, Faculty of Engineering,
University of Benin, Edo State.

Abstract- This paper presents the Comparative Analysis of Base Transceiver Station (BTS) and Power Transmission Lines Effects on the Human Body in Lagos Environs. This was achieved using the measured and calculated values of some electromagnetic parameters such as power density, and electric field intensity. The International Commission on Non-Ionizing Radiation Protection (ICNIRP) exposure limit for BTS antennas is **0.1W/m² (100 mw/m²)**. For values of radiating power of the base station antenna ranging between 33Watts to 100Watts, the power density experienced in the vicinity of the antenna ranges from 0.8 mW/m² to 280 mW/m². The health effect of the antennas is at its peak when the base station antenna is transmitting at 100Watts. At radiating power of 100Watts, the mean power density was found to be 39 mW/m², and the Root Mean Square Error (RMSE) value was 73 mW/m². The distance away from the base station that is safe for residential purposes was found to be 16.m. The safety guideline by ICNIRP for exposure to overhead high voltage power line is **10kv/m**, the electric field around the power line ranges from 0.016KV/m to 0.46 KV/m. The mean electric field was found to be 0.056KV/m, and the Root Mean Square Error (RMSE) value was 0.12KV/m. The highest value of electric field intensity measured in the vicinity of an overhead power line was found to be far below ICNIRP limit of exposure. The results obtained in this research can help in the proper town planning and allocation of land space for residential and commercial purposes, so as to reduce the number of health hazard related to electromagnetic radiation from these two common sources. Also, the health risks associated with exposure to electromagnetic radiation, especially at distances very close to the electromagnetic source are discussed and the public are advised to avoid residing near these sources.

Index terms – Power transmission lines, Environment, Base Transceiver Station, Electromagnetic radiation, Radiating power, Electric field.

I. INTRODUCTION

There is a rise in the use of electric power dependent gadgets in Nigeria. Consequently, several transmission power lines are being installed all over the country to meet electric power demands [3]. Also, in the past decade, because of the need to communicate, the use of mobile telephony has also increased rapidly. There are over a thousand base stations in Lagos. This is so due to the desire of network providers to meet the demands of the increasing

of body parts are some of the effects being reported [3,7]. The International Commission on Non-Ionizing Radiation Protection (ICNIRP) developed a standard for the control of exposure to electromagnetic radiation. The values obtained in this work were compared to the ICNIRP standard to determine the safe proximity to these electromagnetic sources [4,8].

II. MEASUREMENT PROCEDURE

Measurements were made within 100m of a BTS, 132KV power line, and 330KV power

line. The first point of measurement was 10m through to 100m with a 10m interval.

Theoretical calculations were also carried out to estimate the electromagnetic parameters at same distances.

A. Power Density in the Vicinity of a BTS Calculation.

The Power Density (P.D) of an antenna can be mathematically expressed as [11];

$$P_d = \frac{1}{2} Re[\bar{E} \times \bar{H}] \quad 1$$



Figure 1: Pictorial view of a Base Transceiver Station in Ikeja Lagos State



Figure 2: Pictorial view of a Power Line along Ikeja Lagos State

Where, \bar{E} and \bar{H} are the electric and magnetic field intensity of the electromagnetic waves.

$$Z_0 = \sqrt{\frac{\mu_0}{\epsilon_0}} \quad 3$$

$$\mu_0 = 4\pi \times 10^{-7} \frac{H}{m} \quad 4$$

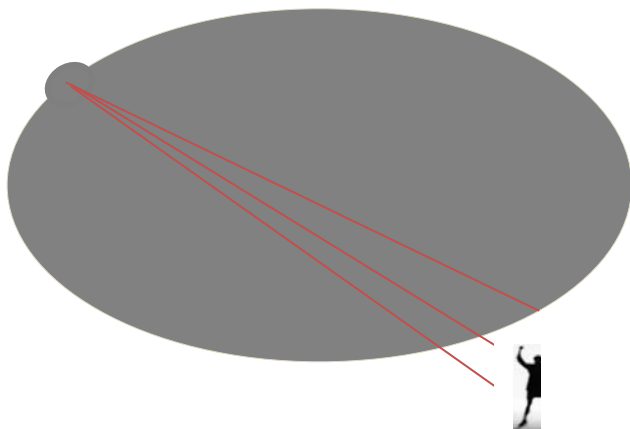


Figure 3: An individual Exposed to Radiation from BTS antenna.

$$\epsilon_0 = \frac{10^{-9}}{36\pi} F/m \quad 5$$

$$\text{Then, } Z_0 = 120\pi \approx 377\Omega \quad 6$$

The total electric field intensity due to the base station antenna is;

$$E_{rms} = \frac{\sqrt{30NP_{rad}G}}{R} \quad 7$$

Where

N is the number of carriers (antennas),

P_{rad} is the radiated power,

G is the radiation gain for a pattern antenna,

R is the distance from the base station.

Then substituting equation (7) in equation (2) it gives:

$$P_d = \frac{30NP_{rad}G}{R^2Z_0} \quad 8$$

The following formula enables the calculation of equivalent power density (P_d) to be made and assumes field impedance [5],

$$P_d = 0.0796N \frac{P_{rad}}{R^2} \times 10^{\frac{G}{10}} \quad 9$$

Where

G in equation (9) is the gain of base station antenna in dB. The simplest case of application is the one when human is exposed to a single base station antenna, ($N=1$).

$$\text{Then: } P_d = 0.0796 \frac{P_{rad}}{R^2} \times 10^{\frac{G}{10}} \quad 10$$

Where

P_{rad} is the radiated power (in Watts) emitted by the base station antenna,

G is the antenna gain (in dB) in the direction where the person is placed relative to the antenna.

B. Electric Field Intensity in the Vicinity of a Power Line.

The electric field intensity around a power line can be estimated by using the Method of Images, the analysis can be calculated from the figure below. The dashed line signifies the earth surface which acts like a mirror. Everything below the dashed line is the mirror image of the elements above it. Because the earth is a perfect conductor (potential at ground level is equal to zero), estimations are made few metres above the ground level [1,6].

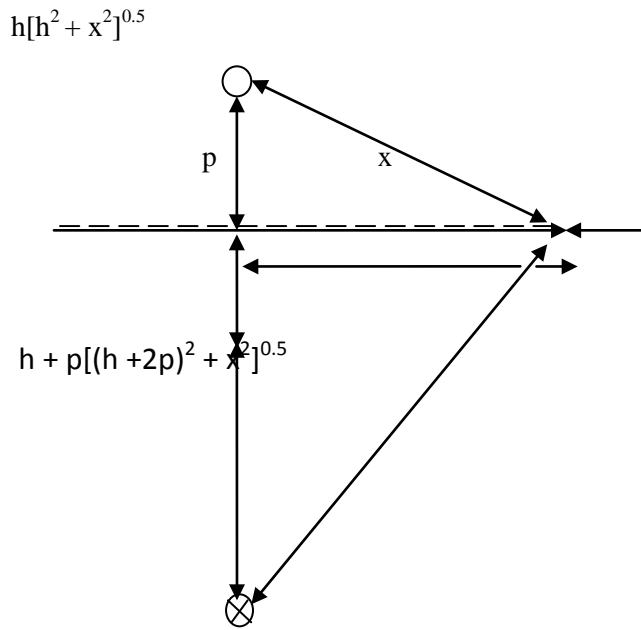


Figure 4: Line current representation of a power line.

$$\text{Let } R = [h^2 + x^2]^{0.5} \quad 11$$

$$\text{and } R' = [(h + 2p)^2 + x^2]^{0.5} \quad 12$$

the expression for the voltage on a power line is given by;

$$V = \frac{Q}{2\pi\epsilon_0} \ln\left(\frac{2(h+p)}{r}\right) \quad 13$$

p is the height of the exposed person.

Where $(h + p)$ is the height of the electric pole,

x is the distance of the exposed person from the power line.

r is the radius of the of the electric conductors used.

Q is the charge per unit length of the conductor.

$$\epsilon_0 = \frac{10^{-9}}{36\pi} \quad F/m \quad 14$$

The electric field intensity that will be felt x metres away from the power line is given by the expression;

$$E = \frac{Q}{2\pi\epsilon_0} \left(\frac{1}{R} - \frac{1}{R'} \right) \quad 15$$

Making charge per unit length Q the subject of the formula in equation 13, we have;

$$Q = \frac{V \times 2\pi\epsilon_0}{\ln\left(\frac{2(h+p)}{r}\right)} \quad 16$$

Substituting equation (16) into equation (15), equation (15) becomes;

$$E = \frac{V}{\ln\left(\frac{2(h+p)}{r}\right)} \times \left(\frac{1}{R} - \frac{1}{R'} \right) \quad 17$$

Equation (17) defines the electric field experienced around an electric overhead power line.

Where V is the voltage along the line conductor in KV.

R is the distance of the observer away from the pole.

R' is the distance of the observer away from the image.

p is the height of the exposed person.

$h+p$ is the height of the electric pole.

r is the radius of the conductor used by the power line.

III. INVESTIGATED ENVIRONMENT

Lagos is the most populous city in Nigeria. It has a population of about 17.5 million people. Its geographical coordinates are $6^{\circ}27'N$ and $3^{\circ}23'E$.



Figure 5: Map of Lagos State

IV. ANALYSIS OF RESULTS

Tables I, and IV show the results of the measured and calculated power density experienced at distances ranging from 10 to 100m with 10m interval away from the BTS, and the power lines. The radiation power (P) of base station antennas is within the range of 33watts and 100watts, at a gain (G) of 5dB. MATLAB software was used for the graphical analysis of the data obtained. Tables II, III, V, and VI show the result of the statistical analysis of the data obtained. The statistical formulae used are given below.

Arithmetic Mean is defined by

$$\bar{x} = \frac{\sum(x)}{n} \quad 18$$

Mean Deviation is defined by

$$M.D = \frac{\sum(x - \bar{x})}{n} \quad 19$$

Table II shows the statistical analysis of the data obtained was also carried out. The results obtained are also tabulated.

Root Mean Square Error is defined by

$$RMSE = \sqrt{\frac{\sum(x - \bar{x})^2}{n}} \quad 20$$

Variance is the square of R.M.S.E, and is defined by

$$\frac{\sum(x - \bar{x})^2}{n} \quad 21$$

Table 4.1: Power density with respect to the distance from base station antenna located at Ikeja Lagos State. for

| Distance From Base Station Antenna (Metres) | P=33W G=5dB Power Density (P.D ₁) (W/m ²) | | P=66.7W G=5dB Power Density (P.D ₂) (W/m ²) | | P=100W G=5dB Power Density (P.D ₃) (W/m ²) | |
|--|---|------------|---|------------|--|------------|
| | Measured | Calculated | Measured | Calculated | Measured | Calculated |
| 10 | 0.074 | 0.0831 | 0.18 | 0.168 | 0.28 | 0.252 |
| 20 | 0.018 | 0.0207 | 0.035 | 0.042 | 0.054 | 0.0629 |
| 30 | 0.0078 | 0.0092 | 0.017 | 0.0186 | 0.023 | 0.028 |
| 40 | 0.0041 | 0.0052 | 0.009 | 0.0105 | 0.016 | 0.0157 |
| 50 | 0.0028 | 0.0033 | 0.0054 | 0.0067 | 0.0091 | 0.0101 |
| 60 | 0.0026 | 0.0023 | 0.0040 | 0.0047 | 0.0066 | 0.0070 |
| 70 | 0.0014 | 0.0017 | 0.0037 | 0.0034 | 0.0055 | 0.0051 |
| 80 | 0.0012 | 0.0013 | 0.0029 | 0.0026 | 0.0031 | 0.0039 |
| 90 | 0.0011 | 0.0010 | 0.0018 | 0.0021 | 0.0028 | 0.0031 |
| 100 | 0.00071 | 0.00083 | 0.0015 | 0.0017 | 0.0022 | 0.0025 |

Table II: Statistical analysis of calculated power density

| Statistical Parameters | P=33W G=5dB (W/m ²) | P=66.7W G=5dB (W/m ²) | P=100W G=5dB (W/m ²) |
|---------------------------|---------------------------------------|---|--|
| Mean | 0.0129 | 0.026 | 0.039 |
| Mean Deviation | 0.0156 | 0.0316 | 0.047 |
| R.M.S.E | 0.0241 | 0.0487 | 0.073 |
| Variance | 0.00058 | 0.00237 | 0.0053 |

Table III: Statistical analysis of calculated power density

| Statistical Parameters | P=33W, G=5dB (W/m ²) | P=66.7W, G=5dB (W/m ²) | P=100W, G=5dB (W/m ²) |
|---------------------------|--|--|---|
| Mean | 0.01137 | 0.02596 | 0.04023 |
| Mean Deviation | 0.0139 | 0.0326 | 0.05071 |
| R.M.S.E | 0.0207 | 0.05226 | 0.0813 |
| Variance | 0.0004 | 0.00273 | 0.00661 |

Table IV: Electric field strength with respect to distance for power lines located at Ikeja Lagos State

| Distance From Power Line (Metres) | Voltage= 132KV | | Voltage=330KV | |
|--|--------------------------|------------|--------------------------|------------|
| | Electric Field (KV/m) | | Electric Filed (KV/m) | |
| | Measured | Calculated | Measured | Calculated |
| 10 | 0.16 | 0.18 | 0.41 | 0.46 |
| 20 | 0.035 | 0.046 | 0.092 | 0.12 |
| 30 | 0.014 | 0.016 | 0.029 | 0.04 |
| 40 | 0.0052 | 0.00745 | 0.015 | 0.019 |
| 50 | 0.0028 | 0.004 | 0.0076 | 0.01 |
| 60 | 0.0016 | 0.0023 | 0.0041 | 0.00573 |
| 70 | 0.0011 | 0.00146 | 0.0020 | 0.00365 |
| 80 | 0.00072 | 0.001 | 0.0015 | 0.0025 |
| 90 | 0.00038 | 0.0007 | 0.00095 | 0.00175 |
| 100 | 0.00022 | 0.00052 | 0.00052 | 0.0013 |

Table V: Statistical analysis calculated electric field intensity

| Statistical Parameters | Voltage 132KV | Voltage 330KV |
|---------------------------|------------------|------------------|
| Mean | 0.026 | 0.066 |
| Mean Deviation | 0.035 | 0.089 |
| R.M.S.E | 0.053 | 0.14 |
| Variance | 0.0028 | 0.018 |

Table VI: Statistical analysis for measured electric field intensity

| Statistical Parameters | Voltage 132KV | Voltage 330KV |
|---------------------------|------------------|------------------|
| Mean | 0.022 | 0.056 |
| Mean Deviation | 0.030 | 0.078 |
| R.M.S.E | 0.047 | 0.12 |
| Variance | 0.0022 | 0.015 |

V. GRAPHICAL ANALYSIS

MATLAB software was used to carry out the graphical analysis of the data obtained.

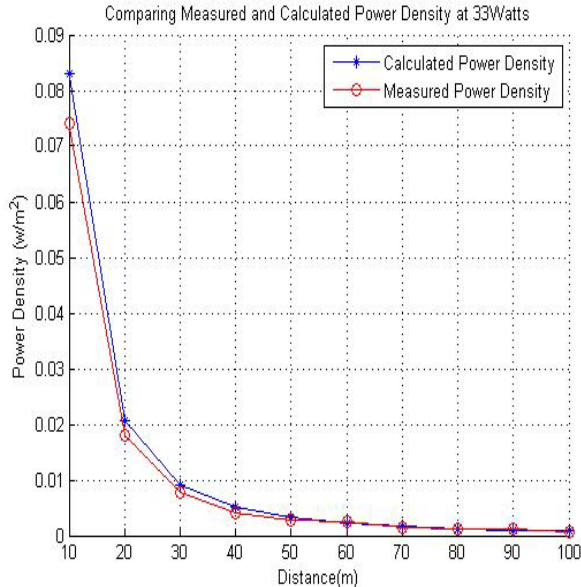


Figure 6: Comparison of calculated and measured Power Density at 33Watts against Distance

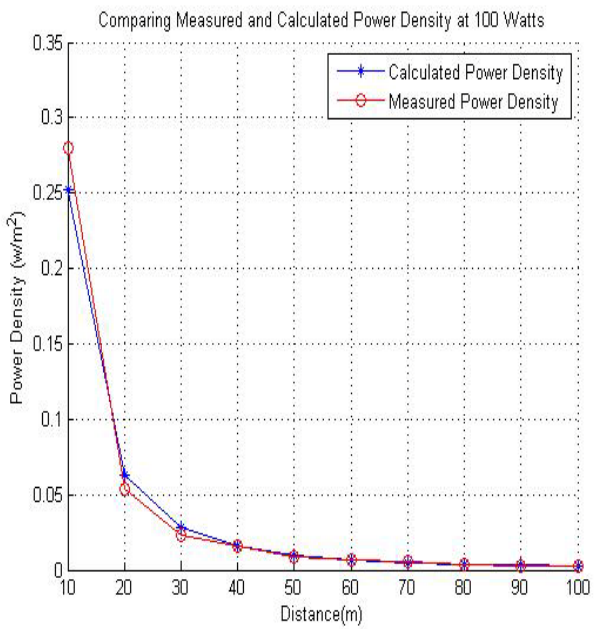


Figure 8: Comparison of calculated and measured Power Density at 100Watts against Distance

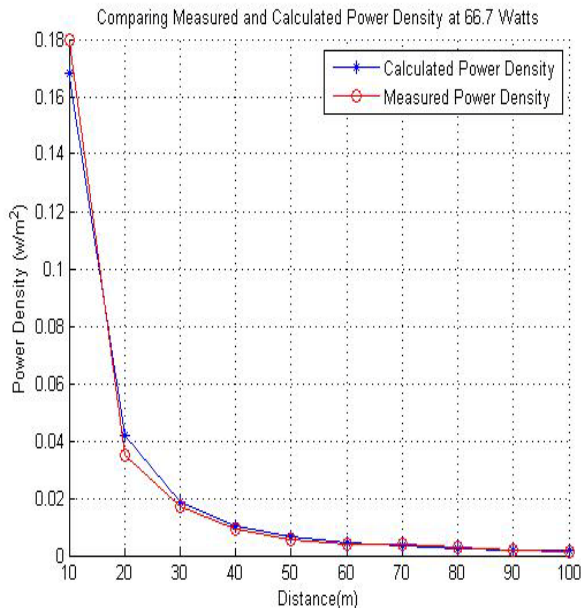


Figure 7: Comparison of calculated and measured Power Density at 66.7Watts against Distance

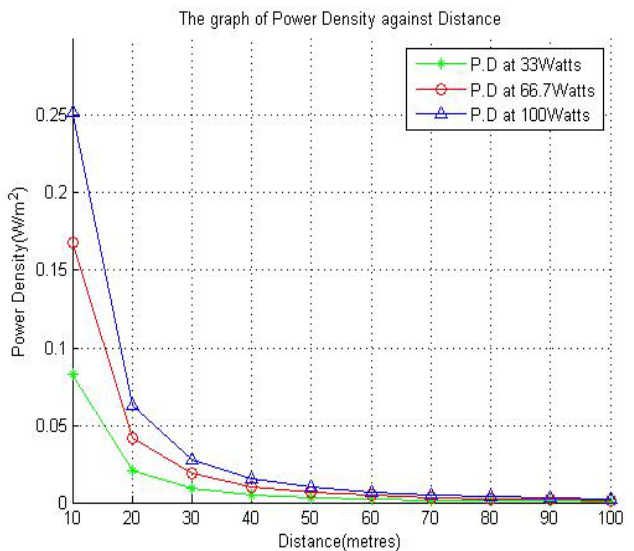


Figure 9: Comparison of Calculated Power Density at 33W, 66.7W, and 100W against Distance

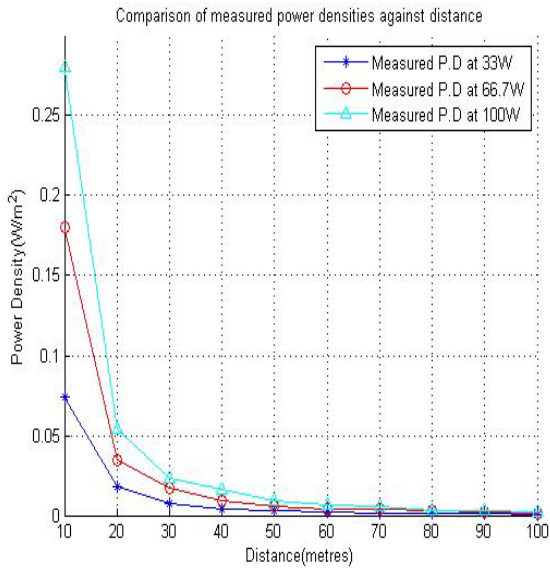


Figure 10: Comparison of Measured Power Density at 33W, 66.7W, and 100W against Distance

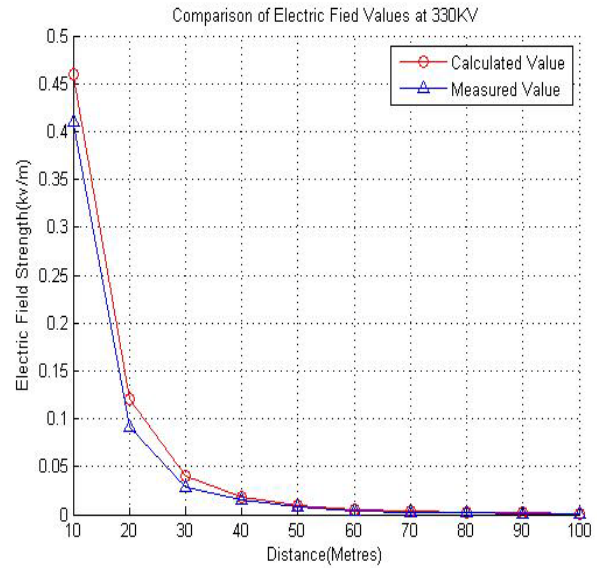


Figure 12: Comparison of measured and calculated Electric Field at 330KV against Distance

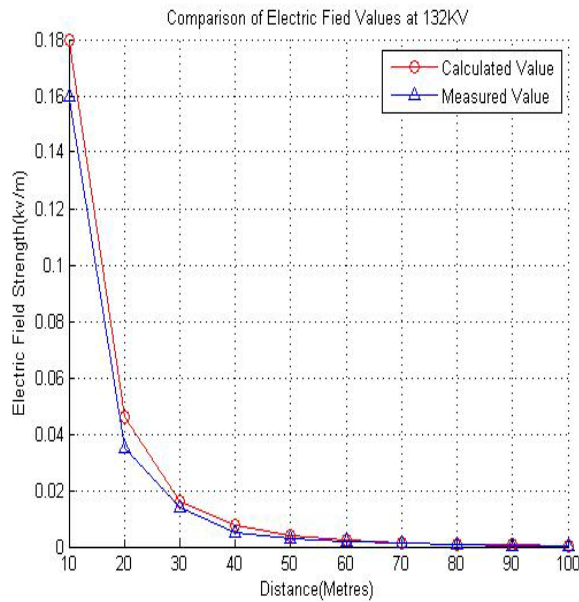


Figure 11: Comparison of measured and calculated Electric Field at 132KV against Distance

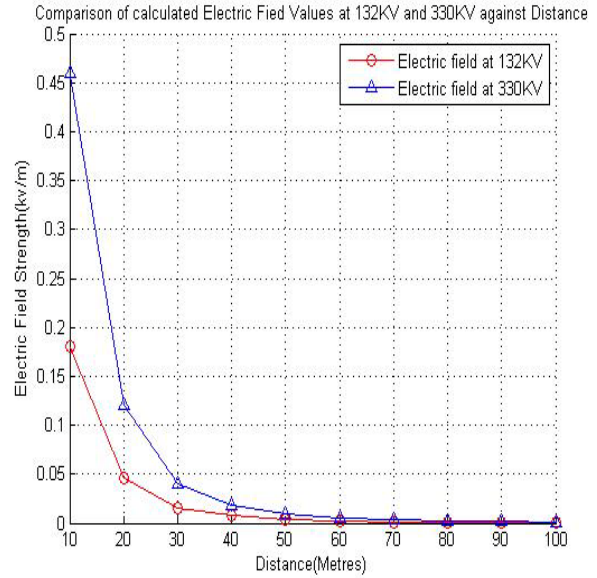


Figure 13: Comparing of calculated Electric Field at 132KV and 330KV against Distance

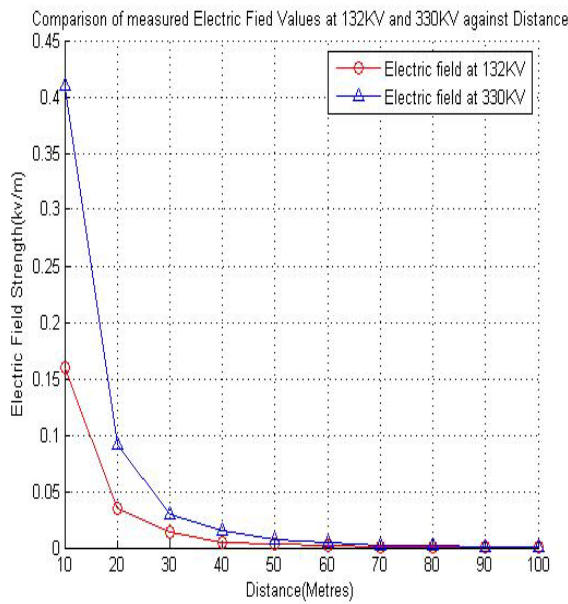


Figure 14: Comparing of measured Electric Field at 132KV and 330KV against Distance

VI. DISCUSSION OF RESULTS

A. Base Station Antennas

The maximum radiating power of base station antennas in Lagos is in the region of 100Watts, and power density at the immediate vicinity of the antenna exceeds ICNIRP exposure guideline of **0.1w/m²**. Most BTS antennas in Lagos environs operate at radiation power P of 100Watts and Antenna gain G of 5dB. The highest value of power density measured is 0.28w/m². This far exceeds the ICNIRP exposure limit (280% of ICNIRP limit), and being exposed to such a value of P.D is totally not safe. The distance at which a power density of 0.1 w/m² will be experienced from a BTS antenna with P=100W and G=5dB is 15.9m. This implies that it is not safe to live within 15.9m (approximately 16m) of a BTS.

Figures 6 to 8 are in the form of decaying graph. It shows that the power density decreases exponentially as the distance from the base station increases. A distance of 100m from the BTS gives a power density of 0.022w/m², which

is just 2.2% of the ICNIRP exposure limit. The farther the exposed person is from the BTS, the safer. The measured value of the power density is lower than the calculated value because of some interference caused by environmental factors [10].

B. High Voltage Power Lines

PHCN (Power Holding Company of Nigeria) is responsible for installation and maintenance of High Voltage power lines in Nigeria has specified 15m and 25m as Right of Way (ROW) for 132KV and 330KV lines, this means no residential or commercial structures should be erected within 15m and 25m of a 132KV and 330KV power line respectively [9]. The ICNIRP exposure limit for overhead power lines is **10KV/m**, the highest value of electric field strength obtained from the results above is 0.46KV/m, which is just 4.6% of the exposure limit. The amount of voltage capable of having an effect of 10KV/m is in the region of 7000KV, which is practically impossible to implement on power lines. Therefore, the electric field in the vicinity of the power line is safe. However, a sizeable number of scientists believe that its thermal effect poses a considerable level of health risk. Also, considering the high voltage flowing through the conductors, if a conductor should snap and fall on an individual or on a building, it will result in damage of property and electrocution[2,9,12].

VII. CONCLUSION

The values of electric field intensity around a 132KV and 330KV power lines have been analyzed, the power density in the vicinity of BTS antenna operating with radiation power of 33Watts, 66.7Watts and 100Watts were also analyzed. The analyses obtained from these cases were compared to the ICNIRP exposure guidelines. The analysis showed that, the Right of Way law given by the PHCN along the power lines have been violated as there are residential

structures less than 15 m and 25 m away from 132 KV and 330 KV lines respectively. The electric field strengths experienced around both power lines are within the ICNIRP safety limits, regardless of the position of the exposed person. However, it is not advisable to live close to power lines because of the risk of electrocution or fire outbreak if one of the conductors should snap. Some studies have shown that a high number of children diagnosed with leukemia, have their houses close to a power line. There is an enormous amount of work to be done by National Environmental Standards and Regulations Enforcement Agency (NESREA), the body responsible for enforcing environmental Laws in Nigeria, and Nigeria Communications Commission, the telecommunication industry regulator in Nigeria, to ensure that the Right of Way is obeyed along the power line. The 10 metre distance from residential homes law given to network operators as regards siting of BTS is still violated by some operators. Some houses even have BTS sited in their compounds. Medical reports have shown that radiations from BTS are carcinogenic; they are capable of generating cancer cells in the human body. Some research reports also suggest that they are also capable of causing genetic mutation in human cells, which can result in having children with some form of physical deformity. Short term effects associated with the exposure to electromagnetic radiation include headaches, fatigue, insomnia, rashes and body pain. Long term exposure to electromagnetic radiation can affect the ability to reproduce, these accumulated radiations is capable of damaging genital cells.

REFERENCES

- [1] Boteler D.H and Pirjola R.J; The Complex-Image Method For Calculating The Magnetic And Electric Fields Produced At The Surface of The Earth By The Auroral Electrojet, Geophys J.Int, 1998.
- [2] www.emfservices.com; EMF Health Effects Research – History and Status. .
- [3] Girish K, Gandhare W.Z; Proximity Effects of High Voltage Transmission Lines on Humans, ACEEE Int J, February 2012.
- [4] Akintonwa A, Busari A. A, Awodele O, and Olayemi S. O; The Hazards of Non-Ionizing Radiation of Telecommunication Mast in an Urban Area of Lagos, Nigeria,African Journal of Biomedical Research, January 2009.
- [5] Sabah H, Saeid A; Theoretical Estimation of Power Density Levels around Mobile Telephone Base Stations, Journal of Science & Technology, 2008.
- [6] Miodrag M, Anamarija J, and Miroslav P; Electric and Magnetic Fields in Vicinity of Overhead Multi-Line Power System, November 2008.
- [7] Boniface O. A and Udochukwu B. A; Electromagnetic Wave Effect on Human Health: Challenges for Developing Countries, CEPA , 2012.
- [8] Ali Z and Cy H; Electromagnetic Radiation and Human Health: A Review of Sources and Effects, Summit Technical Media, July 2005.
- [9] Aliyu O, Maina I, and Ali H; Analysis of Electromagnetic Pollution due to High Voltage Transmission Lines, Journal of Energy Technologies and Policy, 2012.
- [10] Victor U.J, Norbert N, Silas S, Abraham A, and Patrick U;Assessment of Radio-Frequency Radiation Exposure

Level from Selected Mobile Base
Stations (MBS) in Lokoja, Kogi State,
Nigeria, October 2012.

- [11] Santini, R, Santini, P, Le Ruz,P, Danze, J M, Seigne, M ; Survey Study of People Living in the Vicinity of Cellular Phone Base Stations, Journal of Electromagnetic Biology and Medicine, 2003.
- [12] Enyinna P.I, and Awwir G.O; Characterization of the Radiofrequency Radiation Potential of Alakahia and Choba Communities, Nigeria, Working and Living Environmental Protection, June 2010.

A Study of Droplets Division in Circle Shape Micro channel

Maryam Ghelichkhani

Azad School Electrical and Computer Eng University

Saveh, Iran

M_ghelichkhani2007@yahoo.com

Abstract— Micro fluid devices enable the transport nano liters fluids in micro scale channels. Small liquid droplets have many applications in science and technology. In micro fluidics research, microscopic droplets are used to facilitate micro mixing, loading and dispensing reagents from micro-reactors, or to improve the efficiency of cell sorting and fluid sampling systems. The ability to hydro dynamically control the droplet sizes will open new possibilities not only for producing useful emulsions, but also for conducting controlled chemical and biochemical reactions in a confined space. In this paper, a numerical study of the generation of microscopic droplets in a micro-channel of complex geometry is presented. This model is derived of level set method. Furthermore, we investigate volume fraction of micro droplet in this circle micro channel. This device can be used in many applications for example it can be considered as a droplet divider and generate arrays of droplets.

Keywords- *Droplet, Division, Circle micro channel style.*

I. INTRODUCTION

Micro fluidic devices compose micro scale channels that minimize many chemical processes [1]. Monodispersed micro droplets are highly useful for various industrial fields such as the production of polymer particles, pharmaceuticals, and so forth. For example, production of monodispersed polymer particles is essential for column chromatography, while monodispersed emulsions or vesicles are advantageous for accurate drug delivery. To prepare monodispersed particles, synthesized particles are usually separated according to size. Otherwise, specific techniques are employed for the production of monodispersed droplets such as membrane emulsification [2].

It has been demonstrated that precisely fabricated micro fluidic channels with a width or depth of 10–100 μm are suitable for producing monodispersed microdroplets and microparticles [3,4]. Several schemes have hitherto been employed to produce mono dispersed droplets in micro fluidic devices, using T-shaped micro channel confluence [5–13], a micro channel array[14–17]

Numerical modelling fluids in microchannels are a challenging task due to the presence of fluid-fluid interfaces and the limitation of the analytical and numerical methods in dealing with complex geometries. To describe the complex evolution of the fluid-fluid interfaces either the 'Lagrangian', 'Eulerian' or 'hybrid' methods can be used. The Eulerian methods which keep track of the interface motion and deformation using particle, volume, or functional trackers are computationally efficient as they do not require grid deformation or explicitly following the movement of the interface. As a result, they can easily deal with multiple

interface system and topological changes of the interface which happen during interface break-up or coalescence. A method of interface tracking technique based on the use of a level function, which is smooth and is convected by underlying flow on the Eulerian stationary [18]. In this paper, we employed two phase level set method for numerical simulation two fluids transport in a circle micro channel. This valve-less tuning scheme is suitable for producing droplets with precisely controlled sizes, or droplets with small size, which are difficult to generate with the usual micro channel emulsification techniques. This paper is organized as follows, equation governing presented in section II and numerical simulation described in section III.

II. EQUATION GOVERNING

A. Level Set Equation

The level set method (sometimes abbreviated as LSM) which purposed by Sussman and et al, is a numerical technique for tracking interfaces and shapes. The advantage of the level set method is that one can perform numerical computations involving curves and surfaces on a fixed Cartesian grid without having to parameterize these objects (this is called the Eulerian approach) [19]. Also, the level set method makes it very easy to follow shapes that change topology. To describe the droplet motion is necessary to simulate its shape variation and evolution of interface $f(X,t)=0$

between the water and droplet. Driving this expression in time becomes equation (1) [20]:

$$\frac{\partial f}{\partial t} + \mathbf{U} \cdot \nabla f = 0 \quad (1)$$

This method describes the evolution of interface between the two fluids tracing an iso potential curve of level set function ϕ . Zero level set function is demonstrated the interface motion at time. The more dense and more viscous fluids placed in the zone where the level set function is positive ($\phi > 0$) and less dense and less viscous one situated in the domain where the level set function is negative ($\phi < 0$). When the underling velocity field \mathbf{u} is specified, the advection step involves the solution of the scalar transport equation for ϕ [21]:

$$\frac{\partial \phi}{\partial t} + \mathbf{U} \cdot \nabla \phi = 0 \quad (2)$$

U is the fluid velocity.

B. Navier Stock Equation

Furthermore Level set equation, Navier-Stokes equations compose momentum (3) and continuity (4) equations for incompressible fluids are used [20]:

$$\rho \frac{\partial U}{\partial t} - \nabla \cdot [\eta (\nabla U + (\nabla U)^T)] + \rho (U \cdot \nabla) U + \nabla P = F \quad (3)$$

$$\nabla \cdot U = 0 \quad (4)$$

Where p is the pressure, $U = (u; v)^T$ is the velocity, ρ is the density, η is the viscosity and F is a volume force field such as gravity or surface tension

III. NUMERICAL SIMULATION

Droplet generation in micro fluidic devices, a technique to divide droplets into smaller droplets with desired volumes is considered to be attractive for various micro fluidic droplet-base applications. If the volume of the droplets could be precisely altered, and the droplets are mixed with other kind of droplets, a series of droplets with different concentrations can easily be obtained, which will be useful for conducting chemical/biochemical screening. Several researchers have reported on division of droplets using micro fluidic. In this section, A scheme for passive division of produced monodispersed droplets has been reported using circle microchannel .The circle shape micro channel shown in figure1.

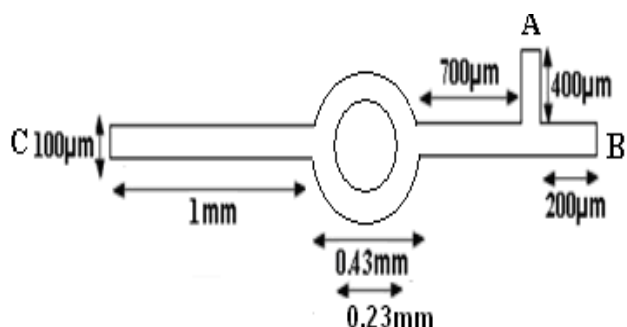


Figure 1. A typical circle shape micro fluidic channel.

The first, water with $\eta=1.95 \times 10^{-3}$ Pa.S and velocity 0.0166 m/s enter in this channel from B inlet. Then droplets with $\eta=6.7 \times 10^{-3}$ Pa.S and velocity =0.0083 m/s enter the channel from A inlet. Surface tension coefficient was considered 5×10^{-3} N/m in this simulation. We investigated droplets motion in length of B-C channel in different step.Schematic of volume fraction fluids in micro channel in this step at $t=0.07s$ shown in figure 2, When the first droplet is entered to micro channel.

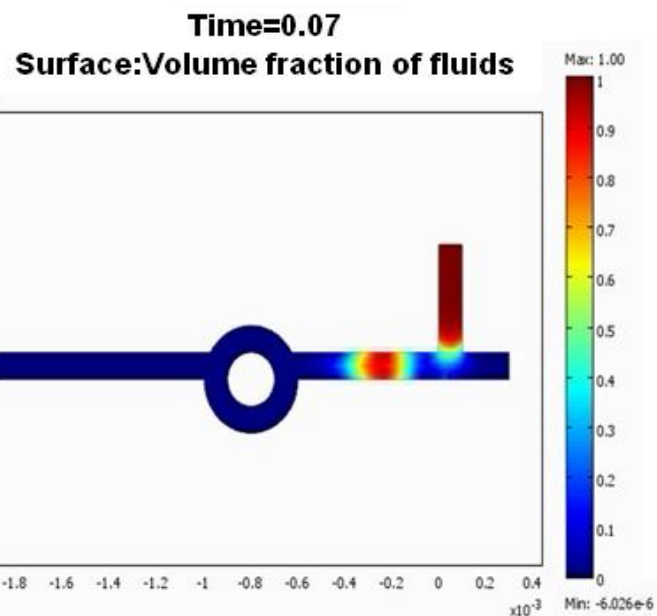


Figure 2. Volume fraction schematic of fluids in micro channel at $t=0.07s$.

At $t= 0.12s$, first droplet received to circle micro channel, micro droplet are divided into two droplets in this channel. Mono dispersed droplets are generated at this stage. And in this time another droplet entered the channel.

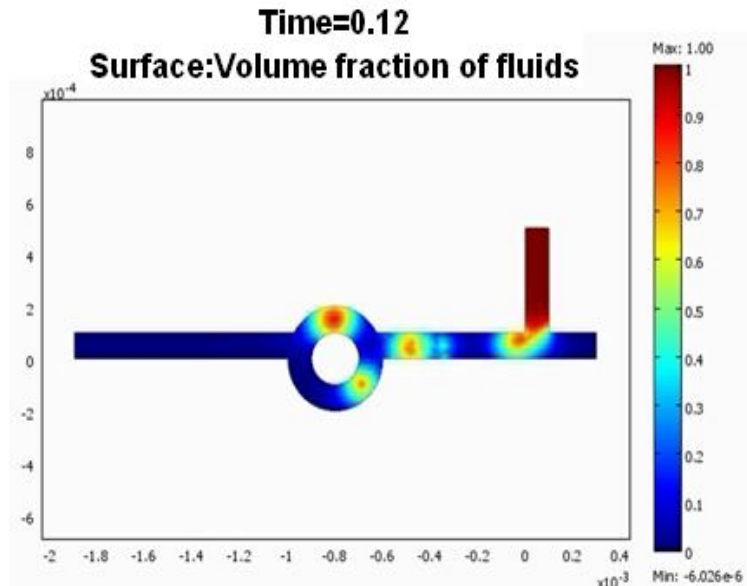


Figure 3. Volume fraction schematic of fluids in micro channel at $t=0.12s$

At $t=0.185\text{s}$, second droplet is divided in circle micro channels and third micro droplet entered the channel. Volume fraction of fluids shown in figure 4. Schematic diagrams show the control of droplet division in circle micro channel.

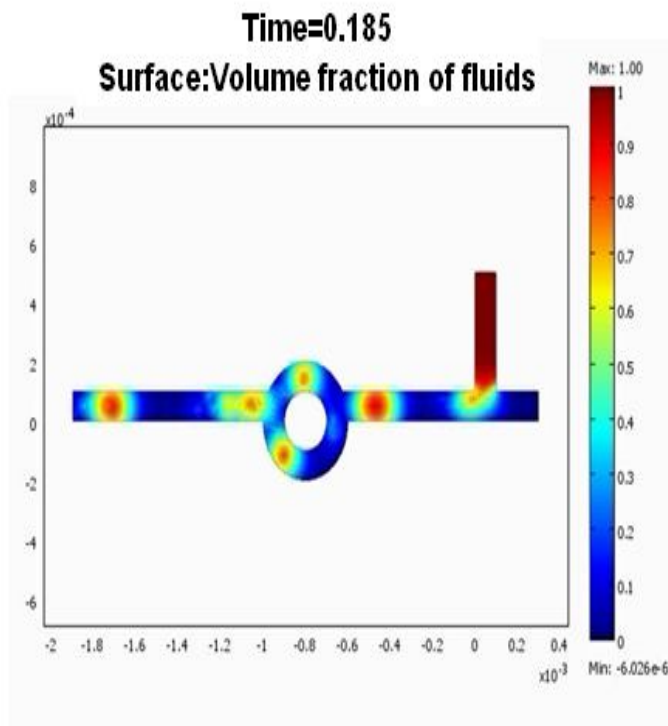


Figure 4. Volume fraction schematic of fluids in micro channel figure 1 at $t=0.185\text{s}$

In the present study, we propose a new scheme for hydro dynamically controlling droplet division using circle micro channel. Figure 5 shown the size distribution of the synthesized particles in micro channel at $t=0.185\text{s}$.

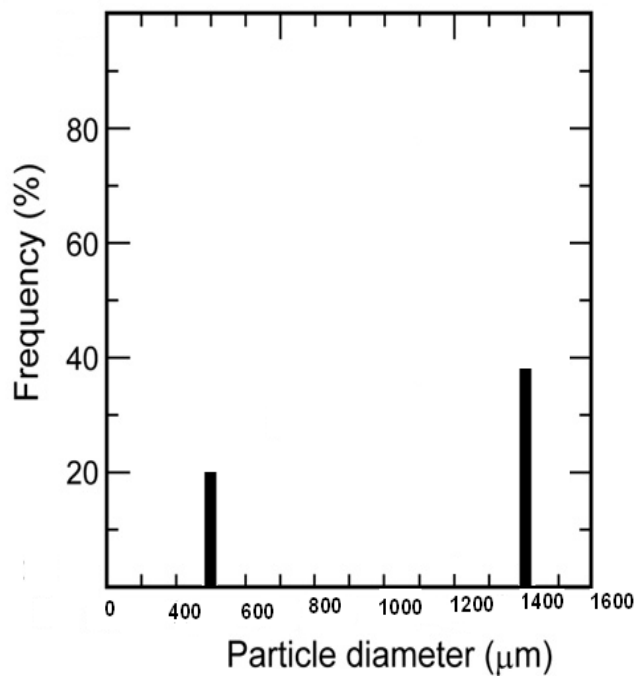


Figure 5. size distribution of the synthesized particles at $t=0.185\text{s}$.

CONCLUSION

A new scheme has been demonstrated for active control of droplets division in a circle microchannel. This valve-less tuning scheme is suitable for producing droplets with precisely controlled sizes, or droplets with small size, which are difficult to generate with the usual micro channel. In addition, this methodology would be extended to the division of monodispersed gas bubbles dispersed in liquid phase, which are also useful for microfluidic reaction systems.

REFERENCES

- [1] Dongdong He. Huaxiong Huang .Yongji Tana, "Numerical simulation for a droplet fusion process of electro wetting on dielectric device", 2009.
- [2] Masumi Yamada, Saki Doi, Hirosuke Maenaka, Masahiro Yasuda, Minoru Seki," Hydrodynamic control of droplet division in bifurcating micro channel and its application to particle synthesis", Journal of Colloid and Interface Science 321 (2008) 401–407.
- [3] H. Song, D.L. Chen, R.F. Ismagilov, Angew. Chem. Int. Ed. 45 (2006) 7336.
- [4] M.S. Seo, Z.H. Nie, S.Q. Xu, M. Mok, P.C. Lewis, R. Graham, E. Kumacheva, Langmuir 21 (2005) 11614.
- [5] T. Thorsen, R.W. Roberts, F.H. Arnold, S.R. Quake, Phys. Rev. Lett. 86 (2001) 4163.
- [6] T. Nisisako, T. Torii, T. Higuchi, Lab Chip 2 (2002) 24.
- [7] B. Zheng, L.S. Roach, R.F. Ismagilov, J. Am. Chem. Soc. 125 (2003)11170.
- [8] H. Song, J.D. Tice, R.F. Ismagilov, Angew. Chem. Int. Ed. 42 (2003)768.
- [9] J.D. Tice, H. Song, A.D. Lyon, R.F. Ismagilov, Langmuir 19 (2003) 9127.
- [10] T. Nisisako, T. Torii, T. Higuchi, Chem. Eng. J. 101 (2004) 23.
- [11] M.Y. He, J.S. Edgar, G.D.M. Jeffries, R.M. Lorenz, J.P. Shelby, D.T.Chiu, Anal. Chem. 77 (2005) 1539.
- [12] J.H. Xu, S.W. Li, J. Tan, Y.J. Wang, G.S. Luo, Langmuir 22 (2006) 7943.
- [13] P. Garstecki, M.J. Fuerstman, H.A. Stone, G.M. Whitesides, Lab Chip 6 (2006) 437.
- [14] S. Sugiura, M. Nakajima, J.H. Tong, H. Nabetani, M. Seki, J. ColloidInterface Sci. 227(2000) 95.
- [15] S. Sugiura, M. Nakajima, H. Itou, M. Seki,Macromol. Rapid Commun. 22(2001) 773.
- [16] S. Sugiura, T. Oda, Y. Izumida, Y. Aoyagi, M. Satake, A. Ochiai, N.Ohkohchi, M. Nakajima, Biomaterials 26 (2005) 3327.
- [17] I. Kobayashi, S. Mukataka, M. Nakajima, Langmuir 21 (2005) 5722.
- [18] A. Bui and Y. Zhu, " Numerical Study of Droplet Generation in A Complex Micro-Channel" , December 2007.
- [19] Osher, S. & J. A. Sethian (1988), "Fronts propagating with curvature-dependent speed: Algorithms based on Hamilton-Jacobi formulations", J. Computer. Phys. 79: 12–49.
- [20] S.Osher and R.Fedkiw. "Level Set Methods and Dynamic Implicit Interfaces", 1st.Edition, Applied Mathematical Sciences, Vol. 153, Springer, 2003.
- [21] E. Bovet, L. Preziosi, B. Chiaia, F. Barpi and Politecnico di Torino" The Level Set Method Applied to Avalanches", 2007.

AQP0 as an atomic machine

Kunihiro Goto, Atsushi Suenaga, Takehiko Ogura, Makoto Taiji, Akira Toyama, Hideo Takeuchi, Mingyu Sun, Kazuyoshi Takayama, Masatoshi Iwamoto, Ikuro Sato, Jay Z. Yeh, Toshio Narahashi, Haruaki Nakaya, and Akihiko Konagaya

Abstract - So far, more than 93,000 protein structures have been reported in the Protein Data Bank, but the driving force and structures that allow for protein functions have not been elucidated at the atomic level for even one protein. We have been able to clarify that the inter-subunit hydrophobic interaction driving the electrostatic opening of the pore in aquaporin 0 (AQP0). Here we show that the AQP0 is an “atomic machine”, and that the engine of the machine is an inter-subunit hydrophobic interaction between proline and histidine residues belonging to different subunit uppermost loops which drives a “stick” portion consisting of four amino acids toward the pore and the tip of the stick portion,

K. Goto Author is with the Department of Molecular Pharmacology and Biological Chemistry, Northwestern University Medical School, 303 East Chicago Avenue, Chicago, IL 60611-3008, USA (corresponding author to provide phone: 312 503 6167; fax: 312503 1700; e-mail: k-goto@northwestern.edu).

A. Suenaga Author is with the Bioinformatics Group, RIKEN Genomic Sciences Center, 61-1 Ono, Tsurumi, Yokohama, Kanagawa 230-0046 Japan (e-mail: suenaga@gsc.riken.jp).

T. Ogura is with the Department of Pharmacology, Chiba University Graduate School of Medicine, Chiba, Japan (e-mail: t.ogura@sa3.so-net.ne.jp).

M. Taiji Author is with the the Bioinformatics Group, RIKEN Genomic Sciences Center, 61-1 Ono, Tsurumi, Yokohama, Kanagawa 230-0046 Japan (e-mail: taiji@gsc.riken.jp).

A. Toyama Author is with the Division of Pharmacy, Medical and Dental Hospital, Niigata University, 1-754 Asahimachi-dori, Niigata 951-8520, Japan (e-mail: toyama@med.niigata-u.ac.jp).

H. Takeuchi Author is with the Department of Pharmaceuticals, Graduate School of Pharmaceutical Sciences, Tohoku University, Aobayama, Sendai 980-8578, Japan (e-mail: takeuchi@mail.pharm.tohoku.ac.jp).

M. Sun Author is with the Shock Wave Research Center, Institute of Fluid Science, Tohoku University, 2-1-1, Katahira, Sendai 980-8577, Japan (e-mail: sun@cir.tohoku.ac.jp).

K. Takayama Author is with the Shock Wave Research Center, Institute of Fluid Science, Tohoku University, 2-1-1, Katahira, Sendai 980-8577, Japan (e-mail: k.takayama@mac.com).

M. Iwamoto Author is with the Department of Applied Physics, Tohoku Gakuin University, 1-13-1, Tagajyo, Miyagi 985-8537, Japan (e-mail: masa@tjcc.tohoku-gakuin.ac.jp).

I. Sato is with the Miyagi Prefecture Cancer Center, Natori, Miyagi, Japan (e-mail: sato-ik510@pref.miyagi.jp).

J. Z. Yeh Author is with the Department of Molecular Pharmacology and Biological Chemistry, Northwestern University Medical School, 303 East Chicago Avenue, Chicago, IL 60611-3008, USA (e-mail: j-yeh@northwestern.edu).

T. Narahashi Author is with the Department of Molecular Pharmacology and Biological Chemistry, Northwestern University Medical School, 303 East Chicago Avenue, Chicago, IL 60611-3008, USA (e-mail: narahashi@northwestern.edu).

H. Nakaya is with the Department of Pharmacology, Chiba University Graduate School of Medicine, Chiba, Japan (e-mail: nakaya@faculty.chiba-u.jp).

A. Konagaya Autho is with the Bioinformatics Group, RIKEN Genomic Sciences Center, 61-1 Ono, Tsurumi, Yokohama, Kanagawa 230-0046 Japan (e-mail: kona@dis.titech.ac.jp).

consisting of a nitrogen atom, opens the pore: that movement is the swing mechanism. The energetics and conformational change of amino acids participating in the swing mechanism confirm this view. The swing mechanism in which inter-subunit

hydrophobic interactions in the tetramer drive the on-off switching of the pore explains why aquaporins consist of tetramers. Here, we report that experimental and molecular dynamics findings using various mutants support this view of the swing mechanism. The finding that mutants of amino acids in AQP2 corresponding to the stick of the swing mechanism cause severe recessive nephrogenic diabetes insipidus (NDI) demonstrates the critical role of the swing mechanism for the aquaporin function.

We report first that the inter-subunit hydrophobic interaction in aquaporin 0 drives the electrostatic opening of the aquaporin pore at the atomic level [1].

Keywords – aquaporin, mechanism, membrane protein, hydrophobic interaction

I. Introduction

Aquaporins are membrane channels for water and small non-ionic solutes found in animals, plants, and microbes [2]-[4]. The structures of aquaporins are known to have high homology and to consist of homotetramers, each monomer of which has one pore for a water channel [5]-[7]. Each pore has two narrow portions: one is the narrowest constriction region consisting of aromatic residues and an arginine (ar/R), and another is two asparagine-proline-alanine (NPA) homolog portions [5]-[7]. Some fundamental questions remain unsolved: Why do they need to be tetramers, though each monomer owns each pore? Are there inter-subunit interactions? If interactions between subunits are present, are they connected to gating mechanisms? AQP0 has one of the lowest water permeabilities among the aquaporins [3]. In AQP0, Cys189, which is most important for mercury sensitivity, is replaced by Ala [6], [7]. However, AQP4 [8] and plant aquaporins [4], having high water permeability, also do not have the cystine corresponding to AQP1 Cys189. AQP0 has low water permeability but does not have Cys189, suggesting that AQP0 has at least one water pathway essential and common to aquaporins. Furthermore, the structure of AQP0 has been determined with high resolution suitable for atomic-level analysis [7]. For these reasons, we have studied the water permeation mechanisms of AQP0 in detail at the atomic level.

In our observations of molecular dynamics simulation images of a bovine AQP0 (Fig. 1), a nitrogen atom of the asparagine sidechain, N119_i.nδ2 (asparagine 119 i subunit. atom), in the upper stream of the narrowest constriction was bound to an oxygen atom of a glycine, G180_i.o, which is one component contributing to the constriction, and, at the same time, the constriction was opened (Fig. 1A). Furthermore, the N119_i was in one uppermost stream random coil, which contained the histidine, H122_i, fourth from the N119_i (see green stick in Fig. 1A). If the random coil moves as a whole, that is, the stick - N119_i, T120_i, L121_i, and H122_i - move together, the movement of the H122_i can make the far N119_i move toward the G180_i.o. In accordance with this reasoning, the H122_i (i chain), must undergo a hydrophobic interaction with a proline, P109_{i-1} (i-1 chain), in the contacting neighboring subunit. Thus, our hypothesis contains a four-fold prediction: (i) the uppermost stream proline, Pro109_{i-1}, in the neighboring subunit, i-1, attracts a H122_i in the subunit, i, by hydrophobic interaction, (ii) by their mutual attraction between P109_{i-1} and H122_i, the four amino acid strand, the stick, in the same random coil, together moves from the periphery toward the pore region, meaning that (iii) the N119_i.nδ2 moves to the pore region, that is, to G180.o, and (iv) the binding of the N119_i.nδ2 to the G180.o of the constriction region causes the separation of electrostatic interaction between G180.o, and arginine nitrogen, R187.mη2, of the constriction region, that is, the constriction is open.

I. Results and Discussion

A. Inter-subunit hydrophobic interaction and conformational changes

In our analyses of 10 ns molecular simulation of wild type bovine AQP0 for clarifying the presence of the “swing mechanisms”, the pore first having opened secondly closed and finally opened again (see Fig. 1A and Video S1 for Ancillary video of [1]). First, it was confirmed that the inter-subunit hydrophobic interaction between P109_{i-1} and H122_i was present, causing the pore to open (Fig. 4A and B). Next, as the inter-subunit hydrophobic interaction became weak, R187.mη2 was bound to G180.o, that is, the pore was closed (Fig. 2Ai [1]). The stronger the inter-subunit hydrophobic interaction was, the nearer was the stick N119 to G180 (Fig. 2Aii - Av [1]). This approach of N119 to G180 caused R187.mη2 to separate from G180.o. Further approach of N119 to G180 induced N119.nδ2 to bind to G180.o and this N119.nδ2 binding to G180.o caused R187.mη2 to further separate

from G180.o (see the blue line of Fig. 2Civ and Fig. 3Bivc), achieving the pore opening (Fig. 2Avi and 7A and B). Thus, we confirmed the swing mechanism (rf. Movie of [1]).

These results showed that inter-subunit hydrophobic interactions drove the electrostatic interaction to open the pore (Fig. 1A). These findings concerning the swing mechanisms indicate that a low Arrhenius activation energy underlies the action of the aquaporins [9]-[12].

B. Energetics of the swing mechanism

Energy increases was a few (1~3) kcal/mol, while the vibration of the entire molecule was large (10~20) kcal/mol. Why, though the driving force is smaller than the vibration, binding or separation are possible, is explained by that the inter-subunit hydrophobic interaction is about 20~30 kcal/mol, making the stick, HLTN, and the tip N119.nd2 move to G180.o.

In these approaches and the large vibration (10 ~ 20 kcal/mol)(Fig. 4A) of the entire molecule, R187_b.mη2 was separated from G180_b.o (Fig. 1A). After that, N119_b.nδ2 was attracted toward G180_b.o by the electrostatic interaction between N119_b.nδ2 and G180_b.o and bound to G180_b.o (Fig. 1A). That is, it did not need to exceed the energy barrier. Thus, actually the inter-subunit hydrophobic interaction was a force that acts an elaborate control to drive the electrostatic interaction to open the pore (Fig. 1B). These phenomena occurred in more than 10 kcal/mol of energy vibration and a few kcal/mol of hydrophobic interaction controlled the swing mechanisms. While the hydrophobic interaction as a force at the macromolecule level has been measured, our calculation would make the atomic level analysis of various molecules possible and supply a useful tool for that analysis.

C. Physiological and simulation results of the wild type and mutants

For further understanding of the fact that in the swing mechanism the inter-subunit hydrophobic interaction is a cause and the pore opening by electrostatic interaction is a result, we examined mutants prepared both for electrophysiological methods and simulations. Each of hydrophobic subsites forming hydrophobic interaction was substituted for each of hydrophilic subsites (P109S and H122S), causing the water permeation to be inhibited (Fig. 1B). Hydrophobic atomic tip was placed instead of hydrophilic one, inducing the water permeation to be inhibited.

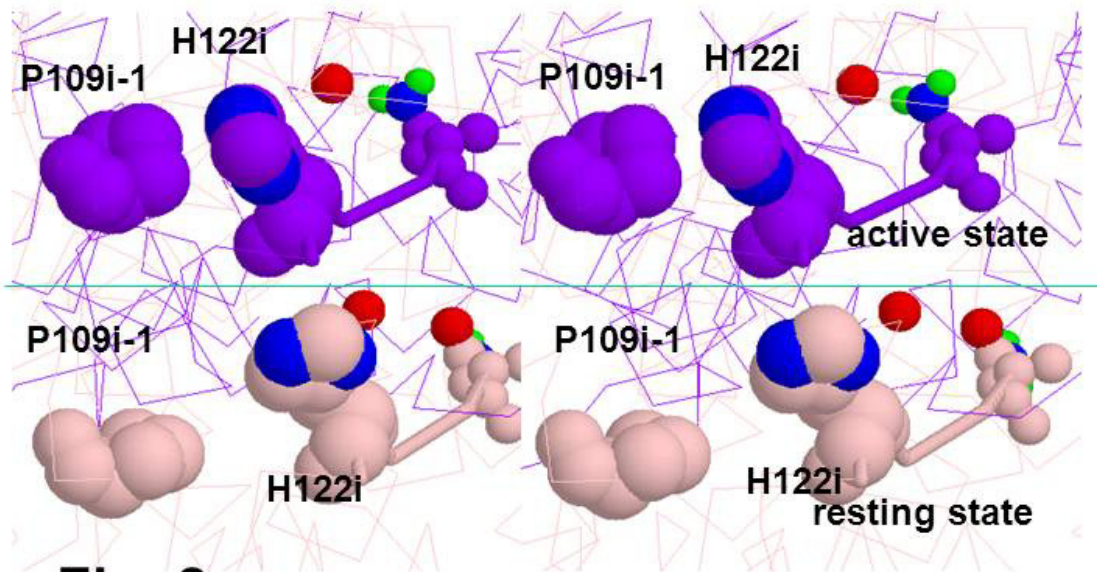
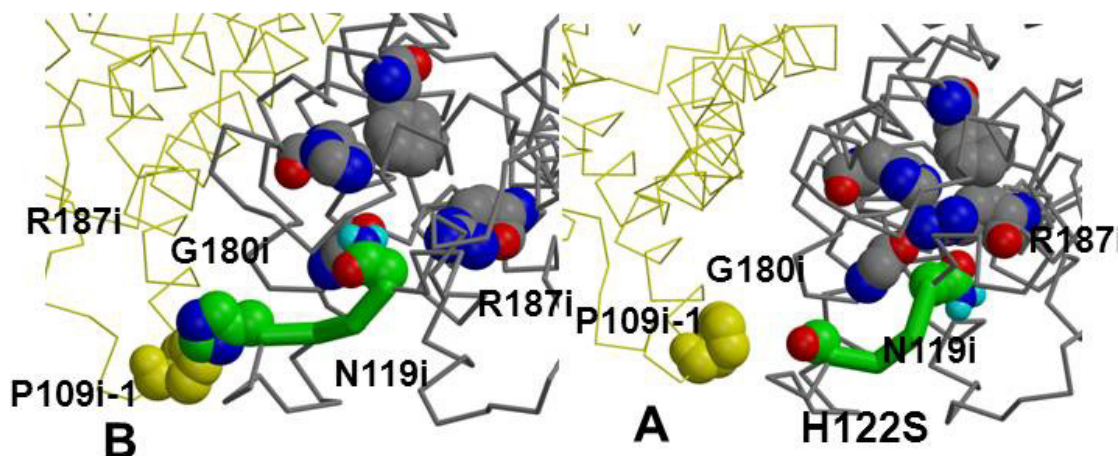
Fig. 1**Fig. 2**

Fig. 1. A. The wild type AQP0. When H122i bound with P109i-1, N119i was binding with G180i, causing the pore to open. B. The H122S mutant. To clarify the mechanism of the pore opening, H122S mutant was chosen. As S122 did not bind with P109i-1, G180i was binding with R187i (cited from [1]).

Fig. 2. The 4th-10th ns average structure ($P109_{\text{c}}.\text{c}-H122_{\text{d}}.\text{c}\varepsilon 1$, 3.84 \AA) of the wild type was superimposed and shifted on the original X-ray structure (lower; $P109_{\text{r1}}.\text{c}-H122_{\text{r1}}.\text{c}\varepsilon 1$, 6.39 \AA). See text. The average 3.84 \AA was very close, because the normal limit of C-C nonbonded contact is 3.0 \AA and the half thickness in the aromatic group (similar to histidine and proline) is 1.7 \AA [30]. Note the $\text{N}119.\text{n}\delta 2-\text{G}180.\text{o}$ hydrogen bonding (cited from [1]). movements, as if hydrophobic interaction between P109i-1 and H122i is shaking like a very heavy golf head.

The fact that hydrophobic interactions play a critical role in cellular functioning is commonly observed, and suggests that hydrophobic interactions should be included in models of the interaction of macromolecules, e.g., in the “rotation model” [13]-[26], and corroborative evidence of this model recently [1], and the predictive features of this model, implicating memory mechanism, most-recently [27].

D. The thermodynamic features of AQP0

As we described in detail about AQP0, in this portion we indicate the force that acts between macromolecules and atoms.

Aquaporin is a homo-tetramer. Why aquaporins have to be a tetramer was clarified by the following experiments: The strong inter-subunit hydrophobic interaction was needed for the opening of the water channel. The reason why a hydrophobic interaction is necessary is that, in water, hydrophobic interactions are the strongest binding force in water. The strength of the hydrophobic interaction was shown to be very strong in the molecular dynamics simulations (Fig. 4). These findings indicate that we can estimate the strength of hydrophobic interaction by using the MD simulation results. The feature of the swing mechanism is like the "golf" stick, that is, hydrophobic interaction between P109i-1 and H122i forces the stick, HLTN, to approach to G180i. As a result of these movements, the stick was bent to the direction opposite these

The interval between P109i-1 and H122i is very close, indicating the strength of hydrophobic interaction to be very strong.

E. Nephrogenic diabetes insipidus.

The substitution of amino acids corresponding amino acids of the stick portion in the swing mechanism and of amino acids corresponding the tip portion caused nephrogenic diabetes insipidus in analytic results of human disease [29]-[32].

II. Conclusions

So far, more than 93,000 protein structures have been reported in the Protein Data Bank, but the driving force and structures that allow for protein functions have not been elucidated at the atomic level for even one protein.

We report first that the inter-subunit hydrophobic interaction in aquaporin 0 drives the electrostatic opening of the aquaporin pore at the atomic level.

III. References

- [1] A. Suenaga, T. Ogura, M. Taiji, A. Toyama, H. Takeuchi, M. Sun, K. Takayama, M. Iwamoto, I. Sato, J. Z. Yeh, T. Narahashi, H. Nakaya, A. Konagaya, and K. Goto, The atomic-level mechanism underlying the functionality of aquaporin-0, *arXiv:1304.5898* (2013) [q-bio.BM]
- [2] G. M. Preston, T. P. Carroll, W. B. Guggino, and P. Agre, Appearance of water channels in Xenopus oocytes expressing red cell CHIP 28 protein, *Science* vol. 256 pp. 385-387 1992.
- [3] P. Agre, L. S. King, M. Yasui, W. B. Guggino, O. P. Ottersen, Y. Fujiyoshi, A. Engel, and D. Nielsen, Aquaporin water channels – from atomic structure to clinical medicine, *J Physiol* vol. 542 pp. 3-16 2002.
- [4] C. Maurel, L. Verdoucq, D-T. Luu, and V. Santoni, Plant aquaporins: membrane channels with multiple integrated functions, *Ann Rev Plant Biol* vol. 59 pp. 595-624 2008.
- [5] K. Murata, K. Mitsuoka, T. Hirai, T. Walz, P. Agre, N. Heymann, A. Engel, and Y. Fujiyoshi, Structural determinants of water permeation through aquaporin-1, *Nature* vol. 407 pp. 599-605 2000.
- [6] T. Gonen, P. Sliz, J. Kistler, Y. Cheng, and T. Walz, (2004) Aquaporin-0 membrane junctions reveal the structure of a closed water pore, *Nature* vol. 429 pp. 193-197 2004.
- [7] W. E. Harries, D. Akhavan, L. J. Mierkes, S. Khademi, and M. Stroud, The channel architecture of aquaporin 0 at a 2.2A resolution, *Proc Natl Acad Sci USA* vol. 101 pp. 14045-14050 2004.
- [8] J. S. Jung, R. V. Bhat, G. M. Preston, W. B. Guggino, J. M. Baraban, and P. Agre, Molecular characterization of an aquaporin cDNA from brain: Candidate osmoreceptor and regulator of water balance, *Proc Natl Acad Sci USA* vol. 91 pp. 13052-13056 1994.
- [9] V. Koefoed-Johnsen, and H. H. Ussing, The contributions of diffusion and flow to the passage of DnO through living membranes. Effect of neurohypophyseal hormone on isolated anuran shin, *Acta Physiol Scand* vol. 28 pp. 60-76 1953.
- [10] C. V. Paganelli, A. K. Solomon, The rate of exchange of tritiated water across the human red cell membrane, *J Gen Physiol* vol. 41 pp. 259-277 1957.
- [11] R. I. Macey, Transport of water and urea in red blood cells, *Am J Physiol* vol. 246 pp. C195-203 1984.
- [12] B-G. Han, A. B. Guliaev, P. J. Walian, and B. K. Jap, Water transport in AQP0 aquaporin: Molecular dynamics studies, *J Mol Biol* vol. 360 pp. 285-296 2006.
- [13] K. Goto, Transmembrane macromolecule rotation model - molecular hypothesis of membrane excitation -, *Tohoku J Exp Med* vol. 139 pp. 159-164 1983.
- [14] K. Goto, and N. Sasano, Molecular mechanism of membrane excitation, *Igakunoayumi* 121: 201-203 1982a (In Japanese)
- [15] K. Goto, N. Sasano, Unificative molecular mechanism of secretion phenomenon, *Igakunoayumi* 122: 971-973 1982b (In Japanese)
- [16] K. Goto, The macromolecule rotation model - the sliding of actin and myosin is due to hydrophobic bonding, *Jap J Pharmacol* vol. 36 pp. 69 1984.
- [17] K. Goto, The on-off mechanisms of the nicotinic acetylcholine receptor ion channel are performed by thermodynamic forces, *J Theor Biol* vol. 170 pp. 267-272 1994.
- [18] K. Goto, Rotation model, *Mebio* vol. 13 no. 12 88-96 1996 (In Japanese)
- [19] K. Goto, Rotation model - Molecular hypothesis not only explaining various phenomena without contradiction, but also predicting various yet-unobserved phenomena -, *Maku (Membrane)* 22: 96-104 1997 (In Japanese)
- [20] K. Goto, Rotation model - A molecular mechanism driven by hydrophobic and hydrophilic interactions, and underlying recognition and ion channels -, *Prog Anesth Mech* vol. 5 pp. 1-22 1998.
- [21] K. Goto, Rotation model - molecular hypothesis elucidating and predicting nAChR, anesthesia, enzyme catalysis, and

- immune signal transduction. *J Clin Anesth* vol. 23 pp. 157-164 1999 (In Japanese).
- [22] K. Goto, Rotation model - Anesthetic agents stop the movement of functioning molecules - *Prog. Anesth. Mech.* vol. 6 pp. 15-18 2000.
- [23] K. Goto, Hydrophobic accessible surface areas are proportional to binding energies of serine protease-protein inhibitor complexes, *Biochem Biophys Res Comm* vol. 206 pp. 497-501 1995.
- [24] K. Goto, and M. Iwamoto, Evidence of α -helix slidings during bacteriorhodopsin photocycle-energetics coupling, *Tohoku J Exp Med* vol. 182 pp. 15-33 1997.
- [25] K. Goto, A. Toyama, H. Takeuchi, K. Takayama, T. Saito, M. Iwamoto, J. Z. Yeh, and T. Narahashi, (2004) Ca⁺⁺ binding sites in calmodulin and troponin C alter interhelical angle movements. *FEBS Lett* vol. 561 pp. 51-57 2004.
- [26] A. Suenaga, Z. J. Yeh, M. Taiji, A. Toyama, H. Takeuchi, M. Son, K. Takayama, M. Iwamoto, I. Sato, T. Narahashi, A. Konagaya, and K. Goto, Bead-like passage of chloride ions through ClC chloride channels. *Biophys Chem* vol. 120 pp. 36-43 2006.
- [27] K. Goto, and T. Nakaye, Dynamic and integrated mechanical movements of a rat brain associated with evoked potentials. arXiv:1404.6932 (2014) [q-bio.NC]
- [28] G. E. Schulz, and R. H. Schirmer, "Principle of Protein Structure", Springer-Verlag GmbH & Co. pp. 10-11 and pp. 21 1979.
- [29] P. M. Deen, M. A. Verdijk, N. V. Knoers, B. Wieringa, L. A. Monnens, C. H. van Os, and B. A. van Oost, (1994) Requirement of human renal water channel aquaporin-2 for vasopressin-dependent concentration of urine. *Science* vol. 264 pp. 92-95 1994.
- [30] K. Goji, M. Kuwahara, Y. Gu, M. Matsuo, F. Marumo, and S. Sasaki, (1998) Novel mutations in aquaporin-2 gene in female siblings with nephrogenic diabetes insipidus: Evidence of disrupted water channel function. *J Clin Endocrinol Metab* vol. 83 pp. 3205-3209, 1998.
- [31] N. Marr, E. J. Kamsteeg, M. van Raak, C. H. van Os, and P. M. Deen, Functionality of aquaporin-2 missense mutants in recessive nephrogenic diabetes insipidus. *Pflugers Arch* vol. 442 pp. 73-77 2001.
- [32] L. Bai, K. Fushimi, S. Sasaki, and F. Marumo, Structure of aquaporin-2 vasopressin water channel. *J Biol Chem* vol. 271 pp. 5171-5176 1996.

Comparison of Segmentation Methods for Accurate Dental Caries Detection

Jackson B.T Pedzisai 210549604

*School of Mathematics,
Statistics and Computer Science
University of KwaZulu-Natal*

Dr Serestina Viriri

*School of Mathematics,
Statistics and Computer Science
University of KwaZulu-Natal*

Abstract

Dental X-ray image analysis applications are important in helping dentist procedures and diagnosis, and in post-mortem identification. The primary step in such applications is the estimation of teeth contour in order to permit efficient feature extraction (segmentation). The increase in the need for teeth segmentation for example as a result of increase in the volumes of cases that need to be investigated by the forensic specialists brings the need for automation of this process. To obtain the proper result, it is required to perform the accurate and efficient segmentation approach which proved itself in the aspect of X-ray image segmentation.

In this paper, we investigated different teeth contour extraction techniques. These include canny edge detector, Laplacian Gaussian, images differences, thresholding.

Keywords: X-ray images,

1 Introduction

Ante mortem (AM) identification, which is identification prior to death, is usually possible through comparison of many biometric identifiers, post-mortem (PM) identification, that is identification after death, is impossible using behavioural biometrics (e.g. speech, gait) especially under severe circumstances, such as those encountered in mass disasters (e.g. airplane crashers) or if identification is being attempted more than a couple of weeks post-mortem, under such circumstances. Most physiological biometrics may not be employed for identification, because of the decay of soft tissues of the body to unidentifiable states. Teeth, being the hardest and the most impregnable part of human body, cannot easily decay. Dental features are biometric identifiers that are resistant to early decays, hence their survivability and diversity, makes them the best candidates for post-mortem

biometric identification. With the evolution in information technology and the huge volume of cases that need to be investigated by forensic specialists, it has become important to automate forensic identification systems.

Dental caries is an infectious, communicable disease resulting in destruction of tooth structure by acid-forming bacteria found in dental plaque, an intra-oral bio film, in the presence of sugar. The infection results in the loss of tooth minerals beginning with the outer surface of the tooth and can progress through the dentine to the pulp, ultimately compromising the vitality of the tooth. The early detection and characterization of caries lesions is very important because surgical restorative procedures could be reduced. If detected at an early stage, the dentist and dental professionals can implement measures to reverse and control caries, such as identifying patients in need of preventive care, implementing fluoride treatments, implementing plaque control measures, and identifying patients that are at high risk of developing dental caries. Also classification of dental caries is important for the diagnosis and treatment planning of the dental disease. Dental imaging allows dentists to be proactive seeing problems before they become visible. It is also helpful for conducting detailed study and investigations about the nature of the dental disease. Automating the process of analysis of dental images is an important application; it helps the dentist procedures and diagnosis. Tooth segmentation from the radiographic images and feature extraction are essential steps.

2 Related work

Several good progresses have been made for teeth segmentation in the past few years. Jain and Chen [1] proposed a semi-automatic contour extraction method for tooth segmentation by using integral projection and Bayes rule, in which an initial valley gap point is required for applying the integral projection to tooth

isolation. Keshtkar and Gueaieb [4] introduced a swarm-intelligence-based and a cellular-automata model approach.

Zhou and Abdel-Mottaleb [2] used active contour models (based on snakes) for extracting the contour of the teeth. Active contour models based on edges are driven by the gradient of the image intensities. In many dental images, the gradient between the teeth and the background is not prominent and, hence, such technique is not able to accurately extract the tooth contour. Also, snake-based schemes rely on a parametric representation of the contour. Parametric representations typically fail to evolve in noisy conditions [6]. Further, parametric contours may not be able to split and merge upon encountering local minima in the region of interest ([7], [8], [9], [10]).

Most of these segmentation algorithms are greatly affected by noise embedded in images, which will lead to poor segmentation performance; hence it is crucial to apply any type of image enhancement before applying the segmentation process. Also due to different ways in which dental curies manifest in different types of teeth, it would be important to classify each tooth.

3 Methodology

In this paper we did thorough reviews of the dental X-ray image segmentation techniques, implemented the segmentation techniques and features extraction methods. The comparison of the segmentation methods is split into a number of processes; the input of an image file, the pre-processing (involves cropping the image), enhancement, teeth segmentation using different segmentation techniques. Figure 1. below shows the pictorial view of the methodology together with the proposed techniques or algorithms.

3.1 Cropping

The first step in segmentation is cropping. We created an interface that shows the image and by simply highlighting the part of the image needed, that part is extracted. Figure 2 and 3 below shows an example of an image and the two cropped images respectively. These images will be used throughout this paper.

3.2 Enhancement

Images Are often corrupted by random variants in intensity values such as salt and pepper noise, impulse noise and Gaussian noise. There is a trade-off between edge

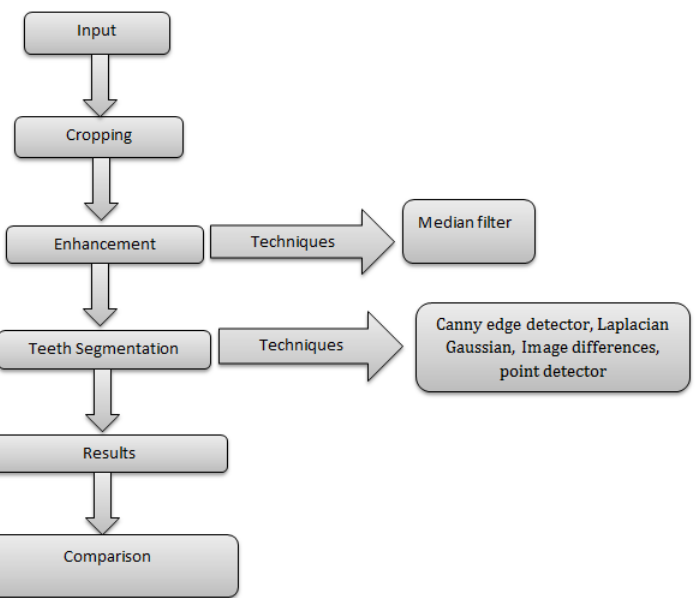


Figure 1: A diagram of the methodology of the teeth segmentation and dental curies detection.

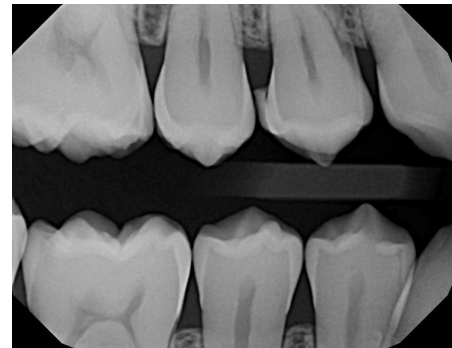


Figure 2: X-ray image

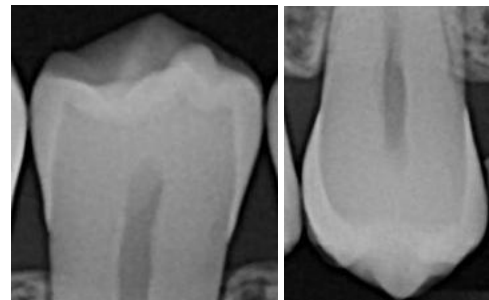


Figure 3: Cropped Images

strength and noise reduction. More filtering to reduce noise results in a loss of edge strength. In this paper a median filter is used, where each pixel is replaced by the median of its neighbourhood [140].

3.3 Detection

Many points in an image have a nonzero value for the gradient, and not all of these points are edges for a particular application. Therefore, some method should be used to determine which points are edge points.

3.3.1 Point Detector

This is achieved by applying a point detecting mask to the image. Each pixel ($g(x,y)$) is given by:

$$g(x,y) = \sum_{s=-m}^m \sum_{t=-n}^n w(s,t)f(x+s, y+t) \quad (1)$$

where function f is the initial image, w is the point detecting mask of size $n \times m$ and g is the resultant image.

$$w = \begin{bmatrix} -1 & -1 & -1 & -1 & -1 \\ -1 & -1 & -1 & -1 & -1 \\ -1 & -1 & 24 & -1 & -1 \\ -1 & -1 & -1 & -1 & -1 \\ -1 & -1 & -1 & -1 & -1 \end{bmatrix}$$

It is clear that any pixel at the edge will have a significantly different value as to that of the average of its neighbours. If the value is approximately the same, then the pixel is not at any edge. Figure 4 below shows the result after applying the point detector filter.

A median filter is applied to the image to remove the noise so that the edges are clear. Figure 5 below shows the results after applying the median filter.

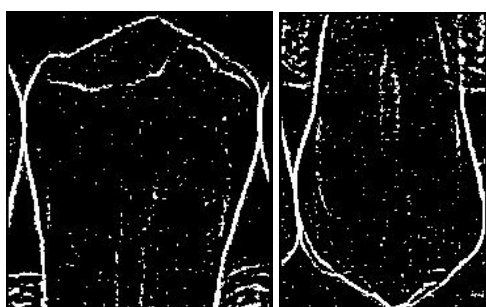


Figure 4: Results of Point detector Filter



Figure 5: Point detector after applying median filter

3.3.2 Laplacian Gausian

The Laplacian generally is not used in its original form for edge detection due to its unacceptable sensitivity to noise. Consider the function:

$$h(r) = -e^{-\frac{r^2}{2\sigma^2}} \quad (2)$$

where $r^2 = x^2 + y^2$ and σ is the standard deviation. Convolving this function with an image blurs the image, with the degree of blurring being determined by the value of σ . The Laplacian of h (second derivative of h with respect to r) is:

$$\nabla^2 h(r) = -\left[\frac{r^2 - \sigma^2}{\sigma^4}\right] e^{-\frac{r^2}{2\sigma^2}} \quad (3)$$

This is the Laplacian of a Gaussian (LoG). The purpose of the Gaussian function in the LoG formulation is to smooth the image, and the purpose of the Laplacian operator is to provide an image with zero crossing used to establish the location of edges. Smoothing reduces the effect of noise and, in principle; it counters the increased effect of noise caused by the second derivative of the laplacian.

Laplacian of Gaussian first smoothes with a low-pass filter to reduce noise. Laplacian of Gaussian kernel is used for this. Figure 6 below shows Laplacian Gausian filter.

$$\begin{bmatrix} 0 & 0 & -1 & 0 & 0 \\ 0 & -1 & -2 & -1 & 0 \\ -1 & -2 & 16 & -2 & -1 \\ 0 & -1 & -2 & -1 & 0 \\ 0 & 0 & -1 & 0 & 0 \end{bmatrix}$$

Figure 6: Laplacian Gausian filter

Figure 7 below shows the results of Laplacian Gausian filter.

Below are the results after filtering the images



Figure 7: Results of Laplacian Gaussian

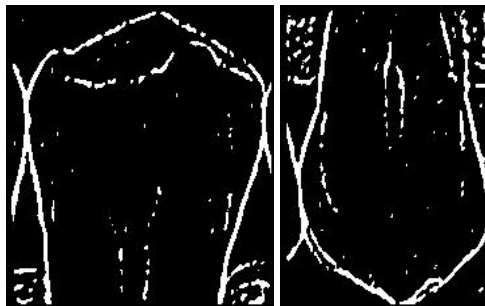


Figure 8: Laplacian of Gaussian after filtering noise

3.3.3 Double Thresholding

This is one of the most simple segmentation techniques, involves thresholding the image intensities [5]. In this paper this technique is done in two steps, thresholding and calculating gradient to determine edges.

Thresholding

Edge pixels stronger than the high threshold, are marked as strong(white); edge pixels weaker than low threshold are suppressed and edges pixels between high and low are marked as weak(grey).

Two threshold values (T_{high} and T_{low}) are chosen. In this paper, the threshold value (T_{high} or T_{low}) is the i^{th} pixels value after all the pixels values are sorted in ascending order, where i is given by the equation:

$$i = \alpha \times N \quad (4)$$

And α in this case is equal 0.4 for T_{high} and 0.26 for T_{low} . This means that for (T_{high}), the threshold groups 40 percent of the pixels to be below T_{high} and the other 60 percent will be above T_{high} . The same is done for T_{low} . These threshold values will group the pixels into three subset, those with pixel values above T_{high} , those with pixels values below T_{low} and those with pixels values below T_{high} and above T_{low} . These three groups of pixels are given different pixel values, 0 for those below T_{low} ,

255 for those with pixel values above T_{high} . The other set is given a value between 0 and 255. Figure 9 below shows the result of double thresholding.



Figure 9: Results of double thresholding

Gradient

From the result shown above, it is clear that the boundaries (edges) can be easily extracted. To determine the edges, gradient magnitude for each pixels is calculated. All the pixels will clearly have the same gradient value of zero, except for those pixels at the edges. Hence any pixels with gradient greater than 0 is categorised as a boundary(is given a value of 1). This draws edges with two pixel thickness

Gradient is computed for every pixels. The gradient of the image $f(x, y)$ at location (x, y) is defined as the vector

$$\nabla f = \begin{bmatrix} G_x \\ G_y \end{bmatrix} = \begin{bmatrix} \frac{\delta f}{\delta x} \\ \frac{\delta f}{\delta y} \end{bmatrix} \quad (5)$$

It is well known from vector analysis that the gradient vector points in the direction of maximum rate of change of at coordinates(x, y). The gradient magnitude is the magnitude of this vector,

$$|\nabla f| = [G_x^2 + G_y^2]^{1/2} \quad (6)$$

In this paper we implemented the Sobel operator to find a first order partial derivative. The Sobel operator computes the approximation of gradients along the horizontal (x) and the vertical (y) directions for each pixels[6]. Any pixel with a gradient magnitude greater than 0 is classified as an edge.

$$\begin{aligned} |G_x| &= \begin{bmatrix} -1 & 0 & 1 \\ -2 & 0 & 2 \\ -1 & 0 & 1 \end{bmatrix} \\ |G_{xy}| &= \begin{bmatrix} -1 & -2 & -1 \\ 0 & 0 & 0 \\ 1 & 2 & 1 \end{bmatrix} \end{aligned} \quad (7)$$

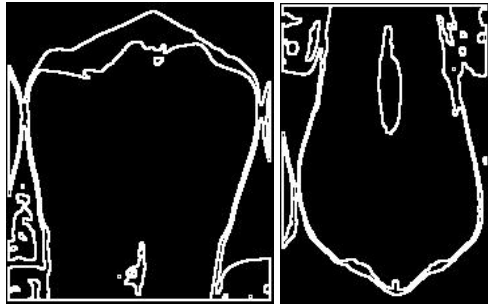


Figure 10: Result of using gradient to determine edges

3.3.4 Image Difference

Gaussian Filter

The image is first smoothed by applying a Gaussian filter with standard deviation of $\sigma = 1.4$. The filter (B) is shown in figure 11 below is a Gaussian filter with $\sigma = 1.4$.

$$B = \frac{1}{159} \cdot \begin{bmatrix} 2 & 4 & 5 & 4 & 2 \\ 4 & 9 & 12 & 9 & 4 \\ 5 & 12 & 15 & 12 & 5 \\ 4 & 9 & 12 & 9 & 4 \\ 2 & 4 & 5 & 4 & 2 \end{bmatrix}$$

Figure 11: Gaussian filter with standard deviation of 1.4

Original image minus filtered image

The smoothed image is subtracted from the original image.

$$g(x,y) = f(x,y) - h(x,y) \quad (8)$$

where $g(x,y)$ is the resultant image, $f(x,y)$ is the original image, and $h(x,y)$ is the filtered image. The results are shown in figure 12 below.



Figure 12: Results of subtracting the filtered image from the original image

Applying averaging filter

The resultant image above has too much noise,hence requires filtering the noise. A lowpass (averaging) filter is applied to the image. Each pixel value is replaced by the the average of the gray levels in the neighbourhood defined by the filter mask. Because random noise typically consists of sharp transitions in gray values these are reduced, together with false contour. On the other hand the filter has an undesirable effect of blurring the edges, but in this case, the edges will not be much affected because they are already clearly defined. The lowpass filter used in this paper is a weighted averaging filter Pixels are multiplied by different coefficients, thus giving more importance to some pixels at the expense of others. The weights are given to the filter depending on the distance from the centre. A median filter is then applied to further clean the image. Figure 13 below shows the results of applying the average filter.



Figure 13: Results of applying the average weighted filter

Erosion/Edge thinning

Because the resultant image has thick contour, there is need to reduce the thickness of the edges. This is acheived by applying erosion on the image. For sets A and B in Z^2 the erosion of A by B, is defined as

$$A \ominus B = \{z | (B)_z \subseteq A\} \quad (9)$$

This indicates that the erosion of A by B is a set of all points z such that B, translated by z, is contained in A. The minimum filter was used to erode the edges. Figure 14 below shows the final results after erosion. It can also be seen that erosion has also removed the noise on the image.

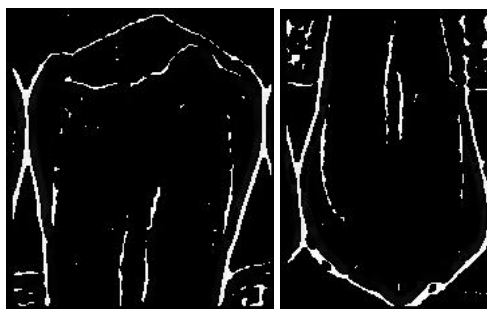


Figure 14: Final image after eroding

3.3.5 Canny Detector

This is a multi-step process, implemented as a sequence of filters. The algorithm involves the following steps:

Noise Filtering

Blurring the image to remove noise. The image is first smoothed by applying a Gaussian filter. In this paper we used a Gaussian filter with a standard deviation of 1.4, shown in figure 11.

Gradient

The edges should be marked where the gradients of the images has large magnitudes (greyscale intensity values changes most). Firstly determined by applying sobel-operator to get the gradient in the x and y direction, then use the law of Pythagoras to determine the resultant gradient. However, the edges are typically broad and thus do not indicate exactly where the edges are. To make it possible to determine this, the direction of the edges must be determined and stored. The direction is determined by the equation below.

$$\theta = \arctan\left(\frac{G_y}{G_x}\right). \quad (10)$$

Non-maximum suppression

Only local maxima should be marked as edges. The purpose of this is to convert the blurred edges in the image of the gradient magnitudes to sharp edges, by preserving

all local maxima in the gradient image and deleting everything else. Firstly, the gradient direction of each pixel is round off to the nearest 45° . The edge strength of each pixel is compared with the edges strength of the pixels in the positive and the negative directions. If the edge strength of that pixel is the largest, its edge strength is preserved, else its is removed.

Double thresholding

Potential edges are determined by thresholding. Many of the resultant edges will probably be true edges in the image, but some maybe as a result of noise. Edges pixels stronger than a chosen high threshold (T_{high}), are marked as strong edges(white); edge pixels weaker than low threshold (T^{low}) are suppressed and edge pixels between high and low are marked as weak edges (grey). The result is shown below.

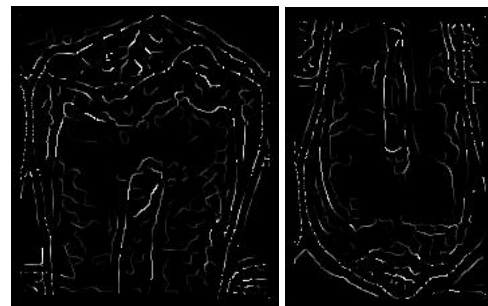


Figure 15: Results of double thresholding

Edge tracking by hysteresis

Final edges are determined by suppressing all edges that are not connected to a very certain (strong) edge. Strong edges are interpreted as certain edges, weak edges are included if and only if they are connected to strong edges. The logic is that noise and other small variations are unlikely to result in a strong edge. The weak edges can either be due to true edges or noise. Edges due to noise will probably be distributed independently of the edges on the entire image, and thus only a small amount will be distributed adjacent to strong edges. Thresholding above would have labelled valid edges as weak (grey) leaving disconnected edges, usually in regions where the gradient fluctuates between above and below the high threshold value (T_{high}). Hysteresis solves the problem by discarding (=0) all pixels with magnitude less than (T_{low}). Pixels with magnitude greater than of equal to (T_{high}) are retained (=1). If a pixel have magnitude between (T_{low}) and (T_{high}), it is retained if any of its neighbours in the 3×3 region around it have gradient magnitude greater than (T_{high}). If none of pixels(x, y)s neighbours have a

magnitude greater than (T_{high}) but at least one falls between (T_{low}) and (T_{high}) a search is made in the 5×5 region and if any of these pixels have a magnitude greater than (T_{high}), it is retained else discarded. Figure below shows the results of hysteresis.

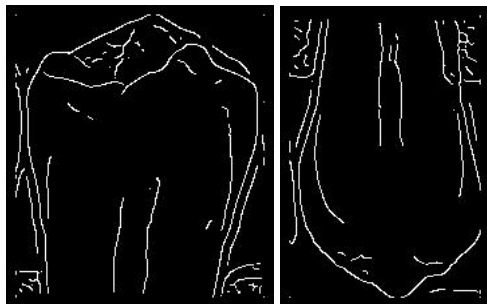


Figure 16: Results of edge tracking by hysteresis

4 Results and comparison

Canny provides better contour in terms of accuracy. It is however affected by illumination variance as shown in figure 17 below. The contour drawn by this technique is 1(one) pixel thick, but sometimes draws lines which are not part of the tooth.



Figure 17: Effects of illumination variance, the first image is the original image where the contour has to be detected. The second and third images show the results of contour detection using canny detector and double thresholding respectively

Most teeth have uneven surfaces and since double thresholding have only 2 threshold values, it can only detect at most two ridges on the surface of a tooth, leaving others. Its is not much affected by illumination variance as shown in figure 17 above. For teeth that are too close to each other, this technique in most cases is unable to detect contour separating the teeth. It is also not so accurate, though able to detect the shape of the contour. Laplacian of Gaussian and point detector have very high failure rates.

The table below shows the percentage of failure for each technique we implemented. We define percentage failure as the number of images from where the technique didn't capture any true segmentation region (tooth) to the total number of images conducted in the experiments.

| Technique | Canny | Difference | Laplacian | Point | Thresholding |
|--------------|--------|------------|-----------|--------|--------------|
| Success rate | 41.18% | 64.71% | 82.35% | 82.35% | 23.53% |

Figure 18: Percentage failure

5 Future work

Implement a new algorithm to accurately detect dental caries.

References

A Critical Study to Enhance the Competitiveness of Engineering Educational Institutions

Ramesh G.M.

Research Scholar, Department of Mechanical Engineering
Anna University,
Chennai -600 025, India
e-mail: gmshreyash@msn.com

Jaiganesh.V

Professor, Department of Mechanical Engineering
S.A Engineering College, Poonamallee-Avadi Road
Chennai – 600 077, India
e-mail :drjai@saec.ac.in

Abstract— India is the third biggest higher education system in the world (after China and the USA) in terms of enrollment. The number of institutions is around 17,973 institutions (348 universities and 17625 colleges – as on June 2005). This means that the average number of students per educational institution in India is also lower than that in the USA and China (Agarwal, Pawan 2006). Presently there are very few technical institutions in India, which provide quality technical education, whereas in many others, the quality of education is a matter of more serious concern. While the demand and supply situation of engineering graduates is satisfactory in terms of quantity, today's young generation has to cope with indifferent quality of education in a large number of institutions. It is one of the contributory factors for many students seeking education outside the country.

Keywords— *Engineering College, Research, Teaching, Administration, Competitiveness*

I. INTRODUCTION

The administrative and management policies of individual institutions are by and large not focused towards the optimal benefits for students and the society. In the prevailing environment, one of the biggest problems is the confusion and stress faced by young technical education aspirants, which may undermine the delicate balance between merit, affordability and equity. The role of high quality teachers, facilities for research and industry-institute and industry-institute-Government interactions need hardly to be emphasized. The role of modern technology in the use of efficient delivery systems for the technical education needs to be assessed fully and exploited. Hence, there is a greater need to study critically the competitiveness of EEIs in the present scenario. The primary focus of the present study is to assess the existing method of governance and management of EEIs in dissemination of engineering knowledge, technology transfer and the innovation process. Three main dimensions of competitiveness of EEIs are the relationships with industry, collaboration through research and consultancy, commercialization of their (Engineering College) research; and linkages made in the perspective of teaching and training.

II. FACTORS FOR BETTER GOVERNANCE AND MANAGEMENT OF EEIs

The major factors to be considered for better governance and management for better competitiveness of EEIs are as follows;

- Professional Ethics and value system of the promoting agency (Society or Trust)
- Quality, Accreditation and Global Competitiveness
- Administration and Management Structure / Empowerment
- Faculty: Quality (Qualification & Competency) and Quantity (Numbers available)
- Students, Admission Policy: Intake Quality of Students
- PG Education and Research and Placement Activities
- Use of Education Technologies / Institutional Methods / Continuous Monitoring of Educational Proces Institute Industry-Interaction
- Collaborative Research Projects with R&D organization / industry
- Networking with Professional Bodies
- In-house Events and Initiatives for Publications and Co curricular Activities e-governance.

III. CRITICAL STUDY

The attitude and professional ethics are the basis of value system of promoting agency of any EEI. Quality Policy of the governing body of any EEI and its keenness to implement the various quality initiatives, such as TQM in line with NBA / NAAC procedures will decide the level of quality consciousness of the promoter(s). Creating suitable administrative structure and governance with proper and adequate empowerment at all levels of management is based on the attitude and professional ethics of the promoters of EEIs.

With reference to the qualification and number of faculty members will be based on the norms of AICTE / UGC /

Affiliating University. Similarly, the admission policy and eligibility criteria are based on the Government Policy / norms of AICTE / UGC / Affiliating University. The real focus for better governance and management of EEIs is depend on the effective Institute-Industry-Interaction, research and development and placement activities apart from better teaching - learning environment.

The findings will be based on the extensive and intensive questionnaire survey and interview conducted by the Author during the course of this research.

3.1 Outcome of the Research Study

The principal objectives of the study are to understand the

- i) effectiveness of existing governance and management of EEIs and how to ensure better governance at these EEIs.
- ii) a comprehensive picture of direct and indirect interactions between EEIs and R&D organizations / industry;
- iii) ensuring the mechanism for updating the knowledge / expertise of existing faculty member, their motivation and retention of these intellectual capital for the betterment of EEIs.
- iv) information enabling the EEIs to benchmark their individual activities in this area and how to enhance the competitiveness of EEIs.

In recent years there has been heightened interest and activity in Institute-industry relationships. The Department of Science and Technology under a Government mandate to facilitate technology transfer. Moreover, it is expected that such cooperation as a way of enhancing national research and development efforts and of helping to make the State and the nation more competitive.

IV. PROPOSED MODEL

The following figure represents the proposed model to asses the competitiveness of EEI.

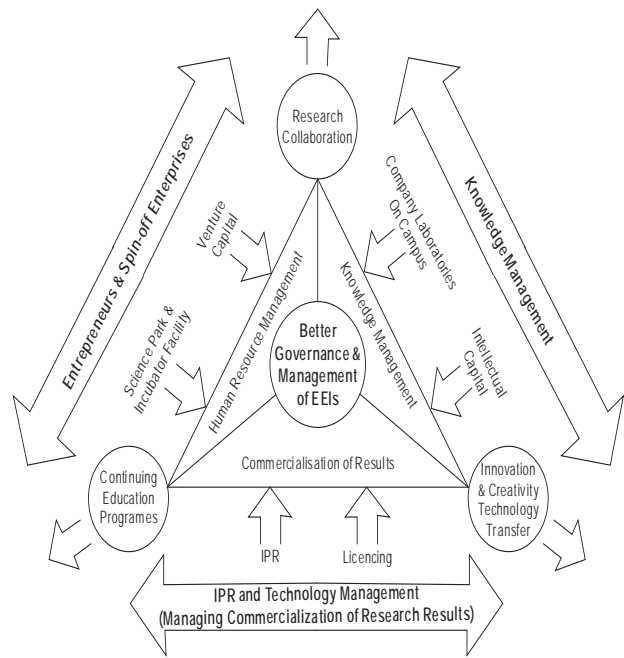


Fig.1 Proposed Model to assess the Competitiveness of IIC

The better governance and management of EEI is possible through addressing the various issues / parameters listed in 2.1 effectively, which in turn will enhance the competitiveness of EEI.

V. CONCLUSION

Much has been made of the emergence of the 'knowledge-based economy' or 'knowledge society', where knowledge and technical acumen form the key foundations of economic success and performance in the global industrial economy in the Liberalisation, Privatisation & Globalisation (LPG) environment. Within the knowledge-based economies, universities and other EEIs play a vital role in the supply of both knowledge and trained people. A third role is emerging as an initiator of entrepreneurial ventures which, after a suitable period of incubation, pass into full industrial ownership in return for financial gain to the institution. The overall finding of this study is that interactions of each type have continued to grow to enhance the competitiveness of EEI and for better governance of EEI.

REFERENCES

- [1] Agarwal, Pawan. "Higher Education in India: A Need For Change". ICRIER Working Paper. June 2006.
- [2]. Dreze, J. & Amartya Sen. "India: Economic Development And Social Opportunity". Oxford University Press, 1998.

Authors Index

| | | | | | |
|--------------------------|---------------|-------------------------|---------------|------------------------|----------|
| Abbas, A. M. J. | 298 | Dimitrov, K. D. | 239 | Khalil, N. S. | 259 |
| Abd El-Aziem, A. H. | 98 | Dolinina, I. | 173 | Khan, A. A. | 309 |
| Abd El-Samie, F. E. | 98 | Dos Santos Filho, D. J. | 51 | Kishore, X. P. | 159 |
| Abramovitch Vaisberg, L. | 220 | Ebibi, M. | 152, 191, 227 | Konagaya, A. | 388 |
| Adami, M. | 326 | Edeko, F. O. | 372 | Kostov, N. T. | 138 |
| Adrian, I. | 216, 270, 282 | Elfarag, A. A. | 259 | Kosun, C. | 183, 224 |
| Ahmed, H. E. H. | 98 | Faizullah, E. | 348 | Kulcsar, R. M. | 168 |
| Akhtar, S. | 309 | Faraj, A. M. | 233 | Li, S. | 117 |
| Akinyemi, L. A. | 372 | Fedosov, V. V. | 166 | Lukas, L. | 142 |
| Albagul, A. M. | 233 | Fedossova, A. | 166 | Makanjuola, N. T. | 372 |
| Aldasouqi, I. | 57 | Ferrarezi, R. C. | 51 | Malaník, D. | 265 |
| Al-Dous, K. K. | 361 | Fetaji, B. | 152, 191, 227 | Maniu, I. | 168 |
| Aloudat, A. | 321 | Fetaji, M. | 152, 191, 227 | Martínez-García, C. G. | 132 |
| Antonov, S. | 66 | Florea, S. | 186 | McGrath, C. H. | 186 |
| Argeşanu, V. | 168 | Garcia-Planas, M. I. | 75 | Milanova Yordanova, S. | 138 |
| Aurelia, P. S. | 159, 197 | George, L. E. | 298 | Miyagi, P. E. | 51 |
| Aurelia, S. | 332 | Ghadi, A. | 367 | Mladenov, V. | 66 |
| Awajan, A. | 57 | Ghelichkhani, M. | 384 | Moscato, L. A. | 51 |
| Aydogan, M. | 114 | Goto, K. | 388 | Muftah, M. A. | 233 |
| Battisti, F. | 70 | Greene, N. | 19 | Mursi, M. F. M. | 98 |
| Beltrán, A. | 286 | Guarini, M. R. | 70 | Muthalif, A. G. A. | 80 |
| Benhaddouche, D. | 87 | Guzman, Y. M. | 204, 286 | Nadimi, M. H. | 326 |
| Benmiloud, T. | 107 | Hamdi, M. | 274 | Nakaya, H. | 388 |
| Benyettou, A. | 87 | Hari, J. | 338 | Narahashi, T. | 388 |
| Bhattacharjee, S. | 355 | Hofreiter, M. | 62 | Ogura, T. | 388 |
| Bilgincan, T. | 224 | Hussain, A. | 348 | Okolnishnikov, V. | 123 |
| Borozan, I. S. | 168 | Ibrahim, D. S. | 80 | Orucevic, F. | 244 |
| Buccarini, C. | 70 | Iftikhar, S. | 309 | Oulehla, M. | 265 |
| Bustamante, F. P. | 204 | Ivanov, K. S. | 220 | Ozdemir, S. | 183, 224 |
| Butkovic, A. | 244 | Iwamoto, M. | 388 | Paduchova, A. | 142 |
| Buzák, P. | 179 | Jaiganesh, V. | 400 | Pastrana, M. I. M. | 286 |
| Castelán-Ortega, O. A. | 132 | Janík, Z. | 179 | Pedzisai, J. B. T. | 393 |
| Castro Rodríguez, V. M. | 204 | Jaramillo, V. | 286 | Petrovski, A. | 152 |
| Caviativa, Y. P. | 204, 286 | Jašek, R. | 210 | Potužák, L. | 92 |
| Chammem, M. | 274 | Johnson-Wahrmann, K. | 117 | Raj, D. | 197, 332 |
| Chan, C.-M. | 342 | Jula, M. | 168 | Ramesh, G. M. | 400 |
| Chaudhury, S. | 355 | Kalyani, S. | 338 | Rano, R. | 290 |
| Daskalov, S. V. | 239 | Kase, W. | 46 | Rayas-Amor, A. A. | 132 |
| Debeleac, C. | 127 | Kaur, M. | 314 | Riaz, A. | 309 |
| Dimchev Kalchev, Y. | 138 | Keller, A. A. | 36 | Rincón, A. M. | 286 |

| | | | | | |
|---------------|---------------|-----------------------|----------|----------------|-----|
| Rudometov, S. | 123 | Simionescu, C.-S. | 127, 146 | Tanovic, A. | 244 |
| Saleh, O. | 159, 197, 332 | Sinkakarmi, A. | 367 | Toyama, A. | 388 |
| Saleh, T. | 80 | Šotnar, J. | 92 | Tsenov, G. | 66 |
| Salman, A. | 309 | Souza, J. A. L. | 51 | Varol, D. | 114 |
| Samaka, M. | 361 | Squillante Júnior, R. | 51 | Viriri, S. | 393 |
| Sarkar, A. | 290 | Stoeva, M. T. | 239 | Vogeltanz, T. | 210 |
| Sato, I. | 388 | Suenaga, A. | 388 | Xu, J. | 117 |
| Saveski, J. | 191 | Sun, M. | 388 | Yeh, J. Z. | 388 |
| Semenescu, A. | 216, 270, 282 | Taberna, J. | 75 | Youssef, S. M. | 259 |
| Shoewu, O. | 372 | Taiji, M. | 388 | Žáková, K. | 179 |
| Šilinger, K. | 92 | Takayama, K. | 388 | Zhuravlev, S. | 123 |
| Silva, J. R. | 51 | Takeuchi, H. | 388 | | |